UNIVERSIDAD POLITÉCNICA DE CARTAGENA

Higher Technical School of Agronomic Engineering

Department of Food Engineering and Agricultural Equipment

ASSOCIATION AMONG AROMA VOLATILES AND OTHER TRAITS IN ONE NEAR-ISOGENIC LINE WITH FIRM FLESH TEXTURE

Mohamed ZARID

2020

Universidad Politécnica de Cartagena | Campus de Excelencia Internacional

ETSIA-UPCT

Ph.D. Thesis:

ASSOCIATION AMONG AROMA VOLATILES AND OTHER TRAITS IN ONE NEAR-ISOGENIC LINE WITH FIRM FLESH TEXTURE

Thesis submitted by:

D. MSc. Ing. Mohamed ZARID

for the degree of

Doctor of Philosophy (PhD)

in

Advanced Techniques in Research and Development of Food Engineering and Agriculture

at

UNIVERSIDAD POLITÉCNICA DE CARTAGENA (ETSIA-UPCT)

Directed by:

Prof. Dr. Juan Pablo Fernández Trujillo

Department of Food Engineering and Agricultural Equipment, ETSIA-UPCT.

Codirected by:

Prof. Dr. María del Carmen Bueso Sánchez

Department of Applied Mathematics and Statistics, ETSII-UPCT.

Cartagena (Spain), 2020.

To Allah, Rasulo Allah

and the spirit of my beloved Mom.

Acknowledgement:

First and foremost, I would like to thank Allah Almighty for giving me the strength, knowledge, ability and opportunity to undertake these research studies.

I would like to give special thanks to the dedication of my supervisor in the development of this PhD Thesis, Prof. Dr. Juan Pablo Fernández Trujillo for allowing me to complete the PhD Thesis under his guidance and support, as well as for the wisdom and counsel he has conveyed to me, also for the trust he has placed in me and my work, for his optimism, and for his ability to guide my ideas, not only in the development of this PhD Thesis but also in my development as a researcher.

Thanks to my Co-director Prof. Dr. María del Carmen Bueso Sánchez, from the Department of Applied Mathematics and Statistics, Universidad Politécnica de Cartagena (UPCT) for her guidance and corrections.

To our dear coordinator Prof. Dr. Francisco Artés Hernández, to Prof. Dr. Francisco Artés Calero and all my colleagues of the "Grupo de Postrecolección y Refrigeración" (ETSIA-UPCT).

To Prof. Dr. Marcos Egea Gutiérrez Cortines, Prof. Encarna Aguayo Giménez, Prof. Perla Gómez Di Marco, Dr. Ginés Benito Martínez Hernández, Dr. Ascensión Martínez Sánchez, Paloma Martínez Martínez, Noelia Castillejo Montoya, Maria Jose Sanchez Martinez, Tâmmila Venze Klug, Elena Collado Marín, Lara Moreno Garcia and to all professors, staff and colleagues of the ETSIA and IBV (UPCT), thanks for your company.

Thanks to María Belén Picó Sirvent and Alicia Gemma Sifres Cuerda from the "Institute for Conservation and Improvement of Valencian Agrodiversity" (COMAV-Universitat Politècnica de València).

I especially express my sincere thanks to Lara Sandrine Koch to Samira Chehab Koch to Lamia Chehab to my brothers/sons Moad and Hamza Zarid and my beloved wife Dr. Sarra Roubi Zarid.

To my family and friends...

To all of you, thank you very much!

Mohamed Taha ZARID

Universidad Politécnica de Cartagena

DT-16

CONFORMIDAD DE SOLICITUD DE AUTORIZACIÓN DE DEPÓSITO DE TESIS DOCTORAL POR LOS DIRECTORES DE LA TESIS

D. **Juan Pablo Fernández Trujillo** y Dña. **María del Carmen Bueso Sánchez,** directores de la Tesis Doctoral **"ASSOCIATION AMONG AROMA VOLATILES AND OTHER TRAITS IN ONE NEAR-ISOGENIC LINE WITH FIRM FLESH TEXTURE"**.

INFORMAN:

Que la referida Tesis Doctoral, ha sido realizada por D. **Mohamed ZARID**, dentro del Programa de Doctorado **Técnicas Avanzadas en Investigación y Desarrollo Agrario y Alimentario (TAIDA)**, dando nuestra conformidad para que sea presentada ante el Comité de Dirección de la Escuela Internacional de Doctorado para ser autorizado su depósito.

La rama de conocimiento en la que esta tesis ha sido desarrollada es:

- ► Ciencias
- □ Ciencias Sociales y Jurídicas
- □ Ingeniería y Arquitectura

En Cartagena, a 13 de febrero de 2020

LOS DIRECTORES DE LA TESIS

FERNANDEZ TRUJILLO JUAN PABLO [redacted]

Fdo.: Juan Pablo Fernández Trujillo

MARIA DEL CARMEN|BUESO SANCHEZ [redacted]

Fdo.: María del Carm

COMITÉ DE DIRECCIÓN ESCUELA INTERNACIONAL DE DOCTORADO

Universidad Politécnica de Cartagena

DT-17

CONFORMIDAD DE DEPÓSITO DE TESIS DOCTORAL

POR LA COMISIÓN ACADÉMICA DEL PROGRAMA

Prof. Dr. Francisco Artés Hernández_____, Presidente/a de la Comisión Académica del Programa __ **Técnicas Avanzadas en Investigación y Desarrollo Agrario y Alimentario (TAIDA)** _____.

INFORMA:

Que la Tesis Doctoral titulada, _**"ASSOCIATION AMONG AROMA VOLATILES AND OTHER TRAITS IN A NEAR-ISOGENIC LINE WITH FIRM FLESH TEXTURE"** __, ha sido realizada, dentro del mencionado Programa de Doctorado, por D._ **Mohamed ZARID**_, bajo la dirección y supervisión del **Prof. Dr. _Juan Pablo Fernández Trujillo** _.

En reunión de la Comisión Académica, visto que en la misma se acreditan los indicios de calidad correspondientes y la autorización del Director/a de la misma, se acordó dar la conformidad, con la finalidad de que sea autorizado su depósito por el Comité de Dirección de la Escuela Internacional de Doctorado.

La Rama de conocimiento por la que esta tesis ha sido desarrollada es:

- ► Ciencias
- □ Ciencias Sociales y Jurídicas
- □ Ingeniería y Arquitectura

En Cartagena, a _13_ de _Febrero_ de _2020_

EL PRESIDENTE DE LA COMISIÓN ACADÉMICA

Fdo: _[redacted]___ Firmado digitalmente por FRANCISCO DE ASIS|ARTES|HERNANDEZ

COMITÉ DE DIRECCIÓN ESCUELA INTERNACIONAL DE DOCTORADO

TABLE OF CONTENTS

List of tables:

postharvest ripening at 20.5 ^{o}C and 88% relative humidity. Effect of postharvest ripening time (RT) or the introgression (I) alone or combined with RT. All the information comes from Melonomics version 4.0, including the chromosome (LG) location except when unavailable (LG 0).

List of figures:

Chapter III:

Chapter IV:

Figure 1. Maximum and minimum temperature, daily rainfall, and average radiation in both growing seasons (S1 and S2, continuous and dotted lines) from plantation to fruit harvest of the melon near-isogenic line (NIL) SC10-2 and the parental 'Piel de Sapo' (PS) line. Mean of temperature, precipitation and radiation are also included in text in the figure.

Figure 2. Discrimination between the melon near-isogenic line (NIL) SC10-2 and the parental 'Piel de Sapo' (PS) line according to individual flesh volatile organic compounds at harvest in two seasons (S1 and S2) according to Partial Least Squares-Discriminant Analysis (PLS-DA). A and B (S1 and S2, respectively): Datasets and the corresponding centroids (x) for the different lines and 65% confidence ellipses. C and D (S1 and S2, respectively): Correlations between the individual volatile compounds, the textural traits and the first two components. The numbers in the graph on the right correspond to the compounds with 50% or more of the variance explained by the two components according to the PLS-DA and numbered according to Table 1.

Figure 3. Random forest (RF) applied for classification of flesh volatile organic compounds of the near-isogenic line (NIL) SC10-2 (n=5 and 4, for S1 and S2, respectively) and the parental 'Piel de Sapo' (PS) line (n=20 and 9, for S1 and S2, respectively). The importance of the compounds for the classification is based on the Mean Decrease in Accuracy and Mean Decrease in the Gini index. (A) Season 1, S1. (B) Season 2, S2.

Figure 4. Correlation network analysis (CNA) based on Pearson coefficient with adjacency defined by cut-off absolute value greater than 0.8. Clusters identified from flesh volatile organic compounds of the near-isogenic line (NIL) SC10-2 and the parental 'Piel de Sapo' (PS) line at harvest in season 1 (S1) and season 2 (S2). The numbers in the graphs correspond to the number assigned for each volatile compound according to Table 1..

Chapter V:

Figure 1. Respiration rate and ethylene production of individual fruit, the near-isogenic line SC10-2 and its parental line 'Piel de Sapo' (PS), harvested in firm-ripe stage of maturity during 18 d of postharvest ripening at 20.5 ^{o}C and 88% relative humidity (mean ± SE, n=6).

Figure 2. Textural traits of melon fruit, the near-isogenic line SC10-2 and its parental line 'Piel de Sapo' (PS) harvested in firm-ripe stage of maturity during 18 d of ripening at 20.5 ^{o}C and 88% relative humidity (mean ± SE, n = 3). A. Flesh firmness B. Whole fruit hardness C. Flesh juiciness.

Figure 3. Main compound classes identified by static headspace solid-phase micro-extraction and gas chromatography–mass spectrometry (HS-SPME/GC-MS) in melon fruit of the near-isogenic line (NIL) SC10-2 and its parental line 'Piel de Sapo' (PS) harvested in firm-ripe stage of maturity and subjected to storage at 20.5 ^{o}C and 88% relative humidity for 18 d. Data are expressed as percentage of each compound class with match quality above 50 with respect to the sum of areas of the identified compounds without considering exogenous ones (mean ±SE, n=3). LSD were calculated after a two-way ANOVA with introgression and ripening time as factors.

Figure 4. Main compound classes identified by the static headspace solid-phase micro-extraction and gas chromatography–mass spectrometry (HS-SPME/GC-MS) technique in melon fruits of the near-isogenic line (NIL) SC10-2 and its parental line 'Piel de Sapo' (PS) (n= 3) subjected to storage at 20.5 ºC and 88% relative humidity for18 d. Data are expressed as percentage of each compound class with respect to the total normalized areas (transformed into log2). Means were statistically significant according to two-way ANOVA with introgression and ripening time as factors.

Figure 5. Gene Ontology (GO) of differentially expressed genes only considering the ripening time factor in melon fruit of the near-isogenic line NIL SC10-2 and its parental 'Piel de Sapo' (PS) harvested in firm-ripe stage of maturity and stored at 20.5 ºC and 88% relative humidity for 18 d.

Figure 6. Gene Ontology (GO) of differentially expressed genes only considering the introgression factor in melon fruit of the near-isogenic line NIL SC10-2 and its parental 'Piel de Sapo' (PS) harvested in firm-ripe stage of maturity and stored at 20.5 ºC and 88% relative humidity for 18 d.

Figure 7. Cluster analysis of the differentially expressed genes only considering the ripening time in fruit of the melon near-isogenic line SC10-2 and its parental control 'Piel de Sapo' (PS). Differentially expressed genes were categorized into six clusters depending on their expression during fruit ripening (0, 4, 8, 12 and 18 d at 20.5 ºC and 88% relative humidity).

Figure 8. Cluster analysis of the differentially expressed genes significant in the comparison between lines over time in fruit of the melon near-isogenic line SC10-2 and its parental control 'Piel de Sapo' (PS). Differentially expressed genes were categorized into seven clusters depending on their expression during fruit ripening (0, 4, 8, 12 and 18 d at 20.5 ºC and 88% relative humidity).

Figure 9. Relative expression of selective genes only considering the ripening time with differential expression involved in primary metabolism or ascorbic acid metabolism in fruit of the melon near-isogenic line SC10-2 and its parental control PS harvested in firm-ripe stage of maturity and stored during 18 d of ripening at 20.5 ºC and 88% relative humidity. *Cm*SDHA: Succinate dehydrogenase [ubiquinone] flavoprotein subunit, mitochondrial/ *Cm*NADP: isocitrate dehydrogenase [NADP]/ *Cm*L-GalDH: L-galactose dehydrogenase/ *Cm*GME: GDP-mannose-3',5'-epimerase/ *Cm*ACLA-1: ATP-citrate synthase alpha chain protein/ *Cm*ACLB-2: ATP-citrate synthase beta chain protein 2-like/ *Cm*SCOA: Succinate--CoA ligase [ADP-forming] subunit alpha, mitochondrial/ *Cm*IIL1: 3-isopropylmalate dehydratase large subunit/ *Cm*NADH1: NADPH:quinone oxidoreductase-like.

Figure 10. Relative expression of selective genes only considering the ripening time involved in quality and physiological process in fruit of the melon near-isogenic line SC10-2 and its parental control PS harvested in firm-ripe stage of maturity and stored during 18 d of ripening at 20.5ºC and 88% relative humidity. *Cm*LOX18: Fruit ripening/ *Cm*ACO2: Ethylene biosynthesis/ *Cm*ADH1 and *Cm*CAD1: Phenylpropanoid biosynthesis/ CmAOS and CmOPR2: Oxylipin biosynthesis/ *Cm*SWEET7: Sugar transporter activity/ *Cm*DFR4: Flavonoid

biosynthesis/ *Cm*NADH1: Oxidoreductase activity/ *Cm*PAL: Phenylpropanoid metabolism/ *Cm*WRKY33, *Cm*GATA5, *Cm*TCP15, *Cm*NAC18: Transcription factor activity/ *Cm*ERF027: Ethylene transcription factor activity/ *Cm*GDSL: Esterase and lipase activity/ *Cm*GDE4: Glycerol metabolism/ *Cm*TAC: Amino acid activity/ *Cm*IPMI3: 3-isopropylmalate dehydratase small subunit 3-like/ *Cm*ALT-2: alanine aminotransferase.

Figure 11. Relative expression of selective genes only mainly considering the comparison between lines over time and involved in different process in fruit of the melon near-isogenic line SC10-2 and its parental control PS harvested in firm-ripe stage of maturity and stored during 18 d of ripening at 20.5 ºC and 88% relative humidity. *Cm*NAC18: Transcription factor activity/ *Cm*WRKY33: Transcription factor activity/ *Cm*CAD1: Phenylpropanoid biosynthesis/ *Cm*MADS-box: MADS-box transcription factor/ *Cm*ACLA-1: ATP-citrate synthase alpha chain protein/ *Cm*IIL1: 3-isopropylmalate dehydratase large subunit/ *Cm*FAH: fumarylacetoacetase/ *Cm*ACO2: Ethylene biosynthesis/ *Cm*SDHA: Succinate dehydrogenase [ubiquinone] flavoprotein subunit, mitochondrial/ *Cm*IPMI3: 3-isopropylmalate dehydratase small subunit 3-like/ C*m*SCOA: Succinate--CoA ligase [ADP-forming] subunit alpha, mitochondrial/ *Cm*L-GalDH: L-galactose dehydrogenase/ C*m*LOX18: Fruit ripening/ *Cm*NADP: isocitrate dehydrogenase [NADP]/ *Cm*ACLB-2: ATP-citrate synthase beta chain protein 2-like.

Figure 12. Relative expression of selective genes only considering the postharvest ripening time factor and involved in different process in fruit of the melon near-isogenic line SC10-2 and its parental control PS harvested in firm-ripe stage of maturity and stored during 18 d of ripening at 20.5ºC and 88% relative humidity. *Cm*DHL92: Polygalacturonase At1g48100/ *Cm*MPC1: Mitochondrial pyruvate carrier/ *Cm*DTX: Protein detoxificatoin/ *Cm*ABREX1: Abscisic acid-insensitive 5-like protein 4 isoform X1/ *Cm*IAA71: auxin-responsive protein SAUR71-like.

List of publications:

***Zarid, M.**, Bueso, M.C., Fernández-Trujillo, J.P. (**2020)**. Seasonal effects on flesh volatile concentrations and texture at harvest in a near-isogenic line of melon with introgression in LG X. Scientia Horticulturae 266, 109244. https://doi.org/10.1016/j.scienta.2020.109244.

***Zarid, M.**, García-Carpintero, V., Esteras, C., Esteva, J., Bueso, M.C., Cañizares, J., Picó, M.B., Monforte, A.J., Fernández-Trujillo, J.P. Transcriptomic analysis of a near-isogenic line of melon with higher fruit flesh firmness during ripening. (Journal of the Science of Food and Agriculture: Under Review)

*****Fernández-Trujillo, J.P.; **Zarid, M.**; Bueso, M.C. (**2018**). Methodology to Remove Strong Outliers of Non-Climacteric Melon Fruit Aroma at Harvest Obtained by HS-SPME GC-MS Analysis. *Separations*, *5*, 30. https://doi.org/10.3390/separations5020030.

List of congress chapters and presentations

***Zarid, M.**, Esteras, C., Sifres, A.G., Cañizares, X., Esteva, J., Bueso, M.C., Picó, M.B., Monforte, A.J., Fernández Trujillo, J.P. (**2020)**. Lower relative differential expression of two genes is associated with delayed ripening in melon. In: Proceedings of the 8th Workshop on Agri-Food Research for young researchers. Editors: Artés-Hernández, F; Fernández-Hernández, J.A.; Zornoza, R.; Periago, P.; Alarcón, J.J.; Cos, J.E. Editorial: CRAI Biblioteca, Universidad Politécnica de Cartagena, Cartagena, Murcia, Spain, pp. 16-19. ISBN: 978-84-17853-08-2. 171 pp. Open access http://hdl.handle.net/10317/8367.

***Zarid, M.**, Esteras, C., Gemma Sifres, A., Cañizares, X., Esteva, J., Picó, M.B., Monforte, A.J., Fernández Trujillo, J.P. (**2019**). High relative expression of two genes of a melon near-isogenic line versus its parental during ripening. In: Proceedings of the 7th Workshop on Agri-Food Research. Editors: Artés-Hernández, F; Fernández-Hernández, J.A.; Cos, J.E., Alarcón, J.J.; Egea-Cortines. M.; Aguayo, E. Editorial: CRAI Biblioteca, Universidad Politécnica de Cartagena, Cartagena, Murcia, Spain, pp. 14-17. ISBN: 978-84-16325-89-4. 167 pp. Open access. http://hdl.handle.net/10317/7652

*** Zarid, M.**, Esteras, C., Gemma Sifres, A., Cañizares, X., Esteva, J., Picó, M.B., Monforte, A.J., Fernández Trujillo, J.P. (**2018)**. Gene expression and volatile production during melon ripening. In: Proceedings of the 6th Workshop on Agri-Food Research. Editors: F. Artés-Hernández, J.E. Cos, J.A. Fernández-Hernández, J. Calatrava, E. Aguayo, J.J. Alarcón, M. Egea. Editorial: CRAI Biblioteca, Technical University of Cartagena, Murcia, España. ISBN: 978-84-16325-64-1. 27-30. 208 pp. Open access http://hdl.handle.net/10317/6706

***Zarid, M.**, Fernández-Trujillo, J.P. (**2017**). Seasonal effect on selected quality traits of a melon near-isogenic line. In: Proceedings of the 5th Workshop on Agri-Food Research. Editors: F. Artés-Hernández, M. Egea-Cortines, J.A. Fernández-Hernández, J. Calatrava, E. Aguayo, J.J. Alarcón, J.E. Cos. Editorial: CRAI Biblioteca. Technical University of Cartagena, pp. 44-47. ISBN: 978-84-16325-29-0. 9-10/05/2016. Cartagena, Murcia, Spain. http://hdl.handle.net/10317/5558

***Zarid, M.**, Fernández-Trujillo, J.P. (**2016**). Association among aroma volatiles and other traits in near-isogenic lines with firm flesh texture. In: Proceedings of the 4th Workshop on Agri-Food Research. Editors: F. Artés-Hernández, J.E. Cos, J.A. Fernández-Hernández, J. Calatrava,

E. Aguayo, J.J. Alarcón, M. Egea. Editorial: CRAI Biblioteca, Technical University of Cartagena, pp. 233-235. ISBN: 978-84-608-5399-2. Cartagena, Murcia, Spain. http://hdl.handle.net/10317/5290

Related publications:

*****Canales, I., Fernández-Trujillo, J.P., Bueso, M.C., **Zarid, M**. (**2016**). Volatile changes in non-climacteric melons with introgression in linkage group X at three stages of maturity. VIII International Postharvest Symposium. Postharvest 2016. Cartagena 21-24 June 2016: Enhancing Supply Chain and Consumer Benefits –Ethical and Technological Issues. Eds.: F. Artés-Hernández et al., pp. 351-356. https://www.actahort.org/members/showpdf?booknrarnr=1194_50

*****Escudero, A.A., **Zarid, M.**, Bueso, M.C., Fernández-Trujillo, J.P. (**2016**). Aroma volatiles during non-climacteric melon ripening and potential association with flesh firmness. VIII International Postharvest Symposium. Postharvest 2016. Cartagena 21-24 June 2016: Enhancing Supply Chain and Consumer Benefits –Ethical and Technological Issues. Eds.: F. Artés-Hernández et al. pp. 363-366. https://www.ishs.org/ishs-article/1194_50

*****Citlalli, P.H., Celso, M., **Zarid, M.**, Benabderrahim, M.A., Bueso, M.C., Fernández-Trujillo, J.P. (**2014**). Textural modifications and differential aroma profile of near-isogenic lines of melon. XII RBMP. XII Reunión Biología Molecular de Plantas. Cartagena, 11-13 June 2014. Actas p. 168. https://www.verticesur.es/congresos/RBMP2014/comunicaciones.php

*****Celso, M., Citlalli, P.H., **Zarid, M.**, Benabderrahim, M.A., Fernández-Trujillo, J.P. (**2014**). Aromatic profile of nearly isogenic lines of melon with firmer pulp than its parental control. II International Congress and XVI National of Agronomic Sciences. Univ. Autonomous Chapingo. Texcoco, Chapingo, Mexico. 23-25 April 2014. Magisterial conference at the agro-industry table. . http://www.chapingo.mx/dgip/eventos/agronomico201/agronomico.html

ABSTRACT :

Quality in melons (*Cucumis melo* L.) is an important criterion for consumer's acceptance. Like any other fruit, melons development and ripening process are linked to a series of biochemical and physiological changes. The goal of these researches has been focused on determination of the global quality and aroma profile of a non-climacteric near-isogenic line (NIL) SC10-2 of melon developed from the Spanish cultivar T111 (ssp. *melo*) of the 'Piel de Sapo' type (PS) and the Korean accession PI 161375 Songwhan Charmi (ssp. *agrestis*) (SC), with different texture than its non-climacteric parental PS, in order to map QTLs associated with fruit quality and, particularly, aroma volatiles.

A methodology for a consistent study of outliers of non-climacteric melon volatile organic compounds at harvest was reported. For extreme outliers, we proposed the study of compound classes in percentage of total area counts by principal component analysis followed by a further verification with box-whisker plot. The presence of esters usually at higher proportions than expected, or an excess of minority compounds such as ketones, alcohols, terpenes or others are usually a sign of volatile results that can be considered outliers. A comparison was performed in two seasons between the melon near-isogenic line SC10-2 and its parental PS in order to identify the most discriminant flesh aroma volatiles at harvest as potential biomarkers of textural differences (especially flesh firmness) due to introgressions in melon chromosome X, examining seasonal effects on these the former traits.

Several univariate and multivariate statistical techniques were used to determine the association between the aroma volatile levels and differences in melon texture. Three methodologies involving different treatments of null values were applied to analyse the effects of introgression on volatile organic compounds (VOCs). Substitution of the zeros with the minimum value of the same VOC variable per season and line is proposed for the analysis of VOC data. SC10-2 showed higher whole fruit hardness, flesh firmness, and fibrousness, but lower juiciness than PS. One hundred sixteen VOCs were identified to evaluate the introgression effect, in which 60 VOCs were detected in two seasons with very different climatic conditions during fruit set and ripening; twenty-eight VOCs were involved in the differences on aroma production in the comparison of the NIL SC10-2 with PS. The environmental effects were more significant than the introgression effect. The environment particularly affected VOCs rather than textural traits, and at least one potential VOC quantitative trait locus (QTL) located in LG X alone and another interacting with the environment are proposed to affect VOC fruit metabolism.

Transcriptomic analysis from RNA-seq revealed 2954 differentially expressed genes (DEGs) having introgression or introgression x ripening time effects and 2068 DEGs postharvest ripening time effect. Only 909 DEGs were exclusive of the introgression, and only 23 DEGs were exclusive of postharvest ripening time. Clusters of ripening time (six) revealed a general upregulation vs. harvest with slight interaction genotype x ripening time in 68.8% DEGs of four clusters, while clusters of the genotype (seven) revealed that the introgression generally produced noticeable differences in DEG upregulation or downregulation vs. the control PS in four clusters and 30% and 7.3% DEGs, respectively. Major functions of the DEGs associated with introgression or ripening time were delimited. About thirty-four genes were affecting direct and/or indirectly in the delay of ripening of SC10-2 versus PS in general and particularly to respiration rate, ethylene production, textural traits and volatile production and probably differential non-climacteric response. Of the former genes, we studied with more detail at least three that mapped in the introgression in linkage group (LG) X, and thirty-one outside it. The former results indicated the control of fruit physiology, but also textural and volatile traits traits, by an eQTL located in LG X. Some genes that mapped within the introgression in LG X that showed differential response between SC10-2 and PS could be associated with these quality differences between lines.

GENERAL INTRODUCTION

I. GENERAL INTRODUCTION:

1. Introduction:

Melon (*Cucumis melo* L.), an important crop worldwide and an annual diploid plant (2n = 2x = 24), has a high intra-specific genetic variation and a small genome size estimated at 454 Mb, which can be technologically exploited in terms of flavour development and textural changes that occur during fruit ripening (Pech et al., 2008). Melon development and ripening process are linked to a series of biochemical, physiological and organoleptic changes (Dos-Santos et al., 2013) including chlorophyll breakdown, cell wall degradation, increase in the sugar content and soluble solids content, pigment biosynthesis, aroma and flavour generation, etc. These changes followed a genetic program with a coordinated cascade on responses starting in the placental tissue of the fruit but ending in the rest of the mesocarp, but with noticeable differences between climacteric and non-climacteric types (Ezura et al., 2008; Guo et al., 2017; Ríos et al., 2017).

Non-climacteric melon fruit ripening is still poorly understood in order to apply several postharvest techniques to delay partly ethylene-indepent processes such as flesh softening or the production of certain aroma (Chaparro-Torres et al., 2016; Pech et al., 2008). One of the main evident changes during melon fruit softening is whole fruit softening but in particularly flesh softening in non-climacteric types (Bianchi et al, 2016; Dos-Santos et al., 2013), among other textural changes such as juiciness (opposite trait to flesh firmness) very appreciated for consumers (Escribano and Lázaro, 2012; Escribano et al., 2010; Obando et al., 2008; Obando-Ulloa et al., 2009). In fact, most of the consumers of non-climactericc melons prefer a fruit of medium firmness, crunchy and outstanding firmness (Fernández-Trujillo et al., 2012a; Lázaro and Lorenzo, 2015).

Non-climacteric melon fruit ripening and quality has been little studied compared with climacteric melons. The melon quality is composed of features that provide value or degree of excellence for the consumer, being firm flesh texture and good flavor and essential nutritional value. The melon aroma is key in the perception of fruit quality perceived by consumers and is due to a mixture of compounds of different degree of volatility (Dos-Santos et al., 2013). The combinations of aroma active compounds determine the melon aroma (Pang, et al., 2012).

The aroma profile and the textural traits discriminate climacteric from non-climacteric near-isogenic lines (NILs) at harvest or after postharvest (Obando-Ulloa et al., 2008 and 2009), but little information is still available about aroma formation in non-climacteric melons particularly during postharvest ripening (Gonda et al., 2010) and in non-climacteric NILs during ripening. The emphasis in the flesh aroma of non-climacteric melons have focused in VOCs at harvest (Obando-Ulloa et al., 2010; Perry et al. 2009; Verzera et al., 2011), and precursors such as branched amino acid and other amino acids (Gonda et al., 2010, 2013 and 2018), fatty acids (Li et al., 2016). In other non-climacteric studies, most of the authors focused in differences between climacteric and non-climacteric types or among types or NILs (Bernillon et al., 2013 ; Güler et al., 2009; Obando-Ulloa et al., 2008), or among different rootstocks (Verzera et al., 2014), because VOC as a part of flavour is also of interest for fresh melon consumption (Escribano et al., 2010; Fernández-Trujillo et al., 2012a).

The development of the melon NILs collection from the cross of the the cv. T111 of the *inodorous* group and 'Piel de Sapo' (PS) type, and the Korean accession 'Songwhan Charmi' (SC) PI 161375 (Eduardo et al., 2005) was economically important because of the fruit traits as the morphology (Eduardo et al., 2007; Fernandez-Silva et al., 2010), climacteric ripening (Vegas et al., 2013) and virus resistance (Essafi et al., 2009), and the genotyping technologies revolution in the last few years allows to identify and localize several quantitative trait loci (QTLs) as in strawberry (Aharoni et al., 2004), tomato (Tieman et al., 2006) and apple (Zini et al., 2005; Dunemann et al., 2009).

New genetic and genomic tools are available for studying fruit ripening including near-isogenic lines, tilling platforms, saturated genetic maps, and the genome sequence, and many QTLs and eQTLs positioned, gene expression atlas, etc. (Dahmani et al., 2010; González et al., 2011; Yano et al., 2018), though again melon is more difficult than tomato because of fruit size and difficulties to establish a proper harvest maturity.

One near-isogenic line (NIL) of melon (SC10-2) contains QTLs of interest for flesh properties, such as for example (and versus PS) higher levels of flesh proportion and flesh firmness at harvest (Dos-Santos et al., 2013; Moreno et al., 2008), and lower levels of flesh juiciness, extractable juice, juice density and titratable acidity but higher pH, dry matter and flesh lightness color index (Obando et al., 2008). The NIL SC10-2 also show differential aroma at harvest with lack of some compounds versus its parental, a pattern associated with delayed ripening at harvest (Dos-Santos et al., 2013), and show reduced juice leakage versus PS in fresh-cut cubes during cold storage (Gomes et al., 2009), and certain risk of cracking during preharvest (Fernández-Trujillo et al., 2013).

The goal of this thesis was to determine global quality and aroma profile of selected near-isogenic lines (NILs) of non-climacteric melons in order to map QTLs associated with fruit quality in the genetic map of melon. Particularly the focus was textural traits and aroma volatile changes due to over ripening and/or season. Using gene expression over time of the parental control and a NIL, the genomic map of melon (MELOGEN) and the sequences previously stored in GenBank, and to position candidate genes in the melon chromosomes and link them with the phenotypic information.

2. Importance of Melon:

2.1 Introduction:

The *Cucurbitaceae* family consists of tendril-bearing vine plants located in sub-tropical and tropical regions (Robinson and Decker-Walters, 1999) some species are resistant to cold and others are adapted to xerophytic conditions (Wien, 1997). According to the geographic origin, the Cucurbits (*Cucurbitaceae* family) can be divided into new world and old-world species. The Cucurbits contain 2 subfamilies, 8 tribes, about 120 genera and more than 800 species (Jeffrey, 1990), mainly cultivated as fruits and vegetables which can be consumed or used in several foodstuff or as medicines, the case of *Cucurbita andreana*, which contain the cucurbitacins important compounds known with anticarcinogen and anti-inflammatory activities (Jayaprakasam et al., 2003). The roots, leaves, seeds and stems could be taken for

hematoma or to reduce hypertension and also as a vomitif or emetic. Also, Cucurbits are used for storing food (Gourd) and as a sponge (Loofah) (Robinson and Decker-Walters, 1999).

2.2 Botany and Origin of *Cucumis melo*:

With 3 ovary sections or locules, melon fruit is an indehiscent 'pepo', a fleshy fruit with a leathery, non-septate rind obtained from an inferior ovary (Robinson and Decker-Walters, 1999). From the placentae or mesocarpic tissue, the edible flesh is derived (Seymour and McGlasson, 1993). Melon fruit has a large diversity as regards form, size, color, etc (Kirkbride, 1993). Fruits as short as 4cm long (*Cucumis melo* L. var. *agrestis*) and as long as 200cm (*Cucumis melo* L. var. *flexuosus*) were reported (Périn et al., 2002b), or a weight interval which oscillate between 50g and more than 15 kg are known (Naudin, 1859). The differences can also be in flesh and rind color and texture (Kirkbride, 1993; Goldman, 2002), and depending also to the attachment to the stem because there is some melon fruit remain attached even after they are ripe (Kirkbride, 1993).

The genetic and environmental (light energy, photoperiod, water supply, and temperature) factors are the main sex expression controllers in *Cucumis melo* (Wien, 1997; Robinson and Decker-Walters, 1999). The female sex expression is promoted generally by some physiological conditions which favor the carbohydrates augmentation, low temperature and nitrogen, short photoperiod and high moisture accessibility (Robinson and Decker-Walters, 1999).

The possible *Cucumis melo* origin is Africa and Asia (Robinson and Decker-Walters, 1999). According to some studies (Kerje and Grum, 2000), crossing with other *Cucumis* species and melon varieties distribution in the world, the origin of melon reported appears to be Africa, and the melon domestication process started in Egypt 3 000 years ago (Pangalo, 1929). Other diversifications and domestications may have occurred throughout the Middle East and Asia (Kerje and Grum, 2000).

2.3 Classification and Cultivars:

Melon classification may be listed as follows (Jeffrey, 1990):

Class: *Dycotyledoneae*	**Tribe**: *Melothrieae*
Subclass: *Dilleniidae*	**Subtribe**: *Cucumerinae*
Superorder: *Violanae*	**Genus**: *Cucumis*
Order: *Cucurbitales*	**Subgenus**: *Melo*
Family: *Cucurbitaceae*	**Species**: *Cucumis melo*

2.4 World production:

The world's leading melon producing countries include China, with an annual production of 15.9 million tonnes and accounting for 50% of global production, Turkey, 1.8M tonnes and finally Iran, with 1.6M tonnes. However, these three countries only represent a percentage of the world melon trade (Source: FAOSTAT- 2016). Within the EU, Spain is by far the largest melon exporter, followed by Italy and Guatemala. However, every year extra-

EU supplies from developing countries are increasing, especially from Costa Rica, Morocco, Brazil, Panama and Turkey (FAOSTAT- 2016).

3. Postharvest Physiology of Melon:

3.1 Physiological Changes during Ripening: Climateric vs. Non-climateric:

A large diversity of melon ripening behaviour was reported, and the varieties may be classified as climacteric or non-climacteric, which is important for genetic studies. *Cantalupensis* cultivars are known with a climacteric ripening which is known by an upsurge in the respiration rate with an autocatalytic ethylene production and consequently a short shelf life.

The *inodorus* cultivars are characterised by non-climacteric fruit ripening behaviour, in which the upregulation of ethylene and respiration are not detected (Lurie and Klein, 1989; Kays and Paull, 2004), and which also characterized by fruit long shelf-life. In melon, the coexistence of two different ripening pathways dependent or independent to ethylene were reported (Flores et al., 2001and 2002; Obando-Ulloa et al., 2009c). Several processes are regulated by ethylene, as the aroma compounds biosynthesis, colour changes and other postharvest aspects (Ayub et al., 1996; Flores et al., 2001 and 2002; EI-Sharkawy et al., 2005; Fernandez-Trujillo et al., 2008; Obando-Ulloa et al., 2008, 2009a and 2009c; Pech et al., 2008a). In contrast to other processes as sugar accumulation, decrease of acidity, pulp coloration and parts of fruit softening are ethylene-independent (Ayub et al., 1996; Pech et al., 2008a). Developing the shelf life is an important breeding objective among others. By decreasing ethylene biosynthesis, shelf life may be improved with a concomitant reduction of aroma and rind colour (Ayub el al., 1996), which can be considered as a commercial disadvantage.

The climacteric ripening is genetically dominant comparing to non-climacteric. According to Perin et al. (2002c), tow genes are responsible of ethylene production and control, which are AI-J and AI-4 (LG VIII and IX, respectively). In addition, some QTLs (LGs I, II, Ill, and XI) affecting climacteric ripening are detected (Perin et al., 2002c; Moreno et al., 2008b).

3.2 Ethylene Production:

Ethylene is a plant gas hormone, and as mentioned before is important for in melon fruit ripening process (Giovannoni, 2001). In climacteric melon fruits, higher levels of ethylene were observed in ripening (Pratt et al., 1977). At or close harvest, some melon fruits such as muskmelon fruits generally synthesized important quantities of ethylene (Kendall and Ng, 1988). In contrast, there is other melon fruit in which the ethylene production start as late as 20 days after harvest. As regards the hybrid melon fruits, the ethylene production rate and time were mostly intermediate to the parental cultivars. According to these results, in *Cucumis melo* ethylene production is regulated and controlled by genetic and developmental factors.

In case of netted fruit melons, exogenous ethylene is not required after harvest as long as it is produced during ripening (Pratt, 1971), but in case of *inodorus* fruits types, exogenous ethylene application after harvest may be required, to accelerate and/or to control the ripening

(Gull, 1988; Suslow et al., 2001), and the harvest of these types of fruits (*inodorus*) depend on soluble solids content, generally sugar content in these types don't increase after harvest (Bianco and Pratt, 1977).

Orange or green fleshed and netted rind fruit melons generally generate higher ethylene quantities comparing to others as green or white fleshed and smooth rind fruits (Zheng and Wolff, 2000; Liu et al., 2004), exceptions may be found especially in netted melons. In other study (Shiomi et al., 1999) measuring ethylene biosynthetic capacity in melon climacteric types revealed that fruit used in the experiment has a non-climacteric fruit behavior.

3.3 Biochemical Changes during Ripening:

3.3.1 Carbohydrate Metabolism:

Among the quality attribute of ripe melon fruits, sweetness is the most important (Yamaguchi et al., 1977; Lester and Shellie, 1992; Artes et al., 1993). In the mesocarp of ripe fruits, sucrose, glucose and fructose are the main sugars detected. The sweetness in melon depend to the sucrose levels (McCollum et al., 1988; Hubbard et al., 1990; Burger et al., 2003; Villanueva et al., 2004).

Differently to other fruits such as apple and banana, Muskmelon fruit don't store starch, and a translocated photoassimilate constant supply is required for using sugar and accumulation during development and ripening (Pratt, 1971; Hubbard et al., 1989 and 1990). Sucrose content reduction depend to photoassimilate translocation during fruit development (Hubbard et al., 1990).

Other translocated photoassimilate carbohydrates than sucrose in *cucumis melo*, can be found in the phloem, such as galactosyl-sucrose oligosaccharides raffinose and stachyose (Mitchell et al., 1992; Gao and Schaffer, 1999; Gao et al., 1999; Volk, et al., 2003).

3.3.2 Sugar and Organic Acids:

In melons, total soluble solids (TSS) are considered as a fruit maturity index, which dependent on soluble sugars, organic acids and soluble pectin. In melon, sucrose is the main sugar responsible for sweetness which is an important quality trait. Sucrose production and accumulation is genetically controlled, and the responsible gene were identified only in sweet varieties of melon fruits (Burger et al., 2002). Several QTLs are involved in sugar regulation in melon (Monforte et al., 2004; Sinclair et al., 2006; Eduardo et al., 2007; Obando-Ulloa et al., 2008 and 2009b; Paris et al., 2008; Park et al., 2009). The genotype-environment interactions affect QTLs expression.

In melon, total acidity is also genetically controlled, precisely by a known gene (Burger et al., 2002). Sweet melons are characterised by lower acidity contrary to some non-sweet melons (*flexuosus* and *acidulus* varieties) with higher acidity. The main organic acids in sweet melons are generally citric acid, malic, ascorbic, succinic, oxalacetic, tartaric, L-glutamic, fumaric, isocitric, pantothenic and so on. Some organic acids QTLs have been previously mapped (Obando et al., 2008).

3.3.3 Aroma Volatiles Compounds, Precursors and Pathways:

The aroma is an important a criterion for consumer (Yamaguchi, 1977), it is implicated in melon fruit ripening (Wang et al., 1996; Beaulieu and Grim, 2001) and continues production after harvest precisely the aroma volatile, unlike sugar accumulation (Wyllie et al., 1995). The aroma volatile profile has been the subject of several research (Kemp et al., 1972; Yabumoto et al., 1977; Yabumoto et al., 1978; Buttery et al., 1982; Yahyaoui et al., 2002; Aubert and Bourger, 2004).

As mentioned before, the melon aroma volatile profile is genetically controlled (Ueda et al., 1997; Yahyaoui et al., 2002), which are synthesized via different pathways of different metabolisms, such as fatty acids, amino acids, phenols and terpenoid (Pech et al., 2008b). The catabolism of amino acids into VOCs in melon fruit tissues, may be triggered by a transamination mechanism, decarboxylation or direct aldehyde synthesis. Using a-ketoglutarate as an amine acceptor, the transaminases converted L-isoleucine, L-leucine, L-valine. L-methionine or L-phenylalanine into their respective a-keto acids (Gonda el al., 2010).

Aroma is different in climacteric comparing to non-climacteric melons. In climacteric melons, aroma is mainly acetate and nonacetate esters and alcohols, and a lower content aldehydes, organic acids, and terpenes which characterise the non-climacteric varieties (Shalit et al., 2001), and that creates differences between cultivars. In aroma profiles, there is other compounds classes such as sulfur-derived compounds, ketones, and aliphatic compounds (Obando-Ulloa et al., 2008, 2009a and 2010; Shalit et al., 2001). Pleiotropic effects of the climacteric behavior QTL are related to differences in aroma profiles (Obando-Ulloa et al., 2008). 4 QTLs of nonethylene dependent aroma were identified and mapped in LGs IV, VlII, and XI (Obando-Ulloa et al., 2008).

3.3.4 Pigments:

Among the important melon quality traits for consumer, the flesh color (Yamaguchi, 1977). Generally, the basic and distinctive observed melon flesh colors are orange, light-orange or pink, green, and white (Watanabe et al., 1991; Goldman, 2002).

In the case of muskmelon, chlorophyll and carotenoid changes in fruit development were previously studied (Reid et al., 1970). In orange-fleshed melons, the principal pigmentsare are: β-carotene (84.7%), δ-carotene (6.8%), α-carotene (1.2%), phytofluene (2.4%), phytoene (1.5%), lutein (1.0%), violaxanthin (0.9%) and traces of other carotenoids (Seymour and McGlasson, 1993). 9 different melon cultivars from the 4 basic and distinctive flesh colors were evaluated (Watanabe et al., 1991). The orange-fleshed melon cultivars ‘Iroquois’, ‘Blenheim Orange’, ‘Birdie Red’, ‘Quincy’ and ‘Tiffany’ contained β-carotene concentrations about 9.2 to 18.0-µg/g as the important pigment, a small amount of phytofluene, α-carotene, ζ-carotene and xanthophylls. In light-orange-fleshed ‘Hale’s Best’ melon, concentrations were measured about 4.0-µg/g β-carotene, and phytofluene; α-carotene, ζ-carotene and xanthophylls were in low concentration. Finally, the principal components in the green-fleshed melon ‘Earl's Favourite’ and ‘Fukunoka’, and white-fleshed melon ‘Barharman’, were β-carotene and xanthophylls.

3.3.5 Nutritional Content:

Also, several important nutrients are contained in melon flesh including mineral, (i.e., K, Ca, Fe, Mg, P, and Zn), a wide variety of antioxidant, fiber, and vitamins, such vitamin A, α-tocopherol (vitamin E), B6 vitamin, and ascorbic acid (vitamin C), niacin, pantothenic acid, folic acid, and carotenoids (β-carotene, lutein. and zeaxanthin). The most important among them is the β-carotene content, which has been described with other carotenoids and ascorbic acid (Burger et al., 2006; Dhillon et al., 2007). β-carotene is regulated by gene wf in the melon flesh, and other QTL regulate its intensity composition (Cuevas et al., 2008). As regards vitamins and antioxidants, three QTLs were previously mapped linked to ascorbic acid content (Sinclair et al., 2004 and 2006; Obando et al., 2009b; Park et al., 2009).

3.3.6 Sensory Aspects:

Sensory characteristics of melon may be described by colour, texture (i.e., juiciness, fibrousness, firmness), aroma (i.e., volatile compounds), and taste (i.e., sweet, sour, sally bitter and umami sensations) additionally to the physical characteristics such as size, colour, and shape (Pardo et al., 2000; Hoberg et al., 2003; Obando et al., 2008), also the global appearance, overall quality and organoleptic quality are evaluated. Sensory tests are important to identify an optimum quality for consumers, because the instrumental measurements don't reflect concretely melon quality. The flesh texture, fruit flavour and generally external and internal aspect are important for consumers (Ferrer et al., 2007; Obando et al., 2008). As regards the global quality evaluation, the retronasal aroma is important in climacteric melon types and the texture in non-climacteric ones. The genetic control of sensory traits was preliminary studied (Obando et al., 2008) Accurate studies are requested to better understand these complex traits.

3.3.7 Texture:

Melon texture is an important trait for consumer acceptance. The crunchy texture is appreciated in some cultivars as ‘Piel de Sapo’ (*inodorus*) (Ferrer et al., 2007), unlike cantaloupes. Several QTLs of melon fruit traits as hardness, flesh firmness, and juiciness and some candidate genes for flesh firmness were recently mapped (Moreno et al., 2008b; Obando et al., 2008; Paris el al., 2008).

Melon fruits are transported to all the continents of the world (e.g., part of the melons consumed in Europe is produced in Latin America and South America), and the physiological disorders during storage and transportation in international markets can be critically important. Among these disorders we find water-soaking texture (i.e., vitreous texture), shrivelling, senescence spot, oxidation, cracking skin, greasiness, over ripening, chilling injury, and flavour loss (Fernandez-Trujillo et al., 2007 and 2008; Martinez et al., 2009; Obando-Ulloa et al., 2009). Because of the complexity of these traits, a few studies were performed to identify QTLs and to understand genetic control (Fernandez-Trujillo et al., 2007 and 2008).

Textural changes during fruit ripening and senescence have a certain correlation due to a matrix effect with aroma biosynthesis (Dos-Santos et al., 2013). Softening is an important determining factor in the fruit quality, which is associated with cell wall polysaccharide changes (Dos-Santos et al., 2011), and fruits with very soft flesh or that are over-mature are not accepted

by consumers (Abrahão et al., 2009), which automatically rejected by market (Amaro et al., 2013). Among the commercial practices to extend fruit post-harvest life and ensure fruit availability in markets is to harvest firm fruits (early mature), but this practice can modify the fruit aroma profile which impact automatically fruit quality traits especially in climacteric fruit (Navarro, 1997; Vallone et al., 2013).

3.3.8 Seasonal effects on fruit quality:

The melon quality is composed of features that provide value or degree of excellence for the consumer, being firm flesh texture and good flavour and essential nutritional value. The melon aroma is key in the perception of fruit quality perceived by consumers and is due to a mixture of compounds of different degree of volatility (Dos-Santos et al., 2013). The fruit melon quality can be affected by many factors, and the seasonal effect is mostly associated with environmental effects but also cultivar x environment effect, for example at the nutritional level. In fact, the insufficient or excessive potassium level negatively affects fruit quality, whereas optimal a K nutrition is involved in the augmentation of yields, soluble solids and ascorbic acid concentrations, fruit size, also, fruit colour, increased shelf life, and shipping quality of many horticultural crops (Tang et al., 2012).

The seasonal effects impact the aroma development (Chaparro-Torres et al., 2016) and may affect at harvest or after cold storage also the aroma perception of some melon fruit as in the case of 'Piel de Sapo' and other melon climacteric near-isogenic lines (NILs) (Fernández-Trujillo et al., 2008). For an optimum melon crop, rain and relatively low temperatures are preferable especially during summer (Dos-Santos et al., 2011). The differences in volatile biosynthesis during fruit growth could explain optimum melon growing conditions (environmental conditions and other potential interferences) (Dos-Santos et al., 2011).

4. Sequencing the Melon Genome and Impact in Fruit QTL mapping:

4.1 Sequencing the Melon Genome:

The genomic and genetic technologies were rare in the past years. Several international research teams contributed to establish in 2005 the International Cucurbit Genomics Initiative (ICuGI) to obtain different genomic tools located in a unique database (Garcia-Mas et al., 2016). Therefore, an ICuGI website was performed (http://www.icugi.org) to centralize the information from genetic maps of melon and expressed sequence tags (ESTs) (Garcia-Mas et al., 2016). Last years the ICuGI was updated adding new data as cucumber, watermelon and squash (Garcia-Mas et al., 2016). In Ezura et al. (2006) some of melon genomic tools are described.

4.1.1 Genetic Maps:

In melon, by using different molecular marker types and backgrounds, several genetic maps were obtained (Garcia-Mas et al., 2016). As a result of the ICuGI initiative, a genetic map considered as the first melon reference was constructed with 8 published genetic maps, containing 1 592 markers and 370 QTLs that controlled 62 traits (Diaz et al., 2011). Initially, a genetic map was constructed with 602 single nucleotide polymorphism (SNP) markers by using

a double haploid line (DHL) mapping population derived from 'Piel de Sapo' line T111 (ssp. *melo*) (PS) and PI 161375 Songwhan Charmi (ssp. *agrestis*) (SC) (Esteras et al., 2013; Garcia-Mas et al., 2012). The objective of this genetic map was anchoring the melon genome sequence to chromosomes (Ezura et al., 2006). In different experiments, some QTLs were mapped in similar genomic locations for the same identified traits (Garcia-Mas et al., 2016).

4.1.2 ESTs and RNA-Seq:

The ICuGI vise to increase the ESTs from different genotypes (Garcia-Mas et al., 2016). A melon transcriptome is available at http://www.icugi.org, assembling all the identified and published melon ESTs, resulted by using Sanger sequencing, accounted 24 444 unigenes, which includes 1 382 full-length transcripts (Clepet et al., 2011). A total of 17 510 of these unigenes allow to develop an oligo-based microarray (Mascarell-Creus et al., 2009) for transcriptome analysis in the melons with some infections as watermelon mosaic virus (Gonzalez-Ibeas et al., 2012) and *Monosporascus cannonballus* (Roig et al., 2012). Using 454 pyrosequencing (Blanca et al., 2011, Portnoy et al., 2011) and SOLiD sequencing (Blanca et al. 2012), a RNA-seq data has been recently performed from different melon genotypes. The melon breeding programmes allows obtaining the simple sequence repeat (SSR) and SNP markers from the sequences, which represent an important and useful genetic markers source (Diaz et al., 2006).

4.1.3 Mutant Collections:

According to Till et al. (2003), the introduced mutations in genes for improvement from mutant populations may be effectively filtered using local lesion in genomes provoked by targeting (TILLING). In the *cantalupensis* and the *inodorus* genetic backgrounds, many mutant populations have been developed (Dahmani-Mardas et al., 2010, Gonzalez-Ibeas et al., 2011) and exploited later for mutations identification in target genes as the sex genes *a* (andromonoecious) and *g* (gynoecious), in addition to others (Dahmani-Mardas et al., 2010; Boualem et al., 2008; Martin et al., 2009).

4.1.4 BAC Libraries:

In melon, more than five bacterial artificial chromosome (BAC) libraries have been used for cloning of important genes and developing the genome assembly (Garcia-Mas et al., 2012, Boualem et al., 2008). According to Gonzalez et al. (2010), before the melon genome sequencing, 454 pyrosequencing was obtained from 1.5% of the genome, permitting to get a preliminary genome structure view, in addition for an efficient melon genome assembly BAC-end sequences from 2 of these BAC libraries (Wang et al., 1997) is useful (Ezura et al., 2006; Garcia-Mas et al., 2012).

4.2 MELONOMICS: Sequencing the Melon Genome:

MELONOMICS is a project funded by the public sector, represented by Genoma España and five Autonomic Governments, and the private sector, in 2009. This project vise to obtain a melon genome draft using next generation sequencing (NGS) technologies. Sequenced DNA material was obtained by using the DHL92 result of PI 161375 (SC) and the PS line T111 hybridization (Garcia-Mas et al., 2012) (http://melonomics.net).

4.2.1 Genome Assembly:

As regards the genome sequencing, Roche 454 pyrosequencing technology was chosen. 14.8 million shotguns and 7.7 million paired-end reads were produced respectively from 3-kb, 8-kb and 20-kb paired-end libraries (Garcia-Mas et al., 2016). In addition, 53 203 BAC-end sequences were included in the genome assembly obtained from 2 BAC libraries from DHL92 (Gonzalez et al., 2010). Before genome assembly, melon chloroplast and mitochondrial genomes were filtered and assembled (Rodriguez-Moreno et al., 2011). The evaluated melon genome size is about 454 Mb, mitochondria genomes contains 2.74 Mb and the melon genome assembly v3.5 spans 375 Mb (83%) (Garcia-Mas et al., 2016). Probably, the unassembled fraction of the genome includes repetitive DNA sequences. The melon genome assembly v3.5 contains 1 594 scaffolds and 29,865 contigs, 78 scaffolds contained 90% of the assembly and the N50 is 4.68 Mb (Garcia-Mas et al., 2016).

The comparison with other Next Generation Sequencing (NGS)-sequenced plant genomes using 454 Titanium technology confirm the quality of the melon genome assembly (Garcia-Mas et al., 2016). The efficient method to sequence a medium-size plant genome is combining the NGS technologies (454 pyrosequencing, Illumina-Solexa, SOLiD) and Sanger sequencing (Ezura et al., 2006).

4.2.2 Genome Anchoring:

The SC × PS double haploid line genetic map (602 SNPs) was used to perform the genome assembly anchor to chromosomes, and 316 Mb of the genome assembly which form 87 scaffolds (84%) to the 12 melon linkage groups. A set of 71 scaffolds which is 292 Mb (78% of the assembly) were carefully arranged (http://melonomics.net). Using Illumina GoldenGate genotyping method, the identification and genotyping of mapped SNPs between SC and PS were performed from 454 transcriptome of melon (Esteras et al., 2013; Blanca et al., 2011). In order to fix the orientation and arranging some scaffolds, the genetic maps and backgrounds of SC × PS and PI 414723 × Dulce were used (Blanca et al., 2012). Five chimerical scaffolds were detected and manually corrected during the genome anchoring, to give another version containing 1,599 scaffolds and 29,865 contigs (Ezura et al., 2006).

Recently, a melon genome anchoring improved version has been obtained, which contain about 12 linkage groups (LG) that constitute 95% of the genome assembly (Garcia-Mas et al., 2016). After the selection of the 150 largest genome scaffolds (95%), SNPs were obtained from not anchored scaffolds in the first version and the SC and PS genomes resequenced were used for SNP mining (Garcia-Mas et al., 2016). For genetic map construction with higher mapping resolution, 150 individuals of an F2 mapping population was used in the SC × PS genetic background (Argyris et al., 2015).

4.2.3 Melon Genome Transposon Content:

It's essential to identify and mask the fraction of transposable elements (TEs) contained in the genome assembly before for an efficient annotation in a plant genome, using ab initio and homology-based methods, a total of 73,787 copies were defined of the 2 major types of TEs the retrotransposons and the DNA transposons (Garcia-Mas et al., 2016). The most

abundant retrotransposon classes were LTR retrotransposons of the Copia and Gypsy superfamilies, which represent respectively 5.5% and 7.2% of the genome assembly, and the DNA transposons, the most abundant class was CACTA superfamily (1.6%) (Garcia-Mas et al., 2016). The underestimation fraction of TEs identified in the melon genome assembly, was probably due to the repetitive sequences of the unassembled genome fraction and the rigorous search parameters used, and the TEs distribution complement the pattern to the gene fraction (Garcia-Mas et al., 2016).

Following a sequence comparison of each LTRs pair in complete elements, the insertion time of major LTR retrotransposon families was obtained (Ezura et al., 2006). An important retrotransposon amplification peak was identified around 2 Myr knowing that the melon and cucumber divergence has been estimated around 10 Myr (Nakata et al., 2005). The Gy14 cucumber genome sequence (1.5%) was identified as retrotransposons applying the transposon annotation criteria in both species (Ezura et al., 2006). The differences of the genome size between melon (454 Mb) and cucumber (367 Mb) was probably due to a high TE amplification in melon (don't exist in cucumber) (Ezura et al., 2006; Garcia-Mas et al., 2016).

4.2.4 Genome Annotation:

As regards the protein-coding genes annotation after masking the repeat content in the melon genome assembly, an association between ab initio and evidence-based approaches (homologous protein databases and EST evidence) was used (Garcia-Mas et al., 2016). About 27 427 protein-coding genes were obtained, which are generally compatible with genes number of other plant as cucumber (26 682) and watermelon (23 440), 69.1% of these genes are supported by ESTs or homologous to protein databases, and 30% are based on ab initio predictions (Garcia-Mas et al., 2016). The increasing of evidence-based protein-coding gene number depend on the availability of the new melon RNA-seq data (Garcia-Mas et al., 2016). Experimentally, some of the gene prognostic identification cannot be confirmed (Ezura et al., 2006).

4.2.5 Phylome Database:

The melon phylome and other 22 plant species were identified using a phylogenomic analysis (algae (4), mosses (2), monocots (5) and dicots (12) figured in the melon phylome) (Garcia-Mas et al., 2016). A set of 22 218 maximum-likelihood (ML) phylogenetic trees were obtained (http://phlylomedb.org). For the protein-coding genes functionality, the orthologous and paralogous sequences identification in addition for inferring whole-genome duplication (WGD) events in the melon genome, the melon phylome was important (Ezura et al., 2006; Garcia-Mas et al., 2016). Since the ancestral WGD eudicots paleohexaploidization recognized after the divergence of monocots and dicots, melon had not a recent one. (Ezura et al., 2006; Garcia-Mas et al., 2012).

4.2.6 Noncoding RNAs:

The noncoding RNA (ncRNA) repertoire annotated by the melon genome sequence, about 1,253 ncRNA genes identified and 140 potential miRNAs were described (Garcia-Mas

et al., 2016), using 454 pyrosequencing, 80 miRNAs of them were expressed comparing to a previous characterization of the small melon RNAome (Dahmani-Mardas et al., 2010). Several genotypes from different plant tissues and miRNAs (known families) were contributed to construct 10 small RNA (sRNA) libraries, and to characterize a new candidate miRNA (Garcia-Mas et al., 2016). In the melon genome many ncRNAs were present in clusters (Ezura et al., 2006; Garcia-Mas et al., 2012).

4.2.7 Disease Resistance Genes:

A total of 411 genes involved in disease resistance, in which 81 melon genes appertain to the plant nucleotide-binding site (NBS)-leucine-rich repeat (LRR) class (R-genes) which are associated to plant pathogens resistance and also are arranged in clusters (Garcia-Mas et al., 2016) two of them are identified in chromosomes V and IX, where some genes of resistance as *Vat* (Luan et al., 2008) and *Fom-1* (Martin et al., 2009) are located.

The R-genes in melon are limited comparing with *Arabidopsis* (212) and grape (302) and other species (Garcia-Mas et al., 2016). It is probably a general trend in cucurbits, in cucumber (61) (Gonzalez et al., 2010; Nakata et al., 2005) and watermelon (44) (Blanca et al., 2012). The R-genes limited number is probably depend to frequent loss and R-gene lineages deficient duplications (Ellis et al., 2000). As a hypothesis, the domestication process caused a R-genes missing in this species after the watermelon wild resequencing and cultivated germplasm (Ezura et al., 2006; Blanca et al., 2012).

4.2.8 Resequencing of Melon Genomes:

Resequencing and mapping reads to the reference genomes depend to reference draft genome availability, which allows to perform additional researches as the genetic diversity assessment in the species using the whole-genome level and the identification of domestication and improvement genes (Blanca et al., 2012). After the watermelon genome sequence publication contained resequencing of 20 accessions belonging to three different subspecies, putative genomic regions were identified that had a selection after domestication (Ezura et al., 2006; Blanca et al., 2012).

The Double-haploid Line 92 genome reconstruction (17 recombination events), was permitted by two parental lines of DHL92 resequenced (SC × PS) (Garcia-Mas et al., 2012). In different genomic studies, the number of identified and validated SNPs between SC and PS, exceed 1 million (Wan et al., 2013). Including PI 124112 (*momordica* type) and Védrantais (*cantalupensis* type), supplementary melon accessions have been recently resequenced from both the *melo* and *agrestis* subspecies (Garcia-Mas et al., 2016). Resequence data analysis allowed the characterization of the genomic variation at the SNPs level, short indels and structural variation (SV), to estimate the chromosomes nucleotide diversity and to distribute TE polymorphism (Ezura et al., 2006; Yang et al., 2013).

4.2.9 Transcriptomic studies:

Thanks to the Spanish Genome Initiative (MELOGENOMICS), he melon genome is being sequenced. In addition, other genetic and genomic tools are available, such as BAC

libraries, high-resolution genetic maps, oligo-based microarrays, and a large number of transcriptome sequences for melon.

Various transcriptome studies allow the detection of the differences between melon cultivars (Saladie et al., 2015; Li et al., 2016; Zhang et al., 2016; Shin et al., 2017). New genetic and genomic tools are available for studying fruit ripening and generally the differentially expressed genes, including near-isogenic lines, tilling platforms, saturated genetic maps, the genome sequence, many QTLs and eQTLs positioned and gene expression atlas, etc. (Dahmani et al., 2010; González et al., 2011; Yano et al., 2018). RNA-Seq technology has been applied for transcriptomic analysis during melon fruit ripening and to determine QTLs, eQTLs and candidate genes of fruit quality traits (Galpaz et al., 2018; Saladié et al., 2015). Genome-wide association study (GWAS) and biparental mapping some SNPs located in β-D-xylosidase, glyoxysomal malate synthase, chloroplastic anthranilate phosphoribosyltransferase, and histidine kinase associated with flesh fruit firmness (Nimmakayala et al., 2016). The most profusely collection studied also for flesh firmness was developed by introgression of the non-climacteric accession PI161375 into the genetic background of the non-climacteric Spanish cultivar 'Piel de Sapo' (Eduardo et al., 2005; Moreno et al., 2008).

4.2.10 QTLs of melon fruit quality at harvest:

The near-isogenic lines (NILs) of melon (*Cucumis melo* L.) obtained through interbreeding between PS × SC, which composed by >95% of the PS, and the rest from SC, have been previously studied in order to identify the QTLs linked to the interesting quality traits for the consumer.

The QTL mapping allowed to identified QTLs located in different linkage groups (Eduardo et al., 2007; Obando et al., 2008 and 2009; Obando-Ulloa et al., 2010; Dos-Santos et al., 2013; Chaparro-Torres et al., 2016), some of them related to the regulation of the aroma volatile compounds production, which permitted to understand aroma synthesis and the relationship between aroma and ethylene production, between aroma and fruit ripening and senescence, and generally between aroma and the fruit quality. Several QTLs were identified majorly associated to melon fruit quality traits (Li et al., 2006; Monforte et al., 2004; Périn et al., 2002a and 2002b; Sinclair et al., 2006; Zalapa et al., 2007).

The QTL mapping compared with other approaches, allows to detect a larger number of QTLs (Eduardo et al., 2007; Eshed and Zamir, 1995), 10–15 QTL of morphological traits, 4–5 for ovary shape, external color, and flesh color (Eduardo et al., 2007), and 11 related to physiological disorders, decay, and flavor loss (Fernández-Trujillo et al., 2007) have been detected.

The QTL mapping allowed also in this case to compare the differences between the NILs and its parental PS as for weight, fruit shape, commercial aspect, texture, taste (Sugar, organic acid and VOCs), nutritional content (ascorbic acid and other vitamins and anti-oxidants content) and sensorial evaluation (sweetness, taste, sourness, bitterness, overall fruit quality) (Moreno et al., 2008; Obando et al., 2008; Tijskens et al., 2009; Obando-Ulloa et al., 2009a, 2009b and 2009c), which can allow to select and develop melon fruit of high quality.

MATERIAL AND METHODS

II. MATERIAL AND METHODS:

This is a general overview of the methodology used in this thesis, though a more detailed description is presented in each chapter of results as in the publication derived from the thesis.

1. Sequencing the Melon Genome and Impact in Fruit QTL mapping:

Fruits obtained from melon plants of the inbred parental 'Piel de Sapo' cv. T111, *inodorus* type, and the NIL SC10-2 derived from the IL collection developed by Eduardo et al. (2005) were analyzed. SC10-2 contains an introgression in homozygosis that covers the entire LG X from the Korean accession 'Songwhan Charmi' (PI 161375) in PS genetic background.

Picture 1. Typical fruit of parental line ´Piel de sapo´ and near-isogenic line SC10-2 (courtesy of J.P. Fernández Trujillo (c)).

Soil preparation, fertigation, plant protection, and other growing practices were those commonly used for melon cultivation in the Mediterranean conditions in Torre Pacheco (Murcia, Spain) (Fernández-Trujillo et al., 2012; Obando-Ulloa et al., 2009). To reduce fruit cracking, measurements reported by Fernández-Trujillo et al. (2013) were followed. The experiment was conducted in 'Centro Experimental de Formación y Experiencias Agrarias' (CIFEA), Torre Pacheco (Murcia, Spain). Field was divided into rows separated by 2.5 m. Each replicate, in parallel rows, consisted in six plants separated 1.5 m in the rows. The separation between rows was 2 m. The plantation was surrounded by a border line of the cultivar 'Nicolás' (Syngenta Seeds). The experiment was conducted in three different seasons (S1, S2, S3), and details about number of replicates are provided in chapter of results I (S1, S2) or chapter II (S3). In both cases the number of replicates in PS exceeded the ones of SC10-2 because is the typical design used for breeding purposes and potential QTL mapping. Additionally, SC10-2 suffers from poor germination or diseases more than PS even during the nursing period, and this is the reason of having sometimes less replicates than expected.

Fruit harvest and maturity index applied were slightly modified from Obando-Ulloa et al. (2009) for non-climacteric melons. Minimum harvest indices were the presence of a well formed and defect-free fruit, firm, well healed and dry epidermis with lignified netting, high

density, absence of trichomes, skin color, withering of the stem and leaf closer to the fruit peduncle suberization, and light yellowing of the ground spot. The most common harvest indices for the SC10-2 and PS were the development of skin netting and sometimes development of annular ring or yellow color around a partly suberized peduncle; the cracking or history of cracking of each NIL (Fernández-Trujillo et al., 2013), light yellowing of the ground spot (particularly in PS), and light crack suberized around the peduncle, and dark blue-green skin color (in SC10-2).

The first harvest season lasted about 2 weeks in both lines, but all the fruits of this experiment (three different biological replicates per line and/or storage time for transcriptomic analysis; more fruit for physiological traits) were collected the same day. PS was harvested about one month earlier than SC10-2 (7 July for PS; 9 August for SC10-2), due to the delay in ripening of this NIL (Dos-Santos et al., 2013) and to the rain during flowering which provoked flower and fruit abscission in May. The results reported in the first chapter of results were conducted in S1 and S2. The results reported in the second chapter (postharvest ripening, gene expression) were conducted in S3. Fruit of S3 were harvested in different replicates though in the field.

In the three seasons, fruits were harvested by one expert in two weeks during morning hours (5:45 to 10 am, temperatures usually from 21-26 ^{o}C). After measuring quality traits, total soluble solids (TSS, in ^{o}Brix) and flesh firmness measured by digital refractometer and according to Dos-Santos et al. (2011), respectively, were also used for verifying the differences in maturity at harvest (Obando et al., 2008). The firm-ripe stage of maturity was used for the experiment of S3 by keeping fruit until 18 d of storage at 20.5 ± 0.6^{o}C and relative humidity of 88.2 ± 5.4 % (means ± SD, n=3 biological replicates).

After harvest, fruits were washed and gently brushed in tap water to remove dust, treatment residues, and other external materials, washed again in tap water, blotted gently, and let dry about 15 minutes on a bed of crushed stone before labelling with a Sharpie® twin tip permanent marker (Newell Rubbermaid Poland S.A., Manieczki, Brodnica, Poland), and packed in polyethylene boxes for transportation in a ventilated car during 30 min to the laboratory in Cartagena.

Fruits were immediately analysed after their arrival to the laboratory. Flesh sampling was carried out following the methodology reported by Obando-Ulloa et al. (2009a). Flesh samples were obtained separately from three different fruits considered as a replicate with a stainless-steel apple cork borer (Valira, Reus, Tarragona, Spain) in cylinders (20 mm length x 15 mm diameter), and immediately frozen in liquid nitrogen. After storage, samples were crushed to reduce pulp size. After about 6 h equilibration time at -35 ^{o}C, lyophilisation progressed with differences between shelves and samples of around 5 ^{o}C according to Dos-Santos et al. (2007) and dry mass calculated. Freeze-dried samples were stored at -25 ^{o}C in hermetic containers containing silica gel.

For the postharvest ripening experiment (S3), two continuous air renewals (30 min every morning and 15 min from 22-23 h) were established daily to ensure an environment with ethylene levels below 0.01 $\mu L \cdot L^{-1}$ during fruit storage.

2. Respiration rate, ethylene production:

Both physiological measurements were conducted on other set of individual fruit (n=6 of different biological replicates in firm-ripe stage of maturity) during postharvest ripening at 20.5ºC and 88% relative humidity during 18 d. The static method was used for gas sampling according with Fernández-Trujillo et al. (2008) using metallic hermetic containers (Sunbox, Barcelona, Spain) of 5.3 L of volume to keep fruit accumulating gases (usually 45 min - 2 h for ethylene and 1-4 h for CO_2 until minimum accumulation of 0.25% v/v of CO_2). After this time, samples of 1 mL for carbon dioxide and 0.5 mL for ethylene were obtained from headspace with disposable hypodermic syringes (Tenemo, Leuven, Belgium) and analysed by gas chromatography. Fruit density necessary to calculate headspace volume was previously calculated by measuring fruit weight and using the distilled water displacement methodology at a measured temperature (Fernández-Trujillo et al., 2005). The final results were calculated by weighing fruits and comparing the results with authentic external gas standards.

3. Textural traits:

Whole fruit hardness (WFH) was determined at the equator (lateral hardness) or at the stylar-end (using a special support to suspend the melon vertically) as previously reported measuring the compression force to achieve 2 mm deformation (Dos-Santos et al., 2013). Flesh firmness (FF) was measured with a puncture test (4,6-mm probe) using cylinders (L = 20 mm; Ø = 15 mm) obtained with stainless steel apple corers from the equator of the fruit and a 4.6 mm wide probe (TG83, SAE Ibertest, Madrid, Spain) adapted to a testing machine (ELIB-5K, SAE Ibertest) (Dos-Santos et al., 2013). Flesh juiciness (FJ) and juice density (JD), were measured according to the methodology described in Dos-Santos et al. (2011) and Obando et al. (2008). The results were expressed in grams of juice per kg fresh weight or kg of juice per m3 juice, respectively.

4. Volatile organic compounds:

For volatile organic compounds, juice extracted from melons were filtered through a four-layer cheesecloth. After 3 min at 23 °C, the mixture containing 28.6% *v*/*v* of saturated $CaCl_2$ solution) was poured into sterile polypropylene vials, which were stored at −80 °C until analysis (Fernández-Trujillo et al., 2018). VOCs were extracted by solid-phase microextraction. The fiber was 1 cm long and coated with 50/30 µm divinylbenzene/carboxen on polydimethylsiloxane (DVB/CAR/PDMS) (57329-U DVB/CarboxenTM/PDMS Stable FlexTM, Supelco, Bellefonte, PA, USA). The peaks were separated by HP-5 MS columns. A retention time locking methodology using pentadecane ensured the same retention time of the VOCs identified. Mass spectra were obtained by electron ionization at 70 eV with a mass spectrometer (5973 Network Mass Selective Detector, Agilent Technologies) that was coupled to the GC. The detector worked in full-scan with data acquisition and ion mass captured between 40 and 450 amu (4 scan·s^{-1}) during the run time (27.5 min). The peaks were compared with the experimental spectra of NIST 11 MS library (National Institute of Standards and Technology, Gaithersburg, MD, USA). The methodology of analysis, calculations and

identification by deconvolution analysis using AMDIS32 and comparison with linear retention index of compounds reported in literature were previously reported in detail (Fernández-Trujillo et al., 2018). Chemical compounds were verified by a comparison of linear retention indices (LRI) calculated with a homologous series of n-alkanes (C6–C20; Sigma-Aldrich) for the HP-5 MS UI column. The concentration of the individual aroma volatile compounds identified (expressed as $ng \cdot mL^{-1}$ of juice) was quantified from the relation between their areas and that of the internal standard (1-phenylethanol, CAS 98-85-1), obtained from the total chromatograms, using a response factor of 1 (Chaparro-Torres et al., 2016).

We classified VOCs in twelve chemical compounds classes during ripening of the NIL SC10-2 and PS which were; acetate esters, acetate non-esters, ketones, acids, terpenes, aliphatic compounds, alcohols, aldehydes, sulfur-derived compounds, exogenous volatiles, other volatile compounds and unidentified volatile compounds.

5. RNA extraction:

The RNA extraction was performed using TRI Reagent RNA isolation protocol (1 mL per 20–30 mg of lyophilized tissue per extraction) that was incubated 5 min at room temperature. After this time, 0.2 mL of chloroform were added and agitated manually by inverting the tube during a few seconds before centrifugation at 12,000 × g for 15 minutes at 4 °C according to the kit protocol. Three phases were separated after centrifugation of the resulting mixture: a red organic phase (containing protein), an interphase which contained DNA), and a colorless upper aqueous phase or supernatant (containing RNA). The supernatant was transferred to a new tube and 0.75 mL of 2-propanol was added before centrifugation at 12,000 × g for 10 minutes at 4 °C.

The pellet (RNA precipitated) was washed with 75% ethanol and centrifuged at 7,000 × g for 5 minutes at 4°C. The supernatant was discarded, and the pellet dried at room temperature and subsequently solved the pellet in 50 µL water (Sigma-Aldrich W-4502).

A volume of 1 µL de DNAaseI (RNAase-free; Roche, city) was added to the RNA sample and incubated for 20 min at 37ºC followed by 10 min at 65ºC. To stop the reaction, 1 µL 0.1 M EDTA was added. Highly pure total RNA was quantified with a NanoDrop ND-1000 spectrophotometers (Thermo Scientific, Germany). RNA quality was verified by calculating two absorbance ratios (260/280 nm and 260/230 nm, respectively) and by electrophoresis analysis. A volume of 5 µL of RNA sample was loaded onto a 1% agarose gel stained with BrEt.

The RNA samples were packed with dry ice (2 kg minimum) and sent to Center of National and Genomics (Barcelona) by SEUR-Frio (Spain). The transportation guarantees a maximum external temperature within the package of 5ºC. The RNA passed the quality control in National Center of Genomic Analysis (CNAG) (Science Park of Barcelona, Spain). A minimum of 2 µg total RNA and RIN value (RIN>6) was used to accept the samples in the quality control.

6. mRNA library preparation and sequencing:

The library from DNA free total RNA was constructed following the TruSeq™ Stranded mRNA Sample Preparation kit protocol (Illumina Inc., Redwood. CA, USA). In short, the polyA fraction of total RNA (0.5 µg) was selected using a magnetic oligo-dT bead-based purification followed by chemical fragmentation resulting into fragments of 80-450 nt, with the major peak at 160 nt. First strand cDNA synthesis by random hexamers and reverse transcriptase was followed by the second strand cDNA synthesis, performed in the presence of dUTP instead of dTTP. Blunt-ended double stranded cDNA was 3'adenylated and the 3'- 'T' nucleotide at the Illumina indexed adapters was used for the adapter´s ligation. The ligation product was amplified with 15 cycles of PCR.

The libraries were sequenced using TruSeq SBS Kit v3-HS, in paired end mode with the read length 2x101bp by CNAG. Fraction of a sequencing lane on Illumina HiSeq2000 sequencing system (Illumina, Inc.) was used to generate 3-6 million paired end reads passing filter for each sample following the manufacturer's protocol. Image analysis, base calling and base quality scoring of the run were processed by integrated primary analysis software as follows: Real Time Analysis (RTA 1.13.48) and followed by generation of FASTQ sequence files by using Illumina CASAVA packaging version 1.8.2.

7. Transcripomic analysis:

The transcriptomic analysis was performed according to Carvajal et al. (2018). The BlastoGO software (v2.8.0) (Conesa et al., 2005) was used for GO term differential analysis. GO terms enrichment for each data set was calculated by a binomial test model with FDR cut off of 0.05. Venn diagram was performed using Microsoft Office 365 ProPlus.

To better understand the transcriptional regulation of the gene expression involved in melon postharvest ripening, we performed a cluster analysis of the differentially expressed genes (DEGs) using the software MEV (2018). The metric used was based on the Pearson correlation and data of sample normalized measurements (in fragment per kilobase of exon per million reads mapped or fpkm) were not adjusted to logarithm for calculations. The number of clusters was established with the analysis of figure of Merit (FOM) and K-means clustering algorithm using means for calculations with the number of clusters obtained (six or seven, depending on the effect considered) and 100 iterations.

A quality read assessment was performed with FastQC package (Andrews et al., 2010). These reads were mapped against the Cucumis melo L. genome CM3.5.1 (http://melonomics.cragenomica.es/) using the Hisat2 mapper (Kim et al., 2015). We counted the number of reads mapped to transcripts with StringTie (Pertea et al., 2015). This counting was guided using the genome annotation and a unified set of transcripts was created for the samples analyzed. Then, a Fragments Per Kilobase of transcript per Million (FPKM) table with gene expression for each sample was generated and used for assessing the expression profiles of each sample by principal component analysis (PCA). Differences within samples were masked by the highly different expression (DE) profiles in ribosomic genes, so these genes were removed from further analyses. Differential expression analyses between both lines over time were run using the Bioconductor package ballgown (Fu et al., 2018), and tables of DEGs considering the effect of the pedigree or the postharvest ripening time were obtained separately.

PCA analyses were run with DE genes and separated in clusters by their expression profiles with RNA-Seq analysis in MeV (Howe et al., 2011). GO terms enrichments analyses were run for each one with Blast2GO package (Conesa et al., 2015).

8. Assessment of introgression effects in textural and VOCs:

The experiment was analyzed by a two-way ANOVA using introgression (I= SC10-2 or PS) and postharvest ripening time (RT= 0, 4, 8, 12, 18 d) as factors followed by LSD test at p=0.05 for main effects or I x RT interaction. We divided the significant effects for the introgression in independent (main effect alone) or dependent (significant interaction I x RT) on the postharvest ripening time. The main introgression effects of SC10-2 were divided into effects above or below PS.

9. Multivariate analysis of VOCs:

Consistent VOC variables were present in more than 25% of the fruits analyzed and 50% or more of the replicates analyzed (Chaparro-Torres et al., 2016). Consistent VOCs with null values were analyzed by three different methodologies, all based on substituting the null-data of each variable by minimum analytical values: i) In each season, the null data were substituted by the minimum non-null value of the VOC variable. ii) The minimum analytical value of VOC found in the entire consistent list of VOCs variables (criteria of Chaparro-Torres et al., 2016). iii) Substitution with the minimum of each line/season (four different cases per VOC).

For individual VOCs, a one-way ANOVA per season (S1 or S2) using introgression (in LG X) as the factor was performed, followed by correction for multiple comparisons using the Benjamini and Hochberg (BH) false discovery rate criterion at a level of $q \leq 0.05$. A two-way ANOVA of the textural traits using introgression (in LG X) and season (S1 or S2) as factors was performed, followed by correction for multiple comparisons using the same criterion reported above at a level of $q \leq 0.05$. Pearson's correlation coefficients were calculated among VOCs, and correlation networks were displayed to visualize the degree of association between variables. Different multivariate statistical techniques, such as Principal Component Analysis (PCA), Random Forest (RF), and Partial Least Squares-Discriminant Analysis (PLS-DA), were applied to the experimental data and conducted with R free software (R Core Team, 2018).

METHODOLOGY TO REMOVE STRONG OUTLIERS OF NON-CLIMACTERIC MELON FRUIT AROMA AT HARVEST OBTAINEDBY HS-SPME GC-MS ANALYSIS:

III. METHODOLOGY TO REMOVE STRONG OUTLIERS OF NON-CLIMACTERIC MELON FRUIT AROMA AT HARVEST OBTAINEDBY HS-SPME GC-MS ANALYSIS:

1. Introduction:

Variability among fruits in the analysis of volatile aroma compounds (VOCs) of non-climacteric melons is usually a problem due to the differential effect of fruit maturity, and the complex interaction between genotype and environment found for other quality attributes (Eduardo et al., 2007). There is even variability among the years in which the fruits of each cultivar or breeding line are harvested because of difficulties in harvesting melons in the same stage of maturity, particularly in non-climacteric types. These visual indices, such as the skin color in contact with the soil, are affected by differences in the environment depending on the season.

Studies of the aroma of the parental line 'Piel de Sapo' have demonstrated the inter-season variability and the lower aromatic potential compared with other climacteric varieties and, to a lesser extent, compared with almost non-climacteric or hybrid isogenic lines of the same type (Obando-Ulloa et al., 2008; Canales et al., 2018). This pattern is typical of the *inodorus* cultivars studied by other authors (Verzera et al., 2011; Verzera et al., 2014). Although certain data considered anomalous for this reference parental are usually discarded, no one methodology has been described for making the decision to remove outliers in a consistent way across years or seasons, although statistical tools, such as Grubbs' test for a single outlier based on the assumption of normality, are available (Grubbs, 1969). However, this type of test is designed to detect the presence of only one outlier, which is why some authors have proposed tests for multiple outliers (e.g., Iglewicz and Hoaglin's two sided and robust test), or outlier high dimensional data analysis (Aggarwal and Yu, 2001; Ro et al., 2015), the latter also applicable to fruit aromas which are composed of many individual chemical compounds.

In previous studies we tested different multivariate and univariate statistical methods for the data analysis of VOCs and other quality traits (Obando-Ulloa et al., 2008 and 2009; Chaparro-Torres et al., 2016; Dos-Santos et al., 2013; Fernández-Trujillo et al., 2009), also considering "zero" type data, when the VOC variable should be considered consistent (Chaparro-Torres et al., 2016), or even the use of deconvolution to reduce this problem (Dos-Santos et al., 2013; Canales et al., 2018). The groups of different compound classes are of interest for the potential discrimination of physiological behavior or for quantitative trait loci (QTL) mapping of VOCs (Chaparro-Torres et al., 2016; Dos-Santos et al., 2013). In particular, principal component analysis (PCA) and partial least-squares discriminant analysis (PLS-DA) were applied to data for unsupervised and supervised dimension reduction, respectively. The projection of data in a lower dimension space is a useful technique for identifying outlier points based on the distance between the rest of the points.

The box-whisker plot, originally introduced by Tukey (Tukey, 1977) as a tool in exploratory data analysis, has become one of the most widely used statistical graphs for the detection of univariate outliers. Outliers in a box-whisker plot are the data with distance to the

box of at least 1.5 times the interquartile range (IQR) while, in the case of extreme outliers, the distance is at least three times the IQR.

Data classified as outliers using different criteria have been considered as strong outliers. The objective of the present work was to develop a methodology for the systematic observation of strong outliers in VOC analysis of samples in an integrated manner that allows some potentially anomalous data to be excluded in the determination of fruit aromas. This is particularly critical for QTL mapping and in the determination of QTL × environment effects because the variability could be higher than in other cases, particularly in plots in open fields for breeding purposes, and/or in fruit where the exact degree of maturity is difficult to assess due to biological variance, e.g., melon (Tijskens et al., 2009). For this, the study was based on the same parental studied in two different seasons.

2. Materials and Methods:

2.1 Plants Material and Experimental Design:

The Spanish melon parental (*Cucumis melo* L., cv. T111, *inodorus* group) of the 'Piel de Sapo' type (PS) was grown in Torre Pacheco (Murcia, Spain) in typical Mediterranean conditions (Dos-Santos et al., 2013) during two consecutive seasons (S1 and S2). The experimental plot consisted of six plants per replicate (three plants located in two adjacent rows) with n = 21 and n = 9 replicates in S1 and S2, respectively. Two to three fruits per replicate were harvested between 07:00 and 10:00 h in one week in each season according to previously-reported minimum and optimum harvest maturity indices for PS (Dos-Santos et al., 2013; Tijskens et al., 2009). The most critical parameters for externally identifying full maturity at harvest in the field were a developed stem scar, followed by peduncle lignification, and the onset of a light yellow color in the skin surrounding the peduncle, a dull dark green skin color, and a minimum light yellow color in the skin in contact with the soil. The total soluble solids (TSS) content, which was regularly monitored, showed a maximum that depended on the season, and fruit with less than 10 °Brix were discarded. Flesh volatiles were analyzed in both seasons.

2.2 Flesh and Juice Sampling for Volatile Analysis:

Flesh cylinder samples (20 mm length × 15 mm diameter) were obtained from the equator of individual fruit using an apple core borer following the previously reported methodology (Obando-Ulloa et al., 2008; Dos-Santos et al., 2013). Each replicate consisted of a single analysis of fruit (usually two different melons) per field replicate. Juice was squeezed from the cylinders with a Simplex Super cast aluminum manual juicer and filtered through a four-layer cheesecloth. After 3 min at 23 °C, the mixture (20 mL juice and 8 mL $CaCl_2$ saturated solution, i.e., 71.4% *v*/*v* of juice) was poured into two 5 mL and one 15 mL sterile polypropylene vials, which were stored at −80 °C until analysis (after around two months). For the analysis, samples were thawed (about 15 min at 20 °C) and 2.32 mL of the mixture was poured into 10-mL vials. After adding 0.02 mL of the internal standard (a solution of 4.27 mgL^{-1} of 1-phenylethanol, CAS 98-85-1, in dichloromethane), the vials were capped hermetically (SU860101 silicone/PTFE 18 mm, 35 shore A, screw cap, Supelco, Bellefonte, PA, USA), and

put into a thermostatted tray at 13 °C. Around 15 samples per day were analyzed in a random order.

2.3 Volatile Analysis: Headspace (HS) Formation, Solid-Phase Micro-Extraction (SPME), and Gas Chromatography-Mass Spectrometry (GC-MS) Analysis:

Solid-phase microextraction was conducted after each season according to the indications of (Amaro et al., 2013) with slight modifications. A retention time-locking gas-chromatography mass-spectrometry method, using *n*-pentadecane (Sigma-Aldrich, Saint Louis, MO, USA; Merck KGaA, Darmstadt, Germany) as reference to block the method (at a retention time of 24.022 min), was used. Therefore, the column operated in constant pressure mode that slightly differed each year in order to keep the retention times constant. This methodology practically avoids the need for alignment (http://www.chem.agilent.com/Library/technicaloverviews/Public/5989-8574EN.pdf), because differences in retention times among chromatograms were negligible.

Volatiles were extracted without stirring during 120 min at 35 °C in the heating tray of the gas chromatograph (6890N, Agilent Technologies, Wilmington, DE, USA) by using static HS-SPME. The fiber was 1 cm long and coated with 50/30 µm divinylbenzene/carboxen on polydimethylsiloxane (DVB/CAR/PDMS) (57329-U DVB/CarboxenTM/PDMS Stable FlexTM, Supelco, Bellefonte, PA, USA). This fiber is recommended for automatic holders and volatile and semi-volatile (C3–C20) analyses. The fiber (20 mm length and 20 gauge needle size) entered 22 mm into the vial headspace and remained for 30 min absorbing volatiles at 35 °C. The volatiles were desorbed from the SPME fiber into the GC injection port (mass spectrum detector transfer line heater) with a bake-out step of 3 min at 280 °C. The analyses were carried out with a MPS2 Gerstel Multipurpose sampler coupled to the GC-MS. The injection port was operated at 260 °C in splitless mode and subjected to a pressure of 13.4 psi adjustable for the retention time of *n*-pentadecane to be the same. The purge flow rate of the inlet was 40 $mL \cdot min^{-1}$ and the purge time was 2 min. The post-run column conditions were 10 min at 220 °C with a pressure of 26.2 psi. The fiber bake-out parameters were 15 min pre-bake-out time, 44 mm of injector penetration, and 1 min post-bake-out time. A solvent delay of 0.5 min was applied. The inlet liner used was a 2637505 SPME/direct (Supelco), 78.5 mm × 6.5 mm × 0.75 mm. Volatiles were separated on a 30 m × 0.25 mm i.d. × 0.25 µm thick capillary column (HP-5MS ultra inert, Agilent Technologies, Wilmington, NC, USA) that contained 5% phenyl-methyl silicone as a stationary phase. The carrier gas was helium (purity > 99.999%) with a flow rate of 1.5 $mL \cdot min^{-1}$. The initial oven temperature was 35 °C, followed by a ramp of 2 $°C \cdot min^{-1}$ up to 75 °C, and then at 50 $°C \cdot min^{-1}$ to reach a final temperature of 250 °C, which was held for 5 min. Oven equilibration time was 0.5 min. Mass spectra were obtained by electron ionization (EI) at 70 eV. The detector worked at 230 °C and in full-scan with data acquisition and ion mass captured between 40 and 450 amu (4 $scan \cdot s^{-1}$) during the run time (27.5 min).

2.4 Identification of Volatile Organic Compound and Data Calculations:

The peaks were identified by a mass spectrometer (5973 Network Mass Selective Detector, Agilent Technologies) coupled to the GC, comparing the experimental spectra with

those of NIST 11 MS library (National Institute of Standards and Technology, Gaithersburg, MD, USA). The chromatographic analysis data for the volatile compounds were automatically integrated using MSD ChemStation software (F.01 001 1903 2013, Agilent Technologies). To reduce the number of additional peaks that would need to be manually introduced in the subsequent deconvolution process, the automatic Chemstation parameters were set as follows: initial area reject 0; initial peak width 0.045; shoulder detection off; initial threshold 14.0. These preliminary data only served as a basis for manual integration, deconvolution, and individual reverification of the peaks based on deconvolution analysis using NIST 11 MS library and the automated mass spectral deconvolution and identification system AMDIS (version 2.7, 2011, National Institute of Standards and Technology, Gaithersburg, MD, USA). Data for the best deconvolution models were selected from those offered by automatic mass spectral deconvolution and identification system (AMDIS) according to the higher match quality index for the target compound (usually 2–3 models, and always less than five models per peak). After several trials with different options, the deconvolution settings of AMDIS were: component width equal to 16, two adjacent peak subtractions, low resolution, very high sensitivity, and low shape requirements. These parameters can be modified, especially to obtain the results for some flat peaks (i.e., some alkanes or poorly detectable compounds) that cannot always be confirmed with the above parameters: for example, by increasing the resolution to high.

Chemical compounds were verified by a comparison of linear retention indices (LRI) calculated with a homologous series of n-alkanes (C6–C20; Sigma-Aldrich) for the HP-5 MS UI column (Van den Dool and Kratz, 1963) and analyzed under the same conditions. Propane, butane, and pentane retention times were estimated based on previous analysis of several seasons. LRI were compared with the literature results compiled by NIST (http://webbook.nist.gov/chemistry/cas-ser/), although sometimes the LRI data were estimated from the non-polar retention index (*n*-alkane scale) offered by NIST MS Search 2.0. We also used a profile of melon VOC LRIs (more than 500 compounds) obtained in hundreds of previous analyses using cultivars of different types and the same methodology, and others with HP-5 MS columns (Fernández-Trujillo et al., 2013). A coefficient of variation for *LRI* was calculated as follows:

$$CV_{LRI} = \frac{(LRI\ calculated - LRI\ literature)}{LRI\ literature} \times 100 \quad (1)$$

The compounds accepted always showed $CV_{LRI} < 1\%$ (usually less than 0.5%). The concentration of the individual aroma volatile compounds identified (expressed as $ng \cdot g^{-1}$ of pulp) was quantified from the relation between their areas and that of the internal standard (1-phenylethanol), obtained from the total chromatograms, using a response factor of 1 (Dos-Santos et al., 2013).

The IUPAC names of individual aroma volatiles were verified with the CAS number of the NIST database (http://webbook.nist.gov/chemistry/cas-ser/) in accordance with several databases(http://www.chemindustry.com/apps/chemicalshttp://www.thegoodscentscompany.com/search2.html).

The chemical volatile compounds were classified into eleven groups, according to Dos-Santos et al. (2013) (Chaparro-Torres et al., 2016): volatile acids (ACD); acetate esters (ACE); alcohols (ALC); aldehydes (ALD); alkanes (AHA); ketones (KET); non-acetate esters (NAE); sulfur-derived compounds (SDC); terpenes (TER); others (OTH). Unidentified (NID) compounds which did not demonstrate a clear comparison with the NIST11 database were not included in the main analysis. Each fruit was classified by the number of replicates (21 in season 1, and nine in season 2) and a letter (A, B, C, or D), and sometimes by adding the letter "r", indicating re-analysis of the same individual fruit sample.

We tested the following six variables calculated automatically by using a Microsoft® Excel 2013 worksheet programmed for this purpose and the calculations of the *LRI* and CV_{LRI}:

- Total area counts (match quality or similarity index MQ > 50).
- Percentage of total area counts of identified compound classes (only classified compounds excluding unidentified and exogenous, with MQ > 50).
- Percentage of total area counts of the whole chromatogram (including compound classes classified as exogenous, with MQ > 50, but not unidentified compounds).
- Total area counts (without MQ criteria).
- Percentage of total area counts of compound classes, including exogenous and unidentified compounds.
- Percentage of total area counts (total area of the chromatogram, without MQ criteria; including exogenous and unidentified ones).

The first and fourth variables expressed in area counts were also examined after normalization of the compound class variables to the response of the internal standard (1-phenylethanol) by multiplying the areas by the corresponding factor calculated for each season, as follows:

$$F_{IE}ij = \frac{Area\ of\ internal\ standard\ of\ the\ sample\ j\ of\ season\ i}{Average\ area\ of\ Internal\ standard\ of\ season\ i} \quad (2)$$

The two former percentage variables showed similar levels. Additionally, the last two percentage variables calculated without MQ criteria showed similar results, and lower levels than the first two percentage variables calculated with the constraint of MQ.

Data of individual fruit aroma analysis computed in Microsoft® Excel were aligned using software specifically developed for this purpose in one of our projects (unpublished). The former software aligned compounds based on names of chemical compounds generated by the NIST library, and CAS numbers were used for further verification and, particularly, to avoid mistakes. Unidentified compounds (NID) were also aligned based on names automatically generated using the concatenate function of Microsoft® Excel with its respective retention time of two decimals (Unidentified (x)). A pseudo CAS number of unidentified compounds was also generated per compounds using its respective x RT and its y linear retention index (LRI) as follows: (NIDxLRIy). This information served for further manual verification in order to identify potential target unidentified compounds for future research. Two Dell® Precision

WorkStations (M6800 and M4400, both with 16 Gb of RAM) were required to perform these processes.

2.5 Total Soluble Solids:

Total soluble solids content were determined using a digital refractometer (Pocket, Atago PAL-1, Tokyo, Japan). The mean of each replicate plus SE are reported.

2.6 Statistical Analysis and Outlier Identification:

Exploratory data analysis consisted of a normal probability plot and box-whisker plot analysis of the six variables obtained for the compound classes of aroma volatiles of both seasons separately, followed by principal component analysis and partial least-squares discriminant analysis applied to the scaled and mean-centered data. For each univariate variable, the Grubbs' test for outlier identification was performed when normality assumption was not rejected according to the Shapiro-Wilk test ($p \leq 0.05$) (Shapiro and Wilk, 1965). Correlation analysis was also carried out for each pair of variables within each type of the former six. Classical and robust 97.5% confidence ellipses of the data were calculated. The robust method used 50% of the observations for MCD (minimum covariance determinant) estimations.

All statistical analyses were performed using the free R software (R Core Team, 2018), the FactoMineR library for the principal component analysis (Lê et al., 2008), and the *caret* library (Kuhn et al., 2016) for the PLS-DA analysis. Grubbs' test and correlation analysis form part of the outliers and mvoutlier packages of R, respectively (Filzmoser et al., 2017; Komsta, et al., 2011).

The first step in the procedure to detect strong outliers consisted of checking PCA and PLS-DA output and marking the potential candidates, then verifying the candidates by correlation analysis, box-whisker plots, and Grubb's test when available. Additionally, dispersion graphs of different quality traits (e.g., TSS vs. the variables of the different VOC compound classes in percentage), served for the final decision on outlier classification and to study their potential origin.

3. Results:

In a previous examination of the data by PCA, there were several mistakes because of a malfunction in our alignment program (two samples) and a sample with many acetate esters and sulfur-derived compounds that were also unique in fruit VOC of both seasons (Supplementary Figure S1 (Annex A)).

In general, the Grubbs' test only allowed detection of a few outliers because the normality assumption was rejected for most of the variables according to the Shapiro-Wilk test at a significance level $p \leq 0.05$ (data not shown).

3.1 Chemical Compounds Classes Based on Total Areas:

All these data were studied visually considering in each fruit sample the other samples of the same or different season. The results for the three groups of variables representing the

total areas of the chromatograms (with or without the MQ criteria, with or without normalizing the areas to the internal standard) were similar and judged by PCA. Finally, the outliers considered with this type of variables were the fruits 2B and 6A (S1), and, to a lesser extent 3B (S2) (Figure 1; Supplementary Figure S2A (Annex A)).

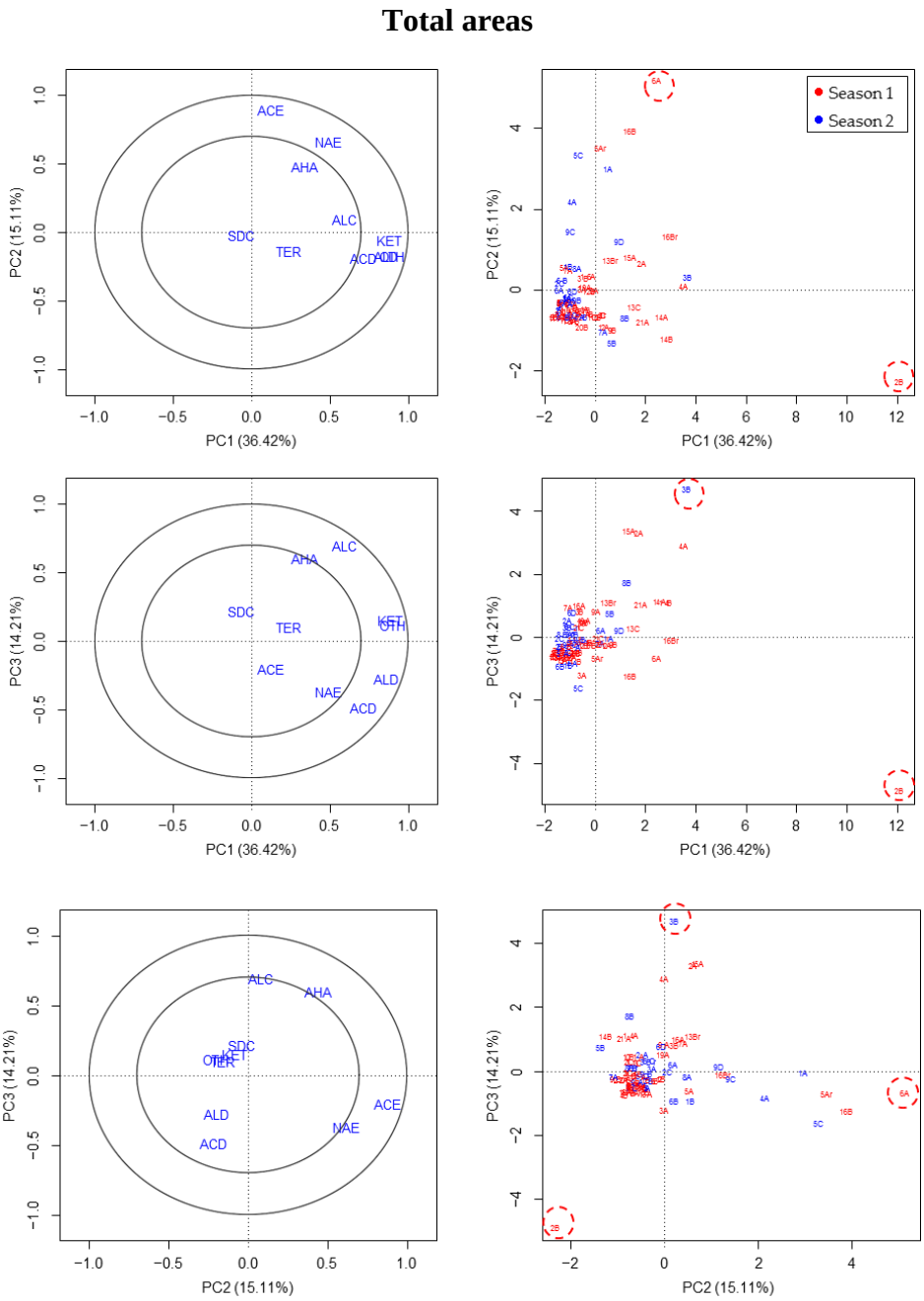

Figure 1. Correlation (**left**) and score (**right**) plots of the first three components of the PCA (with 67.82% of variance explained) applied to compound classes of aroma variable based on total areas (only compounds with match quality >50 without exogenous compounds), obtained in two seasons. The areas of compound classes were normalized to the response of the internal standard (1-phenylethanol) for each season. ACE, acetate ester; NAE, non-acetate ester; ALD, aldehyde; ALC, alcohols, KET, ketones;

SDC, sulfur derived-compounds; TER, terpenes; AHA, alkanes and aliphatic compounds; OTH, other compounds. Circles represent r^2 = 50% and 100% variability explained by the components. Potential outliers are marked by dashed red line.

The outliers observed by using PLS-DA were the same and also 16B (S1) and 2A (S2), and, to a lesser extent, 5B or 6D (S2), because these two were only identified in the case of one of the variables of the total area considered without applying the normalization of areas to the internal standard (Supplementary Figure S2 (Annex A)).

From an observation of the figures and association outlier-centroid of each group of VOC compound class (centroids on the left of each figure for PCA and on the right for PLS-DA; Figure 1; Supplementary Figure S2 (Annex A)), the main reasons identifying the outliers in the first season was the excess of acetate esters (6A (S1), 16B (S1)) and aldehydes, ketones, and others in 2B (S1). In the second season, fruit 2A (S2) and 6D (S2) were considered outliers due to the excess of sulfur-derived compounds, and 5B (S2) due to the unusually high relative abundance and diversity of terpenes.

The main problem with the total area variables was that they did not consider the differences among different fruit analyses that are usually corrected when percentages or total areas are used, sometimes by using internal standards, and this is the reason for verifying the proposed outliers with the variables in percentages.

3.2 Chemical Compound Classes Based on Percentages of Sum of Areas:

The results of the four groups of variables representing percentages of different compound classes based on different total areas of the chromatograms were similar. The reason is that MQ values increased when deconvolution was used, and so the percentages proposed with MQ are not altered much by this limitation.

Essentially, one outlier was detected in the VOCs of fruit 15A (S1) by using PCA and PLS-DA, due to the high proportion of alcohols, while no outliers were detected in S2 (Figure 2). Additionally, fruit 4B (S1) could be an outlier as judged by PLS-DA, due to the greater proportion of terpenes and/or acids than in other fruit (Supplementary Figure S2 (Annex A)). Certain differences between seasons were detected by PCA or the PLS-DA of percentages (e.g., in the graph of the first two axes; Figure 2 and Supplementary Figure S3 (Annex A)). The fruit classified as outliers in the previous section by reference to the area in absolute values were not classified as outliers using PCA, but using variables of compound classes based on percentages of the sum of the areas.

In the last of the percentage variables (without MQ criteria and including total area), fruit 5A (S1) was also considered as outlier (only by PLS-DA) due to a slightly higher proportion of acids, acetate esters and/or alkanes (data not shown). This datum was not finally considered as a strong outlier.

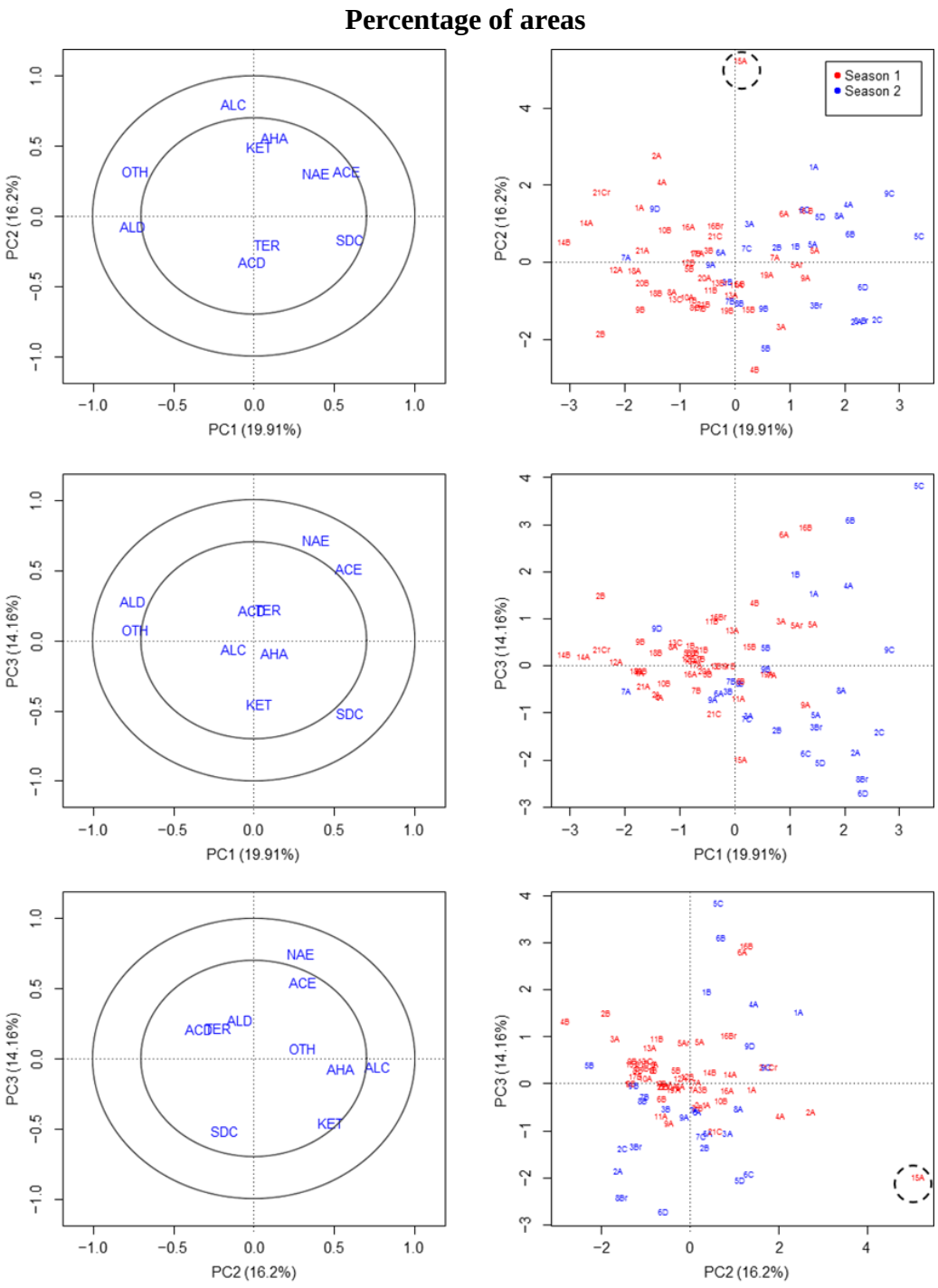

Figure 2. Correlation (**left**) and score (**right**) plots of the first three components of the PCA (with 50.27% of explained variance) applied to compound classes of aroma variable of percentages of different compound classes based on total area counts of such compounds with match quality >50, and without exogenous compounds, obtained in two seasons. ACE, acetate ester; NAE, non-acetate ester; ALD, aldehyde; ALC, alcohols, KET, ketones; SDC, sulfur derived-compounds; TER, terpenes; AHA, alkanes and aliphatic compounds; OTH, other compounds. Circles represent r^2 = 50% and 100% variability explained by the components. Potential outliers are marked by dashed black line.

3.3 Box-Whisker Plots of Both Types of Variables:

A high number of outliers were detected by box-whisker plots based on the lack of normality in most of the variables of the compound classes tested, irrespective of the type of variable considered. The two fruits proposed as strong outlier candidates (15A and 4B of S1) were reassessed by means of box-whisker plots. The outlier of sample 15A (S1) was due to its high relative levels of alcohols, and, after removing this fruit, both variables showed similar behavior in the box-whisker plot (Figure 3A). This was also the case for acids and/or terpenes when the outlier of fruit 4B (S1) was removed (Figure 3B, C). Both outliers were relatively isolated from the rest of S1 and S2 fruits according to the above multivariate analyses and, therefore, can be classified as strong outliers.

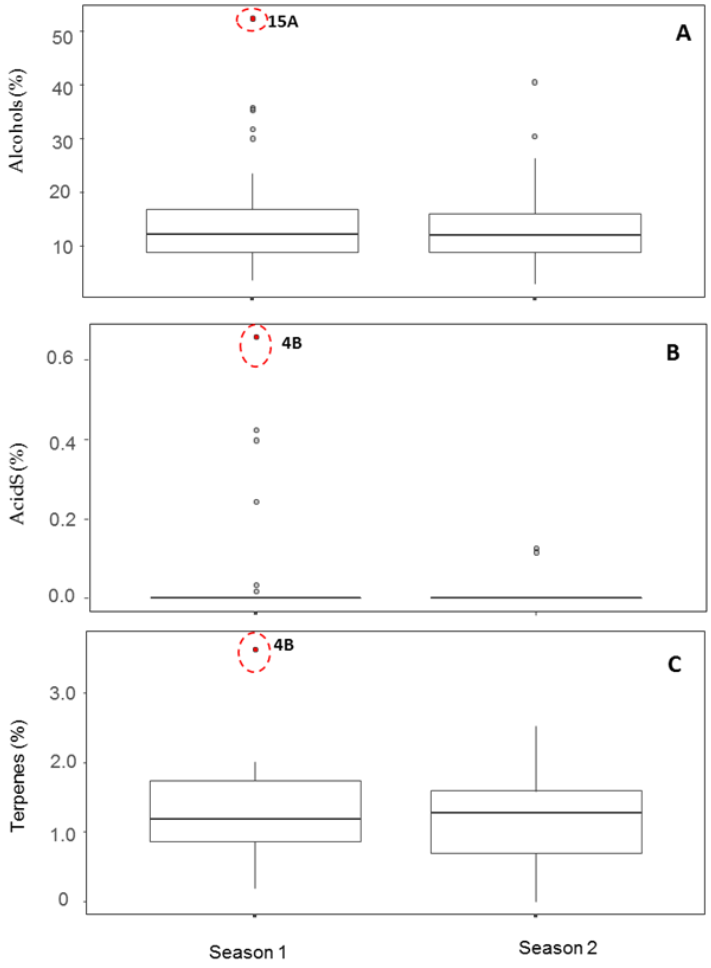

Figure 3. Box whisker-plot of three variables of compound classes (in percentage of area counts of the melon compound **identified** with match quality >50 and without exogenous compounds). (**A**) Alcohols; (**B**) acids; and (**C**) terpenes. Bold red circles indicate the selected outliers (with the fruit code beside this circle).

3.4 Correlation Analysis among Variables:

This type of analysis produced many apparent outliers in each correlation pair (Supplementary Figure S4 (Annex A)), but the strong outliers (15A and 4B of S1) also appeared in graphs when alcohols and terpene variables appeared as percentages (Figure 4; Supplementary Figure S4 A, C, D (Annex A)).

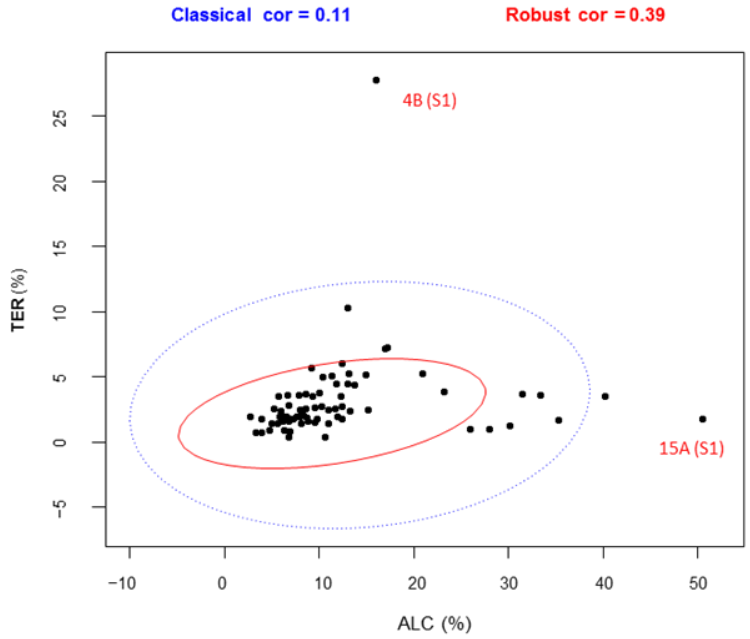

Figure 4. Correlation analysis of alcohol (ALC) and terpene (TER) percentages based on total areas of the melon compounds **identified** with match quality > 50, and without exogenous compounds). Classical and robust 97.5% confidence ellipses of the data (blue and red, respectively). The robust method used 50% of the observations for minimum covariance determinant (MCD) estimations. The strong outliers labeled are the fruits 4B and 15 A from season 1.

3.5 Total Soluble Solids:

Considering all the fruit after discarding outliers, the TSS means ± SD were significantly higher (Tukey test, $p = 0.001$) in season 2 (12.0 ± 0.2 °Brix; $n = 9$) compared with season 1 (9.7 ± 0.3 °Brix; $n = 21$), and the same was true (and with similar values) when they were not removed (data not shown). The TSS did not correlate with any of the variables referring to the total levels of compounds (in area or percentage), although this parameter could be useful for identifying some outliers. The same lack of correlation was found with other quality traits, such as the ratio between TSS and titratable acidity, among others (data not shown).

3.6 PCA of VOCs as Percentage after Removal of Outliers:

The removal of strong outliers did not influence the loss of replicates of the experiment because at least one or two extra fruit can be used to calculate the average per replicate. According to all the PCAs (Figure 5) and PLS-DA (Supplementary Figure S5 (Annex A)), they were able to discriminate between seasons. However, fruit 2B (S1) appeared to be an extra outlier (Figure 5).

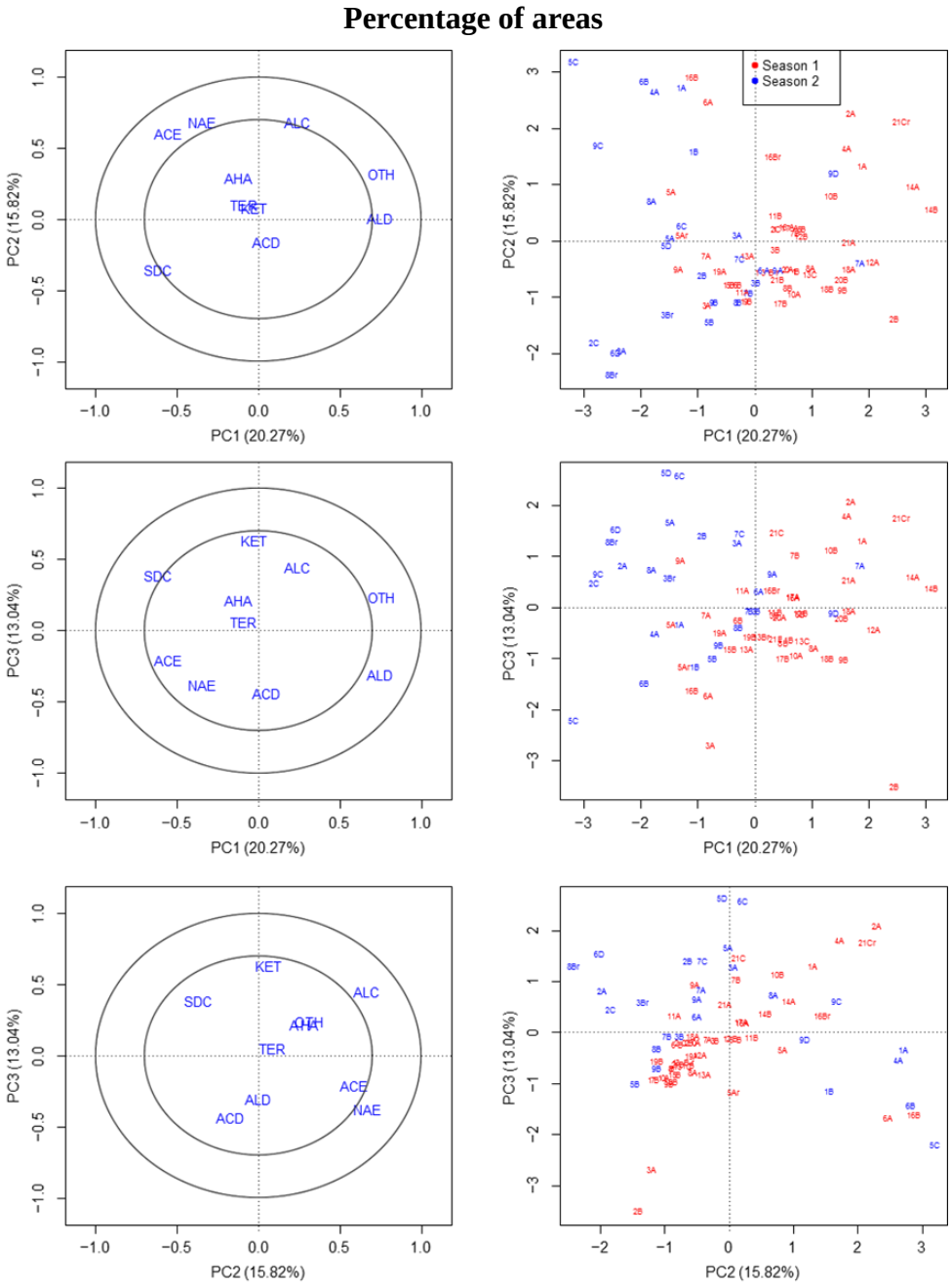

Figure 5. Correlation (**left**) and score (**right**) plots of the first three components of the PCA (with 49.13% of explained variance) applied to variables of different volatile organic compound classes based on percentages of total areas (only compounds with match quality >50) and without exogenous compounds included, obtained in two seasons, after removing the two fruit with outliers of season 1. ACE, acetate ester; NAE, non-acetate ester; ALD, aldehyde; ALC, alcohols, KET, ketones; SDC, sulfur derived-compounds; TER, terpenes; AHA, alkanes and aliphatic compounds; OTH, other compounds. Circles represent r^2 = 50% and 100% variability explained by the components.

Though the outliers reported are not associated with aldehydes, 2B (S1), a potential additional outlier showed a high relative concentration of hexanal or pentanal, and, to a lesser extent, nonanal, together with an unusual diversity of other aldehydes within one sample, but in lower proportions (butanal, heptanal, octanal, decanal, undecanal, dodecanal, tetradecanal, (2E,4E)-hepta-2,4-dienal, (2E,4E)-nona-2,4-dienal, (E)-hept-2-enal, etc.). Additionally, some of these aldehydes were only detected by deconvolution analysis.

3.7 Individual Aroma Volatiles:

The individual aroma volatiles tentatively identified in more than 10% of the fruit analyzed were 126 compounds, irrespective of the season (data not shown). However, only 54 of them appeared in more than 50% of the fruit, and only 21 in more than in 90% of fruits with a similarity index above ninety (Table 1). Of the former, most were aldehydes (particularly hexanal), alcohols, sulfur-derived compounds and, to a lesser extent, other groups.

Table 1. Main volatile organic compounds extracted by headspace solid phase microextraction, measured by gas-chromatography coupled to mass spectrometry and tentatively identified by deconvolution analysis versus NIST11 database. Chemical compound were identified in more than 90% of the melon fruit samples analyzed (outliers excluded from the calculations) in order of retention time. The column used was an HP-5MS UI.

RT Mean	**Chemical Abstract Service**	**Volatile Organic Compound**	**Linear Retention Index Calculated**	**Match Quality Mean**
(Min)	Name	(IUPAC Name)	(ud)	(%)
1.279	000074-93-1	Methanethiol	<400	92
3.572	000624-92-0	Methyldisulfanylmethane	737	94
4.143	000071-41-0	Pentan-1-ol	763	88
4.949	000066-25-1	Hexanal	799	92
7.581	000111-27-3	Hexan-1-ol	867	90
8.974	000111-71-7	Heptanal	902	91
11.951	000100-52-7	Benzaldehyde	954	83
12.427	003658-80-8	Methylsulfanyldisulfanylmethane	962	88
14.814	000124-13-0	Octanal	1004	89
16.607	000104-76-7	2-ethylhexan-1-ol	1033	86
18.709	000098-86-2	1-phenylethanone	1067	92
20.146	000617-94-7	2-phenylpropan-2-ol	1091	81
20.814	000124-19-6	Nonanal	1107	94
20.916	004621-04-9	4-Isopropylcyclohexanol (isomer)	1114	75
21.433	000464-49-3	1,7,7-trimethylbicyclo[2.2.1]heptan-2-one	1151	95
21.629	010340-23-5	(Z)-non-3-en-1-ol	1165	81
22.015	000098-19-1	1-tert-butyl-3,5-dimethylbenzene	1193	72
22.112	000112-40-3	Dodecane	1200	82
22.177	000112-31-2	Decanal	1208	92
22.911	71186-24-8	6Z)-6-[(E)-but-2-enylidene]-1,5,5-trimethylcyclohexene	1305	59
23.463	000629-59-4	Tetradecane	1400	65

The levels of alcohols of the outlier 15A (S1) was 52.4% (percent of identified compounds with MQ > 50), mostly due to the high relative concentration of hexan-1-ol followed by pentan-1-ol (70% of the area counts of alcohols identified), but also to the presence of other alcohols.

The outlier of fruit 4B (S1) has terpene compounds such as alpha-pinene (4,7,7-trimethylbicyclo[3.1.1]hept-3-ene), or beta-pinene (7,7-dimethyl-4-methylidenebicyclo[3.1.1]heptane) or camphene (6,6-dimethyl-5-methylidenebicyclo[2.2.1]heptane), apart from the terpenoid camphor (1,7,7-trimethylbicyclo[2.2.1]heptan-2-one). The acid detected in 4B (S1) was tentatively identified as 2-phenylpropanoic acid.

Other fruit also at the limit of distribution have high relative concentrations of ketones due to 1-phenylethanone, or some ester (isobutyl acetate or phenylmethyl acetate, and, to a lesser extent, isopropyl acetate) or sulfur-derived esters (data not shown).

4. Discussion:

Overall, the outliers detected from the total areas did not match with those detected by the percentages because of the potential variability in the analysis and intensity of aroma among fruits. Transformation of the percentages into logarithms of the variables of compound classes based on percentages is not advisable except for classification or prediction purposes. The PLS-DA of the total area (with or without normalization of each compound class to the response of the internal standard) gave a higher number of outliers compared with PCA (Supplementary Figure S2 (Annex A) vs. Figure 1), while, in percentages, these differences were minimized. Outliers detected by box-whisker plots were also more frequent than in this case because the variables frequently could not be analyzed by assuming normality, as demonstrated by the Shapiro-Wilk test. This problem also meant that Grubb's test could not be used in our case.

The main problem with applying Grubb's test is that individual variables can only be used if they follow a normal distribution, thus losing the perspective of a multivariate analysis. Additionally, this test can only be applied to the two fruits with extreme distribution data (Grubbs, 1969). However, more than one fruit could be considered as an outlier in one extreme, particularly if the variable does not follow a normal distribution.

An important point when two seasons are being compared is that the potential anomaly detected by the box-whisker plot should be in the same range (Figure 3), which probably explains why more outliers were not found in the multivariate statistical analysis compared with box-whisker plots.

The outliers detected by correlation analysis (Figure 4) were more than those finally considered as strong outliers. Removing all of them from certain variables of compound classes using this methodology or box-whisker plot would be problematic for considering the whole aroma of a fruit, and also incorrect from a multivariate point of view.

Variability in melon fruit VOCs could be associated with differences in physiological maturity, but also fruit sampling, particularly the start of the ripening process in the placental tissue containing the seeds (Moing et al., 2011; Nattaporn and Pranee, 2011) because fruit

ripening enhances the presence of alcohols. Some of the alcohols, such as hexan-1-ol, are good substrates for alcohol acetyltransferases or AAT (Shalit et al., 2001), and potential accumulation in some fruits can be a sign of a lack of activity of the enzyme compared with aromatic cultivars (Gonda et al., 2010), or a fruit harvested in a stage when the activity of the enzyme is still low (Shalit et al., 2001). On the other hand, the presence of terpenes or acids is sometimes associated with skin tissue (Portnoy et al., 2008), though terpenes have been found at higher levels in PS than in other cultivars (Condurso et al., 2012). According to our experience and other authors, acids are rarely detected in pulp samples by the HS-SPME test (Chaparro-Torres et al., 2016; Condurso et al., 2012), but, by using stir-bar sorptive extraction (SBSE), it is possible to detect them as a precursor of aromas in whole PS melons, and also in the pulp of climacteric cultivars (Fernández-Trujillo et al., 2013; Fernández-Trujillo et al., 2012) and in other juices (Barba et al., 2017).

Previous publications have applied PCA and PLS-DA to the classification of and comparison between VOCs of melon near-isogenic lines and the corresponding parental (Chaparro-Torres et al., 2016; Dos-Santos et al., 2013), the PLS-DA providing a better classification with fewer variables involved. For a metabolomics approach, PCA combined with multiblock hierarchical PCA has been used (Biais et al., 2009).

Another possibility in the formation of outliers is the onset of analytical artifacts during the process, for example, due to septum bleeding, or the saline solution used (always stored at 2 °C and prepared before each season). No artifacts were observed after a blank SPME of the saturated saline solution or water used to prepare the saline solution alone, in agreement with general recommendations (Verzera et al., 2011; Condurso et al., 2012).

From a physiological point of view, the higher the relative acetate ester concentration in flesh tissue, the more senescent the PS melon flesh (Escudero et al., 2018). This was the case with some samples when area counts were observed, but, in the percentage of total area counts, the outliers apparently disappeared. The esters, particularly isobutyl acetate or phenylmethyl acetate, and, to a lesser extent isopropyl acetate, are typical of climacteric cultivars (Dos-Santos et al., 2013). Other compounds, such as methyl 2-methylpropanoate, or the sulfur-derived esters, which are very specific to some cultivars and more abundant in climacteric ones (Gonda et al., 2013; Esteras et al., 2018), can also help detect outliers. A few esters can develop with certain abundance in some non-climacteric cultivars synthetized by ethylene-independent pathways, (Oh et al., 2011), particularly in certain seasons (Dos-Santos et al., 2013). The high level of these esters dramatically reduced the proportion of the aldehydes typical of non-climacteric cultivars and accessions based on total area counts (Verzera et al., 2011; Verzera et al., 2014; Escudero et al., 2018).

Another factor of importance is whether esters were found in the sampling procedure, particularly in large experiments involving climacteric aromatic and non-climacteric non-aromatic cultivars or lines for breeding purposes (Esteras et al., 2018). In the case of non-climacteric cultivars, placental tissue or local over-mature tissue should be avoided (Obando-Ulloa et al.,2009; Moing et al., 2011; Biais et al., 2009).

Overall, variables in the percentages of total area counts, such as total level of acids, terpenes, or alcohols, increased during PS melon fruit ripening, while aldehydes decreased, although non-acetate esters, alcohols and aldehydes also slightly increased close to senescence (Fernández-Trujillo et al., 2012; Escudero et al., 2018). The detection of the excess of some of these compounds within a sample of different fruit of one parental may help to provide more reliable control data for QTL mapping of this type of compound at harvest using near-isogenic lines (Obando-Ulloa et al., 2010; Chaparro-Torres et al., 2016).

Several strategies are feasible to reduce fruit sampling outliers, although improving the signal to noise ratio in GC-MS analysis is probably the best by using techniques such as *dynamic headspace purge and trap methodology for extraction (*Fredes et al., 2016). The additional validation of the results by SBSE GC-MS is another interesting strategy (Fernández-Trujillo et al., 2012), but deconvolution would be essential for integration (Barba et al., 2017), particularly if full-scan analysis, instead of using quantification, monitoring one or two ions per VOC (Gonda et al., 2013), was used.

Another suggestion for studying outliers using the proposed methodology is to group the compounds according to their metabolic pathways, taking into account their precursors (Wüst et al., 2018). Finally, the methodology proposed can be helpful in association studies of VOCs with aroma obtained by sensorial evaluation, particularly with small datasets in which outliers may or may not control what relationships are found, and some variables show collinearity (Chambers and Koppel, 2013).

5. Conclusions:

We propose a method for detecting outliers using PCA, double-checked with box-whisker plots, using the VOC variables obtained as percentages of chemical compound classes based, for example, on the total area of identified compounds in a chromatogram with an MQ above 50 (without exogenous compounds). The differences with other variables based on percentages were irrelevant. An excess of compounds, such as alcohols, terpenes, acids, or others in fruit samples was typical of some outliers.

SEASONAL EFFECTS ON FLESH VOLATILE CONCENTRATIONS AND TEXTURE AT HARVEST IN A NEAR-ISOGENIC LINE OF MELON WITH INTROGRESSION IN LG X:

IV. SEASONAL EFFECTS ON FLESH VOLATILE CONCENTRATIONS AND TEXTURE AT HARVEST IN A NEAR-ISOGENIC LINE OF MELON WITH INTROGRESSION IN LG X:

1. Introduction:

Melon (*Cucumis melo* L.) is an annual diploid plant that possesses high intra-specific genetic variation and a small genome size (454 Mb), which can be technologically exploited in terms of flavour development and the textural changes that occur during fruit ripening (Pech et al., 2008). One of the main evident changes during melon fruit ripening is softening, particularly the fast flesh softening in climacteric type netted muskmelons, such as cantaloupe, galia, *Ananas* and *Charentais* types (Kyriacou et al., 2018). Nevertheless, softening and other textural changes, such as juiciness (an opposite trait to flesh firmness), are also important and appreciated by consumers of non-climacteric types (Bianchi et al, 2016; Dos-Santos et al., 2013; Escribano and Lázaro, 2012; Escribano et al., 2010; Kyriacou et al., 2018; Obando et al., 2008; Obando-Ulloa et al., 2009a). In fact, most consumers of non-climacteric melons prefer a fruit with a medium firmness or a crunchy and outstanding firmness (Fernández-Trujillo et al., 2012; Lázaro and Lorenzo, 2015).

Volatile compounds are synthesized from fatty acid metabolism, amino acid metabolism, and carbohydrate metabolism (Schwab et al., 2008; Osorio et al., 2010) through several pathways (Schaffer et al., 2007), which are listed below. (i) Straight-chain aldehydes, alcohols and esters are synthesized from lipids, mainly linolenic and linoleic acids, through β-oxidation and lipoxygenase activity (Rowan et al., 1999; Espino-Díaz et al., 2016). (ii) Branched-chain aldehydes, alcohols and esters are derived from isoleucine (Rowan et al., 1996; Matich et al., 2007). (iii) Terpenoids are synthesized via the mevalonate pathway (Schwab et al., 2008; Sanz et al., 2010) and deoxyxylulose phosphate pathway (Eisenreich et al., 2004), and (iv) phenylpropanoids are synthesized from the phenylpropanoid pathway (Gang et al., 2001).

The aroma profile together with textural traits are efficient tools for discriminating climacteric near-isogenic lines (NILs) from non-climacteric lines at harvest or after postharvest senescence (Obando-Ulloa et al. 2008 and 2009a), but little information is available about aroma formation in non-climacteric melons, particularly during postharvest ripening (Gonda et al., 2010), and in non-climacteric NILs during ripening. C9 aliphatic aldehydes have been identified as the key aroma and flavour descriptors of commercial *inodorus* honeydew melons (Kyriacou et al., 2018). The emphasis on the flesh aroma of non-climacteric melons has focused on volatile organic compounds (VOCs) at harvest (Obando-Ulloa et al., 2010, Perry et al. 2009; Verzera et al., 2011), and precursors such as branched amino acids, other amino acids (Gonda et al., 2010, 2013 and 2018), and fatty acids (Li et al., 2016). In other studies of non-climacteric fruit, most authors focused on differences between climacteric and non-climacteric types, among types or NILs (Bernillon et al., 2013; Güler et al., 2013; Obando-Ulloa et al., 2008), or among different rootstocks (Verzera et al., 2014), because VOCs, which contribute to flavour, are also of interest for fresh melon consumption (Escribano et al., 2010; Fernández-Trujillo et al., 2012).

Several factors may affect volatile production and composition, including the genetics of the fruit, its maturity, postharvest handling, storage and seasonal and environmental conditions during production (Bernillon et al., 2013), in addition to the intrinsic variability in melon flesh during sample extraction and analysis (Allwood et al., 2009; Verzera et al., 2011; Kende et al., 2019).

The development of the melon NIL collection from the cross of the donor Korean accession 'Songwhan Charmi' and the 'Piel de Sapo' (PS) strain (Eduardo et al., 2005) has been a topic of interest for mapping quantitative trait loci associated with textural properties and VOCs (Moreno et al., 2008; Obando et al., 2008; Obando-Ulloa et al., 2008). The aim of this paper was to examine introgression (fix effect) and seasonal effects and identify the most discriminant flesh aroma volatiles at harvest as potential biomarkers of textural differences (particularly flesh firmness). Our hypothesis is that the genetic factor (introgression in melon chromosome X present in the NIL SC10-2, but not in PS) and the environment (seasons) differentially contribute to the relative effects on the traits analysed. Additionally, a secondary goal was the study of three methods for analysing the effect of the presence of null values within consistent VOC variables

2. Materials and methods:

The melon near-isogenic line (*Cucumis melo* L.) SC10-2 was obtained by Eduardo et al. (2005) through interbreeding led by molecular markers between a donor [Korean variety 'Songwhan Charmi' PI 161375 (SC)] and the parental Spanish cultivar T111 of the type 'Piel de Sapo' *C. melo* L. subsp. melo, Ibericus Group; based on a recent classification by Pitrat (2017). SC10-2 contains an introgression in homozygosis that covers the entire LG X from SC on a PS genetic background (Eduardo et al., 2005). Melon cultivation occurred under Mediterranean conditions in an experimental orchard of CIFEA (Torre Pacheco, Murcia, Spain). The plot design was randomized, and the number of replicates (three plants per replicate) was n=5 or n=20 (SC10-2 or PS, respectively, in season 1) and n=4 or n=9 (SC10-2 or PS, respectively, in season 2). A minimum of 2 fruits were collected from each replicate.

The fruit harvest and maturity index adopted here were modified slightly from the study Obando-Ulloa et al. (2009a) and were based on the previous experience of three seasons with the non-climacteric fruit of this plant material (Obando et al., 2008; Dos-Santos et al., 2013; Chaparro-Torres et al., 2016). Minimum external harvest indices were defined as the presence of a well formed and defect-free fruit, a firm, well healed and dry epidermis with lignified netting, a high density, the absence of trichomes, skin colour, withering of the stem and leaf closer to the fruit peduncle suberization, risk of cracking, and white to yellow (in SC10-2) or light yellowing (in PS) of the ground spot (if detectable). Soluble solids were monitored during the last two weeks before harvest to ensure minimum harvest maturity. The most common harvest indices for the PS were also the development of a well-lignified skin netting and the occasional development of annular ring or yellow colour surrounding the peduncle. Both lines developed a partly suberized peduncle (stem scar), and dark dull green skin (or dull green spots) in PS or dark blue-green skin colour in SC10-2.

The data for the average, minimum and maximum temperatures, precipitation and average radiation from April to early August (Figure 1) were obtained from SIAM (Agricultural

Information System of Murcia, SIAM, station TP91 or Torre Pacheco; http://siam.imida.es/apex/f?p=101:46:1053892687272425).

The physiological behaviour was determined by measuring the respiration rate and ethylene production during ripening using the static method, and individual fruit from different replicates (n=5) was used to obtain carbon dioxide and ethylene samples that were measured with gas chromatography, as previously reported (Fernández-Trujillo et al., 2008). Firmness in N was measured with a 4.6-mm cylinder probe (TG83, SAE Ibertest, Daganzo de Arriba, Madrid, Spain). The pulp firmness (in N) was measured on melon flesh cylinders (20 mm high and 15 mm diameter) obtained from the fruit equator with a 4.6-mm diameter punch mounted in an ELIB-5K testing machine (Ibertest,) equipped with a 100-N load cell (Ibertest). The probe approached the fruit at a rate of 15 $mm \cdot min^{-1}$ with a 0.1 N preload. Other textural traits were measured using the methods described by Dos-Santos et al. (2013). Equatorial whole fruit hardness (in $N \cdot mm^{-1}$) was defined as the compression force required for a 2 mm deformation obtained with a 2 kN cell with a double scale (only the 0 - 200 N scale was used, with 1/10 of the total graphic scale) mounted in the same testing machine. A 15 $mm \cdot min^{-1}$ compression speed and 1 N preload were applied once on each fruit using a 150-mm round flat compression plate. Juiciness was defined as the amount of juice without pellet (in $g \cdot kg^{-1}$ g of pulp) obtained by squeezing an exact weight of pulp (approximately 200 g) and centrifuging an aliquot of the juice squeezed to obtain a juice free from pellet. Juice density was calculated by weighing 1 mL of juice. Fibrousness was expressed by calculating the grams of pellet per kg of juice after the centrifugation of a juice aliquot (Dos-Santos et al., 2013).

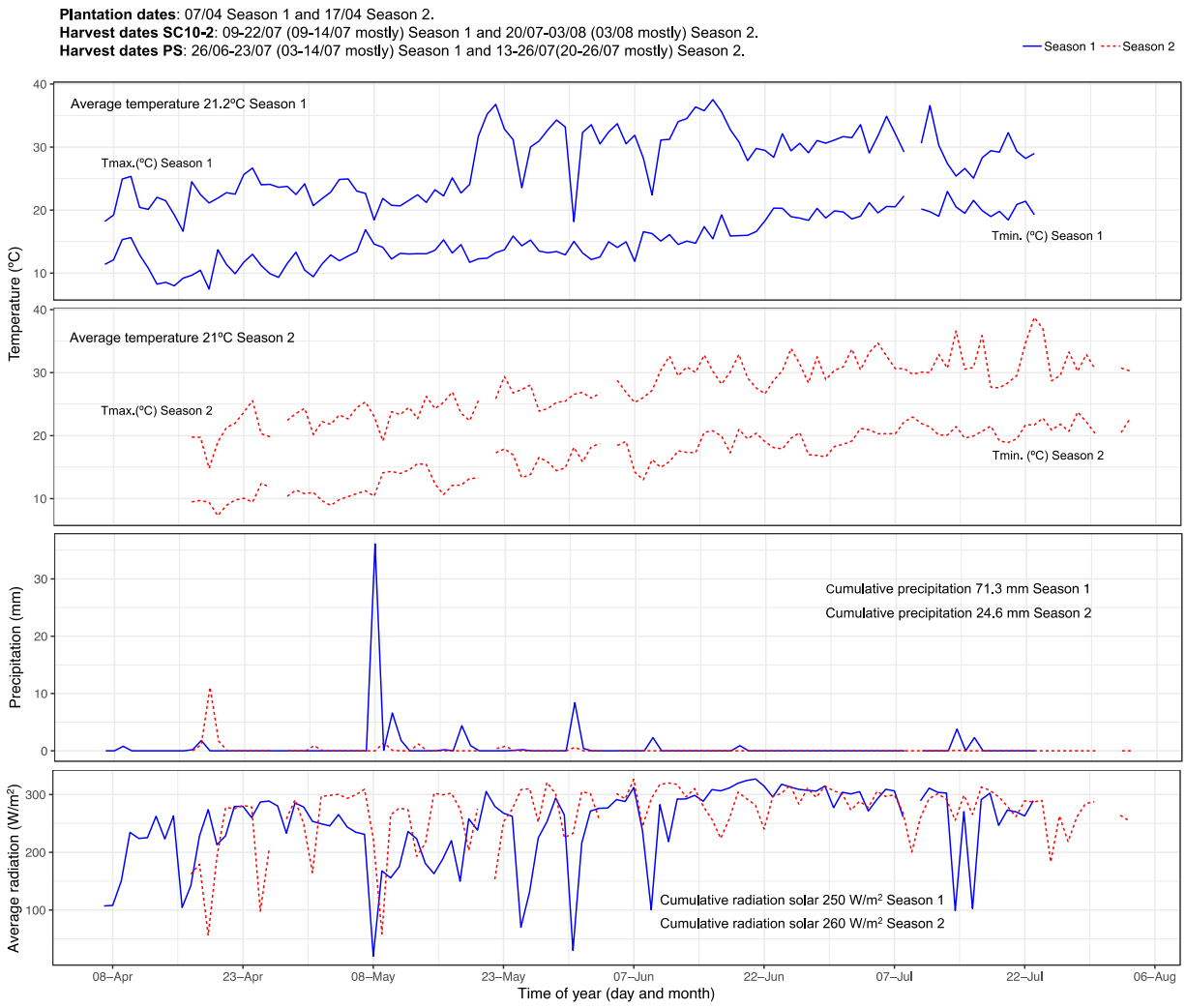

Figure 1. Maximum and minimum temperature, daily rainfall, and average radiation in both growing seasons (S1 and S2, continuous and dotted lines) from plantation to fruit harvest of the melon near-isogenic line (NIL) SC10-2 and the parental 'Piel de Sapo' (PS) line. Mean of temperature, precipitation and radiation are also included in text in the figure.

Before analysing the flesh volatiles, juice was extracted from the flesh and mixed with a saturated calcium chloride solution. The mixture was subsequently analysed in a gas chromatograph equipped with a mass spectrometer using the method of solid-phase microextraction headspace (Dos-Santos et al., 2013; Chaparro-Torres et al., 2016; Fernández-Trujillo et al., 2018). VOC samples consisted of 2.32 mL of a mixture of filtered melon juice and a calcium chloride solution (71.4% *v/v* of juice) poured into 10-mL vials plus 0.02 mL of a solution containing the internal standard (4.27 mg·L^{-1} of 1-phenylethanol, in dichloromethane).

Volatiles were extracted without stirring for 120 min at 35 °C in the heating tray of the gas chromatograph (6890N, Agilent Technologies, Wilmington, DE, USA) using static headspace solid-phase microextraction (HS-SPME). The fibre used for extraction was coated with 50/30 µm divinylbenzene/carboxen on polydimethylsiloxane (DVB/CAR/PDMS) (57329-U DVB/Carboxen™/PDMS Stable Flex™, Supelco, Bellefonte, PA, USA), and volatiles in the vial headspace were absorbed at 35 °C for 30 min. The volatiles were desorbed from the SPME fibre with a bake-out step of 3 min at 280 °C into the GC injection port that operated at 260 °C

in splitless mode. The carrier gas was helium with a flow rate of 1.5 $mL \cdot min^{-1}$. A retention time locking with *n*-pentadecane allowed the comparison of chromatograms and the separation of a homologous series of n-alkanes (C6–C20; Sigma-Aldrich) through the capillary column (30 m × 0.25 mm i.d. × 0.25 µm, HP-5 MS UI) of the gas chromatograph. The initial oven temperature was 35 °C, followed by an increase in temperature to 75 °C at a rate of 2 $°C \cdot min^{-1}$ and then an increase at a rate 50 $°C \cdot min^{-1}$ to reach a final temperature of 250 °C. The mass detector (electron ionization at 70 eV) operated at 230 °C in full-scan mode with data acquisition, and ion masses were captured between 40 and 450 amu.

The integration of the chromatograms, analysis of the individual compounds, separation of aroma groups by chemical compounds, quantification of individual aroma volatile compounds, and removal of strong outliers were performed using the methods described by Fernández-Trujillo et al. (2018). The concentrations were quantified from the relation between the areas of the VOCs and the internal standard (1-phenylethanol) using a response factor of 1. The concentrations of the individual VOCs were reported as $ng \cdot g^{-1}$ of pulp.

The VOC chromatographic data were preintegrated using ChemStation software (G1701DA D.02.00.275, Agilent Technol.), followed by a manual integration step and individual reverification of the peaks based on a deconvolution analysis using NIST 11 MS Library and AMDIS (version 2.7, 2011, National Institute of Standards and Technology, Gaithersburg, MD, USA). VOCs were validated by comparing the linear retention indices (LRI) calculated from a homologous series of n-alkanes (C6-C20; Sigma-Aldrich) separated using an HP-5 MS UI column.

Consistent VOC variables were present in more than 25% of the fruits analysed and 50% or more of the replicates analysed (Chaparro-Torres et al., 2016). Consistent VOCs with null values were analysed using three different methodologies, all of which were based on substituting the null data for each variable with the minimum analytical values before log_2 transformation. i) In each season, the null data were substituted with the minimum non-null value of the VOC variable, ii) the minimum analytical value of VOC detected in the entire consistent list of VOCs variables (criteria adopted in Chaparro-Torres et al., 2016, but also reported by Mathieu et al. (2009) for tomato), and iii) substitution with the minimum value of each line/season (four different cases per VOC).

For individual VOCs, a one-way ANOVA per season (S1 or S2) using introgression (in LG X) as the factor was performed, followed by correction for multiple comparisons using the Benjamini and Hochberg (BH) false discovery rate criterion at a level of $q \leq 0.05$. A two-way ANOVA of the textural traits using introgression (in LG X) and season (S1 or S2) as factors was performed, followed by correction for multiple comparisons using the same criterion reported above at a level of $q \leq 0.05$. Pearson's correlation coefficients were calculated among VOCs, and correlation networks were displayed to visualize the degree of association between variables. Different multivariate statistical techniques, such as Principal Component Analysis (PCA), Random Forest (RF), and Partial Least Squares-Discriminant Analysis (PLS-DA), were applied to the experimental data and conducted with R free software (R Core Team, 2018).

3. Results:

3.1 Seasonal differences:

The average temperature and radiation were similar in both seasons, but precipitation was important only in season 1 (Figure 1). Fruit from season 1 was harvested later than expected (1-2 weeks) due to three abrupt weather events (a decrease in the maximum temperatures for the season and rain during May and June; Figure 1). In Season 1, maximum temperatures were less than 25°C up to the middle of May due to that rain, and two additional rain episodes in June provoked the same effect. In season 2, the maximum temperature from fruit set never decreased below 20°C and the cumulative amount of rain was less than 10 mm (five events) (Figure 1). SC10-2 attained harvest maturity approximately 1-2 weeks later than PS, regardless of the season.

3.2 Physiological behaviour and textural traits:

The physiological behaviour during ripening always showed a non-climacteric pattern (data not shown). The results of the analysis of textural traits at harvest showed similar differences in both seasons and a significant effect of introgression on the traits of fruit harvested in both seasons, with the exception of juice density (any factor was significant) and fibrousness (only season was significant). Additionally, juiciness was higher in the rainiest season regardless of the line (S1; Supplementary Table 1 (Annex B); Figure 1). Juiciness also showed a significant season x introgression interaction, because the differences in juiciness between PS and SC10-2 were substantial in S1 and S2, depending on the season (16 and 34% lower, respectively) (Supplementary Table 1 (Annex B)). In season 1, the melon non-climacteric NIL SC10-2 had a higher firmness (9.2 N) than PS (7.3 N), a higher hardness (58.7 $N \cdot mm^{-1}$ for SC10-2 and 54.7 $N \cdot mm^{-1}$ for PS) and lower juiciness (SC10-2: $\bar{x}$ = 292.8 $g \cdot kg^{-1}$) than PS ($\bar{x}$ = 350.2 $g \cdot kg^{-1}$), and lower fibre presence within the juice, i.e., fibrousness (SC10-2: 27 $g \cdot kg^{-1}$; PS: 29 $g \cdot kg^{-1}$), but a similar density (SC10-2: 1015 $kg \cdot m^{-3}$; PS: 1021 $kg \cdot m^{-3}$). In season 2, the NIL SC10-2 showed a higher flesh firmness (7.5 N), hardness (69.8 $N \cdot mm^{-1}$), fibrousness (24 $g \cdot kg^{-1}$) and lower flesh juiciness ($\bar{x}$ = 194.0 $g \cdot kg^{-1}$) than PS (5.4 N flesh firmness, 64.1 $N \cdot mm^{-1}$ hardness, 23 $g \cdot kg^{-1}$ fibrousness and $\bar{x}$ = 293.8 $g \cdot kg^{-1}$ flesh juiciness), and a similar density as in season 1 (SC10-2: 1020 $kg \cdot m^{-3}$; PS: 1027 $kg \cdot m^{-3}$).

3.3 Aroma volatiles, univariate VOC analysis and detection of introgression effects:

Three hundred eleven melon VOCs were tentatively identified from the melon juice analysis, and another 53 were silanes, siloxane derivatives, or other contaminants of the analysis, which were not considered (data not shown). For example, propylene oxide, toluene and styrene were not considered in the aroma profile. Of the 116 VOCs that were consistently identified, two of them were unidentified compounds (Table 1). All VOCs were subjected to univariate and multivariate analyses (90 compounds for season 1 and 86 for season 2).

Sixty VOCs were detected in both seasons (S1 and S2) and comprised the aroma profile of this experiment (compounds in bold presented in Table 1). The match quality of the tentative

VOCs ranged between 53% and 95%, and the LRI differed by less than 1% from the values reported in the literature.

ANOVA with a correction for multiple testing using the Benjamini and Hochberg false discovery rate criterion revealed two VOCs with a p-value less than 0.05 in S1 and one in S2 (Table 1). Therefore, at least a putative quantitative trait locus was assigned to modify the VOCs pattern at harvest described above. Twenty-eight VOCs differed significantly, regardless of the season, but were attributed to the introgression (Table 2).

Additionally, 30 volatiles (three of which were significant in S1) were absent from S2 but present in S1 (Table 1), including two unidentified compounds (LRI 942 and LRI 1350), three acetate esters, nine aldehydes, four alcohols, seven ketones, two alkanes and three other VOCs (2-methylfuran, (3E)-3-ethyl-2-methylhexa-1,3-diene, and (1S,3aR,4S,8aS)-decahydro-4,8,8-trimethyl-9-methylene-1,4-methanoazulene), some of which are associated, such as C7 and C9 (ketones and alcohols) (Table 1).

Twenty-six other VOCs were absent from S1 but present in S2, including four alcohols, seven alkanes, two acetate esters, one ketones, two sulfur-derived compounds, six non-acetate esters and four other VOCs (1,4-dimethylbenzene, 1,2,3-trimethylbenzene, cyclohex-3-ene-1-carbonitrile, and 1-methyl-4-prop-1-en-2-ylcyclohexene) (Table 1).

3.4 Comparison of the effect of the methods adopted for the treatment of null VOCs:

A greater number of VOCs was affected by the introgression when method ii) or iii) was used, regardless of the season considered. Only three compounds were identified as exerting an introgression effect when the first method (i) of treating null data was used: 2-methylbutanal and naphthalene above PS and (Z)-non-3-en-1-ol below PS (Table 2). These three VOCs also exerted an introgression effect when analysed with the second and third methods for treating null data, but twenty-five more VOCs were also identified (Table 2). Therefore, the third methodology was adopted for this report.

3.5 Multivariate analysis of VOCs:

In both seasons, the use of a supervised PLS-DA method allowed identification of the most influential VOCs to separate the NILs. The PLSDA1 axis discriminated the NIL SC10-2 (right) from PS (left) in S1 and the opposite direction in S2, indicating a general effect of the introgression in LG X on VOCs (Figure 2). Thirty-four compounds were detected in S1 (Table 3 and Figure 2C) and thirty in S2 (Table 4 and Figure 2D), but only 2-methylbutanal, 2-methylpentan-3-one, (E)-hex-2-enal and (E)-5-ethyl-6-methylhept-3-en-2-one were discriminatory factors in both seasons, according to the PLS-DA (Tables 3 and 4).

A correlation analysis was performed by calculating Pearson's correlation coefficients to evaluate the relationship between the VOCs and textural traits. Thirty-two volatile compounds were identified in season 1 (Table 5 and Supplementary Figure 2 (Annex B)) that showed correlations with different textural traits. In season 2, forty-one VOCs were identified (Table 6 and Supplementary Figure 3 (Annex B)), and most VOCs correlated with more than one textural trait, such as nonanal (juice density, juiciness, firmness and hardness) and benzaldehyde

(juiciness, firmness and hardness). Eleven compounds were identified as influential VOCs in both seasons (ethyl acetate, 2-methylbutanal, benzaldehyde, methylsulfanyldisulfanylmethane, undecane, 1,7,7-trimethylbicyclo[2.2.1]heptan-2-one, (Z)-non-3-en-1-ol, 1-tert-butyl-3,5-dimethylbenzene, dodecane, tetradecane and 2,6-di-tert-butylbenzoquinone) (compounds marked in bold in Tables 5 and 6).

In the Random Forest (RF) analysis, slight differences in the order of importance of the VOCs were identified depending on whether the Mean Decrease in Accuracy (MDA) or Mean Decrease in Gini index (MDG) criterion was used to evaluate the influence of the discriminant variables (Figure 3). Multidimensional scaling (MDS) plots of the RF analysis illustrate the discrimination of the NIL SC10-2 and the parental PS (Supplementary Figure 3 (Annex B)).

Finally, heatmaps were constructed to aid in the visualization of the correlation between VOCs identified at harvest in two seasons (1 and 2) and the traits, where the dendrogram on the top of the heatmap showed the clear separation between the NIL and the parental line PS (Supplementary Figs. 4 and 5 (Annex B)).

4. Discussion:

4.1 Introgression and seasonal effects on texture:

The introgression of SC10-2 covered the entire LG X (Eduardo et al., 2005). According to Dos-Santos et al. (2013), the introgressions in LG X did not affect the melon climacteric behaviour, but typical textural traits of a firmer fruit with lower juiciness were observed in LG X. In contrast, our VOC results show clear differences between the NIL SC10-2 and its parental line PS at harvest in both seasons (S1 and S2) and some differences with Dos-Santos et al. (2013), indicating that VOC production may be affected by environmental and seasonal factors. The same NIL can behave differently in different seasons, depending on the environmental conditions during flowering, fruit set and development. This aroma volatile variability is a typical problem that exerts a negative effect when cultivars are grown for the fresh-cut industry and do not reach adequate maturity (Beaulieu, 2005), as was the case in S1 due to increased rainfall and low insolation during melon growth. Our results using NILs contrast the results reported in some well-established commercial cultivars, which show fewer environmental effects on VOCs than on other metabolites (Bernilllon et al., 2013; Kyriacou et al., 2018). In mini-watermelon fruits, Dima et al. (2014) also showed similar results between two seasons, and the authors did not report environmental differences that would affect fruit ripening between seasons.

Table 1
Volatile organic compounds (VOCs) consistently identified at harvest for determination of the introgression effect in two seasons (S1 and S2) using the near-isogenic line (NIL) SC10-2 (n = 5 or n = 4, respectively) and the parental 'Piel de Sapo' (PS) (n = 20 or n = 9, respectively) by static headspace solid-phase microextraction and gas chromatography-mass spectrometry (HS-SPME/GC–MS) technique in melon juice extracted from fruit pulp. Data are VOC equivalent concentration for 1-phenylethanol as standard (ng·g$_{-1}$ of melon pulp). VOCs marked in bold represent the compounds of the aroma profile of the whole experiment (60 compounds).

IDN[a]	CAS[b] number	Volatile organic compound (IUPAC[c] name)	Compound class[d]	RT[e] (min)	MQ[f]	LRI[g] Cal	LRI[g] ref	Season 1 PS		Season 1 SC10-2		Season 1 p[h]	Season 2 PS		Season 2 SC10-2		Season 2 p[h]
1	**000075-07-0**	**Acetaldehyde**	ALD	1.238	90	< 500	381	0.041	± 0.05	0.150	± 0.16	NS	0.117	± 0.03	0.245	± 0.14	NS
2	**000074-93-1**	**Methanethiol**	SDC	1.280	91	< 500	464	0.295	± 0.11	0.315	± 0.22	NS	0.547	± 0.18	0.635	± 0.32	NS
3	**000064-17-5**	**Ethanol**	ALC	1.324	90	< 500	426	0.049	± 0.12	0.172	± 0.22	*	0.476	± 0.41	0.609	± 0.45	NS
4	**000123-72-8**	**Butanal**	ALD	1.795	77	593	595	0.091	± 0.12	0.018	± 0.03	NS	0.030	± 0.04	0.023	± 0.05	NS
5	**000110-54-3**	**Hexane**	AHA	1.810	75	599	600	0.049	± 0.05	0.068	± 0.14	NS	0.075	± 0.07	0.067	± 0.05	NS
6	534-22-5	2-methylfuran	OTH	1.852	86	605	605	0.021	± 0.02	0.034	± 0.04	NS	ND	-	ND	-	ND
7	**000141-78-6**	**Ethyl acetate**	ACE	1.932	85	613	612	0.255	± 0.34	0.355	± 0.22	NS	0.854	± 0.67	0.586	± 0.14	NS
8	**000109-99-9**	**Oxolane**	OTH	2.052	78	625	623	0.009	± 0.01	0.002	± 0.00	NS	0.040	± 0.07	0.048	± 0.04	NS
9	123-73-9	(E)-but-2-enal	ALD	2.249	85	646	645	0.016	± 0.03	0.012	± 0.01	NS	ND	-	ND	-	ND
10	**96-17-3**	**2-methylbutanal**	ALD	2.369	72	658	659	0.008	± 0.02	0.059	± 0.05	**	0.025	± 0.02	0.104	± 0.08	NS
11	000071-36-3	Butan-1-ol	ALC	2.383	80	659	659	0.003	± 0.00	0.014	± 0.02	NS	ND	-	ND	-	ND
12	**000616-25-1**	**Pent-1-en-3-ol**	ALC	2.580	83	680	681	0.039	± 0.03	0.027	± 0.03	NS	0.026	± 0.02	0.005	± 0.00	*
13	**001629-58-9**	**Pent-1-en-3-one**	KET	2.631	82	685	684	0.069	± 0.07	0.072	± 0.05	NS	0.021	± 0.04	0.021	± 0.04	NS
14	**000110-62-3**	**Pentanal**	ALD	2.760	86	699	699	0.715	± 0.57	0.545	± 0.50	NS	0.261	± 0.18	0.262	± 0.08	NS
15	**003208-16-0**	**2-ethyl furan**	OTH	2.812	89	702	702	0.286	± 0.53	0.118	± 0.19	NS	0.096	± 0.11	0.036	± 0.06	NS
16	**000624-92-0**	**Methyldisulfanylmethane**	SDC	3.571	94	737	736	0.255	± 0.31	0.165	± 0.09	NS	1.985	± 2.05	0.747	± 0.69	NS
17	**565-69-5**	**2-methylpentan-3-one**	KET	3.747	79	745	742	0.043	± 0.09	0.023	± 0.02	NS	0.009	± 0.01	0.000	± 0.00	**
18	**001576-87-0**	**(E)-pent-2-enal**	ALD	3.831	82	749	749	0.104	± 0.13	0.066	± 0.04	NS	0.022	± 0.03	0.012	± 0.02	NS
19	**000071-41-0**	**Pentan-1-ol**	ALC	4.141	87	763	764	0.126	± 0.11	0.118	± 0.07	NS	0.162	± 0.14	0.100	± 0.08	NS
20	**000066-25-1**	**Hexanal**	ALD	4.946	92	799	802	4.631	± 5.75	3.376	± 1.28	NS	1.891	± 1.45	0.958	± 0.46	NS
21	**006137-03-7**	**3-ethylpentan-2-one**	KET	6.131	71	831	838	0.058	± 0.09	0.033	± 0.02	NS	0.016	± 0.01	0.001	± 0.00	NS
22	**006728-26-3**	**(E)-hex-2-enal**	ALD	6.825	82	848	850	0.087	± 0.12	0.103	± 0.12	NS	0.011	± 0.01	0.000	± 0.00	****
23	**000111-27-3**	**Hexan-1-ol**	ALC	7.579	91	867	867	0.494	± 0.89	0.417	± 0.41	NS	0.333	± 0.43	0.072	± 0.04	NS
24	000624-41-9	2-methylbutyl acetate	ACE	8.030	77	879	879	0.005	± 0.01	0.009	± 0.01	**	ND	-	ND	-	ND
25	**004466-24-4**	**2-butylfuran**	OTH	8.460	81	890	892	0.048	± 0.05	0.025	± 0.01	NS	0.020	± 0.04	0.000	± 0.00	NS
26	6728-31-0	Hept-4-enal	ALD	8.869	65	900	898	0.003	± 0.00	0.005	± 0.01	NS	ND	-	ND	-	ND
27	**000111-71-7**	**Heptanal**	ALD	8.975	91	902	901	0.258	± 0.27	0.167	± 0.13	NS	0.162	± 0.12	0.135	± 0.02	NS
28	018829-55-5	(E)-hept-2-enal	ALD	11.897	82	953	954	0.151	± 0.21	0.023	± 0.06	NS	ND	-	ND	-	ND
29	**000100-52-7**	**Benzaldehyde**	ALD	11.952	84	954	954	0.116	± 0.10	0.136	± 0.05	NS	0.080	± 0.04	0.169	± 0.03	*
30	**003658-80-8**	**Methylsulfanyldisulfanylmethane**	SDC	12.384	88	961	963	0.075	± 0.08	0.030	± 0.02	NS	0.230	± 0.31	0.150	± 0.17	NS
31	**111-70-6**	**Heptan-1-ol**	ALC	12.942	82	971	970	0.025	± 0.04	0.010	± 0.01	NS	0.013	± 0.01	0.005	± 0.01	NS
32	004312-99-6	Oct-1-en-3-one	KET	13.287	75	977	980	0.022	± 0.03	0.007	± 0.01	NS	ND	-	ND	-	ND
33	**003391-86-4**	**Oct-1-en-3-ol**	ALC	13.405	73	979	980	0.068	± 0.07	0.040	± 0.02	NS	0.016	± 0.02	0.003	± 0.00	NS
34	000585-25-1	Octane-2,5-dione	KET	13.722	73	985	987	0.018	± 0.02	0.011	± 0.01	NS	ND	-	ND	-	ND
35	106-68-3	5-methylheptan-3-one	KET	13.826	79	987	988	0.008	± 0.01	0.014	± 0.03	NS	ND	-	ND	-	ND
36	**000110-93-0**	**6-methylhept-5-en-2-one**	KET	13.877	66	988	988	0.027	± 0.01	0.030	± 0.02	NS	0.002	± 0.00	0.002	± 0.00	****
37	**003777-69-3**	**2-pentylfuran**	OTH	14.021	87	990	993	0.061	± 0.06	0.086	± 0.04	NS	0.042	± 0.05	0.010	± 0.01	NS
38	5910-85-0	(2E,4E)-hepta-2,4-dienal	ALD	14.392	72	996	998	0.026	± 0.04	0.008	± 0.01	NS	ND	-	ND	-	ND
39	**000124-13-0**	**Octanal**	ALD	14.817	95	1004	1005	0.081	± 0.05	0.104	± 0.04	NS	0.038	± 0.02	0.036	± 0.01	NS
40	61142-36-7	(3E)-3-ethyl-2-methylhexa-1,3-diene	OTH	16.429	62	1030	1030	0.016	± 0.04	0.016	± 0.01	NS	ND	-	ND	-	ND
41	**000104-76-7**	**2-ethylhexan-1-ol**	ALC	16.607	86	1033	1031	0.051	± 0.03	0.065	± 0.03	NS	0.083	± 0.03	0.143	± 0.02	*
42	**001193-81-3**	**(2-methylcyclohexyl)methanol**	ALC	17.609	54	1049	1051	0.002	± 0.00	0.003	± 0.00	NS	0.003	± 0.00	0.002	± 0.00	NS
43	**000098-86-2**	**1-phenylethanone**	KET	18.709	92	1067	1068	0.134	± 0.09	0.162	± 0.13	NS	0.402	± 0.16	0.721	± 0.10	NS
44	**000111-87-5**	**Octan-1-ol**	ALC	19.415	77	1079	1080	0.018	± 0.02	0.015	± 0.02	NS	0.011	± 0.02	0.004	± 0.01	NS
45	**000617-94-7**	**2-phenylpropan-2-ol**	ALC	20.147	81	1091	1090	0.040	± 0.01	0.039	± 0.02	NS	0.040	± 0.01	0.059	± 0.00	NS
46	**1120-21-4**	**Undecane**	AHA	20.708	63	1100	1100	0.006	± 0.01	0.010	± 0.01	**	0.009	± 0.01	0.012	± 0.00	NS
47	**4501-58-0**	**2-(2,2,3-trimethylcyclopent-3-en-1-yl) acetaldehyde**	ALD	20.728	59	1101	1109	0.015	± 0.01	0.037	± 0.02	*	0.009	± 0.01	0.011	± 0.01	NS
48	**002277-19-2**	**(Z)-non-6-enal**	ALD	20.775	75	1104	1107	0.032	± 0.02	0.051	± 0.05	NS	0.007	± 0.00	0.027	± 0.02	*
49	**000124-19-6**	**Nonanal**	ALD	20.817	94	1107	1105	0.250	± 0.20	0.236	± 0.14	NS	0.089	± 0.03	0.190	± 0.05	*

(continued on next page)

Table 1 (*continued*)

IDN[a]	CAS[b] number	Volatile organic compound (IUPAC[c] name)	Compound class[d]	RT[e] (min)	MQ[f]	LRI[g] Cal	LRI[g] ref	Season 1 PS		Season 1 SC10-2		Season 1 p[h]	Season 2 PS		Season 2 SC10-2		Season 2 p[h]
50	**NID20.9LRI1114**	**Unidentified**	ALC	20.918	75	1114	ND	0.040	± *0.03*	0.086	± *0.10*	NS	0.024	± *0.01*	0.051	± *0.01*	*
51	3901-95-9	1-methyl-4-propan-2-ylcyclohexan-1-ol	ALC	21.303	63	1142	1138	0.106	± *0.17*	0.080	± *0.08*	NS	ND	-	ND	-	ND
52	**577-16-2**	**1-(2-methylphenyl)ethanone**	KET	21.346	76	1145	1139	0.003	± *0.00*	0.007	± *0.01*	NS	0.001	± *0.00*	0.004	± *0.00*	NS
53	**000464-49-3**	**1,7,7-trimethylbicyclo [2.2.1] heptan-2-one**	KET	21.435	95	1151	1144	0.169	± *0.09*	0.288	± *0.18*	*	0.147	± *0.06*	0.201	± *0.08*	NS
54	77-85-0	2-(hydroxymethyl)-2-methylpropane-1,3-diol	ALC	21.481	58	1155	1162	0.019	± *0.01*	0.032	± *0.02*	NS	ND	-	ND	-	ND
55	**057283-79-1**	**(E)-5-ethyl-6-methylhept-3-en-2-one**	KET	21.521	68	1158	1158	0.046	± *0.05*	0.028	± *0.02*	NS	0.004	± *0.00*	0.000	± *0.00*	**
56	17587-33-6	(2E,6E)-nona-2,6-dienal	ALD	21.611	71	1164	1162	0.026	± *0.02*	0.046	± *0.03*	NS	ND	-	ND	-	ND
57	**010340-23-5**	**(Z)-non-3-en-1-ol**	ALC	21.631	81	1165	1160	0.090	± *0.04*	0.114	± *0.06*	NS	0.031	± *0.01*	0.066	± *0.02*	**
58	**056805-23-3**	**(3Z,6Z)-nona-3,6-dien-1-ol**	ALC	21.666	71	1168	1165	0.081	± *0.08*	0.101	± *0.07*	NS	0.011	± *0.01*	0.026	± *0.03*	NS
59	**018829-56-6**	**(E)-non-2-enal**	ALD	21.684	77	1169	1171	0.067	± *0.05*	0.012	± *0.02*	NS	0.010	± *0.01*	0.005	± *0.01*	NS
60	**000140-11-4**	**Phenylmethyl acetate**	ACE	21.752	86	1173	1172	0.060	± *0.07*	0.133	± *0.09*	NS	0.056	± *0.05*	0.093	± *0.05*	NS
61	**000143-08-8**	**Nonan-1-ol**	ALC	21.855	79	1181	1181	0.075	± *0.05*	0.105	± *0.07*	NS	0.019	± *0.01*	0.019	± *0.01*	NS
62	**91-20-3**	**Naphthalene**	OTH	21.895	70	1184	1185	0.000	± *0.00*	0.002	± *0.00*	****	0.004	± *0.00*	0.006	± *0.00*	NS
63	**000098-19-1**	**1-tert-butyl-3,5-dimethylbenzene**	OTH	22.016	72	1193	1195	0.024	± *0.02*	0.031	± *0.02*	NS	0.019	± *0.02*	0.022	± *0.01*	NS
64	17920-92-2	4,8-dimethylnona-1,7-dien-4-ol	ALC	22.070	57	1197	1191	0.027	± *0.06*	0.023	± *0.01*	NS	ND	-	ND	-	ND
65	**000112-40-3**	**Dodecane**	AHA	22.113	83	1200	1200	0.024	± *0.01*	0.024	± *0.01*	NS	0.015	± *0.00*	0.023	± *0.00*	NS
66	**000112-31-2**	**Decanal**	ALD	22.178	92	1208	1208	0.115	± *0.08*	0.082	± *0.05*	NS	0.045	± *0.02*	0.059	± *0.01*	NS
67	5910-87-2	(2E,4E)-nona-2,4-dienal	ALD	22.249	68	1217	1218	0.050	± *0.08*	0.012	± *0.02*	NS	ND	-	ND	-	ND
68	**NID22.26LRI1219**	**Unidentified**	ALD	22.258	66	1219	ND	0.010	± *0.02*	0.026	± *0.02*	*	0.003	± *0.00*	0.005	± *0.00*	NS
69	NID22.29LRI1222	Unidentified	KET	22.289	71	1222	ND	0.007	± *0.02*	0.002	± *0.00*	NS	ND	-	ND	-	ND
70	000432-25-7	2,6,6-trimethylcyclohexene-1-carbaldehyde 4	ALD	22.308	61	1225	1222	0.015	± *0.02*	0.014	± *0.02*	NS	ND	-	ND	-	ND
71	**000501-92-8**	**4-prop-2-enylphenol**	ALC	22.494	53	1249	1251	0.023	± *0.01*	0.027	± *0.02*	NS	0.010	± *0.00*	0.020	± *0.01*	*
72	**000103-45-7**	**2-phenylethyl acetate**	ACE	22.607	79	1264	1264	0.023	± *0.04*	0.054	± *0.04*	*	0.011	± *0.01*	0.016	± *0.01*	NS
73	6117-99-3	2,4-dimethyldodecane	AHA	22.719	56	1279	1285	0.009	± *0.01*	0.015	± *0.01*	NS	ND	-	ND	-	ND
74	**000629-50-5**	**Tridecane**	AHA	22.876	61	1299	1300	0.017	± *0.02*	0.039	± *0.05*	NS	0.007	± *0.00*	0.008	± *0.00*	NS
75	**71186-24-8**	**6Z)-6-[(E)-but-2-enylidene]-1,5,5-trimethylcyclohexene**	OTH	22.911	59	1305	1317	0.059	± *0.07*	0.030	± *0.02*	NS	0.014	± *0.00*	0.021	± *0.01*	NS
76	000112-44-7	Undecanal	ALD	22.941	63	1310	1315	0.005	± *0.01*	0.003	± *0.01*	*	ND	-	ND	-	ND
77	41436-42-4	(E)-1-(2,6,6-trimethylcyclohex-3-en-1-yl) but-2-en-1-one	KET	23.155	47	1346	1340	0.010	± *0.01*	0.000	± *0.00*	****	ND	-	ND	-	ND
78	122-72-5is	3-phenylpropyl acetate (iso)	ACE	23.261	86	1364	1370	0.026	± *0.05*	0.043	± *0.06*	NS	ND	-	ND	-	ND
79	122-72-5	3-phenylpropyl acetate	ACE	23.356	78	1381	1382	0.032	± *0.06*	0.029	± *0.04*	NS	ND	-	ND	-	ND
80	**74367-34-3**	**(3-hydroxy-2,4,4-trimethylpentyl) 2-methylpropanoate**	NAE	23.369	66	1384	1381	0.021	± *0.02*	0.021	± *0.02*	NS	0.025	± *0.02*	0.029	± *0.02*	NS
81	**000629-59-4**	**Tetradecane**	AHA	23.382	73	1400	1400	0.037	± *0.02*	0.049	± *0.03*	NS	0.012	± *0.00*	0.022	± *0.01*	NS
82	000112-54-9	Dodecanal	ALD	23.525	68	1413	1414	0.007	± *0.01*	0.006	± *0.01*	NS	ND	-	ND	-	ND
83	475-20-7	(1*S*,3a*R*,4*S*,8a*S*)-decahydro-4,8,8-trimethyl-9-methylene-1,4-methanoazulene	OTH	23.649	45	1434	1430	0.002	± *0.00*	0.004	± *0.01*	NS	ND	-	ND	-	ND
84	003796-70-1	(5E)-6,10-dimethylundeca-5,9-dien-2-one	KET	23.781	60	1453	1463	0.022	± *0.01*	0.026	± *0.02*	NS	ND	-	ND	-	ND
85	**000719-22-2**	**2,6-Di-tert-butylbenzoquinone**	KET	23.948	57	1487	1485	0.003	± *0.00*	0.010	± *0.01*	NS	0.009	± *0.01*	0.007	± *0.00*	NS
86	000629-62-9	Pentadecane	AHA	24.013	73	1500	1500	0.013	± *0.01*	0.025	± *0.02*	NS	ND	-	ND	-	ND
87	014901-07-6	(E)-4-(2,6,6-trimethylcyclohexen-1-yl)but-3-en-2-one	KET	24.036	63	1506	1500	0.018	± *0.03*	0.004	± *0.01*	NS	ND	-	ND	-	ND
88	**000544-76-3**	**Hexadecane**	AHA	24.612	71	1601	1600	0.009	± *0.01*	0.008	± *0.01*	NS	0.002	± *0.00*	0.003	± 0.00	NS
89	NID11.3LRI942	Unidentified	NID	11.303	ND	943	ND	0.081	± *0.13*	0.029	± *0.02*	NS	ND	-	ND	-	ND
90	NID23.17LRI1350	Unidentified	NID	23.172	ND	1349	ND	0.024	± *0.07*	0.019	± *0.01*	NS	ND	-	ND	-	ND
91	71-23-8	Propan-1-ol	ALC	1.623	62	527	532	ND	-	ND	-	ND	0.000	± *0.00*	0.079	± *0.03*	**
92	107-83-5	2-Methylpentane	AHA	1.637	74	547	555	ND	-	ND	-	ND	0.000	± *0.00*	0.042	± *0.01*	****
93	78-93-3	2-Butanone	KET	1.821	80	601	602	ND	-	ND	-	ND	0.007	± *0.01*	0.027	± *0.00*	NS

(*continued on next page*)

Table 1 (*continued*)

IDN[a]	CAS[b] number	Volatile organic compound (IUPAC[c] name)	Compound class[d]	RT[e] (min)	MQ[f]	LRI[g]		Season 1				Season 2				
						Cal	ref	PS		SC10-2		p[h]	PS		SC10-2		p[h]
94	000589-34-4	Hexane, 3-methyl-	AHA	2.460	79	667	670	ND	-	ND	-	ND	0.020	± *0.03*	0.087	± *0.03*	NS
95	142-82-5	Heptane	AHA	2.779	73	700	700	ND	-	ND	-	ND	0.040	± *0.04*	0.174	± *0.03*	NS
96	001534-08-3	*S*-methyl ethanethioate	SDC	2.792	74	701	702	ND	-	ND	-	ND	0.053	± *0.05*	0.052	± *0.01*	NS
97	000105-37-3	Ethyl propanoate	NAE	3.016	83	711	714	ND	-	ND	-	ND	0.038	± *0.06*	0.091	± *0.03*	NS
98	000108-87-2	Methylcyclohexane	AHA	3.139	84	717	718	ND	-	ND	-	ND	0.020	± *0.03*	0.090	± *0.02*	NS
99	000123-51-3	3-methylbutan-1-ol	ALC	3.438	76	731	734	ND	-	ND	-	ND	0.012	± *0.01*	0.028	± *0.01*	NS
100	137-32-6	2-methylbutan-1-ol	ALC	3.503	78	733	736	ND	-	ND	-	ND	0.002	± *0.01*	0.015	± *0.00*	NS
101	589-81-1	3-methylheptane	AHA	4.203	62	765	767	ND	-	ND	-	ND	0.000	± *0.00*	0.119	± *0.04*	****
102	000123-86-4	Butyl acetate	ACE	5.537	74	815	815	ND	-	ND	-	ND	0.006	± *0.01*	0.042	± *0.01*	NS
103	106-42-3	1,4-dimethylbenzene	OTH	7.391	83	863	864	ND	-	ND	-	ND	0.002	± *0.00*	0.001	± *0.00*	NS
104	000526-73-8	1,2,3-trimethylbenzene	OTH	13.934	63	988	993	ND	-	ND	-	ND	0.005	± *0.01*	0.031	± *0.00*	NS
105	124-18-5	Decane	AHA	14.605	65	1002	1000	ND	-	ND	-	ND	0.003	± *0.00*	0.007	± *0.00*	*
106	000100-45-8	Cyclohex-3-ene-1-carbonitrile	OTH	15.576	79	1016	1015	ND	-	ND	-	ND	0.025	± *0.03*	0.100	± *0.02*	NS
107	62016-28-8	2,2,6-trimethyloctane	AHA	16.176	79	1026	1029	ND	-	ND	-	ND	0.002	± *0.00*	0.021	± *0.01*	NS
108	000138-86-3	1-methyl-4-prop-1-en-2-ylcyclohexene	OTH	16.208	77	1026	1027	ND	-	ND	-	ND	0.088	± *0.20*	0.040	± *0.02*	NS
109	000103-09-3	2-ethylhexyl acetate	ACE	21.610	74	1164	1159	ND	-	ND	-	ND	0.021	± *0.02*	0.067	± *0.01*	NS
110	93-89-0	Ethyl benzoate	NAE	21.806	61	1178	1180	ND	-	ND	-	ND	0.002	± *0.00*	0.008	± *0.00*	NS
111	000491-02-1	5-methyl-2-propan-2-ylcyclohexan-1-ol	ALC	21.835	58	1180	1182	ND	-	ND	-	ND	0.010	± *0.01*	0.030	± *0.01*	NS
112	95-16-9	1,3-benzothiazole	SDC	22.339	55	1229	1227	ND	-	ND	-	ND	0.000	± *0.00*	0.016	± *0.00*	****
113	054774-91-3	6-methylheptyl prop-2-enoate	NAE	22.383	57	1235	1235	ND	-	ND	-	ND	0.001	± *0.00*	0.002	± *0.00*	NS
114	120-50-3	2-methylpropyl benzoate	NAE	23.101	64	1337	1331	ND	-	ND	-	ND	0.001	± *0.00*	0.001	± *0.00*	NS
115	074367-33-2	(1-hydroxy-2,4,4-trimethylpentan-3-yl) 2-methylpropanoate	NAE	23.255	63	1366	1363	ND	-	ND	-	ND	0.006	± *0.01*	0.014	± *0.01*	NS
116	NID22.5LRI1247	Unidentified	NAE	22.475	51	1247	ND	ND	-	ND	-	ND	0.010	± *0.01*	0.017	± *0.01*	NS

[a] IDN: Identification number assigned for each volatile compound in the correlation plot of PLS-DA.
[b] CAS, chemical abstracts service.
[c] IUPAC, international union of pure and applied chemistry.
[d] Compound Classes: ACE, acetate esters; AHA, alkanes; ALC, alcohols; ALD, aldehydes; KET, ketones; NAE, non-acetate esters; NID, not identified; SDC, sulfur-derived compounds; OTH, other compound class.
[e] RT, retention time in minutes.
[f] MQ: Match quality (0–100 units) of spectra compared with those of the National Institute for Standards and Technology (NIST05a.L, search version 2.0) data bank.
[g] LRI: LRI calculated (mean of both seasons), linear retention indices calculated from the RT of a series of n-alkanes standards (C6–C20). LRI Ref., linear retention referenced (National Institute of Standards and Technology. NIST database. http://www.nist.gov/index.html) or AMDIS32. Absolute difference between both LRI (literature and calculated) should be below 7 units.
[h] The raw p values of the ANOVA were corrected for the multiple test using the Benjamini and Hochberg false discovery rate criterion. *, **, ***, ****: significance at $P \leq 0.05$, 0.01, 0.001 or 0.0001, respectively. NS (non-significant); ND (non-detected).

Table 2
Volatile organic compounds (VOCs) with significant introgression effect using the near-isogenic line (NIL) SC10-2 and the parental 'Piel de Sapo' (PS) at harvest. The corresponding volatile precursors and aromatic notes were included following the literature. The null-data of consistent variables were substituted with the minimum of each line/season, corresponding to the third methodology proposed in VOC data analysis.

IDN[a]	CAS[b] number	Volatile organic compound (IUPAC[c] name)	Compound class[d]	Volatile precursors[f]	Volatile precursors references[g]	Aromatic notes[h]
3	000064-17-5	Ethanol	ALC	FAs	Espino-Díaz et al., 2016	Strong alcoholic ethereal medical.
10	96-17-3	2-methylbutanal	ALD	AA, Iso	Gonda et al., 2010	Green, almond, strong burnt, malty, cocoa.
12	000616-25-1	Pent-1-en-3-ol	ALC	FAs	Juttner et al., 1983	Pungent horseradish green vegetable tropical fruity.
17	565-69-5	2-methylpentan-3-one	KET	TER, FAs	Juttner et al., 1983	Minty.
22	006728-26-3	(E)-hex-2-enal	ALD	AA	Gonda et al., 2010	Green banana aldehydic fatty cheesy.
24	000624-41-9	2-methylbutyl acetate	ACE	Fas, AA	Espino-Díaz et al., 2016	Fruit overripe fruit sweet banana juicy fruit fruity
29	000100-52-7	Benzaldehyde	ALD	Phe, Try, AA	Singh et al., 2003; Gonda et al., 2010; Van et al., 2009	Almond, Burnt sugar, woody, fruity, nutty.
36	000110-93-0	6-methylhept-5-en-2-one	KET	TER, FAs	Juttner et al., 1983	Fruity, apple, musty, ketonic, creamy with slight cheesy.
41	000104-76-7	2-ethylhexan-1-ol	ALC	FAs	Juttner et al., 1983	Citrus fresh floral oily sweet.
46	1120-21-4	Undecane	AHA	TER, FAs	Juttner et al., 1983	Gasoline-like to odorless.
47	4501-58-0	2-(2,2,3-trimethylcyclopent-3-en-1-yl)acetaldehyde	ALD	AA	Gonda et al., 2010	Herbal green woody amber leafy.
48	002277-19-2	(Z)-non-6-enal	ALD	FAs	Hong et al., 2011	Green cucumber and melon with a woody orris-type nuance.
49	000124-19-6	Nonanal	ALD	Iso	Pang et al., 2012	Waxy aldehydic rose fresh orris orange peel fatty peely.
50	NID20.9LRI1114	Unidentified	-	-	-	Leather red rose green dusty weedy metallic.
53	**000464-49-3**	**1,7,7-trimethylbicyclo[2.2.1]heptan-2-one**	KET	AA	Gonda et al., 2010	Camphor minty phenolic herbal woody
55	057283-79-1	(E)-5-ethyl-6-methylhept-3-en-2-one	KET	AA	Chaparro-Torres et al., 2016	N/A literature.
57	010340-23-5	(Z)-non-3-en-1-ol	ALC	FAs	Lingwood et al., 2010	Fresh waxy green melon rind tropical mushroom.
62	91-20-3	Naphthalene	OTH	TER	Negri et al., 2015	Mothball, Medicinal, Pungent, dry, tarry.
68	NID22.26LRI1219	Unidentified	-	-	-	Almond-like.
71	000501-92-8	4-prop-2-enylphenol	ALC	FAs	Lingwood et al., 2010	Phenolic medicinal.
72	000103-45-7	2-phenylethyl acetate	ACE	Iso	Gonda et al., 2010	Fruity, Rose, floral, sweet.
76	000112-44-7	Undecanal	ALD	FAs	Hong et al., 2011	Floral, waxy, citrus odor
77	41436-42-4	(E)-1-(2,6,6-trimethylcyclohex-3-en-1-yl)but-2-en-1-one	KET	AA	Gonda et al., 2010	Floral, rose, apple fruityt, black currant aroma.
91	71-23-8	Propan-1-ol	ALC	FAs	Atsumi et al., 2008	Alcoholic fermented fusel musty.
92	107-83-5	2-Methylpentane	AHA	FAs	Sanz et al., 1997	N/A literature.
101	589-81-1	3-methylheptane	AHA	FAs	Sanz et al., 1997	Odor resembling hexane.
105	124-18-5	Decane	AHA	FAs	Kunst et al., 2006	Colorless liquid with gasoline-like odor.
112	95-16-9	1,3-benzothiazole	SDC	Met, AA	Gonda et al., 2010	Gasoline, rubber.

[a]IDN: Identification number assigned for each volatile compound in the correlation plot of PLS-DA.
[b]CAS, chemical abstracts service.
[c]IUPAC, international union of pure and applied chemistry.
[d]Compound Classes: ACE, acetate esters; AHA, alkanes; ALC, alcohols; ALD, aldehydes; KET, ketones; NAE, non-acetate esters; NID, not identified; SDC, sulfur-derived compounds; OTH, other compound class.
[e]RT, retention time in minutes.
[f]LRI: LRI cal., linear retention indices calculated from the RT of a series of n-alkanes standards (C6–C20). LRI Ref., linear retention referenced (National Institute of Standards and Technology. NIST website database. (http://www.nist.gov/index.html) or scientific literature.
[g]Volatile precursors: AA, amino acid; Iso, L-isoleucine; FAs, fatty acids; TER, terpenes; Phe, L-phenylalanine; Try, L-tryptophan; Met, L-methionine.
[h]http://www.thegoodscentscompany.com.

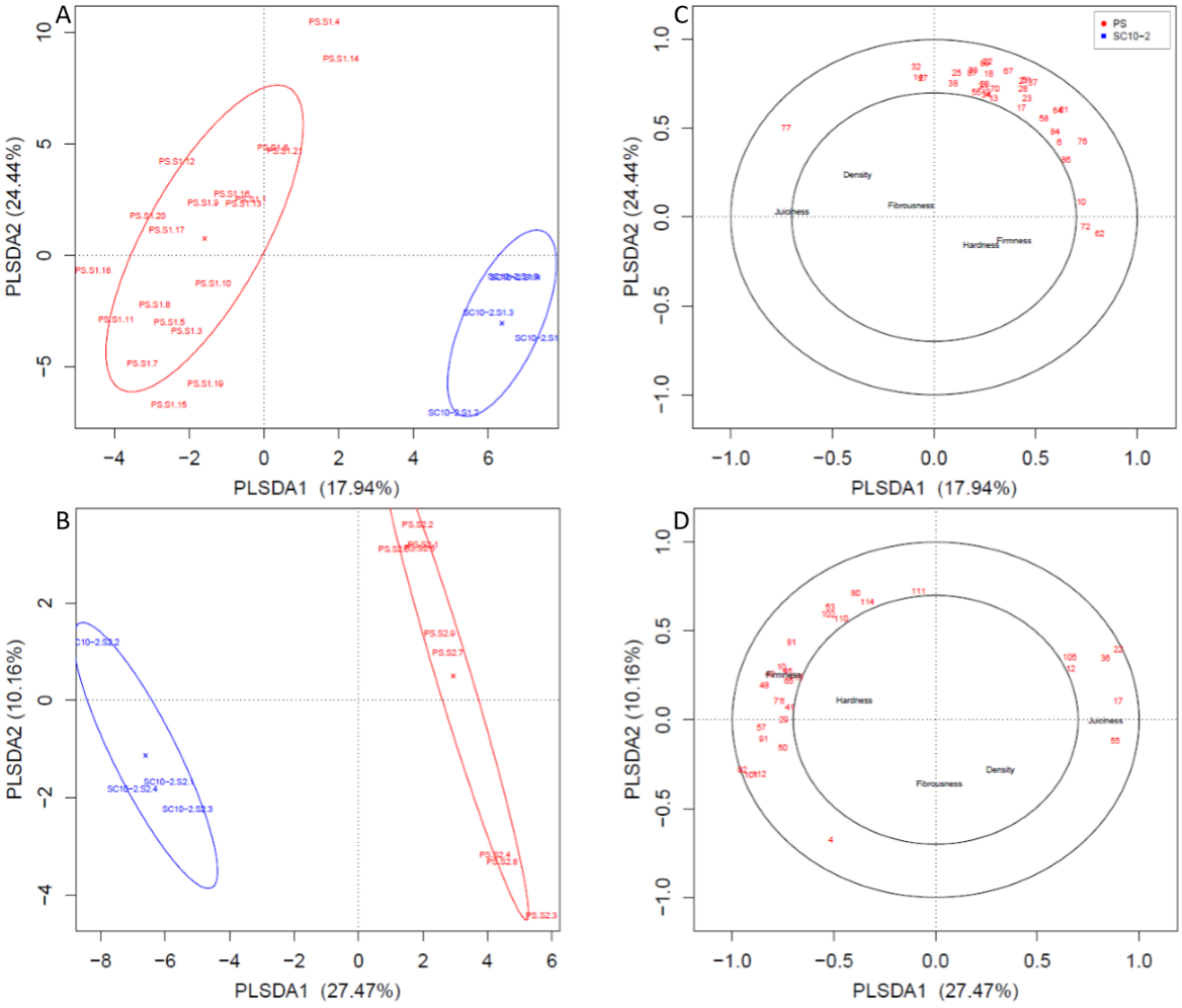

Figure 2. Discrimination between the melon near-isogenic line (NIL) SC10-2 and the parental 'Piel de Sapo' (PS) line according to individual flesh volatile organic compounds at harvest in two seasons (S1 and S2) according to Partial Least Squares-Discriminant Analysis (PLS-DA). A and B (S1 and S2, respectively): Datasets and the corresponding centroids (x) for the different lines and 65% confidence ellipses. C and D (S1 and S2, respectively): Correlations between the individual volatile compounds, the textural traits and the first two components. The numbers in the graph on the right correspond to the compounds with 50% or more of the variance explained by the two components according to the PLS-DA and numbered according to Table 1.

The PS non-climacteric NIL differences in melon fruit textural traits (see above; Tables 5-6) depended on the genotype, but, in contrast with other studies on climacteric NILs (Chaparro-Torres et al., 2016), showed a lower dependency on the season (Aurand et al., 2012; Sams, 1999). However, qualitative and, to a lesser extent, quantitative seasonal differences were particularly noticeable compared with the genotype studied here (Tables 1 and 2). The differences in textural traits might be associated with differences in the cell wall composition between SC10-2 and PS (Gomes et al., 2010), as also revealed in the comparison of other non-climacteric NILs, such as SC7-2 (also with firm texture) vs. PS (Dos-Santos et al., 2011). The textural effect associated with the quantitative trait locus (QTL) *ff10.2* is located in SC10-2 (Moreno et al., 2008; Obando et al., 2008) and is very consistent (Dos-Santos et al., 2013). This QTL has also been mapped in other populations (Perpiñá et al., 2016).

4.2 Methodology of the null zero analysis of VOCs:

Importantly, the first two methodologies proposed to address the null values of VOC variables produced similar results. The second method was proposed by Chaparro-Torres et al. (2016) to compare climacteric NILs and PS, while we compared a non-climacteric NIL with PS (Supplementary Table 2 (Annex B)). The literature rarely provides a detailed analysis of the different possibilities of treating null data for VOC variables. In fact, some authors only quantified the peaks with a minimum signal to noise ratio of five (Verzera et al., 2011) or three (Kende et al., 2019). Another option is simply to select VOC variables without null data, which limits the number of VOCs for analysis (Allwood et al., 2014; Güler, et al., 2013). When the aromatic differences between melon lines are high (i.e., climacteric vs. non-climacteric lines), a consideration of one or the other would be irrelevant (Chaparro-Torres et al., 2016). However, the levels of VOCs in non-climacteric melons are close to their detectable limits in some cases, according to some methodologies, and other factors, such as physiological maturity, fruit sampling, slight damage, a juice matrix effect, etc., potentially produce substantial differences in the VOC profile (Burzynski-Chang et al., 2018; Dos-Santos et al., 2013; Fernández-Trujillo et al., 2018).

Table 3. Discriminant volatile organic compounds (VOCs) identified in 'Piel de Sapo' (PS) (n=20) and the near-isogenic line (NIL) SC10-2 (n=5) identified at harvest in season 1 after multivariate analysis according to PLS-DA and Random Forest (RF). VOCs marked in bold were discriminant in both seasons according to PLS-DA.

IDN[a]	CAS[b] number	Volatile organic compound (IUPAC[c] name)	Compound class[d]	Order RF[e]	
				MDA	MDG
6	534-22-5	2-methylfuran	OTH	18	-
10	**96-17-3**	**2-methylbutanal**	ALD	-	9
13	001629-58-9	Pent-1-en-3-one	KET	-	-
14	000110-62-3	Pentanal	ALD	29	-
17	**565-69-5**	**2-methylpentan-3-one**	KET	-	-
18	**001576-87-0**	**(E)-pent-2-enal**	ALD	-	-
19	000071-41-0	Pentan-1-ol	ALC	-	-
20	000066-25-1	Hexanal	ALD	-	-
21	006137-03-7	3-ethylpentan-2-one	KET	-	-
22	006728-26-3	(E)-hex-2-enal	ALD	-	-
23	000111-27-3	Hexan-1-ol	ALC	-	-
25	004466-24-4	2-butylfuran	OTH	-	-
27	000111-71-7	Heptanal	ALD	-	-
28	018829-55-5	(E)-hept-2-enal	ALD	-	-
31	111-70-6	Heptan-1-ol	ALC	25	-
32	004312-99-6	Oct-1-en-3-one	KET	-	15
33	003391-86-4	Oct-1-en-3-ol	ALC	-	-
34	000585-25-1	Octane-2,5-dione	KET	-	-
37	003777-69-3	2-pentylfuran	OTH	-	-
51	3901-95-9	1-methyl-4-propan-2-ylcyclohexan-1-ol	ALC	-	-
55	**057283-79-1**	**(E)-5-ethyl-6-methylhept-3-en-2-one**	KET	-	-
58	056805-23-3	(3Z,6Z)-nona-3,6-dien-1-ol	ALC	-	-
61	000143-08-8	Nonan-1-ol	ALC	16	-
62	91-20-3	Naphthalene	OTH	2	2
64	17920-92-2	4,8-dimethylnona-1,7-dien-4-ol	ALC	-	-
67	5910-87-2	(2E,4E)-nona-2,4-dienal	ALD	-	-
70	000432-25-7	2,6,6-trimethylcyclohexene-1-carbaldehyde 4	ALD	-	-
72	000103-45-7	2-phenylethyl acetate	ACE	9	3
76	000112-44-7	Undecanal	ALD	4	7
77	41436-42-4	(E)-1-(2,6,6-trimethylcyclohex-3-en-1-yl)but-2-en-1-one	KET	1	1
84	003796-70-1	(5E)-6,10-dimethylundeca-5,9-dien-2-one	KET	-	-
86	000629-62-9	Pentadecane	AHA	-	17
87	014901-07-6	(E)-4-(2,6,6-trimethylcyclohexen-1-yl)but-3-en-2-one	KET	19	-
89	NID11.3LRI942	Unidentified	NID	-	-

[a] IDN: Identification number assigned for each volatile compound in the correlation plot of PLS-DA.

[b] CAS, chemical abstracts service.

[c] IUPAC, international union of pure and applied chemistry.

[d] Compound Classes: ACE, acetate esters; AHA, alkanes; ALC, alcohols; ALD, aldehydes; KET, ketones; NAE, non-acetate esters; NID, not identified; SDC, sulfur-derived compounds; OTH, other compound class.

[e] Order of the main volatile compounds according to Random Forest (RF) analysis. MDA, Mean Decrease Accuracy. MDG, Mean Decrease Gini. Compounds with dash (-) means that they are not represented in the RF diagram (Fig. 3).

4.3 VOC profile and seasonal/introgression effects: pathways associated with VOCs and putative precursors:

Twenty-eight of the VOCs identified here were implicated in differences in aroma production due to the introgression in both seasons. Seven VOCs exerted a positive effect on the VOC content when NIL SC10-2 was compared with PS, and the others (twenty-one) exerted negative effects compared with PS (Table 2). The lack of complete agreement between the VOCs identified or associated with the introgression in previous studies (Dos-Santos et al., 2013) was partially due to the strong seasonal effect, and the difficulties in growing many replicates of SC10-2 (which is sometimes very susceptible to diseases in the nursery and in the field), which reduced the number of plot replicates available.

The compounds associated with the introgression effect on the aroma profile were VOCs typical of other types of non-climacteric melons (Perry et al., 2009; Verzera et al., 2011 and 2014) and were consistent with the VOCs identified in previous studies (Dos-Santos et al., 2013; Obando-Ulloa et al., 2008 and 2010). The compounds included aldehydes (2-methylbutanal, (E)-hex-2-enal, benzaldehyde, 2-(2,2,3-trimethylcyclopent-3-en-1-yl)acetaldehyde, (Z)-non-6-enal, nonanal and unidentified aldehyde NID22.26LRI1219), alcohols (ethanol, pent-1-en-3-ol, 2-ethylhexan-1-ol, unidentified alcohol NID20.9LRI1114, (Z)-non-3-en-1-ol, 4-prop-2-enylphenol and propan-1-ol), ketones (2-methylpentan-3-one, 6-methylhept-5-en-2-one, (E)-5-ethyl-6-methylhept-3-en-2-one and (E)-1-(2,6,6-trimethylcyclohex-3-en-1-yl)but-2-en-1-one), and alkanes (undecane, 2-methylpentane, 3-methylheptane and decane). We even detected an acetate ester compound (2-phenylethyl acetate), a sulfur-derived compound (1,3-benzothiazole) and naphthalene from other compound classes. The identified compounds were generally derived from amino acids (isoleucine, phenylalanine, tryptophan and methionine), fatty acids, and terpenes (Table 2). Overall, the precursors of most of the compounds reported here (Table 2), namely, amino acids such as L-leucine, L-isoleucine and L-valine, generally increased the levels of alcohols and their derivatives, as well as some aldehydes and sulfur-derived compounds (Gonda et al., 2010). These amino acids may also serve as the precursors for some esters (Table 2). The precursor of some sulfur-derived compounds may be L-methionine (Gonda et al., 2010). L-isoleucine is another potential precursor of VOCs such as 2-phenylethyl acetate or 2-ethylhexan-1-ol (Table 1).

The discrimination between the NIL SC10-2 and the parental PS line obtained from the multivariate analysis of VOCs at harvest was more noticeable in S2 (with its better weather) than in S1 (Figures. 2 and 3 and Supplementary Figures. 2, 3 and 4 (Annex B)), even after a detailed integration using AMDIS32. This result may have practical implications, because the production will be more difficult to split into classes in seasons not suited to growing melons of quality, particularly from an aromatic perspective. Another practical application of this result is the possibility of grafting with different rootstocks (Condurso et al., 2012; Verzera et al., 2014) that would contribute to controlling diseases but also mitigate seasonal variability, particularly in areas with climatological risks.

Table 4. Discriminant volatile organic compounds (VOCs) identified in 'Piel de Sapo' (PS) (n= 9) of the near-isogenic line (NIL) SC10-2 (n = 4) identified at harvest in season 2 after multivariate analysis according to PLS-DA and Random Forest (RF). VOCs marked in bold were discriminant in both seasons according to PLS-DA.

IDN[a]	CAS[b] number	Volatile organic compound (IUPAC[c] name)	Compound class[d]	Order RF[e]	
				MDA	MDG
1	000075-07-0	Acetaldehyde	ALD	-	-
4	000123-72-8	Butanal	ALD	19	-
10	**96-17-3**	**2-methylbutanal**	ALD	18	28
12	000616-25-1	Pent-1-en-3-ol	ALC	27	13
17	**565-69-5**	**2-methylpentan-3-one**	KET	7	7
22	**006728-26-3**	**(E)-hex-2-enal**	ALD	2	1
29	000100-52-7	Benzaldehyde	ALD	16	15
36	000110-93-0	6-methylhept-5-en-2-one	KET	3	5
41	000104-76-7	2-ethylhexan-1-ol	ALC	22	14
45	000617-94-7	2-phenylpropan-2-ol	ALC	-	19
48	002277-19-2	(Z)-non-6-enal	ALD	23	19
49	000124-19-6	Nonanal	ALD	10	9
50	NID20.9LRI1114	Unidentified	NID	12	8
53	000464-49-3	1,7,7-trimethylbicyclo[2.2.1]heptan-2-one	KET	-	-
55	**NID21.5LRI1158**	**Unidentified**	NID	1	2
57	010340-23-5	(Z)-non-3-en-1-ol	ALC	8	10
65	000112-40-3	Dodecane	AHA	13	12
71	000501-92-8	4-prop-2-enylphenol	ALC	-	-
80	74367-34-3	(3-hydroxy-2,4,4-trimethylpentyl) 2-methylpropanoate	NAE	-	-
81	000629-59-4	Tetradecane	AHA	-	25
91	71-23-8	Propan-1-ol	ALC	6	4
92	107-83-5	2-Methylpentane	AHA	9	11
101	589-81-1	3-methylheptane	AHA	5	6
102	000123-86-4	Butyl acetate	ACE	-	-
105	124-18-5	Decane	AHA	24	24
110	93-89-0	Ethyl benzoate	NAE	29	-
111	000491-02-1	5-methyl-2-propan-2-ylcyclohexan-1-ol	ALC	-	-
112	95-16-9	1,3-benzothiazole	SDC	4	3
114	120-50-3	2-methylpropyl benzoate	NAE	-	-
115	074367-33-2	(1-hydroxy-2,4,4-trimethylpentan-3-yl) 2-methylpropanoate	NAE	-	-

[a] IDN: Identification number assigned for each volatile compound in the correlation plot of PLS-DA.

[b] CAS, chemical abstracts service.

[c] IUPAC, international union of pure and applied chemistry.

[d] Compound Classes: ACE, acetate esters; AHA, alkanes; ALC, alcohols; ALD, aldehydes; KET, ketones; NAE, non-acetate esters; NID, not identified; SDC, sulfur-derived compounds; OTH, other

[e] Order of the main volatile compounds according to Random Forest (RF) analysis. MDA, Mean Decrease Accuracy. MDG, Mean Decrease Gini. Compounds with dash (-) means that they are not represented in the RF diagram (Fig. 3).

Table 5. Pearson's correlation coefficients between textural traits and volatile organic compounds (VOCs) in season 1 at harvest in near-isogenic lines (NILs) SC10-2 (n=5) of melon and the parental line 'Piel de Sapo' (PS) (n=20). Only significant correlations ($p<0.05$) are shown. VOCs in bold were detected in both seasons.

IDN[a]	CAS[b] number	Volatile organic compound (IUPAC[c] name)	Density	Juiciness	Firmness	Hardness	Fibrousness
6	534-22-5	2-methylfuran		-0,49			
7	**000141-78-6**	**Ethyl acetate**			-0,39		
8	000109-99-9	Oxolane			0,43	0,64	
9	123-73-9	(E)-but-2-enal		-0,45			
10	**96-17-3**	**2-methylbutanal**	-0,43		0,42		
16	000624-92-0	Methyldisulfanylmethane				-0,41	
26	6728-31-0	Hept-4-enal	-0,4				
29	**000100-52-7**	**Benzaldehyde**		-0,61	0,41		
30	**003658-80-8**	**Methylsulfanyldisulfanylmethane**			-0,52		
35	106-68-3	5-methylheptan-3-one		-0,38			
42	001193-81-3	(2-methylcyclohexyl)methanol					-0,49
44	000111-87-5	Octan-1-ol					-0,41
46	**1120-21-4**	**Undecane**			0,45		
53	**000464-49-3**	**1,7,7-trimethylbicyclo[2.2.1]heptan-2-one**	-0,39				
56	17587-33-6	(2E,6E)-nona-2,6-dienal	-0,47	-0,45			
57	**010340-23-5**	**(Z)-non-3-en-1-ol**		-0,54			
60	000140-11-4	Phenylmethyl acetate		-0,63			
62	91-20-3	Naphthalene		-0,56			
63	**000098-19-1**	**1-tert-butyl-3,5-dimethylbenzene**	-0,52				
65	**000112-40-3**	**Dodecane**		-0,54			
68	NID22.26LRI1219	Unidentified	-0,57	-0,43			
72	000103-45-7	2-phenylethyl acetate		-0,62			
74	000629-50-5	Tridecane					0,45
75	71186-24-8	6Z)-6-[(E)-but-2-enylidene]-1,5,5-trimethylcyclohexene				-0,39	
76	000112-44-7	Undecanal		-0,54		0,41	
77	41436-42-4	(E)-1-(2,6,6-trimethylcyclohex-3-en-1-yl)but-2-en-1-one	0,54	0,52	-0,52		
78	122-72-5is	3-phenylpropyl acetate (iso)	-0,4		0,43		
81	**000629-59-4**	**Tetradecane**		-0,49			
82	000112-54-9	Dodecanal		-0,45			
85	**000719-22-2**	**2,6-Di-tert-butylbenzoquinone**		-0,38			
86	000629-62-9	Pentadecane		-0,43			
88	000544-76-3	Hexadecane					0,43

[a] IDN: Identification number assigned for each volatile compound in the correlation plot of PLS-DA.

[b] CAS, chemical abstracts service.

[c] IUPAC, international union of pure and applied chemistry.

The PLS-DA result agrees with results of the ANOVA and most of the RF analysis. Thirty-four aroma volatile compounds in S1 (Table 3 and Figure 2C) and thirty in S2 (Table 4, Figure 2D) helped discriminate the NIL SC10-2 from PS at harvest, and four of these compounds (2-methylbutanal, 2-methylpentan-3-one, (E)-pent-2-enal, and (E)-5-ethyl-6-methylhept-3-en-2-one) were detected in both seasons (S1 and S2), as reported in other studies on melon aroma (Dos-Santos et al., 2013) and on fruit aroma in general (Polster and Schieberle, 2017). The PLS-DA showed better discrimination between the NIL SC10-2 and PS than the RF

analysis, as has been proposed in a study using a smaller number of input variables (Obando-Ulloa et al., 2008). The RF analysis exhibits better discrimination than PLS-DA for other melon quality traits, including sensory traits at harvest (Fernández-Trujillo et al., 2009; Obando-Ulloa et al., 2009b).

A correlation network analysis (CNA) has been used in previous studies to group VOCs, to associate the resulting components with VOC biosynthetic pathways, and to study the biosynthetic pathways of fruit aroma in fruit such as melons and peaches (Moing et al., 2011). In our experiment, three components were detected in S1 using the CNA (Figure 4 and S1) and eleven were detected in S2 (Figure 4 and S2), with high correlations observed in S2 (Figure 4 and S1). Most of these compounds were aldehydes and alcohols, followed by ketones and compounds from other compound classes (Table 1), which were derived from different metabolic pathways, including fatty acids, amino acids and terpenes (Table 2).

Table 6. Pearson's correlation coefficients among textural traits and volatile organic compounds (VOCs) in season 2 at harvest in near-isogenic lines (NIL) SC10-2 (n = 4) of melon and the parental line 'Piel de Sapo' (PS) (n = 9). Only significant correlations ($p<0.05$) are shown. VOCs marked in bold were detected in both seasons.

IDN[a]	CAS[b] number	Volatile organic compound (IUPAC[c] name)	Density	Juiciness	Firmness	Hardness	Fibrousness
7	**000141-78-6**	**Ethyl acetate**	0,56				0,58
10	**96-17-3**	**2-methylbutanal**		-0,81	0,71		
12	000616-25-1	Pent-1-en-3-ol		0,59			
13	001629-58-9	Pent-1-en-3-one			0,58		
14	000110-62-3	Pentanal			0,66		
17	565-69-5	2-methylpentan-3-one		0,61			
18	001576-87-0	(E)-pent-2-enal		-0,57	0,62	0,78	
22	006728-26-3	(E)-hex-2-enal		0,71			
27	000111-71-7	Heptanal			0,57	0,64	
29	**000100-52-7**	**Benzaldehyde**		-0,81	0,65	0,64	
30	**003658-80-8**	**Methylsulfanyldisulfanylmethane**					-0,63
36	000110-93-0	6-methylhept-5-en-2-one		0,66			
39	000124-13-0	Octanal			0,59		
41	000104-76-7	2-ethylhexan-1-ol		-0,84	0,86	0,57	
43	000098-86-2	1-phenylethanone			0,77	0,45	
45	000617-94-7	2-phenylpropan-2-ol		-0,86	0,8		
46	**1120-21-4**	**Undecane**		-0,62			
48	002277-19-2	(Z)-non-6-enal			0,64		
49	000124-19-6	Nonanal	-0,57	-0,74	0,88	0,65	
50	NID20.9LRI1114	Unidentified		-0,84	0,75		
52	577-16-2	1-(2-methylphenyl)ethanone		-0,58	0,62		
53	**000464-49-3**	**1,7,7-trimethylbicyclo[2.2.1]heptan-2-one**		-0,62	0,7		
55	057283-79-1	(E)-5-ethyl-6-methylhept-3-en-2-one		0,57	-0,58		
57	**010340-23-5**	**(Z)-non-3-en-1-ol**		-0,7			
61	000143-08-8	Nonan-1-ol					-0,65
63	**000098-19-1**	**1-tert-butyl-3,5-dimethylbenzene**		-0,59			
65	**000112-40-3**	**Dodecane**		-0,77	0,87		
66	000112-31-2	Decanal			0,62	0,79	
71	000501-92-8	4-prop-2-enylphenol		-0,77	0,71		
81	**000629-59-4**	**Tetradecane**		-0,67	0,59		
85	**000719-22-2**	**2,6-Di-tert-butylbenzoquinone**				0,62	
91	71-23-8	Propan-1-ol		-0,74			
92	107-83-5	2-Methylpentane		-0,81	0,65		
93	78-93-3	2-Butanone			0,66		
96	001534-08-3	S-methyl ethanethioate				-0,61	
101	589-81-1	3-methylheptane		-0,78	0,64		
102	000123-86-4	Butyl acetate			0,56		
105	124-18-5	Decane		0,58			
112	95-16-9	1,3-benzothiazole		-0,73	0,64		
113	054774-91-3	6-methylheptyl prop-2-enoate		0,62		-0,57	
114	120-50-3	2-methylpropyl benzoate	-0,7				

[a] IDN: Identification number assigned for each volatile compound in the correlation plot of PLS-DA.

[b] CAS, chemical abstracts service.

[c] IUPAC, international union of pure and applied chemistry.

The introgression negatively affected 2-methylbutanal levels (Tables 1 and 2), a VOC whose putative precursor L-isoleucine increased its levels, similar to the effects of another amino acid (L-methionine) on butan-1-ol, 2-methylbutan-1-ol, nonanal and 1,3-benzothiazole levels (Gonda et al., 2010; Singh et al., 2003). Additionally, the application of exogenous L-

isoleucine into strawberry peduncles increased the levels of the structurally similar 2-methylbutyl volatile derivatives in fruits, and deuterated L-isoleucine was converted into the corresponding 2-methylbutyl volatile derivatives in apples (Rowan et al., 1996; Matich and Rowan, 2007), which probably explains the presence of some compounds, such as 2-methylbutanal, in PS in both seasons.

Benzaldehyde levels were also negatively affected by the introgression in LG X (Table 1), consistent with previous results obtained in a single season (Obando-Ulloa et al., 2010), which might exert a negative effect on the pleasant melon flavour because it is associated with a higher degree of melon ripening (Beaulieu, 2006; Beaulieu and Grimm, 2001). The application of exogenous L-phenylalanine increases the levels of benzaldehyde (Gonda et al., 2010). Benzaldehyde also serves as a precursor of some of the aroma volatiles produced (Boatright et al., 2004).

The differences in VOCs caused by the introgression may be related to the amino acid metabolism pathways. The amino acids phenylalanine, isoleucine, valine and leucine are considered aroma precursors in free L-amino acid metabolism (Gonda et al., 2010; Qi et al., 2012; Smit et al., 2009). The L-amino acid L-phenylalanine and fatty acids are the important metabolic precursors of the VOCs that discriminate the introgression, such as aldehydes and alcohols (Table 2). The conversion of aldehydes into alcohols and the subsequent conversion into esters potentially explain the difference in the aldehyde content between PS and the NIL SC10-2, as has been observed in other cultivars (Mahmuda and Ueda, 2008).

The ketone 6-methylhept-5-en-2-one, whose presence correlates with a high beta-carotene content (Galpaz et al., 2013), was also negatively affected by the introgression. The ketone apparently is derived from the oxidative cleavage of open-chain carotenes (Galpaz et al., 2013). The α,β-unsaturated ketone mesityl oxide, which was also negatively affected by the introgression, might also have the same carotenoid origin (Juttner et al., 1983).

The VOCs associated with introgression were also linked to the aroma pathways of distinctive melon aromas, such as sulfur-containing VOCs that have L-methionine as the precursor (Gonda et al., 2013). The aforementioned pathway may involve the enzymatic degradation of the amino acid cysteine from methionine, producing methanethiol, and the subsequent production of sulfur-derived compounds, such as S-methyl ethanethioate (Gonda et al., 2013).

The introgression also showed higher levels other compounds, such as naphthalene, than PS (Table 2). Some of its derivatives, such as 1-naphthaleneacetic acid, are used as plant growth regulators to increase yield and fruit quality in climacteric and non-climacteric fruit (Hairdry et al., 1997; El-Shewy, 1999; Iqbal et al., 2009). Some authors have claimed that hydrocarbons with a ring structure, such as naphthalene, potentially arise from the degradation of β-carotene (Irigoyen et al., 2007; Baron et al., 2007). Naphthalene was also detected in the aroma profile of the NIL collection (Obando-Ulloa et al., 2010) and the climacteric NIL SC3-5-1 (also containing the introgression of SC, but is classified into linkage groups III and VI; Ríos et al., 2017) at harvest using polydimethylsiloxane stir bar absorption (Fernández-Trujillo et al., 2013).

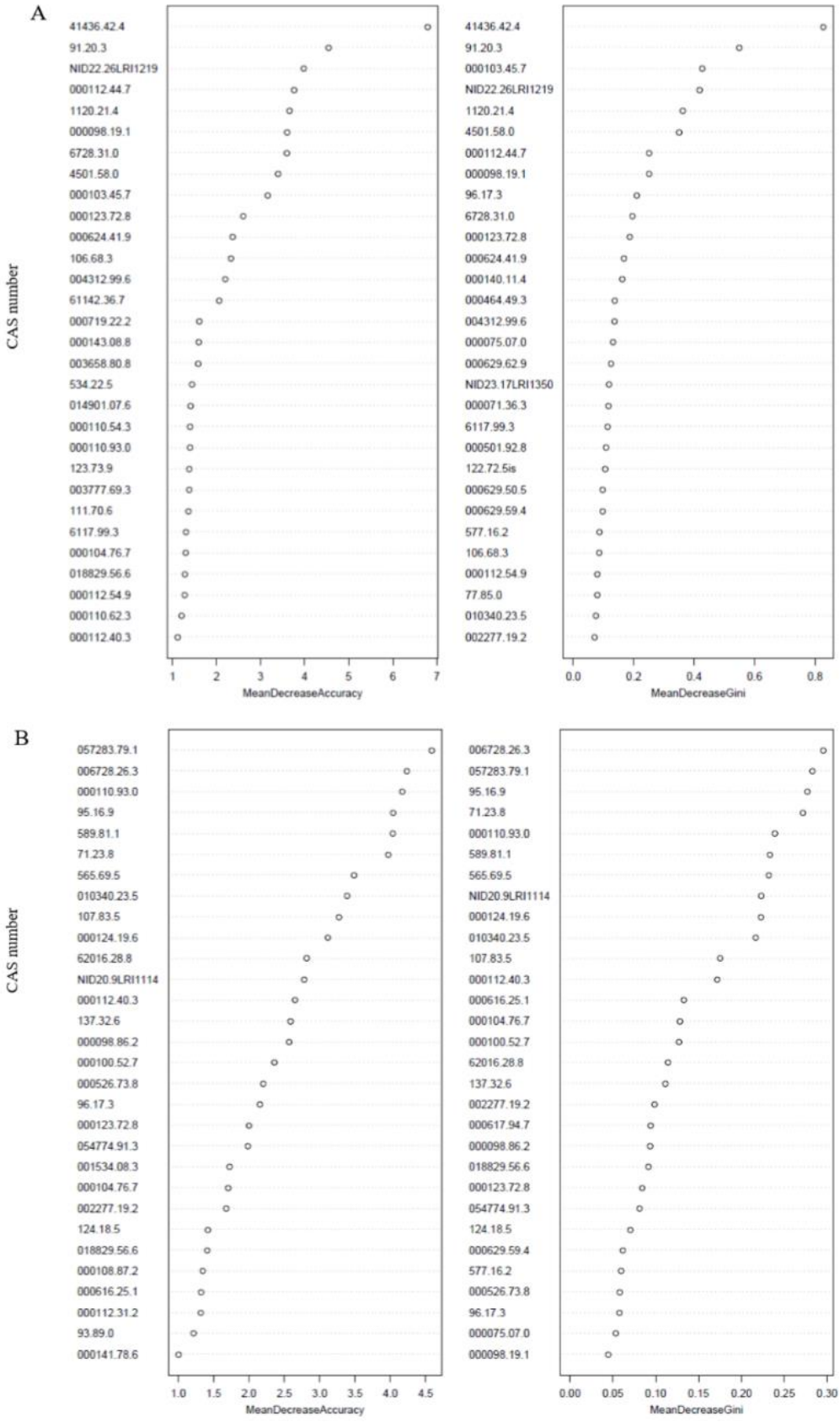

Figure 3. Random Forest (RF) applied for classification of flesh volatile organic compounds of the near-isogenic line (NIL) SC10-2 (n=5 and 4, for S1 and S2, respectively) and the parental Piel de Sapo' (PS) line (n=20 and 9, for S1 and S2, respectively). The importance of the compounds for the classification is based on the Mean Decrease in Accuracy and Mean Decrease in the Gini index. (A) Season 1, S1. (B) Season 2, S2.

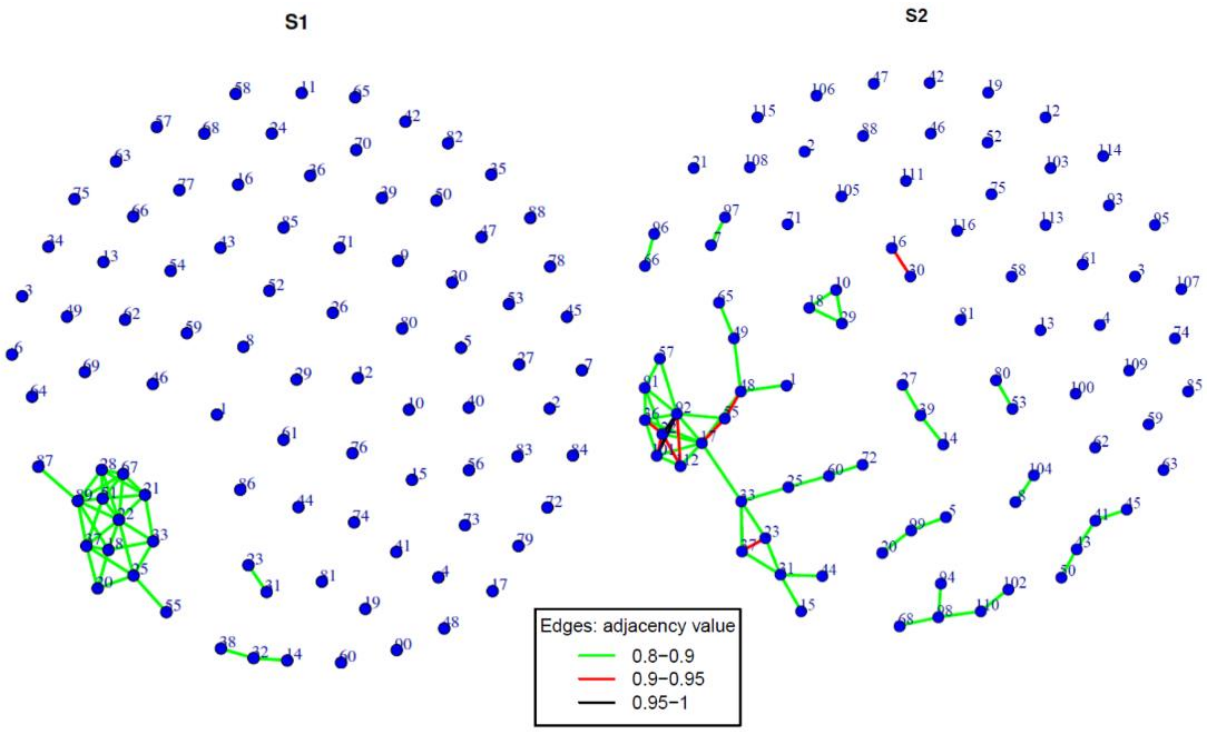

Figure 4. Correlation network analysis (CNA) based on Pearson coefficient with adjacency defined by cut-off absolute value greater than 0.8. Clusters identified from flesh volatile organic compounds of the near-isogenic line (NIL) SC10-2 and the parental 'Piel de Sapo' (PS) line at harvest in season 1 (S1) and season 2 (S2). The numbers in the graphs correspond to the number assigned for each volatile compound according to Table 1.

4.4 Link between aroma and textural traits at harvest:

Compared with other studies (Causse et al., 2002) in which the correlation between texture and aroma has generally been reported to be low and not modelled, in our experiment (and even with limited number of replicates of SC10-2), a higher correlation was observed between flesh texture (firmness and hardness) and the VOCs identified (Tables 5 and 6). Apparently, some associations between textural traits and VOCs remains, regardless of the season. The NIL SC10-2 had a higher firmness and higher hardness, along with other textural properties that showed correlations among flesh firmness and VOCs (Tables 5-6). Because the VOC concentrations were potentially modified in the headspace because of the differences in the juice matrix (Bezman et al., 2003), the VOC measurements may have been confounded by a matrix effect (Dos-Santos et al., 2013). Additionally, all eleven compounds identified in both seasons (S1 and S2) exhibited negative correlations with juiciness (Tables 5-6). The negative correlations (a juicy melon is preferred, as is a pleasant aroma) indicate certain problems in non-climacteric ripening. A juicy melon (more ripe) will display a reduced benzaldehyde content. An optimal relation should exist between juiciness and benzaldehyde aroma. Some lower correlations were detected, but only in S1 (Table 5).

Some aldehydes, such as 2-methylbutanal, benzaldehyde, pentanal, (E)-pent-2-enal, heptanal, (Z)-non-6-enal, and nonanal (Tables 5-6), were also linked to the introgression effect (Tables 3-4) due to their association with flesh firmness, consistent with previous results (Dos-Santos et al., 2013). Some of these C9 aldehydes are also present at relatively high concentrations in other cucurbits where flesh firmness is very important, such as the watermelon

(Dima et al., 2014). In honeydew melon, C9 aliphatic aldehydes are key aroma and flavour descriptors (Kyriacou et al., 2018). In another previous study (Dos-Santos et al., 2013), the higher flesh firmness of the NIL SC10-2 was mainly associated with volatiles linked to pathways whose putative precursors are L-amino acids (such as 2-methylbutanal, (E)-hex-2-enal, benzaldehyde, NID22.26LRI1219, (E)-5-ethyl-6-methylhept-3-en-2-one, 2-(2,2,3-trimethylcyclopent-3-en-1-yl)acetaldehyde and (E)-1-(2,6,6-trimethylcyclohex-3-en-1-yl)but-2-en-1-one in our experiment), or fatty acids (ethanol, pent-1-en-3-ol, 2-methylpentan-3-one, 6-methylhept-5-en-2-one, undecane, (Z)-non-6-enal, (Z)-non-3-en-1-ol, 4-prop-2-enylphenol, propan-1-ol, 2-methylpentane, 3-methylheptane and decane in our experiment). The VOC 2-methylbutanal is considered a key flavour compound in many fruits (Smit et al., 2009), as well as in melon (Gonda et al., 2010). 2-Methylbutanal is obtained from the sequential conversion of L-isoleucine into the branched-chain alcohol 2-methylbutanol and its corresponding ester butanol-2-methyl acetate, a typical acetic ester present in climacteric melon fruits (Gonda et al., 2010; Pang et al., 2012; Qi et al., 2012).

4.5 Importance in the field:

The effect of the season on non-climacteric melon aroma reinforces the need for the adequate selection of open field locations or greenhouse environments for the growth of non-climacteric melons due to the effects on aroma volatiles. The textural traits of the introgression of NIL SC10-2, particularly flesh firmness and juiciness, are also commercially important. Firmness correlates positively with cell density in watermelon (Soteriou et al., 2019), and this density and juiciness might exert a noticeable effect on the quality-oriented breeding of new breeding lines of cucurbits (Fernández-Trujillo et al., 2012). The presence of genes involved in fruit ripening (including textural traits) in LG X has been confirmed by several authors (Moreno et al., 2008; Perpiñá et al., 2016 and 2017). Therefore, the NIL SC10-2 or subNILs with a shorter introgression (Argyris et al., 2015) could be used for breeding programs to develop new cultivars from elite parentals with enhanced textural traits. However, the process of developing new cultivars should carefully consider the potential effects of variability in the environmental factors across seasons on aroma before recommending the growth of these enhanced cultivars. The methodology of treating null data for studying volatiles in non-climacteric melons is of particular research interest. Finally, a careful textural study (from instrumental to sensorial perspectives) is suggested before introducing the QTLs of texture present in LG X into melon breeding programs.

5. Conclusions:

The differences in the textural profile at harvest between the NIL SC10-2 and the PS parental line were consistent between seasons and resulted in increased flesh firmness and whole fruit hardness, but reduced juiciness (particularly in S2) due to the introgression in LG X. The strong effect of the introgression on VOCs was also observed, but seasonal effects were even more noticeable than the introgression itself. The season best suited to growing melons resulted in the presence of more VOCs (acetate esters, non-acetate esters, alkanes, alcohols, sulfur-derived compounds and other compound classes) and a more typical melon aroma, regardless of the non-climacteric line considered.

TRANSCRIPTOMIC ANALYSIS OF A NEAR-ISOGENIC LINE OF MELON WITH HIGH FRUIT FLESH FIRMNESS DURING RIPENING:

V. TRANSCRIPTOMIC ANALYSIS OF A NEAR-ISOGENIC LINE OF MELON WITH HIGH FRUIT FLESH FIRMNESS DURING RIPENING:

1. Introduction:

Fruit ripening in melon (*Cucumis melo* L.) is characterized by a series of physiological, biochemical and organoleptic changes, as a consequence of a genetic program involving a coordinated cascade of responses that start in the placental tissue of the fruit and end in the rest of the mesocarp, with noticeable differences between climacteric and non-climacteric types (Ríos et al., 2017; Ezura et al., 2008; Guo et al., 2017). Non-climacteric melon fruit ripening is still poorly understood, hindering the application of postharvest techniques to delay ethylene-independent processes such as flesh softening or the production of certain aromas (Chaparro-Torres et al., 2016; Pech et al., 2008).

New genetic and genomic tools are available in melon for studying fruit ripening including collections of near-isogenic lines, tilling platforms, saturated genetic maps, the genome sequence, and many Quantitative Trait Loci (QTLs) and eQTLs positioned on the genetic map, gene expression atlas, etc (Dahmani-Mardas et al., 2010; González et al., 2011; Yano et al., 2018). However, this species still presents a challenge because of the size of its fruit and the difficulties in establishing the exact degree of maturity for harvesting.

Several collections of near-isogenic lines have recently been developed in this species. One of them was obtained by crossing the *Charentais* type *Védrantais* (*C. melo* L. subsp. *melo*, Cantalupensis Group) with the Japanese Ginsen makuwa cultivar (*C. melo* L. subsp. *agrestis*, Makuwa group) (Perpiñá et al., 2016), several QTLs related to quality traits were reported in introgressions in linkage group (LG) X. Another involved crossing 'Piel de Sapo' (*C. melo* L. subsp. *melo*, Ibericus Group; based on a recent classification (Pitrat et al., 2017) with dudaim (*C. melo* sp. *agrestis*, Dudaim group) (Castro et al., 2016). Recently, Pereira et al., *2018* obtained two QTLs more in LG X. However, the most widely studied collection for flesh firmness was developed using exotic non-climacteric accession PI161375 (ssp. *agrestis*) as donor and the non-climacteric Spanish cultivar PS as recurrent parental (Eduardo et al., 2005; Moreno et al., 2008).

RNA-Seq technology has also been applied for transcriptomic analysis during melon fruit ripening and to determine QTLs, expression QTLs (eQTLs) and candidate genes related to fruit quality (Galpaz et al., 2018; Saladié et al., 2015; Zhang et al., 2016). These authors concluded that the upregulation and downregulation of multiple set of genes act coordinately during fruit ripening, although environmental and seasonal effects need to be taken into account (Chaparro-Torres et al., 2016; Eduardo et al., 2007). Also, genes of β-D-xylosidase, glyoxysomal malate synthase, chloroplastic anthranilate phosphoribosyltransferase, and histidine kinase have been associated with flesh firmness (Nimmakayala et al., 2016).

The aroma profile together with textural traits are efficient traits for discriminating climacteric NILs from non-climacteric ones at harvest or during postharvest (Fernández-Trujillo et al., 2012; Obando-Ulloa et al., 2008; Obando-Ulloa et al., 2009b), but little

information is available about aroma formation in non-climacteric melons, particularly during postharvest ripening (Gonda et al., 2010) and in non-climacteric NILs during ripening.

One near-isogenic line (NIL) developed by Eduardo et al. (2005) (SC10-2) contains QTLs that affect flesh properties: for example, PI161375 allele (vs. PS) increases flesh firmness and flesh proportion vs. placental tissue at harvest (Moreno et al., 2008; Dos-Santos et al., 2013) and reduces flesh juiciness, extractable juice, juice density and titratable acidity but increases pH, dry matter and the flesh lightness colour parameter (Obando et al., 2008). SC10-2 also shows differential volatile organic compounds (VOCs) at harvest, lacking some compounds that are present in the PS parental, a pattern which is associated with delayed ripening at harvest (Dos-Santos et al., 2013). Finally, SC10-2 in fresh-cut cubes also showed reduced juice leakage compared with PS during cold storage (Gomes et al., 2010), but a certain risk of cracking during preharvest (Fernández-Trujillo et al., 2013).

The aim of this study was to analyze and compare the transcriptomes of the NIL SC10-2 and its PS parental during ripening to reveal the genes associated with the introgression during melon postharvest ripening (particularly those associated with textural traits and VOCs), and also to provide further insights for identifying key potential pathways and regulators.

2. Materials and methods:

2.1 Plant material, crop management experimental design and sampling:

Fruits obtained from plants of the inbred parental *C. melo* 'Piel de Sapo' (PS), *inodorus* type, and the NIL SC10-2 from the collection developed by Eduardo et al. (2005) were analysed. SC10-2 contains an introgression in homozygosis that covers the entire LG X from the Korean accession 'Songwhan Charmi' (PI 161375) in a PS genetic background (Eduardo et al., 2005). Soil preparation, fertigation, plant protection, and other growing practices were those commonly used for melon cultivation in the Mediterranean conditions in Torre Pacheco (Murcia, Spain) (Fernández-Trujillo et al., 2012; Obando-Ulloa et al., 2009b). To reduce fruit cracking, the measures reported by Fernández-Trujillo et al. (2013) were followed. The experiment was conducted in the 'Centro Experimental de Formación y Experiencias Agrarias' (CIFEA) located in Torre Pacheco (Murcia, Spain). The field was divided into rows 2 m apart, in which each replicate consisted of six plants 1.5 m apart, in parallel rows. Twelve replicates of PS and seven of SC10-2 were planted. The plantation was surrounded by a border of the cultivar 'Nicolás' (Syngenta Seeds).

The fruit harvest and maturity indexes were slightly modified versions of those reported for non-climacteric melons (Chaparro-Torres et al., 2016). Minimum harvest indexes were the presence of a well formed and defect-free fruit, firm, well healed and dry epidermis with lignified netting, high density, absence of trichomes, dark-green skin color, withering of the stem and leaf close to the fruit peduncle, peduncle suberization, and light yellowing of the ground spot. The most common harvest indices for both SC10-2 and PS were the rind netting and, in some fruit, an annular ring or yellow color around a partly suberized peduncle (Fernández-Trujillo et al., 2013), light yellowing of the ground spot (particularly in PS), and a slight suberized crack around the peduncle, and dark blue-green skin color (in SC10-2).

The harvest season lasted about 2 weeks in both lines, but all the fruit for this experiment (three different biological replicates per line and/or storage time for transcriptomic analysis; more fruit for the study of physiological traits) were collected on the same day. PS was harvested about one month later than SC10-2 (7 July for PS; 9 August for SC10-2), due to the later ripening of this NIL (Dos-Santos et al., 2013) and to the rain that fell during flowering, which provoked flower and fruit abscission in May. Fruits were harvested by an expert over a period of two weeks during morning hours (05.45 h to 10.00 h, at a usual temperature of 21-26 ^{o}C. Total soluble solids and flesh firmness were used to assess the differences in maturity at harvest (Obando et al., 2008; Dos-Santos et al., 2011). Fruit in the firm-ripe stage of maturity were used in this experiment after storing fruit for 18 days at 20.5 ± 0.6 ^{o}C and a relative humidity of 88.2 ± 5.4 % (means ± SD, n=3 biological replicates).

Fruits were immediately analysed after their arrival in the laboratory or during the postharvest storage. Flesh sampling was carried out following the methodology previously reported (Obando et al., 2008). After storage, samples lyophilised according to Dos-Santos et al. (2007).

2.2 Respiration rate, ethylene production:

Both physiological measurements were made in another lot of individual fruit (n=6 of different biological replicates in firm-ripe stage of maturity) during postharvest ripening of 18 d at 20.5 ^{o}C and 88% relative humidity. The static method30 was followed for gas sampling and analysis by gas chromatography of carbon dioxide and ethylene.

2.3 Textural traits:

Whole fruit hardness (WFH) was determined at the equator (lateral hardness) as previously reported for measuring the compression force (in N) to achieve 2 mm deformation (Dos-Santos et al., 2013). Flesh firmness (FF), flesh juiciness (FJ) and juice density (JD) were measured according to the methodology previously reported (Obando et al., 2008; Dos-Santos et al., 2011). The results were expressed in N, grams of juice per kg fresh weight or kg juice per m^3 juice, respectively.

2.4 Volatile organic compounds (VOCs):

To analyze volatile organic compounds, the juice extracted from melons was filtered through a four-layer cheesecloth. After 3 min at 23 °C, the mixture containing 28.6% *v*/*v* of saturated $CaCl_2$ solution and the rest of the juice was poured into sterile polypropylene vials, which were stored at −80 °C until solid-phase microextraction and analysis by gas chromatography mass spectrometry (Chaparro-Torres et al., 2016; Fernández-Trujillo et al., 2018).

2.5 RNA extraction:

The RNA extraction was performed using the TRI Reagent RNA isolation protocol (1 mL per 20–30 mg of lyophilized tissue per extraction) and treated with DNAse.

2.6 mRNA library preparation and sequencing:

The library from DNA free total RNA was constructed following the TruSeq™ Stranded mRNA Sample Preparation kit protocol (Illumina Inc., Redwood. CA, USA).

The libraries were sequenced using TruSeq SBS Kit v3-HS, in paired end mode with a read length ranging from 35 to 76 bp by the National Centre of Genomics Analysis (CNAG) in Barcelona (Spain). A fraction of a sequencing lane on the Illumina HiSeq2000 sequencing system (Illumina, Inc.) was used to generate 6-12 million Paired End reads Passing Filter for each sample.

A quality read assessment was performed with FastQC package (Andrews et al., 2010). These reads were mapped against the *C. melo* genome CM3.5.1 (http://melonomics.cragenomica.es/) using the Hisat2 mapper (Kim et al., 2015), counting the number of reads mapped to transcripts with StringTie (Pertea et al., 2015). This counting was guided using the genome annotation, and a unified set of transcripts was created for the samples analyzed. Then, a Fragments Per Kilobase of transcript per Million (FPKM) table with gene expression for each sample was generated and used to assess the expression profiles of each sample by principal components analysis (PCA). Expression profiles showed high differences between samples due to ribosomal genes expression, so this were removed from further analysis steps. Differential expression analyses of both lines over time were run using the Bioconductor package Ballgown (Fu et al., 2018), using FPKMs as measurement of gene expression. Tables of DEGs, considering the effect of the introgression or the postharvest ripening time, were obtained separately. Mev (RNA-Seq analysis in MeV (Howe et al., 2011; MEV, 2018) was used to run PCA analyses on DEGs and separate those genes into expression profile clusters. These clusters were calculated by k-means algorithm with Pearson correlation as metric and FPKMs as measurement. GO terms enrichment analyses were run for each one with the Blast2GO package (Conesa et al., 2008).

2.7 Assessment of introgression effects on textural traits and VOCs

The experiment was analyzed by a two-way ANOVA using introgression (I= SC10-2 or PS) and postharvest ripening time (RT= 0, 4, 8, 12, 18 d) as factors followed by an LSD test at p=0.05 for the main effects or I x RT interaction. For the DEGs, the significant effects of the introgression (effect I alone) or the combined effect of postharvest ripening time and the interaction I x RT were calculated. The main introgression effects of SC10-2 were grouped into effects above or below the PS.

3. Results:

3.1 Physiological behaviour and textural traits:

The depletion in respiration rate and ethylene production were most pronounced during the first four days of postharvest ripening and the rates of SC10-2, particularly of ethylene production, were generally below those of PS (Figure 1). Early or late harvested fruits showed, respectively, higher or lower respiration and ethylene production rates irrespective of the line (data not shown). SC10-2 could be stored for more than 40 d and PS for around 30 d. The main problem of extending fruit storage further, particularly at high relative humidity levels, is flesh sugar loss and fungal decay (*Fusarium* sp.), particularly at the peduncle (data not shown).

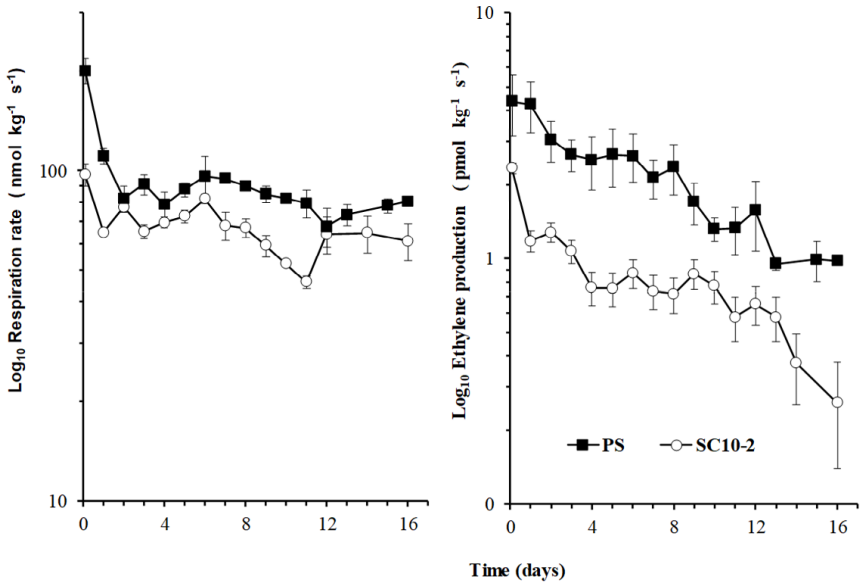

Figure 1. Respiration rate and ethylene production of individual fruit, the near-isogenic line SC10-2 and its parental line 'Piel de Sapo' (PS), harvested in firm-ripe stage of maturity during 18 d of postharvest ripening at 20.5 ºC and 88% relative humidity (mean ± SE, n=6).

Flesh firmness and whole fruit hardness were always higher in SC10-2 than in PS (Figure 2). The firm-ripe fruit of the NIL SC10-2 was slower to ripen postharvest than PS, as revealed by its slower softening (higher whole fruit hardness and flesh firmness during ripening and reduced juiciness (introgression and postharvest ripening time significant at $P<0.05$; Figure 2). Juice density (overall 1017 ± 4 $kg \cdot m^{-3}$) did not change significantly in either line.

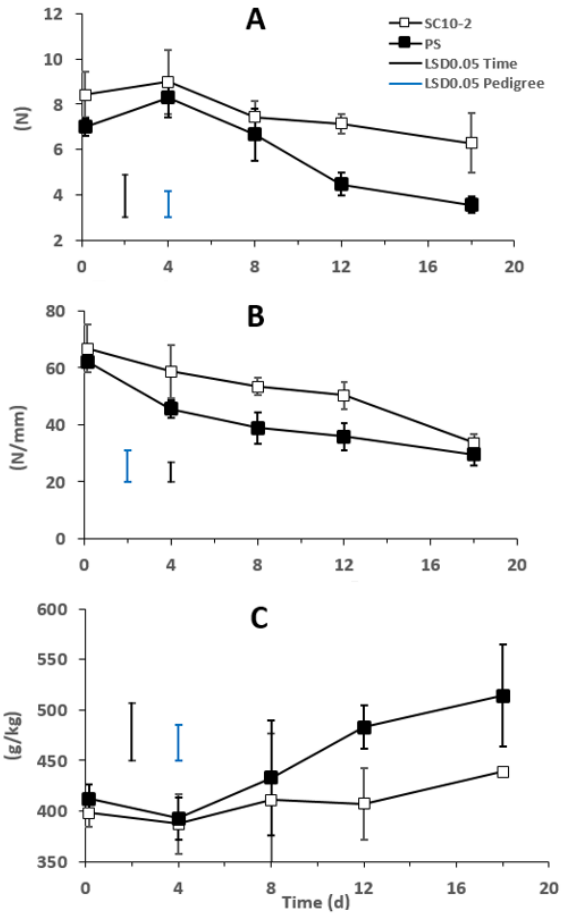

Figure 2. Textural traits of melon fruit, the near-isogenic line SC10-2 and its parental line 'Piel de Sapo' (PS) harvested in firm-ripe stage of maturity during 18 d of ripening at 20.5 ºC and 88% relative humidity (mean ± SE, n = 3). A. Flesh firmness B. Whole fruit hardness C. Flesh juiciness.

3.2 Volatile organic compounds:

During postharvest storage (Figure 3) two significant introgression x ripening time interactions ($P<0.05$) were observed for some groups of VOCs. After 4 d, the relative levels of acetate esters were higher in PS than in SC10-2. The same was true for non-acetate esters but after 8 d, while the concentration of other VOCs abruptly also increased after 12 d of storage in SC10-2 compared with PS levels. The relative levels of aldehydes, alcohols, acids and terpenes showed generally higher levels in SC10-2 than in PS (introgression significant, $P<0.05$; Figure 3). Aldehydes, alcohols and terpenes followed a similar pattern during ripening, with a maximum after 4-8 days and decreasing thereafter (time significant, $P<0.05$; Figure 3).

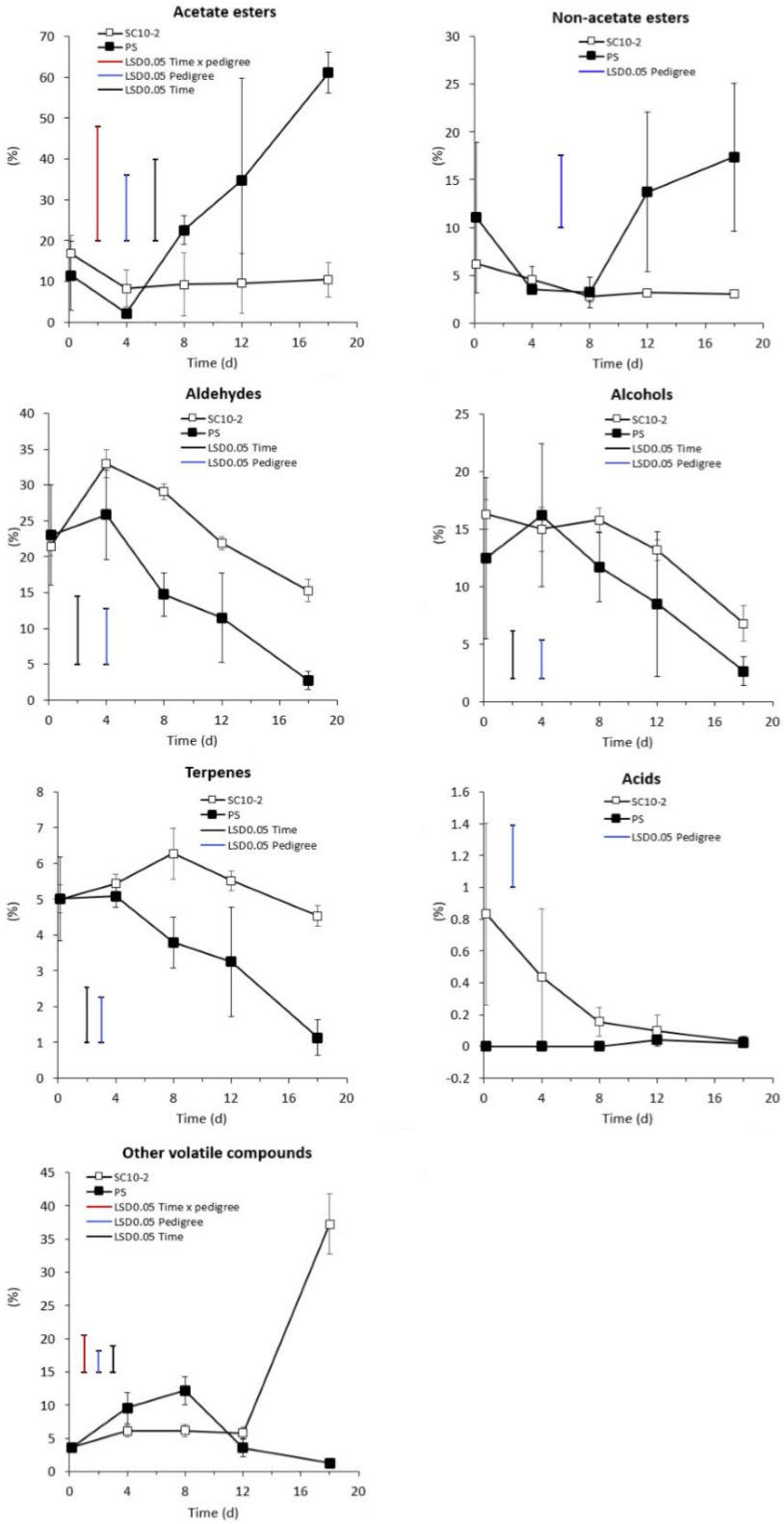

Figure 3. Main compound classes identified by static headspace solid-phase micro-extraction and gas chromatography–mass spectrometry (HS-SPME/GC-MS) in melon fruit of the near-isogenic line (NIL) SC10-2 and its parental line 'Piel de Sapo' (PS) harvested in firm-ripe stage of maturity and subjected to storage at 20.5 ºC and 88% relative humidity for 18 d. Data are expressed as percentage of each compound class with match quality above 50 with respect to the sum of areas of the identified compounds without considering exogenous ones (mean ±SE, n=3). LSD were calculated after a two-way ANOVA with introgression and ripening time as factors.

A total of thirteen individual VOCs showed significant effects for the factors studied during storage (Figure 4), all of them belonging to four compound classes (aldehydes, ketones, alcohols and sulphur-derived compounds). Two compounds (1-phenylethanone and dodecanal) showed significant introgression x ripening time effects ($P<0.05$), because of the differences in their respective patterns of ripening in both lines (convex for SC10-2; concave for PS). A total of eleven individual VOCs of different classes showed a significant introgression effect according to the two-way ANOVA (Figure 4), most of them alcohols or aldehydes with lower levels in PS than in SC10-2 during ripening (methanethiol, S-methyl ethanethioate, hexanal, octanal, (Z)-non-6-enal, nonanal, decanal, 4-isopropylcyclohexanol (isomer 1), 2-ethylhexan-1-ol, nonan-1-ol, (E)-4-phenylbut-3-en-2-one). Decanal and hexanal also showed a significant time effect together with nonanal but decreased with the ripening time ($P<0.05$).

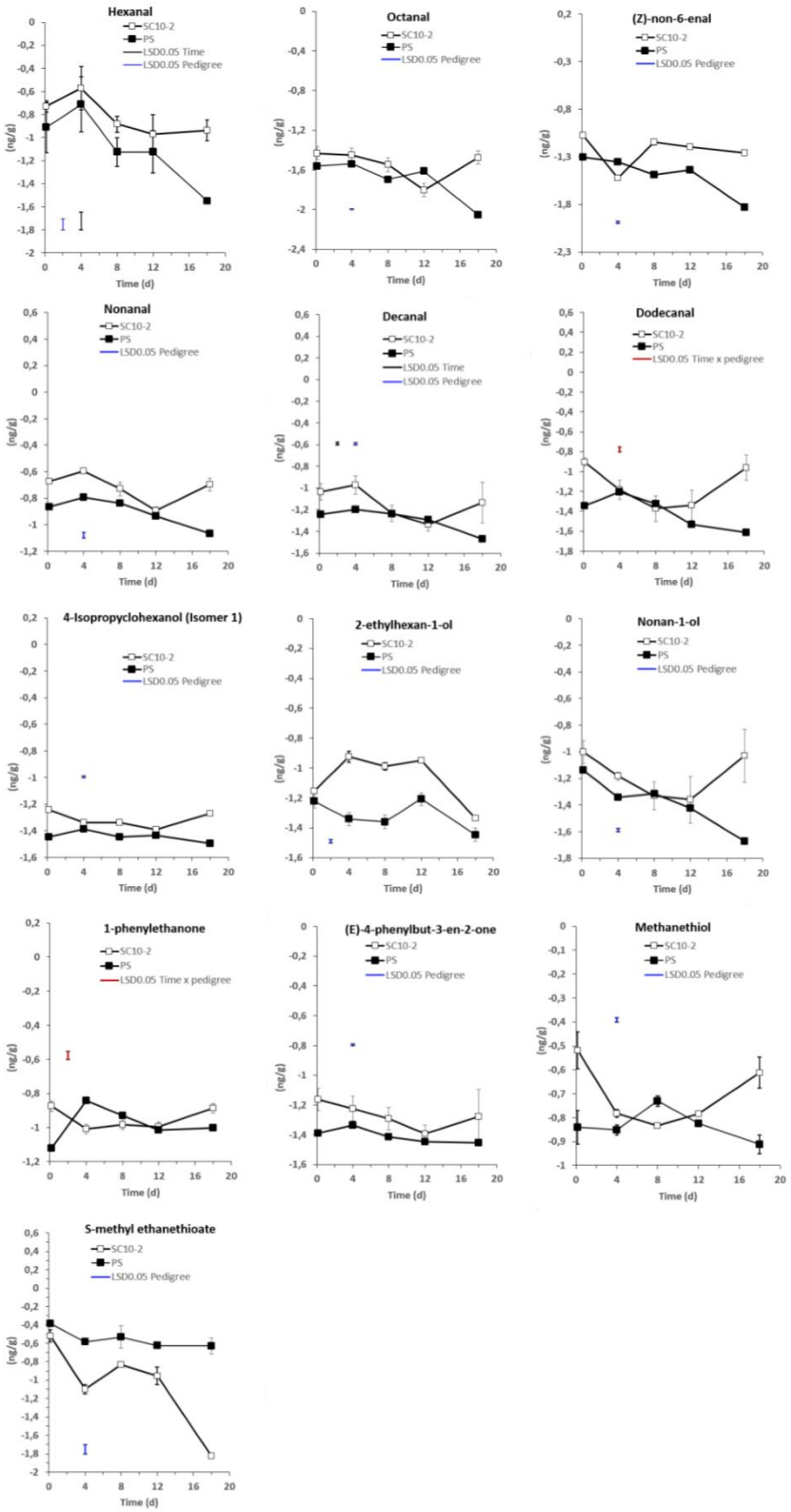

Figure 4. Main compound classes identified by the static headspace solid-phase micro-extraction and gas chromatography–mass spectrometry (HS-SPME/GC-MS) technique in melon fruits of the near-isogenic line (NIL) SC10-2 and its parental line 'Piel de Sapo' (PS) (n= 3) subjected to storage at 20.5 ºC and 88% relative humidity for18 d. Data are expressed as percentage of each compound class with respect to the total normalized areas (transformed into log2). Means were statistically significant according to two-way ANOVA with introgression and ripening time as factors.

3.3 Effect of LG X introgression on textural traits and VOCs during ripening:

Negative effects on the mean respiration rate and ethylene production rates and flesh juiciness were found in PS, while flesh firmness and whole fruit hardness showed an opposite trend**.** As regards the VOCs and taking into account the effects reported in the previous section, the introgression affected aldehydes (hexanal, octanal, (Z)-non-6-enal, nonanal, decanal); alcohols (4-isopropylcyclohexanol (isomer 1); 2-ethylhexan-1-ol; nonan-1-ol), ketones ((E)-4-phenylbut-3-en-2-one) and sulphur-derived compounds (methanethiol, and S-methyl ethanethioate). Two time-dependent effects were observed for 1-phenylethanone and dodecanal.

3.4 Differential expression analysis:

PCA analysis showed expression differences between groups and low variability within groups, so further steps in the analysis could be done without any concern about samples' expression profiles. As expected, the PCA based on a comparison between lines with time separated SC10-2 from PS better than the other PCA involving ripening time (Supplementary Figs. 1 and 2 (Annex C), respectively).

A total of 2954 DEGs were found by comparing both lines (i.e. considering the introgression factor or the interaction introgression x ripening time; Supplementary Table 1 (Annex C)). A total of 2068 DEGs changed during postharvest ripening in both lines (Supplementary Tables 2 and 3 (Annex C)), while 2045 of the formers were also DEGs, as seen from the comparison between lines over time. Therefore, 23 DEGs were exclusive to the postharvest ripening time effect and with no introgression or introgression x ripening time effects (Supplementary Table 3 (Annex C)). Only 909 of the 2954 DEGs found for introgression showed a significant effect for introgression but did not appear in the DEGs when the factor ripening time was analyzed (Supplementary Table 4 (Annex C)), making them the most interesting ones for this study.

During postharvest ripening, most of the identified DEGs were downregulated to a greater degree in SC10-2 than in PS but accounted for a smaller proportion of the total DEGs than in PS (Figure 5). Comparing lines during ripening time (introgression effect), most of the upregulated DEGs in almost all of the functional categories were more abundant in SC10-2 than in PS (Figure 6), but, in contrast to the first factor studied (ripening time effect), some DEGs were upregulated in some biological processes (such as the negative regulation of cell growth, the biosynthesis of indole-containing compound, mRNA 3'-end processing, jasmonic acid mediated signaling and the initiation of DNA replication (Figure 6).

Figure 5. Gene Ontology (GO) of differentially expressed genes only considering the ripening time factor in melon fruit of the near-isogenic line NIL SC10-2 and its parental ´Piel de Sapo´ (PS) harvested in firm-ripe stage of maturity and stored at 20.5 ºC and 88% relative humidity for 18 d.

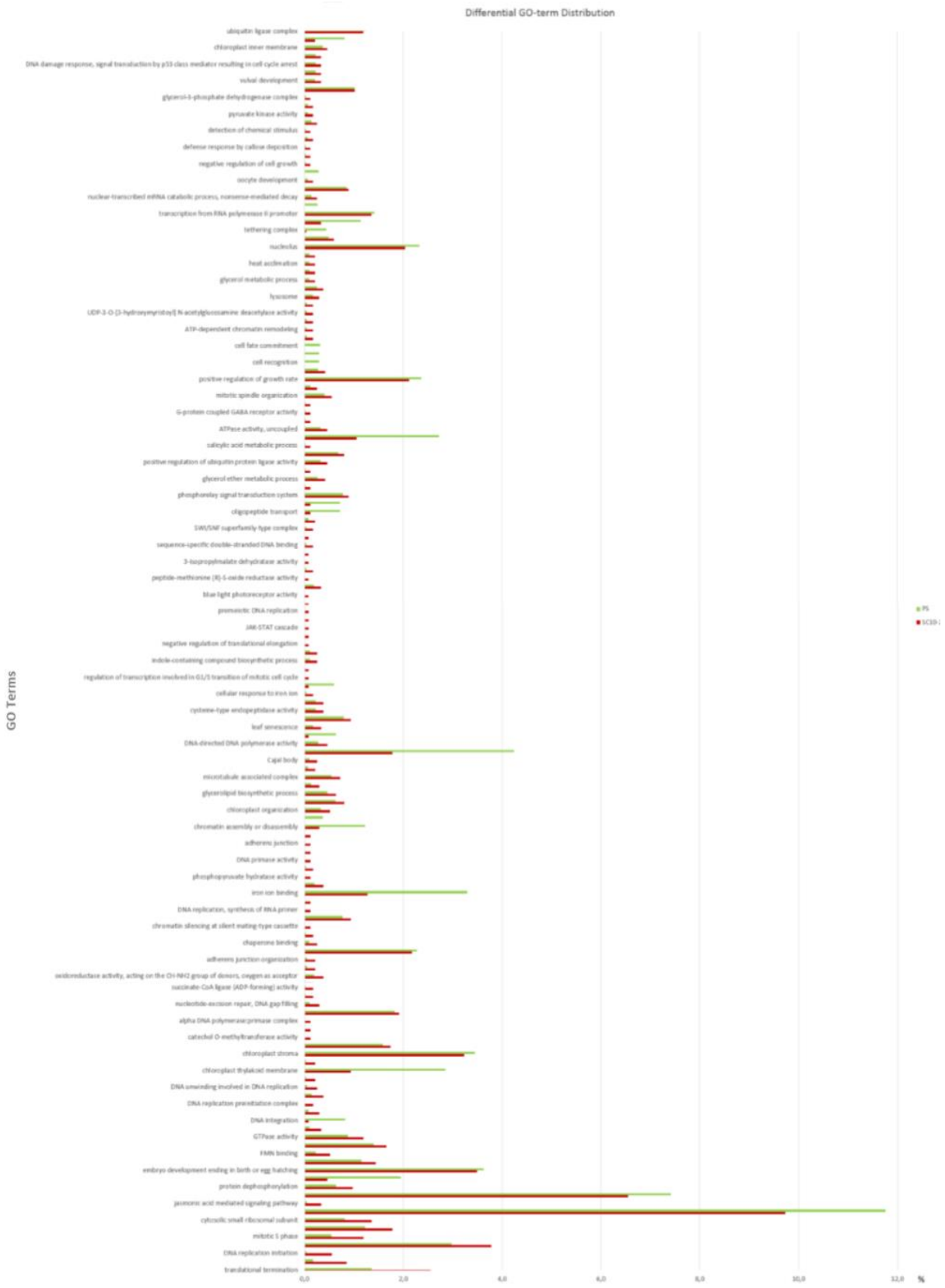

Figure 6. Gene Ontology (GO) of differentially expressed genes only considering the introgression factor in melon fruit of the near-isogenic line NIL SC10-2 and its parental 'Piel de Sapo' (PS) harvested in firm-ripe stage of maturity and stored at 20.5 ºC and 88% relative humidity for 18 d.

Overall, the functions of the most abundant DEGs associated with the postharvest ripening time factor or I x RT interaction (Figure 5) were mRNA metabolic process; lipid A biosynthetic process; mitotic S phase; glycolytic process and gluconeogenesis (Supplementary Figure 3 (Annex C)).

On the other hand, the most abundant functions of the DEGs associated with the introgression were as follows: DNA strand elongation involved in DNA replication; zinc ion binding; RNA binding; chloroplast stroma; oxidoreductase activity, acting on paired donors, with incorporation or reduction of molecular oxygen; hydrolase activity, acting on glycosylic bonds; monooxygenase activity; positive regulation of growth rate; transcription from RNA polymerase II promoter (Figure 6).

Cluster analysis. Seven clusters were found when the introgression effect was studied in a comparison of lines over time (Figure 7; Supplementary Table 1 (Annex C)). However, considering the expression patterns during postharvest ripening time, we classified the DEGs into six main clusters (Figure 8; Supplementary Table 2 (Annex C)).

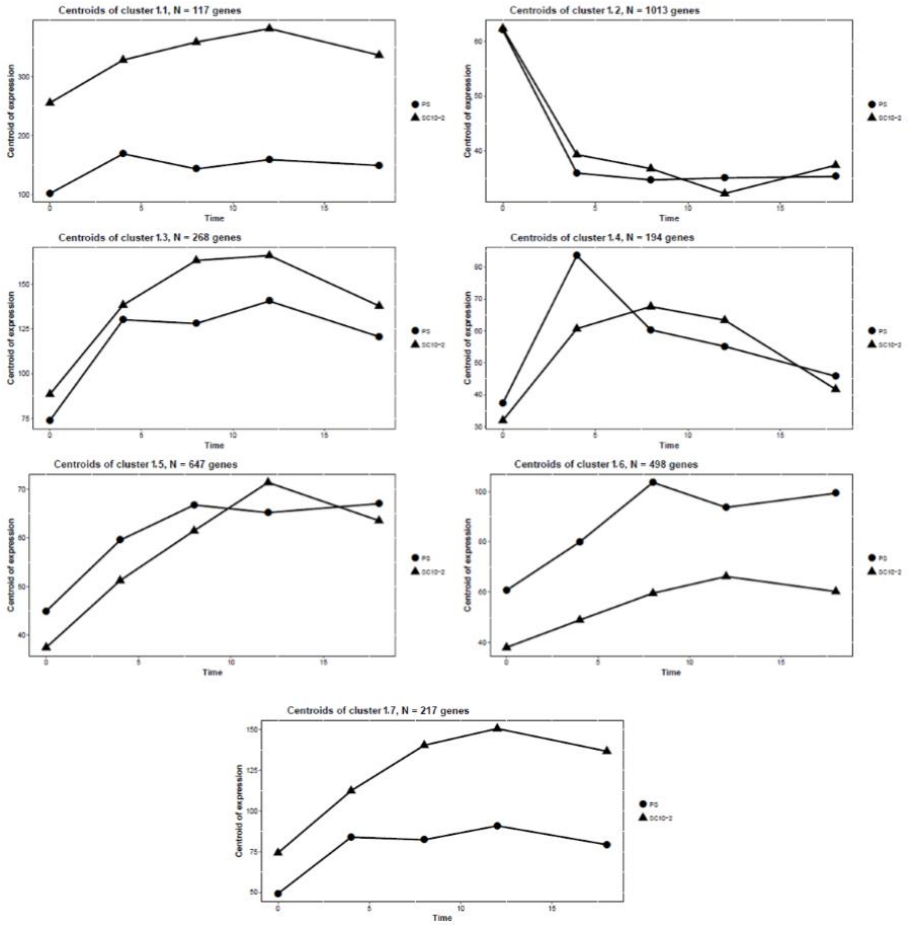

Figure 7. Cluster analysis of the differentially expressed genes only considering the ripening time in fruit of the melon near-isogenic line SC10-2 and its parental control 'Piel de Sapo' (PS). Differentially expressed genes were categorized into six clusters depending on their expression during fruit ripening (0, 4, 8, 12 and 18 d at 20.5 ºC and 88% relative humidity).

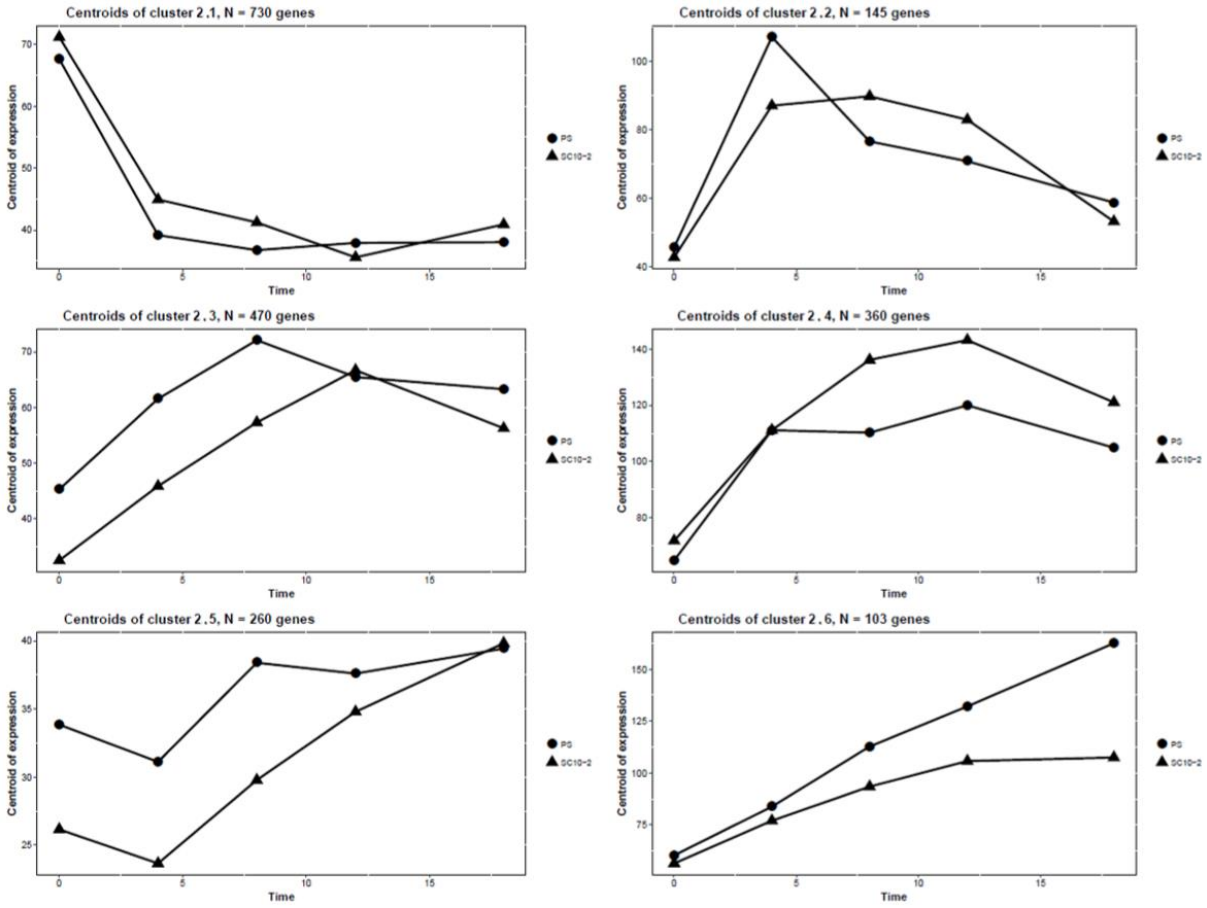

Figure 8. Cluster analysis of the differentially expressed genes significant in the comparison between lines over time in fruit of the melon near-isogenic line SC10-2 and its parental control 'Piel de Sapo' (PS). Differentially expressed genes were categorized into seven clusters depending on their expression during fruit ripening (0, 4, 8, 12 and 18 d at 20.5 ºC and 88% relative humidity).

As regards the study of clusters involving introgression differences over time (Figure 7), the most noticeable differences were the presence of 30% of total DEGs with upregulation of SC10-2 vs PS (clusters 1.1, 1.3 and 1.6) and 34.3% with minor differences but the same trend except at harvest and after 12 days of ripening (cluster 1.2). These clusters were associated with the mRNA metabolic process, the response to abscisic acid, kinase activity, carbohydrate derivative biosynthetic processes, etc. (Supplementary Figure 4 (Annex C)). By contrast, only 7.3% of DEGs (cluster 1.7) were clearly upregulated in PS compared with SC10-2, which was associated with the nucleolus, small molecule metabolic processes and lyase activity. However, 28.5% of DEGs (clusters 1.4 and 1.5) showed the same trend but only from harvest up to 4 or 8 d, probably due to different responses between lines to oxidative stress, the polysaccharide metabolic process or zinc ion binding, etc. (Supplementary Figure 4 (Annex C)). Clusters 1.2, 1.4 and 1.5 showed a noticeable introgression x ripening time interaction (Figure 7).

Generally, the genes expressed in the clusters were more abundant in PS than in SC10-2 considering both factors (Supplementary Figures 3 and 4, Annex C). In general, the study of clusters referring to postharvest ripening time revealed that most of the DEGs related with this factor were upregulated from harvest levels, peaking after 4, 8 or 12 d of postharvest ripening

(clusters 2.2, 2.3, and 2.4; 47.1% DEGs; Figure 8). Also, clusters 2.5 and 2.6 represent genes highly expressed after 4 d of ripening and peaking after 18 d (17.6% DEGs; Figure 8). In all the clusters except cluster 2.1 (35.3% of total DEGs, downregulated since harvest), slight introgression x ripening time interactions were evident (the lines during ripening tending to cross). Cluster 2.1 reflects downregulation of the mRNA metabolic process, the RNA biosynthetic process or cellular macromolecule biosynthetic process, among others (Supplementary Table 2, Annex C). By contrast, the rest of the clusters mostly represent upregulated genes associated with processes such as transferase of hexosyl groups, binding (ATP, metal ion, RNA, zinc ion, coenzyme), mRNA metabolic process, glycolytic process, cell wall, gluconeogenesis, etc. (Supplementary Figure 3 (Annex C)).

Selected DEGs study. Overall, we selected and studied a total of twenty-eight differentially expressed genes (DEGs) as a result of the introgression and/or postharvest ripening time factors (fourteen of the selected ones) that were involved in different pathways and functions (Table 1; Supplementary Tables 4 and 5 (Annex C)). Among them, two selected DEGs involved in primary metabolism, ATP-citrate synthase alpha chain protein (*Cm*ACLA-1), which is involved in ligase and catalytic activity, Succinate--CoA ligase [ADP-forming] subunit alpha, mitochondrial (*Cm*SCOA) involved in pyruvate metabolism and Citric Acid (TCA) cycle, were generally upregulated in SC10-2 compared with PS (Figure 9). However, some slight differences in expression between NIL SC10-2 and PS, particularly as regards postharvest ripening time, were found in three DEGs (*Cm*NADP, *Cm*ACLB-2, and *Cm*SDHA).

Table 1. Differentially expressed genes transcripts from RNA-seq of the near-isogenic line (NIL) SC10-2 fruit (n = 3) of melon and its parental control ´Piel de Sapo´ (PS) during 18 d postharvest ripening at 20.5 ºC and 88% relative humidity. Effect of postharvest ripening time (RT) or the introgression (I) alone or combined with RT. All the information comes from Melonomics version 4.0, including the chromosome (LG) location except when unavailable (LG 0).

Gene	Transcript name	LG	Locus start	Locus end	Gene description	Code	Factor
MELO3C024348	MELO3C024348 2 1	1	36244644	36249009	Lipoxygenase	*Cm*LOX18	RT/ I
MELO3C019735	MELO3C019735 2 1	11	23244951	23246562	1-aminocyclopropane-1-carboxylate oxidase	*Cm*ACO2	RT/ I
MELO3C019548	MELO3C019548 2 1	6	12928441	12930407	Cinnamyl alcohol dehydrogenase	*Cm*ADH1	RT
MELO3C018492	MELO3C018492 2 1	1	614743	617080	Cinnamyl alcohol dehydrogenase	*Cm*CAD1	RT/ I
MELO3C010910	MELO3C010910 2 1	3	30073454	30075374	Allene oxide synthase	*Cm*AOS	RT
MELO3C016259	MELO3C016259 2 1	7	22840158	22843162	Bidirectional sugar transporter SWEET	*Cm*SWEET7	RT
MELO3C008075	MELO3C008075 2 1	3	159591	162626	12-oxophytodienoate reductase-like protein	*Cm*OPR2	RT
MELO3C020508	MELO3C020508 2 1	12	399308	402564	Cinnamoyl-CoA reductase 1/ Bifunctional dihydroflavonol 4-reductase	*Cm*DFR4	RT
MELO3C012476	MELO3C012476 2 1	10	214914	216424	NADPH:quinone oxidoreductase-like	*Cm*NADH1	RT
MELO3C017811	MELO3C017811 2 1	7	27322473	27324829	Phenylalanine ammonia-lyase-like	*Cm*PAL	RT
MELO3C009127	MELO3C009127 2 1	4	34052833	34055772	WRKY family transcription factor family protein	*Cm*WRKY33	RT/ I
MELO3C023350	MELO3C023350 2 1	11	1856000	1857792	GATA transcription factor	*Cm*GATA5	RT
MELO3C005630	MELO3C005630 2 1	9	23110939	23111708	Ethylene-responsive transcription factor ERF027	*Cm*ERF027	RT
MELO3C012086	MELO3C012086 2 1	10	2703625	2705396	Transcription factor TCP15	*Cm*TCP15	RT
MELO3C011939	MELO3C011939 2 1	10	3788375	792148	GDSL esterase/lipase At3g26430	*Cm*GDSL esterase/ lipase	RT
MELO3C013101	MELO3C013101 2 1	1	12324577	12332243	Glycerophosphodiester phosphodiesterase GDPDL4-like	*Cm*GDPDL4	RT
MELO3C016540	MELO3C016540 2 1	6	27663292	27665351	NAC domain protein	*Cm*NAC18	RT/ I
MELO3C005591	MELO3C005591 2 1	9	22744057	22747399	ACT domain-containing family protein	*Cm*ACT	RT
MELO3C017560	MELO3C017560 2 1	7	25124825	25133417	Succinate dehydrogenase flavoprotein subunit, mitochondrial	*Cm*SDHA	RT/ I
MELO3C021563	MELO3C021563 2 1	9	3808841	3816628	isocitrate dehydrogenase [NADP]	*Cm*NADP	RT/ I
MELO3C018576	MELO3C018576 2 1	1	1201943	1207142	L-galactose dehydrogenase	*Cm*L-GalDH	RT/ I
MELO3C004377	MELO3C004377 2 1	5	26991180	26994294	GDP-mannose-3',5'-epimerase	*Cm*GME	RT
MELO3C010675	MELO3C010675 2 1	3	31551192	31555805	ATP-citrate synthase alpha chain protein	*Cm*ACLA-1	RT/ I
MELO3C011482	MELO3C011482 2 1	3	25714081	25722118	ATP-citrate synthase beta chain protein 2-like	*Cm*ACLB-2	RT/ I
MELO3C002167	MELO3C002167 2 1	12	25867931	25872728	Succinate--CoA ligase [ADP-forming] subunit alpha, mitochondrial	*Cm*SCOA	RT/ I
MELO3C005518	MELO3C005518 2 1	9	22123330	22124520	3-isopropylmalate dehydratase small subunit 3-like	*Cm*IPMI3	RT/ I
MELO3C003344	MELO3C003344 2 1	4	456132	464549	3-isopropylmalate dehydratase large subunit	*Cm*IIL1	RT/ I
MELO3C007433	MELO3C007433 2 1	8	2763982	2767562	Fumarylacetoacetase	*Cm*FAH	I
MELO3C009970	MELO3C009970 2 1	4	27614894	27618780	Polygalacturonase At1g48100	*Cm*DHL92	RT
MELO3C007517	MELO3C007517 2 1	8	3320368	3322511	Mitochondrial pyruvate carrier	*Cm*MPC1	RT
MELO3C017343	MELO3C017343 2 1	2	24148159	24152142	Protein DETOXIFICATION	*Cm*DTX	RT
MELO3C014384	MELO3C014384 2 1	5	2954394	2961074	ABSCISIC ACID-INSENSITIVE 5-like protein 4 isoform X1	*Cm*ABREX	RT
MELO3C000885	MELO3C000885 2 1	0	20311284	20311754	auxin-responsive protein SAUR71-like	*Cm*IAA71	RT
MELO3C024001	MELO3C024001 2 1	4	23817884	23822674	MADS-box transcription factor	*Cm*MADS-box	I
MELO3C010686	MELO3C010686 2 1	3	31468671	31472617	Alanine aminotransferase 2	*Cm*ALT-2	I

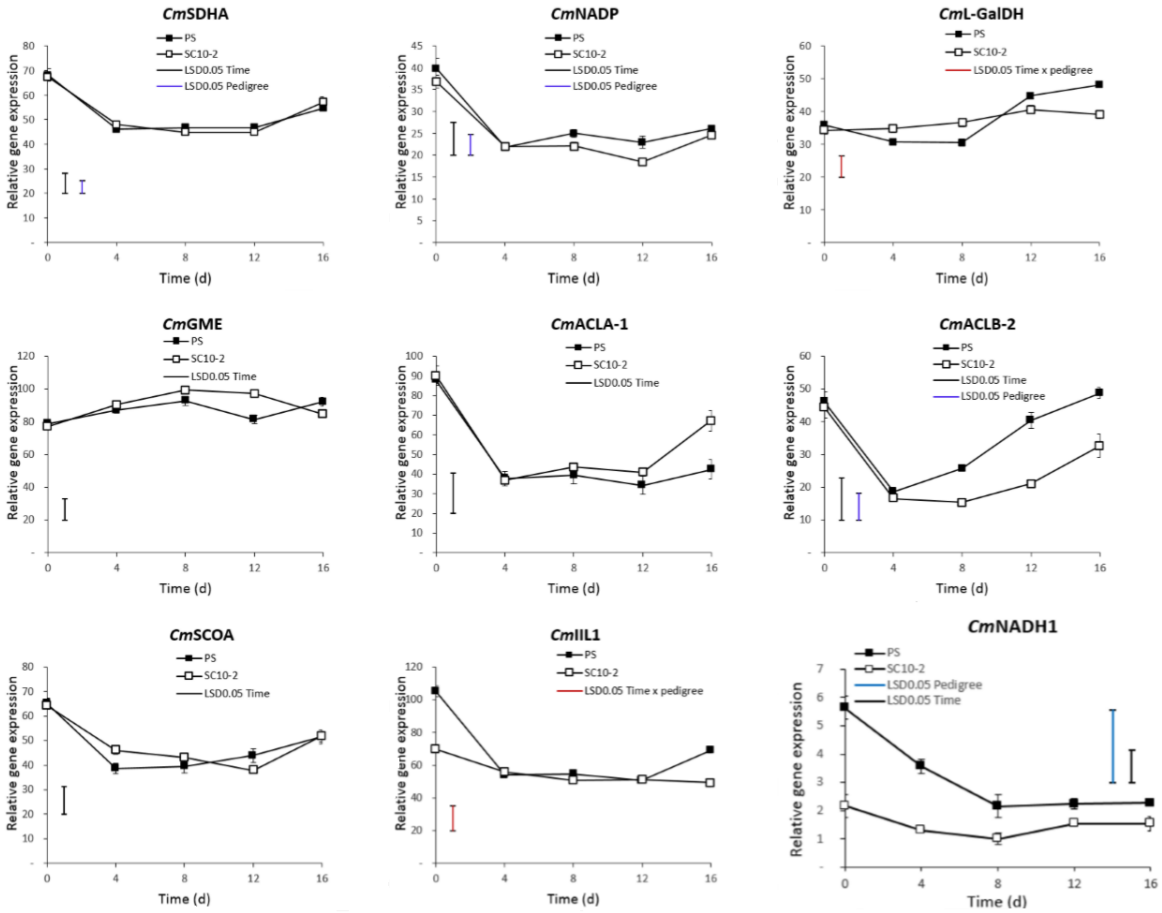

Figure 9. Relative expression of selective genes only considering the ripening time with differential expression involved in primary metabolism or ascorbic acid metabolism in fruit of the melon near-isogenic line SC10-2 and its parental control PS harvested in firm-ripe stage of maturity and stored during 18 d of ripening at 20.5 ºC and 88% relative humidity. *Cm*SDHA: Succinate dehydrogenase [ubiquinone] flavoprotein subunit, mitochondrial/ *Cm*NADP: isocitrate dehydrogenase [NADP]/ *Cm*L-GalDH: L-galactose dehydrogenase/ *Cm*GME: GDP-mannose-3',5'-epimerase/ *Cm*ACLA-1: ATP-citrate synthase alpha chain protein/ *Cm*ACLB-2: ATP-citrate synthase beta chain protein 2-like/ *Cm*SCOA: Succinate--CoA ligase [ADP-forming] subunit alpha, mitochondrial/ *Cm*IIL1: 3-isopropylmalate dehydratase large subunit/ *Cm*NADH1: NADPH:quinone oxidoreductase-like.

An additional twenty-eight DEGs were selected considering the traits studied and postharvest fruit ripening: *Cm*LOX18, *Cm*AOS, *Cm*OPR2, *Cm*SWEET7, *Cm*DFR4, *Cm*PAL, *Cm*WRKY33, *Cm*GATA5, *Cm*TCP15, *Cm*GDSL esterase/lipase, *Cm*ERF027, *Cm*GDE4 and *Cm*ATC were generally upregulated in SC10-2 compared with PS (Figure 10) with some exceptions in the expression of *Cm*GDE4 and *Cm*ATC. In contrast, the genes of *Cm*ACO2, *Cm*ADH1, *Cm*CAD1, *Cm*NADH1 and *Cm*NAC18 were downregulated (Figure 10). Only *Cm*NADH1, *Cm*TCP15 and *Cm*GDSL esterase/lipase were located in LG (Table 1), while for the other differentially expressed genes, some eQTLs could be found within LG X). Two genes involved in aminoacid metabolism *(Cm*IIL1 and *Cm*FAH were downregulated in SC10-2 vs. PS, while *Cm*IPMI3 was upregulated (Figure 10). Another two selected DEGs (*Cm*L-GalDH and *Cm*GME) involved in ascorbic acid metabolism were generally upregulated in SC10-2 vs. PS (Figure 10).

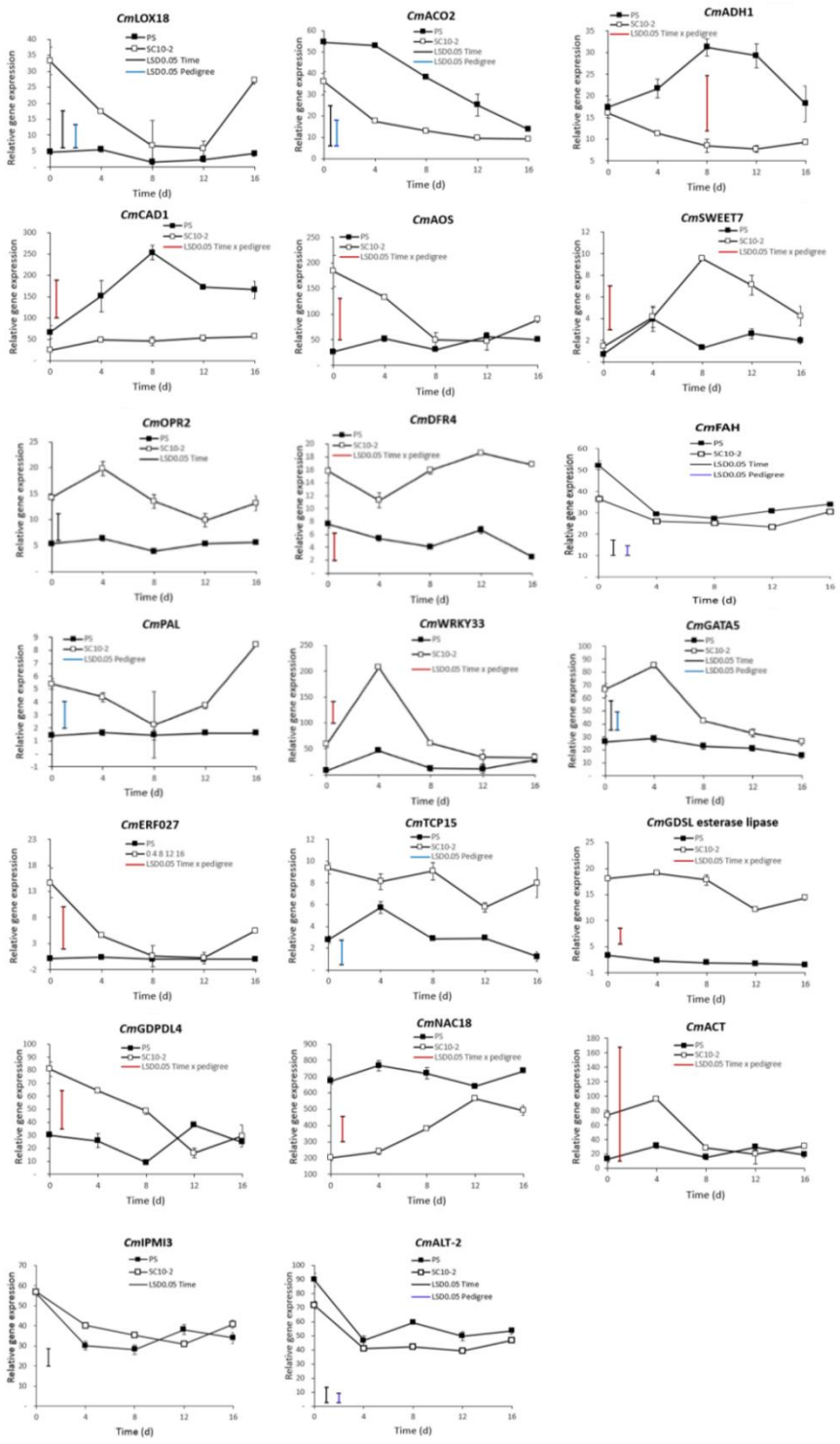

Figure 10. Relative expression of selective genes only considering the ripening time involved in quality and physiological process in fruit of the melon near-isogenic line SC10-2 and its parental control PS harvested in firm-ripe stage of maturity and stored during 18 d of ripening at 20.5 ºC and 88% relative humidity. *Cm*LOX18: Fruit ripening/ *Cm*ACO2: Ethylene biosynthesis/ *Cm*ADH1 and *Cm*CAD1: Phenylpropanoid biosynthesis/ CmAOS and CmOPR2: Oxylipin biosynthesis/ *Cm*SWEET7: Sugar transporter activity/ *Cm*DFR4: Flavonoid biosynthesis/ *Cm*NADH1: Oxidoreductase activity/ *Cm*PAL: Phenylpropanoid metabolism/ *Cm*WRKY33, *Cm*GATA5, *Cm*TCP15, *Cm*NAC18: Transcription factor activity/ *Cm*ERF027: Ethylene transcription factor activity/ *Cm*GDSL: Esterase and lipase activity/ *Cm*GDE4: Glycerol metabolism/ *Cm*TAC: Amino acid activity/ *Cm*IPMI3: 3-isopropylmalate dehydratase small subunit 3-like/ *Cm*ALT-2: alanine aminotransferase.

Fourteen selected DEGs were significant for the introgression: *Cm*MADS-box, *Cm*NAC18, *Cm*CAD1, *Cm*NADP, *Cm*ACLB-2, *Cm*IIL1 and *Cm*ACO2, which were generally downregulated in SC10-2 vs. PS (Figure 11) with some exceptions in *Cm*NADP, *Cm*ACLB-2 and *Cm*IIL1 and some introgression x ripening time interactions (levels of SC10-2 increased over time and remained constant in PS) such as in *Cm*NAC18 (Figure 11). As regards *Cm*WRKY33, *Cm*ACLA-1, *Cm*FAH, *Cm*SDHA, *Cm*IPMI3, *Cm*SCOA, *Cm*L-GalDH and *Cm*LOX18, they were generally upregulated in SC10-2 vs. PS (Figure 11) with some exceptions in *Cm*ACLA-1, *Cm*SDHA, *Cm*IPMI3, *Cm*SCOA and *Cm*L-GalDH was downregulated after 12 d (Figure 11).

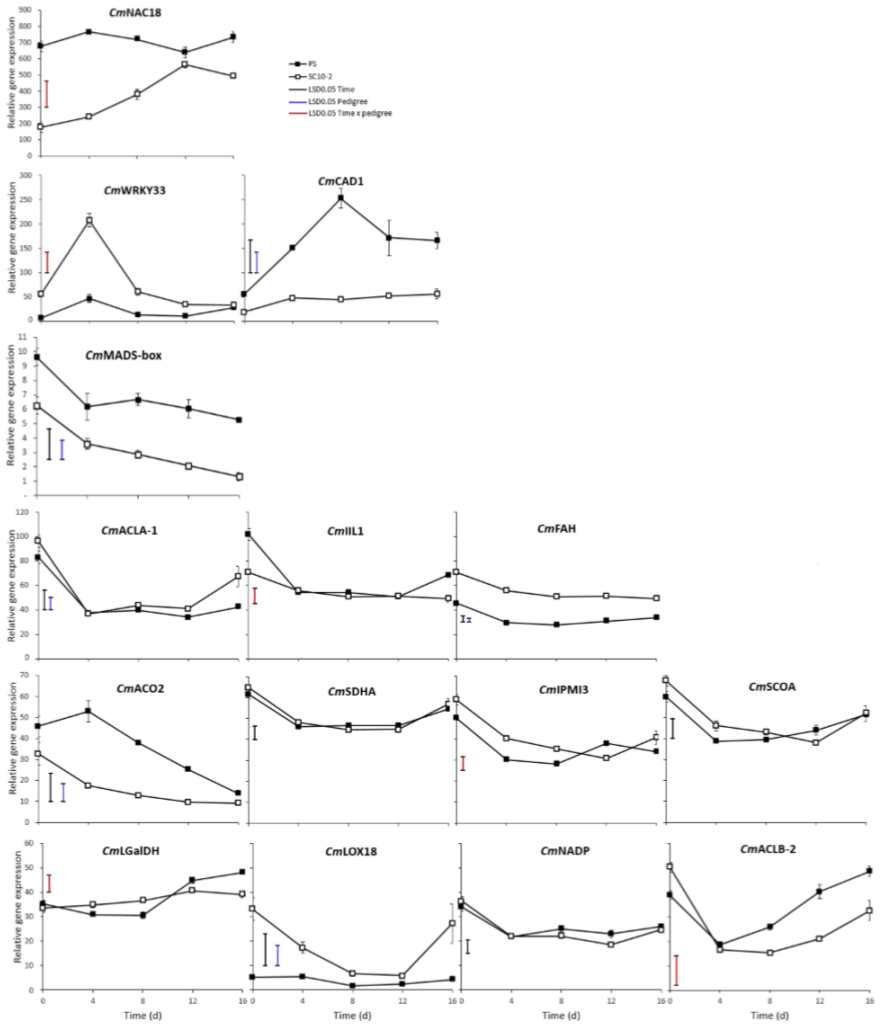

Figure 11. Relative expression of selective genes only mainly considering the comparison between lines over time and involved in different process in fruit of the melon near-isogenic line SC10-2 and its parental control PS harvested in firm-ripe stage of maturity and stored during 18 d of ripening at 20.5oC and 88% relative humidity. *Cm*NAC18: Transcription factor activity/ *Cm*WRKY33: Transcription factor activity/ *Cm*CAD1: Phenylpropanoid biosynthesis/ *Cm*MADS-box: MADS-box transcription factor/ *Cm*ACLA-1: ATP-citrate synthase alpha chain protein/ *Cm*IIL1: 3-isopropylmalate dehydratase large subunit/ *Cm*FAH: fumarylacetoacetase/ *Cm*ACO2: Ethylene biosynthesis/ *Cm*SDHA: Succinate dehydrogenase [ubiquinone] flavoprotein subunit, mitochondrial/ *Cm*IPMI3: 3-isopropylmalate dehydratase small subunit 3-like/ C*m*SCOA: Succinate--CoA ligase [ADP-forming] subunit alpha, mitochondrial/ *Cm*L-GalDH: L-galactose dehydrogenase/ C*m*LOX18: Fruit ripening/ *Cm*NADP: isocitrate dehydrogenase [NADP]/ *Cm*ACLB-2: ATP-citrate synthase beta chain protein 2-like.

Some evident introgression x ripening time interactions were identified in some DEGs using ANOVA: *Cm*IIL1, *Cm*ADH1, *Cm*CAD1, *Cm*AOS, *Cm*SWEET7, *Cm*DFR4, *Cm*WRK33, *Cm*GDSL esterase/lipase, *Cm*ERF027, *Cm*GDPDL4, *Cm*NAC18, *Cm*ACT, *Cm*LGalDH and *Cm*ACLB-2 (Figures 9-11).

About 23 DEGs changed as time progressed and followed the typical trend to decrease from high harvest levels, or the contrary after 4-8 d of ripening (Table 1; Supplementary Tables 1 and 4 (Annex C); Figure 12).

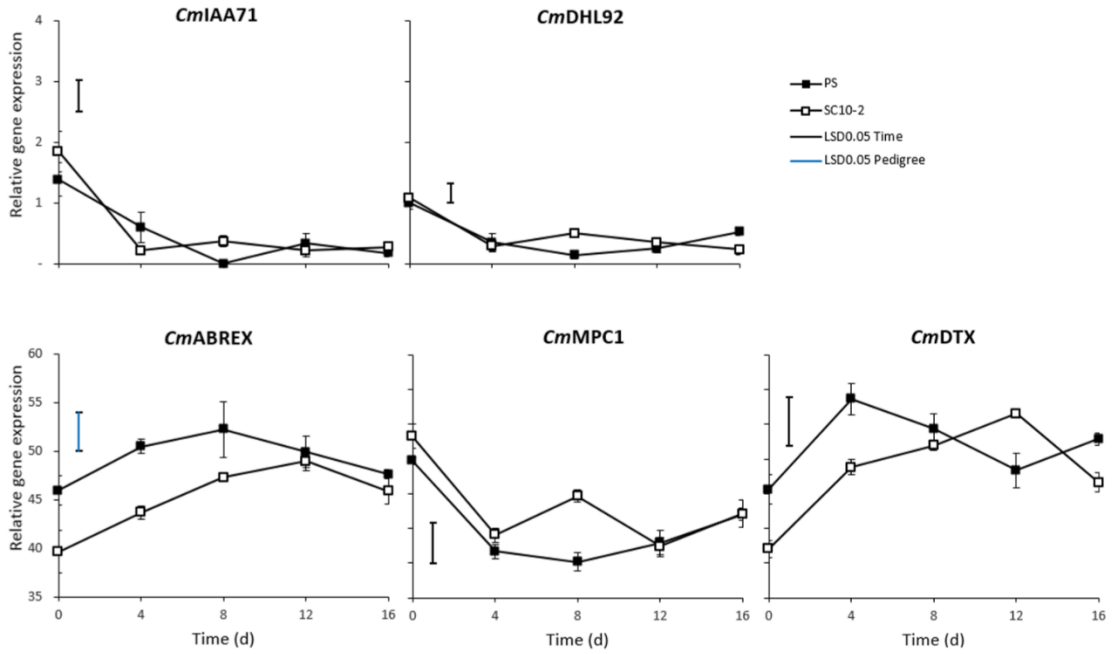

Figure 12. Relative expression of selective genes only considering the postharvest ripening time factor and involved in different process in fruit of the melon near-isogenic line SC10-2 and its parental control PS harvested in firm-ripe stage of maturity and stored during 18 d of ripening at 20.5 ºC and 88% relative humidity. *Cm*DHL92: Polygalacturonase At1g48100/ *Cm*MPC1: Mitochondrial pyruvate carrier/ *Cm*DTX: Protein detoxificatoin/ *Cm*ABREX1: Abscisic acid-insensitive 5-like protein 4 isoform X1/ *Cm*IAA71: auxin-responsive protein SAUR71-like.

4. DISCUSSION:

4.1 Quality and physiological traits vs. gene expression:

Primary metabolic changes vs gene expression. As is known, fruit ripening is classified as climacteric and non-climacteric, depending on the presence or absence of a transient rise in the respiration rate and the production of autocatalytic ethylene (Pech et al., 2008; Obando-Ulloa et al., 2008; Paul et al., 2012). Because the respiration rate was lower in SC10-2 than in PS (Figure 1), it was thought to be of interest to check some genes of mitochondrial enzymatic activities, transporters that are involved in metabolic changes during fruit development (Perotti et al., 2014), and genes of the tricarboxylic acid (TCA) cycle (Araújo et al., 2012). For example, NADH:quinone oxidoreductase *Cm*NADH1 (MELO3C012476) expression, the largest complex of the respiratory chain (Melo et al., 2004), was higher in PS than in SC10-2 throughout the experimental time (Figure 10), which would partly explain the higher respiration rate of PS (Figure 1). This difference could also be attributed to several genes that codify for proteins that act as enzymes of the aerobic respiratory chains (Moller, 2001; Yagi et al., 2004). For example, isocitrate dehydrogenase (*Cm*NADP; MELO3C021563) expression was generally higher in PS than in NIL SC10-2 throughout the postharvest ripening time (Figure 9). However, the mitochondrial succinate dehydrogenase (*Cm*SDHA) first decreased before increasing during the last few days of ripening, but differences between lines were negligible when both factors (introgression and ripening time) were considered (Figure 11).

For ATP-citrate synthase, two genes were differentially expressed in our experiment: ATP-citrate synthase alpha chain protein (*Cm*ACLA-1; MELO3C010675) and ATP-citrate synthase beta chain protein 2-like (*Cm*ACLB-2; MELO3C011482) (Figure 9). After decreasing from harvest to 4 d *Cm*ACLA-1 was higher in the NIL SC10-2 than in PS. By contrast, *Cm*ACLB-2 expression was higher in PS (Figure 11), probably because of the contribution of ACL, which is necessary for the generation of the cytosolic pool of acetyl-CoA (Fatland et al., 2002; Sánchez et al., 2000).

The expression of succinate--CoA ligase [ADP-forming] subunit alpha, mitochondrial gene (*Cm*SCOA; MELO3C002167) associated with GTP binding, ATP binding, succinate-CoA ligase (GDP-forming) activity, succinate-CoA ligase (ADP-forming) activity and ATP citrate synthase activity (Fraser et al., 1999), was not significantly different between PS and SC10-2 but the respiration rate followed a similar pattern (Figs. 1 and 9).

Postharvest ripening delay and textural traits vs gene expression. This paper confirms the effect of the long introgression covering the entire LG X (Eduardo et al., 2005) that contained the previously reported QTL *ff10.2* of flesh firmness and textural traits at harvest (Moreno et al., 2008; Dos-Santos et al., 2013; Obando et al., 2008). The introgression also delayed fruit ripening in general, as seen from by physiological traits (respiration rate, ethylene production, volatile production; Figs.1-4). Perpiñá et al. (2016) reported QTLs affecting fruit ripening in a climacteric melon genetic background, including *ff.10* for flesh firmness at harvest, *al.10* for the suppression of the formation of abscission layer, *ar.10* that produced less aroma at harvest, or QTLs affecting soluble solids and sugar content. Due to the length of these introgressions in LG X, the effects on the aroma volatiles and textural traits could be due to

independent genes, or to pleiotropic effects due to a unique gene (Dos-Santos et al., 2013). The candidate genes for *ff10.2* were *CmXTH5* and *CmEXP3* (Moreno et al., 2008), but during postharvest ripening these genes did not show differential expression. Other authors did not map QTLs or candidate genes on LG X (Immakayala et al., 2016). In tomato, QTLs affecting texture at harvest are distinguished from those affected softening and other ripening-associated textural traits during postharvest (Causse et al., 2008).

Several potential candidate genes have been proposed as being associated with melon textural traits during ripening (mostly firmness, *ffr10.2*, whole fruit hardness *wfhr10.2*, or flesh juiciness *fjr10.2*). This is common, as observed by the negative correlation between flesh firmness and juiciness (Obando et al., 2008), because firmer fruit are usually less juicy (Obando et al., 2008). Moreno et al. (2008) reported *ff10.2* at harvest and the unpublished results of these experiments (Obando et al., 2008) would also confirm *wfh10.2*. However, juice density was not affected during ripening in contrast with the results of Obando et al. (2008) who also reported the effect of the QTL of flesh firmness *fj10.2* but only at harvest time.

The expression of GDSL esterase/lipase (MELO3C011939) located in LG X was higher in SC10-2 than in PS (Figure 10), and SC10-2 also showed lower ethylene production (Figure 1). The expression of this gene could be associated with a delay or partial inhibition of some ethylene-dependent flesh or whole fruit softening in SC10-2 compared with PS, because GDSL expression in apple correlated negatively with ethylene production (Zhang et al., 2015b) and in tomato it was expressed in the epidermis of developing fruit (Girard et al., 2012).

Of the potential candidate genes responsible for the increase in textural traits in SC10-2 compared with PS (Figure 2), the glycerophosphoryl diester phosphodiesterase (*Cm*GDE1; MELO3C013101) gene has been found to play a role in plant cell wall remodelling (Hayashi et al., 2008; Ge et al., 2011).

DEGs exclusive to postharvest ripening time. Of the 23 genes that changed over time (Table 1; Supplementary Tables 1 and 4, Annex C; Figure 12), we found typical ones in melon ripening changes such as polygalacturonase (*Cm*DHL92; MELO3C009970) (Table 1; Supplementary Tables 1 and 4 (Annex C); Figure 12) associated with cell-wall disassembly (Rose et al., 1998) or other ongoing processes typical of maintaining homeostasis or hydrolase activity and hydrolyzing O-glycosyl compounds. For example, processes such as providing feed for diminished mitochondrial respiration during postharvest ripening (*Cm*MPC1; MELO3C007517) (Table 1; Supplementary Tables 1 and 4 (Annex C); Figure 12), or increased protein detoxification (*Cm*DTX; MELO3C017343) (Table 1; Supplementary Tables 1 and 4 (Annex C); Figure 12). Some of these genes, such as the one that is responsible for the increase of ABA receptors such as abscisic acid-insensitive 5-like protein 4 isoform X1 (*Cm*ABREX; MELO3C014384) (Table 1; Supplementary Tables 1 and 4, Annex C; Figure 12), or the gene that decreases in auxin-responsive protein (*Cm*IAA71; MELO3C000885) (Table 1; Supplementary Tables 1 and 4 (Annex C); Figure 12), would deserve further investigation due to the possible similarity of non-climacteric ripening with the antagonist interaction of auxin and abscisic acid with ethylene during ripening in other non-climacteric and climacteric fruits (Daminato et al., 2013; Lu et al., 2018).

Physiological traits and gene expression. The expression of *Cm*ACO2 (MELO3C019735) increased during ripening, a trend that was more pronounced in PS than in SC10-2 (Figure 10) (Figure 11), which agrees with the faster ripening of PS (including higher level of respiration, ethylene production, and the synthesis of some ethylene-dependent VOCs, such as acetate esters and non-acetate esters; Figures 1 and 4) in PS. The melon 1-aminocyclopropane-1-carboxylic acid oxidase gene (*Cm*ACO) is an ethylene-responsive gene that catalyses the conversion of ACC to ethylene during fruit ripening and is of greater importance in climacteric fruit (Ezura et al., 2008; Barry et al., 2000). However, *Cm*ACO2 has been mapped in LG VIII (Moreno et al., 2008), and consequently some eQTLs upstream of *Cm*ACO2 but affecting its expression should be mapping in LG X. On the other hand, other genes with no differential expression in our non-climacteric experiment such as *CmACO1* have been associated with ethylene biosynthesis, together with *CmACS1* and *CmACS5* in climacteric melon fruit ripening (Guo et al., 2017).

More than four transcription factors were identified in our experiment; *Cm*WRKY33 (MELO3C009127), *Cm*TCP15 (MELO3C01208), *Cm*GATA5 (MELO3C023350) and *Cm*ERF027 (MELO3C005630) (Table 1). Almost all of them increased in SC10-2 more than in PS during the ripening time and therefore could be partially responsible for the delay of ripening in the NIL SC10-2 compared with PS.

The expression of *Cm*WRKY33 (ethylene-responsive gene during climacteric ripening (Wang et al., 2017), *Cm*GATA5 (transcriptional regulators involved in metabolism regulation) (Zhang et al., 2015a), and *Cm*ERF027 (ethylene-inducible genes during fruit ripening) (Sharma et al., 2010; Pirrello et al., 2011; Liu et al., 2014) decreased from their highest level of expression before 4 d of ripening but remained higher in SC10-2 than in PS throughout the postharvest ripening time (Figures 10 and 11). The behaviour of these genes was apparently opposite to that of ethylene production, particularly during the first 4 days of non-climacteric melon ripening of both lines (Figure 1), and so they could be associated with the ripening differences between climacteric and non-climacteric melon fruit (Obando-Ulloa et al., 2008). *Cm*GATA5 could interact with cis-acting elements involved in the light regulation of nuclear genes encoding chloroplast glyceraldehyde-3-phosphate dehydrogenase (GAPDH) and therefore glycolysis (Jeong and Shih, 2003) or other processes such as ribosome biogenesis, mRNA metabolism or lipid A biosynthesis (Tarze et al., 2018; Zala et al., 2018).

Glycerophosphodiester phosphodiesterases (*Cm*GDPDL4; MELO3C013101) showed similar gene expression to GATA5 in our experiment, with higher levels after 8 d of ripening in SC10-2 than in PS (Figure 10). This gene could be involved in fatty acid metabolism to further provide glycerol phosphate and alcohol resulting from the hydrolysis of deacylated glycerophospholipids (Yanaka et al., 2007).

*Cm*NAC18 (MELO3C016540) expression was stable in SC10-2 but was present at higher levels than in PS, where it increased after harvest to reach levels similar to that of SC10-2 (Figure 10). This *CmNAC-NOR* domain transcription factor was expressed in the flesh of both climacteric and non-climacteric melon types, but is probably transcriptionally regulated in non-climacteric types because it has been considered a candidate gene for the QTL *ETHQV6.3* of climacteric fruit ripening (Guo et al., 2013). NAC transcription factor is a positive regulator of

fruit ripening, affecting ethylene synthesis and carotenoid accumulation (Guo et al., 2013; Zhu et al., 2013), but NAC also interacts with other genes in the complex regulatory network of fruit ripening in tomato (Zhu et al., 2013). All the above information suggests a potential association of higher NAC levels with the delayed fruit ripening of the NIL SC10-2 compared with PS.

In our experiment, a MADS-box transcription factor was identified among the DEGs with higher relative expression in PS than in SC10-2 and decreasing with ripening time (Figure 11). Some MADS-box genes are involved in the development and ripening of non-climacteric fruits such as bilberry (Jaakola et al., 2010) and strawberry (Daminato et al., 2014; Seymour et al., 2011).

Postharvest VOCs vs gene expression. In previous investigations, noticeable differences were found between the aroma profile of NIL SC10-2 and the control PS at harvest (Dos-Santos et al., 2013; Obando-Ulloa et al., 2010). Some VOCs were lacking from the NIL SC10-2 compared with PS [some ketones and alcohols, and one acid (e.g. 2-phenylpropanoic acid)], but also the concentration of aldehydes (e.g. 2,4-dimethylbenzaldehyde, 2-methylpropanal and 2-methylbutanal) were higher in the NIL (Dos-Santos et al., 2013). In our experiment, too, the levels of many aldehydes (C6-up to C12) remained high during ripening (Figure 4), in agreement with the above results at harvest, but ketone levels were similar, and acids were hardly present (data not shown). The NIL SC10-2 was characterized by a lower ketone content than PS (Dos-Santos et al., 2013). In our experiment, aldehydes, alcohols, acids and terpenes were higher in SC10-2 than in PS during postharvest ripening, while the opposite trend was seen for acetate and non-acetate esters (Figure 3). As regards other VOCs, they increased in SC10-2 and were higher than in PS at the end of the experiment (Figure 3), which could be due to senescence processes (Obando-Ulloa et al., 2009b).

As regards other metabolic pathways associated with the differences between PS and SC10-2 QTLs and volatiles, these were related in part to the free L-amino acid metabolism, in which phenylalanine, valine, isoleucine and leucine (Dos-Santos et al., 2013) are considered aroma precursors (Gonda et al., 2010). The higher aldehyde content was typical of the NIL SC10-2 and associated with its high flesh firmness at harvest compared with PS (Dos-Santos et al., 2013), in agreement with our results (Figs. 2 and 3). Aldehydes are key-flavor compounds synthesized from α-keto acids particularly in melon fruit (Gonda et al., 2010).

The expression of GDPDL4 (MELO3C013101) in our experiment also was higher in SC10-2 than in PS from harvest to 8 d of postharvest ripening (Figure 10), which might explain the abundance of alcohols in this NIL (Figure 3), as explained above for *Cm*GDPDL4 gene. In this case, glycerophosphodiester phosphodiesterase (GDPD) hydrolyzes the glycerophosphodiesters into sn-glycerol-3-phosphate (G-3-P) and the corresponding alcohols (Gaude et al., 2008), particularly in fruit tissue (Cheng et al., 2011). GDPD have also been seen to be involved in the generation of phosphatidic acid, a precursor of diacylglycerol and inorganic phosphate by phosphatidate phosphatase (Li et al., 2006; Nakamura et al., 2009), or in the degradation of phospholipids into diacylglycerol and inorganic phosphate (Nakamura et al., 2005).

*Cm*LOX18 (MELO3C024348) was highly expressed in the NIL SC10-2 compared with PS, which had higher levels of aldehydes, terpenes, alcohols and other VOCs than PS (Figs. 3; 10 and 11). *Cm*LOX genes are involved in generating fruit aroma in melon (Tang et al., 2015; Zhang et al., 2017). Our results support that this is the LOX family gene responsible for producing LOX enzyme during ripening to form C6 VOCs such as hexanal, (Z)-3-hexenal, and (Z)-3-hexenol in fruit, and is also possibly involved in the formation of straight-chain ester (Zhang et al., 2017).

The enzymatic reaction of LOX causes polyunsaturated fatty acids, such as linoleic acid and linolenic acid, to generate hydroperoxide (HPO) (Liavonchanka et al., 2006; Andreou et al., 2009). HPO is catalyzed by hydroperoxide lyase (HPL) to produce aldehydes, which are catalyzed by alcohol dehydrogenases (ADH) to produce alcohols (Tang et al., 2015; Jin et al., 2016). The final step in ester biosynthesis is catalyzed by alcohol acyl-transferase (AAT) (Tijet et al., 2011; Manríquez et al., 2006). Apparently, the higher expression of *Cm*ADH1 (MELO3C019548) in PS than in SC10-2 would explain the differences in aroma production between lines because in PS the former volatile metabolism would be more advanced and produce alcohols as precursors of the esters (Figure 3). In fact, Chen et al. *(2016)* observed the upregulation of *Cm*ADH1 after the addition of aldehydes, which indicated its potential function in aroma volatile or ester synthesis. Also, in climacteric tomato fruit, Moummou et al. (2012*)* suggested a function of ADH1 of supplying C5 and C6 volatiles from the lipoxygenase pathway. Alcohol acetyl transferases (*Cm*AAT1 and *Cm*AAT2) showed similar relative expression in both lines in our experiment (data not shown), and it is known that the expression of AAT in PS is very low (Gonda et al., 2010). Therefore, we conclude that *Cm*ADH1 is a key enzyme, particularly in PS aroma formation.

12-oxophytodienoate reductase 2 (*Cm*OPR2; MELO3C008075) expression was also higher in SC10-2 than in PS (Figure 10). Therefore, *Cm*OPR2 may increase the activity of the β-oxidation pathway because the oxophytodienoate reductase family (OPR) is expressed throughout the plant and co-localises with enzymes involved in the β-oxidation of very long fatty acids in peroxisomes (Strassner et al., 2002). In fact, the levels of most of the aldehydes in SC10-2 were higher than in PS (Figure 3), and, consequently, alcohol dehydrogenase 1 (*Cm*ADH1; MELO3C019548) and cinnamyl alcohol dehydrogenase 1 (*Cm*CAD1; MELO3C018492) genes showed lower expression in SC10-2 than in PS. *Cm*CAD1 expression was also lower in SC10-2 than in PS (Figure 11), which might have some influence in the conversion of cinnamyl aldehydes into alcohols, using NADPH (quinone oxidoreductase) as a cofactor (Sattler et al., 2010).

In our experiment, the expression of allene oxide synthase gene (*Cm*AOS; MELO3C010910) was higher in SC10-2 than in PS (Figure 10). *Cm*AOS could be involved in the jasmonic acid metabolism from hydroperoxides because AOS and allene oxide cyclase mediated in the branch of α-linolenic acid metabolism for the formation of jasmonic acids (Ezura et al., 2008; Wasternack et al., 2002). Two AOS isozymes identified in oriental melon fruit catalysed 10-OPDA and 12-OPDA formation, and other AOS isozymes, identified in different ripening stages, are differently regulated by genetic and environmental factors (Ezura et al., 2008). Concomitant with jasmonic acid biosynthesis and ethylene production, AOS was

downregulated during fruit development but increased again in the last stage of peach fruit development (Torrigiani et al., 2012). However, in SC10-2 the hypothetical stimulation of ethylene production by *Cm*AOS during the first 8 d of ripening was not evident (Figures 1 and 10).

Aminoacid metabolism. The 3-isopropylmalate dehydratase small subunit 3-like (*Cm*IPMI3; MELO3C005518) was generally higher in the NIL SC10-2 than in PS, except at 12 d (Figures 10 and 11), in contrast to the behaviour of 3-isopropylmalate dehydratase large subunit (*Cm*IIL1; MELO3C003344) at harvest and in senescence (Figures 9 and 11). Generally, 3-isopropylmalate dehydratase catalyses the stereo-specific isomerisation of 2-isopropylmalate and 3-isopropylmalate, via the formation of 2-isopropylmaleate, which is the second step in the biosynthesis of the aminoacid leucine (Gruer et al., 1997), a potential precursor of some VOCs of interest here, such as 2-ethylhexan-1-ol, nonanol, or 4-Isopropylhexanol (isomer 1) (Figure 4; Table 1).

By contrast, fumarylacetoacetase (*Cm*FAH; MELO3C007433) expression and alanine aminotransferase (CmALT-2; MELO3C010686) expression were always higher in PS than in NIL SC10-2 (Figures 10 and 11). FAH is involved in the metabolism of amino acids (phenylalanine and tyrosine) and the catabolism of its derivatives (Gruer et al., 1997), Phe being of interest as a potential precursor of some VOCs of interest here such as methanetiol or S-methyl ethanethioate (Figure 4; Table 1). ALT is active during melon ripening and it has positive correlation with chlorophyllase and carotenoid accumulation (Freilich et al., 2015).

Gene expression and other postharvest changes. Dihydroflavonol 4-reductase (*Cm*DFR4; MELO3C020508), the first committed enzyme of the flavonoid biosynthetic pathway including VOC regulation (Hua et al., 2013), showed higher expression in SC10-2 compared with PS particularly after 4 days of postharvest ripening (Figure 10).

Apparently in SC10-2, *Cm*PAL (MELO3C017811) gene expression is a response to late fruit ripening, which contrast with the lack of changes during ripening in PS (Figure 10). Melon fruit phenylalanine ammonia-lyase (PAL), the first enzyme of phenylpropanoid biosynthesis, is transcriptionally induced in response to fruit ripening and *Cm*PAL gene expression follows the expression kinetics of the ethylene biosynthetic genes during fruit development (Diallinas et al., 1994).

*Cm*ACT (MELO3C005591) regulatory domain expression showed higher levels in SC10-2 than PS during the first 8 days of postharvest ripening (Figure 10), and the ACT was generally found in enzymes involved in amino acid and purine metabolism (Aravind et al., 1999; Chipman et al., 2001), some of them probably associated with the formation of volatile precursors.

*Cm*TCP15 (MELO3C012086) expression was always higher in SC10-2 than in PS (Figure 10). TCP proteins are involved in biological processes of potential interest for future studies in other aspects of factors affecting melon fruit ripening, such as hormone pathways (Aguilar-Martinez et al., 2007), mitochondrial biogenesis (Hammani et al., 2011), and regulation of the circadian clock (Giraud et al., 2010).

The higher expression of the bidirectional sugar transporter *Cm*SWEET7 (MELO3C016259) in SC10-2 compared with PS after 4 days of ripening (Figure 10) could be related with fruit senescence, environmental adaptation, the sugar accumulation pattern, or other essential fruit biological processes (Zhou et al., 2014; Guo et al., 2014; Shammai et al., 2018). Some QTLs in LG X associated with the soluble solids content and individual sugars (sucrose, fructose) in other genetic backgrounds have also been mapped (Perpiñá et al., 2016). Although sugars are not discussed here, SC10-2 is less sweet than PS at harvest. In fact, several QTLs that negatively affect sensory traits have been mapped at harvest in LG X (sweetness, taste and global sensorial quality appreciation) compared with PS, due to lower sucrose, total sugars and sucrose equivalents (Obando-Ulloa et al., 2009a). One hypothesis for the mechanism of *Cm*SWEET7 gene would be to delay ripening in order to supply additional sugar resources to the fruit metabolism in SC10-2. This hypothesis would agree with results in tomato, where SWEET transporter was also upregulated in the lines with a high fructose-to-glucose ratio (Shammai et al., 2018).

GalLDH catalyses the oxidation of the last precursor, L-galactono-γ-lactone, to ascorbic acid (Hancock et al., 2005). In our experiment, evidence of differences in ascorbate metabolism would include lower L-galactono-1, 4-lactone dehydrogenase (*Cm*L-GalLDH; MELO3C018576) relative expression with higher expression in PS than in SC10-2 until 8 d (Figures 9 and 11). Other evidence is the report on one QTL that reduced levels of ascorbic at harvest in LG X (Obando-Ulloa et al., 2009a).

As regards GDP-mannose-3',5'-epimerase (*Cm*GME; MELO3C004377), in our experiment it showed higher expression in NIL SC10-2 than in PS but it decreased after 12 d (Figure 9). The GME, which converts GDP-d-mannose to GDP-l-galactose, is generally considered to be a central enzyme of the major ascorbate biosynthesis pathway in higher plants (Gilbert et al., 2009). The formation of GDP-d-mannose is the initial step in the pathway of ascorbate biosynthesis, and GDP-d-mannose is also a known precursor for the synthesis of d-mannose, l-fucose and l-galactose, and therefore for hemicelluloses such as (galacto)glucomannans and for the pectin rhamnogalacturonan II (Reiter et al., 2001). This biosynthesis could be of importance for maintaining melon flesh firmness during ripening (Figure 2).

4.2 General processes deduced from transcriptome analysis:

As regards the comparison between lines, many of the genes downregulated in cluster 1.1 (Supplementary Table 1 (Annex C)) were related with regulation of the cellular macromolecule biosynthetic process, the RNA biosynthetic process and other genes depending to the photosynthesis processes. The genes related to photosynthesis during fruit ripening are also downregulated in non-climacteric grape (Pilati et al., 2007).

As regards the postharvest ripening time effect (Supplementary Table 2 (Annex C)), clusters 2.2 and 2.4 were the most closely associated with this effect (Figure 8), a sharp rise in the expression of DEGs being evident in the two non-climacteric genotypes. The same is true for clusters 1.4, 1.5 and 1.6, considering the comparison between lines (Figure 8; Supplementary Table 1 (Annex C)). Most genes of both group of clusters were related to

biosynthetic processes (Supplementary Tables 1 and 2 (Annex C)), for example those related to ethylene-regulated and ripening-related genes (Alexander et al., 2002), including those involved in ethylene synthesis, fruit texture, and aroma volatile production (Pech et al., 2008).

Considering the postharvest ripening time effect, most DEGs of clusters 2.3, 2.5 and 2.6 showed higher expression in PS than in SC10-2 and a trend to increase (Figure 8). The same is true for clusters 1.5 and 1.6, but considering the comparison between lines over time (Figure 7). The DEGs of the above mentioned clusters were generally related to molecular function and cellular components (Supplementary Tables 1 and 2 (Annex C)), and these genes affected in one way or another to flesh firmness and whole fruit hardness because they showed the opposite trend and led to fruit softening. As regards other non-climacteric NILs (i.e. SC7-2) with firm flesh and other climacteric melons and fruits in general, it has been reported that flesh textural changes are accompanied by loss of neutral sugars, solubilisation and depolymerisation of the polysaccharides of the cell wall, and rearrangements of their associations, as the result of the combined action of several cell wall-modifying enzymes such as polygalacturonase and others (see above), acting in both pectic and hemicellulosic fractions (Dos-Santos et al., 2011; Rose et al., 1998). Consequently, it is these changes that probably make the PS fruit texture less resistant and juicier than SC10-2.

4.3 Implications for the future:

The genetic changes described not only explain new aspects of the non-climacteric fruit ripening - such as the control of non-climacteric ripening, respiration and ethylene biosynthesis and action, texture, or aroma production - but also provide a few new ideas about the changes in different metabolic pathways. These could help growers and researchers to develop new melon varieties with good quality traits with a long shelf life, for example by manipulating genes such as *CmNAC18* or *CmSWEET7*.

To better understand the effect of introgressions in LG X and the transcriptional regulation of metabolic genes during fruit ripening, other specific development and textural transcriptome analyses are necessary, probably using NILs with shorter introgressions such as SC10-1, SC10-3 or SC10-4, or the development of NILs with shorter introgressions that are more useful for melon breeding (Argyris et al., 2015a and 2015b). Recently, Perpiñá et al. (2017) developed a breeding line with a short introgression (between markers CMPSNP172 and CMPSNP65) in LG X from the cultivar Ginsen Makuwa (closely related to SC) (Monforte et al., 2003), that also extended fruit shelf-life and maintained flesh firmness but in the *Charentais* genetic background (a climacteric type). This would confirm the presence of genes involved in fruit ripening in LG X from different germplasm sources which effects are stable in different genetic backgrounds and, therefore, with a potential for breeding. Unfortunately, the DEGs studied here with more detail that mapped in LG X (MELO3C012476, MELO3C012086 or MELO3C011939) were not within the LG X region flanked by the above mentioned SNPs).

5. Conclusions:

The introgressions in LG X delayed non-climacteric fruit ripening as demonstrated by physiological and textural traits: reduced ethylene production and respiration rates, and, consequently delayed softening and loss of whole fruit hardness and an increase in flesh juiciness. The ripening delay consequently delayed senescence processes, which impacted on volatile production in the NIL SC10-2 compared with PS, as evidenced by acetate esters and non-acetate esters levels in this experiment. The clusters of the DEGs associated with the factor postharvest ripening time show that most genes are upregulated over time, while the comparison between lines showed noticeable gene upregulation in SC10-2 compared with PS at harvest or after 8 d of ripening) and downregulation in 29% of the DEGs.

The transcriptome of the melon NIL SC10-2 and its parental PS suggest that the genes involved in the ripening pathways are regulated dynamically to activate the expression of some genes during ripening time (e.g. *Cm*LOX18, *Cm*AOS, *Cm*DFR4, *Cm*OPR2, *Cm*GATA5, *Cm*TCP15 and *Cm*GDSL esterase/lipase process genes) and to delay the expression of others (genes related to cellular component such as *Cm*NAC18, *Cm*NADH1, *Cm*CAD1, *Cm*ACO2 and *Cm*ADH1) during fruit ripening.

The identified genes differentially expressed during the ripening time and located in different linkage group (other than LG X in the case of *Cm*NADH1, *Cm*TCP15 and *Cm*GDSL esterase/lipase) might be controlled by an expression QTL (eQTL) located in LG X that would contribute to, or be involved in, crosstalk with other QTLs associated with differential textural traits and aroma volatile production in NIL SC10-2 and PS during postharvest ripening. Generally, all the genes identified in this experiment (whether or not located in the LG X) were affected by the introgression in LG X.

GENERAL DISCUSSION:

VI. GENERAL DISCUSSION:

Melon fruit texture depends on the environmental conditions and the genotype (Aurand et al., 2012; Dos-Santos et al., 2011 and 2013; Sams, 1999), as confirmed our researches conducted during three seasons reported before using different textural traits (mainly flesh firmness, hardness and juiciness). Also, it was demonstrated the association among aroma volatile organic compounds and these traits which are ripening-dependent also in non-climacteric fruit. However, it is evident that the seasonal effects dramatically affected aroma volatiles to a higher extent that textural traits, probably due to alterations in biochemical pathways affecting fruit ripening (Ezura et al., 2008; Guo et al. 2017; Ríos et al., 2017). In fact, noticeable differences in gene expression were found between PS and SC10-2 during postharvest ripening of both non-climacteric lines, as it has been evidenced in climacteric ones (Lu et al., 2018).

Also, according to Dos-Santos et al. (2013), the introgressions in LG X did not affect the melon climacteric behavior but higher flesh firmness, lower whole fruit hardness and different juice textural properties were observed in LG X. In contrast, our results show clear differences comparing the NIL SC10-2 and its parental PS at harvest in both seasons (S1 and S2) and some differences comparing with Dos-Santos et al. (2013) results, which means that the VOCs production may be affected by the environmental and seasonal effects. The same NIL can behave differentially in different seasons depending to the environmental growth conditions.

Textural traits were important from harvest to postharvest point of view in this experiment using non-climacteric melons, but sometimes the effect of the introgression in LG X was not only affecting textural traits at harvest or aroma volatiles as previously reported (Dos-Santos et al., 2013; Moreno et al., 2008; Obando et al., 2008), but also during postharvest ripening, in contrast with other QTLs mapped in tomato (Causse et al., 2002) or melon. Probably the reason for that is the large introgression covering almost the entire LG X (Argyris et al., 2015a; Eduardo et al., 2005), that could be the reason of its effect on respiration rate and ethylene production during fruit ripening (Figure 1, Chap. V.). Due to the length of these introgressions in LG X, some of the QTLs of the aroma volatiles could be independent of textural traits (Dos-Santos et al., 2013).

The putative QTL identified for texture in the introgression in LG X was somehow linked to aroma pathways. In Dos-Santos et al. (2013) as in our experiment, a QTL for benzaldehyde was mapped in LG X. In other experiment, exogenous L-phenylalanine increased the levels of aromatic volatiles such as benzaldehyde (Gonda et al., 2010). Therefore, it is possible that benzaldehyde, is a precursor of some of the aromatic volatiles formed (Boatright et al., 2004), and that this QTL may be associated with phenylalanine supply as precursor.

In a previous study (Dos-Santos et al., 2013), the higher flesh firmness of the NIL SC10-2 was mainly associated with volatiles linked to pathways which putative precursors are L-amino acids (2-methylbutanal), fatty acids ((Z)-non-6-enal; (Z)-non-3-en-1-ol) and alfa-methylstyrene (1-phenylethanone). On the other hand, in our study we found also discriminant compounds associated with textural traits. For example, some aldehydes (2-methylbutanal;

benzaldehyde; (Z)-non-6-enal; nonanal), alcohols (4-Isopropylcyclohexanol (Isomer 1); (Z)-non-3-en-1-ol) and ketones (1-phenylethanone) are generally derived from the L-amino acids phenylalanine, isoleucine, valine and leucine pathways (Dos-Santos et al., 2013). L-isoleucine one of the putative precursors of some discriminant compounds in our experiments (Pang et al., 2012; Gonda et al., 2006 and 2010; Table 2, Chap. IV., Figure 2, Chap. IV.) increase the levels of 2-methylbutanal and nonanal (Gonda et al., 2010; Singh et al., 2003), and feeding of exogenous L-*Ile* into strawberry peduncles or in apples resulted in enhanced levels of the structurally corresponding 2-methylbutyl volatile derivatives. in fruits (Rowan et al., 1996; Matich and Rowan, 2007).

According to Baldwin et al. (2000), the aliphatic compounds (2-Methylpentane) and alcohols are derived from free fatty acids and by β-oxidation fatty acids can also produce shorter chains compounds (Sanz et al., 1997). Both pathways the aldehydes can be reduced to alcohols by alcohol dehydrogenase catalyzation (Speirs et al., 1998).

Differences in volatiles among NIL SC10-2 and PS were probably mainly associated with differences in enzymatic activities (Dos-Santos et al., 2013). In previous investigations (Obando-Ulloa et al., 2010), noticeable differences were found between the aroma profile of NIL SC10-2 and control PS. The NIL SC10-2 was characterized by a lower ketones content than PS (Dos-Santos et al., 2013). In our experiment, aldehydes, alcohols, acids, terpenes, increased significantly in SC10-2 comparing with PS during ripening, in contrary of acetate esters, non-acetate esters were higher PS while other VOCs were increased in SC10-2 to overtake PS in the finale of the experiment, which could be associated with differences in the metabolism (Dos-Santos et al., 2013).

As regards other metabolic pathways associated with the differences between PS and SC10-2 QTLs and volatiles, these were related in part to the free L-amino acid metabolism, in which phenylalanine, valine, isoleucine and leucine (Dos-Santos et al., 2013) are considered aroma precursors (Gonda et al., 2010; Qi et al., 2012; Smit et al., 2009). The higher aldehyde content characterized the firmer NIL SC10-2 (Dos-Santos et al., 2013). The aldehydes are potent flavor compounds obtained via the corresponding α-keto acid and are regarded as key-flavor compounds in many foods (Smit et al., 2009), particularly in melon fruit (Gonda et al., 2010).

Transcriptomic analysis from RNA-seq revealed 2954 differentially expressed genes (DEGs) having introgression or introgression x ripening time effects and 2068 DEGs postharvest ripening time effect. Only 909 DEGs were exclusive of the introgression, and only 23 DEGs were exclusive of postharvest ripening time. Clusters of ripening time (six) revealed a general upregulation vs. harvest with slight interaction genotype x ripening time in 68.8% DEGs of four clusters, while clusters of the genotype (seven) revealed that the introgression generally produced noticeable differences in DEG upregulation or downregulation vs. the control PS in four clusters and 30% and 7.3% DEGs, respectively. Major functions of the DEGs associated with introgression or ripening time were delimited. About thirty-four genes were affecting direct and/or indirectly in the delay of ripening of SC10-2 versus PS in general and particularly to respiration rate, ethylene production, textural traits and volatile production and probably differential non-climacteric response. Of the former genes, we studied with more

detail at least three that mapped in the introgression in linkage group (LG) X, and thirty-one outside it. The apparent control by an eQTL located in LG X of genes such as *Cm*NAC18, a candidate for climacteric pattern (Ríos et al., 2017), suggest certain link between climacteric and non-climacteric ripening control.

By summarizing according to our results, the melon non-climacteric NIL SC10-2 behavior at harvest was different than during postharvest ripening. With higher flesh firmness, higher hardness and lower juiciness comparing to the parental PS, the NIL SC10-2 was characterized at harvest of two seasons, but during postharvest ripening, the melon non-climacteric NIL SC10-2 behaved differentially with differentially expressed genes than different enzymatic activity which affect the VOCs production and the fruit traits comparing to PS.

The physiological changes not only revealed new aspects of the non-climacteric fruit ripening such as aroma production and maturity but provided an important link with changes in these pathways and could be used in the selection of new biomarkers of melon at different stages of maturity. The introgression in the linkage group X allows to the NIL SC10-2 to behave differently provoking a maturity and senescence delay. These findings provide an understanding of metabolism pathways, which help to develop new approaches for exploring the pathways that are controlling non-climacteric melon ripening in the different ripening stages and also with the non-climacteric melon NIL SC10-2 commercially important traits can help to develop new melon varieties with good quality traits with a long shelf life.

GENERAL CONCLUSIONS:

VII. GENERAL CONCLUSIONS:

We intended in these researches to study the association among aroma volatiles and other traits in near-isogenic line SC10-2 with firm flesh texture comparing to the parental PS and to study the seasonal effects on QTLs specially located on LG X of texture and aroma volatiles, using multivariate statistics applying to differentiate aroma volatiles and to map texture and aroma QTLs, and transcriptomic analysis during postharvest ripening. As general conclusions of these researches we found:

- The introgression in the LG X in the NIL SC10-2 delayed fruit ripening compared with the non-climacteric parental PS, as evidenced in physiological behavior (reduced ethylene production and respiration rate), fruit textural (higher whole fruit hardness and firmness, reduced flesh juiciness) and reduced and delayed presence of some type of aroma volatiles (esters).

- The seasonal effects on the introgression were less important in textural traits but more relevant in volatile organic compound production.

- The season with better environmental conditions had more volatile compounds than season with worse growing conditions irrespective of the presence or not of introgression in LG X. VOCs of different classes showed a significant introgression effect, most of them alcohols and aldehydes with lower levels in PS than in SC10-2 during ripening (methanethiol, S-methyl ethanethioate, hexanal, octanal, (Z)-non-6-enal, nonanal, decanal, 4-isopropylcyclohexanol (isomer 1), 2-ethylhexan-1-ol, nonan-1-ol, (E)-4-phenylbut-3-en-2-one). Decanal and hexanal also showed a significant time effect together with nonanal but decreased with the ripening time.

- The transcriptome of the melon NIL SC10-2 and its parental PS suggest that the genes involved in the ripening pathways are regulated dynamically to activate the expression of some genes (i.e biosynthesis *Cm*LOX18, *Cm*AOS, *Cm*DFR4, *Cm*OPR2, *Cm*GATA5, *Cm*TCP15 and *Cm*GDSL esterase/lipase process genes) and to delay the expression of others (i.e genes related to cellular component such as *Cm*NAC18, *Cm*NADH1, *Cm*CAD1, *Cm*ACO2 and *Cm*ADH1) during fruit ripening.

- The identified genes differentially expressed located in different linkage group (others than LG X) might be controlled by an expression QTL (eQTL) located in LG X that would have a contribution in differential textural traits and aroma volatile production between the NIL SC10-2 and PS during ripening.

ANNEXES:

Annex A:

Supplementary Material:

Methodology to remove strong ouliers of non-climacteric melon fruit aroma at harvest obtained by HS-SPME GC-MS analysis.

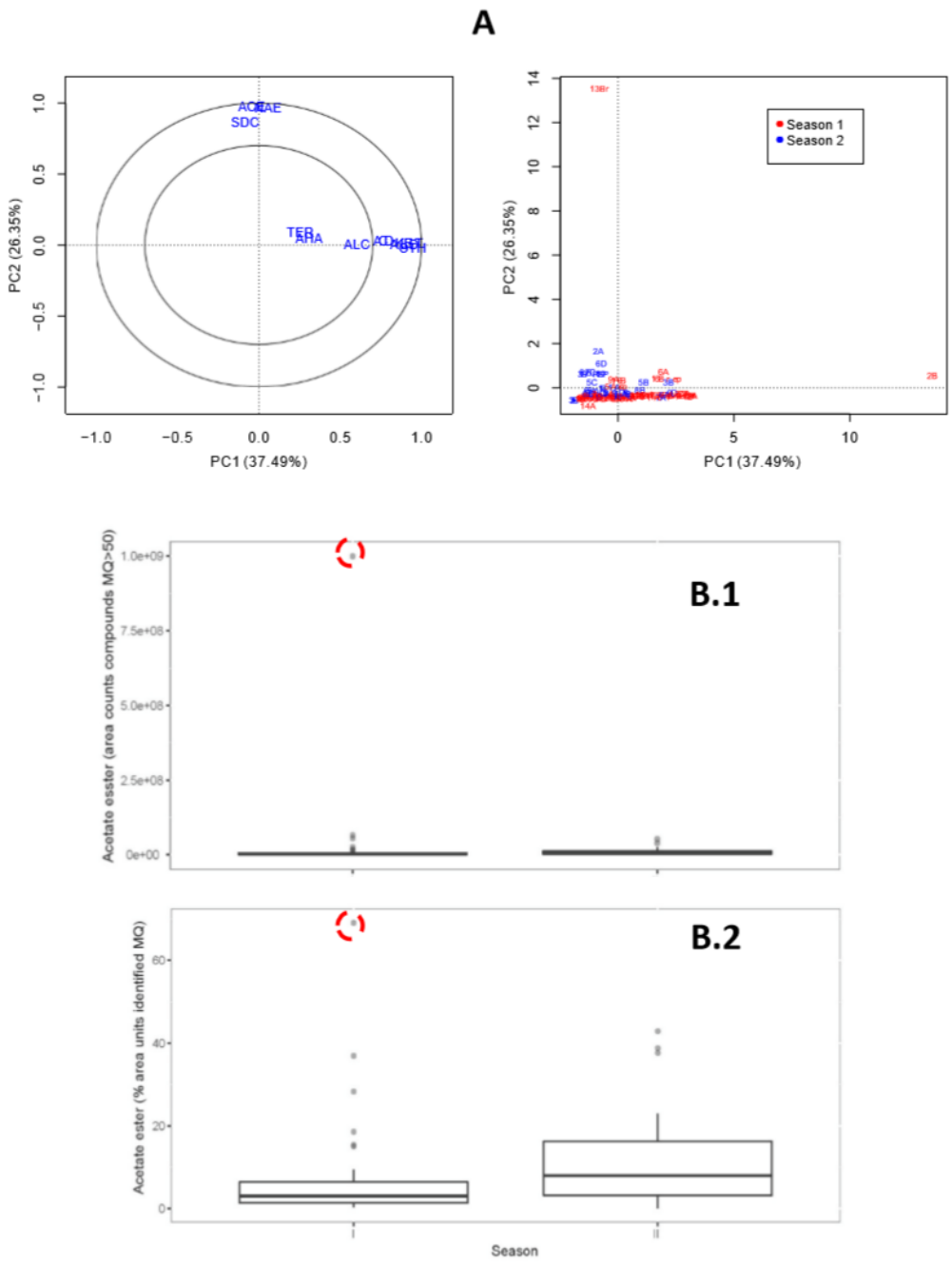

Supplementary Figure 1. A. Correlation (left) and score (right) plots of the first two components of the PCA (with 63.84% of variance explained) applied to compound classes of aroma variable based on total areas (only compounds with match quality > 50 without exogenous compounds), obtained in two seasons. This graph contained an outlier (former 13Br, S1) removed in a previous version of this manuscript because it was a mistake due to the confusion with a climacteric cultivar of melon with abundance of esters and sulfur derived compounds. Another data (2B, S2) was considered a real outlier. AEC, acetate ester; NAE, non-acetate ester; ALD, aldehyde; ALC, alcohols, KET, ketones; SDC, sulfur derived-compounds; TER, terpenes; AHA, alkanes and aliphatic compounds; OTH, other compounds. Circles represent r^2 = 50% and 100% variability explained by the components. **B.** Example of outliers in acetate esters (ACE) of two aroma variables obtained in two seasons. Bold red circles indicate the fruit 13Br fruit of season 1. **B.1.** Box whisker plot of area counts of ACE with MQ>50. **B.2.** Box whisker plot of percentages of ACE based on total areas of compounds with match quality >50 and without exogenous compounds.

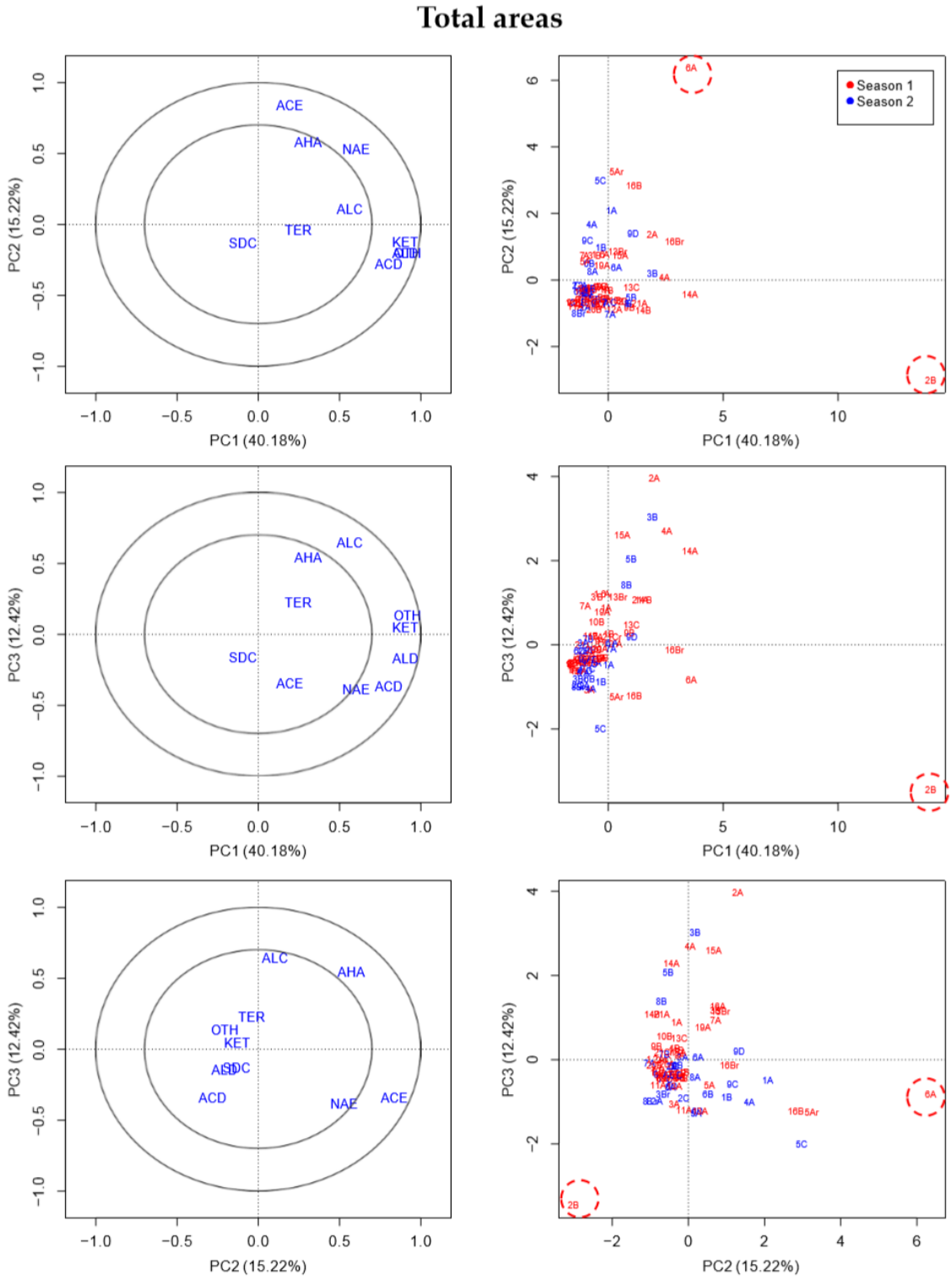

Supplementary Figure 2.A Results of the principal component analysis (PCA) to verify potential outliers (dashed lines in different colors) in compound classes of aroma variable based on total areas (only compounds with match quality > 50), obtained in two seasons. The areas of compound classes were not normalized to the response of the internal standard (1-phenylethanol). ACE, acetate ester; NAE, non-acetate ester; ALD, aldehyde; ALC, alcohols, KET, ketones; SDC, sulfur derived-compounds; TER, terpenes; AHA, alkanes and aliphatic compounds; OTH, other compounds. Circles represent r^2 = 50% and 100% variability explained by the components.

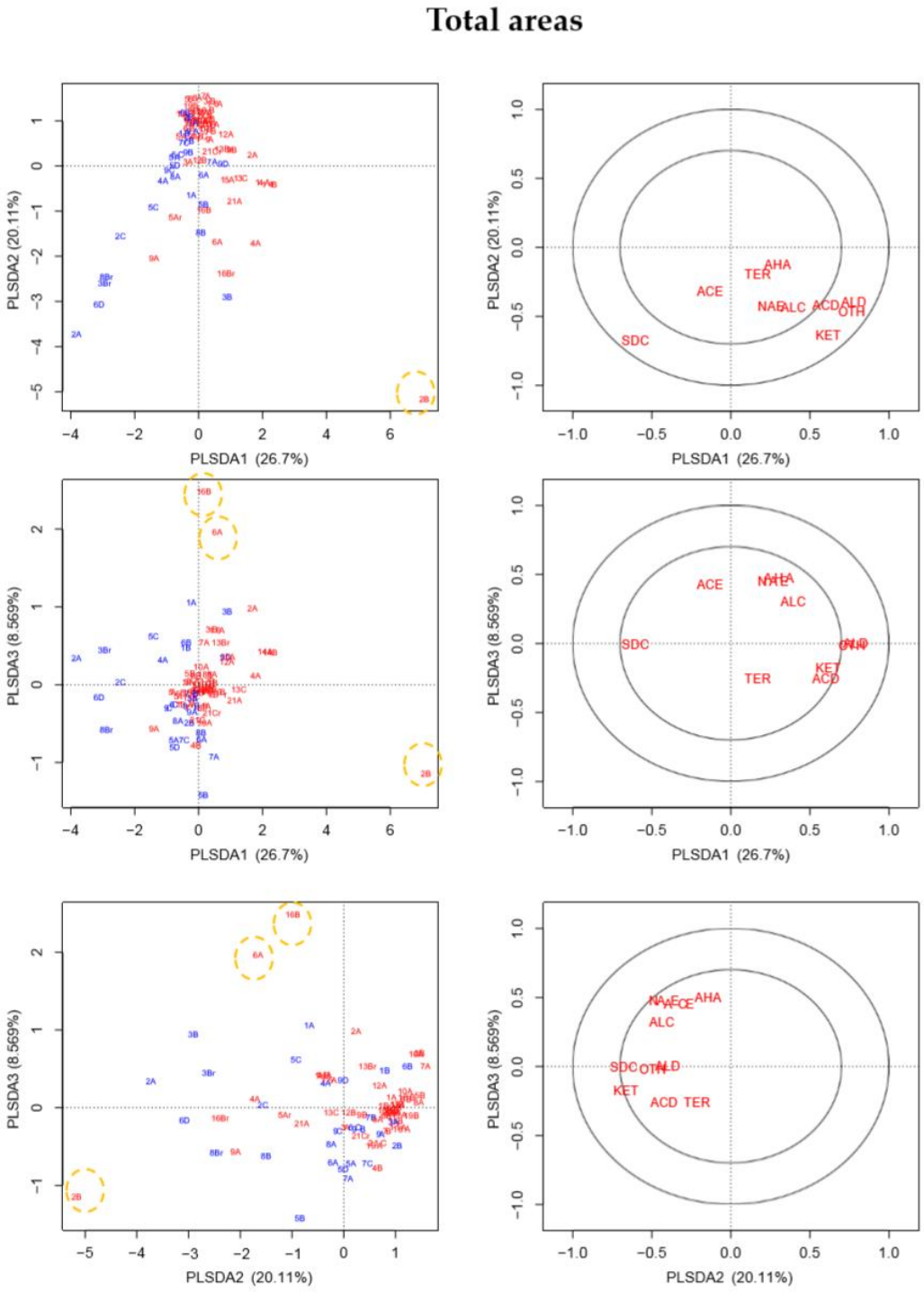

Supplementary Figure 2.B Results of the partial least-squares discriminant analysis (PLS-DA) to verify potential outliers (dashed lines in different colors) in compound classes of aroma variable based on total areas (only compounds with match quality > 50), obtained in two seasons. The areas of the compound classes were normalized to the response of the internal standard (1-phenylethanol) each season. ACE, acetate ester; NAE, non-acetate ester; ALD, aldehyde; ALC, alcohols, KET, ketones; SDC, sulfur derived-compounds; TER, terpenes; AHA, alkanes and aliphatic compounds; OTH, other compounds. Circles represent r^2 = 50% and 100% variability explained by the components.

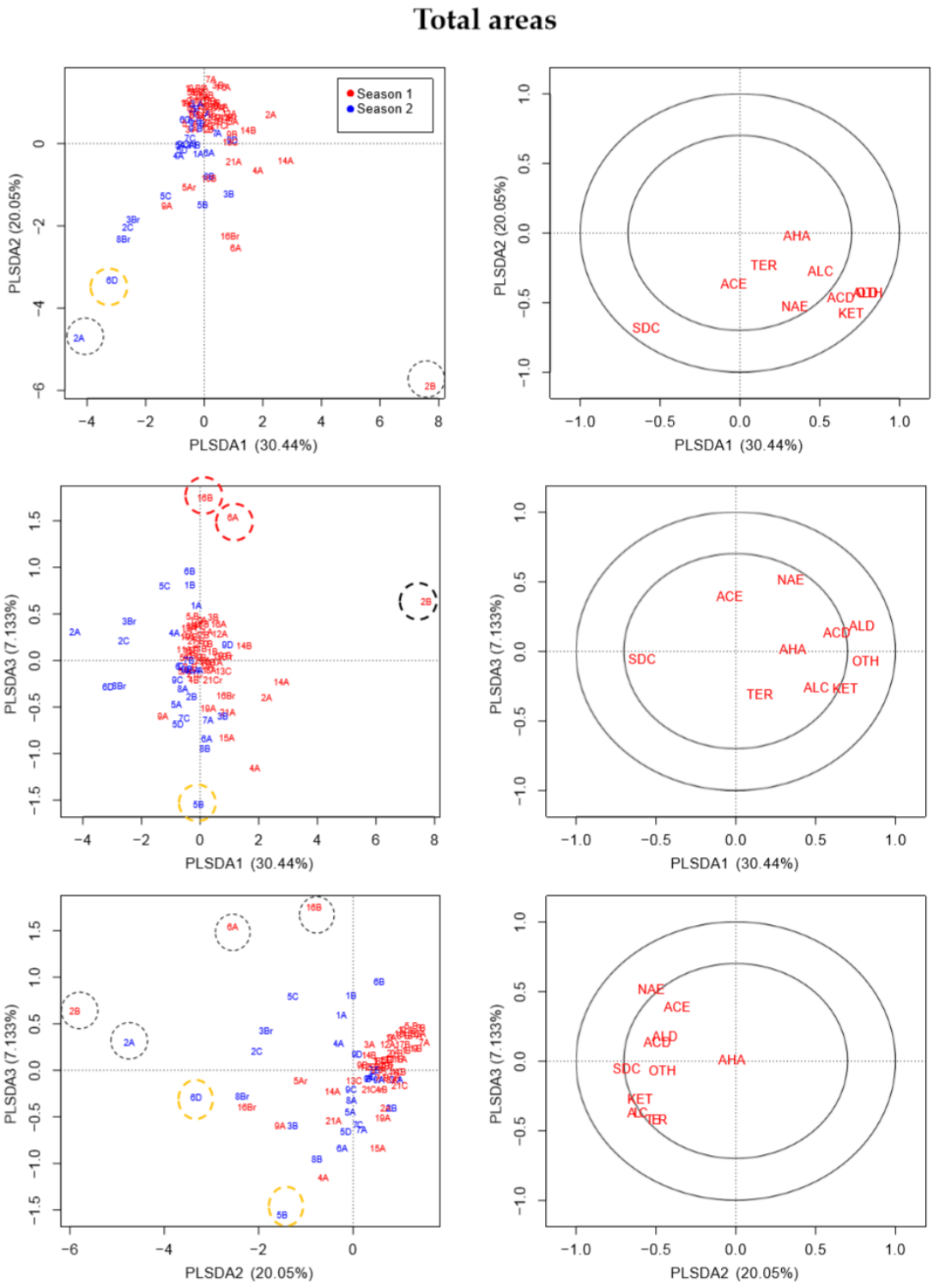

Supplementary Figure 2.C Results of the partial least-squares discriminant analysis (PLS-DA) to verify potential outliers (dashed lines in different colors) in compound classes of aroma variable based on total areas (only compounds with match quality > 50), obtained in two seasons. The areas of the compound classes were not normalized to the response of the internal standard (1-phenylethanol) each season. ACE, acetate ester; NAE, non-acetate ester; ALD, aldehyde; ALC, alcohols, KET, ketones; SDC, sulfur derived-compounds; TER, terpenes; AHA, alkanes and aliphatic compounds; OTH, other compounds. Circles represent r^2 = 50% and 100% variability explained by the components.

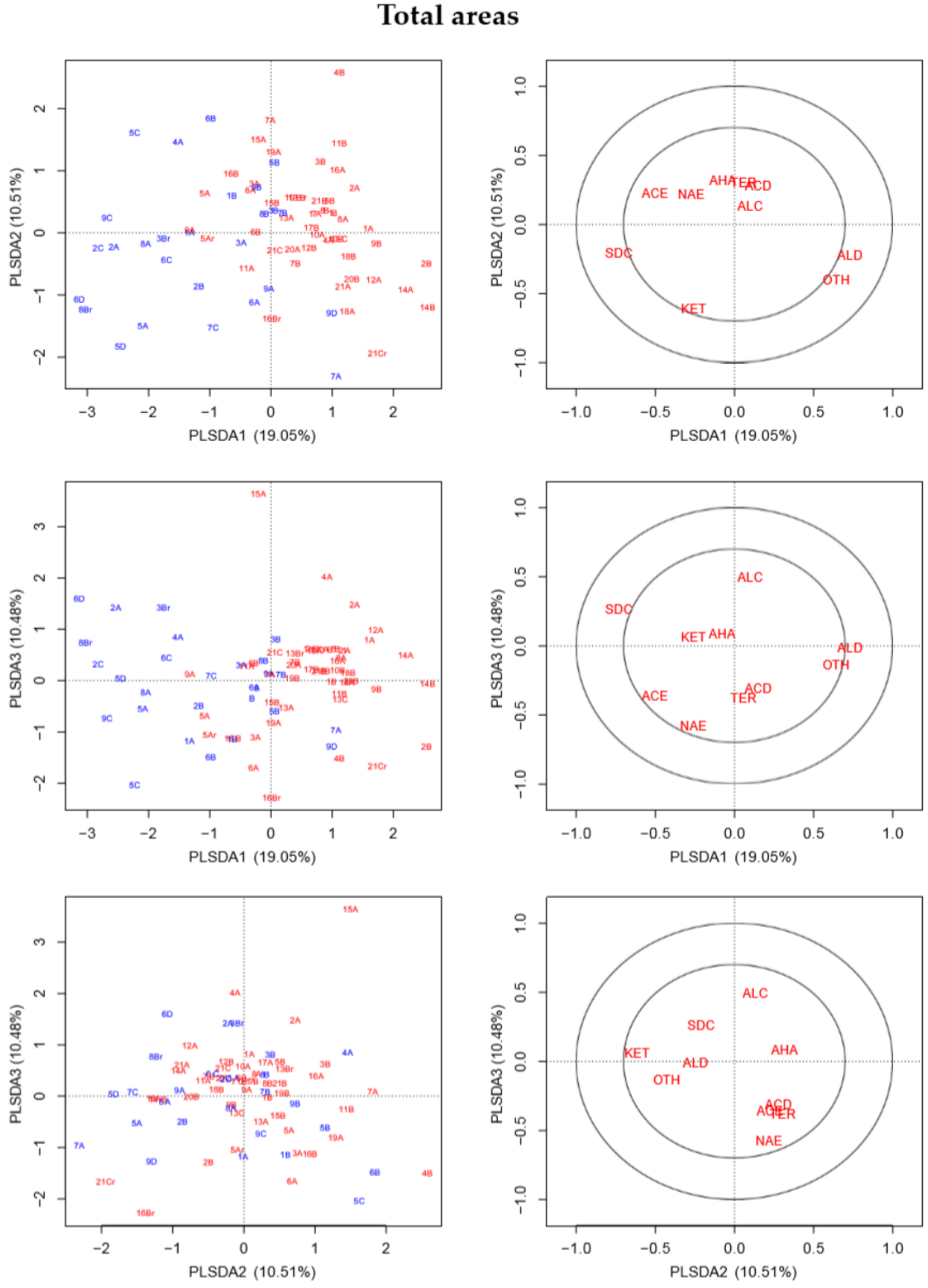

Supplementary Figure 3. Results of the partial least-squares discriminant analysis (PLS-DA) to verify potential outliers in compound classes of aroma variable based on total area counts of such compounds with match quality >50, and without exogenous compounds, obtained in two seasons. ACE, acetate ester; NAE, non-acetate ester; ALD, aldehyde; ALC, alcohols, KET, ketones; SDC, sulfur derived-compounds; TER, terpenes; AHA, alkanes and aliphatic compounds; OTH, other compounds. Circles represent r^2 = 50% and 100% variability explained by the components.

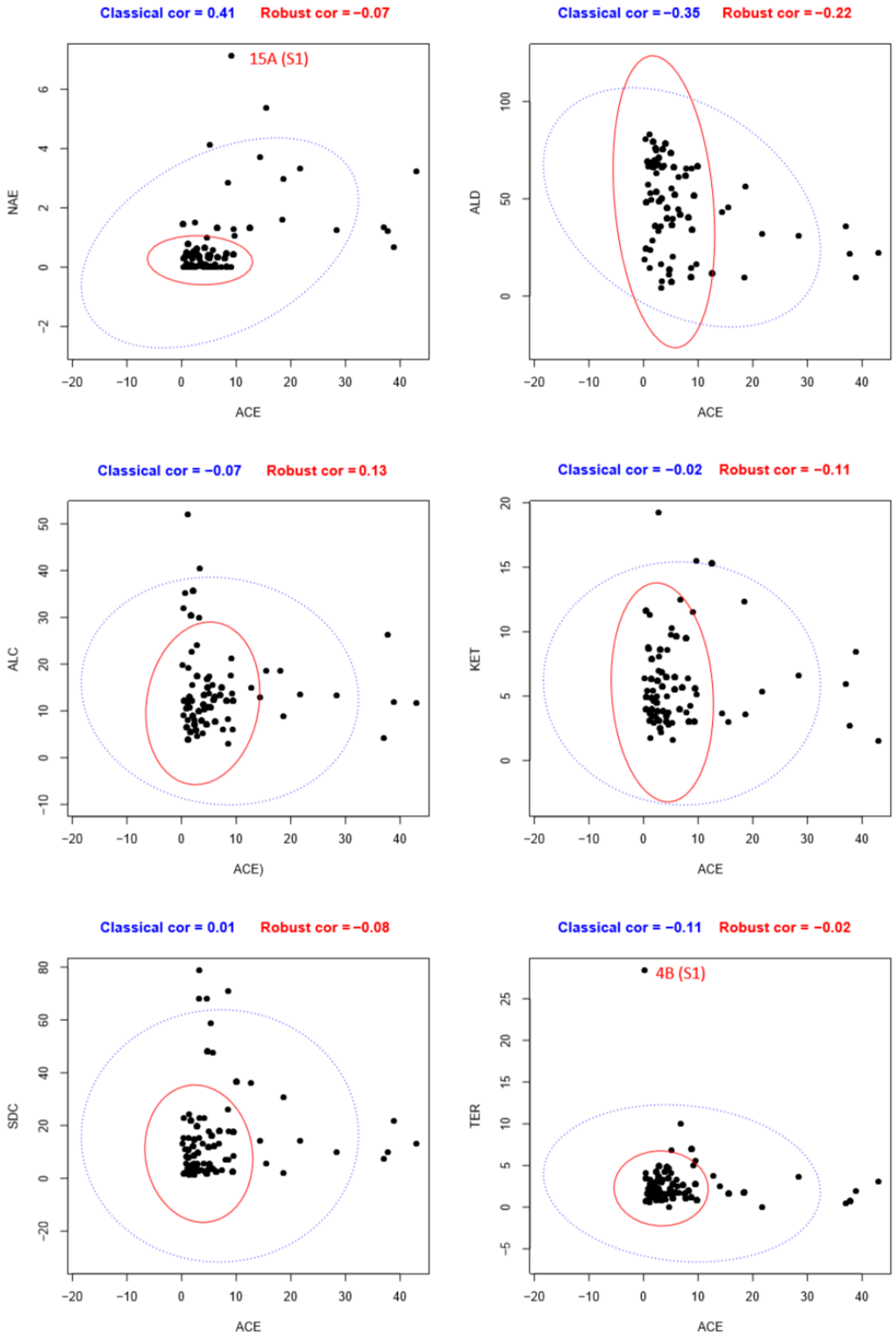

Supplementary Figure 4.A. Results of the correlation analysis to verify potential outliers in compound classes of aroma variable of percentages of different compound classes based on total areas of such compounds with match quality >50, and without exogenous compounds, obtained in two seasons. ACE, acetate ester; NAE, non-acetate ester; ALD, aldehyde; ALC, alcohols, KET, ketones; SDC, sulfur derived-compounds; TER, terpenes; AHA, alkanes and aliphatic compounds; OTH, other compounds. Classical and robust 97.5% confidence ellipses of the data (blue and red, respectively). Robust method used 50% of the observations for Minimum Covariance Determinant (MCD estimations. The strong outliers labeled are the fruits 4B and 15A from season 1.

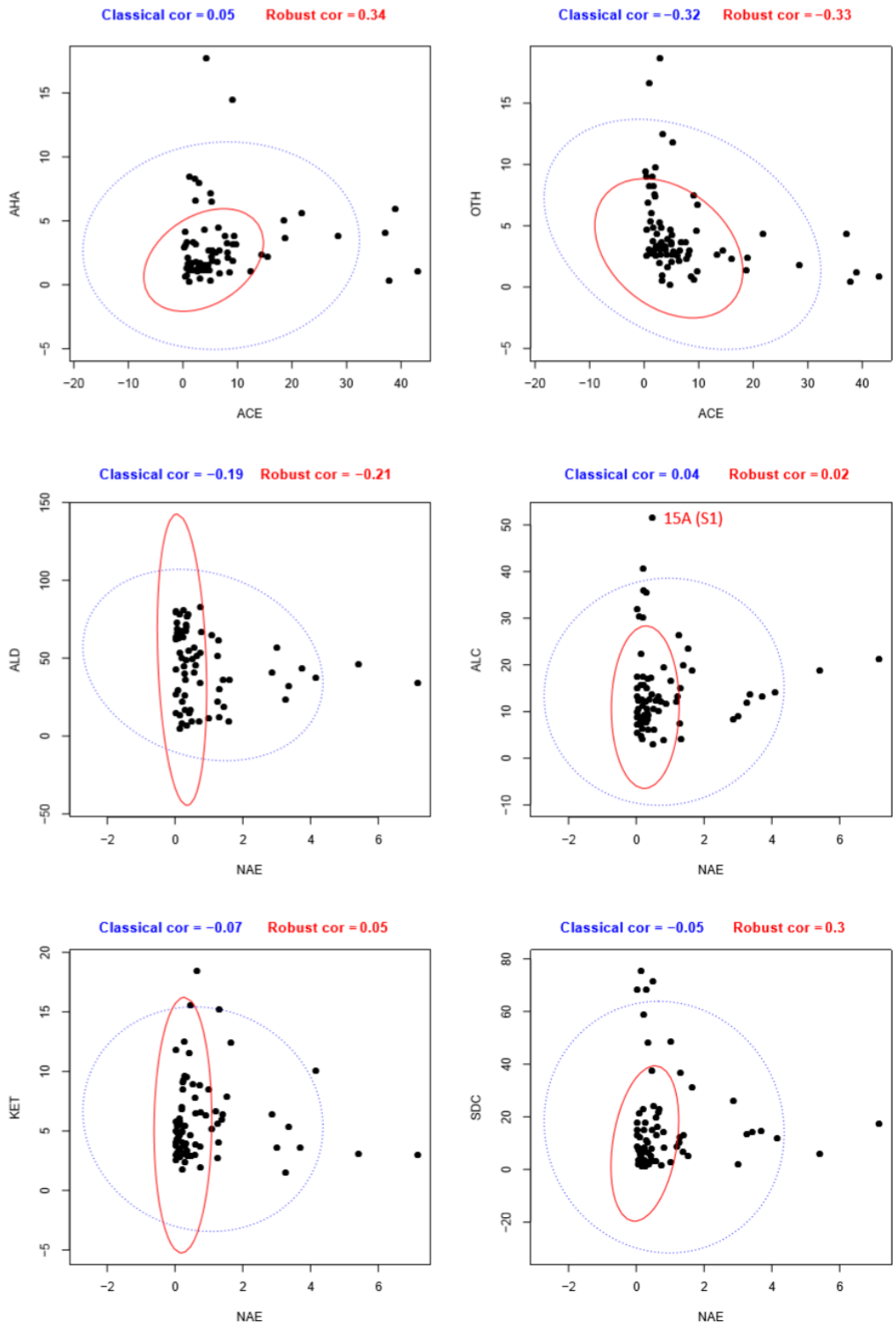

Supplementary Figure 4.B. Results of the correlation analysis to verify potential outliers in compound classes of aroma variable of percentages of different compound classes based on total areas of such compounds with match quality >50, and without exogenous compounds, obtained in two seasons. ACE, acetate ester; NAE, non-acetate ester; ALD, aldehyde; ALC, alcohols, KET, ketones; SDC, sulfur derived-compounds; TER, terpenes; AHA, alkanes and aliphatic compounds; OTH, other compounds. Robust method used 50% of the observations for Minimum Covariance Determinant (MCD estimations. The strong outliers labeled are the fruits 4B and 15A from season 1.
Strong outliers labeled are the fruits 4B and 15A of season 1.

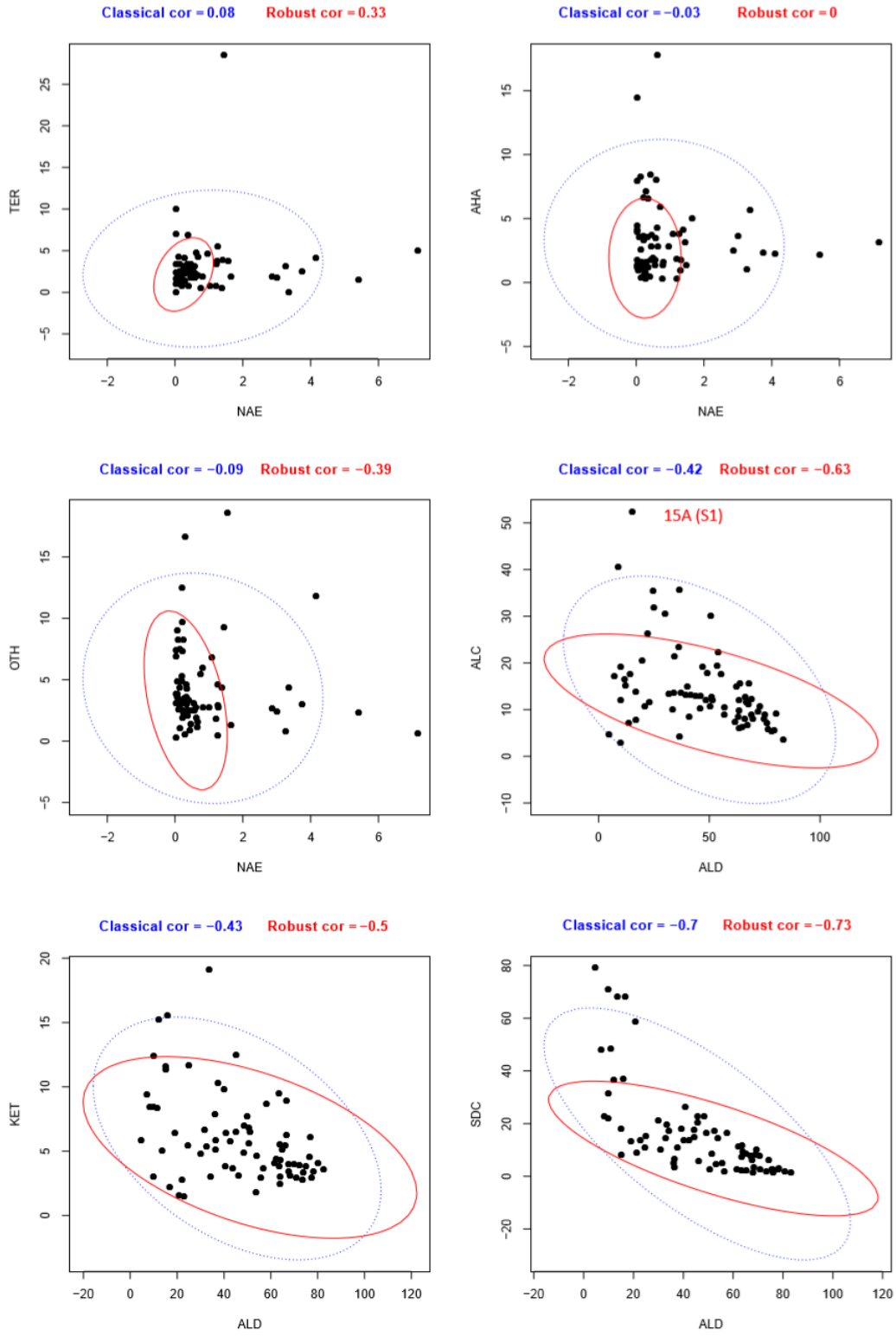

Supplementary Figure 4.C. Results of the correlation analysis to verify potential outliers in compound classes of aroma variable of percentages of different compound classes based on total areas of such compounds with match quality >50, and without exogenous compounds, obtained in two seasons. ACE, acetate ester; NAE, non-acetate ester; ALD, aldehyde; ALC, alcohols, KET, ketones; SDC, sulfur derived-compounds; TER, terpenes; AHA, alkanes and aliphatic compounds; OTH, other compounds. Robust method used 50% of the observations for Minimum Covariance Determinant (MCD estimations. The strong outliers labeled are the fruits 4B and 15A of season 1.

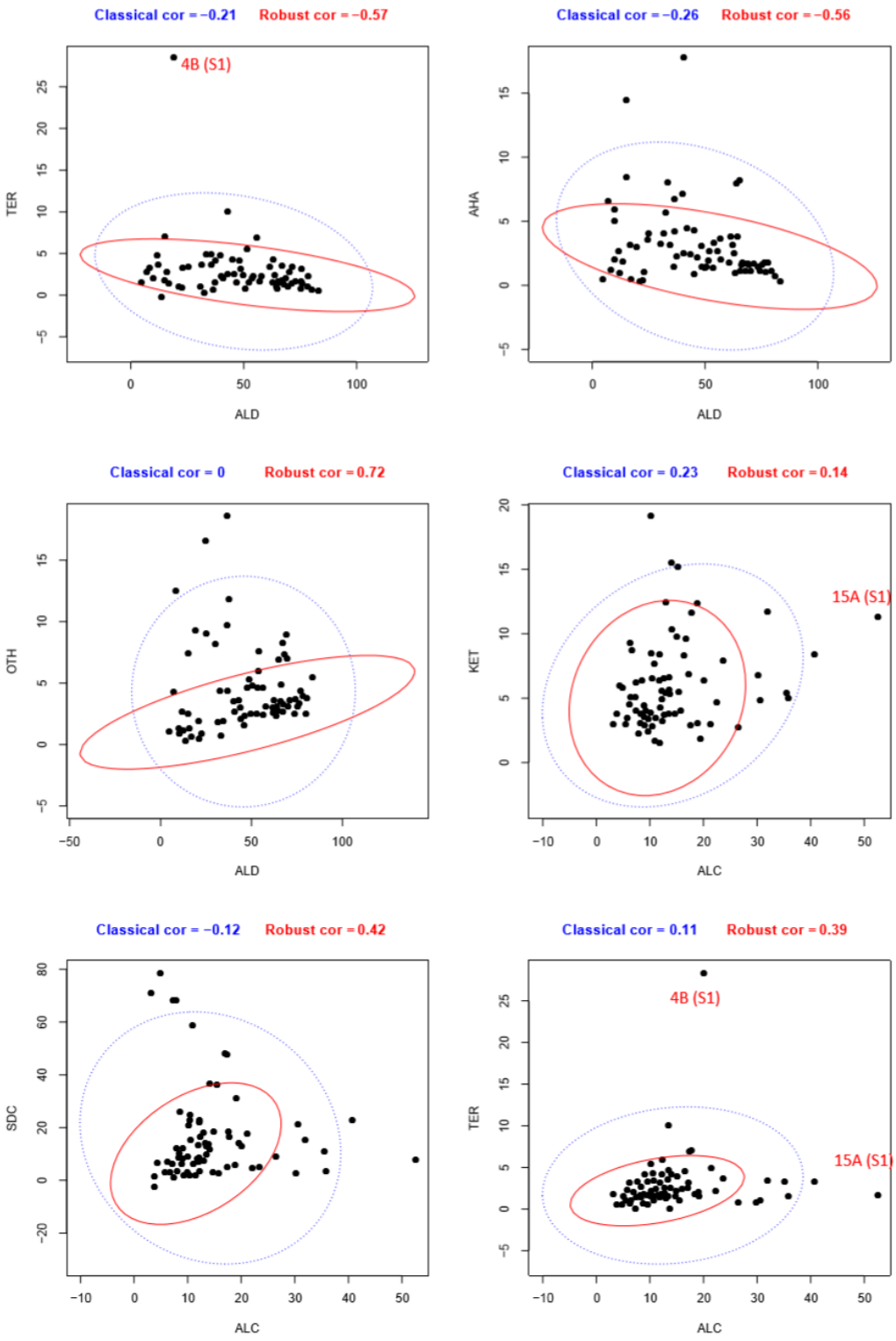

Supplementary Figure 4.D. Results of the correlation analysis to verify potential outliers in compound classes of aroma variable of percentages of different compound classes based on total areas of such compounds with match quality >50, and without exogenous compounds, obtained in two seasons. ACE, acetate ester; NAE, non-acetate ester; ALD, aldehyde; ALC, alcohols, KET, ketones; SDC, sulfur derived-compounds; TER, terpenes; AHA, alkanes and aliphatic compounds; OTH, other compounds. Classical and robust 97.5% confidence ellipses of the data (blue and red, respectively). Robust method used 50% of the observations for Minimum Covariance Determinant (MCD estimations. . Strong outliers labeled are the fruits 4B and 15A of season 1.

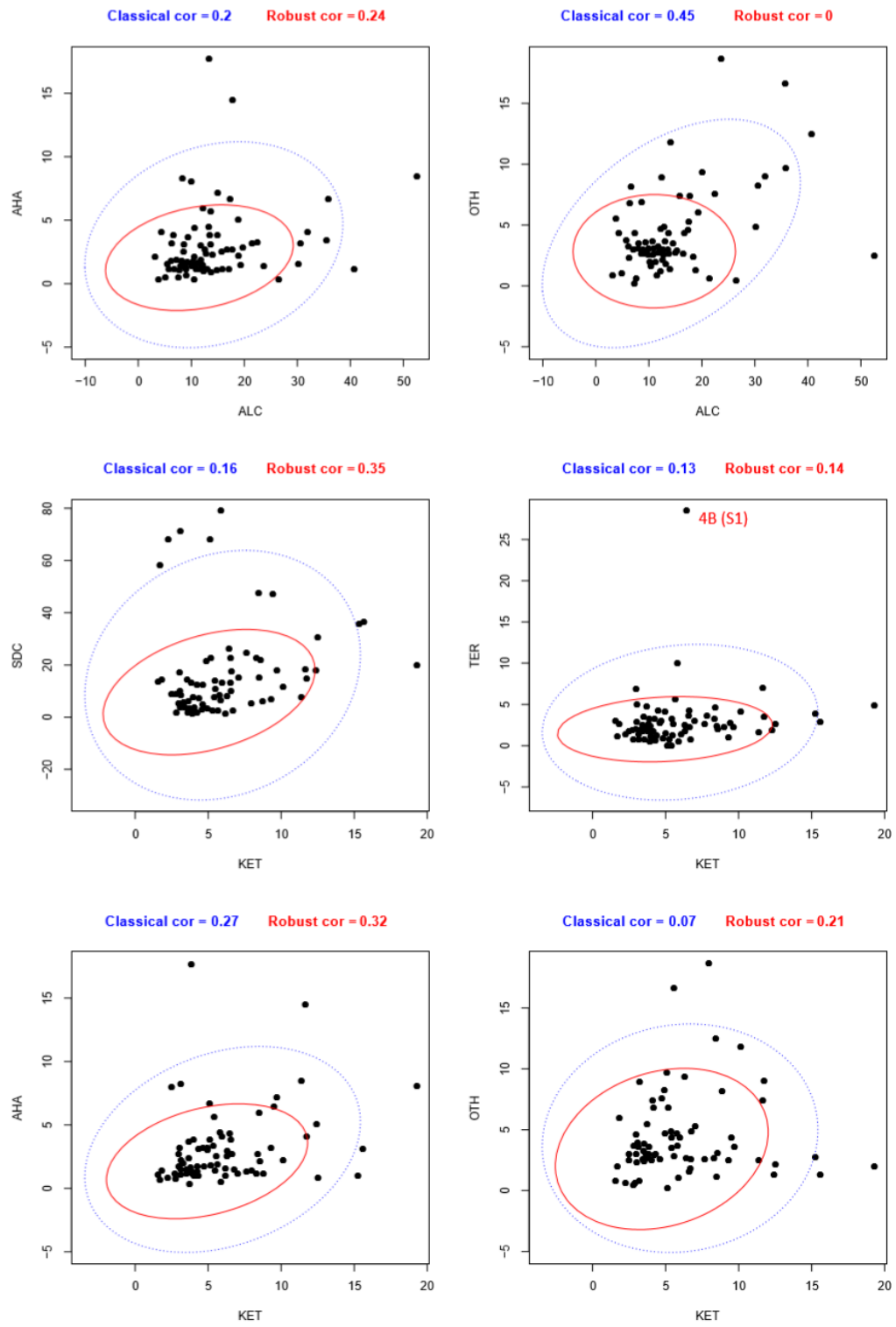

Supplementary Figure 4.E. Results of the correlation analysis to verify potential outliers in compound classes of aroma variable of percentages of different compound classes based on total areas of such compounds with match quality >50, and without exogenous compounds, obtained in two seasons. ACE, acetate ester; NAE, non-acetate ester; ALD, aldehyde; ALC, alcohols, KET, ketones; SDC, sulfur derived-compounds; TER, terpenes; AHA, alkanes and aliphatic compounds; OTH, other compounds. Classical and robust 97.5% confidence ellipses of the data (blue and red, respectively). Robust method used 50% of the observations for Minimum Covariance Determinant (MCD estimations. The strong outlier labeled is the fruits 4B of season 1.

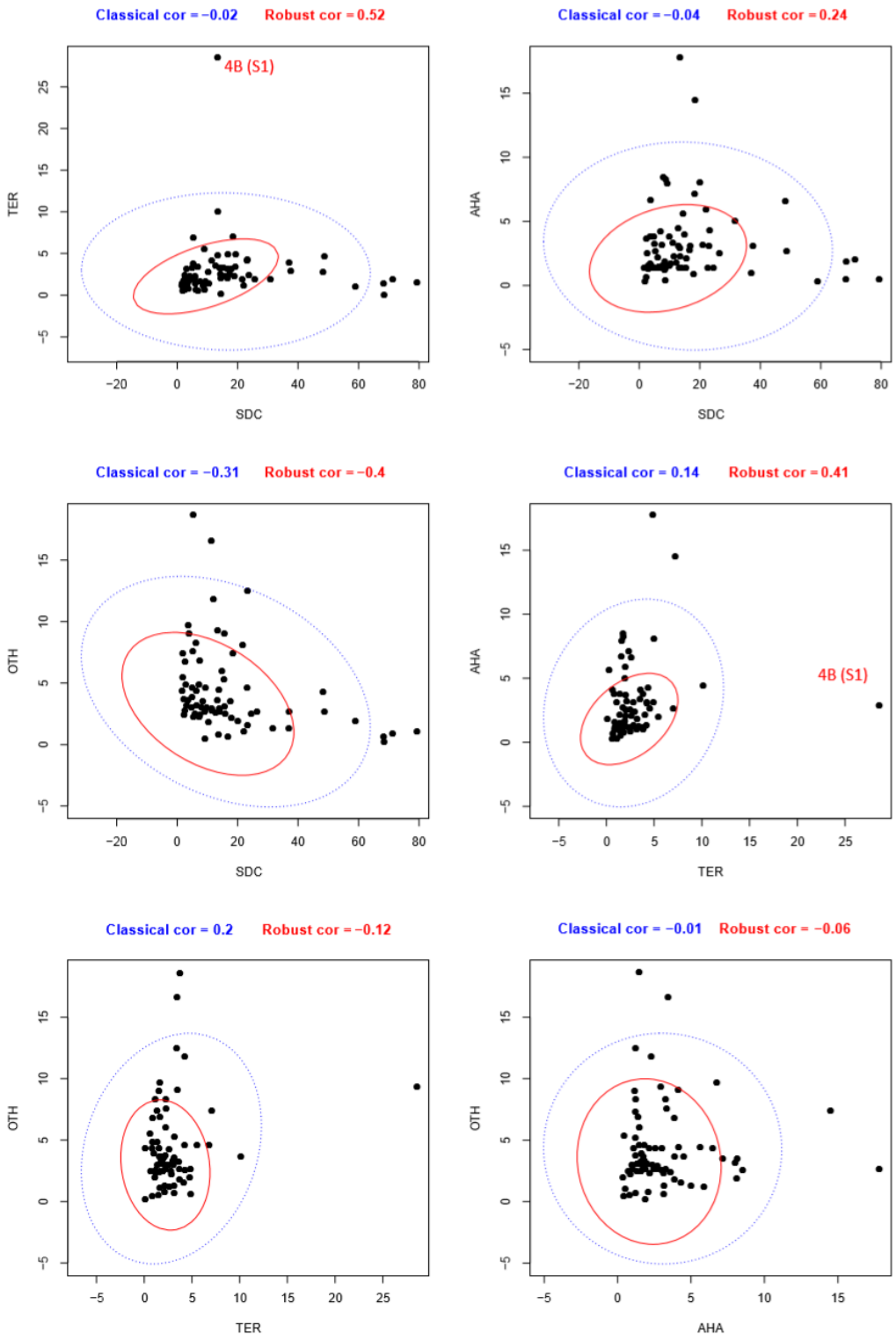

Supplementary Figure 4.F. Results of correlation analysis to verify potential outliers in compound classes of aroma variable of percentages of different compound classes based on total areas of such compounds with match quality >50, and without exogenous compound. ACE, acetate ester; NAE, non-acetate ester; ALD, aldehyde; ALC, alcohols, KET, ketones; SDC, sulfur derived-compounds; TER, terpenes; AHA, alkanes and aliphatic compounds; OTH, other compounds. Classical and robust 97.5% confidence ellipses of the data (blue and red, respectively). Robust method used 50% of the observations for Minimum Covariance Determinant (MCD estimations. The strong outlier labeled is the fruits 4B of season 1.

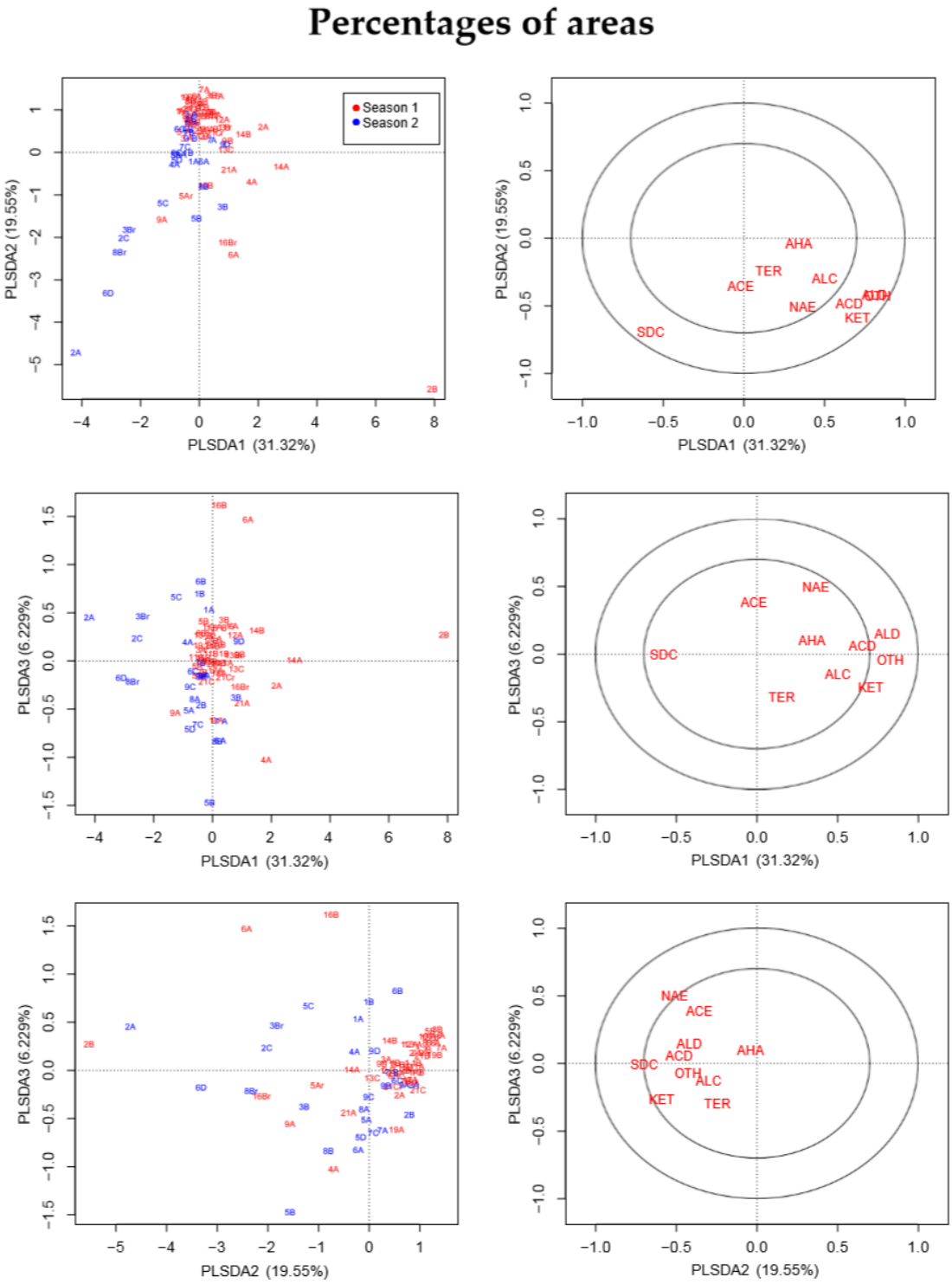

Supplementary Figure 5. Results of partial least-squares discriminant analysis (PLS-DA) after removing strong outliers of fruits 4B and 15A (season 1) in compound classes of aroma variable of percentages of different compound classes based on total areas of such compounds with match quality >50, and without exogenous compounds, obtained in two seasons. ACE, acetate ester; NAE, non-acetate ester; ALD, aldehyde; ALC, alcohols, KET, ketones; SDC, sulfur derived-compounds; TER, terpenes; AHA, alkanes and aliphatic compounds; OTH, other compounds. Circles represent r^2 = 50% and 100% variability explained by the components.

Annex B:

Supplementary Material:

Seasonal effects on flesh volatile concentrations and texture at harvest in a near-isogenic line of melon with introgression in LG X

Supplementary Table 1. Analysis of Variance (ANOVA) with introgression and season (S1 and S2) as factors with interaction applied to the textural traits (mean ± SD) measured at the near-isogenic line (NIL) SC10-2 (n = 5 and n=4, for S1 and S2, respectively) and the parental 'Piel de Sapo' (PS) (n = 20 and n=9, for S1 and S2, respectively). Original data were log2-transformed.

Textural traits	Season 1		Season 2		Mean Squares (Df[a])				Percentage of explained variance			p-values[b]		
	PS	SC10-2	PS	SC10-2	Introgression (I)	Season (S)	Interaction (I xS)	Residuals	Introgression (I)	Season (S)	Interaction (I x S)	Introgression (I)	Season (S)	Interaction (I x S)
Fibrousness (g·kg^{-1})	28.8 ± 6	27 ± 4	23± 7	2.4± 0.6	0.0235 (1)	0.9054 (1)	0.0352 (1)	0.027 (34)	0.43%	16.61%	0.65%	NS	*	NS
Firmness (N)	7.3 ± 1.1	9.2± 2.2	5.4± 1.2	7.5± 0.5	0.7872 (1)	1.4064 (1)	0.0741 (1)	0.073 (34)	16.58%	29.62%	1.56%	**	***	NS
Hardness (N·mm^{-1})	54.7 ± 5.3	58.7 ± 5.9	64.1± 7.3	69.8± 8.2	0.1408 (1)	0.4555 (1)	0.0007 (1)	0.022 (34)	10.43%	33.73%	0.05%	*	***	NS
Juiciness (g·kg^{-1})	350.2 ± 29.6	292.8 ± 33.8	293.8± 49.1	194.0± 12.7	1.3297 (1)	1.0421 (1)	0.1693 (1)	0.132 (34)	38.45%	30.13%	4.89%	****	****	*

[a]Df: Degree freedom.

[b]The raw p values of the ANOVA were corrected for the multiple test using the Benjamini and Hochberg false discovery rate criterion. NS: non-significant. *, **; ***, ****: significance at P 0.05, 0.01, 0.001 or 0.0001, respectively.

Supplementary Table 2. Comparative table of volatiles with significant introgression effect obtained from three different methods using the near-isogenic line (NIL) SC10-2 or the parental line 'Piel de Sapo' (PS) at harvest. The corresponding volatile precursors and aromatic notes are included following the literature. Consistent VOC variables were present in more than 25% of the fruits analyzed and 50% or more of the replicates analyzed (Chaparro-Torres et al., 2016). Consistent VOCs with null values were analyzed by three different methodologies, all based on substituting the null-data of each variable by minimum analytical values before log2 transformation: method 1) in each season, the null data were substituted by the minimum non-null value of the VOC variable; method 2) the minimum analytical value of VOC found in the entire consistent list of VOCs variables (criteria adopted in Chaparro-Torres et al., 2016 but also reported by Mathieu et al. (2009) for tomato); and method 3) substitution with the minimum of each line/season (four different cases per VOC).

	CAS[a] number	Volatile organic compound (IUPAC[b] name)	Compound class[c]	RT[d] (min)	LRI[e] Cal	LRI[e] ref	Volatile precursors[f]	Volatile precursors references	Aromatic notes[g]	Effect vs. PS
Method 1	96-17-3	2-methylbutanal	ALD	2.369	658	662	AA, Iso	Gonda et al., 2010/Goff et a	Green, almond, strong burnt, malty, cocoa.	+
	010340-23-5	(Z)-non-3-en-1-ol	ALC	21.631	1165	1160	FAs	Lingwood et al., 2010	Fresh waxy green melon rind tropical mushroom.	-
	91-20-3	Naphthalene	OTH	21.895	1184	1189	TER	Negri et al., 2015	Mothball, Medicinal, Pungent, dry, tarry	+
Method 2	000064-17-5	Ethanol	ALC	1.324	354	426	FAs	Espino-Diaz et al., 2016	Strong alcoholic ethereal medical.	-
	96-17-3	2-methylbutanal	ALD	2.369	658	662	AA, Iso	Gonda et al., 2010/Goff et a	Green, almond, strong burnt, malty, cocoa.	+
	000616-25-1	Pent-1-en-3-ol	ALC	2.580	680	686	FAs	Juttner et al., 1983	Pungent horseradish green vegetable tropical fruity.	-
	565-69-5	2-methylpentan-3-one	KET	3.747	745	748	TER, FAs	Juttner et al., 1983	Minty.	-
	006728-26-3	(E)-hex-2-enal	ALD	6.825	848	853	AA	Gonda et al., 2010	Green banana aldehydic fatty cheesy.	-
	000100-52-7	Benzaldehyde	ALD	11.952	954	961	Phe, Try, AA	Singh et al., 2003/Gonda et	Almond, Burnt sugar, woody, fruity, nutty.	-
	000110-93-0	6-methylhept-5-en-2-one	KET	13.877	988	988	TER, FAs	Juttner et al., 1983	Fruity, apple, musty, ketonic, creamy with slight cheesy.	-
	000104-76-7	2-ethylhexan-1-ol	ALC	16.607	1033	1029	FAs	Juttner et al., 1983	Citrus fresh floral oily sweet.	-
	1120-21-4	Undecane	AHA	20.708	1100	1100	TER, FAs	Juttner et al., 1983	Gasoline-like to odorless.	-
	4501-58-0	2-(2,2,3-trimethylcyclopent-3-en-1-yl)acetaldehyde	ALD	20.728	1101	1109	AA	Gonda et al., 2010	Herbal green woody amber leafy.	-
	002277-19-2	(Z)-non-6-enal	ALD	20.775	1104	1107	FAs	Hong et al., 2011	Green cucumber and melon with a woody orris-type nuance.	-
	000124-19-6	Nonanal	ALD	20.817	1107	1105	Iso	Pang et al., 2012	Waxy aldehydic rose fresh orris orange peel fatty peely.	-
	004621-04-9-is1	4-Isopropylcyclohexanol (Isomer 1)	ALC	20.918	1114	1103	TER	Dos-santos et al., 2013	Leather red rose green dusty weedy metallic.	-
	057283-79-1	(E)-5-ethyl-6-methylhept-3-en-2-one	KET	21.521	1158	1144	AA	UM-BBD (2013)	N/A literature.	-
	010340-23-5	(Z)-non-3-en-1-ol	ALC	21.631	1165	1160	FAs	Lingwood et al., 2010	Fresh waxy green melon rind tropical mushroom.	-
	91-20-3	Naphthalene	OTH	21.895	1184	1189	TER	Negri et al., 2015	Mothball, Medicinal, Pungent, dry, tarry.	-
	005779-94-2	2,5-dimethylbenzaldehyde	ALD	22.258	1219	1208	AA, Phe	Gonda et al., 2010/Van Mo	Almond-like.	-
	000501-92-8	4-prop-2-enylphenol	ALC	22.494	1249	1251	FAs	Lingwood et al., 2010	Phenolic medicinal.	-
	000103-45-7	2-phenylethyl acetate	ACE	22.607	1264	1264	Iso	Gonda et al., 2010	Fruity, Rose, floral, sweet.	-
	41436-42-4	(E)-1-(2,6,6-trimethylcyclohex-3-en-1-yl)but-2-en-1-one	KET	23.155	1346	1340	AA	UM-BBD (2013)	Floral, rose, apple fruityt, black currant aroma.	-
	71-23-8	Propan-1-ol	ALC	1.623	527	521	FAs	Wills et al., 2012	Alcoholic fermented fusel musty.	+
	107-83-5	2-Methylpentane	AHA	1.637	539	558	FAs	Sanz et al., 1997	N/A literature.	+
	589-81-1	3-methylheptane	AHA	4.203	765	767	FAs	Sanz et al., 1997	Odor resembling hexane.	+
	124-18-5	Decane	AHA	14.605	1002	1000	FAs	Kunst et al., 2006	Colorless liquid with gasoline-like odor.	-
	95-16-9	1,3-benzothiazole	SDC	22.339	1229	1235	Met, AA	Gonda et al., 2010	Gasoline, rubber.	+
Method 3	000064-17-5	Ethanol	ALC	1.324	354	426	FAs	Espino-Diaz et al., 2016	Strong alcoholic ethereal medical.	-
	96-17-3	2-methylbutanal	ALD	2.369	658	662	AA, Iso	Gonda et al., 2010/Goff et a	Green, almond, strong burnt, malty, cocoa.	+
	000616-25-1	Pent-1-en-3-ol	ALC	2.580	680	686	FAs	Juttner et al., 1983	Pungent horseradish green vegetable tropical fruity.	-
	565-69-5	2-methylpentan-3-one	KET	3.747	745	748	TER, FAs	Juttner et al., 1983	Minty.	-
	006728-26-3	(E)-hex-2-enal	ALD	6.825	848	853	AA	Gonda et al., 2010	Green banana aldehydic fatty cheesy.	-
	000100-52-7	Benzaldehyde	ALD	11.952	954	961	Phe, Try, AA	Singh et al., 2003/Gonda et	Almond, Burnt sugar, woody, fruity, nutty.	-
	000110-93-0	6-methylhept-5-en-2-one	KET	13.877	988	988	TER, FAs	Juttner et al., 1983	Fruity, apple, musty, ketonic, creamy with slight cheesy.	-
	000104-76-7	2-ethylhexan-1-ol	ALC	16.607	1033	1029	FAs	Juttner et al., 1983	Citrus fresh floral oily sweet.	-
	1120-21-4	Undecane	AHA	20.708	1100	1100	TER, FAs	Juttner et al., 1983	Gasoline-like to odorless.	-
	4501-58-0	2-(2,2,3-trimethylcyclopent-3-en-1-yl)acetaldehyde	ALD	20.728	1101	1109	AA	Gonda et al., 2010	Herbal green woody amber leafy.	-
	002277-19-2	(Z)-non-6-enal	ALD	20.775	1104	1107	FAs	Hong et al., 2011	Green cucumber and melon with a woody orris-type nuance.	-
	000124-19-6	Nonanal	ALD	20.817	1107	1105	Iso	Pang et al., 2012	Waxy aldehydic rose fresh orris orange peel fatty peely.	-
	004621-04-9-is1	4-Isopropylcyclohexanol (Isomer 1)	ALC	20.918	1114	1103	TER	Dos-santos et al., 2013	Leather red rose green dusty weedy metallic.	-
	057283-79-1	(E)-5-ethyl-6-methylhept-3-en-2-one	KET	21.521	1158	1144	AA	UM-BBD (2013)	N/A literature.	-
	010340-23-5	(Z)-non-3-en-1-ol	ALC	21.631	1165	1160	FAs	Lingwood et al., 2010	Fresh waxy green melon rind tropical mushroom.	-
	91-20-3	Naphthalene	OTH	21.895	1184	1189	TER	Negri et al., 2015	Mothball, Medicinal, Pungent, dry, tarry.	-
	005779-94-2	2,5-dimethylbenzaldehyde	ALD	22.258	1219	1208	AA, Phe	Gonda et al., 2010/Van Mo	Almond-like.	-
	000501-92-8	4-prop-2-enylphenol	ALC	22.494	1249	1251	FAs	Lingwood et al., 2010	Phenolic medicinal.	-
	000103-45-7	2-phenylethyl acetate	ACE	22.607	1264	1264	Iso	Gonda et al., 2010	Fruity, Rose, floral, sweet.	-
	41436-42-4	(E)-1-(2,6,6-trimethylcyclohex-3-en-1-yl)but-2-en-1-one	KET	23.155	1346	1340	AA	UM-BBD (2013)	Floral, rose, apple fruityt, black currant aroma.	-
	71-23-8	Propan-1-ol	ALC	1.623	527	521	FAs	Wills et al., 2012	Alcoholic fermented fusel musty.	+
	107-83-5	2-Methylpentane	AHA	1.637	539	558	FAs	Sanz et al., 1997	N/A literature.	+
	589-81-1	3-methylheptane	AHA	4.203	765	767	FAs	Sanz et al., 1997	Odor resembling hexane.	+
	124-18-5	Decane	AHA	14.605	1002	1000	FAs	Kunst et al., 2006	Colorless liquid with gasoline-like odor.	-
	95-16-9	1,3-benzothiazole	SDC	22.339	1229	1235	Met, AA	Gonda et al., 2010	Gasoline, rubber.	+

[a] CAS, chemical abstracts service.

[b] IUPAC, international union of pure and applied chemistry.

[c] Compound Classes: ACE, acetate esters; AHA, alkanes; ALC, alcohols; ALD, aldehydes; KET, ketones; NAE, non-acetate esters; NID, not identified; SDC, sulfur-derived compounds; OTH, other compound class.

[d] RT, retention time in minutes.

[e] LRI: LRI cal., linear retention indices calculated from the RT of a series of n-alkanes standards (C6–C20). LRI Ref., linear retention referenced (National Institute of Standards and Technology. NIST database. http://www.nist.gov/index.html).

[f] Volatile precursors: AA, amino acid; Iso, L-isoleucine; FAs, fatty acids; TER, terpenes; Phe, L-phenylalanine; Try, L-tryptophan; Met, L-methionine.

[g] http://www.thegoodscentscompany.com

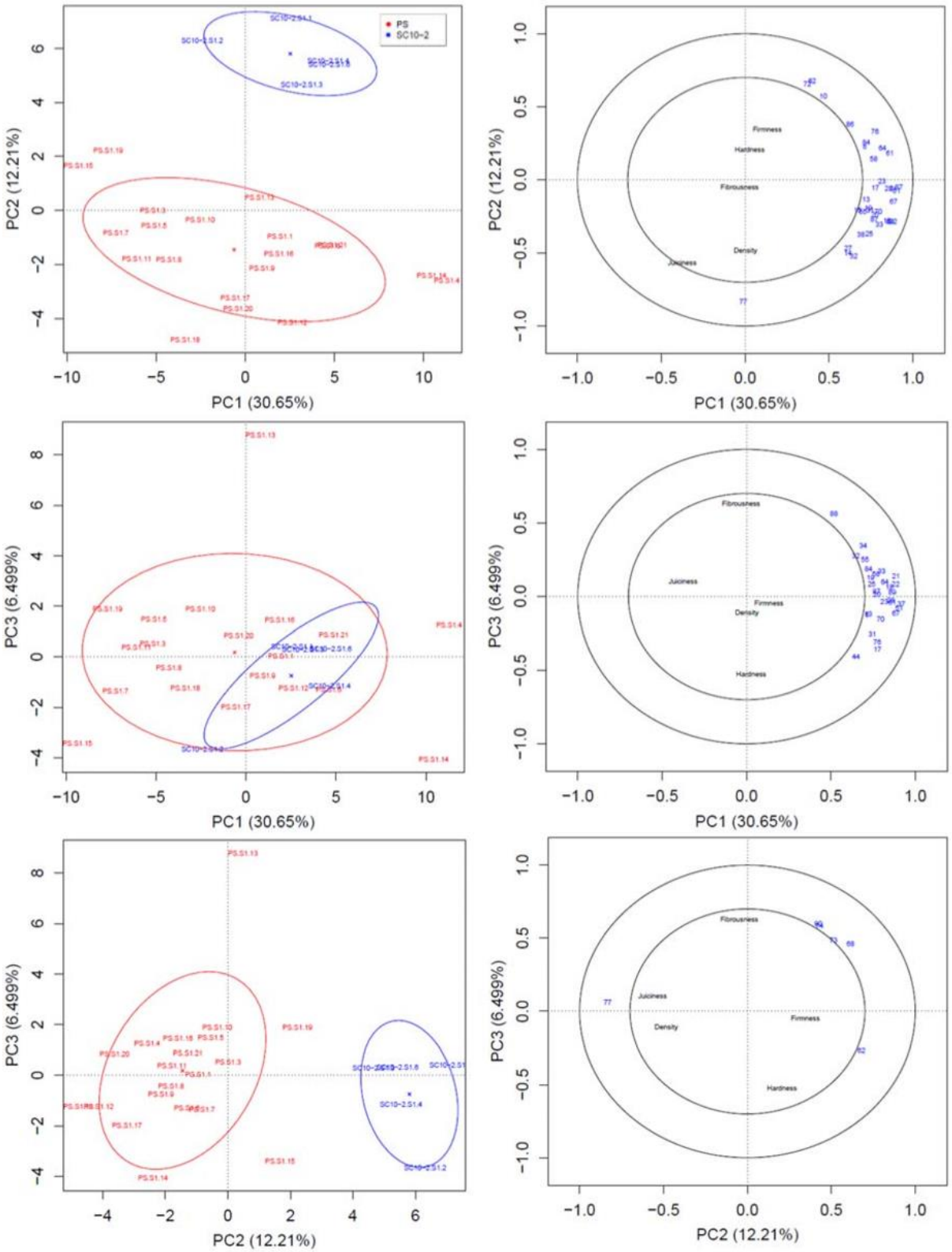

Suppl. Fig. 1. Scores and correlation plots obtained by Principal Component Analysis (PCA) of the aroma volatiles identified in the near-isogenic line (NIL) SC10-2 (n=5) of melon and the parental 'Piel de Sapo' (PS) (n=20) at harvest in season 1 (S1). Datasets and the corresponding centroids for the different lines and 65% confidence ellipses.

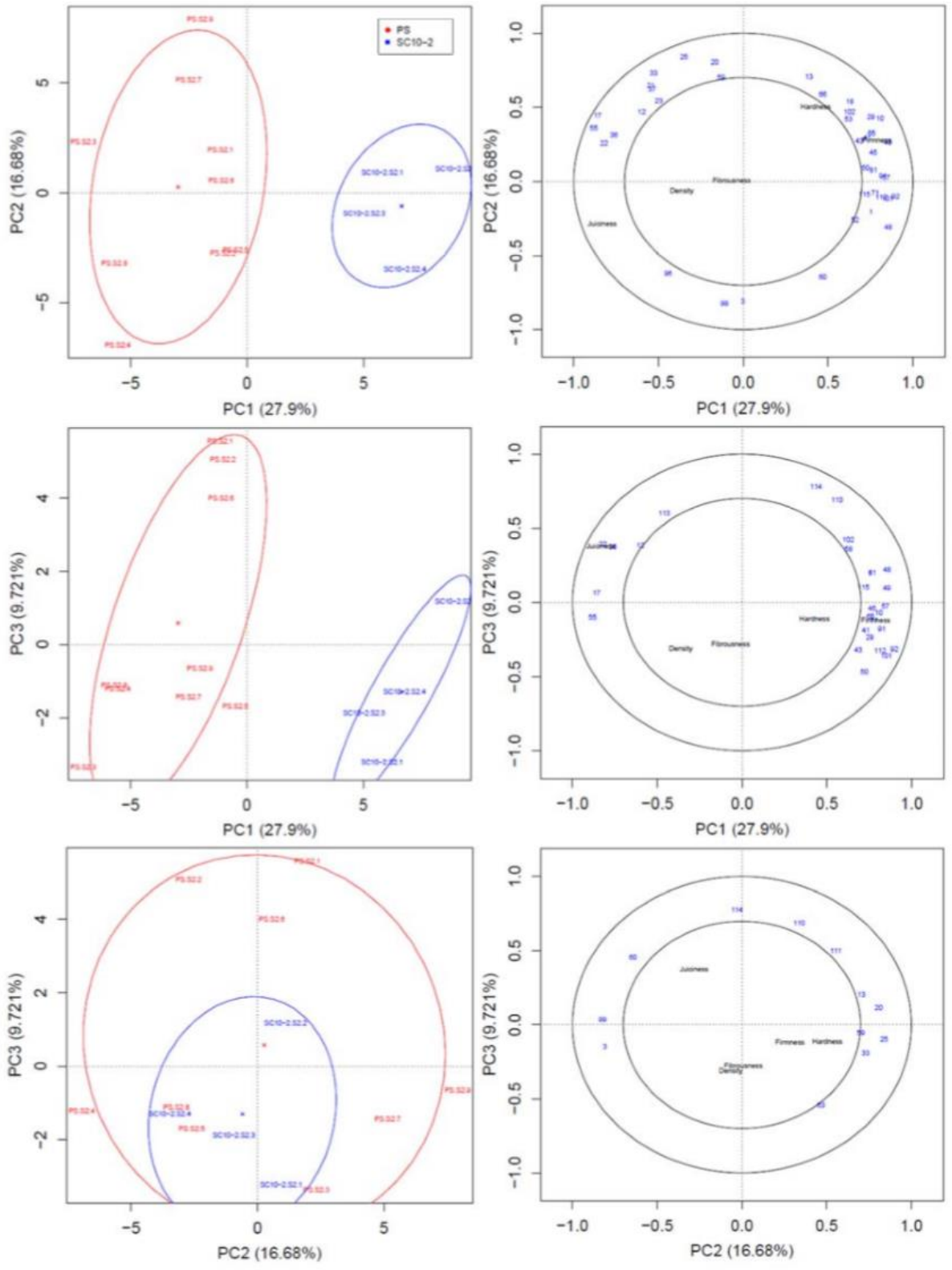

Suppl. Fig. 2. Scores and correlation plots obtained by Principal Component Analysis (PCA) of the aroma volatiles identified in the near-isogenic line (NIL) SC10-2 (n=4) of melon and the parental 'Piel de Sapo' (PS) (n=9) at harvest in season 2 (S2). Datasets and the corresponding centroids for the different lines and 65% confidence ellipses.

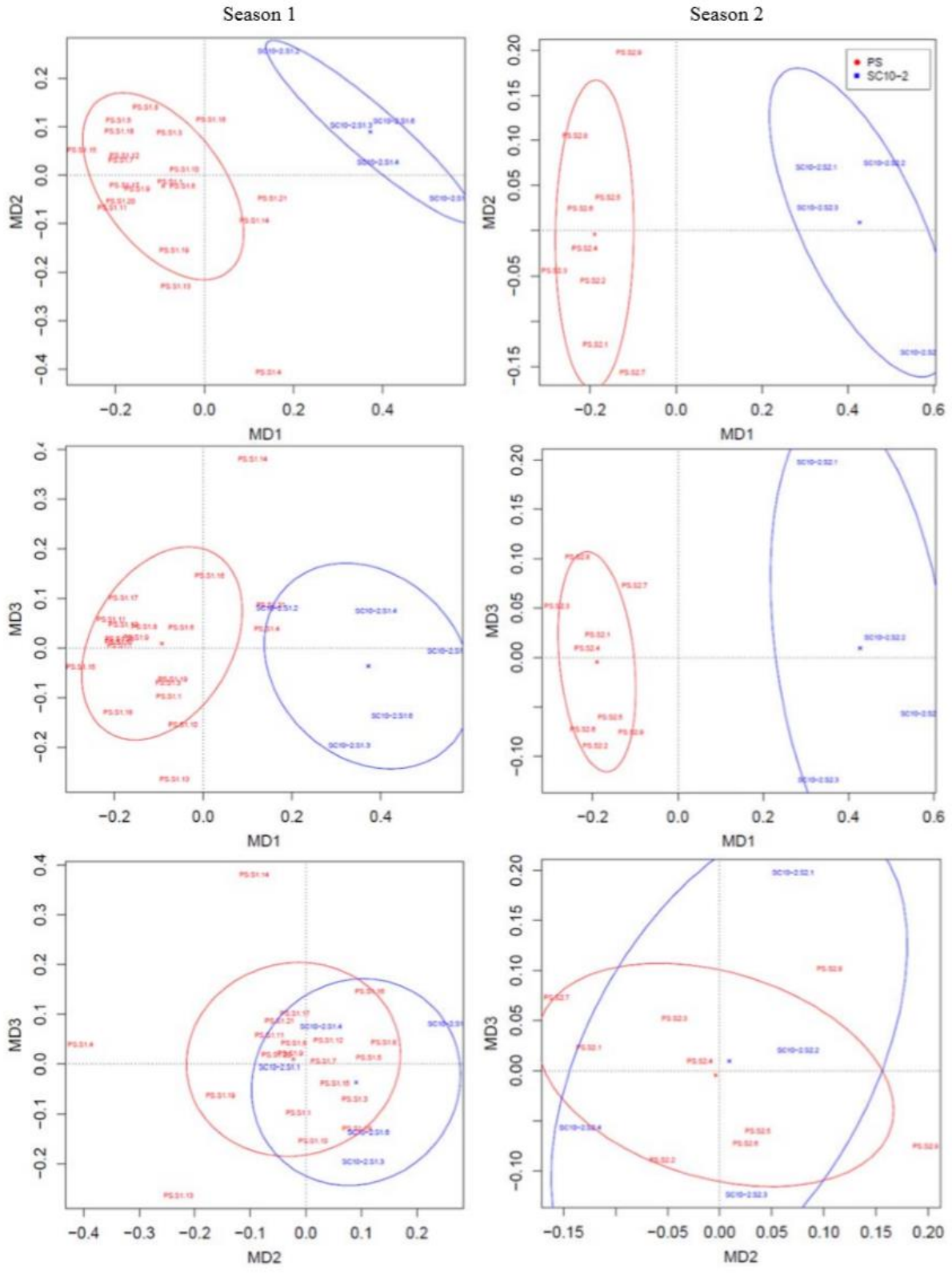

Suppl. Fig. 3. Discrimination of the near-isogenic line (NIL) SC10-2 (n=5 or n=4, for S1 and S2, respectively) of melon and the parental 'Piel de Sapo' (PS; n=20 or n=9, for S1 and S2, respectively) using Multidimensional scaling (MDS) plots based on Random Forest (RF) analysis applied to the flesh volatile organic compounds identified at harvest in two seasons (S1 and S2). Datasets and the corresponding centroids for the different lines and 65% confidence ellipses.

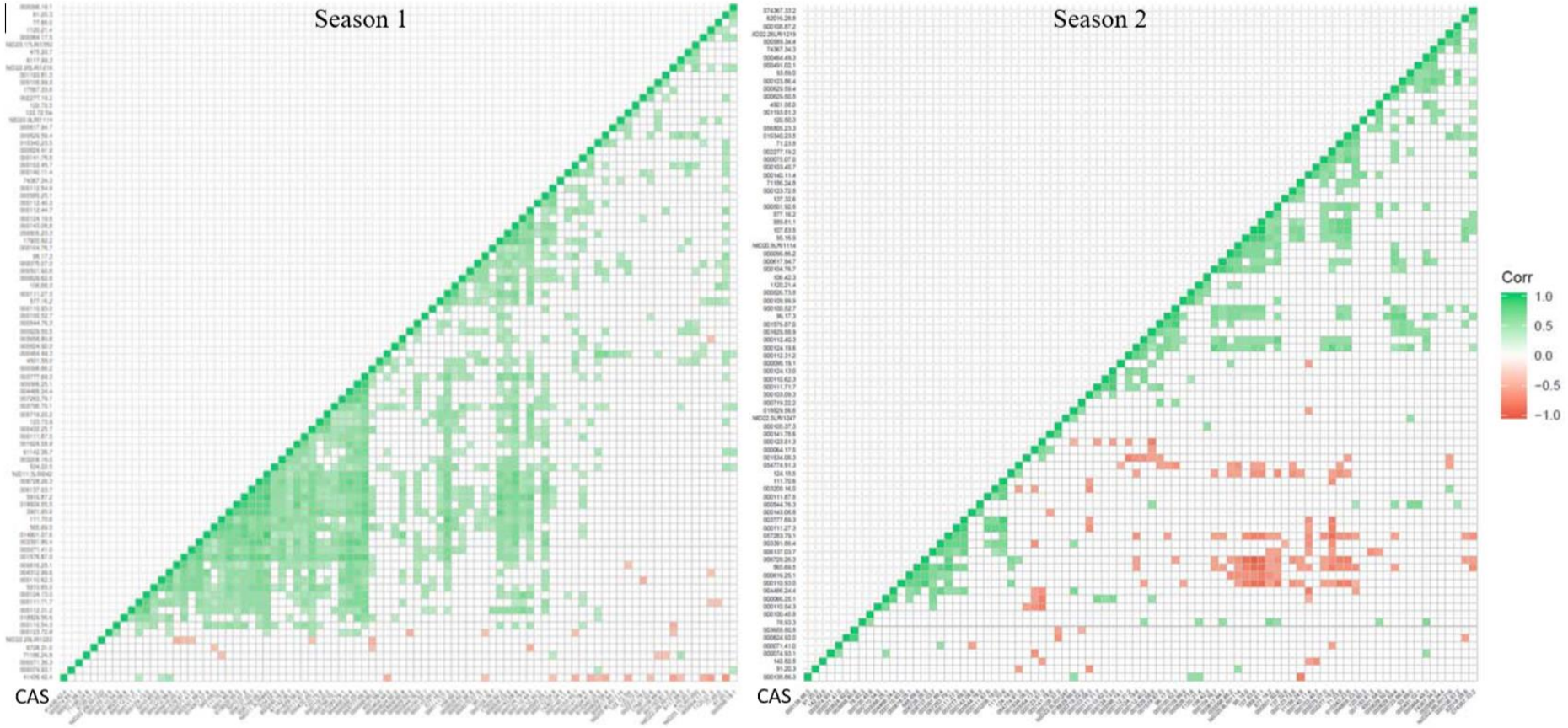

Suppl. Fig. 4. Correlation (Corr) between volatile compounds identified at harvest in two seasons (S1 and S2) of the near-isogenic line (NILs) SC10-2 (n=5 or n=4, respectively) of melon and the parental 'Piel de Sapo' (PS) (n=20 or n=9, respectively). Main discriminant melon aroma volatile compounds presented in the figure by its number in the Chemical Abstracts Service (CAS) had a $p<0.05$.

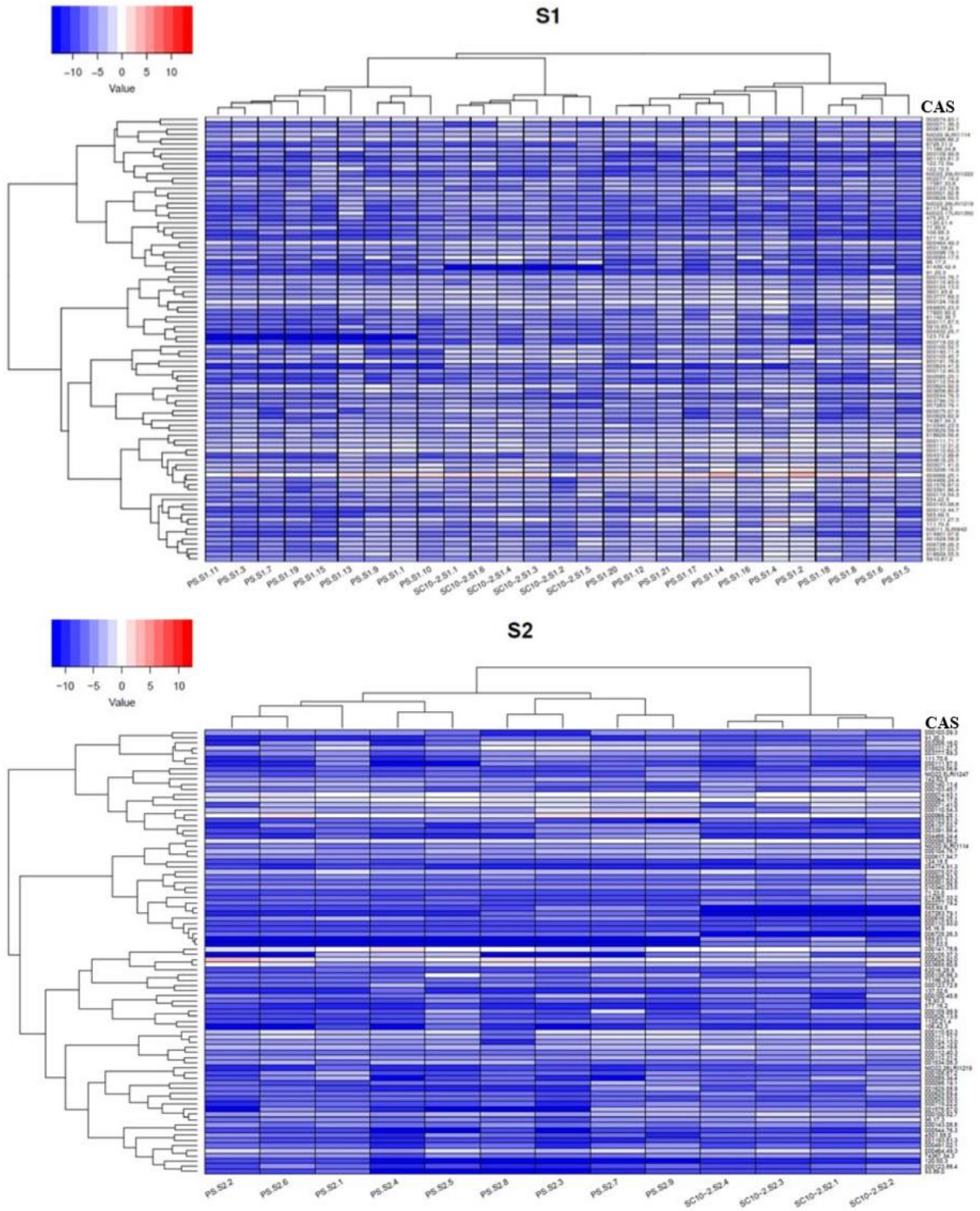

Suppl. Fig. 5: Heatmaps of the volatile compounds identified at harvest in two seasons (S1 and S2) of the near-isogenic line (NIL) SC10-2 (n=5 and n=4, for S1 and S2, respectively) of melon and the parental 'Piel de Sapo' (PS) (n=20 and n=9, for S1 and S2, respectively). Main discriminant melon aroma volatile compounds presented on the figure by its Chemical Abstracts Service (CAS) number.

Annex C:

Supplementary Material:

Transcriptomic analysis of a near-isogenic line of melon with high fruit flesh firmness during ripening:

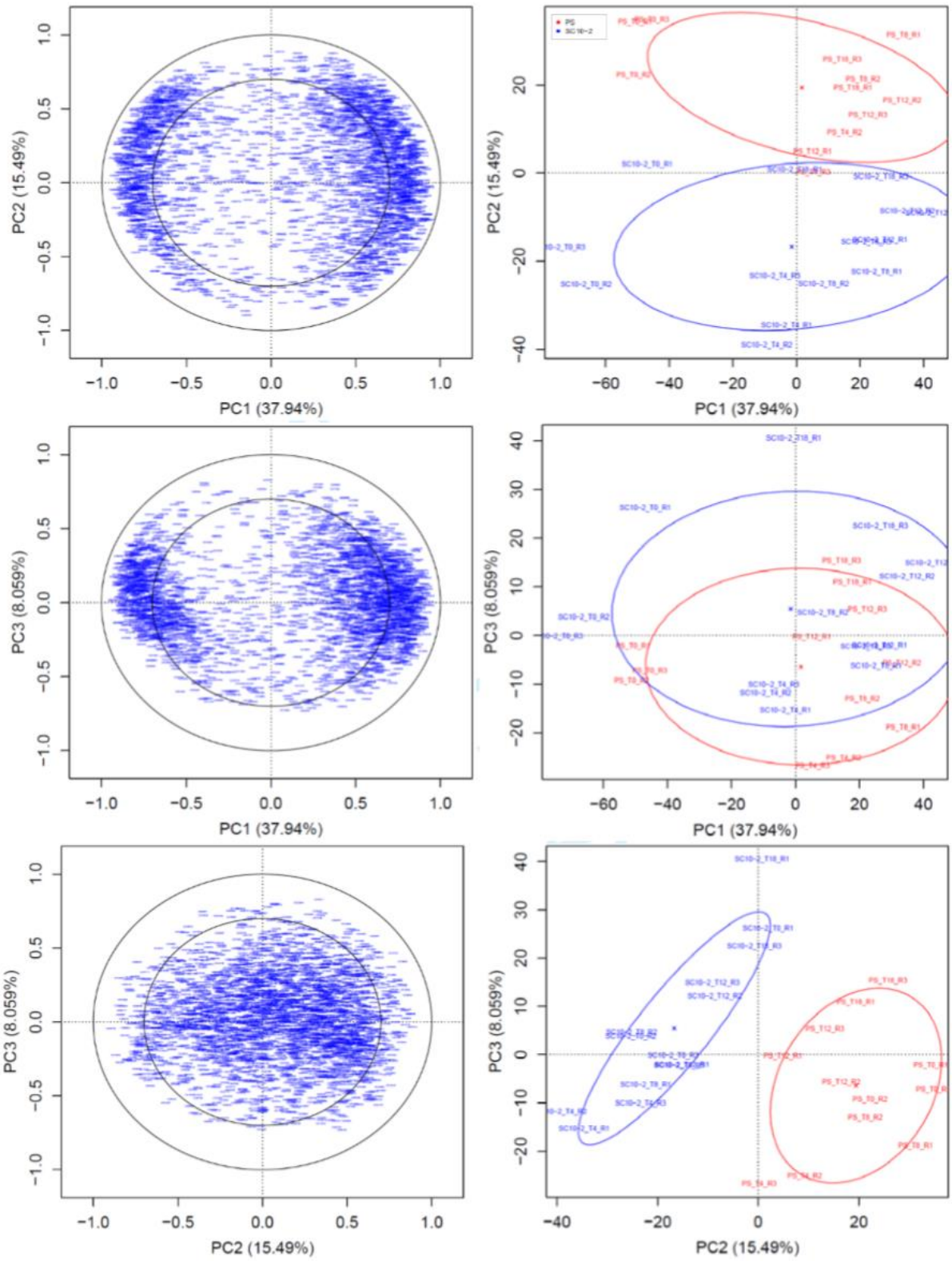

Supplementary Figure 1. Plot of the centroids of scores and loading plots of the Principal Component Analysis (PCA) of the expressed genes significant in introgression and identified in the near-isogenic line (NIL) SC10-2 and the parental control ´Piel de Sapo´ (PS)). Datasets and the corresponding centroids for the different lines and 65% confidence ellipses. Tx (x = 0, 4, 8, 12, 18) indicates the postharvest ripening time in days and Rn (n = 1-3) the corresponding replicate

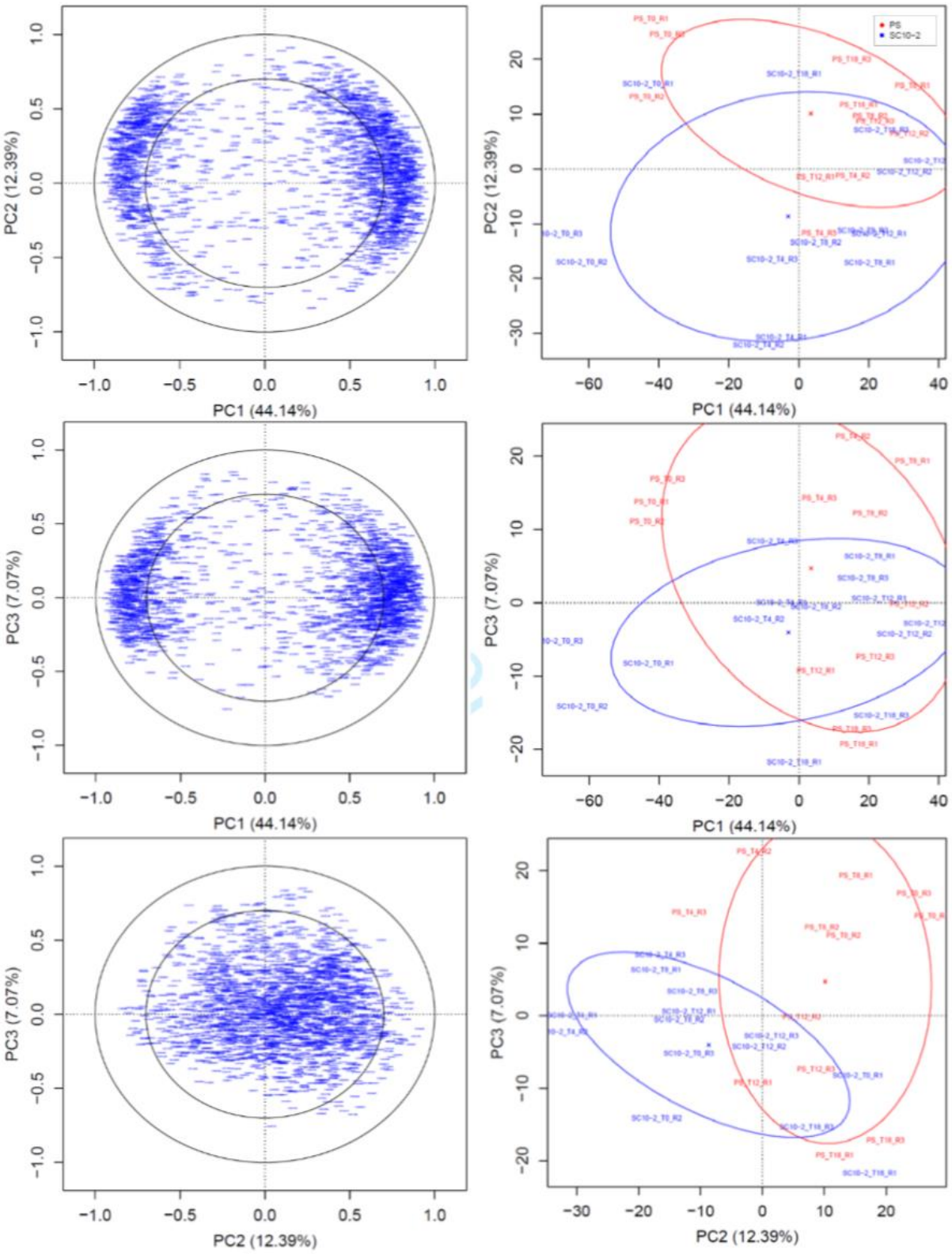

Supplementary Figure 2. Plot of the centroids of scores and loading plots of the Principal Component Analysis (PCA) of the expressed genes significant in ripening time identified in the near-isogenic line (NIL) SC10-2 and the parental control ´Piel de Sapo´ (PS). Datasets and the corresponding centroids for the different lines and 65% confidence ellipses. Tx (x = 0, 4, 8, 12, 18) indicates the postharvest ripening time in days and Rn (n = 1-3) the corresponding replicate.

Supplementary Figure 3. Gene Ontology (GO) of the different clusters obtained using differentially expressed genes, only considering the postharvest ripening factor in melon fruit of the near-isogenic line NIL SC10-2 and its parental ´Piel de Sapo´ (PS) harvested in firm-ripe stage of maturity and stored at 20.5 ºC and 88% relative humidity for 18 d.

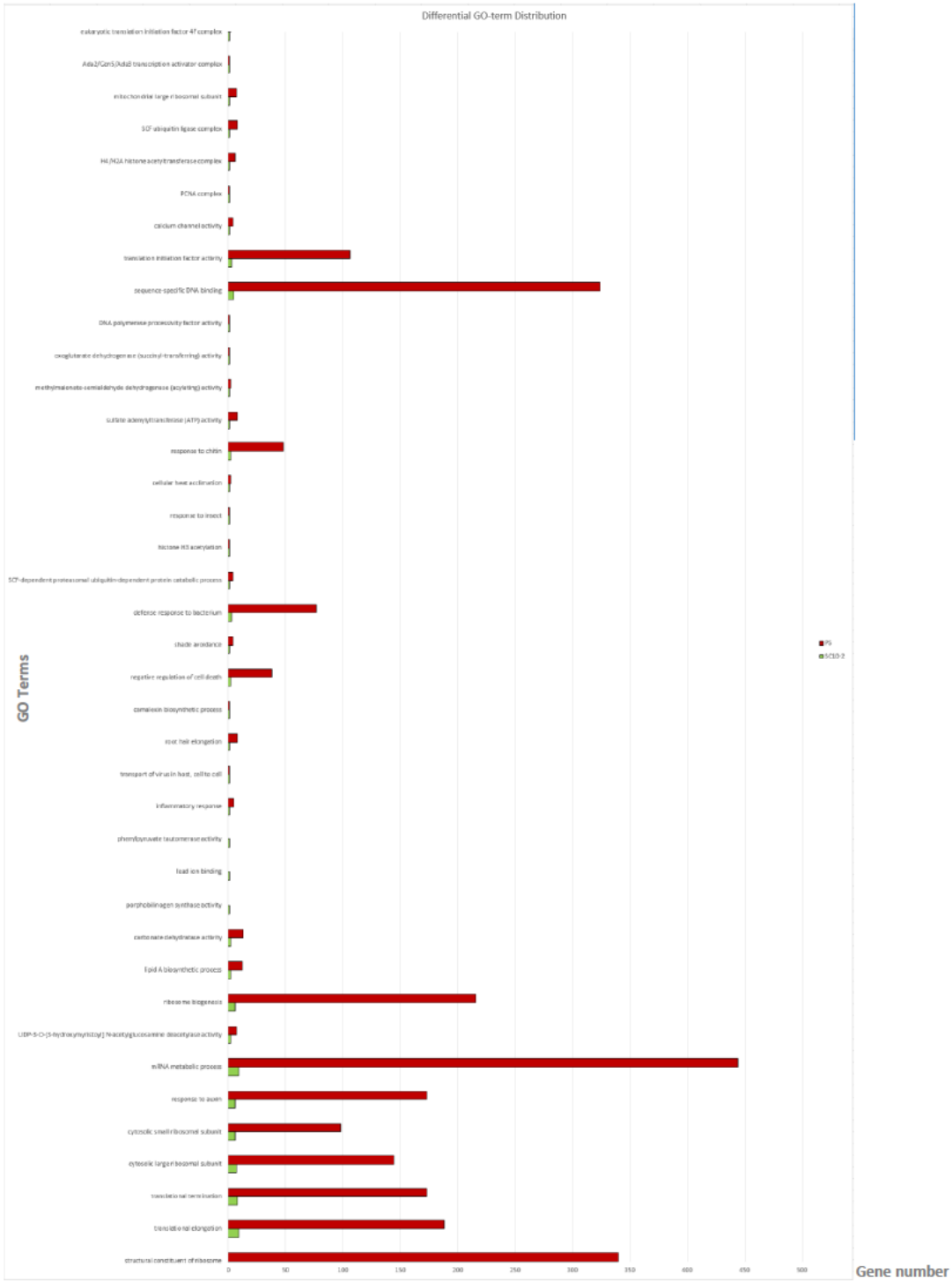
Differential GO-term Distribution
eukaryotic translation initiation factor 4F complex
Ada2/Gcn5/Ada3 transcription activator complex
mitochondrial large ribosomal subunit
SCF ubiquitin ligase complex
H4/H2A histone acetyltransferase complex
PCNA complex
calcium channel activity
translation initiation factor activity
sequence-specific DNA binding
DNA polymerase processivity factor activity
oxoglutarate dehydrogenase (succinyl-transferring) activity
methylmalonate-semialdehyde dehydrogenase (acylating) activity
sulfate adenylyltransferase (ATP) activity
response to chitin
cellular heat acclimation
response to insect
histone H3 acetylation
SCF-dependent proteasomal ubiquitin-dependent protein catabolic process
defense response to bacterium
shade avoidance
negative regulation of cell death
coniferin biosynthetic process
root hair elongation
transport of virus in host, cell to cell
inflammatory response
phenylpyruvate tautomerase activity
lead ion binding
porphobilinogen synthase activity
ketone reductase activity
lipid A biosynthetic process
ribosome biogenesis
UDP-3-O-[3-hydroxymyristoyl] N-acetylglucosamine deacetylase activity
mRNA metabolic process
response to auxin
cytosolic small ribosomal subunit
cytosolic large ribosomal subunit
translational termination
translational elongation
structural constituent of ribosome
GO Terms
0
50
100
150
200
250
300
350
400
450
500
Gene number
PS
SC10-2

GO. Cluster 1

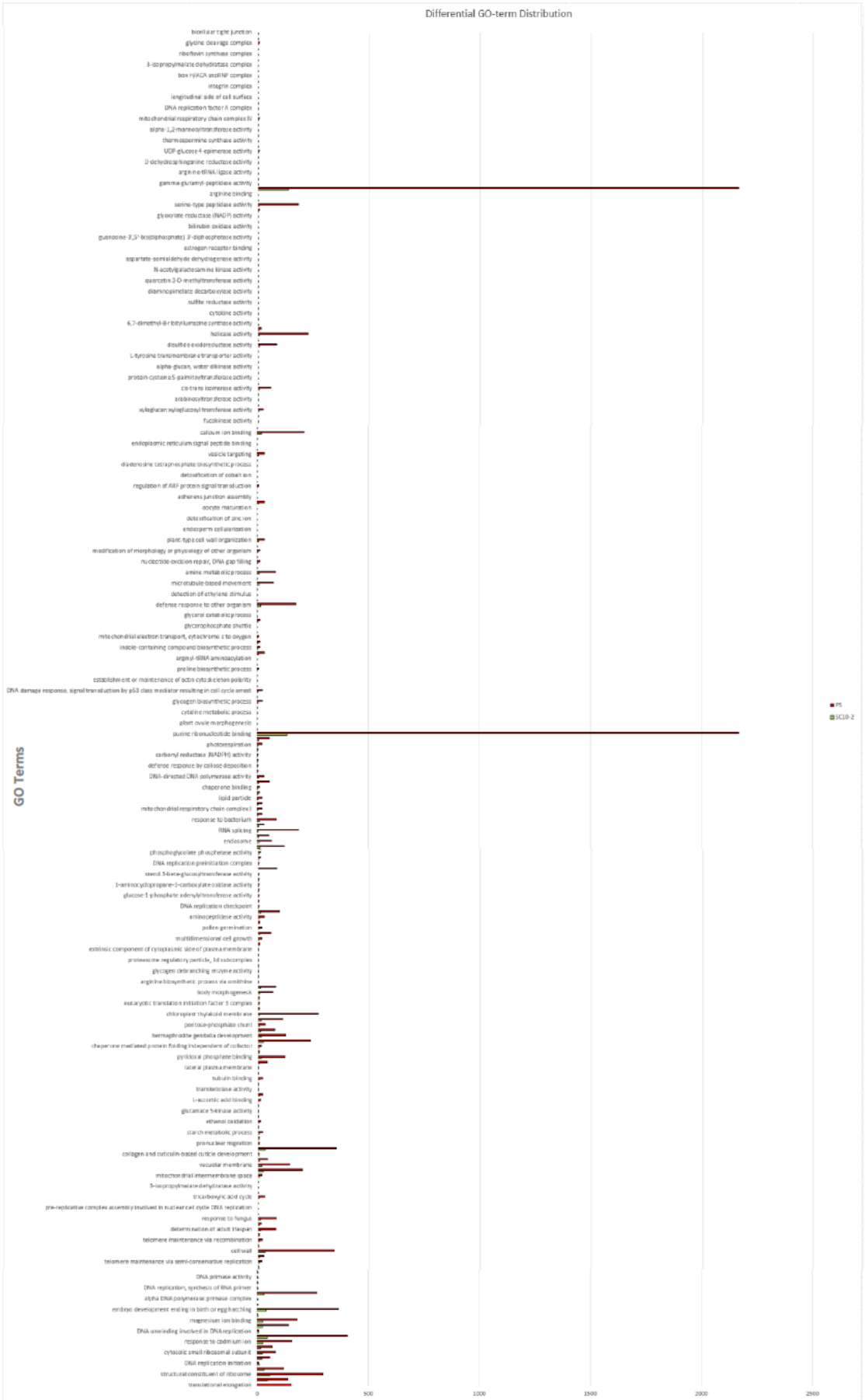
Differential GO-term Distribution
bicellular tight junction
glycine cleavage complex
riboflavin synthase complex
3-isopropylmalate dehydratase complex
box H/ACA snoRNP complex
integrin complex
longitudinal side of cell surface
DNA replication factor A complex
mitochondrial respiratory chain complex IV
alpha-1,2-mannosyltransferase activity
thermospermine synthase activity
UDP-glucose 4-epimerase activity
3-dehydrosphinganine reductase activity
arginine-tRNA ligase activity
gamma-glutamyl-peptidase activity
arginine binding
serine-type peptidase activity
glyoxylate reductase (NADP) activity
bilirubin oxidase activity
guanosine-3',5'-bis(diphosphate) 3'-diphosphatase activity
estrogen receptor binding
aspartate-semialdehyde dehydrogenase activity
N-acetylgalactosamine kinase activity
quercetin 3-O-methyltransferase activity
diaminopimelate decarboxylase activity
sulfite reductase activity
cytokinin activity
6,7-dimethyl-8-ribityllumazine synthase activity
helicase activity
disulfide oxidoreductase activity
L-tyrosine transmembrane transporter activity
alpha-glucan, water dikinase activity
protein-cysteine S-palmitoyltransferase activity
cis-trans isomerase activity
arabinosyltransferase activity
xyloglucan xylosyltransferase activity
fucokinase activity
calcium ion binding
endoplasmic reticulum signal peptide binding
vesicle targeting
diadenosine tetraphosphate biosynthetic process
detoxification of cobalt ion
regulation of ARF protein signal transduction
adherens junction assembly
oocyte maturation
detoxification of zinc ion
endosperm cellularization
plant-type cell wall organization
modification of morphology or physiology of other organism
nucleotide-excision repair, DNA gap filling
amine metabolic process
microtubule-based movement
detection of ethylene stimulus
defense response to other organism
glycerol catabolic process
glycerophosphate shuttle
mitochondrial electron transport, cytochrome c to oxygen
indole-containing compound biosynthetic process
arginyl-tRNA aminoacylation
proline biosynthetic process
establishment or maintenance of actin cytoskeleton polarity
DNA damage response, signal transduction by p53 class mediator resulting in cell cycle arrest
glycogen biosynthetic process
cytidine metabolic process
plant ovule morphogenesis
purine ribonucleotide binding
photorespiration
carbonyl reductase (NADPH) activity
defense response by callose deposition
DNA-directed DNA polymerase activity
chaperone binding
lipid particle
mitochondrial respiratory chain complex I
response to bacterium
RNA splicing
endosome
phosphoglycolate phosphatase activity
DNA replication preinitiation complex
sterol 3-beta-glucosyltransferase activity
1-aminocyclopropane-1-carboxylate oxidase activity
glucose-1-phosphate adenylyltransferase activity
DNA replication checkpoint
aminopeptidase activity
pollen germination
multidimensional cell growth
extrinsic component of cytoplasmic side of plasma membrane
proteasome regulatory particle, lid subcomplex
glycogen debranching enzyme activity
arginine biosynthetic process via ornithine
body morphogenesis
eukaryotic translation initiation factor 5 complex
chloroplast thylakoid membrane
pentose-phosphate shunt
hermaphrodite genitalia development
chaperone mediated protein folding independent of cofactor
pyridoxal phosphate binding
lateral plasma membrane
tubulin binding
transketolase activity
L-ascorbic acid binding
glutamate 5-kinase activity
ethanol oxidation
starch metabolic process
pronuclear migration
collagen and cuticulin-based cuticle development
vacuolar membrane
mitochondrial intermembrane space
3-isopropylmalate dehydratase activity
tricarboxylic acid cycle
pre-replicative complex assembly involved in nuclear cell cycle DNA replication
response to fungus
determination of adult lifespan
telomere maintenance via recombination
cell wall
telomere maintenance via semi-conservative replication
DNA primase activity
DNA replication, synthesis of RNA primer
alpha DNA polymerase:primase complex
embryo development ending in birth or egg hatching
magnesium ion binding
DNA unwinding involved in DNA replication
response to cadmium ion
cytosolic small ribosomal subunit
DNA replication initiation
structural constituent of ribosome
translational elongation
GO Terms
0
500
1000
1500
2000
2500
Gene number
PS
SC10-2

GO. Cluster 2

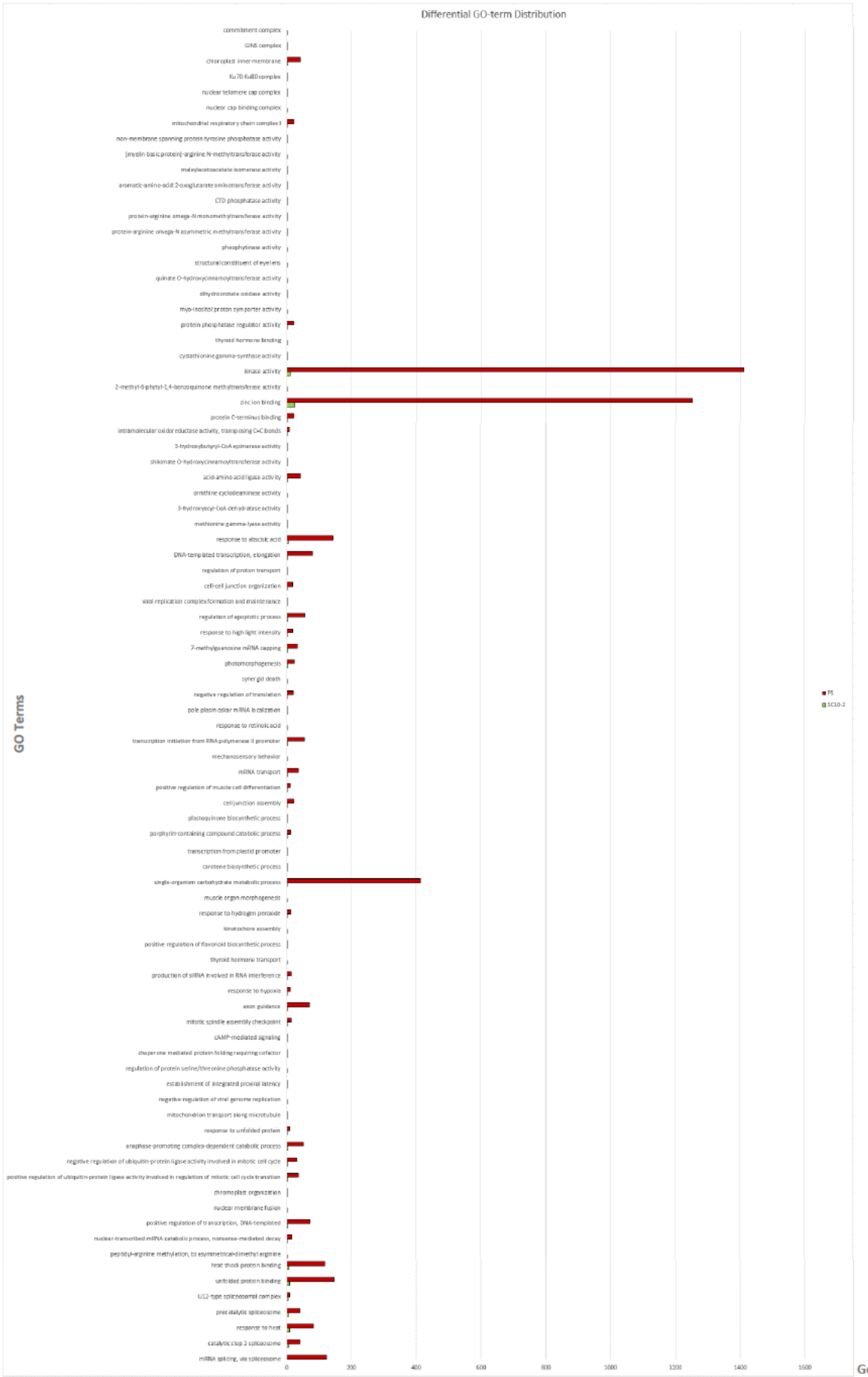
Differential GO-term Distribution
commitment complex
GINS complex
chloroplast inner membrane
Ku70-Ku80 complex
nuclear telomere cap complex
nuclear cap binding complex
mitochondrial respiratory chain complex II
non-membrane spanning protein tyrosine phosphatase activity
[myelin basic protein]-arginine N-methyltransferase activity
malylacetoacetate isomerase activity
aromatic-amino-acid 2-oxoglutarate aminotransferase activity
CTD phosphatase activity
protein-arginine omega-N monomethyltransferase activity
protein-arginine omega-N asymmetric methyltransferase activity
phosphatase activity
structural constituent of eye lens
quinate O-hydroxycinnamoyltransferase activity
dihydrocoriate oxidase activity
myo-inositol proton symporter activity
protein phosphatase regulator activity
thyroid hormone binding
cystathionine gamma-synthase activity
kinase activity
2-methyl-6-phytyl-1,4-benzoquinone methyltransferase activity
zinc ion binding
protein C-terminus binding
intramolecular oxidoreductase activity, transposing C=C bonds
3-hydroxybutyryl-CoA epimerase activity
shikimate O-hydroxycinnamoyltransferase activity
acid-amino acid ligase activity
ornithine cyclodeaminase activity
3-hydroxyacyl-CoA dehydratase activity
methionine gamma-lyase activity
response to abscisic acid
DNA-templated transcription, elongation
regulation of proton transport
cell-cell junction organization
viral replication complex formation and maintenance
regulation of apoptotic process
response to high light intensity
7-methylguanosine mRNA capping
photomorphogenesis
synergid death
negative regulation of translation
pole plasm oskar mRNA localization
response to retinoic acid
transcription initiation from RNA polymerase II promoter
mechanosensory behavior
mRNA transport
positive regulation of muscle cell differentiation
cell junction assembly
plastoquinone biosynthetic process
porphyrin-containing compound catabolic process
transcription from plastid promoter
carotene biosynthetic process
single-organism carbohydrate metabolic process
muscle organ morphogenesis
response to hydrogen peroxide
kinetochore assembly
positive regulation of flavonoid biosynthetic process
thyroid hormone transport
production of siRNA involved in RNA interference
response to hypoxia
axon guidance
mitotic spindle assembly checkpoint
cAMP-mediated signaling
chaperone-mediated protein folding-requiring cofactor
regulation of protein serine/threonine phosphatase activity
establishment of integrated proviral latency
negative regulation of viral genome replication
mitochondrion transport along microtubule
response to unfolded protein
anaphase-promoting complex-dependent catabolic process
negative regulation of ubiquitin-protein ligase activity involved in mitotic cell cycle
positive regulation of ubiquitin-protein ligase activity involved in regulation of mitotic cell cycle transition
chromoplast organization
nuclear membrane fusion
positive regulation of transcription, DNA-templated
nuclear-transcribed mRNA catabolic process, nonsense-mediated decay
peptidyl-arginine methylation, to asymmetrical-dimethyl arginine
heat shock protein binding
unfolded protein binding
U12-type spliceosomal complex
precatalytic spliceosome
response to heat
catalytic step 2 spliceosome
mRNA splicing, via spliceosome
GO Terms
PS
SC10-2
0
200
400
600
800
1000
1200
1400
1600
Gene number

GO. Cluster 3

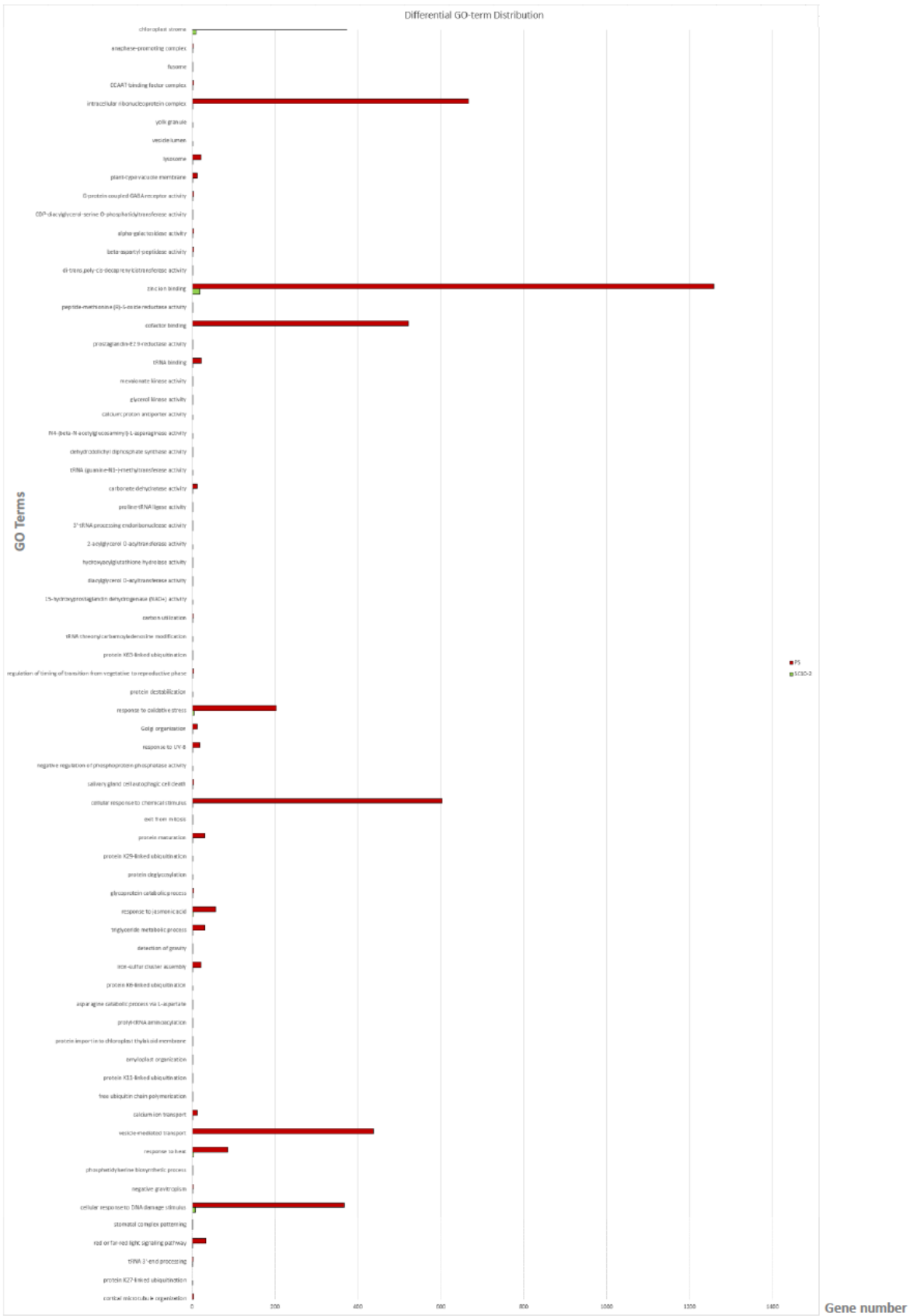
Differential GO-term Distribution
GO Terms
chloroplast stroma
anaphase-promoting complex
fusome
CCAAT-binding factor complex
intracellular ribonucleoprotein complex
yolk granule
vesicle lumen
lysosome
plant-type vacuole membrane
G-protein coupled GABA receptor activity
CDP-diacylglycerol--serine O-phosphatidyltransferase activity
alpha-galactosidase activity
beta-aspartyl-peptidase activity
all-trans-poly-cis-decaprenyl-diphosphate synthase activity
zinc ion binding
peptide-methionine (R)-S-oxide reductase activity
cofactor binding
prostaglandin-E2 9-reductase activity
tRNA binding
mevalonate kinase activity
glycerol kinase activity
calcium:proton antiporter activity
N4-(beta-N-acetylglucosaminyl)-L-asparaginase activity
dehydrodolichyl diphosphate synthase activity
tRNA (guanine-N1-)-methyltransferase activity
carbonate dehydratase activity
proline-tRNA ligase activity
3'-tRNA processing endoribonuclease activity
2-acylglycerol O-acyltransferase activity
hydroxyacylglutathione hydrolase activity
diacylglycerol O-acyltransferase activity
15-hydroxyprostaglandin dehydrogenase (NAD+) activity
carbon utilization
tRNA threonylcarbamoyladenosine modification
protein K63-linked ubiquitination
regulation of timing of transition from vegetative to reproductive phase
protein destabilization
response to oxidative stress
Golgi organization
response to UV-B
negative regulation of phosphoprotein phosphatase activity
salivary gland cell autophagic cell death
cellular response to chemical stimulus
exit from mitosis
protein maturation
protein K29-linked ubiquitination
protein deglycosylation
glycoprotein catabolic process
response to jasmonic acid
triglyceride metabolic process
detection of gravity
iron-sulfur cluster assembly
protein K6-linked ubiquitination
asparagine catabolic process via L-aspartate
prolyl-tRNA aminoacylation
protein import in to chloroplast thylakoid membrane
amyloplast organization
protein K11-linked ubiquitination
free ubiquitin chain polymerization
calcium ion transport
vesicle-mediated transport
response to heat
phosphatidylserine biosynthetic process
negative gravitropism
cellular response to DNA damage stimulus
stomatal complex patterning
red or far-red light signaling pathway
tRNA 3'-end processing
protein K27-linked ubiquitination
cortical microtubule organization
PS
SC10-2
0
200
400
600
800
1000
1200
1400
Gene number

GO. Cluster 4

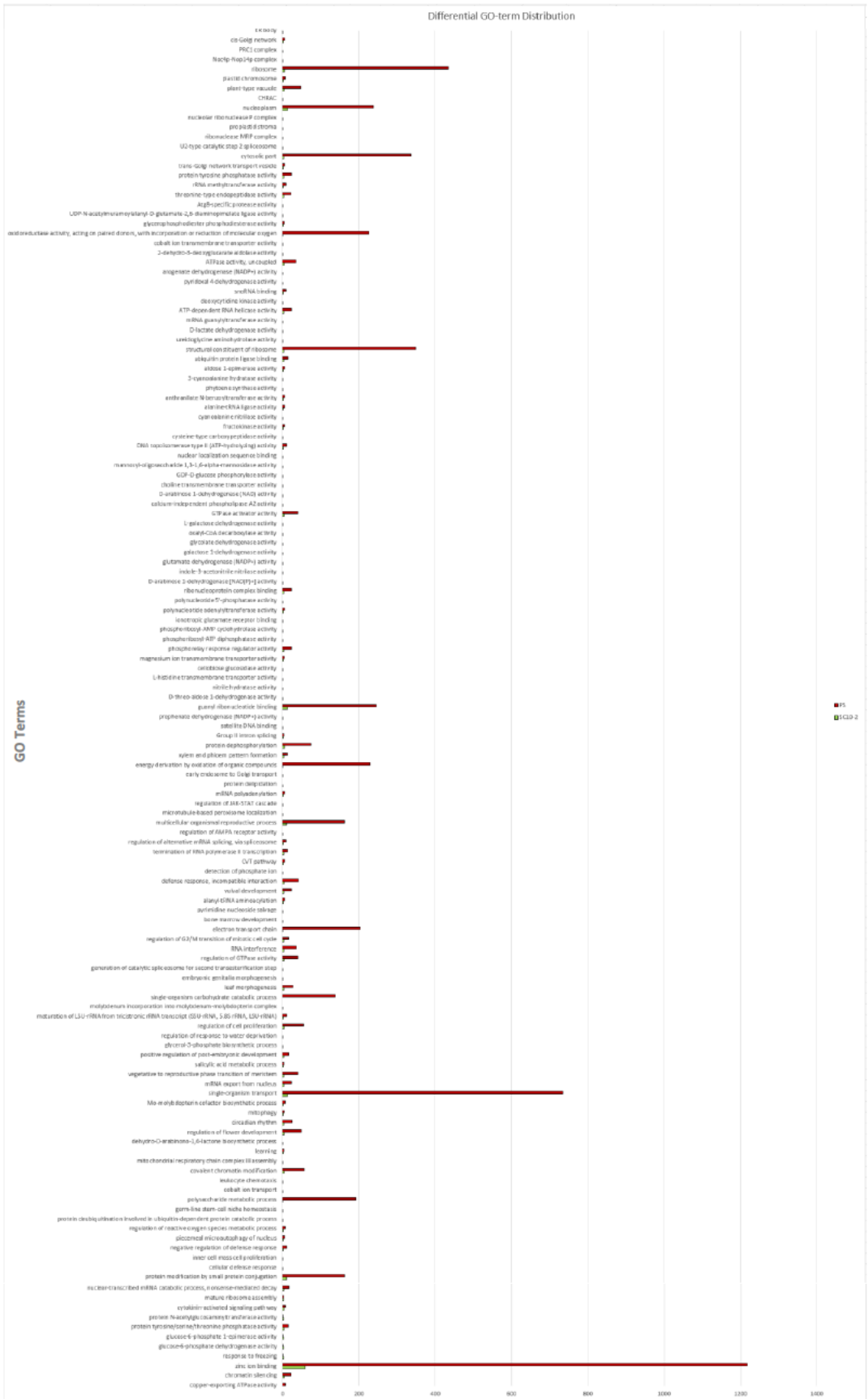
Differential GO-term Distribution
exocyst
cis-Golgi network
PAC1 complex
Nup84-Nup145 complex
ribosome
plastid chromosome
plant-type vacuole
CHRAC
nucleoplasm
nucleolar ribonuclease P complex
pro-plastid stroma
ribonuclease MRP complex
U2-type catalytic step 2 spliceosome
cytosolic part
trans-Golgi network transport vesicle
protein-tyrosine phosphatase activity
rRNA methyltransferase activity
threonine-type endopeptidase activity
Atg8-specific protease activity
UDP-N-acetylmuramoylalanyl-D-glutamate-2,6-diaminopimelate ligase activity
glycerophosphodiester phosphodiesterase activity
oxidoreductase activity, acting on paired donors, with incorporation or reduction of molecular oxygen
cobalt ion transmembrane transporter activity
2-dehydro-3-deoxyglucarate aldolase activity
ATPase activity, uncoupled
asparagine dehydrogenase (NADP+) activity
pyridoxal 4-dehydrogenase activity
snoRNA binding
deoxycytidine kinase activity
ATP-dependent RNA helicase activity
mRNA guanylyltransferase activity
D-lactate dehydrogenase activity
Leukoglycine aminohydrolase activity
structural constituent of ribosome
ubiquitin protein ligase binding
aldose 1-epimerase activity
3-cyanoalanine hydratase activity
phytoene synthase activity
anthranilate N-benzoyltransferase activity
alanine-tRNA ligase activity
cyanoalanine nitrilase activity
fructokinase activity
cysteine-type carboxypeptidase activity
DNA topoisomerase type II (ATP-hydrolyzing) activity
nuclear localization sequence binding
mannosyl-oligosaccharide 1,3-1,6-alpha-mannosidase activity
GDP-D-glucose phosphorylase activity
choline transmembrane transporter activity
D-arabinose 1-dehydrogenase (NAD) activity
calcium-independent phospholipase A2 activity
GTPase activator activity
L-galactose dehydrogenase activity
acetyl-CoA decarboxylase activity
glycolate dehydrogenase activity
galactose 1-dehydrogenase activity
glutamate dehydrogenase (NADP+) activity
indole-3-acetonitrile nitrilase activity
D-arabinose 1-dehydrogenase (NADP+) activity
ribonucleoprotein complex binding
polynucleotide 5'-phosphatase activity
polynucleotide adenylyltransferase activity
ionotropic glutamate receptor binding
phosphatidyl-myo-cyclohydrolase activity
phosphoribosyl-ATP diphosphatase activity
phosphorelay response regulator activity
magnesium ion transmembrane transporter activity
cellobiose glucosidase activity
L-histidine transmembrane transporter activity
nitrilase hydratase activity
D-threo-aldose 1-dehydrogenase activity
guanyl-ribonucleotide binding
prephenate dehydrogenase (NADP+) activity
satellite DNA binding
Group II intron splicing
protein dephosphorylation
xylem and phloem pattern formation
energy derivation by oxidation of organic compounds
early endosome to Golgi transport
protein delipidation
mRNA polyadenylation
regulation of JAK-STAT cascade
microtubule-based peroxisome localization
multicellular organismal reproductive process
regulation of AMPA receptor activity
regulation of alternative mRNA splicing, via spliceosome
termination of RNA polymerase II transcription
CVT pathway
detection of phosphate ion
defense response, incompatible interaction
vulval development
alanyl-tRNA aminoacylation
pyrimidine nucleoside salvage
bone marrow development
electron transport chain
regulation of G2/M transition of mitotic cell cycle
RNA interference
regulation of GTPase activity
generation of catalytic spliceosome for second transesterification step
embryonic genitalia morphogenesis
leaf morphogenesis
single-organism carbohydrate catabolic process
molybdenum incorporation into molybdenum-molybdopterin complex
maturation of LSU-rRNA from tricistronic rRNA transcript (SSU-rRNA, 5.8S rRNA, LSU-rRNA)
regulation of cell proliferation
regulation of response to water deprivation
glycerol-3-phosphate biosynthetic process
positive regulation of post-embryonic development
salicylic acid metabolic process
vegetative to reproductive phase transition of meristem
mRNA export from nucleus
single-organism transport
Mo-molybdopterin cofactor biosynthetic process
mitophagy
circadian rhythm
regulation of flower development
dehydro-D-arabinono-1,4-lactone biosynthetic process
learning
mitochondrial respiratory chain complex III assembly
covalent chromatin modification
leukocyte chemotaxis
cobalt ion transport
polysaccharide metabolic process
germ line stem cell niche homeostasis
protein ubiquitination involved in ubiquitin-dependent protein catabolic process
regulation of reactive oxygen species metabolic process
pericentriolar microautophagy of nucleus
negative regulation of defense response
inner cell mass cell proliferation
cellular defense response
protein modification by small protein conjugation
nuclear-transcribed mRNA catabolic process, nonsense-mediated decay
mature ribosome assembly
cytokinin-activated signaling pathway
protein-N-acetylglucosaminyltransferase activity
protein tyrosine/serine/threonine phosphatase activity
glucose-6-phosphate 1-isomerase activity
glucose-6-phosphate dehydrogenase activity
response to freezing
zinc ion binding
chromatin silencing
copper-exporting ATPase activity
0
200
400
600
800
1000
1200
1400
GO Terms
Gene number
FS
SCLD-2

GO. Cluster 5

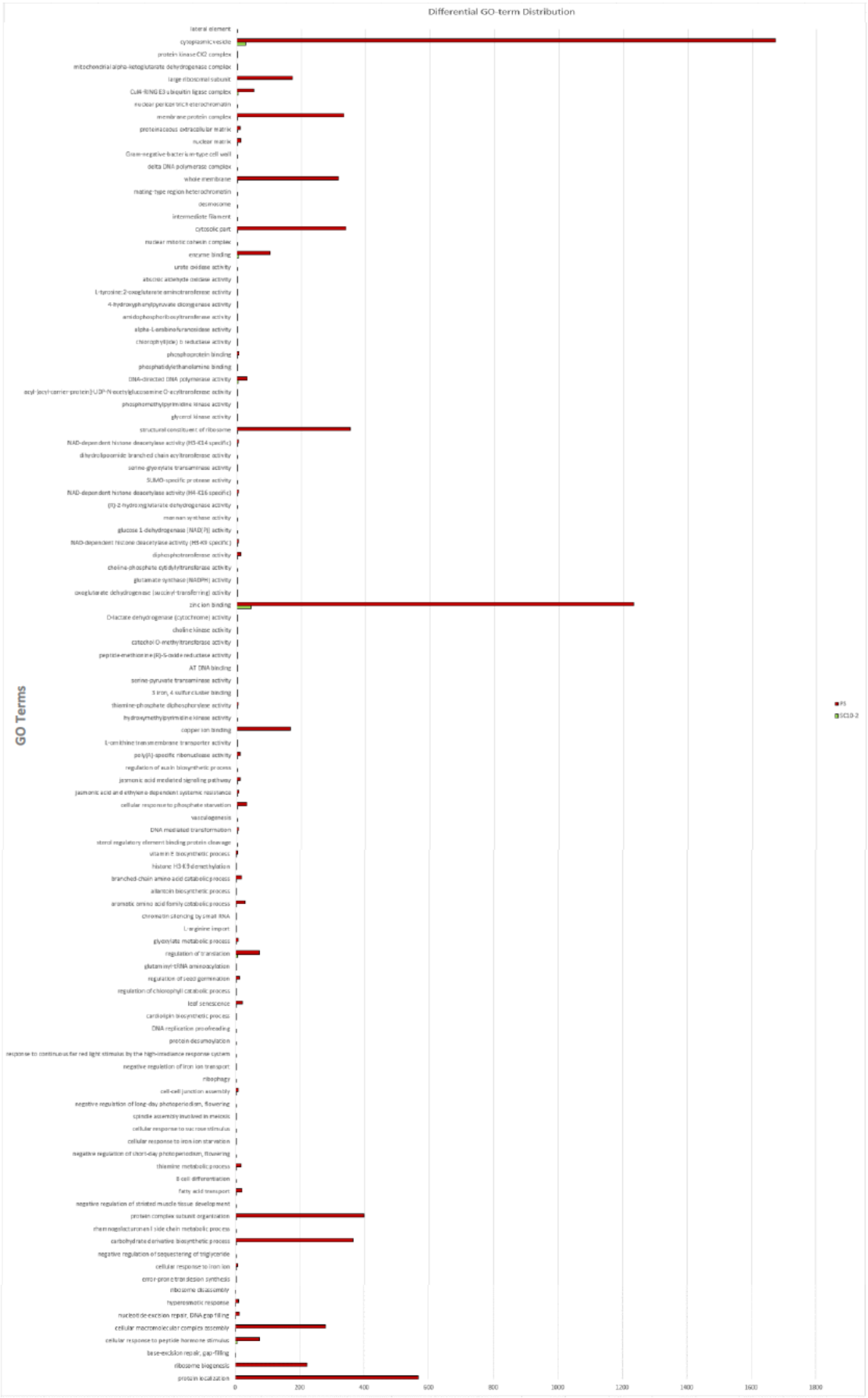
Differential GO-term Distribution
GO Terms
Gene number
F5
SC10-2
lateral element
cytoplasmic vesicle
protein kinase CK2 complex
mitochondrial alpha-ketoglutarate dehydrogenase complex
large ribosomal subunit
CUL4-RING E3 ubiquitin ligase complex
nuclear periphery euchromatin
membrane protein complex
proteinaceous extracellular matrix
nuclear matrix
Gram-negative-bacterium-type cell wall
delta DNA polymerase complex
whole membrane
mating-type region heterochromatin
desmosome
intermediate filament
cytosolic part
nuclear mitotic cohesin complex
enzyme binding
urate oxidase activity
abscisic aldehyde oxidase activity
L-tyrosine:2-oxoglutarate aminotransferase activity
4-hydroxyphenylpyruvate dioxygenase activity
amidophosphoribosyltransferase activity
alpha-L-arabinofuranosidase activity
chlorophyllide b reductase activity
phosphoprotein binding
phosphatidylethanolamine binding
DNA-directed DNA polymerase activity
acyl-[acyl-carrier-protein]-UDP-N-acetylglucosamine O-acyltransferase activity
phosphomethylpyrimidine kinase activity
glycerol kinase activity
structural constituent of ribosome
NAD-dependent histone deacetylase activity (H3-K14 specific)
dihydrolipoamide branched chain acyltransferase activity
serine-glyoxylate transaminase activity
SUMO-specific protease activity
NAD-dependent histone deacetylase activity (H4-K16 specific)
(S)-2-hydroxyglutarate dehydrogenase activity
mannan synthase activity
glucose 1-dehydrogenase (NAD(P)) activity
NAD-dependent histone deacetylase activity (H3-K9 specific)
diphosphotransferase activity
choline-phosphate cytidylyltransferase activity
glutamate synthase (NADPH) activity
oxoglutarate dehydrogenase (succinyl-transferring) activity
zinc ion binding
D-lactate dehydrogenase (cytochrome) activity
choline kinase activity
catechol O-methyltransferase activity
peptide-methionine (R)-S-oxide reductase activity
AT DNA binding
serine-pyruvate transaminase activity
3 iron, 4 sulfur cluster binding
thiamine-phosphate diphosphorylase activity
hydroxymethylpyrimidine kinase activity
copper ion binding
L-ornithine transmembrane transporter activity
poly(U)-specific ribonuclease activity
regulation of auxin biosynthetic process
jasmonic acid mediated signalling pathway
jasmonic acid and ethylene dependent systemic resistance
cellular response to phosphate starvation
vasculogenesis
DNA mediated transformation
sterol regulatory element binding protein cleavage
vitamin E biosynthetic process
histone H3-K9 demethylation
branched-chain amino acid catabolic process
allantoin biosynthetic process
aromatic amino acid family catabolic process
chromatin silencing by small RNA
L-arginine import
glyoxylate metabolic process
regulation of translation
glutaminyl-tRNA aminoacylation
regulation of seed germination
regulation of chlorophyll catabolic process
leaf senescence
cardiolipin biosynthetic process
DNA replication proofreading
protein desumoylation
response to continuous far red light stimulus by the high-irradiance response system
negative regulation of iron ion transport
ribophagy
cell-cell junction assembly
negative regulation of long-day photoperiodism, flowering
cytokinetic process involved in meiosis
cellular response to sucrose stimulus
cellular response to iron ion starvation
negative regulation of short-day photoperiodism, flowering
thiamine metabolic process
B cell differentiation
fatty acid transport
negative regulation of striated muscle tissue development
protein complex subunit organization
rhamnogalacturonan I side chain metabolic process
carbohydrate derivative biosynthetic process
negative regulation of sequestering of triglyceride
cellular response to iron ion
error-prone translesion synthesis
ribosome disassembly
hyperosmotic response
nucleotide-excision repair, DNA gap filling
cellular macromolecular complex assembly
cellular response to peptide hormone stimulus
base-excision repair, gap-filling
ribosome biogenesis
protein localization
0
200
400
600
800
1000
1200
1400
1600
1800

GO. Cluster 6

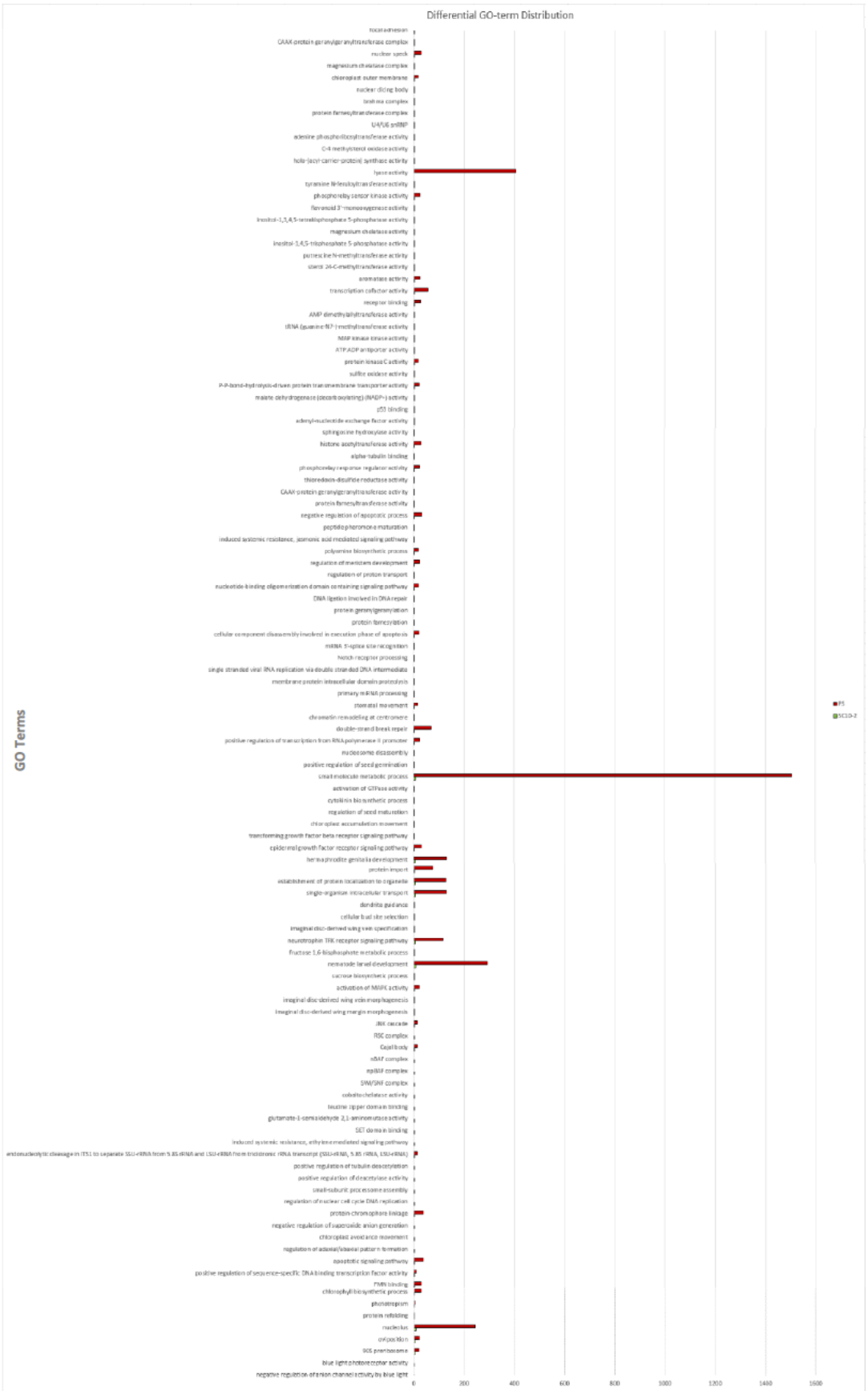
Differential GO-term Distribution
focal adhesion
CAAX-protein geranylgeranyltransferase complex
nuclear speck
magnesium chelatase complex
chloroplast outer membrane
nuclear dicing body
brahma complex
protein farnesyltransferase complex
U4/U6 snRNP
adenine phosphoribosyltransferase activity
C-4 methysterol oxidase activity
holo-[acyl-carrier-protein] synthase activity
lyase activity
tyramine N-feruloyltransferase activity
phosphorelay sensor kinase activity
flavanoid 3'-monooxygenase activity
inositol-1,3,4,5-tetrakisphosphate 5-phosphatase activity
magnesium chelatase activity
inositol-1,4,5-trisphosphate 5-phosphatase activity
putrescine N-methyltransferase activity
sterol 24-C-methyltransferase activity
aromatase activity
transcription cofactor activity
receptor binding
AMP dimethylallyltransferase activity
tRNA (guanine-N7-)-methyltransferase activity
MAP kinase kinase activity
ATP:ADP antiporter activity
protein kinase C activity
sulfite oxidase activity
P-P-bond-hydrolysis-driven protein transmembrane transporter activity
malate dehydrogenase (decarboxylating) (NADP+) activity
t53 binding
adenyl-nucleotide exchange factor activity
sphingosine hydroxylase activity
histone acetyltransferase activity
alpha-tubulin binding
phosphorelay response regulator activity
thioredoxin-disulfide reductase activity
CAAX-protein geranylgeranyltransferase activity
protein farnesyltransferase activity
negative regulation of apoptotic process
peptidyl-pheromone maturation
induced systemic resistance, jasmonic acid mediated signaling pathway
polyamine biosynthetic process
regulation of meristem development
regulation of protein transport
nucleotide-binding oligomerization domain containing signaling pathway
DNA ligation involved in DNA repair
protein geranylgeranylation
protein farnesylation
cellular component disassembly involved in execution phase of apoptosis
mRNA 5'-splice site recognition
Notch receptor processing
single-stranded viral RNA replication via double-stranded DNA intermediate
membrane protein intracellular domain proteolysis
primary miRNA processing
stomatal movement
chromatin remodeling at centromere
double-strand break repair
positive regulation of transcription from RNA polymerase II promoter
nucleosome disassembly
positive regulation of seed germination
small molecule metabolic process
activation of GTPase activity
cytokinin biosynthetic process
regulation of seed maturation
chloroplast accumulation movement
transforming growth factor beta receptor signaling pathway
epidermal growth factor receptor signaling pathway
hermaphrodite genitalia development
protein import
establishment of protein localization to organelle
single-organism intracellular transport
dendrite guidance
cellular bud site selection
imaginal disc-derived wing vein specification
neurotrophin TRK receptor signaling pathway
fructose 1,6-bisphosphate metabolic process
nematode larval development
sucrose biosynthetic process
activation of MAPK activity
imaginal disc-derived wing vein morphogenesis
imaginal disc-derived wing margin morphogenesis
JNK cascade
RISC complex
Cajal body
nBAF complex
npBAF complex
SWI/SNF complex
cobalt chelatase activity
leucine zipper domain binding
glutamate-1-semialdehyde 2,1-aminomutase activity
SET domain binding
induced systemic resistance, ethylene mediated signaling pathway
endonucleolytic cleavage in ITS1 to separate SSU-rRNA from 5.8S rRNA and LSU-rRNA from tricistronic rRNA transcript (SSU-rRNA, 5.8S rRNA, LSU-rRNA)
positive regulation of tubulin deacetylation
positive regulation of deacetylase activity
small-subunit processome assembly
regulation of nuclear cell cycle DNA replication
protein-chromophore linkage
negative regulation of superoxide anion generation
chloroplast avoidance movement
regulation of adaxial/abaxial pattern formation
apoptotic signaling pathway
positive regulation of sequence-specific DNA binding transcription factor activity
FMN binding
chlorophyll biosynthetic process
phototropism
protein refolding
nucleolus
cytoplasm
90S preribosome
blue light photoreceptor activity
negative regulation of ion channel activity by blue light
GO Terms
Gene number
0
200
400
600
800
1000
1200
1400
1600
P5
SC10-2

GO. Cluster 7

Supplementary Figure 4. Gene Ontology (GO) of the different clusters obtained using differentially expressed genes, only considering the introgression differences over time in melon fruit of the near-isogenic line NIL SC10-2 and its parental ´Piel de Sapo´ (PS) harvested in firm-ripe stage of maturity and stored at 20.5 ^{o}C and 88% relative humidity for18 d.

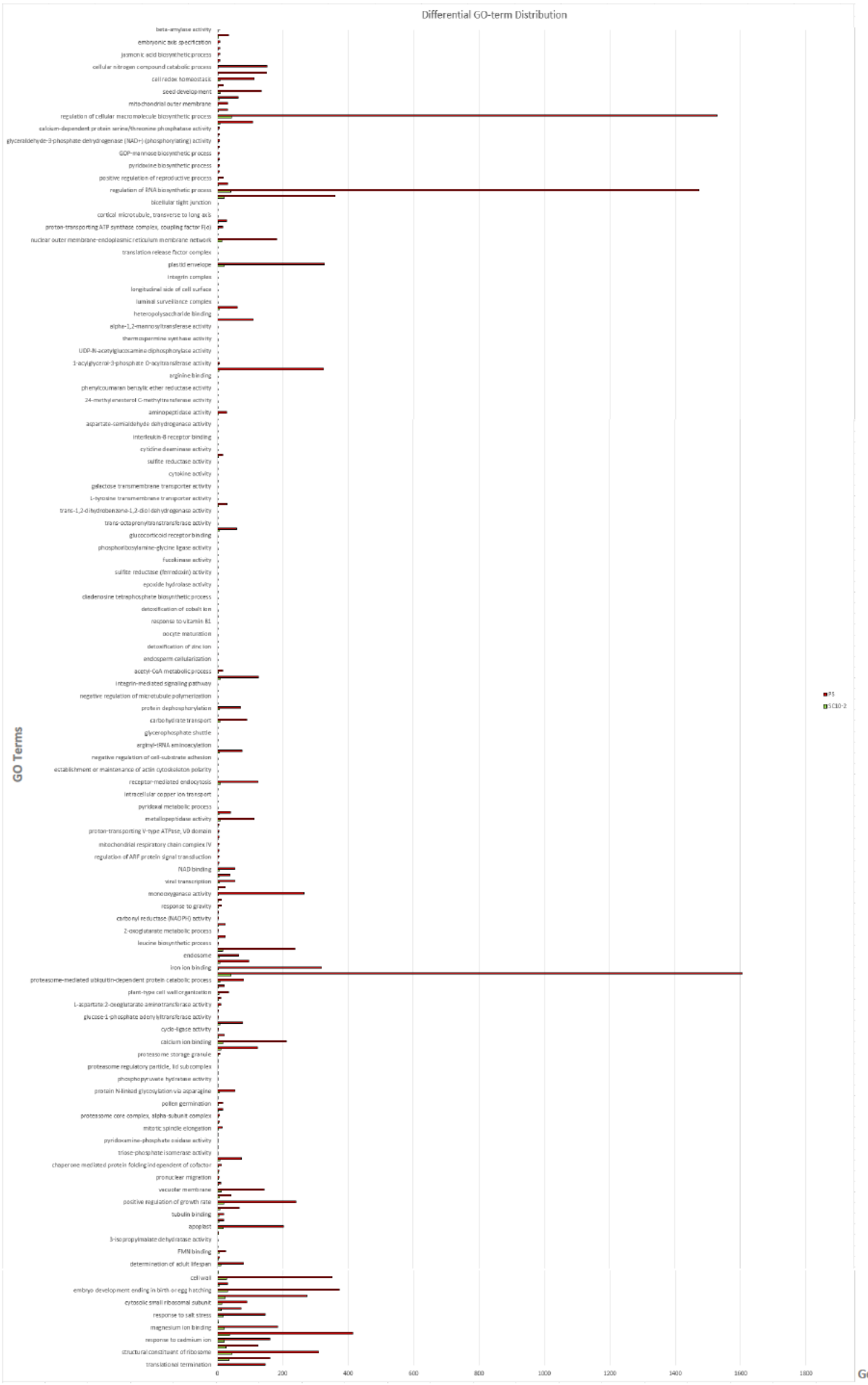
Differential GO-term Distribution
beta-amylase activity
embryonic axis specification
jasmonic acid biosynthetic process
cellular nitrogen compound catabolic process
cell redox homeostasis
seed development
mitochondrial outer membrane
regulation of cellular macromolecule biosynthetic process
calcium-dependent protein serine/threonine phosphatase activity
glyceraldehyde-3-phosphate dehydrogenase (NAD+) (phosphorylating) activity
GDP-mannose biosynthetic process
pyridoxine biosynthetic process
positive regulation of reproductive process
regulation of RNA biosynthetic process
bicellular tight junction
cortical microtubule, transverse to long axis
proton-transporting ATP synthase complex, coupling factor F(o)
nuclear outer membrane-endoplasmic reticulum membrane network
translation release factor complex
plastid envelope
integrin complex
longitudinal side of cell surface
luminal surveillance complex
heteropolysaccharide binding
alpha-1,2-mannosyltransferase activity
thermospermine synthase activity
UDP-N-acetylglucosamine diphosphorylase activity
1-acylglycerol-3-phosphate O-acyltransferase activity
arginine binding
phenylcoumaran benzylic ether reductase activity
24-methylenesterol C-methyltransferase activity
aminopeptidase activity
aspartate-semialdehyde dehydrogenase activity
interleukin-8 receptor binding
cytidine deaminase activity
sulfite reductase activity
cytokine activity
galactose transmembrane transporter activity
L-tyrosine transmembrane transporter activity
trans-1,2-dihydrobenzene-1,2-diol dehydrogenase activity
trans-octaprenyltranstransferase activity
glucocorticoid receptor binding
phosphoribosylamine-glycine ligase activity
Fucokinase activity
sulfite reductase (ferredoxin) activity
epoxide hydrolase activity
cladenosine tetraphosphate biosynthetic process
detoxification of cobalt ion
response to vitamin B1
oocyte maturation
detoxification of zinc ion
endosperm cellularization
acetyl-CoA metabolic process
integrin-mediated signaling pathway
negative regulation of microtubule polymerization
protein dephosphorylation
carbohydrate transport
glycerophosphate shuttle
arginyl-tRNA aminoacylation
negative regulation of cell-substrate adhesion
establishment or maintenance of actin cytoskeleton polarity
receptor-mediated endocytosis
intracellular copper ion transport
pyridoxal metabolic process
metallopeptidase activity
proton-transporting V-type ATPase, V0 domain
mitochondrial respiratory chain complex IV
regulation of ARF protein signal transduction
NAD binding
viral transcription
monooxygenase activity
response to gravity
carbonyl reductase (NADPH) activity
2-oxoglutarate metabolic process
leucine biosynthetic process
endosome
iron ion binding
proteasome-mediated ubiquitin-dependent protein catabolic process
plant-type cell wall organization
L-aspartate:2-oxoglutarate aminotransferase activity
glucose-1-phosphate adenylyltransferase activity
cyclo-ligase activity
calcium ion binding
proteasome storage granule
proteasome regulatory particle, lid subcomplex
phosphopyruvate hydratase activity
protein N-linked glycosylation via asparagine
pollen germination
proteasome core complex, alpha-subunit complex
mitotic spindle elongation
pyridoxamine-phosphate oxidase activity
triose-phosphate isomerase activity
chaperone mediated protein folding independent of cofactor
pronuclear migration
vacuolar membrane
positive regulation of growth rate
tubulin binding
apoplast
3-isopropylmalate dehydratase activity
FMN binding
determination of adult lifespan
cell wall
embryo development ending in birth or egg hatching
cytosolic small ribosomal subunit
response to salt stress
magnesium ion binding
response to cadmium ion
structural constituent of ribosome
translational termination
GO Terms
0
200
400
600
800
1000
1200
1400
1600
1800
Gene number
R9
SC10-2

GO. Cluster 1

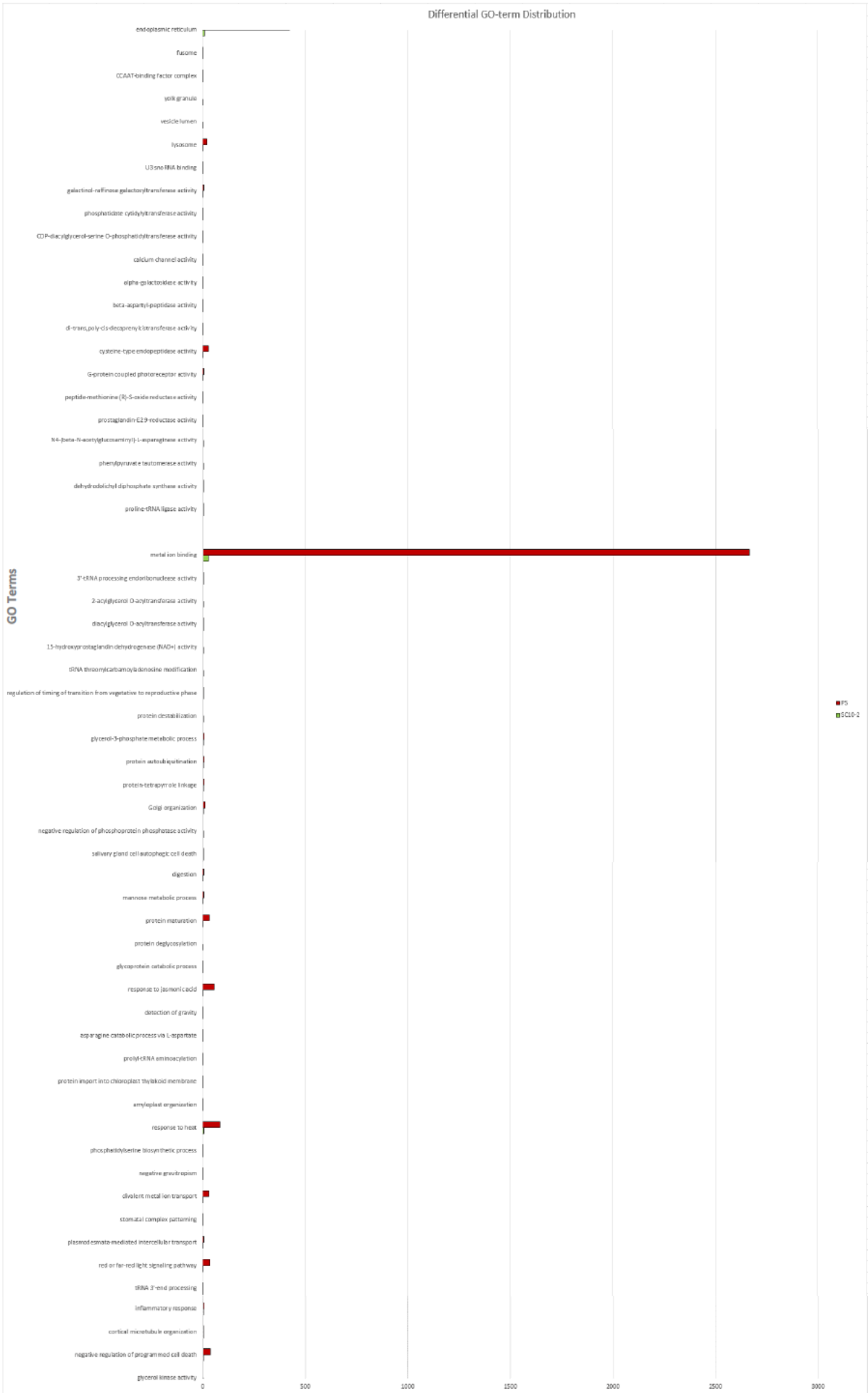
Differential GO-term Distribution
endoplasmic reticulum
fusome
CCAAT-binding factor complex
yolk granule
vesicle lumen
lysosome
U3 snoRNA binding
galactinol-raffinose galactosyltransferase activity
phosphatidate cytidylyltransferase activity
CDP-diacylglycerol-serine O-phosphatidyltransferase activity
calcium channel activity
alpha-galactosidase activity
beta-aspartyl-peptidase activity
di-trans,poly-cis-decaprenylcistransferase activity
cysteine-type endopeptidase activity
G-protein coupled photoreceptor activity
peptide-methionine (R)-S-oxide reductase activity
prostaglandin-E2 9-reductase activity
N4-(beta-N-acetylglucosaminyl)-L-asparaginase activity
phenylpyruvate tautomerase activity
dehydrodolichyl diphosphate synthase activity
proline-tRNA ligase activity
metal ion binding
3'-tRNA processing endoribonuclease activity
2-acylglycerol O-acyltransferase activity
diacylglycerol O-acyltransferase activity
15-hydroxyprostaglandin dehydrogenase (NAD+) activity
tRNA threonylcarbamoyladenosine modification
regulation of timing of transition from vegetative to reproductive phase
protein destabilization
glycerol-3-phosphate metabolic process
protein autoubiquitination
protein-tetrapyrrole linkage
Golgi organization
negative regulation of phosphoprotein phosphatase activity
salivary gland cell autophagic cell death
digestion
mannose metabolic process
protein maturation
protein deglycosylation
glycoprotein catabolic process
response to jasmonic acid
detection of gravity
asparagine catabolic process via L-aspartate
prolyl-tRNA aminoacylation
protein import into chloroplast thylakoid membrane
amyloplast organization
response to heat
phosphatidylserine biosynthetic process
negative gravitropism
divalent metal ion transport
stomatal complex patterning
plasmodesmata-mediated intercellular transport
red or far-red light signaling pathway
tRNA 3'-end processing
inflammatory response
cortical microtubule organization
negative regulation of programmed cell death
glycerol kinase activity
GO Terms
0
500
1000
1500
2000
2500
3000
Gene number
FS
SC10-2

GO. Cluster 2

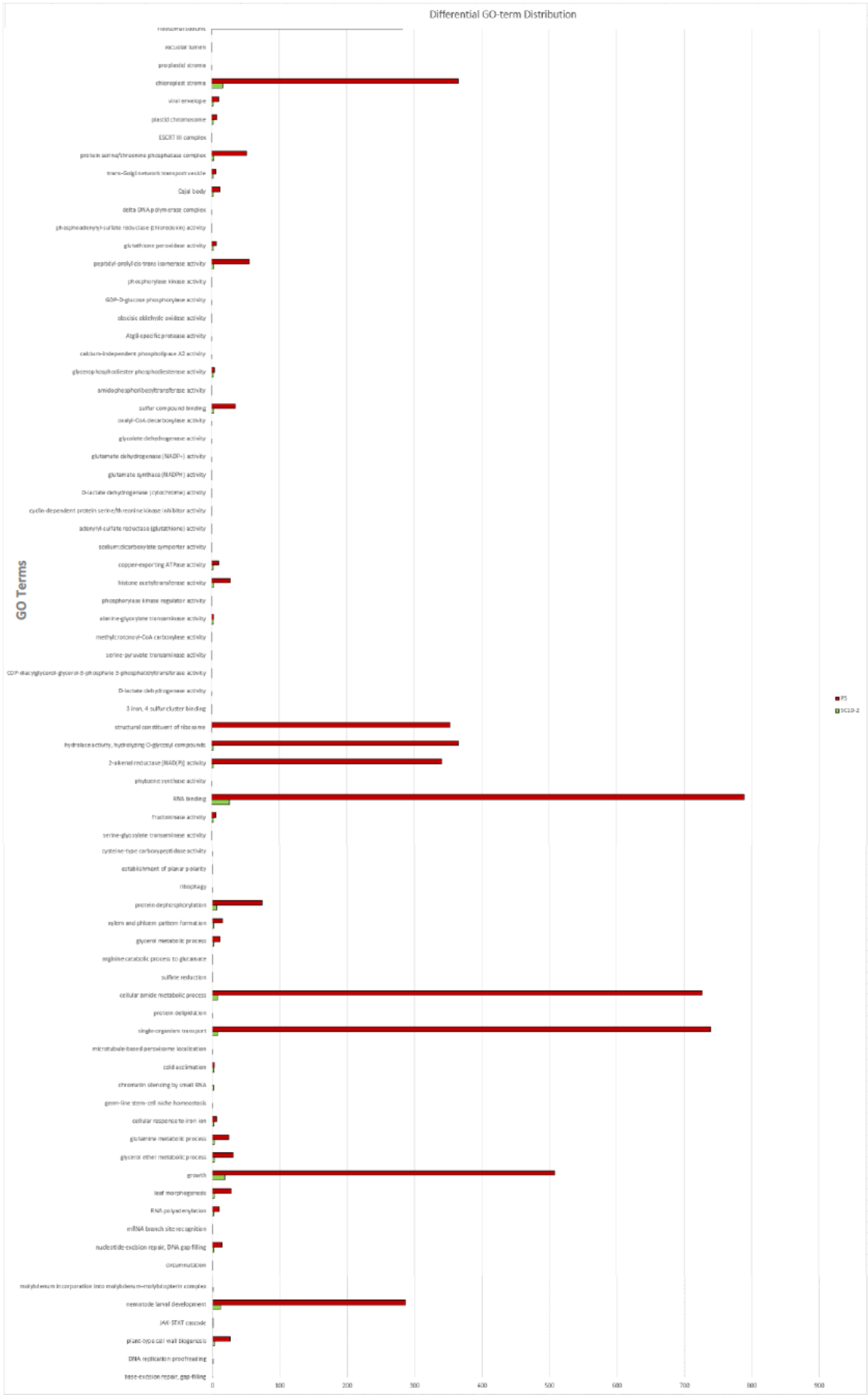
Differential GO-term Distribution
vacuolar lumen
proplastid stroma
chloroplast stroma
viral envelope
plastid chromosome
ESCRT III complex
protein serine/threonine phosphatase complex
trans-Golgi network transport vesicle
Cajal body
delta DNA polymerase complex
phosphoadenylyl-sulfate reductase (thioredoxin) activity
glutathione peroxidase activity
peptidyl-prolyl cis-trans isomerase activity
phosphorylase kinase activity
GDP-D-glucose phosphorylase activity
abscisic aldehyde oxidase activity
Atg8-specific protease activity
calcium-independent phospholipase A2 activity
glycerophosphodiester phosphodiesterase activity
amidophosphoribosyltransferase activity
sulfur compound binding
oxalyl-CoA decarboxylase activity
glycolate dehydrogenase activity
glutamate dehydrogenase (NADP+) activity
glutamate synthase (NADPH) activity
D-lactate dehydrogenase (cytochrome) activity
cyclin-dependent protein serine/threonine kinase inhibitor activity
adenylyl-sulfate reductase (glutathione) activity
sodium:dicarboxylate symporter activity
copper-exporting ATPase activity
histone acetyltransferase activity
phosphorylase kinase regulator activity
alanine-glyoxylate transaminase activity
methylcrotonoyl-CoA carboxylase activity
serine-pyruvate transaminase activity
CDP-diacylglycerol-glycerol-3-phosphate 3-phosphatidyltransferase activity
D-lactate dehydrogenase activity
3 iron, 4 sulfur cluster binding
structural constituent of ribosome
hydrolase activity, hydrolyzing O-glycosyl compounds
2-alkenal reductase [NAD(P)] activity
phytoene synthase activity
RNA binding
fructokinase activity
serine-glyoxylate transaminase activity
cysteine-type carboxypeptidase activity
establishment of planar polarity
ribophagy
protein dephosphorylation
xylem and phloem pattern formation
glycerol metabolic process
arginine catabolic process to glutamate
sulfate reduction
cellular amide metabolic process
protein delipidation
single-organism transport
microtubule-based peroxisome localization
cold acclimation
chromatin silencing by small RNA
germ line stem cell niche homeostasis
cellular response to iron ion
glutamine metabolic process
glycerol ether metabolic process
growth
leaf morphogenesis
RNA polyadenylation
mRNA branch site recognition
nucleotide-excision repair, DNA gap filling
circumnutation
molybdenum ion transport
nematode larval development
JAK-STAT cascade
plant-type cell wall biogenesis
DNA replication proofreading
base-excision repair, gap-filling
GO Terms
P5
SC10-2
0
100
200
300
400
500
600
700
800
900
Gene number

GO. Cluster 3

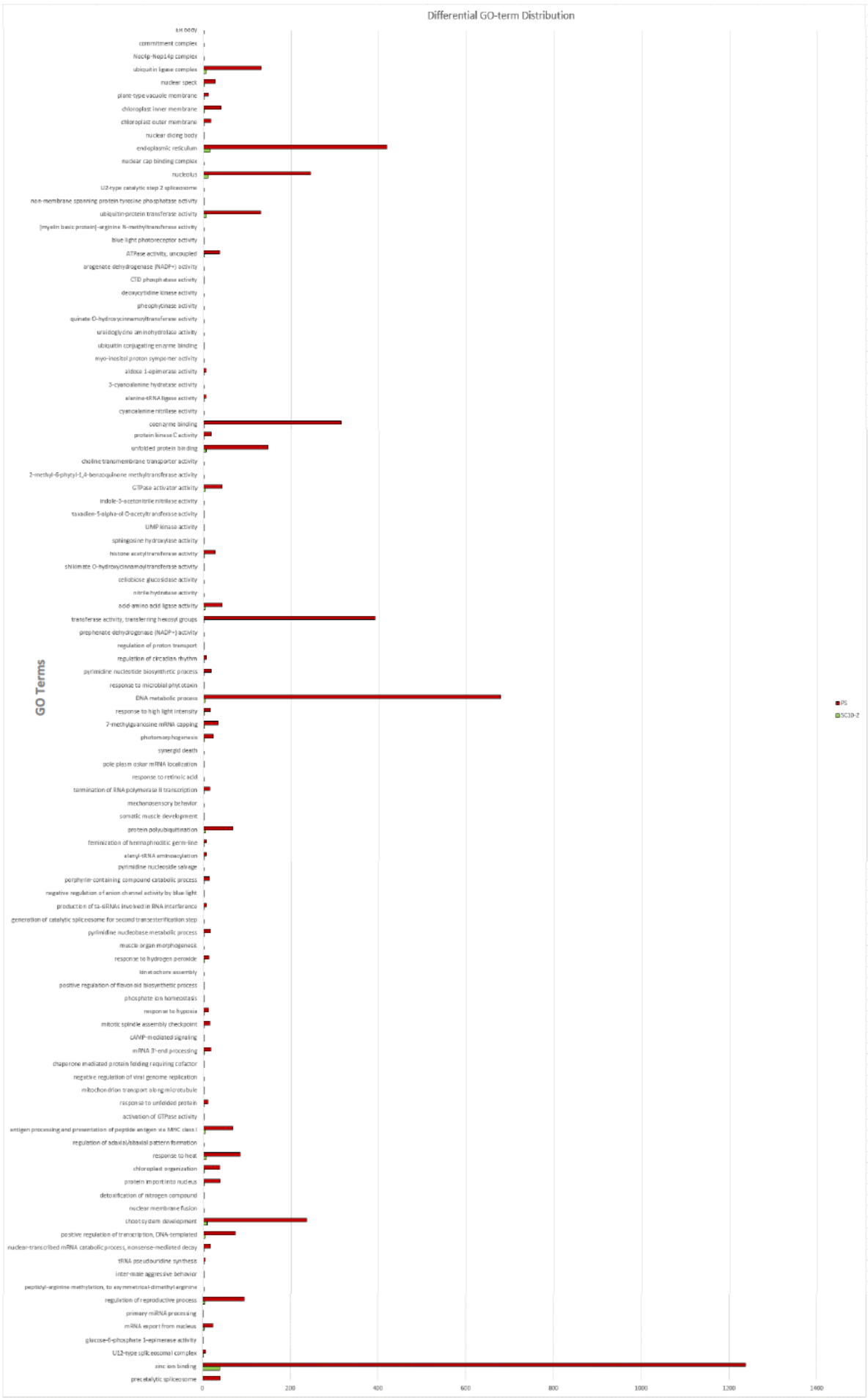
Differential GO-term Distribution
GO Terms
Gene number
PS
SG10-2
LH body
commitment complex
Noc4p-Nop14p complex
ubiquitin ligase complex
nuclear speck
plant-type vacuole membrane
chloroplast inner membrane
chloroplast outer membrane
nuclear dicing body
endoplasmic reticulum
nuclear cap binding complex
nucleolus
U2-type catalytic step 2 spliceosome
non-membrane spanning protein tyrosine phosphatase activity
ubiquitin-protein transferase activity
[myelin basic protein]-arginine N-methyltransferase activity
blue light photoreceptor activity
ATPase activity, uncoupled
arogenate dehydrogenase (NADP+) activity
CTD phosphatase activity
deoxycytidine kinase activity
pheophytinase activity
quinate O-hydroxycinnamoyltransferase activity
ureidoglycine aminohydrolase activity
ubiquitin conjugating enzyme binding
myo-inositol proton symporter activity
aldose 1-epimerase activity
3-cyanoalanine hydratase activity
alanine-tRNA ligase activity
cyanoalanine nitrilase activity
coenzyme binding
protein kinase C activity
unfolded protein binding
choline transmembrane transporter activity
2-methyl-6-phytyl-1,4-benzoquinone methyltransferase activity
GTPase activator activity
indole-3-acetonitrile nitrilase activity
taxadien-5-alpha-ol O-acetyltransferase activity
UMP kinase activity
sphingosine hydroxylase activity
histone acetyltransferase activity
shikimate O-hydroxycinnamoyltransferase activity
cellobiose glucosidase activity
nitrile hydratase activity
acid-amino acid ligase activity
transferase activity, transferring hexosyl groups
prephenate dehydrogenase (NADP+) activity
regulation of proton transport
regulation of circadian rhythm
pyrimidine nucleotide biosynthetic process
response to microbial phytotoxin
DNA metabolic process
response to high light intensity
7-methylguanosine mRNA capping
photomorphogenesis
synergid death
pole plasm oskar mRNA localization
response to retinoic acid
termination of RNA polymerase II transcription
mechanosensory behavior
somatic muscle development
protein polyubiquitination
feminization of hermaphroditic germ-line
alanyl-tRNA aminoacylation
pyrimidine nucleoside salvage
porphyrin-containing compound catabolic process
negative regulation of anion channel activity by blue light
production of ta-siRNAs involved in RNA interference
generation of catalytic spliceosome for second transesterification step
pyrimidine nucleobase metabolic process
muscle organ morphogenesis
response to hydrogen peroxide
kinetochore assembly
positive regulation of flavonoid biosynthetic process
phosphate ion homeostasis
response to hypoxia
mitotic spindle assembly checkpoint
cAMP-mediated signaling
mRNA 3'-end processing
chaperone mediated protein folding requiring cofactor
negative regulation of viral genome replication
mitochondrion transport along microtubule
response to unfolded protein
activation of GTPase activity
antigen processing and presentation of peptide antigen via MHC class I
regulation of adaxial/abaxial pattern formation
response to heat
chloroplast organization
protein import into nucleus
detoxification of nitrogen compound
nuclear membrane fusion
shoot system development
positive regulation of transcription, DNA-templated
nuclear-transcribed mRNA catabolic process, nonsense-mediated decay
tRNA pseudouridine synthesis
inter-male aggressive behavior
peptidyl-arginine methylation, to asymmetrical-dimethylarginine
regulation of reproductive process
primary miRNA processing
mRNA export from nucleus
glucose-6-phosphate 1-epimerase activity
U12-type spliceosomal complex
zinc ion binding
precatalytic spliceosome
0
200
400
600
800
1000
1200
1400

GO. Cluster 4

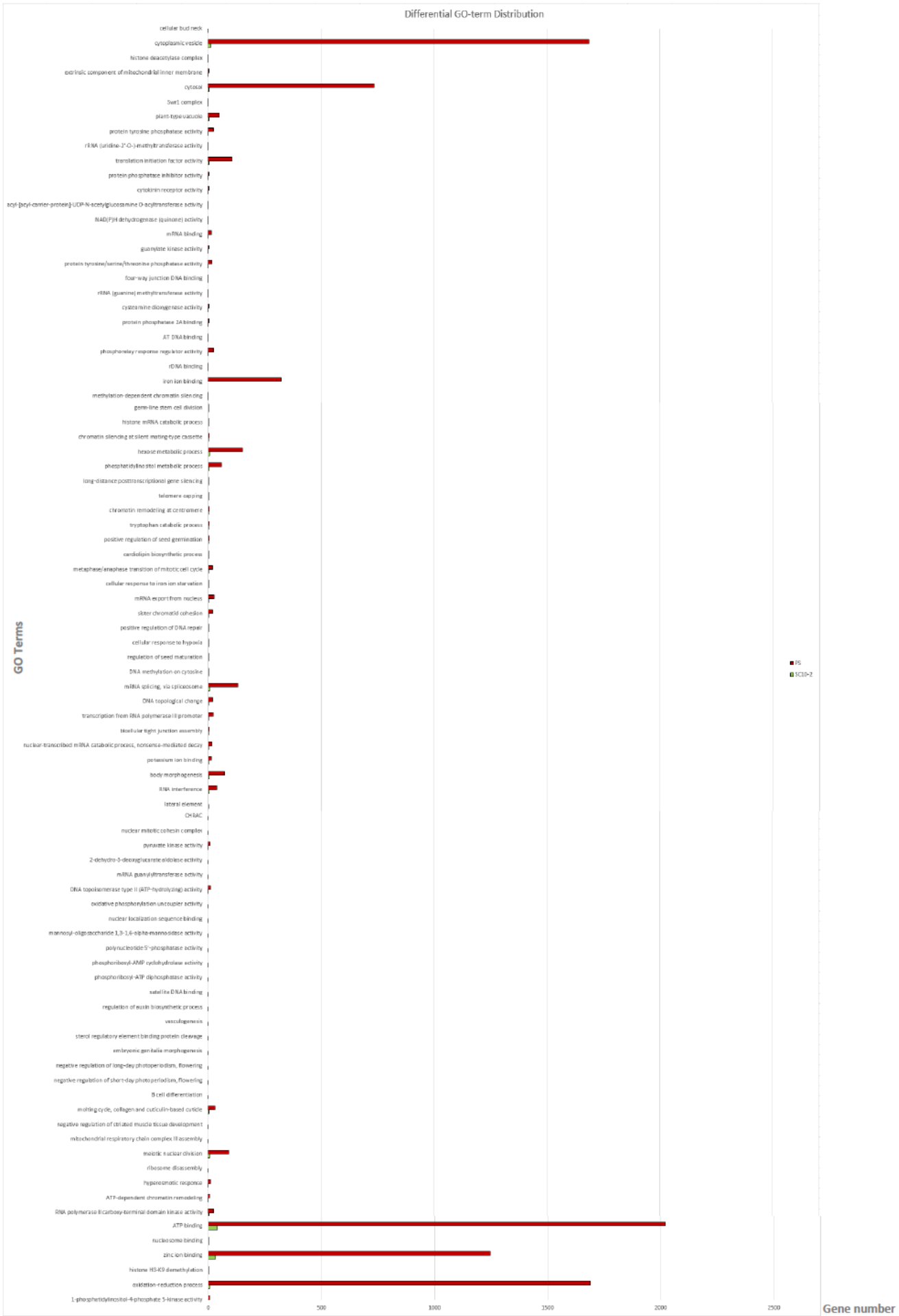
Differential GO-term Distribution
GO Terms
Gene number
IR
SC10-2
0
500
1000
1500
2000
2500
cellular bud neck
cytoplasmic vesicle
histone deacetylase complex
extrinsic component of mitochondrial inner membrane
cytosol
Swr1 complex
plant-type vacuole
protein tyrosine phosphatase activity
rRNA (uridine-2'-O-)-methyltransferase activity
translation initiation factor activity
protein phosphatase inhibitor activity
cytokinin receptor activity
acyl-[acyl-carrier-protein]-UDP-N-acetylglucosamine O-acyltransferase activity
NAD(P)H dehydrogenase (quinone) activity
mRNA binding
guanylate kinase activity
protein tyrosine/serine/threonine phosphatase activity
four-way junction DNA binding
rRNA (guanine) methyltransferase activity
cysteamine dioxygenase activity
protein phosphatase 2A binding
AT DNA binding
phosphorelay response regulator activity
rDNA binding
iron ion binding
methylation-dependent chromatin silencing
germ-line stem cell division
histone mRNA catabolic process
chromatin silencing at silent mating-type cassette
hexose metabolic process
phosphatidylinositol metabolic process
long-distance posttranscriptional gene silencing
telomere capping
chromatin remodeling at centromere
tryptophan catabolic process
positive regulation of seed germination
cardiolipin biosynthetic process
metaphase/anaphase transition of mitotic cell cycle
cellular response to iron ion starvation
mRNA export from nucleus
sister chromatid cohesion
positive regulation of DNA repair
cellular response to hypoxia
regulation of seed maturation
DNA methylation on cytosine
mRNA splicing, via spliceosome
DNA topological change
transcription from RNA polymerase III promoter
bicellular tight junction assembly
nuclear-transcribed mRNA catabolic process, nonsense-mediated decay
potassium ion binding
body morphogenesis
RNA interference
lateral element
CHRAC
nuclear mitotic cohesin complex
pyruvate kinase activity
2-dehydro-3-deoxyglucarate aldolase activity
mRNA guanylyltransferase activity
DNA topoisomerase type II (ATP-hydrolyzing) activity
oxidative phosphorylation uncoupler activity
nuclear localization sequence binding
mannosyl-oligosaccharide 1,3-1,6-alpha-mannosidase activity
polynucleoside 5'-phosphatase activity
phosphoribosyl-AMP cyclohydrolase activity
phosphoribosyl-ATP diphosphatase activity
satellite DNA binding
regulation of auxin biosynthetic process
vasculogenesis
sterol regulatory element binding protein cleavage
embryonic genitalia morphogenesis
negative regulation of long-day photoperiodism, flowering
negative regulation of short-day photoperiodism, flowering
B cell differentiation
molting cycle, collagen and cuticulin-based cuticle
negative regulation of striated muscle tissue development
mitochondrial respiratory chain complex III assembly
meiotic nuclear division
ribosome disassembly
hyperosmotic response
ATP-dependent chromatin remodeling
RNA polymerase II carboxy-terminal domain kinase activity
ATP binding
nucleosome binding
zinc ion binding
histone H3-K9 dimethylation
oxidation-reduction process
1-phosphatidylinositol-4-phosphate 5-kinase activity

GO. Cluster 5

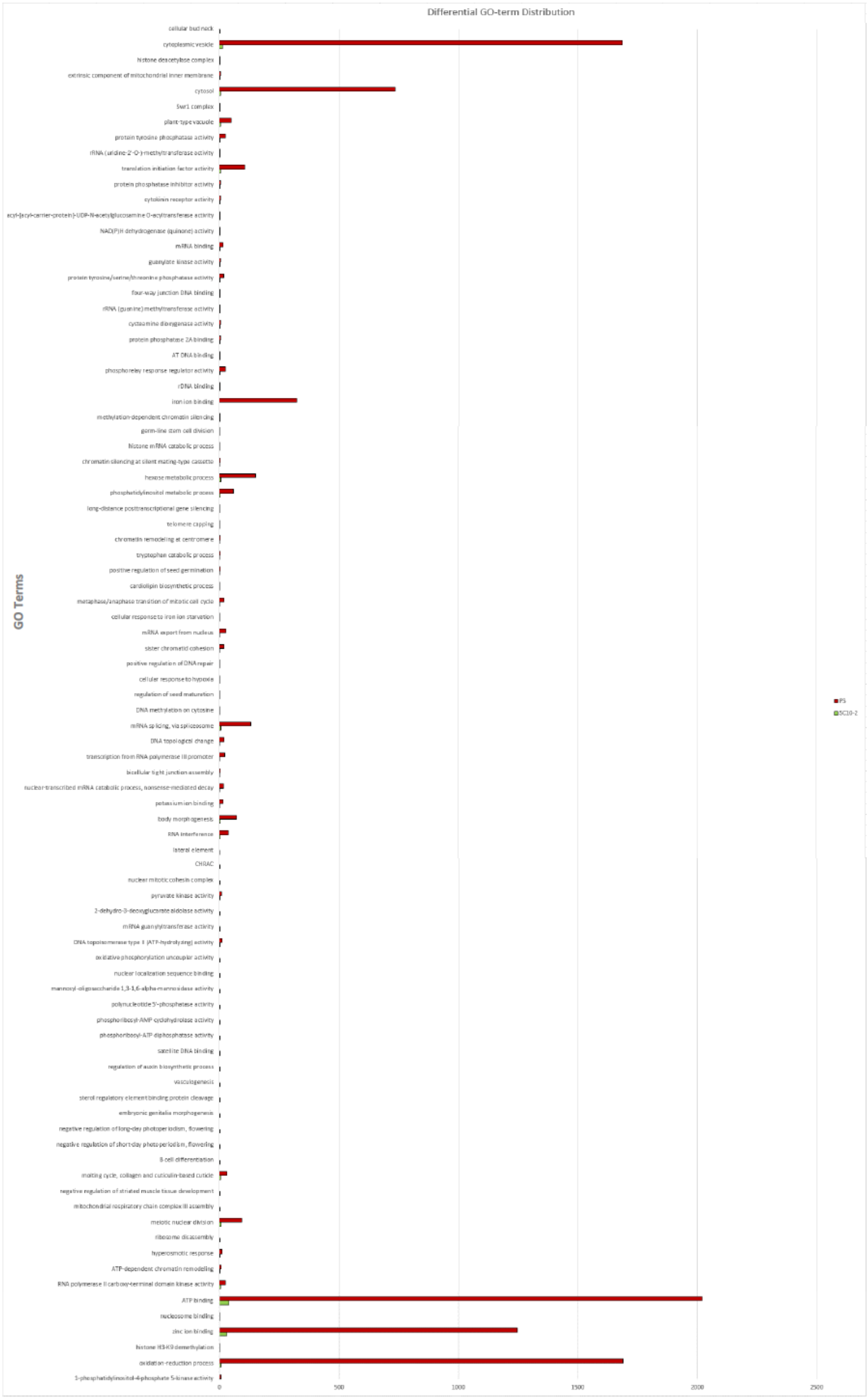
Differential GO-term Distribution
GO Terms
cellular bud neck
cytoplasmic vesicle
histone deacetylase complex
extrinsic component of mitochondrial inner membrane
cytosol
Swr1 complex
plant-type vacuole
protein tyrosine phosphatase activity
rRNA (uridine-2'-O-) methyltransferase activity
translation initiation factor activity
protein phosphatase inhibitor activity
cytokinin receptor activity
acyl-[acyl-carrier-protein]-UDP-N-acetylglucosamine O-acyltransferase activity
NAD(P)H dehydrogenase (quinone) activity
mRNA binding
guanylate kinase activity
protein tyrosine/serine/threonine phosphatase activity
four-way junction DNA binding
rRNA (guanine) methyltransferase activity
cysteamine dioxygenase activity
protein phosphatase 2A binding
AT DNA binding
phosphorelay response regulator activity
rDNA binding
iron ion binding
methylation-dependent chromatin silencing
germ-line stem cell division
histone mRNA catabolic process
chromatin silencing at silent mating-type cassette
hexose metabolic process
phosphatidylinositol metabolic process
long-distance posttranscriptional gene silencing
telomere capping
chromatin remodeling at centromere
tryptophan catabolic process
positive regulation of seed germination
cardiolipin biosynthetic process
metaphase/anaphase transition of mitotic cell cycle
cellular response to iron ion starvation
mRNA export from nucleus
sister chromatid cohesion
positive regulation of DNA repair
cellular response to hypoxia
regulation of seed maturation
DNA methylation on cytosine
mRNA splicing, via spliceosome
DNA topological change
transcription from RNA polymerase III promoter
bicellular tight junction assembly
nuclear-transcribed mRNA catabolic process, nonsense-mediated decay
potassium ion binding
body morphogenesis
RNA interference
lateral element
CHRAC
nuclear mitotic cohesin complex
pyruvate kinase activity
2-dehydro-3-deoxyglucarate aldolase activity
mRNA guanylyltransferase activity
DNA topoisomerase type II (ATP-hydrolyzing) activity
oxidative phosphorylation uncoupler activity
nuclear localization sequence binding
mannosyl-oligosaccharide 1,3-1,6-alpha-mannosidase activity
polynucleotide 5'-phosphatase activity
phosphoribosyl-AMP cyclohydrolase activity
phosphoribosyl-ATP diphosphatase activity
satellite DNA binding
regulation of auxin biosynthetic process
vasculogenesis
sterol regulatory element binding protein cleavage
embryonic genitalia morphogenesis
negative regulation of long-day photoperiodism, flowering
negative regulation of short-day photoperiodism, flowering
B cell differentiation
molting cycle, collagen and cuticulin-based cuticle
negative regulation of striated muscle tissue development
mitochondrial respiratory chain complex III assembly
meiotic nuclear division
ribosome disassembly
hyperosmotic response
ATP-dependent chromatin remodeling
RNA polymerase II carboxy-terminal domain kinase activity
ATP binding
nucleosome binding
zinc ion binding
histone H3-K9 demethylation
oxidation-reduction process
1-phosphatidylinositol-4-phosphate 5-kinase activity
0
500
1000
1500
2000
2500
Gene number
IPS
SC10-2

GO. Cluster 6

Supplementary Table 1. List of total Differentially Expressed Genes (2954 DEGs) only considering the comparison between lines over time fruit during postharvest storage at 20.5 ^{o}C and 88% relative humidity for 18 d of the near-isogenic line SC10-2 and its parental control ´Piel de Sapo´ (PS). 1 Presence 0 Absence in the list of DEGs during postharvest ripening time. Gene Ontology terms (GO terms) of the seven different clusters (named 1.x) obtained according to the differentially expressed gene pattern.

Gene ID	pval	qval	Description	
MELO3C010748	2.12940776123105e-12	4.2053673876552e-08	Heat shock transcription factor	1
MELO3C023889	1.64774860422767e-11	1.62706935924462e-07	Ultraviolet-B receptor UVR8	1
MELO3C005540	7.05828728797542e-11	4.64647052167422e-07	14 kDa proline-rich protein dc2.15	1
MELO3C026975	4.80710693473441e-10	1.99977760837466e-06	40S ribosomal protein S15a	1
MELO3C012728	5.06298447611186e-10	1.99977760837466e-06	Vacuolar sorting-associated protein 2-like protein	1
MELO3C003298	1.04465369688e-09	3.43847764328054e-06	high mobility group B protein 1	1
MELO3C013974	1.49749790345766e-09	4.22486944219789e-06	Hsp70-Hsp90 organizing protein 3	1
MELO3C026279	2.1098163216493e-09	5.20834531703152e-06	cell division cycle protein 48 homolog	1
MELO3C018265	2.94331214956145e-09	5.28431560378992e-06	ADP-ribosylation factor GTPase-activating protein	1
MELO3C020533	2.81429302084746e-09	5.28431560378992e-06	Ran-binding protein 1	1
MELO3C026613	2.4889622585178e-09	5.28431560378992e-06	Tubulin alpha chain	1
MELO3C015733	4.18112777733626e-09	6.88109103955115e-06	Pre-mRNA-splicing factor ATP-dependent RNA helicase	1
MELO3C016101	4.9076187558228e-09	6.92289734348174e-06	UBP1-associated protein 2C	1
MELO3C022036	4.56549242855431e-09	6.92289734348174e-06	protein LONGIFOLIA 2	1
MELO3C019941	6.56920629005242e-09	8.62635084597496e-06	T-complex protein 11	1
MELO3C018099	6.98878999116914e-09	8.62635084597496e-06	No data found	0
MELO3C023417	1.0827110208389e-08	1.25779176179691e-05	DUF4050 family protein	1
MELO3C002468	1.31388873114702e-08	1.44155491952347e-05	Tobamovirus multiplication protein 1	1
MELO3C003282	1.38912555902593e-08	1.44388635080016e-05	cleft lip and palate transmembrane protein 1 homolog	1
MELO3C024028	1.65297714405099e-08	1.63223228089315e-05	DEAD-box ATP-dependent RNA helicase	1
MELO3C014090	1.74401538766134e-08	1.6401218995678e-05	No data found	1
MELO3C008669	2.53079915912835e-08	2.11626693401623e-05	RING-type E3 ubiquitin transferase	1
MELO3C018038	2.64090955770513e-08	2.11626693401623e-05	proline iminopeptidase	1
MELO3C001317	2.67895454708622e-08	2.11626693401623e-05	Coiled-coil protein (DUF572)	1
MELO3C003752	2.55143854932527e-08	2.11626693401623e-05	gibberellin-regulated protein 11-like	1
MELO3C010731	2.89443125023325e-08	2.19854318310987e-05	cyclin-dependent kinase G-2 isoform X1	1
MELO3C008209	3.06606515732e-08	2.24265632562639e-05	Ankyrin	1
MELO3C013868	3.65972404603454e-08	2.41181691777337e-05	Cytochrome P450 family ent-kaurenoic acid oxidase	1
MELO3C019616	3.66370487281387e-08	2.41181691777337e-05	E3 ubiquitin-protein ligase RGLG2	1
MELO3C003444	3.45134805179725e-08	2.41181691777337e-05	transcription factor IWS1	1
MELO3C004023	4.57532089992441e-08	2.82368788914397e-05	NADPH--cytochrome P450 reductase	1
MELO3C019369	4.44710406277693e-08	2.82368788914397e-05	50S ribosomal protein L9	1
MELO3C015789	4.94272753837066e-08	2.84560916498596e-05	sucrose-binding protein-like	1
MELO3C024775	4.86891227335917e-08	2.84560916498596e-05	Bud13	1
MELO3C022533	5.04310703197675e-08	2.84560916498596e-05	shaggy-related protein kinase theta	1
MELO3C018195	6.19554454406313e-08	3.30691376218115e-05	Arf GTPase activating protein	1
MELO3C026898	6.14242697816181e-08	3.30691376218115e-05	Cathepsin B-like cysteine protease	1
MELO3C004204	6.59174723693923e-08	3.42580042585034e-05	Importin subunit alpha	1
MELO3C002485	7.36338064966091e-08	3.63548511125383e-05	Transmembrane protein, putative	1
MELO3C003812	7.18805542865297e-08	3.63548511125383e-05	Glucose-1-phosphate adenylyltransferase	1
MELO3C021514	8.24147254885332e-08	3.77341577131167e-05	No data found	0
MELO3C023342	8.40702283344541e-08	3.77341577131167e-05	kinesin-related protein 11-like	1
MELO3C002104	8.08121399797912e-08	3.77341577131167e-05	Receptor-like kinase	1
MELO3C015197	8.2265061651654e-08	3.77341577131167e-05	Translocation protein Sec62	1
MELO3C000452	9.44282844139721e-08	4.14414264198119e-05	Coiled-coil protein (DUF572)	1
MELO3C016073	9.75029128547078e-08	4.18605440427744e-05	Tudor/PWWP/MBT superfamily protein	1
MELO3C006028	1.07972809137991e-07	4.53692554822591e-05	cyclic nucleotide-gated ion channel 1	1
MELO3C007022	1.11002842029251e-07	4.56707318174099e-05	UDP-N-acetylglucosamine diphosphorylase 2-like	1
MELO3C003570	1.13579167182465e-07	4.57770402589081e-05	Protein ROOT PRIMORDIUM DEFECTIVE 1	1
MELO3C007499	1.18439269947146e-07	4.58638655330624e-05	protein DA1-related 1-like	1
MELO3C017271	1.17156354062509e-07	4.58638655330624e-05	Acetyl-coenzyme A synthetase	1
MELO3C014089	1.3594595926758e-07	5.16307067226047e-05	caffeic acid 3-O-methyltransferase 1-like	1
MELO3C012331	1.44328094586754e-07	5.37799158489398e-05	dnaJ protein homolog	0
MELO3C002508	1.4915760315759e-07	5.45502500881343e-05	thioredoxin-like protein CXXS1	1
MELO3C003905	1.80851489561817e-07	6.39831774649798e-05	glycine--tRNA ligase, mitochondrial 1	1
MELO3C021108	1.84669660008296e-07	6.39831774649798e-05	Peptidylprolyl isomerase	1
MELO3C005293	1.82100714729572e-07	6.39831774649798e-05	Phosphoglucomutase, putative	1

MELO3C017963	1.99110337106845e-07	6.77970697848806e-05	Lycopene beta-cyclase	1
MELO3C016475	2.08360193654222e-07	6.97441604148684e-05	Chloride channel protein	1
MELO3C019973	2.2593505843993e-07	7.4366524485503e-05	2-C-methyl-D-erythritol 4-phosphate cytidylyltransferase	1
MELO3C013123	2.50657820832778e-07	7.98426016713957e-05	Syntaxin-51	1
MELO3C017095	2.50064974283148e-07	7.98426016713957e-05	CASP-like protein	1
MELO3C007204	2.70307014549331e-07	8.47348131799166e-05	60S ribosomal protein L11-like	0
MELO3C022213	2.95504305247718e-07	8.82741693322043e-05	Myb family transcription factor family protein	1
MELO3C025783	2.88477511212193e-07	8.82741693322043e-05	receptor-like serine/threonine-protein kinase NCRK	1
MELO3C003875	2.90642418132592e-07	8.82741693322043e-05	Protein phosphatase 2c, putative	1
MELO3C012788	2.99476902387852e-07	8.82741693322043e-05	Transcription initiation factor IIF alpha subunit family protein	1
MELO3C002464	3.08444173202638e-07	8.82820866170854e-05	polyadenylate-binding protein RBP45-like	1
MELO3C003563	3.07599423821081e-07	8.82820866170854e-05	No data found	1
MELO3C002736	3.17503783264783e-07	8.957688879566e-05	Calcyclin-binding protein	1
MELO3C026304	3.34660603895642e-07	9.30874967089442e-05	nuclear cap-binding protein subunit 2	1
MELO3C023110	3.42064934821806e-07	9.37785766616996e-05	Alkaline alpha galactosidase	1
MELO3C020989	3.46642163973065e-07	9.37785766616996e-05	phosphatidylinositol 4-kinase alpha 1	1
MELO3C017380	3.55206742130854e-07	9.4796999328949e-05	zinc finger CCHC domain-containing protein 7 isoform X3	1
MELO3C014061	3.64245731243606e-07	9.59131859510665e-05	WPP domain interacting protein, putative	1
MELO3C012356	3.74511264888966e-07	9.73187232933183e-05	Aspartyl aminopeptidase	1
MELO3C023146	4.04118919106189e-07	0.000102319801710617	villin-2-like	1
MELO3C023449	4.03846042607015e-07	0.000102319801710617	UPF0481 plant-like protein	1
MELO3C024278	4.11229531316337e-07	0.000102802177391979	Mitochondrial carrier protein	1
MELO3C015720	4.28536336860574e-07	0.000105789551458244	Smr (Small MutS-related) domain protein	1
MELO3C004433	4.57582358448505e-07	0.000111565357987648	calcium uptake protein 1, mitochondrial-like isoform X1	1
MELO3C010244	5.04511900589755e-07	0.000121507384448135	Temperature-induced lipocalin	1
MELO3C024910	5.28152974021978e-07	0.000125668591373013	FRIGIDA-like protein	1
MELO3C023537	5.4337361676815e-07	0.00012691733086263	zinc finger A20 and AN1 domain-containing stress-associated protein 8-like	0
MELO3C015590	5.46254145694647e-07	0.00012691733086263	protochlorophyllide-dependent translocon component 52, chloroplastic-like	1
MELO3C012930	5.68072576645484e-07	0.000130451922281066	Zinc knuckle family protein	1
MELO3C011379	5.84145015025683e-07	0.00013260091841083	Chaperone protein dnaJ	1
MELO3C017213	5.98506860738368e-07	0.000134317181735478	UDP-glucose 6-dehydrogenase	1
MELO3C014359	6.34542943744876e-07	0.000140804366247388	Calcium-binding EF-hand family protein	1
MELO3C011117	6.51958590447421e-07	0.00014284228791607	receptor-like protein kinase HSL1	1
MELO3C003581	6.58192728764107e-07	0.00014284228791607	signal peptide peptidase	1
MELO3C006120	7.02155050880116e-07	0.000148453468702257	MYB-related transcription factor	1
MELO3C011085	6.97631587276426e-07	0.000148453468702257	Argininosuccinate lyase	1
MELO3C003506	7.06599121880203e-07	0.000148453468702257	Rhamnogalacturonate lyase family protein	1
MELO3C012146	7.17645318282223e-07	0.000149187130429007	14-3-3 protein, putative	0
MELO3C023559	7.44244884831602e-07	0.000153105127401451	40S ribosomal protein S27	1
MELO3C011089	7.54406601521929e-07	0.000153595628592336	O-fucosyltransferase family protein	1
MELO3C016717	7.90376939896476e-07	0.00015927708353077	COP1-interacting protein, putative	1
MELO3C007177	8.23092384139024e-07	0.000164194459539006	Transcription factor GTE12	1
MELO3C011324	8.36300357853759e-07	0.000165160957672539	No data found	1
MELO3C004799	8.70907565730938e-07	0.000170292609065548	splicing factor U2af small subunit B-like	1
MELO3C006297	9.06615200468863e-07	0.000172160996096727	RNA recognition motif (RRM) containing protein	1
MELO3C007072	9.03693317066967e-07	0.000172160996096727	Caffeoylshikimate esterase	1
MELO3C025061	9.00795385505582e-07	0.000172160996096727	V-type proton ATPase subunit C	1
MELO3C005262	9.43659170360434e-07	0.000177488809099507	PLATZ transcription factor family protein, putative	1
MELO3C004194	9.58587341726158e-07	0.000178595673695754	calreticulin	1
MELO3C022416	9.74627697658548e-07	0.000179887125243539	Ubiquitin family protein	1
MELO3C021903	1.01411382180672e-06	0.000183740677677623	Alpha/beta hydrolase-3	1
MELO3C015327	1.01389569406862e-06	0.000183740677677623	isoaspartyl peptidase/L-asparaginase	1
MELO3C013136	1.03190995592861e-06	0.000185265361087583	GDP-L-galactose phosphorylase 1	1
MELO3C003448	1.2097755952567e-06	0.000215241966042564	Methyltransferase-related family protein	1
MELO3C024862	1.29411787552769e-06	0.000228192267176753	Plant peroxidase	1
MELO3C019120	1.32913722605821e-06	0.00023229319537543	R3H domain-containing protein 1-like isoform X1	1
MELO3C021462	1.37274241240881e-06	0.000237809560549663	DDT domain-containing protein PTM	1
MELO3C017749	1.39039915902917e-06	0.000238773852101452	BAG family molecular chaperone regulator 6-like	1
MELO3C015067	1.43038817013164e-06	0.000243523585964911	transcription factor LHW	1
MELO3C016754	1.51495070621621e-06	0.000253548826246305	Cold regulated gene 27, putative isoform 3	1
MELO3C005731	1.50559889966484e-06	0.000253548826246305	Intracellular protein transport protein USO1-like protein	1
MELO3C017884	1.52819748255872e-06	0.000253616572126489	DUF4050 family protein	1

MELO3C013622	1.60432891793683e-06	0.000264032431669453	mannan endo-1,4-beta-mannosidase 2	1
MELO3C022408	1.62486392341066e-06	0.000265201963830059	UV-stimulated scaffold protein A homolog	1
MELO3C024626	1.7288799445403e-06	0.000279865983809232	Protein LIKE COV 1	1
MELO3C009967	1.75992938844516e-06	0.000282575979613036	cyclin-dependent kinase C-2-like	1
MELO3C020570	1.778215225956e-06	0.000283209455624235	Maternal effect embryo arrest protein	1
MELO3C022066	1.8187769972311e-06	0.000287352215346536	Zinc finger CCHC domain-containing protein 8	1
MELO3C013988	1.86327363427274e-06	0.000292045960343273	Myelodysplasia-myeloid leukemia factor 1-interacting protein	1
MELO3C027330	1.90953358347734e-06	0.000294620146406984	Caffeic acid O-methyltransferase	1
MELO3C001987	1.90165617108828e-06	0.000294620146406984	cyclic dof factor 3	1
MELO3C006997	1.975027581258e-06	0.000302362943428406	galactan beta-1,4-galactosyltransferase GALS3-like	1
MELO3C018525	2.01982641567788e-06	0.000306842706794019	Myosin heavy chain-like protein	1
MELO3C021940	2.06217394693731e-06	0.00031088452884019	Cold acclimation protein	1
MELO3C025488	2.10223959085098e-06	0.000312158869772302	transcription initiation factor TFIID subunit 1-like	1
MELO3C020880	2.09783662086238e-06	0.000312158869772302	Pathogenesis-related protein 1	0
MELO3C009091	2.15805440451078e-06	0.000318055346527488	50S ribosomal protein L17	1
MELO3C007139	2.23241586572165e-06	0.000324832030554499	la-related protein 6A	1
MELO3C012149	2.23693129552949e-06	0.000324832030554499	PLASMODESMATA CALLOSE-BINDING PROTEIN 3	1
MELO3C007547	2.28760654796822e-06	0.000327376389245105	AT3g50560/T20E23_160	1
MELO3C007735	2.28658548895311e-06	0.000327376389245105	E3 ubiquitin-protein ligase RING1	1
MELO3C002689	2.36888940319258e-06	0.000336569761321224	serine/threonine-protein kinase STY8-like	1
MELO3C010985	2.3905490020848e-06	0.00033722108744409	B-box zinc finger protein 20-like	1
MELO3C009579	2.41978410275845e-06	0.000338924228690614	Myosin-binding protein 7	1
MELO3C003975	2.4639976213825e-06	0.000342686542427345	protein CHLOROPLAST IMPORT APPARATUS 2 isoform X2	1
MELO3C003331	2.48646479494852e-06	0.000343392959688379	BAX inhibitor-1	1
MELO3C021782	2.59632473731397e-06	0.000356075119702872	alpha-glucosidase	1
MELO3C014555	2.65481477645935e-06	0.000359109157673258	splicing factor 3B subunit 6-like protein	1
MELO3C022488	2.65025887680181e-06	0.000359109157673258	tubulin-folding cofactor D	1
MELO3C026045	2.71888340064308e-06	0.000365273661763947	alanine--glyoxylate aminotransferase 2 homolog 2, mitochondrial-like	0
MELO3C006929	2.74598986926833e-06	0.000366422661676893	BAHD acyltransferase DCR	1
MELO3C024188	2.78370137918316e-06	0.000368961869379115	ribulose-1,5 bisphosphate carboxylase/oxygenase large subunit N-methyltransferase, chloroplastic	1
MELO3C023188	2.84005641981722e-06	0.000373921828233135	Beta-galactosidase	1
MELO3C013183	2.90970862626416e-06	0.000379146148603654	elongation factor-like GTPase 1	1
MELO3C026090	2.91813330233204e-06	0.000379146148603654	Sec14p-like phosphatidylinositol transfer family protein	1
MELO3C012737	2.98116016383965e-06	0.00037983827145593	F21O3.15 protein	1
MELO3C021100	2.94284546042967e-06	0.00037983827145593	Heat shock 70 kDa protein	1
MELO3C018644	2.96391440057775e-06	0.00037983827145593	serine/arginine-rich splicing factor SC35	1
MELO3C022819	3.01520986245585e-06	0.000381713971625901	Myosin heavy chain-like protein, putative	1
MELO3C006921	3.11710684453015e-06	0.000389618627041936	No data found	1
MELO3C018149	3.10182773133327e-06	0.000389618627041936	Beta-glucosidase, putative	1
MELO3C008069	3.14379035937229e-06	0.000390482489353732	Phosphoinositide phosphatase family protein	1
MELO3C013712	3.18040612723447e-06	0.00039256150379221	Fact complex subunit spt16	1
MELO3C022511	3.22910355765593e-06	0.000396096684224516	synaptotagmin-5	1
MELO3C026068	3.27213557271833e-06	0.000398338562635824	Transcriptional adapter ADA2b-like protein	1
MELO3C010675	3.28772017366141e-06	0.000398338562635824	ATP-citrate synthase alpha chain protein	1
MELO3C009296	3.38391772602975e-06	0.000405601118255557	Energy-coupling factor transporter ATP-binding EcfA 1	1
MELO3C010235	3.38873788607863e-06	0.000405601118255557	No data found	1
MELO3C002056	3.41335219067318e-06	0.000406086098877136	O-fucosyltransferase family protein	1
MELO3C007008	3.47097234532079e-06	0.000408989535555527	cytochrome c6, chloroplastic	1
MELO3C022204	3.47917575438395e-06	0.000408989535555527	SART-1 family protein DOT2 isoform X2	1
MELO3C019002	3.51510799601051e-06	0.000410768448598885	Annexin	1
MELO3C002674	3.53997063085032e-06	0.000411240470521547	BnaA04g24650D protein	1
MELO3C008598	3.67564570480372e-06	0.000424504836398647	Lecithin:cholesterol acyltransferase family protein	1
MELO3C012074	3.70429519958027e-06	0.000425326313351806	Ubiquitin-conjugating enzyme, E2	0
MELO3C012400	3.73601575998084e-06	0.000426488874241974	pentatricopeptide repeat-containing protein At2g22070	1
MELO3C012597	3.76446955963061e-06	0.000427267295018074	Defective in cullin neddylation protein	1
MELO3C017897	3.79392199290063e-06	0.000428149516787397	Plant/protein	1
MELO3C005069	4.07248831202356e-06	0.000456974839057689	GEM-like protein 4	1
MELO3C013128	4.09613167873246e-06	0.000457031099001624	Golgin family A protein	1
MELO3C004439	4.20919038268686e-06	0.000467007308245409	Protein phosphatase 2c, putative	1
MELO3C007827	4.27775306732769e-06	0.00047169877077526	pyridine nucleotide-disulfide oxidoreductase domain-containing protein 2-like	0
MELO3C026614	4.29924445488616e-06	0.00047169877077526	WD repeat-containing protein 55	1

MELO3C013870	4.40428128078985e-06	0.000477912917661092	Chloroplast 40 kDa outer membrane envelope protein	1
MELO3C015804	4.40195694373369e-06	0.000477912917661092	heat stress transcription factor A-6b-like isoform X1	1
MELO3C010295	4.43891109647154e-06	0.000478586239136045	Armadillo-like helical	1
MELO3C013000	4.45895326350865e-06	0.000478586239136045	Malic enzyme	0
MELO3C006926	4.53250933496463e-06	0.000480700689972296	Divalent ion symporter	1
MELO3C016805	4.5614759661694e-06	0.000480700689972296	No data found	0
MELO3C017908	4.58576324779969e-06	0.000480700689972296	No data found	1
MELO3C015891	4.59599066471306e-06	0.000480700689972296	U1 small nuclear ribonucleoprotein C	1
MELO3C004732	4.62469649575858e-06	0.000480700689972296	Alpha/beta-Hydrolases superfamily protein	1
MELO3C001976	4.62163323611264e-06	0.000480700689972296	Pentatricopeptide repeat-containing family protein	1
MELO3C015764	4.69261976665525e-06	0.000482679936310805	F-box/LRR-repeat protein 17	1
MELO3C000673	4.68826114552456e-06	0.000482679936310805	ATP-dependent zinc metalloprotease FtsH	0
MELO3C014178	4.90082299253736e-06	0.00049501531360691	Trigger factor	1
MELO3C016366	4.84117746490931e-06	0.00049501531360691	Phosphatidylcholine transfer protein	1
MELO3C022210	4.87671299553849e-06	0.00049501531360691	regulator of nonsense transcripts UPF3-like	1
MELO3C011196	4.91280578596154e-06	0.00049501531360691	ABC1 family protein, expressed	1
MELO3C002469	4.96222207591046e-06	0.000497456465873887	BnaC01g13120D protein	1
MELO3C025257	5.17156136781161e-06	0.000515824067943997	KH domain-containing family protein	1
MELO3C021534	5.25036197840389e-06	0.000517501450917762	homeobox-leucine zipper protein HAT5-like	1
MELO3C023408	5.26699031011546e-06	0.000517501450917762	Lactoylglutathione lyase	1
MELO3C025798	5.24348350627868e-06	0.000517501450917762	cytochrome P450 71A1-like	1
MELO3C015929	5.35053621086856e-06	0.000523107621922986	GTP-binding protein SAR1A	1
MELO3C017521	5.38464579769027e-06	0.000523849112603868	No data found	1
MELO3C006836	5.46398631773304e-06	0.000526381784336145	Activating transcription factor 7-interacting 2	1
MELO3C002148	5.44726792994776e-06	0.000526381784336145	NF-X1-type zinc finger protein NFXL1	1
MELO3C023857	5.61354392358826e-06	0.000538164460907498	GATA zinc finger domain-containing protein 10-like isoform X2	1
MELO3C024270	5.74599306712997e-06	0.000548201048708936	Terpene cyclase/mutase family member	1
MELO3C017104	5.97652550948791e-06	0.000567453857148446	Trehalose-6-phosphate synthase, putative	1
MELO3C005382	6.01113701315104e-06	0.0005680093056111	luc7-like protein 3	1
MELO3C023409	6.14485843719592e-06	0.000576681512004752	BEL1-like homeodomain protein 7	1
MELO3C020612	6.16131444797219e-06	0.000576681512004752	Unknown protein	1
MELO3C024316	6.22303370301225e-06	0.000579710814154665	Late embryogenesis abundant protein, LEA-14	1
MELO3C018948	6.26667399727943e-06	0.000581035421466063	Alpha-1,4 glucan phosphorylase	1
MELO3C009879	6.36776455420485e-06	0.000587649449443886	Cullin family protein	1
MELO3C026738	6.6257926438773e-06	0.000608617576390385	Acyl-CoA N-acyltransferase (NAT) superfamily protein	0
MELO3C007207	6.76358441276115e-06	0.000615548518744792	Kinase family protein	1
MELO3C024545	6.75704541253097e-06	0.000615548518744792	Transmembrane 9 superfamily member	1
MELO3C016298	7.03896222753464e-06	0.000634760114299459	Ribosome maturation factor	1
MELO3C010136	7.03790217027045e-06	0.000634760114299459	Glycogenin-1	1
MELO3C016877	7.08417712036447e-06	0.000635933699773081	Beta-fructofuranosidase, insoluble isoenzyme CWINV1	1
MELO3C013630	7.27915942988488e-06	0.000650480179098627	switch 2 isoform X1	1
MELO3C009482	7.35514913974278e-06	0.000651375965743409	Rho GTPase-activating protein	1
MELO3C004305	7.32999088659536e-06	0.000651375965743409	Pre-mRNA-splicing factor SLU7	1
MELO3C002767	7.40044993308153e-06	0.00065246198985905	Nuclear-interacting partner of ALK	1
MELO3C011284	7.49379739761746e-06	0.000657755576913543	Aspartate aminotransferase	1
MELO3C004591	7.82543966471039e-06	0.0006773432768121	Phosphotransferase	1
MELO3C003146	7.76221228304674e-06	0.0006773432768121	L-type lectin-domain containing receptor kinase IV.1-like	1
MELO3C022065	7.89187488892118e-06	0.0006773432768121	Nuclear matrix constituent protein 1	0
MELO3C023513	7.92274530070358e-06	0.0006773432768121	Metal tolerance protein C2	1
MELO3C011963	7.81226541701763e-06	0.0006773432768121	anthranilate phosphoribosyltransferase	0
MELO3C017093	7.90303656583724e-06	0.0006773432768121	Kinesin light chain	1
MELO3C025813	8.03564289664216e-06	0.000684034101576664	Polyadenylate-binding protein-interacting protein 3	1
MELO3C006383	8.19423848996692e-06	0.000685711931942189	acid phosphatase 1-like	1
MELO3C005211	8.1839472017009e-06	0.000685711931942189	Zinc finger, CCCH-type	1
MELO3C011984	8.09410918967135e-06	0.000685711931942189	pyrrolidone-carboxylate peptidase	1
MELO3C020001	8.17250552875848e-06	0.000685711931942189	Mini-chromosome maintenance complex-binding protein	1
MELO3C026410	8.27649747914272e-06	0.000689673201331601	transcription factor PIF4-like	0
MELO3C026629	8.48234927142144e-06	0.000703856788913034	potassium channel AKT1	1
MELO3C005952	8.62960587788564e-06	0.000713079859758843	60S acidic ribosomal protein P1-like	1
MELO3C026239	8.8767811139423e-06	0.000730448125913527	Protein tipD, putative	1
MELO3C020244	9.03752558945037e-06	0.000737638866316949	UTP--glucose-1-phosphate uridylyltransferase	1
MELO3C014083	9.07089525736815e-06	0.000737638866316949	Transmembrane protein, putative	1
MELO3C002302	9.07621877133113e-06	0.000737638866316949	Kinase family protein	1
MELO3C017657	9.15025518799517e-06	0.000738148417531329	branchpoint-bridging protein	1

MELO3C025502	9.15724149552766e-06	0.000738148417531329	Pentatricopeptide repeat-containing protein	1
MELO3C009423	9.29697871865365e-06	0.000746365986645085	Uridylate kinase	1
MELO3C005252	9.39636883812156e-06	0.000751291045279606	Ankyrin repeat-containing protein, putative	1
MELO3C020444	9.46083891961713e-06	0.000753301154100758	Purple acid phosphatase	1
MELO3C005301	9.59131909827882e-06	0.000753301154100758	At1g70780	1
MELO3C027060	9.50844332436862e-06	0.000753301154100758	Pectinesterase	1
MELO3C015322	9.61222800310857e-06	0.000753301154100758	cyclin-L1-1	1
MELO3C017346	9.60276551809081e-06	0.000753301154100758	alpha-dioxygenase 2	1
MELO3C014575	9.6661640416329e-06	0.000754533887977107	Saccharopine dehydrogenase	1
MELO3C013703	1.01872779812995e-05	0.000788974717069347	diacylglycerol O-acyltransferase 2-like	1
MELO3C026689	1.01759043160676e-05	0.000788974717069347	LRR receptor-like kinase, putative	0
MELO3C009339	1.05713260298845e-05	0.000815519991266366	Glycosyl transferase, family 31	1
MELO3C017385	1.078928932019e-05	0.000829096010834364	pollen receptor-like kinase 1	1
MELO3C008596	1.10425164834282e-05	0.000845266116400095	S-adenosyl-L-methionine-dependent methyltransferase	1
MELO3C024844	1.11280763014365e-05	0.000848526559370927	At5g24610	1
MELO3C013792	1.13111690041023e-05	0.000859170294853912	Ribosomal protein L28	1
MELO3C012136	1.13801551119286e-05	0.000861098403469263	Nodulin-related protein 1	1
MELO3C009461	1.15575520555078e-05	0.00086458369524327	Protein LITTLE ZIPPER 4	1
MELO3C007614	1.15006113516891e-05	0.00086458369524327	Leucine-rich repeat family protein	0
MELO3C010714	1.15230725494797e-05	0.00086458369524327	two-component response regulator ARR11	1
MELO3C014019	1.16203737828835e-05	0.000866002874861004	Rhomboid-like protein	1
MELO3C026749	1.20811670227816e-05	0.000896958524559827	DNA helicase	0
MELO3C021119	1.21310338159208e-05	0.00089728759112592	Cytochrome b561 and domon domain-containing protein	1
MELO3C011747	1.22550755131678e-05	0.000903080172796835	Protein FAR1-RELATED SEQUENCE 5	1
MELO3C009315	1.23509541338773e-05	0.00090491340308527	Ribosomal protein S12	0
MELO3C014678	1.2388353868964e-05	0.00090491340308527	Kelch repeat-containing F-box family protein	1
MELO3C016855	1.24174151722167e-05	0.00090491340308527	CRG16	0
MELO3C002700	1.24733027745405e-05	0.000905644325347061	Serine/threonine-protein kinase PLK4	1
MELO3C014174	1.25786625135849e-05	0.000909948739856364	(S)-ureidoglycine aminohydrolase	1
MELO3C003916	1.26667633769673e-05	0.000910771796448124	Cellulose synthase	1
MELO3C023590	1.2682274749265e-05	0.000910771796448124	Pheophytinase, chloroplastic	1
MELO3C017364	1.27819750068703e-05	0.000914605885545946	Ribosomal protein L19	1
MELO3C007033	1.28479493655131e-05	0.000916007769023535	protein SUPPRESSOR OF FRI 4 isoform X2	1
MELO3C014749	1.29109006289374e-05	0.000917184807629082	Acetyl-coenzyme A synthetase	1
MELO3C006107	1.32783063222508e-05	0.000939904199133086	RNA polymerase I-specific transcription initiation factor RRN3	1
MELO3C008910	1.34152483453054e-05	0.000942838930859203	transcription termination factor MTEF18, mitochondrial-like	1
MELO3C023986	1.33894728500117e-05	0.000942838930859203	DNA topoisomerase 2	1
MELO3C007432	1.35509775082143e-05	0.000949000903580584	Phosphatidate cytidylyltransferase	1
MELO3C003915	1.36025675472329e-05	0.000949247726114142	Pentatricopeptide repeat-containing protein	1
MELO3C022707	1.38477429754147e-05	0.000962954493033326	Ubiquitin-conjugating enzyme family protein	1
MELO3C009222	1.39431327602635e-05	0.000963333195559096	Protein RETICULATA, chloroplastic	1
MELO3C025451	1.39726341720214e-05	0.000963333195559096	Actin-depolymerizing factor family protein	1
MELO3C016016	1.39995254000436e-05	0.000963333195559096	xyloglucan 6-xylosyltransferase 1	1
MELO3C025977	1.4120841748122e-05	0.000968307304457158	OBERON-like protein	1
MELO3C020875	1.4385688624774e-05	0.000983055241005747	CLK4-associating serine/arginine-rich protein	1
MELO3C009276	1.46222781025607e-05	0.000995777138784382	Acyl-CoA N-acyltransferase with RING/FYVE/PHD-type zinc finger domain-containing protein	1
MELO3C022342	1.4755856923232e-05	0.00100142068170759	NAC domain-containing protein 83	1
MELO3C006313	1.50251507858856e-05	0.00101325938561605	Myb family transcription factor APL	1
MELO3C024262	1.5032913058155e-05	0.00101325938561605	activating signal cointegrator 1 complex subunit 1	1
MELO3C014825	1.52073123453889e-05	0.00102152793030301	Steroid nuclear receptor, ligand-binding	1
MELO3C004636	1.56355188315471e-05	0.00103625657153415	T-complex protein 1 subunit beta	1
MELO3C016380	1.55814578131075e-05	0.00103625657153415	Laccase	1
MELO3C024447	1.56364604950721e-05	0.00103625657153415	Protein SEC13 like	1
MELO3C011160	1.54835320682611e-05	0.00103625657153415	2-on-2 hemoglobin	1
MELO3C017720	1.5829999835848e-05	0.00104557413631492	protein farnesyltransferase/geranylgeranyltransferase type-1 subunit alpha	0
MELO3C006959	1.59256922638296e-05	0.0010483883217279	Reticulon-like protein	1
MELO3C009591	1.61324199619006e-05	0.0010508747649051	IQ domain-containing protein IQM6	1
MELO3C004553	1.60189519178289e-05	0.0010508747649051	multiprotein-bridging factor 1c	1
MELO3C025526	1.62295206489471e-05	0.0010508747649051	Pollen Ole e 1 allergen/extensin	1
MELO3C003813	1.61832411422758e-05	0.0010508747649051	Mannan endo-1,4-beta-mannosidase-like protein	1
MELO3C013093	1.62023783316645e-05	0.0010508747649051	glyoxylate/succinic semialdehyde reductase 2, chloroplastic-like	0
MELO3C013925	1.63110244950637e-05	0.00105270072795102	Myb transcription factor	1

MELO3C011731	1.65099639795052e-05	0.00106206931150244	Ubiquitin carboxyl-terminal hydrolase	1
MELO3C006948	1.66519377275964e-05	0.00106409276491677	Protein SGT1 homolog	1
MELO3C025282	1.67030612752139e-05	0.00106409276491677	SCARECROW	1
MELO3C025799	1.66160070578236e-05	0.00106409276491677	Alpha-ketoglutarate-dependent dioxygenase AlkB	1
MELO3C001954	1.67788745651931e-05	0.00106548551057234	Glycosyltransferase	1
MELO3C021588	1.71895920806353e-05	0.00108113775159384	CRS1/YhbY (CRM) domain protein	1
MELO3C021279	1.70987463855576e-05	0.00108113775159384	GTP-binding protein SAR1A-like	1
MELO3C008321	1.71502866039841e-05	0.00108113775159384	Biotin carboxyl carrier protein of acetyl-CoA carboxylase	1
MELO3C012083	1.73075270275547e-05	0.00108509952783231	Actin-binding LIM protein 1, putative	1
MELO3C024407	1.74182752812335e-05	0.00108858708395279	Charged multivesicular body 1	1
MELO3C015627	1.76483058498267e-05	0.00109948388715529	serrate RNA effector molecule	1
MELO3C018053	1.80475750266584e-05	0.00112082251321219	Costars family protein At4g33640	1
MELO3C006602	1.86668661633638e-05	0.00115252448748568	serine/threonine-protein kinase RUNKEL	1
MELO3C017677	1.86747600382509e-05	0.00115252448748568	chitinase-like protein 1	1
MELO3C019451	1.89781614502449e-05	0.00116760034417722	Unknown protein	1
MELO3C008933	1.9062906662648e-05	0.00116917187478458	Zinc finger family protein	1
MELO3C021107	1.93475282579403e-05	0.00118295459927574	Peptidylprolyl isomerase	0
MELO3C023442	1.95211350888513e-05	0.00118988548416582	glycerol kinase	1
MELO3C004593	1.95826094848695e-05	0.00118995986066673	OXS3	1
MELO3C020394	1.97117608555786e-05	0.00119048185057132	Phospholipid-transporting ATPase	1
MELO3C012088	1.97023626935522e-05	0.00119048185057132	sphinganine C4-monooxygenase 2	1
MELO3C014649	2.00030745243218e-05	0.00120138093791952	Metal tolerance protein C2	1
MELO3C007069	2.00138907577863e-05	0.00120138093791952	Protein phosphatase 2c, putative	1
MELO3C012243	2.02363198715805e-05	0.00121105176104195	tetraketide alpha-pyrone reductase 2-like	0
MELO3C025855	2.11718078086953e-05	0.00125940371209013	Alkyl transferase	1
MELO3C020589	2.11652532021711e-05	0.00125940371209013	17.5 kDa class I heat shock protein	1
MELO3C011138	2.13686692861481e-05	0.00126729684604246	Ultraviolet-B receptor UVR8	1
MELO3C019527	2.14406552635493e-05	0.00126775898443065	CBS domain-containing protein CBSX1, chloroplastic	1
MELO3C015263	2.16246135184006e-05	0.00127481938022356	Werner syndrome-like exonuclease	1
MELO3C017683	2.17107562363594e-05	0.00127608846699959	Clathrin interactor EPSIN 2	1
MELO3C011825	2.18256773739656e-05	0.00127903650581141	nifU-like protein 2, chloroplastic	1
MELO3C008690	2.20750108673728e-05	0.00128982067934836	splicing factor 3B subunit 2	1
MELO3C022786	2.23215132971744e-05	0.00130037630119733	Phd finger protein, putative	1
MELO3C007075	2.28317060992911e-05	0.001326186363985	ADP-ribosylation factor GTPase-activating protein AGD12	1
MELO3C009187	2.32460548075242e-05	0.00134235770875379	Transferase family protein	1
MELO3C010761	2.32330067020392e-05	0.00134235770875379	far upstream element-binding protein 1	1
MELO3C024385	2.38134500429865e-05	0.00137028743648528	protein indeterminate-domain 7	1
MELO3C012378	2.39378786565103e-05	0.00137028743648528	phosphoglucan phosphatase DSP4, amyloplastic	1
MELO3C019633	2.39288368943935e-05	0.00137028743648528	Glyceraldehyde-3-phosphate dehydrogenase	1
MELO3C014114	2.42431211936456e-05	0.00137976196096054	RPM1-interacting protein 4	1
MELO3C011271	2.4241787024426e-05	0.00137976196096054	14 kDa proline-rich protein DC2.15	1
MELO3C025111	2.43574415158543e-05	0.00138228480602473	CoA ligase	1
MELO3C007673	2.49104628767816e-05	0.00140884079117347	tubulin alpha chain-like	1
MELO3C005467	2.49680630366456e-05	0.00140884079117347	At5g07590	1
MELO3C008520	2.63403040063892e-05	0.00144498517728383	Cysteine protease	1
MELO3C013369	2.6235044301437e-05	0.00144498517728383	Methyltransferase-like protein	1
MELO3C007265	2.60273344152573e-05	0.00144498517728383	Protein DEHYDRATION-INDUCED 19	1
MELO3C019056	2.61549670041994e-05	0.00144498517728383	two-component response regulator ARR8-like	1
MELO3C023560	2.58082812095717e-05	0.00144498517728383	PsaB RNA-binding protein	1
MELO3C012196	2.62297140761758e-05	0.00144498517728383	Phospholipid-transporting ATPase	1
MELO3C025859	2.62944593677483e-05	0.00144498517728383	zinc finger CCCH domain-containing protein 25	1
MELO3C021670	2.5745984559733e-05	0.00144498517728383	Nuclear inhibitor of protein phosphatase 1	1
MELO3C010119	2.58387265157367e-05	0.00144498517728383	U11/U12 small nuclear ribonucleoprotein 48 kDa protein	1
MELO3C009886	2.60319997607006e-05	0.00144498517728383	plant cysteine oxidase 2	1
MELO3C006493	2.65023384483642e-05	0.00144950576797161	ATP sulfurylase	1
MELO3C016552	2.6816575519617e-05	0.00144950576797161	Fiber expressed protein	1
MELO3C017856	2.66462100604326e-05	0.00144950576797161	extensin-like	1
MELO3C025079	2.6770532013165e-05	0.00144950576797161	universal stress protein A-like protein	1
MELO3C022436	2.67748264992651e-05	0.00144950576797161	Amaranthin-like lectin	1
MELO3C010042	2.68630872994891e-05	0.00144950576797161	endoribonuclease Dicer homolog 2 isoform X2	1
MELO3C024214	2.70940042867984e-05	0.0014579822633787	Cytochrome b561 and domon domain-containing protein	1
MELO3C004278	2.78234834507618e-05	0.00147094913094369	mevalonate kinase-like	1
MELO3C006705	2.79177989914725e-05	0.00147094913094369	Binding protein	1
MELO3C005490	2.77615447602519e-05	0.00147094913094369	U-box domain-containing protein 35-like isoform X2	1

MELO3C020109	2.78415158727618e-05	0.00147094913094369	Nop53 protein	1
MELO3C026470	2.79308280978219e-05	0.00147094913094369	Potassium transporter	1
MELO3C000817	2.77390788183673e-05	0.00147094913094369	Magnesium transporter MRS2-like protein	1
MELO3C002677	2.7819366417603e-05	0.00147094913094369	NAD(P)-binding Rossmann-fold superfamily protein	1
MELO3C002044	2.78036725491759e-05	0.00147094913094369	DNA polymerase alpha subunit B	1
MELO3C021398	2.8164374234807e-05	0.00147930379458299	serine incorporator 3	1
MELO3C014530	2.84013662230631e-05	0.00148385868132083	Nuclear transcription factor Y subunit C8	1
MELO3C012748	2.83333883075443e-05	0.00148385868132083	Lysine-specific demethylase	0
MELO3C014507	2.84858782809705e-05	0.00148434725638756	F-box family protein	1
MELO3C006260	2.87159989742491e-05	0.0014878051459065	Dynamin, putative	1
MELO3C025345	2.88485624249102e-05	0.0014878051459065	Polyol transporter 5-like protein	1
MELO3C010686	2.88107005061988e-05	0.0014878051459065	Alanine aminotransferase 2	1
MELO3C013022	2.88535809854773e-05	0.0014878051459065	Serine/threonine-protein kinase ATM	1
MELO3C016541	2.93398141502088e-05	0.00150893747305332	Peroxisomal membrane 22 kDa (Mpv17/PMP22) family protein	1
MELO3C017836	2.96642891901566e-05	0.00152166246030235	UPF0326 protein	1
MELO3C003313	2.99724595917983e-05	0.00153348731730162	Membrane steroid-binding protein	1
MELO3C020701	3.0080522178122e-05	0.00153503936045408	Myb transcription factor	1
MELO3C016074	3.02469208611766e-05	0.00153552012010767	No data found	1
MELO3C024292	3.02042248422341e-05	0.00153552012010767	O-fucosyltransferase family protein	0
MELO3C008367	3.03231984830621e-05	0.00153552012010767	serine/threonine-protein kinase STY8-like	1
MELO3C013104	3.07867267796968e-05	0.00155028543425578	Upstream activation factor subunit spp27	1
MELO3C007083	3.07940069153023e-05	0.00155028543425578	187-kDa microtubule-associated protein AIR9	1
MELO3C022499	3.08502797945476e-05	0.00155028543425578	Myeloid leukemia factor	1
MELO3C012967	3.09977807957384e-05	0.00155374409374375	At5g57230	1
MELO3C009171	3.14944790682503e-05	0.00157464422055412	Mitochondrial carrier protein	1
MELO3C023731	3.17116579537924e-05	0.00157825662440481	phosphatidylcholine transfer protein-like isoform X1	1
MELO3C017474	3.17265623519525e-05	0.00157825662440481	Zinc finger protein	1
MELO3C007767	3.23184251792563e-05	0.00160365974589229	Lipoxygenase y domain-containing protein 1	1
MELO3C026235	3.25468898165759e-05	0.00161094868919188	haloacid dehalogenase-like hydrolase domain-containing protein At3g48420	1
MELO3C013383	3.32537247063058e-05	0.00163772521003699	Calcium-binding EF hand family protein	1
MELO3C005849	3.3214611836252e-05	0.00163772521003699	p-loop containing nucleoside triphosphate hydrolases superfamily protein	1
MELO3C023526	3.33581295046681e-05	0.00163878034723306	chaperone protein dnaJ GFA2, mitochondrial	1
MELO3C009996	3.39940585575293e-05	0.00166587757432419	dnaJ protein homolog	1
MELO3C016253	3.42100392104472e-05	0.00167231204051268	Zinc finger protein, putative	1
MELO3C013470	3.44618684419151e-05	0.00168046281446761	Ankyrin repeat domain-containing 2-like protein	0
MELO3C022144	3.4767194971419e-05	0.0016911756982526	TMV resistance protein N-like	1
MELO3C015277	3.55894665726719e-05	0.00172691984113931	GATA transcription factor 16-like	1
MELO3C020830	3.59045646862732e-05	0.00173793933330689	BZIP transcription factor, putative (DUF630 and DUF632)	1
MELO3C004542	3.60642823011847e-05	0.00174140222778997	tRNA (guanine(37)-N1)-methyltransferase	1
MELO3C004366	3.62660963766359e-05	0.00174687594473703	Prenylyltransferase superfamily protein	1
MELO3C009495	3.67311633746592e-05	0.00175067140545441	CASP-like protein	1
MELO3C013248	3.66059451775147e-05	0.00175067140545441	nucleolar complex protein 4 homolog	1
MELO3C014150	3.65614978239392e-05	0.00175067140545441	Fimbrin, putative	1
MELO3C024450	3.69654147589493e-05	0.00175067140545441	nuclear pore complex protein NUP35	1
MELO3C023306	3.68811505284672e-05	0.00175067140545441	adoMet-dependent rRNA methyltransferase spb1 isoform X1	1
MELO3C013664	3.66656130084131e-05	0.00175067140545441	Transcriptional elongation regulator MINIYO	1
MELO3C022386	3.69238571342745e-05	0.00175067140545441	50S ribosomal protein L14	1
MELO3C025256	3.74632503545858e-05	0.00176764322254611	protein RETICULATA-RELATED 3, chloroplastic-like	1
MELO3C005565	3.75027854699894e-05	0.00176764322254611	Elongation factor G, chloroplastic	1
MELO3C003911	3.78070399631447e-05	0.00177774102912415	protein BONZAI 3	1
MELO3C007825	3.79500651352949e-05	0.0017802276398027	random slug protein 5-like	1
MELO3C004492	3.83150140621513e-05	0.00179308818178537	methyl-CpG-binding domain-containing protein 11-like	1
MELO3C024005	3.84547735918783e-05	0.00179537428762649	Acyl-CoA--sterol O-acyltransferase 1	1
MELO3C017898	3.89913539624587e-05	0.00180760621925962	F-box family protein	1
MELO3C024586	3.89204117599018e-05	0.00180760621925962	Ribosomal protein S8e/ribosomal biogenesis NSA2	0
MELO3C002154	3.88440754720554e-05	0.00180760621925962	Monoglyceride lipase	1
MELO3C021113	3.92616078019881e-05	0.00180901640460669	asparagine--tRNA ligase, cytoplasmic 2	1
MELO3C001175	3.92192487606025e-05	0.00180901640460669	Glutathione s-transferase	1
MELO3C018502	3.92965738810203e-05	0.00180901640460669	MAR-binding filament-like protein	1
MELO3C013891	4.00972913509046e-05	0.00184140770420847	AT5g47090/K14A3_4	1
MELO3C020824	4.01866788451999e-05	0.00184140770420847	Pre-mRNA-splicing factor syf2	1
MELO3C024596	4.07119270215972e-05	0.00186115705266093	DNA polymerase	1

MELO3C002115	4.08557565708678e-05	0.0018634187910348	Poly(A) polymerase	1
MELO3C014175	4.15915338907169e-05	0.00189178845108025	Phospho-2-dehydro-3-deoxyheptonate aldolase	1
MELO3C014009	4.16693491427367e-05	0.00189178845108025	PGR5-like protein 1A, chloroplastic	1
MELO3C013366	4.18519287170849e-05	0.00189571958769199	Protein nuclear fusion defective 4	1
MELO3C024435	4.20256696651577e-05	0.00189923329569153	Poly(A) polymerase	1
MELO3C006736	4.24021129614705e-05	0.00191187061387233	Beta-1,3-galactosyltransferase-like protein	1
MELO3C015860	4.25403537831492e-05	0.00191373450310573	Calcium permeable stress-gated cation channel 1	1
MELO3C020132	4.28311459950148e-05	0.00192243705058079	Potassium transporter	1
MELO3C002226	4.29674849788952e-05	0.00192418335793243	polynucleotide 5'-hydroxyl-kinase NOL9	1
MELO3C010275	4.36787795317084e-05	0.00195161135061473	Serine-rich protein-like protein	1
MELO3C017620	4.38789811226803e-05	0.00195172522115273	BnaA10g17500D protein	1
MELO3C020780	4.38459148834891e-05	0.00195172522115273	Triosephosphate isomerase	1
MELO3C008330	4.42680489831648e-05	0.00196460606599668	S-acyltransferase	1
MELO3C004641	4.4476178534758e-05	0.00196941715220389	Protein BREVIS RADIX	1
MELO3C009595	4.45835594083954e-05	0.00196975551399642	serine/arginine-rich SC35-like splicing factor SCL33	1
MELO3C013455	4.49710978889239e-05	0.00197627470685878	Calcium ion-binding protein	1
MELO3C010297	4.49064579863823e-05	0.00197627470685878	Purple acid phosphatase	1
MELO3C003471	4.50313240207834e-05	0.00197627470685878	protein SAWADEE HOMEODOMAIN HOMOLOG 1-like isoform X2	1
MELO3C010997	4.52420342280657e-05	0.00198111958751678	Protein IQ-DOMAIN 32	1
MELO3C018394	4.6087660756533e-05	0.00201368409796631	Abscisic acid receptor	0
MELO3C004669	4.6537154970494e-05	0.00202648542403205	Pentatricopeptide repeat-containing protein	1
MELO3C026502	4.65858718168288e-05	0.00202648542403205	Phytochrome	1
MELO3C015043	4.71004272699638e-05	0.00204436557836157	DnaJ-like protein	0
MELO3C025034	4.73219853005524e-05	0.00204582515146751	peroxiredoxin Q, chloroplastic	1
MELO3C022721	4.73412372383741e-05	0.00204582515146751	Ninja-family protein AFP3	1
MELO3C005245	4.79549976355464e-05	0.00206782368625416	Xyloglucan endotransglucosylase/hydrolase	1
MELO3C024885	4.83734309704165e-05	0.00207353939040731	ATP-dependent DNA helicase	1
MELO3C025391	4.83084956899305e-05	0.00207353939040731	No data found	0
MELO3C025056	4.8402534760128e-05	0.00207353939040731	zinc finger CCCH domain-containing protein 53-like	0
MELO3C023753	4.85878972154019e-05	0.00207697485304539	BnaC06g27400D protein	1
MELO3C025784	4.88195283186998e-05	0.0020823690383715	Zinc finger (C3HC4-type RING finger) family protein	1
MELO3C024376	4.90235715564502e-05	0.00208656576437141	Eukaryotic initiation factor 4A (ATP-dependent RNA helicase eIF4A)	0
MELO3C024863	4.93566951739188e-05	0.00209622660858005	No data found	1
MELO3C021587	5.05070902130367e-05	0.00214048181248339	NAC domain-containing protein 8 isoform X1	1
MELO3C011705	5.07150635979947e-05	0.00214469334260556	Pyruvate dehydrogenase E1 component subunit alpha	1
MELO3C021999	5.12860701999962e-05	0.00215959189846423	Expansin protein	1
MELO3C025308	5.12768922132922e-05	0.00215959189846423	auxin-responsive protein IAA16-like	1
MELO3C025887	5.14003217724213e-05	0.00215979777592244	No data found	1
MELO3C023727	5.20365869023376e-05	0.00218189077438273	CDT1-like protein a, chloroplastic	1
MELO3C022647	5.23411990736022e-05	0.0021900134332724	UDP-glycosyltransferase 89A2-like	1
MELO3C023808	5.24853113137436e-05	0.00219140045060279	SAC3/GANP/Nin1/mts3/eIF-3 p25 family isoform 1	1
MELO3C024514	5.27174142808118e-05	0.00219644771019357	enolase	1
MELO3C026107	5.30162818748181e-05	0.00220424958051744	No data found	1
MELO3C006189	5.33192345207878e-05	0.00220818488486918	Glutathione S-transferase	1
MELO3C007609	5.33345582096612e-05	0.00220818488486918	Subtilisin-like protease	1
MELO3C009292	5.42517615724769e-05	0.00222633555573646	ABC transporter G family member 20	0
MELO3C023475	5.42682466746491e-05	0.00222633555573646	pre-mRNA-splicing factor ISY1 homolog	1
MELO3C011843	5.43007606186308e-05	0.00222633555573646	No data found	1
MELO3C020783	5.43366113658905e-05	0.00222633555573646	protein XAP5 CIRCADIAN TIMEKEEPER	1
MELO3C011285	5.41233647706196e-05	0.00222633555573646	60S ribosomal protein L39	1
MELO3C016696	5.44683324148476e-05	0.00222711200178225	PROTON PUMP INTERACTOR 1 family protein	1
MELO3C007010	5.52589988974672e-05	0.00225477266369025	phosphatidate cytidylyltransferase, mitochondrial isoform X1	1
MELO3C011003	5.59736594196725e-05	0.00227922432964765	transcription factor E2FC isoform X3	1
MELO3C022693	5.60978884305285e-05	0.00227958271319858	GDSL esterase/lipase 5	0
MELO3C016002	5.719334841503e-05	0.00231457261854186	Arginine/serine-rich splicing factor, putative	1
MELO3C020957	5.70871739773438e-05	0.00231457261854186	GDSL esterase/lipase 5-like	1
MELO3C007653	5.75656860861695e-05	0.00232040749860482	Protein PHLOEM PROTEIN 2-LIKE A10	1
MELO3C026835	5.75725188270981e-05	0.00232040749860482	Pentatricopeptide repeat-containing protein At2g30100, chloroplastic	1
MELO3C019411	5.82043706141011e-05	0.00234109595775536	Kinase superfamily protein	1
MELO3C007562	5.83480571787476e-05	0.00234210524638839	Lipase	1
MELO3C006145	5.87198712955761e-05	0.00235224896189925	F-box protein PP2-A13	1

MELO3C009338	5.94246730396542e-05	0.00235658206397616	60S ribosomal protein L12	1
MELO3C006854	5.93200212051226e-05	0.00235658206397616	transcription factor bHLH118-like	1
MELO3C019522	5.92040129191451e-05	0.00235658206397616	Exocyst complex component	1
MELO3C016186	5.91282394308834e-05	0.00235658206397616	No data found	1
MELO3C002384	5.94135676414975e-05	0.00235658206397616	Coiled-coil domain-containing protein SCD2	1
MELO3C018749	5.95836233487912e-05	0.00235815025554164	Phosphatase 2C family protein	1
MELO3C004273	6.01342544248595e-05	0.0023751827812731	Mitochondrial Rho GTPase	1
MELO3C021332	6.05753663890374e-05	0.00238547596635887	40S ribosomal protein S21	0
MELO3C015339	6.06364340023369e-05	0.00238547596635887	UDP-N-acetylglucosamine transferase subunit ALG13 homolog	1
MELO3C014260	6.11461584065776e-05	0.00240074648582803	Interactor of constitutive active ROPs-like protein	1
MELO3C003278	6.17486979386239e-05	0.0024195933245831	PHD finger protein At1g33420	1
MELO3C013736	6.21357963599412e-05	0.00242994028180689	basic endochitinase C	1
MELO3C021207	6.30709811876295e-05	0.00246163795943576	Signal peptide peptidase-like protein	1
MELO3C005992	6.3408310252755e-05	0.00246211971008436	homeobox-leucine zipper protein ATHB-7	0
MELO3C015734	6.34573361908419e-05	0.00246211971008436	No data found	1
MELO3C015439	6.32324988869559e-05	0.00246211971008436	Protein PLASTID MOVEMENT IMPAIRED 1-RELATED 1	1
MELO3C022162	6.40116656055456e-05	0.00247390681808986	mannan endo-1,4-beta-mannosidase 1-like	1
MELO3C011408	6.39667592298165e-05	0.00247390681808986	nucleolar protein 14 isoform X2	1
MELO3C013738	6.49744440790467e-05	0.00249335090143193	Ganglioside-induced differentiation-associated protein 2	1
MELO3C010439	6.49361610987054e-05	0.00249335090143193	structure-specific endonuclease subunit SLX4-like isoform X2	1
MELO3C027375	6.50197840010858e-05	0.00249335090143193	Pectinesterase	1
MELO3C011144	6.49593068970944e-05	0.00249335090143193	Translation initiation factor IF-2	1
MELO3C017813	6.58591244822038e-05	0.00251576760038499	ADP-ribosylation factor GTPase-activating protein AGD3	1
MELO3C025582	6.5766423634761e-05	0.00251576760038499	Ribosomal protein S5/S7	1
MELO3C011422	6.60698899755952e-05	0.0025189464423321	Pentatricopeptide repeat-containing protein	1
MELO3C020255	6.65873213148149e-05	0.00253378229026258	3-phosphoinositide-dependent protein kinase-1	0
MELO3C016660	6.74206308142189e-05	0.00255074719913795	Flavin-binding kelch domain F box protein	1
MELO3C008046	6.73044786470012e-05	0.00255074719913795	zinc finger CCCH domain-containing protein 38 isoform X1	1
MELO3C012391	6.73894846392464e-05	0.00255074719913795	NAC domain-containing protein 16	1
MELO3C008513	6.82229065330775e-05	0.00257616478225956	FAST kinase domain-containing 3	1
MELO3C022074	6.86128717086731e-05	0.00258102019690397	Tryptophan synthase-related	1
MELO3C016019	6.84870669735993e-05	0.00258102019690397	heat shock factor-binding protein 1	1
MELO3C013946	6.88829284867243e-05	0.00258625276555954	Small heat shock protein, chloroplastic	1
MELO3C021771	6.96161904623072e-05	0.00260882380538919	exocyst complex component EXO84C	1
MELO3C005703	6.97949721109037e-05	0.00261056989435272	Beta-carotene 3-hydroxylase	1
MELO3C011011	7.00407553777538e-05	0.00261481073337478	Transducin/WD40 repeat-like superfamily protein	1
MELO3C019135	7.0205236232912e-05	0.00261600605729015	4-alpha-glucanotransferase DPE2	1
MELO3C024138	7.04960768541651e-05	0.00262189646288683	Auxin response factor	1
MELO3C020860	7.10014079137178e-05	0.00263572707685717	DNA polymerase	1
MELO3C016468	7.31467793237961e-05	0.00271027344252467	No data found	1
MELO3C014658	7.36569729663517e-05	0.00271924112679749	Peroxidase	1
MELO3C005581	7.39243833014491e-05	0.00271924112679749	Ankyrin repeat/KH domain protein (DUF1442)	1
MELO3C017384	7.39395658053699e-05	0.00271924112679749	tRNA pseudouridine synthase	1
MELO3C025026	7.38424094659518e-05	0.00271924112679749	abscisic stress-ripening protein 2-like	0
MELO3C014419	7.56717115111272e-05	0.0027671089367998	Unknown protein	1
MELO3C014309	7.59720866843061e-05	0.0027671089367998	Magnesium transporter MRS2-like protein	1
MELO3C004308	7.65458843351441e-05	0.0027671089367998	Photosystem II reaction center PsbP family protein	1
MELO3C014027	7.6019752883516e-05	0.0027671089367998	Cytochrome P450 family protein	1
MELO3C021979	7.63281862419252e-05	0.0027671089367998	Glutaredoxin family protein, putative	1
MELO3C012242	7.65118129815168e-05	0.0027671089367998	ethylene-responsive transcription factor ERF118	1
MELO3C015202	7.64393255101581e-05	0.0027671089367998	zinc finger A20 and AN1 domain-containing stress-associated protein 4-like	1
MELO3C020003	7.64967470061606e-05	0.0027671089367998	40S ribosomal protein S26	1
MELO3C013084	7.63203350274688e-05	0.0027671089367998	Aminopeptidase	0
MELO3C009827	7.66422901630204e-05	0.0027671089367998	No data found	1
MELO3C004186	7.71375798698237e-05	0.00277519988206223	Unknown protein	1
MELO3C016917	7.71474370981906e-05	0.00277519988206223	Damaged dna-binding 2, putative isoform 1	1
MELO3C002821	7.79612487069592e-05	0.00279937581947952	Unknown protein	1
MELO3C015603	7.8575539132153e-05	0.00281631274468401	E3 ubiquitin-protein ligase RING1-like	1
MELO3C011173	7.89147137463253e-05	0.00282334543800032	Gamma-glutamylcyclotransferase	1
MELO3C006158	7.91940140983938e-05	0.00282821443838911	lysophospholipid acyltransferase LPEAT2 isoform X1	1
MELO3C010737	7.96416118012955e-05	0.00283906532755196	RING-type E3 ubiquitin transferase	1
MELO3C025265	8.02798553996009e-05	0.00284737098364442	Unknown protein	1
MELO3C015594	8.04513144398999e-05	0.00284737098364442	No data found	1

MELO3C008076	8.00977753115939e-05	0.00284737098364442	No data found	1
MELO3C003393	8.0430383471497e-05	0.00284737098364442	Plant intracellular ras group-related LRR protein	1
MELO3C019730	8.11006363776734e-05	0.00286521729485272	zinc finger CCCH domain-containing protein 3-like	1
MELO3C009560	8.21626649760709e-05	0.00289444859730923	Polyketide cyclase/dehydrase/lipid transport superfamily protein	1
MELO3C023161	8.22211586961608e-05	0.00289444859730923	nuclear transcription factor Y subunit A-7-like	1
MELO3C023018	8.26704742665774e-05	0.00290468115089194	splicing factor U2af large subunit B isoform X1	1
MELO3C021786	8.280598956667e-05	0.00290468115089194	Cyclin-T1-like protein	1
MELO3C015704	8.32907324128662e-05	0.00291193049597952	Protein trigalactosyldiacylglycerol 2, chloroplastic	1
MELO3C025307	8.33075462164379e-05	0.00291193049597952	Transmembrane 19	1
MELO3C016262	8.34670928354653e-05	0.00291235267916538	26S proteasome non-ATPase regulatory subunit 8	1
MELO3C025654	8.41080056708243e-05	0.00292498547025566	Transmembrane protein	0
MELO3C010913	8.4125360631182e-05	0.00292498547025566	Protein DA1-related 1	1
MELO3C023419	8.4525555592907e-05	0.00293373496907613	methyl-CpG-binding domain-containing protein 11	1
MELO3C022998	8.50718977087883e-05	0.00294235535525545	Malate dehydrogenase	1
MELO3C003977	8.50368989402384e-05	0.00294235535525545	Microtubule-associated family protein	1
MELO3C008197	8.52787411298461e-05	0.00294435289960373	Chloride channel protein	1
MELO3C016126	8.64520687487991e-05	0.00296335514244293	Pathogen-related protein	1
MELO3C005754	8.61995591473486e-05	0.00296335514244293	PHD finger family protein	1
MELO3C005828	8.65793669142523e-05	0.00296335514244293	SKP1-like protein 21	0
MELO3C025956	8.6286284875392e-05	0.00296335514244293	No data found	1
MELO3C021232	8.63064375860034e-05	0.00296335514244293	Novel plant snare, putative	1
MELO3C007483	8.75097762822463e-05	0.0029900182903081	ABC transporter family protein	1
MELO3C008879	8.77609174688709e-05	0.00299342030931387	Triosephosphate isomerase	1
MELO3C025073	8.93035963320798e-05	0.00303555374175946	GRIP and coiled-coil domain-containing protein 1	1
MELO3C005872	8.92453339496058e-05	0.00303555374175946	Polypyrimidine tract binding protein, putative	0
MELO3C019225	8.99096474886729e-05	0.00304860401862575	Formin-like protein	1
MELO3C003659	8.9996260208558e-05	0.00304860401862575	Glucan endo-1,3-beta-glucosidase, putative	1
MELO3C014565	9.04686218434758e-05	0.00304891606277612	Homeobox domain-containing protein	1
MELO3C022494	9.03951638639988e-05	0.00304891606277612	No data found	1
MELO3C010877	9.02100101682901e-05	0.00304891606277612	Phosphatidate phosphatase PAH2	1
MELO3C004610	9.15000192608373e-05	0.003067019032385	zinc finger CCCH domain-containing protein 20-like	1
MELO3C022068	9.14387798359728e-05	0.003067019032385	proline-rich receptor-like protein kinase PERK8	1
MELO3C021228	9.16269800550484e-05	0.003067019032385	tRNA pseudouridine synthase	1
MELO3C003638	9.1278293153696e-05	0.003067019032385	replication protein A 32 kDa subunit A-like	1
MELO3C006670	9.20264952706251e-05	0.00307398449987238	Translationally-controlled tumor protein homolog	0
MELO3C026234	9.21463782431742e-05	0.00307398449987238	elongator complex protein 3	1
MELO3C025779	9.2346093012563e-05	0.00307545192395465	Nucleotide/sugar transporter family protein	1
MELO3C007571	9.30114872104149e-05	0.00309239707225334	OTU domain-containing protein	1
MELO3C024850	9.32171318644981e-05	0.00309402544065878	60S ribosomal protein L9-like	1
MELO3C012943	9.46720039655125e-05	0.00313704262804514	ADP,ATP carrier protein	0
MELO3C013810	9.56120904125335e-05	0.00316288638786788	At3g49990	1
MELO3C021436	9.61451448351358e-05	0.00317520144707207	60S acidic ribosomal protein P2B-like	1
MELO3C010021	9.6358700537813e-05	0.00317694153075337	ER membrane protein complex subunit 10	0
MELO3C022901	9.65210274401773e-05	0.00317698961819344	Alpha/beta-Hydrolases superfamily protein, putative	1
MELO3C021923	9.72721588077263e-05	0.00319638579749382	CCG-binding protein 1	1
MELO3C017755	9.79998273007432e-05	0.00321494782286109	zinc finger protein CONSTANS-LIKE 15-like	1
MELO3C009312	9.82774985767154e-05	0.00321871031408218	Pentatricopeptide repeat-containing protein At3g09650, chloroplastic	1
MELO3C017946	9.85155856012554e-05	0.00322116605966754	bifunctional epoxide hydrolase 2-like	1
MELO3C016303	9.87452484355611e-05	0.00322333869645272	ATP-dependent zinc metalloprotease FtsH	1
MELO3C002041	9.90924691245398e-05	0.00322933526854874	RHOMBOID-like protein 12, mitochondrial	1
MELO3C009572	0.00010010530796678	0.00324566590511127	ABC transporter family protein	1
MELO3C006316	9.98384531540886e-05	0.00324566590511127	cytochrome b5	1
MELO3C020557	0.000100154739182123	0.00324566590511127	Tetratricopeptide repeat (TPR)-like superfamily protein	1
MELO3C023996	0.000100250959649495	0.00324566590511127	RNA polymerase sigma factor sigD, chloroplastic	1
MELO3C024366	0.000100516259118888	0.00324892897109479	Mitochondrial carrier protein	1
MELO3C017255	0.000101150217111434	0.00326407783943417	BSD domain-containing protein	1
MELO3C017754	0.000102643919310808	0.00328012097486915	NAC domain-containing protein	1
MELO3C025278	0.00010184182706352	0.00328012097486915	Emp24/gp25L/p24 family/GOLD family protein	1
MELO3C005405	0.000102359121522122	0.00328012097486915	CDGSH iron-sulfur domain-containing protein NEET	1
MELO3C021901	0.000102486479856445	0.00328012097486915	Alpha/beta hydrolase-3	0
MELO3C025903	0.000102095232691002	0.00328012097486915	At5g59460	1
MELO3C012956	0.00010262148165241	0.00328012097486915	Protein MARD1	1
MELO3C003145	0.000103066071958313	0.00328829055751975	Cyclin d, putative	1

MELO3C006853	0.000103656565781596	0.00329094438804991	receptor-like serine/threonine-protein kinase isoform X2	1
MELO3C013261	0.000104022481609345	0.00329094438804991	No data found	0
MELO3C013440	0.000103896359409772	0.00329094438804991	PHD domain-containing protein/BAH domain-containing protein	1
MELO3C021116	0.000104315721652704	0.00329094438804991	No data found	1
MELO3C015563	0.000103478026248882	0.00329094438804991	TATA-box-binding protein	1
MELO3C008332	0.000104296975344309	0.00329094438804991	5-formyltetrahydrofolate cyclo-ligase-like protein COG0212	1
MELO3C025812	0.000103525632135115	0.00329094438804991	ATP-dependent zinc metalloprotease FtsH	1
MELO3C024396	0.000104622452385073	0.00329535695718149	Cytochrome p450	1
MELO3C003906	0.000107750928353134	0.00338431427849777	Ethylene receptor	0
MELO3C021258	0.00010778944155021	0.00338431427849777	flowering time control protein FCA isoform X2	1
MELO3C015373	0.000108200386231605	0.0033918244883936	40S ribosomal protein S25	1
MELO3C009776	0.000108425898432851	0.00339350723954101	DNA-directed RNA polymerase II, putative	1
MELO3C013031	0.000108816587797156	0.00340034619051587	Glutamate dehydrogenase, putative	1
MELO3C005869	0.000108994104927262	0.00340051276178279	Bidirectional sugar transporter SWEET	1
MELO3C009354	0.000109747032851715	0.00340558652863798	Glutathione gamma-glutamylcysteinyltransferase 1	1
MELO3C016198	0.000109404821318382	0.00340558652863798	No data found	1
MELO3C009076	0.000109755888868523	0.00340558652863798	Nucleolar protein gar2-like protein	1
MELO3C022658	0.000109846504569466	0.00340558652863798	Ubiquitin-specific protease family C19 protein	1
MELO3C007433	0.000111052139491363	0.00342197323004645	fumarylacetoacetase	1
MELO3C007572	0.000110860800119461	0.00342197323004645	AP2-like ethylene-responsive transcription factor TOE3	1
MELO3C005299	0.000110942650853096	0.00342197323004645	C2 domain-containing protein	1
MELO3C011955	0.000111068147271243	0.00342197323004645	Tetratricopeptide-like helical	1
MELO3C008752	0.00011157295959352	0.0034321719299259	TATA box-binding protein-associated factor RNA polymerase I subunit B	1
MELO3C014730	0.000111888076964051	0.00343651264690986	N utilization substance B	1
MELO3C025853	0.000112716329796925	0.00345657577198675	protein DAMAGED DNA-BINDING 2	1
MELO3C002085	0.000113224239913556	0.00346676823884159	ethylene-responsive transcription factor ERF071	0
MELO3C020294	0.000113888702424569	0.00348171514579384	DNA-directed RNA polymerase subunit beta	1
MELO3C023310	0.000114261528182169	0.00348771394137505	Glucose-1-phosphate adenylyltransferase	1
MELO3C022773	0.00011559372525527	0.00352293283960852	Transmembrane protein, putative	1
MELO3C012529	0.000116333438386462	0.00352495494601283	Ras-related Rab7	1
MELO3C002885	0.000116374025256993	0.00352495494601283	transcription factor GTE1	1
MELO3C024324	0.000116198570528248	0.00352495494601283	Chaperone protein DnaJ	0
MELO3C019844	0.000116328959425371	0.00352495494601283	ras-related protein RABC2a-like	1
MELO3C022837	0.000116753774780598	0.00352564265770953	Cysteine-rich repeat secretory protein 60	0
MELO3C010776	0.000116715602386908	0.00352564265770953	Branched-chain-amino-acid aminotransferase	0
MELO3C010102	0.000117010176775678	0.00352799081090514	O-linked n-acetylglucosamine transferase, ogt, putative	1
MELO3C019470	0.000118662693332494	0.00355835651190511	glutelin type-A 2-like	1
MELO3C005094	0.000118738009081243	0.00355835651190511	histidine biosynthesis bifunctional protein hisIE, chloroplastic	1
MELO3C012180	0.000118248526876918	0.00355835651190511	ruBisCO large subunit-binding protein subunit beta, chloroplastic-like	1
MELO3C003658	0.000118704100653622	0.00355835651190511	Protein MARD1	1
MELO3C025049	0.000119458467457201	0.00357452314213979	transcription factor TCP21-like	1
MELO3C005331	0.000120522869021755	0.00359934712416343	Acyl-[acyl-carrier-protein] hydrolase	1
MELO3C001323	0.000120652579684855	0.00359934712416343	transmembrane protein 184C	1
MELO3C015024	0.000121409478646695	0.00361646424403254	RING-type E3 ubiquitin transferase	1
MELO3C014719	0.00012160994411281	0.00361698009982514	Aldehyde oxidase, putative	1
MELO3C012622	0.000122331082063387	0.00363295720251103	peptidyl-prolyl cis-trans isomerase CYP59	1
MELO3C019012	0.000123020613497338	0.00364794909303142	peptidyl-prolyl cis-trans isomerase CYP59	1
MELO3C011773	0.00012378596496454	0.00366514096264573	Oxidoreductase/transition metal ion-binding protein (DUF3531)	1
MELO3C011099	0.000124519937175549	0.00368135365161664	Universal stress protein A-like protein	1
MELO3C001165	0.000124820210286147	0.00368471499692246	eukaryotic translation initiation factor 3 subunit M	0
MELO3C005945	0.000125956652920811	0.00369128273352684	Dihydroorotate dehydrogenase (DUF3598)	1
MELO3C014016	0.000125606445577908	0.00369128273352684	Phospholipase D	1
MELO3C016924	0.000125729655771067	0.00369128273352684	pentatricopeptide repeat-containing protein At4g33170-like	0
MELO3C011550	0.000125977242513398	0.00369128273352684	transcription factor HBP-1b(C38) isoform X2	1
MELO3C003326	0.000125964577002202	0.00369128273352684	Ataxin-10	1
MELO3C005679	0.000126310862371914	0.00369557514219695	Tyrosine--tRNA ligase	1
MELO3C003768	0.000126536742464767	0.00369670728836787	Auxin response factor	1
MELO3C023989	0.000126739273406784	0.00369715496382656	Methyltransferase	0
MELO3C018203	0.000127875492985874	0.00372479809878764	Lysine-specific histone demethylase 1-like protein	1
MELO3C024226	0.000128758289654418	0.00374498889894713	Sulfate transporter 3.1	1
MELO3C022501	0.00012898932198635	0.00374619135280652	SNARE-interacting protein KEULE	1
MELO3C013591	0.000130542508120834	0.0037857327355042	Sugar transporter, putative	1

MELO3C007450	0.000130883346322275	0.0037900516224613	No data found	1
MELO3C016245	0.00013277895743391	0.00382810456987195	Glycosyl transferase family 1 family protein	1
MELO3C005812	0.000132585965774146	0.00382810456987195	ARM repeat superfamily protein	1
MELO3C010286	0.000132474750104805	0.00382810456987195	pyrophosphate-energized vacuolar membrane proton pump	1
MELO3C005656	0.000133662942434221	0.00383121836013559	Protein LURP-one-related 11	1
MELO3C011868	0.000133236508693457	0.00383121836013559	Rubber elongation factor protein (REF)	1
MELO3C024004	0.000133474638887243	0.00383121836013559	No data found	1
MELO3C009836	0.000133335849776817	0.00383121836013559	Saccharopine dehydrogenase-like protein	1
MELO3C026097	0.000133883793933309	0.00383198702375207	Hexosyltransferase	1
MELO3C009272	0.000136632869338404	0.00384148920539927	UNC93-like protein 3	1
MELO3C004354	0.000136084094665589	0.00384148920539927	Cc-nbs-lrr resistance protein	1
MELO3C004448	0.000135177309396939	0.00384148920539927	DNA helicase	1
MELO3C006344	0.000136358697194305	0.00384148920539927	GDT1-like protein	1
MELO3C016879	0.000135264956713455	0.00384148920539927	Cytochrome P450, putative	1
MELO3C010548	0.000135760565941778	0.00384148920539927	Receptor-like protein kinase	1
MELO3C007153	0.000136188957985395	0.00384148920539927	No data found	1
MELO3C007246	0.000136437561226055	0.00384148920539927	28 kDa heat/acid-stable phosphoprotein-like protein	0
MELO3C023322	0.000135847690136526	0.00384148920539927	BnaC07g46810D protein	0
MELO3C017248	0.000136096223293025	0.00384148920539927	ATP-dependent helicase hrq1 isoform X6	1
MELO3C018521	0.000136744488905549	0.00384148920539927	DNA polymerase kappa	1
MELO3C010798	0.000136566235940494	0.00384148920539927	NADH dehydrogenase (Ubiquinone) iron-sulfur protein 4, mitochondrial	1
MELO3C009895	0.000134705562194748	0.00384148920539927	Actin cross-linking protein	1
MELO3C003344	0.000137728859039843	0.00386364664371855	3-isopropylmalate dehydratase large subunit	1
MELO3C020622	0.000138697018806866	0.00388528712683233	Rab5-interacting family protein	1
MELO3C021529	0.000139532513883989	0.00390315526444036	NHL domain-containing protein, putative	1
MELO3C013254	0.000140084319380063	0.0039130484065585	Kinase family protein	1
MELO3C015431	0.000140582970614034	0.00392084191800449	40S ribosomal protein S30	1
MELO3C011444	0.000140928428675302	0.00392084191800449	Mitogen-activated protein kinase	1
MELO3C011256	0.00014095892256738	0.00392084191800449	DEAD-box ATP-dependent RNA helicase-like protein	1
MELO3C023033	0.000141418977736452	0.00392810603560785	heterogeneous nuclear ribonucleoprotein 1-like	0
MELO3C002381	0.000142522202502882	0.00395318957476041	Bidirectional sugar transporter SWEET	1
MELO3C014860	0.000143769670123084	0.00395998216912243	Transcription factor GTE8	1
MELO3C017753	0.000143619980119469	0.00395998216912243	Glycerophosphodiester phosphodiesterase, putative	1
MELO3C027408	0.000143675590806192	0.00395998216912243	polygalacturonase-like	1
MELO3C011905	0.000143275905241325	0.00395998216912243	RING finger protein	1
MELO3C021273	0.000143610156909224	0.00395998216912243	Seed maturation protein PM36	1
MELO3C021552	0.000144105408032114	0.00396370153652676	universal stress protein A-like protein	1
MELO3C012410	0.000144501796441432	0.00396907646442537	thioredoxin-like 3-2, chloroplastic isoform X8	1
MELO3C009350	0.000144748238125936	0.00397032354826265	TSL-kinase interacting protein 1	1
MELO3C019087	0.000146130882510365	0.00398610331311767	UDP-glycosyltransferase 76E2-like	0
MELO3C013563	0.000146093610227327	0.00398610331311767	Metacaspase-5	0
MELO3C020626	0.000145762787050252	0.00398610331311767	Expansin	1
MELO3C003332	0.000145611556127134	0.00398610331311767	BAX inhibitor-1	1
MELO3C005692	0.000146809861828023	0.00399910063619536	E3 ubiquitin-protein ligase At3g02290-like	0
MELO3C023195	0.000147031826110533	0.00399963021192413	NAC domain-containing protein 2	1
MELO3C015186	0.000147641124904396	0.00400517112051775	Sulfite reductase	1
MELO3C026248	0.000147597711079306	0.00400517112051775	E3 ubiquitin-protein ligase RGLG2	1
MELO3C005182	0.000148326223665451	0.00401823675057476	Short-chain dehydrogenase/reductase family protein	1
MELO3C022443	0.000148550255063884	0.00401879313322828	flowering time control protein FPA	1
MELO3C003561	0.000149095804355959	0.00402803425475489	VQ motif-containing protein 9	1
MELO3C016354	0.000150065092783924	0.00404868240080563	Short-chain dehydrogenase TIC 32, chloroplastic	1
MELO3C024861	0.000151226502948631	0.00407445048667466	Caffeic acid O-methyltransferase	0
MELO3C014129	0.000151454412625762	0.00407503160074411	THO complex subunit 3	1
MELO3C017700	0.000151785072965982	0.00407691511311494	disease resistance protein RGA2-like	1
MELO3C000065	0.000151961111964471	0.00407691511311494	V-type proton ATPase proteolipid subunit	1
MELO3C018160	0.000152143725675513	0.00407691511311494	factor of DNA methylation 1-like	0
MELO3C010420	0.000153349701356276	0.00409707057209984	DUF581 family protein, putative (DUF581)	1
MELO3C016246	0.000153294831223838	0.00409707057209984	Kinase family protein	1
MELO3C015930	0.000153518265398445	0.00409707057209984	Translation initiation factor IF-2	1
MELO3C011402	0.000153953444997246	0.00410313979116141	D-aminoacyl-tRNA deacylase	1
MELO3C017560	0.000155454272554256	0.00413387924224256	Succinate dehydrogenase [ubiquinone] flavoprotein subunit, mitochondrial	1
MELO3C008974	0.000155525458351624	0.00413387924224256	60S ribosomal protein L35a	0

MELO3C023979	0.000156378911793542	0.00415097732393906	Cellulose synthase	1
MELO3C021064	0.000157428826421557	0.00417323744026756	malonyl-CoA:anthocyanidin 5-O-glucoside-6"-O-malonyltransferase	1
MELO3C006645	0.000158263172499673	0.00417852860119792	No data found	1
MELO3C003147	0.000158254093796217	0.00417852860119792	LOW QUALITY PROTEIN: L-type lectin-domain containing receptor kinase S.4-like	1
MELO3C001121	0.00015812671487514	0.00417852860119792	Aspartate aminotransferase	1
MELO3C010760	0.000158563073288098	0.00418085732225187	Pollen specific protein sf21	1
MELO3C024871	0.000160253718284764	0.00421980090987441	serine/threonine-protein phosphatase 4 regulatory subunit 2 isoform X1	1
MELO3C017653	0.000160928051555986	0.00422261443857199	Isoaspartyl peptidase/L-asparaginase	1
MELO3C008785	0.000160986249053918	0.00422261443857199	BTB/POZ domain protein	1
MELO3C024222	0.000161002008822964	0.00422261443857199	aldo-keto reductase family 4 member C9-like	1
MELO3C025594	0.000161236287363531	0.00422315044979094	C2 domain-containing protein	1
MELO3C019722	0.000162089692921086	0.00423791057130512	Protein disulfide-isomerase like 2-2	1
MELO3C015230	0.000162228993463298	0.00423791057130512	Pectin acetylesterase	1
MELO3C018510	0.000162585414409389	0.00424161076508721	somatic embryogenesis receptor kinase 1-like	1
MELO3C013260	0.000162887802810818	0.00424389342705917	protein LAZ1 isoform X1	1
MELO3C009203	0.000165437336013374	0.00426283287985112	tubulin beta chain-like	1
MELO3C023685	0.000165296367253043	0.00426283287985112	alcohol dehydrogenase-like	1
MELO3C006088	0.000165137396803905	0.00426283287985112	50S ribosomal protein L5, chloroplastic	1
MELO3C006974	0.000165557386138326	0.00426283287985112	Plastid division protein PDV1	1
MELO3C023255	0.000164791051848967	0.00426283287985112	DNA-directed RNA polymerase subunit beta-beta protein, putative (DUF506)	1
MELO3C002817	0.000164407991422699	0.00426283287985112	No data found	1
MELO3C002163	0.000164730021437798	0.00426283287985112	E3 ubiquitin-protein ligase RING1-like	0
MELO3C010165	0.000165256170291617	0.00426283287985112	Cyclic nucleotide-gated ion channel-like protein	1
MELO3C026141	0.000165134912869958	0.00426283287985112	ADP-ribosylation factor-like	1
MELO3C014128	0.000165992853658037	0.00426848029543303	Calcium-dependent protein kinase	1
MELO3C012572	0.000166407907161714	0.00427358876272652	CTP synthase	1
MELO3C003973	0.000167132576897933	0.00427592256812336	SNW/SKI-interacting protein-like	1
MELO3C017838	0.000166939205969663	0.00427592256812336	Ubiquitin system component Cue	1
MELO3C014217	0.000167148322577915	0.00427592256812336	Telomere repeat-binding protein 4	0
MELO3C009063	0.000169160970210358	0.00432181112637045	serine/threonine-protein kinase Nek6 isoform X1	1
MELO3C018306	0.000169535131114396	0.00432577429506227	Mitogen-activated protein kinase	1
MELO3C005001	0.000170562545132369	0.00434637381137955	dof zinc finger protein DOF5.3-like	0
MELO3C005882	0.000171637761367083	0.00436813679025582	Eukaryotic translation initiation factor 3 subunit 10	1
MELO3C015374	0.000172882858217371	0.00439416160480678	Superoxide dismutase [Cu-Zn]	1
MELO3C012201	0.000173729943490741	0.0044017019494474	Isoprenylcysteine alpha-carbonyl methylesterase ICME protein	1
MELO3C020583	0.000173737441671706	0.0044017019494474	Neutral ceramidase	0
MELO3C002566	0.000173848170569091	0.0044017019494474	Katanin p80 WD40 repeat-containing subunit B1 homolog	1
MELO3C014799	0.000175285251514445	0.00442673712552274	TRANSPORT INHIBITOR RESPONSE 1 protein, putative	0
MELO3C015185	0.000175088311723859	0.00442673712552274	MP domain-containing protein	1
MELO3C022562	0.00017556921672901	0.00442824579972059	protein CHROMATIN REMODELING 19 isoform X1	0
MELO3C010421	0.000176144776798615	0.00443709591453551	Random slug protein 5	1
MELO3C014379	0.000177515142250728	0.00446023733372727	Protein RETICULATA-RELATED 1, chloroplastic	1
MELO3C001948	0.000177457027202066	0.00446023733372727	Short-chain dehydrogenase, putative	1
MELO3C003508	0.000178471292703875	0.00447856360814335	UDP-glycosyltransferase 91C1	1
MELO3C005673	0.000183514922535988	0.00459928452431881	tubulin beta chain-like	1
MELO3C009561	0.000183781133722527	0.00460011864370873	iron-sulfur cluster co-chaperone protein HscB, mitochondrial	1
MELO3C006651	0.000184318937710204	0.00460191491888599	No data found	1
MELO3C017358	0.000184207700662187	0.00460191491888599	C2 domain-containing protein	1
MELO3C013346	0.000185552097884845	0.0046268540165755	Phospholipase-like protein (PEARLI 4) family protein	1
MELO3C015111	0.000188240908695514	0.00468798197456205	rho GTPase-activating protein 7	1
MELO3C010245	0.000189301601007941	0.00470846009862194	Two-component response regulator	1
MELO3C012076	0.00019072837700751	0.00473798077675636	UDP-galactose/UDP-glucose transporter family protein	1
MELO3C025468	0.000191221524523888	0.00474349870973502	ABC transporter B family protein	1
MELO3C004833	0.000191430881141263	0.00474349870973502	crooked neck-like protein 1	1
MELO3C015350	0.000191817108435632	0.0047471128753074	Sugar transporter ERD6-like protein	1
MELO3C006239	0.000194745937404539	0.0048075468972528	Receptor protein kinase, putative	0
MELO3C022684	0.000194616340531306	0.0048075468972528	peroxisomal (S)-2-hydroxy-acid oxidase GLO4-like	0
MELO3C011588	0.000195838236416002	0.00482847606863872	Phosphatidylinositol-4-phosphate 5-kinase 1-like protein	1
MELO3C003733	0.000196244446180049	0.00483245831372793	ribonuclease P protein subunit p25-like protein isoform X1	1
MELO3C000826	0.000197316742958864	0.00484075572260199	Transcription factor	1

MELO3C021280	0.000197073655135882	0.00484075572260199	Calmodulin-binding transcription activator	1
MELO3C018455	0.000197093459462172	0.00484075572260199	thioredoxin M3, chloroplastic	1
MELO3C024902	0.000197626941677576	0.00484235046053404	ABC subfamily C transporter	0
MELO3C005808	0.000198080417585844	0.00484539295425683	No data found	1
MELO3C024344	0.000198241810068334	0.00484539295425683	DUF1677 family protein (DUF1677)	1
MELO3C025606	0.000198581595278524	0.00484769830056313	Unknown protein	1
MELO3C016360	0.00019959105733458	0.00486632566827238	Transferring glycosyl group transferase	1
MELO3C019026	0.000200262784349703	0.00487668277203734	Phosphate transporter	1
MELO3C019564	0.000201417398875803	0.00489273334612328	High chlorophyll fluorescence phenotype 173	1
MELO3C000994	0.000201282242801692	0.00489273334612328	wall-associated receptor kinase 2-like	1
MELO3C013841	0.000206757258935486	0.00501012160333364	nucleolar protein 12	1
MELO3C003817	0.00020674784003627	0.00501012160333364	DNA polymerase epsilon catalytic subunit A	1
MELO3C004551	0.000207150930850553	0.00501350947716613	ARF guanine-nucleotide exchange factor GNL2	1
MELO3C005035	0.000208333784670112	0.00503596562233786	E3 SUMO-protein ligase SIZ1	1
MELO3C011395	0.000212015636750662	0.00511870025695455	Hydroxyproline O-arabinosyltransferase 1	1
MELO3C009566	0.000212899672441647	0.0051337675592797	Protein WVD2-like 4	1
MELO3C007624	0.00021680183247641	0.00519433149706969	Acyl-CoA N-acyltransferases (NAT) superfamily protein	1
MELO3C005520	0.000216989391112588	0.00519433149706969	Ribosomal protein L15	1
MELO3C023503	0.000216126270384365	0.00519433149706969	Unknown protein	1
MELO3C022540	0.000216005163480082	0.00519433149706969	NADH dehydrogenase [ubiquinone] 1 beta subcomplex subunit 7	0
MELO3C013615	0.00021629852461702	0.00519433149706969	E3 ubiquitin-protein ligase RMA1H1	1
MELO3C003842	0.000216935765092741	0.00519433149706969	Dead box ATP-dependent RNA helicase, putative	1
MELO3C026764	0.000217488779697295	0.00519998294218144	Magnesium transporter MRS2-like protein	1
MELO3C020601	0.000218758247361506	0.00522354898241223	Protein phosphatase 2C	1
MELO3C017432	0.000219003420802943	0.00522354898241223	At1g16840/F17F16.27	1
MELO3C019629	0.000220238525441285	0.00524667145831115	ALA-interacting subunit 3-like	0
MELO3C004999	0.000222439350828108	0.00529271655361963	nicotinamide adenine dinucleotide transporter 1, chloroplastic-like	1
MELO3C010189	0.00022317153203999	0.00529927201732925	lactation elevated protein 1	1
MELO3C017165	0.000223376505001038	0.00529927201732925	HVA22-like protein	1
MELO3C009914	0.000223519853685517	0.00529927201732925	Alpha-mannosidase	1
MELO3C021308	0.00022430380657712	0.00530926236936354	Multiple organellar RNA editing factor 8, chloroplastic/mitochondrial	1
MELO3C019921	0.000224478914295334	0.00530926236936354	Phospholipid-transporting ATPase	0
MELO3C019139	0.000225618022833496	0.00532485097703111	Nascent polypeptide-associated complex subunit alpha-like protein	1
MELO3C026027	0.000225677263039903	0.00532485097703111	Macrophage migration inhibitory factor family protein	1
MELO3C012869	0.000228239696927757	0.00537888517258504	Adaptin ear-binding coat-associated protein, putative	1
MELO3C013214	0.000232109115587242	0.00546355533221984	DNA damage-inducible protein 1	1
MELO3C017043	0.000233289549711801	0.00547828218461161	Glutamate receptor	1
MELO3C011682	0.00023316957210473	0.00547828218461161	Fructose-1,6-bisphosphatase	0
MELO3C009429	0.000234027845987472	0.00548351994895583	peroxiredoxin-2E-2, chloroplastic	1
MELO3C005111	0.00023446163867713	0.00548351994895583	Coiled-coil protein	0
MELO3C005745	0.000234311765738404	0.00548351994895583	Abhydrolase_5 domain-containing protein	1
MELO3C023464	0.000234798570744266	0.00548351994895583	sister chromatid cohesion protein PDS5 homolog B-B-like	1
MELO3C021339	0.000234900900137558	0.00548351994895583	60S ribosomal protein L13a, putative	1
MELO3C014614	0.000235860026803869	0.00549292413838397	Leucine-rich repeat receptor-like protein kinase family	0
MELO3C010705	0.000235766264270243	0.00549292413838397	T-complex protein 1 subunit epsilon	1
MELO3C019435	0.000236976943461809	0.00550595018403207	MLO-like protein 4	1
MELO3C015852	0.000236938477880977	0.00550595018403207	adenylate isopentenyltransferase 3, chloroplastic	1
MELO3C002886	0.000237461224858571	0.00551071883634772	Alpha-taxilin	1
MELO3C017008	0.000239417539566356	0.00552722123260604	Ubiquitin family protein	0
MELO3C026804	0.000239213874166588	0.00552722123260604	histone-lysine N-methyltransferase, H3 lysine-9 specific SUVH1-like	1
MELO3C000201	0.000239277857855269	0.00552722123260604	dof zinc finger protein DOF1.5-like	1
MELO3C021461	0.000239571693509077	0.00552722123260604	No data found	1
MELO3C021742	0.000238546835302778	0.00552722123260604	Glycine cleavage system H, mitochondrial	1
MELO3C024688	0.000240582824529545	0.00554407258066976	TATA-binding protein-associated factor 2N	0
MELO3C009127	0.000241609568591317	0.00556124402110712	WRKY family transcription factor family protein	0
MELO3C004441	0.000242392300670469	0.00557276547839475	RING-H2 finger protein ATL16	1
MELO3C016707	0.000243440104488402	0.00557737659343555	Choline transporter-like protein 2	1
MELO3C012173	0.00024337823626408	0.00557737659343555	DNA-directed RNA polymerase	1
MELO3C011044	0.000243145665177247	0.00557737659343555	cytochrome c oxidase subunit 6b-1-like	1
MELO3C003120	0.000244375341807102	0.00559231590422763	SLT1	1
MELO3C012004	0.000244992421164048	0.00559765608210468	Xyloglucan endotransglucosylase/hydrolase	1
MELO3C018437	0.000245175579068335	0.00559765608210468	Pentatricopeptide repeat-containing protein At5g39710	1

MELO3C002075	0.00024584132238592	0.00559990804590489	No data found	1
MELO3C011507	0.00024562707592301 6	0.00559990804590489	Vesicle transport protein GOT1	1
MELO3C024192	0.00024731600777605 5	0.0056205337601488	Fasciclin-like arabinogalactan protein	1
MELO3C007425	0.00024728316081834 6	0.0056205337601488	1-aminocyclopropane-1-carboxylate oxidase 1	0
MELO3C015496	0.00025133641912544 7	0.00570533671414766	Plant/F27B13-30 protein	1
MELO3C021292	0.00025195642650854 8	0.00571284439393493	Protein DEHYDRATION-INDUCED 19	1
MELO3C011986	0.00025266878831753 4	0.00572242649137956	Polygalacturonase	1
MELO3C013600	0.00025614310001709 2	0.00574837509345177	O-methyltransferase, putative	1
MELO3C005797	0.00025528909842986 7	0.00574837509345177	Unknown protein	1
MELO3C012033	0.00025552162754083 3	0.00574837509345177	Neurofilament heavy protein	1
MELO3C022354	0.00025494492787436 8	0.00574837509345177	Light-regulated protein, putative	1
MELO3C017242	0.00025602726417806	0.00574837509345177	protein COBRA-like	1
MELO3C026522	0.00025569069952724 5	0.00574837509345177	monosaccharide-sensing protein 2-like	1
MELO3C011105	0.00025566909574714 6	0.00574837509345177	Chaperone protein dnaJ	1
MELO3C009782	0.00025472239308277 4	0.00574837509345177	5-methyltetrahydropteroyltriglutamate-- homocysteine methyltransferase	1
MELO3C026803	0.00025845091568699 2	0.00578701489104581	S-acyltransferase	1
MELO3C022442	0.00025843778781919 9	0.00578701489104581	At1g08760	1
MELO3C002351	0.00025952776688131 8	0.00580454571703188	Receptor protein kinase-like protein	0
MELO3C008058	0.00026162609819291 3	0.00581198404185809	mitogen-activated protein kinase kinase kinase YODA isoform X1	1
MELO3C022196	0.00026154962293545 3	0.00581198404185809	Kinase family protein	1
MELO3C010214	0.00026161008367320 3	0.00581198404185809	Nucleoid-associated protein At2g24020, chloroplastic	1
MELO3C026201	0.00026084211648180 8	0.00581198404185809	non-specific phospholipase C6	1
MELO3C011601	0.00026098620099357 4	0.00581198404185809	No data found	1
MELO3C011107	0.00026160953134102 3	0.00581198404185809	Serine hydroxymethyltransferase	1
MELO3C005967	0.00026498483475578 8	0.005879983709654	At3g15351	1
MELO3C022114	0.00026544762787983 3	0.00588364220314122	RmlC-like cupins superfamily protein	1
MELO3C003186	0.00026665888002941 76	0.00588910762529048	Proteasome inhibitor-related	1
MELO3C011622	0.00026608518732795 8	0.00588910762529048	Receptor-like kinase	1
MELO3C010958	0.00026633997274461 1	0.00588910762529048	Gamma carbonic anhydrase 1, mitochondrial	1
MELO3C011482	0.00026699412311226 3	0.00589147143837328	ATP-citrate synthase beta chain protein 2-like	1
MELO3C016601	0.00026804757406839 7	0.00590561416358361	No data found	1
MELO3C002470	0.00026823312090407 1	0.00590561416358361	Patatin	1
MELO3C003294	0.00026896786022034 8	0.00591519629342055	vacuolar cation/proton exchanger 3	1
MELO3C017993	0.00027153216554065 6	0.00596494853978021	40S ribosomal protein S29	1
MELO3C025255	0.00027327109676833 5	0.00599647876675316	Zinc transporter	1
MELO3C006594	0.00027565284089270 4	0.00602044287082797	Inosine-uridine preferring nucleoside hydrolase	1
MELO3C022014	0.00027473352176254 9	0.00602044287082797	WRKY transcription factor, putative	1
MELO3C005588	0.00027576175649812 7	0.00602044287082797	No data found	1
MELO3C002223	0.00027588742711526 2	0.00602044287082797	hydroxyproline O-galactosyltransferase GALT6	1
MELO3C024975	0.00027551687458338 1	0.00602044287082797	DUF3511 domain protein	1
MELO3C013766	0.00027704788195737 1	0.00602295331887094	Translocase of chloroplast	0
MELO3C017544	0.00027686204683130 5	0.00602295331887094	DNA-directed RNA polymerase III subunit RPC5	1
MELO3C018441	0.00027722236907457	0.00602295331887094	presequence protease 1, chloroplastic/mitochondrial-like	1
MELO3C022679	0.00027718310493640 7	0.00602295331887094	oligouridylate-binding protein 1B-like	0
MELO3C013188	0.00027787228047226 9	0.00602381961256513	Pentatricopeptide repeat-containing protein	1
MELO3C002118	0.00027783604314279 8	0.00602381961256513	Elongation factor 1 alpha	1
MELO3C013046	0.00027818083088737 6	0.0060238960846434	Kinase family protein	1
MELO3C005002	0.00028104085958569 1	0.00607916312810274	Interactor of constitutive active ROPs-like protein	0
MELO3C012349	0.00028211508638220 6	0.00609572302074638	replication protein A 14 kDa subunit B-like	0
MELO3C008097	0.00028289118341373 6	0.00610581200135287	Polyprotein	0
MELO3C022353	0.00028347677461315 6	0.0061117716395581	tRNA dimethylallyltransferase	0
MELO3C008236	0.00028385781345763 3	0.00611331293127022	S-adenosyl-L-methionine-dependent methyltransferases superfamily protein isoform 1	1
MELO3C007082	0.00028560147257095 1	0.00613952992528879	No data found	1
MELO3C012218	0.00028569689611324 1	0.00613952992528879	Two-component response regulator	1
MELO3C009779	0.00028706342501905 2	0.00616219084858832	S-adenosyl-L-methionine-dependent methyltransferases superfamily protein	1
MELO3C020850	0.00028741527379527 7	0.00616304477978603	Filament-like plant protein 7	0
MELO3C009539	0.00028893531346940 7	0.00616328919688229	NC domain-containing protein	1
MELO3C008986	0.00028802166158015 1	0.00616328919688229	No data found	1
MELO3C023484	0.00028885238373110 9	0.00616328919688229	AP2-like ethylene-responsive transcription factor At1g16060	1
MELO3C010053	0.00028960765020635 8	0.00616328919688229	Isopentenyl diphosphate isomerase	1
MELO3C017226	0.00028961123979476 3	0.00616328919688229	glycine-rich RNA-binding protein 2, mitochondrial-like	1

MELO3C010630	0.000289461750767162	0.00616328919688229	40S ribosomal protein S8	1
MELO3C003771	0.000289095891857327	0.00616328919688229	Mitochondrial 39S ribosomal protein L53	0
MELO3C007084	0.000290601122250878	0.00617769813060558	BTB/POZ domain-containing protein	0
MELO3C008295	0.000291253199451558	0.0061849026193213	ABC1-like protein	1
MELO3C023251	0.000292832830838363	0.00621176753622646	callose synthase 5	1
MELO3C025232	0.000294396155300802	0.00623822926076775	Ubiquitin-conjugating enzyme, E2	1
MELO3C016288	0.000296833075818848	0.00628245353684985	F-box/LRR-repeat protein 14	1
MELO3C003487	0.0002971194290049	0.00628245353684985	receptor-like protein kinase HAIKU2	1
MELO3C006785	0.00030098724067229	0.00634386020921778	U11/U12 small nuclear ribonucleoprotein 35 kDa protein	1
MELO3C016573	0.000300781649135162	0.00634386020921778	Serine/threonine-protein kinase	1
MELO3C012335	0.00030093175099899	0.00634386020921778	Uricase	0
MELO3C002298	0.00030226452811033	0.00635973082156247	Methylthioribose-1-phosphate isomerase	0
MELO3C008469	0.00030238428484719	0.00635973082156247	Kinase family protein	1
MELO3C015385	0.000304250502092929	0.00638538062256456	Pentatricopeptide repeat-containing protein	1
MELO3C019777	0.000304243646278235	0.00638538062256456	U4/U6 small nuclear ribonucleoprotein PRP4-like protein	1
MELO3C025091	0.000304781112087205	0.0063897263085034	protein REVEILLE 1-like isoform X1	1
MELO3C017939	0.000306345373478512	0.00641571026598847	Ribosomal protein L19	1
MELO3C007011	0.000307586424169948	0.00642904807225306	No data found	1
MELO3C007611	0.000307633319574618	0.00642904807225306	Prolyl 4-hydroxylase alpha-like protein	1
MELO3C013883	0.000308162688031799	0.00643330330437632	BOI-related E3 ubiquitin-protein ligase 1	1
MELO3C022514	0.000309803504096484	0.00645779523213418	UTP:RNA uridylyltransferase 1	1
MELO3C002328	0.000310299011578308	0.00645779523213418	zinc finger CCCH domain-containing protein 43	1
MELO3C011090	0.000310316860362314	0.00645779523213418	Unknown protein	1
MELO3C008440	0.000311127156138014	0.00646784232270487	wall-associated receptor kinase 2-like	1
MELO3C004818	0.000313659812932854	0.00651363579980119	S-adenosyl-L-methionine-dependent methyltransferase superfamily protein	0
MELO3C014557	0.000316734499387072	0.00655680254548773	Peptidyl-prolyl cis-trans isomerase	1
MELO3C010478	0.000316303353062986	0.00655680254548773	Protein-methionine-s-oxide reductase	1
MELO3C013527	0.000316579852200904	0.00655680254548773	1D-myo-inositol 2-amino-2-deoxy-alpha-D-glucopyranoside ligase	1
MELO3C001849	0.000317464593990291	0.00656503483425577	No data found	1
MELO3C025628	0.000319630051430653	0.00660290155408364	Aspartyl/glutamyl-tRNA (Asn/Gln) amidotransferase subunit B	0
MELO3C017799	0.000320760795404995	0.00661242687729984	F2P16.20 protein, putative isoform 1	1
MELO3C011882	0.000320479602688328	0.00661242687729984	RING-type E3 ubiquitin transferase	1
MELO3C019053	0.000321423875051297	0.00661859054599197	Ectonucleotide pyrophosphatase/phosphodiesterase family member 3	1
MELO3C021608	0.00032173005844105	0.00661859054599197	zinc finger protein CONSTANS-LIKE 6	1
MELO3C022345	0.000322137578457116	0.00662007808215357	somatic embryogenesis receptor kinase 2-like	1
MELO3C011110	0.000324177713222018	0.00665507864700794	transcription factor bHLH93-like	1
MELO3C008732	0.000326177477364187	0.00668529463580516	No data found	1
MELO3C016284	0.000326326600279314	0.00668529463580516	BnaC06g13730D protein	0
MELO3C013949	0.000326936864283978	0.00669085609610806	Ribosomal protein L20	1
MELO3C025848	0.000329847364902602	0.00674343230793115	Peptidyl-prolyl cis-trans isomerase	1
MELO3C016213	0.00033459521642587	0.00683342391850518	Beta-amylase	1
MELO3C018956	0.000335707153891862	0.00683492843526844	Ubiquitin carboxyl-terminal hydrolase, putative	1
MELO3C007152	0.000335088922765014	0.00683492843526844	Leucine-rich receptor-like protein kinase family protein	1
MELO3C010769	0.000335478511820808	0.00683492843526844	Protein EARLY FLOWERING 3	1
MELO3C015450	0.000340086584732724	0.00691696185570192	Pollen-specific protein SF21	1
MELO3C006413	0.000342652819556477	0.00696198614549472	Clathrin interactor EPSIN 2	1
MELO3C017698	0.00034384648671526	0.00697905885523091	Vesicle transport protein GOT1	0
MELO3C018478	0.000344872724779233	0.00698552968375904	kynurenine formamidase	1
MELO3C011104	0.00034473878406005	0.00698552968375904	Glucose-6-phosphate isomerase	1
MELO3C021510	0.000345680560706607	0.00699471864077334	Ferredoxin-thioredoxin reductase catalytic chain	0
MELO3C011212	0.000351043049657718	0.00709595617982627	Photosystem II reaction center PsbP family protein	1
MELO3C006983	0.000353401205477111	0.00713631943452705	Protein phosphatase 2C	1
MELO3C014307	0.000354028631387227	0.00714168686544059	PRA1 family protein	1
MELO3C026030	0.000355478001607956	0.00716360719770972	Protein phosphatase-2c, putative	1
MELO3C019462	0.000356006879700388	0.00716695195433533	Membralin, putative	1
MELO3C010774	0.000360111028847587	0.00724219216773014	Zinc finger CCCH domain-containing protein	1
MELO3C010329	0.000361489058516851	0.0072625100881478	methyl-CpG-binding domain-containing protein 11-like	1
MELO3C007086	0.000362295746433317	0.00727131981332476	ABC transporter C family member 12-like	1
MELO3C014306	0.000362983932115979	0.00727773571102382	signal recognition particle 9 kDa protein	1
MELO3C007119	0.000364741286312031	0.00730555341113216	E3 ubiquitin-protein ligase arkadia-A, putative	0
MELO3C022212	0.000369332025183966	0.00739000827290592	Deoxycytidine kinase	1
MELO3C002722	0.000370088987242112	0.00739765932089521	3-oxoacyl-[acyl-carrier-protein] synthase	1

MELO3C002607	0.000370819442000903	0.00740476558147202	Sulfate/thiosulfate import ATP-binding protein cysA, putative	1
MELO3C014272	0.000376517115107222	0.00750665144381306	Pyruvate kinase	1
MELO3C017784	0.000376681937354739	0.00750665144381306	Pentatricopeptide repeat-containing family protein	1
MELO3C026155	0.000378623549355916	0.00753773838329637	(+)-neomenthol dehydrogenase	1
MELO3C006598	0.000380672496428369	0.00757089741386089	serine/arginine-rich SC35-like splicing factor SCL28	1
MELO3C008040	0.000381908918189233	0.00758784630313799	RING-type E3 ubiquitin transferase	1
MELO3C012525	0.000384064071674795	0.00762299633317137	Receptor-like kinase	1
MELO3C026919	0.000385875008708902	0.00765125054918887	RuBisCO large subunit-binding protein subunit alpha, chloroplastic	0
MELO3C003242	0.000388061894538216	0.0076868950403563	Clathrin light chain	1
MELO3C006096	0.000388869747816378	0.00769517900764094	DNA replication complex GINS protein SLD5	0
MELO3C008925	0.000389715645112587	0.00770419847380229	GTPase LSG1-2-like	1
MELO3C007691	0.000390499220882301	0.00771196911320456	Auxin-responsive protein	1
MELO3C018720	0.000391460927158693	0.00772323861184519	F-box protein MAX2	1
MELO3C006726	0.000393613047360519	0.00775021343202681	Galactokinase	0
MELO3C023350	0.000393498277305726	0.00775021343202681	GATA transcription factor	0
MELO3C017960	0.00039484077823515	0.00775296869722632	NADH dehydrogenase [ubiquinone] iron-sulfur protein 5-B	1
MELO3C007833	0.000394930705828633	0.00775296869722632	ATPase family AAA domain-containing protein 3	1
MELO3C005861	0.000394326202309614	0.00775296869722632	Hexosyltransferase	0
MELO3C019503	0.000397224747742952	0.00776020694699844	zinc-binding alcohol dehydrogenase domain-containing protein 2	1
MELO3C027373	0.000398384892281056	0.00776020694699844	ADP-ribosylation factor GTPase-activating protein AGD12-like	1
MELO3C022007	0.000397071538311811	0.00776020694699844	transmembrane emp24 domain-containing protein p24delta9	1
MELO3C024444	0.000395871151194438	0.00776020694699844	Avr9/Cf-9 rapidly elicited protein	1
MELO3C012447	0.00039769110672716	0.00776020694699844	Scarecrow-like 3	1
MELO3C020610	0.000397760016506599	0.00776020694699844	protein TOC75-3, chloroplastic	0
MELO3C002609	0.000398442951251021	0.00776020694699844	serine/threonine-protein kinase HT1-like	1
MELO3C024644	0.000397462342182631	0.00776020694699844	50S ribosomal protein L18	1
MELO3C019816	0.000399693237937981	0.00777688842959329	Amino acid transporter family protein	1
MELO3C009758	0.000402735654175146	0.00780045318224247	Amino acid transporter family protein	1
MELO3C009408	0.000402832046479062	0.00780045318224247	Tetratricopeptide repeat (TPR)-like superfamily protein	1
MELO3C016817	0.000402351344261254	0.00780045318224247	Calcium-transporting ATPase	1
MELO3C026025	0.000402879246842236	0.00780045318224247	Dehydration responsive element binding transcription factor	1
MELO3C017480	0.000401515371484806	0.00780045318224247	Xyloglucan endotransglucosylase/hydrolase	1
MELO3C024544	0.000404108671178793	0.00781659367983349	Cell division FtsZ-1, chloroplastic-like protein	1
MELO3C005517	0.0004077385948561	0.00787908953993455	Tryptophan RNA-binding attenuator protein-like	1
MELO3C007043	0.000408454688791027	0.00788521177803909	UDP-glucose 4-epimerase, putative	1
MELO3C013773	0.000410427524175638	0.00790881113427016	Mediator of RNA polymerase II transcription subunit	1
MELO3C003426	0.000410478070415055	0.00790881113427016	Inositol-tetrakisphosphate 1-kinase	1
MELO3C014619	0.000416573957624733	0.00798238170586701	IRK-interacting protein-like	1
MELO3C021139	0.000416728063664884	0.00798238170586701	No data found	0
MELO3C005875	0.000415414077330256	0.00798238170586701	Curved DNA-binding protein	0
MELO3C012171	0.000417125825128095	0.00798238170586701	phosphatidylinositol 4-kinase gamma 5	0
MELO3C025940	0.000416422648866988	0.00798238170586701	CONSTANS-like zinc finger protein	1
MELO3C002382	0.000417101743036552	0.00798238170586701	Kinase family protein	1
MELO3C017207	0.000416952793157011	0.00798238170586701	LYR motif-containing protein 4	1
MELO3C002312	0.000421192848875096	0.00805240810497025	cytochrome P450 71A1-like	1
MELO3C026966	0.00042238849588494	0.00806745687159737	2-oxoglutarate (2OG) and Fe(II)-dependent oxygenase superfamily protein	1
MELO3C017319	0.000423412418095515	0.00807919985021093	BnaA06g03540D protein	1
MELO3C023667	0.000425142227014508	0.00809656108130136	Tetratricopeptide repeat-containing protein	1
MELO3C008086	0.00042505111070712	0.00809656108130136	Delta-aminolevulinic acid dehydratase	0
MELO3C010565	0.000429306516313455	0.00815720266161301	No data found	1
MELO3C007254	0.000428996821239314	0.00815720266161301	guanylate-binding protein 2	1
MELO3C026249	0.000429565586514635	0.00815720266161301	E3 ubiquitin-protein ligase RGLG2	1
MELO3C022021	0.00043037785930633	0.00816477650666735	Lysine--trna ligase	1
MELO3C016868	0.00043226379708261	0.00819268496025381	serine/threonine-protein kinase EDR1	1
MELO3C020924	0.000436769436912066	0.00827014344158809	zinc finger protein 830 isoform X1	1
MELO3C022005	0.000438006177052808	0.00828561684924894	Phosphate transporter PHO1-like protein	1
MELO3C025753	0.000438646630847916	0.0082897916867134	elongation factor 1-alpha	0
MELO3C022975	0.000440378076259629	0.00830959014615144	At1g04330	0
MELO3C018718	0.000440535768039929	0.00830959014615144	At2g42760	1
MELO3C005757	0.000442811253232867	0.00834454145047317	Luminal binding heat shock protein 70	1
MELO3C006289	0.000446332049387155	0.00840287096601232	Unknown protein	0
MELO3C020049	0.000448014525992635	0.00842651321317005	Ribosomal protein S5/S7	1
MELO3C007494	0.000451721422672913	0.00848815069112022	Hexosyltransferase	1

MELO3C023370	0.000452977173029057	0.00850365607428787	No data found	1
MELO3C000425	0.000455936542064439	0.00855108335159602	alanine--tRNA ligase-like	1
MELO3C023876	0.000456434521640348	0.00855230110804101	glycerol-3-phosphate acyltransferase 5-like	0
MELO3C016308	0.000457945081585698	0.00857247148458383	myosin-11-like	1
MELO3C009542	0.00046017704841339	0.00859657502875971	BEL1-like homeodomain protein 1	0
MELO3C016542	0.000460538578177516	0.00859657502875971	peptidyl-prolyl cis-trans isomerase CYP37, chloroplastic	1
MELO3C011208	0.000460347156840069	0.00859657502875971	acetylglutamate kinase, chloroplastic	1
MELO3C006160	0.000462267098868541	0.00861871471817833	Histone deacetylase complex subunit SAP18	1
MELO3C020721	0.000462597478417592	0.00861871471817833	triacylglycerol lipase SDP1	1
MELO3C007106	0.000465408661012523	0.00864826228616565	Remorin family protein	1
MELO3C015502	0.000465497129484738	0.00864826228616565	Integral membrane protein	1
MELO3C025336	0.000465391273717142	0.00864826228616565	BnaC03g47530D protein	0
MELO3C009550	0.000471294734155636	0.0087265283090437	33 kDa ribonucleoprotein, chloroplastic	1
MELO3C005109	0.000470509180352852	0.0087265283090437	alpha-mannosidase	1
MELO3C022406	0.000471916705171882	0.0087265283090437	phosphatidylinositol 4-kinase gamma 4	1
MELO3C019873	0.000471726154005148	0.0087265283090437	3-oxoacyl-[acyl-carrier-protein] synthase-like protein	1
MELO3C003825	0.00047191919763323	0.0087265283090437	Cysteine/Histidine-rich C1 domain family protein, putative	1
MELO3C000237	0.000472801986159843	0.00873467392392025	Major facilitator superfamily domain-containing protein 12	1
MELO3C007821	0.000476474174394781	0.00879428828983414	U1 small nuclear ribonucleoprotein 70 kDa	1
MELO3C009490	0.000477551177120339	0.00880593669182967	Ribosomal protein S11	0
MELO3C026433	0.000478847432524576	0.00882160256056703	U4/U6 small nuclear ribonucleoprotein PRP4-like protein	0
MELO3C026780	0.000482363906618488	0.00886692143153668	Ribosomal protein S19	0
MELO3C010512	0.000482211167430746	0.00886692143153668	Plastid transcriptionally active 6	1
MELO3C015867	0.00048265433889827	0.00886692143153668	E3 ubiquitin ligase-like protein	1
MELO3C007421	0.000484638644706603	0.00888684177744727	pyrophosphate--fructose 6-phosphate 1-phosphotransferase subunit beta	1
MELO3C019813	0.000484275792564381	0.00888684177744727	Lysine-specific demethylase REF6	1
MELO3C018368	0.000485361148193419	0.00889183424459354	omega-hydroxypalmitate O-feruloyl transferase	1
MELO3C021408	0.000486240439558361	0.00889968715554965	Protein trichome birefringence-like 10	1
MELO3C007181	0.00048750090623062	0.00891449573810048	MADS box transcription factor AGAMOUS	1
MELO3C013476	0.000489273029856685	0.00893862448347796	phototropin-2	1
MELO3C006813	0.000492228148743612	0.00894906064744133	monocopper oxidase-like protein SKS1	1
MELO3C023222	0.000492403978258671	0.00894906064744133	ABC transporter-like protein	1
MELO3C019735	0.000492040262321525	0.00894906064744133	1-aminocyclopropane-1-carboxylate oxidase	0
MELO3C021759	0.000492563113259847	0.00894906064744133	lecithin-cholesterol acyltransferase-like 4	1
MELO3C011484	0.000491054220355669	0.00894906064744133	Spermidine synthase	1
MELO3C026705	0.000490305274858382	0.00894906064744133	Vesicle-associated membrane protein, putative	0
MELO3C012651	0.00049485375550895	0.00898241435436238	FRIGIDA-like protein	1
MELO3C021368	0.000495830343627213	0.00899187645206044	DnaJ subfamily B member 14	1
MELO3C009670	0.000496738100771443	0.00900007408452774	PHD-finger protein	1
MELO3C020386	0.000500316681290025	0.00902351976145818	E3 ubiquitin-protein ligase LAP	1
MELO3C013938	0.000499419243035093	0.00902351976145818	Protein transport protein Sec16B	0
MELO3C009005	0.000499727849437859	0.00902351976145818	Unknown protein	1
MELO3C005238	0.000499204461091307	0.00902351976145818	GAGA-binding transcriptional activator	1
MELO3C011070	0.000500007962388027	0.00902351976145818	Rhamnogalacturonate lyase	0
MELO3C006420	0.000501794482363316	0.00903935208658677	Cotton fiber protein	1
MELO3C013436	0.000502109941717843	0.00903935208658677	DNA helicase	0
MELO3C012073	0.000503847273066516	0.00906236775572916	SNF1-related kinase regulatory subunit gamma 1	0
MELO3C006280	0.000504505272682865	0.00906236922916473	60S ribosomal protein L37a	1
MELO3C008245	0.000504765109731187	0.00906236922916473	Delta-1-pyrroline-5-carboxylate synthetase	0
MELO3C014007	0.000506074895368025	0.00907763225124716	Superoxide dismutase 1	1
MELO3C026398	0.000506910045428688	0.00908436160360359	APO protein 1, chloroplastic	1
MELO3C023998	0.000507430810900544	0.00908544975927003	Protein RETICULATA-RELATED 4, chloroplastic	0
MELO3C009506	0.000508124357512574	0.00908962675409042	secoisolariciresinol dehydrogenase-like	1
MELO3C003541	0.000510134406861762	0.00911732524987596	NAD(P)H-hydrate epimerase	1
MELO3C019404	0.000510767191047368	0.00912038088245431	phytosulfokine receptor 2	1
MELO3C021846	0.00051267436100022	0.00913791151208787	cytochrome P450 89A2-like	1
MELO3C019688	0.000512648137834137	0.00913791151208787	Peroxisomal and mitochondrial division factor 2	1
MELO3C006430	0.000517174720864766	0.00920981385244208	ethylene-responsive transcription factor 1B	0
MELO3C008866	0.000517893399529346	0.00921430337595049	Plasma-membrane choline transporter family protein	0
MELO3C020562	0.000520045834638383	0.00924427109655574	No data found	1
MELO3C009261	0.000521943976709904	0.0092563001622102	Peptide transporter family protein	1
MELO3C004505	0.000521802144234362	0.0092563001622102	Ribosomal protein L31	1
MELO3C025989	0.000522128633384078	0.0092563001622102	Kinase superfamily protein	1

MELO3C023163	0.000524847951735463	0.00928783351149074	Kinase superfamily protein	1
MELO3C026263	0.000524589257258512	0.00928783351149074	DEAD-box ATP-dependent RNA helicase-like protein	1
MELO3C014273	0.000526136935624533	0.00929398778322799	Pentatricopeptide repeat-containing protein family	1
MELO3C003695	0.00052583296602382	0.00929398778322799	ethylene-responsive transcription factor SHINE 2-like	1
MELO3C022609	0.000527154911452721	0.00930364820936531	No data found	1
MELO3C000279	0.000528395036966334	0.00930889704286184	Late cornified envelope protein 1E	1
MELO3C023830	0.000528124502867655	0.00930889704286184	protein-tyrosine-phosphatase MKP1 isoform X1	1
MELO3C007909	0.000529760023340375	0.00932462629318099	Armadillo repeat only protein	1
MELO3C005720	0.000530338114349549	0.0093264892433564	Late embryogenesis abundant protein	0
MELO3C008491	0.000531797074916351	0.00934382600758276	Zinc finger protein CONSTANS	0
MELO3C016775	0.000532384973778277	0.00934584075301973	Leucine-rich repeat receptor-like protein kinase family	1
MELO3C003292	0.000535229738756193	0.00938743526704801	protein N-methyltransferase NNT1 isoform X1	1
MELO3C015375	0.000536261199456822	0.00939718050405748	Sodium/hydrogen exchanger	1
MELO3C009346	0.000538853443754816	0.00942651619399203	translin	0
MELO3C009994	0.000538889907489848	0.00942651619399203	MD-2-related lipid recognition domain-containing protein / ML domain-containing protein	1
MELO3C007391	0.000540671539647652	0.00944931171371813	Glycosyl transferase, family 31	0
MELO3C002332	0.000541447285320018	0.00945450259751108	Telomere length regulation TEL2	1
MELO3C024016	0.000542761100591038	0.00946907153319118	Metal-dependent phosphohydrolase	1
MELO3C017902	0.000543462838672237	0.00947294580841837	monothiol glutaredoxin-S15, mitochondrial	1
MELO3C006175	0.000544486571854463	0.00947406635026766	ankyrin repeat and zinc finger domain-containing protein 1	1
MELO3C025062	0.000544142102876677	0.00947406635026766	transcription initiation factor TFIID subunit 11-like	0
MELO3C003567	0.000545821213981501	0.00948892883355692	Glycosyltransferase	0
MELO3C011576	0.000546754914670933	0.00949680106406003	zinc finger protein CONSTANS-LIKE 6	1
MELO3C012178	0.000548063155305423	0.00951115927427662	protein PHYLLO, chloroplastic isoform X1	0
MELO3C016015	0.000549275667963922	0.00952383245532879	AAA-type ATPase family protein	1
MELO3C022260	0.000550317736865757	0.00952517527200863	CDPK-related kinase 3 isoform X1	0
MELO3C026636	0.000550273723547212	0.00952517527200863	Protein arginine N-methyltransferase	1
MELO3C008806	0.000551102874571718	0.00953041214528622	Echinoderm microtubule-associated protein-like 6	0
MELO3C023776	0.000553621720863151	0.00955723371094962	Laminin subunit gamma-1	1
MELO3C026221	0.000553304287941092	0.00955723371094962	protein PLASTID TRANSCRIPTIONALLY ACTIVE 10-like	1
MELO3C023047	0.000555357376203602	0.00957882342589078	glutamyl-tRNA(Gln) amidotransferase subunit B, chloroplastic/mitochondrial	1
MELO3C021456	0.000557011378721106	0.00959059958008991	histone deacetylase HDT1-like	1
MELO3C002180	0.000556955335141218	0.00959059958008991	mRNA splicing factor, Cwf18	1
MELO3C015290	0.000557828007353156	0.00959629383032881	peptidyl-prolyl cis-trans isomerase G	1
MELO3C019497	0.000558942859338996	0.00960710402879532	Tubby-like F-box protein	1
MELO3C023291	0.000560242444828107	0.00962106786340025	glycine-rich RNA-binding protein 1-like	1
MELO3C017572	0.00056405672942228	0.00967815495165995	transcription factor TGA1 isoform X1	1
MELO3C006950	0.000566029637463883	0.0097035757901686	Pentatricopeptide repeat-containing protein At4g21190	1
MELO3C014394	0.000567251287668546	0.00971608471827071	Ribosomal N-lysine methyltransferase 5	1
MELO3C005706	0.000567796577401691	0.00971699705988388	40S ribosomal protein S10-1	0
MELO3C027308	0.000574051466060821	0.00981006784135699	alanine--tRNA ligase-like	1
MELO3C021404	0.000574228488764428	0.00981006784135699	Heavy metal-associated isoprenylated plant protein 21	1
MELO3C012284	0.000578777758954763	0.00987924110769024	Zinc finger, B-box	1
MELO3C002714	0.000579702326297893	0.00988647775652598	60S ribosomal protein L18a-like protein	0
MELO3C022359	0.000581911996475948	0.00991559967075366	F3H9.20 protein	1
MELO3C024951	0.000582445935391473	0.00991614205003984	cellulose synthase-like protein E6	1
MELO3C014321	0.000584951558469826	0.00993311120225331	2-methyl-6-phytyl-1,4-hydroquinone methyltransferase, chloroplastic	1
MELO3C017623	0.000584098236359187	0.00993311120225331	Metacaspase-1	1
MELO3C023413	0.000584468800800653	0.00993311120225331	Signal peptidase I	1
MELO3C004105	0.000588504749103658	0.00995066805654806	Cytochrome c oxidase subunit	1
MELO3C013315	0.000587711132197466	0.00995066805654806	O-methyltransferase, putative	1
MELO3C016140	0.000588364468219194	0.00995066805654806	Solanesyl diphosphate synthase, putative	1
MELO3C003017	0.000587375958133851	0.00995066805654806	Alpha/beta-Hydrolases superfamily protein	1
MELO3C025102	0.000587683965674879	0.00995066805654806	Phytoene synthase	1
MELO3C008018	0.000589155695845944	0.0099531529831151	Like-COV protein	1
MELO3C013760	0.000589668535514898	0.0099533024853707	26S proteasome non-ATPase regulatory subunit 4 homolog	1
MELO3C004944	0.000591070098526769	0.00996844011597367	polyadenylation and cleavage factor homolog 4 isoform X2	1
MELO3C024760	0.000592163910059229	0.00997836609194515	RNA polymerase sigma factor sigA	0
MELO3C011805	0.000592819805662836	0.00998090225237456	No data found	0
MELO3C014315	0.000595152627668183	0.00998400707837636	Bifunctional DNA-directed RNA polymerase subunit beta-beta	1
MELO3C013921	0.000595531942798488	0.00998400707837636	Protein-tyrosine phosphatase mitochondrial 1-like protein	1

MELO3C010524	0.000594398368218396	0.00998400707837636	arabinosyltransferase XEG113	1
MELO3C002757	0.000594856562811885	0.00998400707837636	signal recognition particle 14 kDa protein	1
MELO3C018461	0.00059493992894244	0.00998400707837636	E3 ubiquitin-protein ligase MARCH6	1
MELO3C020276	0.000599313743151031	0.0100354207566094	Tobamovirus multiplication 1	1
MELO3C012960	0.000599614992799591	0.0100354207566094	BZIP protein, putative	1
MELO3C011787	0.000601120982774539	0.0100436026132101	No data found	1
MELO3C018462	0.000600683577282934	0.0100436026132101	Polyadenylate-binding protein	0
MELO3C016314	0.00060235623438154	0.0100557339584117	Aldose 1-epimerase, putative	1
MELO3C006412	0.00060289070656494	0.0100561558817154	60S ribosomal protein L14, putative	1
MELO3C007492	0.000606809347387105	0.0101086526857278	elongation of fatty acids protein 3-like	1
MELO3C005899	0.000607220982714818	0.0101086526857278	Protein yippee-like	0
MELO3C025346	0.00060757358539465	0.0101086526857278	Sugar/inositol transporter	1
MELO3C010928	0.000609112966384107	0.0101257339841075	PPPDE putative thiol peptidase family protein	1
MELO3C025449	0.000611945427998251	0.0101642643040685	Zinc finger C3H1 domain-containing protein, putative	1
MELO3C024474	0.000615373567698807	0.0102126156205746	zinc finger protein 593	1
MELO3C005518	0.000616382245133273	0.0102207665483938	3-isopropylmalate dehydratase small subunit 3-like	1
MELO3C010055	0.000619950377860445	0.0102713087352063	4-hydroxy-4-methyl-2-oxoglutarate aldolase	1
MELO3C006418	0.000621568353065705	0.0102808654980692	Ankyrin repeat-containing protein	1
MELO3C011873	0.000621061425400415	0.0102808654980692	60S ribosomal protein L17	0
MELO3C024108	0.000623760788199368	0.0103084952352714	OBERON-like protein	1
MELO3C004100	0.000624466041786231	0.010311521621435	WD-repeat protein, putative	1
MELO3C006875	0.000627322932097107	0.0103500422606397	BAG family molecular chaperone regulator 1-like	1
MELO3C006051	0.000629690258800331	0.0103733540615013	BTB/POZ domain-containing protein POB1	1
MELO3C014161	0.000629786395247356	0.0103733540615013	aspartic proteinase A1-like	1
MELO3C017030	0.000630415357957714	0.0103750607535891	Bromodomain-containing protein	0
MELO3C012411	0.000630978450257835	0.0103756814439151	pumilio homolog 4	1
MELO3C015514	0.000632477107366913	0.0103916725402572	12-oxophytodienoate reductase 3	1
MELO3C017300	0.000634855988458249	0.0104220872120216	AT-rich interactive domain-containing protein 5A, putative	1
MELO3C018406	0.000637480217704711	0.0104564757636631	Cytochrome c biogenesis protein	1
MELO3C006154	0.000639515485286957	0.0104811546215204	Cyclin-D-binding Myb-like transcription factor 1	1
MELO3C013710	0.000641723438790986	0.0104878954442637	Auxin efflux carrier	1
MELO3C015270	0.000642051019905554	0.0104878954442637	single-stranded DNA-binding protein, mitochondrial	0
MELO3C003726	0.000640546691929922	0.0104878954442637	Methyltransferase	1
MELO3C009966	0.000641231456532054	0.0104878954442637	ADP-ribosylation factor-like	1
MELO3C011640	0.00064292610395178	0.0104935104354907	Zinc finger, C6HC-type	1
MELO3C018027	0.000645454282273139	0.0105173899510002	Pyruvate kinase	0
MELO3C007441	0.000645005876675375	0.0105173899510002	RING-type E3 ubiquitin transferase	1
MELO3C013429	0.000649935677337288	0.0105752863095764	kinesin-related protein 11	1
MELO3C002144	0.00065007836243991	0.0105752863095764	Receptor-like kinase 1	1
MELO3C006005	0.000651967117786256	0.0105972828058936	Bifunctional fucokinase/fucose pyrophosphorylase	1
MELO3C011675	0.000653292394574789	0.0106100916944552	Cmp-sialic acid transporter, putative	1
MELO3C015151	0.000654376429938264	0.0106189647615865	Alanine:glyoxylate aminotransferase	1
MELO3C024457	0.000656618608750104	0.010646601727591	ATP-dependent zinc metalloprotease FtsH	1
MELO3C021845	0.000659542009912029	0.0106852298226027	Cytochrome P450	1
MELO3C019630	0.000661812702282605	0.0107132287355567	ribosomal RNA large subunit methyltransferase I	1
MELO3C009148	0.000666792796674809	0.0107850048661186	Methionine aminopeptidase,related	1
MELO3C014722	0.000668654842860272	0.0107902195406569	ethylene-responsive transcription factor RAP2-11	1
MELO3C012452	0.000667682946013937	0.0107902195406569	CSC1-like protein isoform X1	0
MELO3C001971	0.000668754302383112	0.0107902195406569	HVA22-like protein	0
MELO3C007934	0.000669504598248771	0.010793507192502	methyltransferase-like protein 23 isoform X3	1
MELO3C019163	0.000671672363601994	0.0108196227640912	ABC transporter F family-like protein	1
MELO3C009771	0.000672773809379912	0.0108285329759119	Ectonucleotide pyrophosphatase/phosphodiesterase family member 3	1
MELO3C004434	0.000674552868131673	0.0108483262155801	Serine-rich protein-like protein	1
MELO3C007012	0.000677563644158052	0.0108878799092574	DNA polymerase eta	0
MELO3C019820	0.000678838654992631	0.0108994996727231	Glycerol-3-phosphate dehydrogenase	1
MELO3C014297	0.000679949464106544	0.0109084662604713	type I inositol polyphosphate 5-phosphatase 4	1
MELO3C002872	0.000681526249681097	0.0109232372222944	Short-chain dehydrogenase/reductase family protein	1
MELO3C008099	0.00068197637830214	0.0109232372222944	eukaryotic translation initiation factor 2D	1
MELO3C012283	0.000684239705449396	0.0109506077333226	Small ubiquitin-related modifier	1
MELO3C017651	0.000689957443399614	0.0110331737244526	Receptor-like kinase	1
MELO3C017711	0.000692222789745456	0.0110604432643066	Proline--tRNA ligase	1
MELO3C009624	0.000694814321152259	0.0110660387326097	Actin family protein	1
MELO3C008494	0.000693792651051739	0.0110660387326097	E3 ubiquitin-protein ligase	1

MELO3C005367	0.000694218350740128	0.0110660387326097	dehydration-responsive element-binding protein 1D-like	1
MELO3C023990	0.000694276492963164	0.0110660387326097	Methyltransferase	1
MELO3C000881	0.000697534212565021	0.0111004054504002	Unknown protein	0
MELO3C020587	0.000701975152042733	0.0111620831543413	No data found	1
MELO3C007103	0.000705517478176043	0.0111962038589772	Protein plastid transcriptionally active 12	1
MELO3C022868	0.000706077302177532	0.0111962038589772	No data found	1
MELO3C005147	0.000706388678327285	0.0111962038589772	NADPH:QUINONE OXIDOREDUCTASE family protein	1
MELO3C013007	0.000705481661930962	0.0111962038589772	profilin-like	0
MELO3C008775	0.000711395060906339	0.0112574848219866	Elongation factor 4	0
MELO3C018120	0.000710958527238903	0.0112574848219866	Purple acid phosphatase	1
MELO3C025349	0.000711969357716224	0.0112575523182848	subtilisin-like protease SBT6.1	1
MELO3C005942	0.000713428603669519	0.0112716011950955	Kinase family protein	1
MELO3C013779	0.000715958032653785	0.0112844813941577	2-keto-3-deoxy-L-rhamnonate aldolase	1
MELO3C008959	0.000715790240196523	0.0112844813941577	1-acyl-sn-glycerol-3-phosphate acyltransferase	1
MELO3C003078	0.000715397659275085	0.0112844813941577	Protein MODIFIER OF SNC1 11	1
MELO3C017880	0.0007166424359909	0.0112862611390624	Glucan endo-1,3-beta-glucosidase	1
MELO3C007667	0.000719402723322826	0.0113207046875717	Epidermal patterning factor-like protein	0
MELO3C013343	0.000720118690283433	0.0113229490560569	FAD-dependent urate hydroxylase-like	1
MELO3C009128	0.000720765197783857	0.0113240985608858	F-box/LRR-repeat protein 15	0
MELO3C019871	0.00072164473946712	0.0113289045784866	Phytol kinase	1
MELO3C014358	0.000722535218217302	0.0113338745230925	transcription initiation factor TFIID subunit 6-like	1
MELO3C003394	0.000724782540440172	0.011360103485042	Protein LSD1	1
MELO3C012722	0.000725794860899187	0.0113669490149866	Pentatricopeptide repeat-containing family protein	1
MELO3C018052	0.000727486395143639	0.0113844126923072	dynamin-related protein 3A-like	1
MELO3C007899	0.000728120600503868	0.0113853157081163	WD repeat-containing protein 82	1
MELO3C010223	0.000729141268915101	0.0113922554745287	WRKY transcription factor	1
MELO3C019498	0.000730368821527216	0.0113934074694637	Tubby-like F-box protein	0
MELO3C007248	0.000730214662693074	0.0113934074694637	Transcription factor VOZ1	1
MELO3C003418	0.000731189926678533	0.0113972137821423	PLATZ transcription factor family protein	1
MELO3C018487	0.000731828295116532	0.0113981679812748	Lipase	1
MELO3C009133	0.0007353585541372	0.0114437336587229	Receptor-like kinase	1
MELO3C001997	0.000735912792879545	0.0114437336587229	Galactoside 2-alpha-L-fucosyltransferase	1
MELO3C014062	0.000737302663945227	0.0114563259718759	Tir-nbs resistance protein	0
MELO3C004589	0.000738241873302403	0.0114619015376173	Mitochondrial import inner membrane translocase subunit Tim17-like protein	0
MELO3C014459	0.000741853945029902	0.0114728845422048	Serine/threonine phosphatase	1
MELO3C013245	0.000740135031843447	0.0114728845422048	40S ribosomal protein S11-like	1
MELO3C017561	0.000741241733906883	0.0114728845422048	Gras family transcription factor	0
MELO3C015750	0.000739717212356328	0.0114728845422048	No data found	1
MELO3C001996	0.000741526118682501	0.0114728845422048	No data found	1
MELO3C017968	0.000742732357898568	0.0114774814836767	LOW QUALITY PROTEIN: translocase of chloroplast 159, chloroplastic-like	1
MELO3C003678	0.000746920851982136	0.0115331820999181	DNA-directed RNA polymerase subunit beta	0
MELO3C009747	0.000752031580646517	0.0116030247548344	Zinc finger (C3HC4-type RING finger) family protein, putative	1
MELO3C003086	0.000755050317633899	0.0116405064191662	protein GPR107	0
MELO3C002741	0.000764731490141668	0.0117805633376036	Protein TIFY 5A	1
MELO3C021326	0.000766461351612402	0.0117888202749169	Peroxisomal fatty acid beta-oxidation multifunctional protein	0
MELO3C015233	0.000766447720925711	0.0117888202749169	ABC1-like kinase	0
MELO3C015304	0.00076794260535884	0.0118024112943438	60S ribosomal protein L22-2	1
MELO3C014991	0.000770621360316692	0.0118343711080049	MLP-like protein 28	1
MELO3C025645	0.000773924241273871	0.0118566152606867	gamma-glutamyl hydrolase 2-like	0
MELO3C015686	0.000774471299118229	0.0118566152606867	Lectin receptor kinase	0
MELO3C024241	0.00077368783366849	0.0118566152606867	Kinesin-like protein	1
MELO3C013645	0.000774280158386098	0.0118566152606867	Alanine--tRNA ligase	1
MELO3C011793	0.000775832531782594	0.0118682545857277	transcription termination factor MTERF9, chloroplastic-like	1
MELO3C019253	0.000776921270584152	0.0118757106600359	thioredoxin domain-containing protein 9 homolog	1
MELO3C023481	0.000777841519056355	0.011880038253785	nudix hydrolase 3-like	1
MELO3C020808	0.000778407489006927	0.011880038253785	Choline transporter-related family protein	1
MELO3C009250	0.000782324663164635	0.0119187750503673	Laccase	1
MELO3C005971	0.000782531579639922	0.0119187750503673	E3 ubiquitin-protein ligase BRE1-like 1	1
MELO3C002662	0.00078275615172041	0.0119187750503673	Receptor kinase, putative	0
MELO3C023644	0.000784187854190543	0.0119225443154391	subtilisin-like protease SBT3.17	0
MELO3C007281	0.00078421110262572	0.0119225443154391	Transmembrane protein, putative	0
MELO3C016152	0.000786489841811733	0.0119479906814922	Gibberellin 2-oxidase	1

MELO3C016884	0.000792002683039694	0.0120040375958181	Methyltransferase	1
MELO3C007328	0.000791713477300116	0.0120040375958181	Wound-responsive family protein	1
MELO3C025585	0.000791107901455534	0.0120040375958181	bifunctional nitrilase/nitrile hydratase NIT4A	1
MELO3C023114	0.000793652645098342	0.0120106539547994	Cellulose synthase	1
MELO3C021548	0.000793655547673966	0.0120106539547994	BnaC05g50840D protein	0
MELO3C021170	0.00079612896994774	0.0120388598985436	BTB/POZ domain-containing protein POB1	0
MELO3C015844	0.000797345327828602	0.012048028216746	DNA repair helicase	0
MELO3C025549	0.000799268560659261	0.0120678553550915	vesicle-fusing ATPase	1
MELO3C011847	0.000801855921626515	0.0120792163205203	60S ribosomal protein L5	1
MELO3C024982	0.000801587460503073	0.0120792163205203	Farnesyl diphosphate synthase	1
MELO3C013076	0.000801616547371209	0.0120792163205203	casein kinase I	1
MELO3C013761	0.000803412442861307	0.0120892909496463	MLO-like protein	0
MELO3C007931	0.000803749000804377	0.0120892909496463	Protein preY, mitochondrial, putative	1
MELO3C021620	0.000804655961069711	0.0120937218989085	transcription initiation factor TFIID subunit 7	1
MELO3C012670	0.000806556187156526	0.0120946682916889	Ribosomal protein S5/S7	1
MELO3C026224	0.000806198958957616	0.0120946682916889	Aspartyl aminopeptidase family protein	0
MELO3C009797	0.000806319229198271	0.0120946682916889	HSP20-like chaperones superfamily protein	1
MELO3C023412	0.000810590269652245	0.0121374241605471	O-fucosyltransferase family protein	1
MELO3C019815	0.000810636612879723	0.0121374241605471	Receptor-like protein kinase	1
MELO3C011018	0.000812005118265402	0.0121487038489571	Thaumatin-like protein 1	0
MELO3C012730	0.00081283392472975	0.0121518979405661	Structural maintenance of chromosomes protein	1
MELO3C016522	0.000815966088231534	0.0121714739300738	Unknown protein	0
MELO3C005332	0.000815992277250377	0.0121714739300738	CDP-diacylglycerol--serine O-phosphatidyltransferase 1	1
MELO3C002819	0.000815110446897416	0.0121714739300738	eukaryotic translation initiation factor 3 subunit A-like	1
MELO3C006925	0.000817431595872442	0.0121837408202905	mitogen-activated protein kinase kinase kinase YODA-like	1
MELO3C017131	0.000818103995706476	0.0121845669767777	General negative regulator of transcription subunit 4	1
MELO3C007143	0.000819606583127408	0.0121977471063928	NAD(P)-binding domain-containing protein	0
MELO3C024558	0.000823867542946388	0.0122519277903978	sorting nexin 1	1
MELO3C005650	0.000828101492612809	0.0123056255662983	Dead box ATP-dependent RNA helicase, putative	1
MELO3C019948	0.000830095547025289	0.0123259826753402	Oxidoreductase family protein	1
MELO3C007495	0.000833697338175732	0.0123668718316225	protein LYK5-like	1
MELO3C005360	0.000834453426250992	0.0123668718316225	mediator of RNA polymerase II transcription subunit 36a-like	1
MELO3C013541	0.000834727841994676	0.0123668718316225	No data found	1
MELO3C018010	0.0008354022801359	0.012367585929838	At3g19650	0
MELO3C009687	0.000836070000848177	0.012368199585581	No data found	1
MELO3C003222	0.000839084099028331	0.012403496909963	mRNA-capping enzyme	1
MELO3C001947	0.000841859856859473	0.0124352208774254	eukaryotic translation initiation factor 3 subunit G-like	0
MELO3C025499	0.00084299621236239	0.0124426996995103	Gb|AAD43168.1	0
MELO3C006241	0.000846579502224443	0.0124676350405895	protein NRT1/ PTR FAMILY 7.3-like	1
MELO3C013173	0.000846446048688998	0.0124676350405895	NAC domain-containing protein 17-like	1
MELO3C017320	0.000846271674169286	0.0124676350405895	Zinc finger protein, putative	1
MELO3C003945	0.00085012626266634	0.0124919222927065	Protein trichome birefringence	1
MELO3C022639	0.000849764070270709	0.0124919222927065	No data found	1
MELO3C016408	0.000849878202600962	0.0124919222927065	D-2-hydroxyglutarate dehydrogenase, mitochondrial-like	0
MELO3C015796	0.000854500203095521	0.0125375367837544	Acetyl-CoA carboxylase, putative	1
MELO3C018591	0.00085408519847574	0.0125375367837544	Transcription factor, putative	1
MELO3C013338	0.000857578253785185	0.0125439869644173	RNA-binding protein 39 isoform X1	1
MELO3C024287	0.000858057790619982	0.0125439869644173	GATA transcription factor 24-like	0
MELO3C022319	0.000857819419544437	0.0125439869644173	DNA primase large subunit	0
MELO3C020710	0.000855996771340739	0.0125439869644173	THO complex subunit 4A	0
MELO3C011139	0.000858115671118931	0.0125439869644173	Nuclear pore complex protein NUP85	1
MELO3C013139	0.000862543291056284	0.0125993842123303	prohibitin-1, mitochondrial	1
MELO3C003439	0.000864308651512991	0.0126158400286253	NAD(P)-binding rossmann-fold protein	0
MELO3C013707	0.000869260816383277	0.0126787532221221	Thioredoxin reductase	0
MELO3C026026	0.000872361768709862	0.0127145923027683	PRA1 family protein	1
MELO3C014888	0.000874915018815425	0.012742401701022	yrdC domain-containing protein, mitochondrial isoform X2	1
MELO3C026198	0.000877911808357279	0.0127766251313544	Gamma carbonic anhydrase-like 1, mitochondrial	1
MELO3C002816	0.000879193317881222	0.0127858533393492	obg-like ATPase 1	1
MELO3C011944	0.000880749748052967	0.0127990631157454	Beta-1,4-mannosyl-glycoprotein 4-beta-N-acetylglucosaminyltransferase	1
MELO3C016558	0.000881863372467206	0.0128058233403345	Cyclic nucleotide-gated ion channel, putative	1
MELO3C006320	0.000883864838401527	0.0128254567917647	Type 1 membrane protein, putative isoform 1	1
MELO3C015098	0.000890296667866552	0.012909301684065	Tubulin beta chain	1
MELO3C018689	0.000892082156492835	0.0129257010334387	nuclear transcription factor Y subunit C-2	0

MELO3C010693	0.000893079815306175	0.0129306695546053	Lysine ketoglutarate reductase trans-splicing protein (DUF707)	1
MELO3C010903	0.00089679269942633	0.0129749150336781	thylakoidal processing peptidase 1, chloroplastic-like	0
MELO3C012634	0.000897600518375397	0.0129755749429774	Receptor-like protein kinase	1
MELO3C020806	0.000898152359463777	0.0129755749429774	Peptidyl-prolyl cis-trans isomerase	1
MELO3C013437	0.000905985501302276	0.0129920969393496	V-type proton ATPase subunit a	1
MELO3C007398	0.000902959644092149	0.0129920969393496	5'-adenylylsulfate reductase	1
MELO3C007472	0.000905497264532817	0.0129920969393496	LRR receptor-like serine/threonine-protein kinase GSO1 isoform X1	1
MELO3C003057	0.00090625881451678	0.0129920969393496	Phosphatidylinositol-4-phosphate 5-kinase, putative	1
MELO3C016033	0.000904166343776214	0.0129920969393496	glutathione S-transferase-like	1
MELO3C024333	0.000905840775861422	0.0129920969393496	DNA-binding protein, putative	1
MELO3C025720	0.00090037014311295	0.0129920969393496	phototropin-1	0
MELO3C015198	0.000903708398408365	0.0129920969393496	Pentatricopeptide repeat-containing protein	1
MELO3C010183	0.000904336723108301	0.0129920969393496	glycine-rich cell wall structural protein 2-like	0
MELO3C017091	0.000906532461513176	0.0129920969393496	Pleckstrin homology domain-containing family M member 3	1
MELO3C003312	0.000901569386704937	0.0129920969393496	Protein kinase superfamily protein	1
MELO3C013403	0.000911652577039623	0.0130465411188083	auxin-responsive protein SAUR36-like	1
MELO3C026102	0.000911617325186298	0.0130465411188083	Rhodanese-like domain-containing protein 6	1
MELO3C003139	0.000913198703413887	0.013059204340131	ATP-dependent zinc metalloprotease FtsH	0
MELO3C014849	0.000914437911399668	0.0130674633228886	Alpha/beta hydrolase-3	1
MELO3C020172	0.000915802238327545	0.0130774970388508	Hydroxyacylglutathione hydrolase	0
MELO3C014258	0.000917959386003142	0.0130968989268235	IQ-domain 1	1
MELO3C004142	0.000918487265869183	0.0130968989268235	Unknown protein	1
MELO3C007144	0.000921378557700914	0.0131286472842968	DNA helicase	0
MELO3C019858	0.000923438376700947	0.0131485108157657	No data found	1
MELO3C018046	0.000926412561525591	0.0131718658585809	Zinc transport ZntB	0
MELO3C021858	0.000925765305583526	0.0131718658585809	WEB family protein At3g02930, chloroplastic	1
MELO3C025347	0.000928175455473412	0.0131874367411111	Short-chain dehydrogenase/reductase	0
MELO3C009770	0.000931788216151919	0.0132197453166553	two-component response regulator ORR9-like	0
MELO3C005244	0.000931247853704242	0.0132197453166553	ABC transporter F family member 3	1
MELO3C002159	0.000933740659770033	0.013237935599281	Nascent polypeptide-associated complex subunit beta	1
MELO3C015926	0.000935266432297022	0.0132500550727646	DNA helicase	0
MELO3C008149	0.000936996534496304	0.0132650498636326	LEAF RUST 10 DISEASE-RESISTANCE LOCUS RECEPTOR-LIKE PROTEIN KINASE-like 1.4 isoform X1	1
MELO3C017347	0.000938758613047153	0.0132804755365818	Actin-interacting protein 1-2	1
MELO3C007917	0.000939995495577994	0.013286163190543	thiosulfate sulfurtransferase 18 isoform X1	0
MELO3C025885	0.000940506159318399	0.013286163190543	ras-related protein Rab11C	1
MELO3C004539	0.000946307413841607	0.0133322132934015	serine/threonine protein phosphatase 2A 57 kDa regulatory subunit B' iota isoform-like	0
MELO3C006569	0.000945446689776475	0.0133322132934015	Cytochrome P450 family protein	1
MELO3C013757	0.000947021349863686	0.0133322132934015	Proteasome subunit alpha type	1
MELO3C017581	0.000945962882874185	0.0133322132934015	inositol-3-phosphate synthase	1
MELO3C005046	0.000947141386938188	0.0133322132934015	protein indeterminate-domain 2	0
MELO3C024673	0.000950133026605071	0.0133647985344897	Trihelix transcription factor	1
MELO3C001994	0.000950855162021425	0.0133654367222499	thioredoxin-like 1-2, chloroplastic	1
MELO3C016464	0.00095330453726683	0.0133903352108696	No data found	1
MELO3C007646	0.000954499819987076	0.0133975955543175	heptahelical transmembrane protein 4-like	0
MELO3C020749	0.000958357604638915	0.0134231236411446	amidophosphoribosyltransferase, chloroplastic-like	1
MELO3C002897	0.000957057417631413	0.0134231236411446	Nuclear receptor corepressor 1	1
MELO3C012906	0.000957862608659155	0.0134231236411446	CDT1-like protein a, chloroplastic	1
MELO3C004480	0.000959813634533235	0.0134339897012026	No data found	1
MELO3C011759	0.000962693217067989	0.0134501480567726	transcription factor DIVARICATA	1
MELO3C026443	0.000961972935031419	0.0134501480567726	No data found	1
MELO3C002092	0.000963011258913182	0.0134501480567726	Receptor-like kinase	1
MELO3C020835	0.000965408283639557	0.0134740976633199	Unknown protein	1
MELO3C005939	0.000969123816900619	0.0135164027259677	nucleoside diphosphate kinase	1
MELO3C027064	0.000971938273088613	0.0135460895943733	Pentatricopeptide repeat-containing protein	1
MELO3C008088	0.000973514744218917	0.0135584927246681	phospholipase SGR2	1
MELO3C003880	0.000975348030759493	0.0135744526141432	Histone deacetylase complex subunit	1
MELO3C012016	0.00097897348711995	0.0136153150684027	MLP-like protein 423	0
MELO3C016915	0.000983430844025079	0.0136484720580824	copper-transporting ATPase PAA2, chloroplastic isoform X1	1
MELO3C007613	0.000983096242711756	0.0136484720580824	acyl-CoA-binding domain-containing protein 3	1
MELO3C017416	0.000982464041033859	0.0136484720580824	Cyclin-dependent protein kinase inhibitor SMR15	1

			Mitochondrial import inner membrane translocase subunit	
MELO3C005915	0.000986201687010468	0.0136581326204556	Tim17/Tim22/Tim23 family protein	0
MELO3C025944	0.000985917354598187	0.0136581326204556	ABC1 family protein	0
MELO3C010599	0.000985933718972154	0.0136581326204556	Gamma-glutamylcyclotransferase	1
MELO3C016811	0.000987087449194402	0.0136608199258166	Ubiquitin system component Cue	0
MELO3C012695	0.000991906014960131	0.0137178934800053	la-related protein 6B isoform X1	1
MELO3C005439	0.000993351291647127	0.0137282677807831	NO-associated protein 1, chloroplastic/mitochondrial	1
MELO3C009735	0.000998956915092108	0.0137301972062592	NF-kappa-B-activating protein	1
MELO3C009562	0.00100183372192109	0.0137301972062592	Pentatricopeptide repeat-containing protein	1
MELO3C013175	0.00100051618365293	0.0137301972062592	Pentatricopeptide repeat-containing family protein	1
MELO3C014176	0.000996507629712262	0.0137301972062592	30S ribosomal protein S6	1
MELO3C016139	0.00099980979828429	0.0137301972062592	Mitogen-activated protein kinase	1
MELO3C017878	0.00100181581724934	0.0137301972062592	Protein LURP-one-related 17	1
MELO3C018042	0.000996419011577765	0.0137301972062592	Phosphoglycerate mutase-like protein 1	1
MELO3C015770	0.000999619597627954	0.0137301972062592	phospholipase A1-Igamma1, chloroplastic-like isoform X1	0
MELO3C017467	0.000996740137645613	0.0137301972062592	Syntaxin/T-SNARE family protein	1
MELO3C010964	0.000998038684778546	0.0137301972062592	Cyclin-T1-like protein	1
MELO3C012873	0.000995473042618045	0.0137301972062592	NAC domain protein	1
MELO3C009961	0.000997510371846033	0.0137301972062592	At1g23710	1
MELO3C003951	0.00100473081766883	0.0137603529252023	No data found	0
MELO3C007467	0.00100905049094524	0.0138099363448909	No data found	0
MELO3C015523	0.00101538983608185	0.0138870733191	Cysteine protease	1
MELO3C007316	0.00101829843398527	0.0139089177661161	Transmembrane protein, putative	0
MELO3C010601	0.00101839561951511	0.0139089177661161	LysM domain-containing GPI-anchored protein 1	1
MELO3C025590	0.00102358772268074	0.0139605206734958	NF-kappa-B inhibitor-like protein 2 isoform 2	1
MELO3C010273	0.0010234211073139	0.0139605206734958	Transmembrane protein	1
MELO3C015727	0.00102505641861605	0.0139628570857366	Maternal effect embryo arrest 60	1
MELO3C001962	0.00102517306062677	0.0139628570857366	protein REVEILLE 2-like	1
MELO3C013125	0.00103621741953086	0.0140667073781726	Lipid-binding serum glycoprotein family protein, putative	1
MELO3C007127	0.00103536298460694	0.0140667073781726	9-cis-epoxycarotenoid dioxygenase	1
MELO3C005201	0.00103600206925747	0.0140667073781726	multicopper oxidase LPR1-like	1
MELO3C001943	0.00103568118847042	0.0140667073781726	17. class I heat shock protein	0
MELO3C010755	0.00103635927060819	0.0140667073781726	At5g11810	1
MELO3C009038	0.00103983524063711	0.0140953069960971	adenylosuccinate synthetase, chloroplastic	1
MELO3C024239	0.0010406075041931	0.0140953069960971	Mitochondrial carrier protein	0
MELO3C018758	0.00104031520097592	0.0140953069960971	Secretory carrier-associated membrane protein	1
MELO3C010959	0.00104181627537914	0.014102007966047	Adenosine kinase, putative	0
MELO3C002016	0.00104357250065368	0.0141161050105544	zinc finger protein ZAT4-like	1
MELO3C004597	0.0010513769558067	0.0142119394252064	DUF1005 family protein (DUF1005)	1
MELO3C014116	0.0010524633137019	0.0142168932847461	poly(A)-specific ribonuclease PARN	0
MELO3C007647	0.0010600013683566	0.0142852160059244	xyloglucan 6-xylosyltransferase 1	1
MELO3C021598	0.0010608705730426	0.0142852160059244	pre-rRNA-processing protein ESF2	0
MELO3C005286	0.00106186121305873	0.0142852160059244	Mediator of RNA polymerase II transcription subunit 23	1
MELO3C021366	0.00106142095838846	0.0142852160059244	Acyl carrier protein	1
MELO3C010052	0.00106101733938158	0.0142852160059244	Basic leucine zipper/W2 domain protein	1
MELO3C011488	0.00106087293661083	0.0142852160059244	ylmG homolog protein 2, chloroplastic	1
MELO3C010821	0.00106381826751312	0.0143018018823121	Glutamyl-tRNA (Gln) amidotransferase subunit A	0
MELO3C013824	0.00106573213139216	0.0143080515723071	inactive poly [ADP-ribose] polymerase RCD1-like	0
MELO3C005300	0.0010652510900182	0.0143080515723071	BnaC07g20870D protein	0
MELO3C000254	0.00107265318236205	0.014391187295155	Auxin response factor	0
MELO3C013964	0.00107467152470697	0.0144084778964277	Flavin-containing monooxygenase	0
MELO3C019125	0.00107877740647	0.0144537143828874	WAT1-related protein At5g07050-like	0
MELO3C013406	0.00108795323877697	0.0145667718729535	tRNA-dihydrouridine(47) synthase [NAD(P)(+)]	1
MELO3C017833	0.00109169981020196	0.0145872662731249	Golgi SNAP receptor complex member 1-1	1
MELO3C002134	0.00109141215498465	0.0145872662731249	protection of telomeres protein 1a-like isoform X1	0
MELO3C018732	0.00109122951858942	0.0145872662731249	Histone-lysine N-methyltransferase, H3 lysine-36 specific	1
MELO3C002171	0.00109283685930461	0.0145925862977734	LOW QUALITY PROTEIN: probable metal-nicotianamine transporter YSL5	1
MELO3C008124	0.0010950939938712	0.0146128454628124	SNARE associated Golgi protein family	0
MELO3C020616	0.00110160610411703	0.0146898169819089	Haloacid dehalogenase-like hydrolase	0
MELO3C009334	0.00111024230362466	0.0147850136576423	Methyltransferase type 11	1
MELO3C016951	0.00110990724649795	0.0147850136576423	Glutathione peroxidase	1
MELO3C019907	0.00111354912043438	0.0148190576680987	40S ribosomal protein S17	1
MELO3C013702	0.00111548535806738	0.0148269770804629	kinesin-like calmodulin-binding protein	1

MELO3C021370	0.00111564575125667	0.0148269770804629	PAX-interacting protein 1	1
MELO3C004713	0.00111704118586142	0.0148355389237238	Ribosomal protein	0
MELO3C020825	0.00111940322596316	0.0148569182187812	Phospholipase-like protein	1
MELO3C012628	0.00112110321793302	0.0148595083563484	BOI-related E3 ubiquitin-protein ligase 1-like	1
MELO3C019140	0.00112109638180102	0.0148595083563484	Nascent polypeptide-associated complex subunit alpha-like protein	0
MELO3C009380	0.00112906693300263	0.0149353473849775	ras-related protein RABC2a	1
MELO3C013859	0.00112932514486075	0.0149353473849775	CAAX amino terminal protease	1
MELO3C006995	0.00112951941137085	0.0149353473849775	DNA helicase	0
MELO3C007743	0.00112985006801136	0.0149353473849775	Polyadenylate-binding 2	1
MELO3C008318	0.00113812614307651	0.0150346844144602	Dehydration-responsive element-binding protein 2C	1
MELO3C008052	0.00114026869495676	0.0150529187544793	No data found	1
MELO3C023492	0.00114758708393703	0.0151394103678506	Receptor kinase	1
MELO3C020963	0.00114885976832013	0.0151460824863513	WRKY family transcription factor	1
MELO3C008233	0.00115122999267281	0.0151672055538995	Thylakoid lumenal 15 kDa protein 1, chloroplastic	1
MELO3C024505	0.00115519001740017	0.0152092317690906	SRSF protein kinase 1-like	1
MELO3C022000	0.00115848232083415	0.0152424166250191	KH domain-containing protein	1
MELO3C025511	0.00116227454348072	0.0152506151645319	elongation factor 1-alpha-like	0
MELO3C005511	0.00116090537302926	0.0152506151645319	palmitoyl-protein thioesterase 1-like	1
MELO3C023317	0.00116296655211834	0.0152506151645319	phosphatidylinositol/phosphatidylcholine transfer protein SFH8-like	1
MELO3C003305	0.00116254711149832	0.0152506151645319	Protein CDI	1
MELO3C003420	0.0011601994899415	0.0152506151645319	Ring finger protein, putative	0
MELO3C018616	0.0011655704891641	0.0152746195026555	Alkyl transferase	1
MELO3C010482	0.00117143822600851	0.0153396734280064	F-box protein 7	1
MELO3C017259	0.0011720880653634	0.0153396734280064	Protoheme IX farnesyltransferase, mitochondrial	1
MELO3C024554	0.00117317342071144	0.0153437098580332	Chaperone dnaJ-like protein	0
MELO3C004437	0.0011762151255299	0.0153529891038268	Methyltransferase-related family protein	1
MELO3C018981	0.00117475910333109	0.0153529891038268	UNC93-like protein	0
MELO3C026230	0.00117574360508321	0.0153529891038268	Ribonuclease J	0
MELO3C023200	0.00117863846732424	0.015374459109106	Receptor-like protein kinase	1
MELO3C017757	0.00118580073769048	0.0154474793988452	Inositol transporter 1	1
MELO3C010651	0.00118541624822299	0.0154474793988452	No data found	1
MELO3C016562	0.00118807502290619	0.0154669041709784	At4g33560	1
MELO3C006802	0.00118904758520466	0.0154693680897278	Protein DEHYDRATION-INDUCED 19	1
MELO3C025917	0.00119861897500195	0.0155836248435244	CAX-interacting protein 4	1
MELO3C009101	0.00120197975122283	0.0156170382282234	B3 domain-containing transcription repressor VAL2	1
MELO3C018950	0.00120877376552109	0.015694985598472	Chaperone protein DNAj, putative	1
MELO3C011752	0.00121308127110931	0.0157405663752547	E3 ubiquitin ligase BIG BROTHER-related	1
MELO3C026886	0.00121509032211076	0.0157562828439694	Chaperone DnaJ	0
MELO3C002651	0.00121668506400485	0.0157666097959526	protein SCAR3	1
MELO3C022930	0.0012198997375259	0.0157772101613615	mitotic spindle checkpoint protein MAD1	1
MELO3C002363	0.00121933620530013	0.0157772101613615	TITAN-like protein	1
MELO3C017254	0.00121947301870651	0.0157772101613615	Sterile alpha motif domain-containing family protein	1
MELO3C014732	0.00122174468221292	0.0157907301891512	Pyruvate kinase	1
MELO3C006268	0.00122376359873888	0.015796148569604	10 kDa chaperonin isoform X1	1
MELO3C007914	0.00122356487409925	0.015796148569604	calmodulin-lysine N-methyltransferase isoform X1	0
MELO3C017945	0.00122821280365626	0.015832881631467	bifunctional epoxide hydrolase 2-like	1
MELO3C018617	0.00122760195676008	0.015832881631467	Pentatricopeptide repeat-containing protein	1
MELO3C023725	0.00123619916806539	0.0158993585323115	Protein ROOT PRIMORDIUM DEFECTIVE 1	1
MELO3C007724	0.00123610608361802	0.0158993585323115	Pesticidal crystal cry8Ba protein	0
MELO3C007986	0.00123446337349731	0.0158993585323115	Histidine phosphatase family (Branch 1) protein	1
MELO3C010353	0.00123739501059106	0.0158993585323115	protein NRT1/ PTR FAMILY 6.2-like	1
MELO3C003675	0.00123674154707298	0.0158993585323115	Protein TIFY 8	0
MELO3C003249	0.00124444883017238	0.0159795968446518	target of Myb protein 1 isoform X1	1
MELO3C024088	0.00124664245485939	0.0159973631195699	F-box family protein, putative	1
MELO3C014877	0.00124810334608227	0.0160057097284278	DNA/RNA-binding protein KIN17	1
MELO3C013822	0.0012520996871519	0.0160361327636594	Unknown protein	1
MELO3C025637	0.00125177019058254	0.0160361327636594	Mannosyltransferase	1
MELO3C022009	0.00125751310639199	0.0160950267907553	Vesicle transport v-SNARE family protein	0
MELO3C010375	0.00126258066098428	0.0161389679441932	DNA ligase	0
MELO3C026013	0.00126215947958241	0.0161389679441932	Plectin-like protein	0
MELO3C012713	0.00126675355311634	0.016174344703256	Zinc finger, CCCH-type	1
MELO3C008252	0.00126698624011023	0.016174344703256	Protease inhibitor/seed storage/lipid transfer family protein	0
MELO3C014398	0.00127170983656311	0.0162085217333131	Myosin-binding protein 1	0

MELO3C019504	0.00127161606417181	0.0162085217333131	Meiosis arrest female protein 1-like protein	1
MELO3C002271	0.00127212561074663	0.0162085217333131	F-box protein SKIP16	1
MELO3C008801	0.00127339795929893	0.0162142722747869	H/ACA ribonucleoprotein complex subunit	1
MELO3C002687	0.00127622712446374	0.0162398256965427	dynamin-related protein 4C-like	1
MELO3C012470	0.00127972386650055	0.0162738355695553	two-component response regulator ORR9-like	1
MELO3C007690	0.00128234955404771	0.0162967318808805	No data found	1
MELO3C015518	0.00128401665288447	0.0163074243587237	Acyl-CoA N-acyltransferase (NAT) superfamily protein	1
MELO3C016882	0.00128643995485178	0.0163277009436811	Magnesium transporter NIPA	0
MELO3C023961	0.00128738672658923	0.0163292231621135	ras-related protein RABA4c isoform X1	0
MELO3C011040	0.00129103487176252	0.0163649856755058	40S ribosomal protein S6-like	0
MELO3C023304	0.00129224801413341	0.0163698563381147	Isoflavone reductase like	1
MELO3C006507	0.00129529568976838	0.0163979452418178	40S ribosomal protein S3a	0
MELO3C015862	0.00129679606732103	0.0164064225070615	Unknown protein	1
MELO3C011193	0.00130134505932378	0.0164534337878267	COP9 signalosome complex subunit 5b	1
MELO3C014190	0.00130600334466013	0.0165017658692853	DUF4408 domain protein	0
MELO3C016890	0.00131018435614794	0.0165440094946072	aminopeptidase M1	1
MELO3C017808	0.00131120432915433	0.0165463094546126	Protein NEOXANTHIN-DEFICIENT 1	1
MELO3C018360	0.00131240394258225	0.0165508719425651	No data found	1
MELO3C016300	0.00132248461135576	0.0166461877352294	UDP-glucose 4-epimerase family protein	0
MELO3C012715	0.00132243173147539	0.0166461877352294	mediator of RNA polymerase II transcription subunit 19a-like	0
MELO3C005294	0.00132249068593726	0.0166461877352294	Myosin-binding protein 2	0
MELO3C021556	0.00132370263701453	0.0166508301773249	ADP-ribosylation factor-like	0
MELO3C006249	0.00132556843054021	0.0166636861456007	No data found	1
MELO3C009467	0.001327686515185	0.0166786633326799	Alpha/beta-Hydrolases superfamily protein	1
MELO3C016114	0.00132956872636503	0.0166786633326799	Protein ROOT INITIATION DEFECTIVE 3	1
MELO3C012296	0.00133013796895898	0.0166786633326799	Unknown protein	0
MELO3C026175	0.00132851382917032	0.0166786633326799	Long chain base biosynthesis protein	1
MELO3C002646	0.00133518613930561	0.0167313395083417	Transcription initiation factor IIB	1
MELO3C011088	0.00133656832394879	0.0167380392071431	mechanosensitive ion channel protein 3, chloroplastic-like	1
MELO3C004475	0.00133894602167994	0.016746576936135	arogenate dehydrogenase 1, chloroplastic-like	1
MELO3C012100	0.00133814393390308	0.016746576936135	ribonuclease 3-like	1
MELO3C015409	0.00134065781250059	0.0167467749140254	ABC transporter B family protein	0
MELO3C018106	0.0013404763400835	0.0167467749140254	ABC transporter B family protein	1
MELO3C014018	0.00134463174948718	0.0167857979902796	Pentatricopeptide repeat-containing protein family	1
MELO3C003846	0.00135074087660314	0.0168514097106983	Glucan endo-1,3-beta-glucosidase, putative	0
MELO3C020978	0.00135752330090511	0.0169253331247317	Adenylyl cyclase-associated protein	1
MELO3C011952	0.00136365991062004	0.0169911164510001	UDP-galactose:fucoside alpha-3-galactosyltransferase	1
MELO3C009873	0.00136459747634987	0.0169920779069569	zinc-finger homeodomain protein 9-like	0
MELO3C004461	0.00136807981374421	0.017024705886348	protein TOPLESS	1
MELO3C015398	0.00136911537600959	0.017026863703283	cysteine synthase-like	0
MELO3C018573	0.00137461012268614	0.017084440096242	Inorganic pyrophosphatase	1
MELO3C009172	0.00137678127435881	0.0171006625077434	RING finger protein	1
MELO3C016608	0.00137878915949885	0.0171148379075693	Transmembrane protein, putative	1
MELO3C003926	0.00138073092069713	0.0171179590713092	No data found	0
MELO3C005199	0.00138077415568361	0.0171179590713092	charged multivesicular body protein 7 isoform X1	1
MELO3C008375	0.00138251768956899	0.0171288217385809	Unknown protein	0
MELO3C008114	0.00138405655359919	0.017137136600019	TSA: Wollemia nobilis Ref_Wollemi_Transcript_28887_1569 transcribed RNA sequence	1
MELO3C017272	0.00138518236716068	0.0171403299304863	Ethylene-responsive transcription factor	0
MELO3C019561	0.00138619118409045	0.0171420724449607	At1g78995	1
MELO3C006587	0.0013871485080218	0.0171431763985747	Endonuclease/exonuclease/phosphatase family protein	0
MELO3C006136	0.00139306498415936	0.0171625953662903	Signal recognition particle 54 kDa protein	1
MELO3C019011	0.00139215182628716	0.0171625953662903	copper-transporting ATPase PAA1, chloroplastic isoform X1	1
MELO3C005696	0.00139171797478665	0.0171625953662903	E3 ubiquitin-protein ligase RHA1B	1
MELO3C021247	0.0013904593458578	0.0171625953662903	Dihydrolipoyl dehydrogenase	1
MELO3C018688	0.00139270363874489	0.0171625953662903	dynamin-like protein ARC5	1
MELO3C006754	0.0013989936942238	0.0171921631272379	SWI/SNF-related matrix-associated actin-dependent regulator of chromatin subfamily A-like protein 1	1
MELO3C027346	0.00139863809916196	0.0171921631272379	Indole-3-acetic acid-amido synthetase GH3.3	0
MELO3C015791	0.0013969561102013	0.0171921631272379	Pentatricopeptide repeat-containing protein	1
MELO3C022388	0.00139981762664432	0.0171921631272379	Pre-mRNA-processing factor 39	1
MELO3C026711	0.00139804378035702	0.0171921631272379	Protein FAM32A-like	1

MELO3C016623	0.00140078931774978	0.0171934047459543	NAD(P)H dehydrogenase (Quinone)	1
MELO3C016965	0.00140646424613533	0.0172416278069067	Formin-like protein	0
MELO3C015422	0.00140579592416201	0.0172416278069067	Arginine--tRNA ligase	1
MELO3C021047	0.00140828800908288	0.0172532753668597	nucleolin-like	1
MELO3C009663	0.00141290977451258	0.0172561584703465	1-acyl-sn-glycerol-3-phosphate acyltransferase-like protein	1
MELO3C004467	0.00141258546588374	0.0172561584703465	Exostosin family protein	1
MELO3C013359	0.00141108727208694	0.0172561584703465	Ubiquitin-conjugating enzyme, E2	1
MELO3C005079	0.00141241328020525	0.0172561584703465	protein ASPARTIC PROTEASE IN GUARD CELL 2	1
MELO3C021384	0.00141376598334197	0.0172561584703465	Cox19-like CHCH family protein	1
MELO3C026760	0.00141223060883444	0.0172561584703465	Arabinogalactan protein	1
MELO3C017133	0.00141800169024686	0.0172971682400774	No data found	0
MELO3C020927	0.00141984372965775	0.0173089468006241	Molybdenum cofactor sulfurase	1
MELO3C014895	0.00142136942562132	0.0173168567468202	squamosa promoter-binding-like protein 13A	1
MELO3C017703	0.00142356391852405	0.0173305233976508	disease resistance protein RGA2-like	1
MELO3C008096	0.00142424626433679	0.0173305233976508	Galactose-binding domain-like protein	0
MELO3C016382	0.00142850587618693	0.0173645781687618	small nuclear ribonucleoprotein Sm D2-like	1
MELO3C022448	0.00142880345963026	0.0173645781687618	Metal tolerance protein	1
MELO3C019524	0.0014304129339574	0.017373447129597	40S ribosomal protein S16	0
MELO3C023309	0.00143156903792496	0.0173768020466995	SNF1-related protein kinase regulatory subunit gamma-1-like	1
MELO3C011834	0.00143661881258605	0.0174273863204926	Protein EI24 like	0
MELO3C025593	0.00144052700680608	0.0174509693332693	Pentatricopeptide repeat-containing family protein	1
MELO3C013587	0.00144121378209339	0.0174509693332693	No data found	1
MELO3C003416	0.00144044124356046	0.0174509693332693	Unknown protein	1
MELO3C016383	0.00144678432164969	0.0175025482951149	RING-type E3 ubiquitin transferase	1
MELO3C017844	0.00144724600566726	0.0175025482951149	calcineurin subunit B	1
MELO3C014454	0.00145093122867479	0.0175329893825102	Receptor-like protein kinase	1
MELO3C007047	0.0014515386926125	0.0175329893825102	Protein kinase	1
MELO3C023367	0.00145318824654184	0.0175421850128085	DNA repair protein XRCC1	1
MELO3C004576	0.00145859722393693	0.0175954172565851	sugar transport protein 14-like	1
MELO3C022932	0.00145937989094569	0.0175954172565851	Auxin response factor	0
MELO3C021360	0.00146048979136648	0.0175980554543604	Pentatricopeptide repeat-containing family protein	1
MELO3C015477	0.00146228225489542	0.0176089099097132	No data found	0
MELO3C003375	0.00146380420207692	0.0176164955434596	Two-component response regulator-like protein APRR2	1
MELO3C014281	0.0014702360035872	0.0176508758874429	Aldo/keto reductase, putative	0
MELO3C005421	0.00146899146702206	0.0176508758874429	GTF2H2	1
MELO3C021914	0.00146823354847903	0.0176508758874429	peroxidase 10-like	0
MELO3C018768	0.00146951190071176	0.0176508758874429	Wound-responsive family protein	1
MELO3C023985	0.00147349210060765	0.0176792196202312	RNA/RNP complex-1-interacting phosphatase, putative	1
MELO3C007497	0.0014780779626572	0.0177234740039569	Transcription termination factor family protein	0
MELO3C002227	0.00147953668231926	0.0177302002057786	Unknown protein	1
MELO3C014008	0.00148146067848454	0.0177424905636089	Adenosine monophosphate-protein transferase and cysteine protease ibpA	1
MELO3C020591	0.00148245648757772	0.0177436564685893	Glycosyltransferase	1
MELO3C002416	0.00148622342396076	0.017777968746094	Ankyrin repeat family protein	0
MELO3C004577	0.00148880872396417	0.0177981134924749	CRS2-associated factor 1, chloroplastic	1
MELO3C018494	0.00150424303608299	0.0179717457468862	Protein TIC 21, chloroplastic	1
MELO3C000075	0.0015064080353504	0.0179867305260793	Myosin heavy chain-like protein, putative	1
MELO3C027219	0.00150762899745338	0.0179904320668923	Hydroxycinnamoyl-CoA shikimate/quinate hydroxycinnamoyltransferase	1
MELO3C020942	0.00150894782427158	0.0179952962448909	PQ-loop repeat family protein / transmembrane family protein	1
MELO3C022059	0.00151061562675903	0.0180043138279203	Pentatricopeptide repeat-containing protein	1
MELO3C005651	0.00151252537705282	0.0180162024556189	30S ribosomal S1	1
MELO3C009588	0.00151414543658712	0.0180196286456078	Downstream neighbor of Son	1
MELO3C022783	0.00151463788301731	0.0180196286456078	transmembrane protein 50A	1
MELO3C021536	0.00151639341105281	0.0180296529048055	Quinone oxidoreductase-like protein	0
MELO3C015130	0.00152015005154871	0.0180417327932905	polygalacturonase-like	1
MELO3C025354	0.00151869336680555	0.0180417327932905	Late embryogenesis abundant protein	1
MELO3C008285	0.00151933283763561	0.0180417327932905	eukaryotic translation initiation factor 3 subunit F	1
MELO3C003457	0.00152415156525021	0.018078359917193	protein EMBRYONIC FLOWER 1-like isoform X3	0
MELO3C003826	0.00152506826935495	0.0180783753010149	No data found	1
MELO3C014604	0.0015283132911843	0.0181059743176957	F16F4.11 protein	1
MELO3C016826	0.00153179476841669	0.0181146196894978	At4g33800	1
MELO3C021148	0.00153136859350866	0.0181146196894978	Autophagy-related protein	0

MELO3C025035	0.00153071881752509	0.0181146196894978	lecithin-cholesterol acyltransferase-like 1	0
MELO3C020427	0.00153376154089113	0.018127023740909	DEAD-box ATP-dependent RNA helicase 42-like	0
MELO3C021563	0.00153757354735573	0.0181612081260337	isocitrate dehydrogenase [NADP]	1
MELO3C022392	0.00153951311588807	0.018173248371592	Cytochrome oxidase complex assembly protein	0
MELO3C011439	0.00154415748059011	0.0182171840407253	6,7-dimethyl-8-ribityllumazine synthase	0
MELO3C006294	0.00154543307012311	0.0182213478817083	Dna repair helicase xpb1	1
MELO3C013965	0.00154666283116955	0.0182249667379281	Flavin-containing monooxygenase	1
MELO3C014230	0.00155245603648058	0.0182793157660068	Ethylene insensitive 2	1
MELO3C017115	0.00155312632818672	0.0182793157660068	succinate dehydrogenase subunit 7B, mitochondrial-like	1
MELO3C004279	0.00156216413039512	0.0183747346105856	RING zinc finger family protein	1
MELO3C010197	0.00157227802397697	0.0184785490735071	Tetratricopeptide repeat (TPR)-like superfamily protein	0
MELO3C026288	0.00157286146096336	0.0184785490735071	Serine/threonine-protein phosphatase 2A 55 kDa regulatory subunit B	1
MELO3C010403	0.00157447526897514	0.0184865113477943	LOW QUALITY PROTEIN: LEAF RUST 10 DISEASE-RESISTANCE LOCUS RECEPTOR-LIKE PROTEIN KINASE-like 1.4	0
MELO3C016483	0.00158023620980208	0.0185349689647406	phosphoribosylamine--glycine ligase	1
MELO3C008947	0.00158137311774076	0.0185349689647406	CBS domain-containing protein	1
MELO3C024313	0.00158260126212806	0.0185349689647406	AT-rich interactive domain-containing protein 4-like	0
MELO3C002034	0.00158329498422793	0.0185349689647406	ninja-family protein 6-like isoform X2	1
MELO3C010600	0.00158218164950008	0.0185349689647406	DNA ligase 1 isoform X3	1
MELO3C013750	0.00158688511649507	0.0185356656353381	SKP1-like protein 1B	1
MELO3C015747	0.00158659415425944	0.0185356656353381	At3g60850	1
MELO3C005214	0.00158559844227557	0.0185356656353381	Defensin	1
MELO3C020906	0.00158710874420764	0.0185356656353381	60S ribosomal protein L26-1-like	1
MELO3C014944	0.00158975633025693	0.0185423015211278	homeobox-leucine zipper protein HAT22-like	0
MELO3C016193	0.00158896575333467	0.0185423015211278	Lysine-specific histone demethylase 1	0
MELO3C022042	0.00159143253219463	0.0185423015211278	DUF2039 family protein	0
MELO3C021348	0.00159087168485317	0.0185423015211278	E3 ubiquitin-protein ligase Topors	1
MELO3C010688	0.00159627418691699	0.0185877470031979	F-box protein At1g70590	1
MELO3C018476	0.0016042694552616	0.0186698394059878	cyclin-D3-3	1
MELO3C019491	0.00160887864625414	0.0186904378734547	Nucleolar complex protein 2 homolog	0
MELO3C007099	0.00160852551941759	0.0186904378734547	Nucleoporin protein Ndc1-Nup	0
MELO3C020159	0.00160703147890584	0.0186904378734547	transmembrane protein 87A	0
MELO3C023469	0.00161398184714412	0.0187386992940912	Protein LOW PSII ACCUMULATION 3, chloroplastic	1
MELO3C012604	0.00161829168735006	0.018777698315791	Phosphoglycerate kinase	1
MELO3C008773	0.00161989152750242	0.0187788394496662	Succinate dehydrogenase assembly factor 2, mitochondrial	1
MELO3C013829	0.00162029178298806	0.0187788394496662	Calmodulin family protein	1
MELO3C003734	0.00162208649782969	0.0187886136338056	T4O12.20	0
MELO3C009234	0.00162371681969942	0.0187964733131558	SUPERMAN-like zinc finger protein	1
MELO3C020789	0.00162576706990036	0.0188054398657658	Nucleoporin NUP188 like	1
MELO3C010960	0.0016263958322309	0.0188054398657658	Proteasome subunit alpha type	1
MELO3C023338	0.00163648326242916	0.018911005236813	cysteine proteinase RD19a-like	1
MELO3C010456	0.00163788891852379	0.0189161802642844	Phosphatidylinositol-4-phosphate 5-kinase, putative	1
MELO3C023852	0.00164327417852994	0.0189672833148964	Actin family protein	0
MELO3C014850	0.00164799342509903	0.0189971298758232	No data found	1
MELO3C015748	0.00164874579002283	0.0189971298758232	transcription factor EMB1444	1
MELO3C005404	0.00164747201365656	0.0189971298758232	LOW QUALITY PROTEIN: xyloglucan galactosyltransferase XLT2	1
MELO3C005918	0.00164998656602089	0.0190003409284819	NPL4 family protein	1
MELO3C008092	0.00165607824610392	0.01905937603864	50S ribosomal protein L14, putative	1
MELO3C014611	0.00166499764807648	0.0191508669492501	Pre-mRNA-splicing factor CWC22	1
MELO3C009455	0.00166599357714137	0.0191511683090599	BZIP transcription factor family protein	1
MELO3C015946	0.00166733441386024	0.0191554318437033	GATA transcription factor-like protein	1
MELO3C004391	0.00167241694262599	0.0192026524418143	PRA1 family protein	1
MELO3C013753	0.00168358970314475	0.0193016055803562	Vacuolar protein sorting-associated protein 35	0
MELO3C002314	0.00168227509520191	0.0193016055803562	cytochrome P450 71A1-like	1
MELO3C002117	0.00168396710795249	0.0193016055803562	T-complex protein 1 subunit delta	1
MELO3C008313	0.0016862201830351	0.0193162194865199	UTP--glucose-1-phosphate uridylyltransferase 3, chloroplastic	1
MELO3C024001	0.00169134873987065	0.0193637369644669	MADS-box transcription factor	0
MELO3C011109	0.00169484210432513	0.0193924894080632	Octicosapeptide/Phox/Bem1p	1
MELO3C018434	0.00169761795586676	0.019401769103248	Armadillo repeat-containing protein, putative	1
MELO3C003770	0.0016973381454457	0.019401769103248	TLD-domain nucleolar protein	0
MELO3C026046	0.00170144999900546	0.0194343181205082	alpha-ketoglutarate-dependent dioxygenase AlkB-like	1

MELO3C014346	0.00170775748623742	0.0194843255499909	protein PALE CRESS, chloroplastic	1
MELO3C020369	0.00170878788052986	0.0194843255499909	60S ribosomal protein L37a	1
MELO3C005759	0.00170806862709461	0.0194843255499909	30S ribosomal protein S6 alpha, chloroplastic	1
MELO3C026518	0.00171160126017267	0.0195051432701385	Photosystem II reaction center PsbP family protein	1
MELO3C005711	0.00171342810463715	0.0195147010602532	heavy metal-associated isoprenylated plant protein 3-like	1
MELO3C019488	0.00171945922624073	0.0195665520250788	Pentatricopeptide repeat-containing protein	1
MELO3C007617	0.00171996224191284	0.0195665520250788	At5g67390	1
MELO3C003852	0.00172185560495652	0.0195768142442639	DNA ligase-like protein	1
MELO3C004139	0.0017260170705593	0.0196128372419308	Ubiquitin carboxyl-terminal hydrolase, putative	1
MELO3C009090	0.00173121000396637	0.0196392051611116	Kinase family protein	0
MELO3C004645	0.00173460385515178	0.0196392051611116	40S ribosomal S3-like protein	1
MELO3C006409	0.0017350513931752	0.0196392051611116	Glycolipid transfer protein domain-containing protein	1
MELO3C019490	0.00173728752931601	0.0196392051611116	40S ribosomal protein S16	0
MELO3C008815	0.00173564949107596	0.0196392051611116	nucleolar MIF4G domain-containing protein 1	1
MELO3C005455	0.00173406833228484	0.0196392051611116	origin of replication complex subunit 3	0
MELO3C017223	0.00173331296437929	0.0196392051611116	Mitochondrial carrier protein, putative	1
MELO3C008195	0.00173319093407187	0.0196392051611116	Katanin p60 atpase-containing subunit a1	0
MELO3C018180	0.00173648133509596	0.0196392051611116	tRNA (guanine(37)-N1)-methyltransferase	1
MELO3C007601	0.00174263062211799	0.0196883364738033	Lysine-rich arabinogalactan protein 18	1
MELO3C016494	0.00174848962342988	0.019709430121642	Polygalacturonase	0
MELO3C007269	0.00174774945217715	0.019709430121642	Auxin repressed protein	1
MELO3C023451	0.00174626345788564	0.019709430121642	BRCA1-associated protein	1
MELO3C017294	0.00174730515676302	0.019709430121642	Carbon catabolite repressor protein 4 like 3	0
MELO3C003671	0.0017542994104538	0.0197636389372801	SPOC domain/transcription elongation factor S-II, putative	1
MELO3C015470	0.00175565135908395	0.0197675933241442	beta-galactosidase	0
MELO3C013769	0.0017643629105647	0.0198543607525597	Seven transmembrane receptor	1
MELO3C005913	0.00176561299034728	0.0198571132951984	Auxin-responsive family protein	1
MELO3C002390	0.001768224463224	0.0198751650109338	At5g44650	1
MELO3C015695	0.00176927873858901	0.0198757029626816	Expansin	1
MELO3C021264	0.00177097699103468	0.0198834704922933	Ubiquitin-conjugating enzyme, E2	0
MELO3C017440	0.00177258734143249	0.0198902428442899	U3 small nucleolar RNA-associated protein 25-like	1
MELO3C008115	0.0017806901857147	0.01996981855632	5'-3' exonuclease	1
MELO3C011496	0.00178431101807353	0.0199990682723803	BRCT domain DNA repair protein	1
MELO3C021452	0.00179794402675915	0.0201216026456491	No data found	1
MELO3C015692	0.00179684828190319	0.0201216026456491	Brefeldin A-inhibited guanine nucleotide-exchange protein	1
MELO3C018459	0.00179830009973014	0.0201216026456491	40S ribosomal protein S16	0
MELO3C026143	0.00179937326870028	0.0201222099000916	Unknown protein	1
MELO3C009032	0.00180618680062949	0.020186974038275	fructokinase-like 2, chloroplastic	1
MELO3C025142	0.00180918499272109	0.0202090466183534	Proliferating cell nuclear antigen	0
MELO3C017149	0.00181586970268244	0.0202722502873236	Pentatricopeptide repeat-containing protein	1
MELO3C007800	0.00181959699758183	0.0203023848052223	Receptor protein kinase, putative	1
MELO3C013929	0.0018284576743629	0.0203897293116844	Unknown protein	1
MELO3C002604	0.00183522225955302	0.0204536142234269	DUF2921 family protein	0
MELO3C019168	0.00184600708229754	0.0205622074835274	Metacaspase-9	1
MELO3C008786	0.00185244710486099	0.0206223099627394	Rhomboid protein, putative	0
MELO3C016694	0.00186271795353732	0.0207238791076526	VQ motif-containing protein	1
MELO3C007935	0.0018647188806673	0.0207238791076526	Peroxidase	1
MELO3C005389	0.00186395168082631	0.0207238791076526	NADH dehydrogenase [ubiquinone] 1 alpha subcomplex subunit 12	1
MELO3C026593	0.00186878067212692	0.0207573394228541	Surfeit locus protein 2 (SURF2)	0
MELO3C012493	0.00187295993871484	0.0207687174787643	Choline/ethanolamine kinase	0
MELO3C012420	0.00187233804376197	0.0207687174787643	No data found	0
MELO3C003456	0.00187113290658125	0.0207687174787643	Alpha/beta-Hydrolases superfamily protein	1
MELO3C016923	0.00187914670450451	0.0208203232473985	No data found	1
MELO3C026058	0.00188077657974373	0.0208203232473985	Non-specific serine/threonine protein kinase	1
MELO3C012852	0.00188039613797097	0.0208203232473985	Protein BREAST CANCER SUSCEPTIBILITY 1-like protein	0
MELO3C015177	0.00188263980533365	0.0208292736781705	60S ribosomal protein L13a, putative	0
MELO3C008032	0.00188467890401967	0.020840158832858	Actin	0
MELO3C019226	0.00188936224392533	0.0208569116575077	transcription factor ILR3-like	1
MELO3C018413	0.00188895876601003	0.0208569116575077	Allene oxide synthase	0
MELO3C015664	0.00188866569845136	0.0208569116575077	RING-type E3 ubiquitin transferase	1
MELO3C020988	0.00189735927898682	0.020933490726654	Unknown protein	1
MELO3C014447	0.00190474460798895	0.0210027680620675	Nuclear ribonuclease Z	1
MELO3C023862	0.0019068491527422	0.0210027680620675	Factor of DNA methylation 1	0
MELO3C025744	0.00190635644741377	0.0210027680620675	Zinc finger family protein, putative	0

MELO3C002219	0.00190789234408573	0.0210027680620675	HIPL1 protein-like isoform X1	1
MELO3C025651	0.00193151944245629	0.0212510180886179	Intracellular protein transport protein USO1, putative	1
MELO3C026194	0.00193480153015102	0.0212752758457419	No data found	1
MELO3C004459	0.0019419027908818	0.0213410737977304	actin-related protein 6	1
MELO3C014099	0.00194294651315607	0.0213410737977304	BnaC03g71690D protein	1
MELO3C017167	0.00194967540488111	0.0214030792501374	Transmembrane protein	1
MELO3C009583	0.00195706642749194	0.0214493569525252	E3 ubiquitin-protein ligase BAH1-like protein, putative	1
MELO3C023799	0.00195756025201366	0.0214493569525252	12-oxophytodienoate reductase 3	1
MELO3C014091	0.00195604462548404	0.0214493569525252	caffeic acid 3-O-methyltransferase-like	1
MELO3C022124	0.00195823538333095	0.0214493569525252	Glycerophosphodiester phosphodiesterase GDPD4	1
MELO3C024926	0.00196315683099746	0.0214806908923386	two-pore potassium channel 1 isoform X1	1
MELO3C020588	0.00196327140921926	0.0214806908923386	17.5 kDa class I heat shock protein	0
MELO3C008516	0.00196685604928237	0.0214960930366782	Guanosine nucleotide diphosphate dissociation inhibitor	0
MELO3C024337	0.00196598778055268	0.0214960930366782	transmembrane protein 87B isoform X2	1
MELO3C017730	0.0019724064548432	0.0215448313477314	Pentatricopeptide repeat-containing family protein	1
MELO3C025272	0.00197489363397907	0.021549925840151	AT3g54190/F24B22_150	1
MELO3C008116	0.00197505523169139	0.021549925840151	Magnesium transporter NIPA	1
MELO3C014488	0.00198659047530292	0.0216518627465548	Cyclin T1 family protein	1
MELO3C022477	0.00198647332954294	0.0216518627465548	Protein nuclear fusion defective 4	1
MELO3C016469	0.00198908132816278	0.0216670530335834	zinc finger CCCH domain-containing protein 5	1
MELO3C023622	0.00199024853339758	0.0216678160342165	Short-chain dehydrogenase/reductase	1
MELO3C005260	0.00200197408497349	0.0217834634733562	Vacuolar iron transporter 1	1
MELO3C021345	0.00200657619838918	0.0218215161574823	cullin-1	1
MELO3C006870	0.0020155939407539	0.0218719472185081	ethylene-responsive transcription factor ERF027	1
MELO3C020834	0.00201564352309913	0.0218719472185081	Unknown protein	1
MELO3C002717	0.00201365744032933	0.0218719472185081	prefoldin subunit 6	1
MELO3C019814	0.00201274196770884	0.0218719472185081	ABC transporter G family member	0
MELO3C008766	0.00202108742744311	0.021892587246618	sister chromatid cohesion 1 protein 4 isoform X1	1
MELO3C006934	0.00202201822291359	0.021892587246618	protein REVEILLE 6-like isoform X2	0
MELO3C018999	0.00202098577629739	0.021892587246618	Transmembrane protein, putative	1
MELO3C007228	0.00202308834498344	0.021892587246618	GDSL esterase/lipase	0
MELO3C022845	0.00201915646106055	0.021892587246618	RING-type E3 ubiquitin transferase	1
MELO3C021622	0.00202499337392292	0.021901201610955	Elicitor-responsive protein 1	1
MELO3C013411	0.0020279124270397	0.0219207676637149	NADP dependent sorbitol 6-phosphate dehydrogenase family protein	1
MELO3C014706	0.00203201183773705	0.0219530644329699	Argonaute	1
MELO3C026657	0.00203570078237614	0.0219808937950499	Glycine-rich protein	1
MELO3C027092	0.00204005247370298	0.0220158449744045	DExH-box ATP-dependent RNA helicase DExH12-like	1
MELO3C014417	0.00204144586045041	0.0220188499716194	sugar transporter ERD6-like 7	0
MELO3C023473	0.00204448889464182	0.0220396349237343	Phosphatase 2C family protein	1
MELO3C019899	0.00204636292220117	0.0220478021552378	AMMECR1 family	1
MELO3C009149	0.00205119616259886	0.0220878260715184	Copper chaperone SCO1/SenC	1
MELO3C011654	0.00205279144184656	0.0220929581389797	RING zinc finger protein-like	1
MELO3C018781	0.0020542658700694	0.0220967846775603	Leucine-rich repeat family protein	0
MELO3C012131	0.00207255568294284	0.0222813838772119	eukaryotic translation initiation factor 5A-like	1
MELO3C003423	0.00207648623644074	0.0223114943870883	Zinc finger CCCH domain protein	1
MELO3C016550	0.00207952457836447	0.0223176578137305	Unknown protein	1
MELO3C011972	0.00208045004987989	0.0223176578137305	Alpha-glucan water dikinase, chloroplastic	0
MELO3C015616	0.00208012082145714	0.0223176578137305	BnaA04g07840D protein	1
MELO3C009119	0.00208260743603428	0.0223286722335727	Protein LURP-one-related 15	1
MELO3C006314	0.00208855728757984	0.0223803135498721	60S ribosomal protein L13a, putative	1
MELO3C019818	0.00209071289150375	0.0223912629578675	DVL8	1
MELO3C009600	0.00209252401614957	0.022398513167988	60S ribosomal protein L21	0
MELO3C013539	0.00209583349110565	0.0224217852740224	vesicle-associated protein 4-2-like	0
MELO3C010198	0.00210011636188545	0.0224554401899706	DNA-directed RNA polymerase subunit beta	0
MELO3C002372	0.00211176063197727	0.022567727662835	heavy metal-associated isoprenylated plant protein 3-like	1
MELO3C002268	0.00211346018252012	0.0225736750376365	Iron-sulfur cluster assembly protein	0
MELO3C026887	0.00212116551042296	0.022643728467753	Tryptophan synthase, alpha chain	0
MELO3C004015	0.00212540410728268	0.0226746301857241	Pentatricopeptide repeat-containing family protein	1
MELO3C011763	0.0021263565296451	0.0226746301857241	LRR receptor-like kinase	0
MELO3C021153	0.00213199409674547	0.0227224778287244	Arginine--tRNA ligase	0
MELO3C005926	0.00213685711803191	0.0227347077752584	protein BONZAI 1	1
MELO3C006092	0.00213681237477381	0.0227347077752584	Glycoside hydrolase family 28 protein/polygalacturonase family protein	1

MELO3C012052	0.00213774633341712	0.0227347077752584	dnaJ homolog subfamily B member 1	1
MELO3C009872	0.0021356274309372	0.0227347077752584	Gibberellin-regulated family protein	1
MELO3C025491	0.00215106029913348	0.0228516889981641	transcription initiation factor TFIID subunit 1-like	0
MELO3C023221	0.00215059543241081	0.0228516889981641	DNA cross-link repair family protein	1
MELO3C001656	0.00215343807777302	0.0228646497838383	Unknown protein	1
MELO3C015457	0.00216212621458034	0.0229445623921263	K(+) efflux antiporter	0
MELO3C020836	0.00216873957663433	0.0229900364460286	transportin-1	1
MELO3C025710	0.00216856106267871	0.0229900364460286	Nuclear factor related to kappa-B-binding protein	1
MELO3C002598	0.00217096035433062	0.0230012317798688	E3 ubiquitin-protein ligase RMA1H1-like	0
MELO3C005704	0.00217420806065527	0.0230232895388101	Beta-carotene hydroxylase	1
MELO3C004533	0.00218101748222876	0.0230830194300835	GDP-mannose transporter, putative	1
MELO3C005821	0.0021861903058622	0.0231253735139114	mRNA, clone: RTFL01-46-D12	1
MELO3C009489	0.0021885277242305	0.0231377055812785	Ribosomal protein S11	0
MELO3C024916	0.00219277810808238	0.0231525705960907	Agenet domain-containing protein / bromo-adjacent domain-containing protein, putative	1
MELO3C010727	0.00219323526137982	0.0231525705960907	3-oxoacyl-[acyl-carrier-protein] reductase 4	1
MELO3C003496	0.00219345078663657	0.0231525705960907	Phosphoglycerate mutase-like protein 1	0
MELO3C021777	0.00219600458758573	0.0231671445514052	Vesicle-associated membrane protein, putative	1
MELO3C011042	0.00220196138837392	0.0232175843347552	VQ motif-containing protein 9	0
MELO3C019361	0.00220806422194508	0.0232695092418321	fasciclin-like arabinogalactan protein 7	0
MELO3C016149	0.00220997904778486	0.0232772673145084	Cationic amino acid transporter, putative	1
MELO3C009308	0.00221549861231163	0.023322964869159	LRR receptor-like kinase	1
MELO3C006759	0.00221808743540164	0.023337777710041	Ca2+-activated RelA/SpoT-like protein	1
MELO3C007340	0.00222103371849125	0.023356333816019	NAD(P)H dehydrogenase (Quinone) FQR1-like	1
MELO3C006212	0.00222542135216774	0.0233900193102506	tRNA (Guanine-N(7)-)-methyltransferase	0
MELO3C009757	0.00222821468022771	0.0234069211275623	Amino acid transporter family protein	0
MELO3C008970	0.00223264451449334	0.023440986983907	vacuolar protein sorting-associated protein 20 homolog 2-like	0
MELO3C015292	0.00225207974747366	0.0236199272081026	Epoxide hydrolase 2	0
MELO3C020002	0.00225192014674969	0.0236199272081026	Protein IDA	1
MELO3C005976	0.00225640094494073	0.0236526869753898	Protein AATF	0
MELO3C007466	0.00225882808818756	0.0236530201026597	RNA cytidine acetyltransferase	0
MELO3C003532	0.00225770592718466	0.0236530201026597	Pesticidal crystal cry8Ba protein	1
MELO3C007270	0.00226366852216031	0.023678596209822	Ring finger protein, putative	0
MELO3C026053	0.00226283308011266	0.023678596209822	WEB family protein At2g38370	1
MELO3C010806	0.0022690529645768	0.0237223541542759	DNA excision repair protein ERCC-8	1
MELO3C013780	0.00227310793406177	0.0237475211628624	Early nodulin-like protein 1	1
MELO3C025943	0.00227386513337247	0.0237475211628624	RPM1-interacting protein 4	1
MELO3C014588	0.00227553039129758	0.0237523518486976	Calcium-dependent protein kinase	1
MELO3C018569	0.00229013798537503	0.0238909923541539	peptide methionine sulfoxide reductase B5-like	1
MELO3C026897	0.00229123193674452	0.0238909923541539	thioredoxin-like 1-1, chloroplastic	1
MELO3C011885	0.00229709778793552	0.0239287608363609	Lipoxygenase	1
MELO3C008100	0.00229727735813157	0.0239287608363609	gibberellin receptor GID1B	0
MELO3C006202	0.00230065370872889	0.0239386776046823	Peptidase_M22 domain-containing protein	1
MELO3C024312	0.00229967510877782	0.0239386776046823	At1g53885	0
MELO3C019333	0.00230343015017287	0.0239549457797599	DUF679 domain membrane protein	1
MELO3C008037	0.00230496063997476	0.0239582461467693	Ubiquinol-cytochrome C chaperone family protein	1
MELO3C013489	0.00230717829032479	0.0239686817757097	monosaccharide-sensing protein 2	1
MELO3C022165	0.00231035379912992	0.0239890521445934	Actin-binding LIM protein 1, putative	0
MELO3C018492	0.00231232472788601	0.0239969001844565	Cinnamyl alcohol dehydrogenase	0
MELO3C016031	0.0023175934401175	0.0240389458239919	glutathione S-transferase-like	1
MELO3C006106	0.00232061450614851	0.0240576461322451	U-box domain-containing protein kinase family protein, putative	0
MELO3C011216	0.00232275821897354	0.0240672361314315	Photosynthetic NDH subcomplex B 3	1
MELO3C012445	0.0023251385175671	0.0240792661685541	ATP synthase subunit d, mitochondrial	1
MELO3C018264	0.00232641112745924	0.0240798183208556	No data found	1
MELO3C009318	0.00234066344919559	0.0241830573770045	Ribonuclease P protein subunit p29	1
MELO3C016952	0.00234128339180883	0.0241830573770045	eukaryotic translation initiation factor-like	0
MELO3C023445	0.00234094296969889	0.0241830573770045	F-box/LRR-repeat protein 14	1
MELO3C015103	0.00233825502701834	0.0241830573770045	Histone deacetylase	1
MELO3C021217	0.00234540104667236	0.0242129248670844	MACPF domain-containing CAD1-like protein	1
MELO3C007793	0.00235058569176971	0.0242537705468966	cytochrome P450 CYP736A12-like	1
MELO3C010517	0.00235527000820146	0.0242640727135997	WAT1-related protein	1
MELO3C023224	0.00235334258523257	0.0242640727135997	Glutathione-S-transferase	1
MELO3C026247	0.00235451557099309	0.0242640727135997	Raffinose synthase	1

MELO3C019947	0.00236105137720877	0.0243109508073493	Oxidoreductase family protein	1
MELO3C011167	0.00236258553874436	0.0243140707684535	basic leucine zipper 9	1
MELO3C005136	0.00236472222389739	0.0243233849998695	Protein EARLY RESPONSIVE TO DEHYDRATION 15	1
MELO3C017817	0.0023669444389276	0.0243335688310157	transaldolase	0
MELO3C003722	0.00237262336257049	0.0243792605553614	serine/threonine-protein kinase STY46-like isoform X1	0
MELO3C020532	0.0023744538022763	0.0243853812486504	Potassium transporter	1
MELO3C009984	0.00237666292726679	0.0243953826146527	Zinc finger CCCH domain-containing protein 41	1
MELO3C017462	0.00238451283574159	0.0244603094659689	(DL)-glycerol-3-phosphatase 2	1
MELO3C013034	0.00238546539224549	0.0244603094659689	Charged multivesicular body 1	0
MELO3C004281	0.00239189379534643	0.0245134979576008	mevalonate kinase-like	1
MELO3C019725	0.00239709679529321	0.0245540791546917	ethylene-responsive transcription factor 3-like	0
MELO3C023404	0.00240231684114978	0.0245947927920513	DNA replication complex GINS protein PSF1	0
MELO3C004084	0.00240477987021892	0.0246043393730093	No data found	1
MELO3C021521	0.00240698686863405	0.0246043393730093	WAT1-related protein	0
MELO3C003593	0.00240673840906169	0.0246043393730093	Bromo-adjacent-like (BAH) domain protein	1
MELO3C016970	0.00240841038837392	0.0246061545576805	Chaperone protein	1
MELO3C026286	0.00240990356136972	0.0246086791279682	Protein MICRORCHIDIA 6	0
MELO3C008847	0.00241118052862543	0.0246089944495213	M50 family peptidase	1
MELO3C019724	0.00241443701091759	0.0246295023391588	Triacylglycerol lipase 2, putative	1
MELO3C023540	0.00242100412623403	0.024683743153844	Unknown protein	1
MELO3C027184	0.00242276758035198	0.0246889767514816	DNA primase	0
MELO3C021295	0.00243412618990746	0.0247919330193308	Transducin family protein/WD-40 repeat protein	1
MELO3C004761	0.00243983236026302	0.0248134188898108	CBS domain-containing protein CBSX1, chloroplastic	0
MELO3C021783	0.00244000503742026	0.0248134188898108	Peroxisome biogenesis protein 1	1
MELO3C018797	0.00243837045809947	0.0248134188898108	Cysteine-rich receptor-kinase-like protein	0
MELO3C022094	0.00244379917129034	0.024839212472369	T-complex protein 1 subunit zeta 1	1
MELO3C009908	0.00245124923270912	0.0249021199057471	Type I inositol polyphosphate 5-phosphatase, putative	0
MELO3C009019	0.00245329237328473	0.0249100622519281	Rhodanese-like domain-containing family protein	1
MELO3C015210	0.00245634052673682	0.0249280206155854	ETHYLENE INSENSITIVE 3-like 3 protein	1
MELO3C011264	0.00245758550501518	0.0249280206155854	Histone acetyltransferase	0
MELO3C009639	0.00246576674180576	0.0249496524561083	Squamosa promoter binding protein	0
MELO3C013353	0.00246544497319956	0.0249496524561083	heavy metal-associated isoprenylated plant protein 26-like	1
MELO3C010493	0.00246180150676134	0.0249496524561083	Aldehyde dehydrogenase	0
MELO3C012545	0.0024685614916824	0.0249496524561083	phosphatidylinositol 4-kinase alpha 1-like	1
MELO3C021185	0.00246257535260708	0.0249496524561083	Peptidase M48	1
MELO3C019827	0.00246720498745034	0.0249496524561083	MEF2BNB-like protein	0
MELO3C010794	0.00246827361479818	0.0249496524561083	No data found	1
MELO3C017333	0.00247027858353721	0.0249542361873536	BnaC05g35140D protein	0
MELO3C002785	0.00247438794712673	0.0249829691041952	epimerase family protein SDR39U1 homolog, chloroplastic-like	1
MELO3C012428	0.0024886778630655	0.0251144093600821	mRNA-decapping enzyme subunit 2-like	1
MELO3C019500	0.00249021021586082	0.0251170385868414	Protein-protein interaction regulator family protein	0
MELO3C018683	0.00249307436724266	0.0251330912091247	Actin	0
MELO3C011084	0.00250020007177665	0.0251920669477128	Ribosomal RNA small subunit methyltransferase A	0
MELO3C009268	0.00250588454406664	0.0252175084867174	SLT1	1
MELO3C013149	0.00250643639339809	0.0252175084867174	UPF0505 protein C16orf62 homolog isoform X1	1
MELO3C006957	0.0025065557324131	0.0252175084867174	DUF21 domain-containing protein	1
MELO3C009290	0.00251076561525454	0.0252470010874042	Phosphatidate phosphatase PAH1	1
MELO3C004381	0.00251245552795387	0.025251137008428	Auxin-responsive protein	0
MELO3C016067	0.00252103326446729	0.0253107646948902	Mitochondrial processing peptidase beta subunit	1
MELO3C023844	0.00252223327356038	0.0253107646948902	2-oxoglutarate dehydrogenase E1 component family protein	0
MELO3C019704	0.00252200355091303	0.0253107646948902	Serine/threonine protein phosphatase 7 long form	0
MELO3C013745	0.00252732137778466	0.0253372598900947	Phosphatase 2C family protein	1
MELO3C022231	0.00252743946445322	0.0253372598900947	Corepressor	1
MELO3C004564	0.00253284738789272	0.0253659355931144	protein NUCLEAR FUSION DEFECTIVE 6, chloroplastic/mitochondrial-like isoform X2	1
MELO3C018460	0.00253286875232273	0.0253659355931144	O-acyltransferase WSD1-like	0
MELO3C005779	0.00253841918105957	0.025395765150327	Metal-dependent protein hydrolase	1
MELO3C025725	0.00253729953931148	0.025395765150327	RNA binding (RRM/RBD/RNP motifs) family protein	1
MELO3C004423	0.00253995268287976	0.0253982407768063	protease 2	1
MELO3C018716	0.00254246520730694	0.025410498673636	ras-related protein Rab11D	1
MELO3C019673	0.00254436052110441	0.0254165786197728	BOI-related E3 ubiquitin-protein ligase 1-like	1
MELO3C004321	0.00255025674306286	0.0254625987961317	Vat protein	1
MELO3C016014	0.0025571448957098	0.0255184712205016	thiamine pyrophosphokinase 1	0
MELO3C003874	0.00255880335336345	0.0255221249624115	cytochrome P450 734A1-like	1

MELO3C010640	0.00256492543970355	0.0255702738559845	zinc finger CCCH domain-containing protein 1	1
MELO3C015459	0.0025681230640956	0.0255892343051584	Cytidine deaminase	1
MELO3C010716	0.00256975248916946	0.0255925576947089	Protein HHL1, chloroplastic	1
MELO3C002167	0.0025805609976346	0.0256872475515553	Succinate--CoA ligase [ADP-forming] subunit alpha, mitochondrial	1
MELO3C002589	0.00258385469115019	0.0257070762194081	At2g47960/T9J23.10	1
MELO3C024357	0.0025853839593345	0.0257093392814184	transcription initiation factor TFIID subunit 12b	1
MELO3C002277	0.0025908406468802	0.0257506350957408	Glutathione transport system permease protein gsiD	0
MELO3C022399	0.00259592798474784	0.0257882202066323	alcohol dehydrogenase-like	1
MELO3C016434	0.00260306171692859	0.0258067871092464	protein STICHEL	1
MELO3C015825	0.00260506410889971	0.0258067871092464	F-box protein, putative	1
MELO3C026572	0.00260563742446895	0.0258067871092464	Proline transporter	0
MELO3C008389	0.0026054713783954	0.0258067871092464	RNA-binding protein 2	1
MELO3C019810	0.00260464821668416	0.0258067871092464	Adenosine kinase	1
MELO3C003818	0.00260420294403418	0.0258067871092464	Tubby-like F-box protein	0
MELO3C007660	0.00260875272791905	0.0258116902544923	DUF21 domain-containing-like protein	1
MELO3C019661	0.00260850482660091	0.0258116902544923	No data found	1
MELO3C023969	0.00261005344261589	0.0258116902544923	Unknown protein	1
MELO3C024244	0.00261508509481012	0.0258485062749775	Ribosomal protein L37	0
MELO3C009587	0.00261788420547349	0.0258632292015487	S-adenosyl-L-methionine-dependent methyltransferases superfamily protein	1
MELO3C000251	0.00262134113062928	0.0258844329943989	Protein LAZ1	1
MELO3C018344	0.00262491390901554	0.0258938185759979	No data found	1
MELO3C017158	0.00262413446791454	0.0258938185759979	Serine/threonine-protein kinase atr	0
MELO3C007785	0.00263134950686683	0.0259431666044565	RING-H2 zinc finger protein RHA2a	0
MELO3C011498	0.00263254371742017	0.0259431666044565	Splicing factor u2af large subunit, putative	1
MELO3C009532	0.0026377958393965	0.025943562933669	NDR1/HIN1-like protein 12	0
MELO3C021618	0.00263523784937714	0.025943562933669	ribosomal RNA large subunit methyltransferase E-like	0
MELO3C027119	0.00263408267344634	0.025943562933669	1-aminocyclopropane-1-carboxylate oxidase 2	0
MELO3C026901	0.00263783859288103	0.025943562933669	HNH endonuclease	0
MELO3C026222	0.00264225576370025	0.0259740712181763	Transcription factor GTE10	1
MELO3C004385	0.00265207979831772	0.0260253671353869	pathogenesis-related protein PR-4-like	0
MELO3C006055	0.00265102172481946	0.0260253671353869	Aldose 1-epimerase	1
MELO3C010522	0.00264977766937746	0.0260253671353869	Zinc knuckle family protein	1
MELO3C018365	0.00265274515385761	0.0260253671353869	GDP-Man:Man(3)GlcNAc(2)-PP-Dol alpha-1,2-mannosyltransferase	1
MELO3C021604	0.00265591567654666	0.0260435346058193	glycerol-3-phosphate dehydrogenase [NAD(+)]	1
MELO3C024086	0.00266368909276027	0.0261052559442443	70 kDa heat shock protein	1
MELO3C017481	0.00266485371328151	0.0261052559442443	Xyloglucan endotransglucosylase/hydrolase	1
MELO3C004519	0.00267496625574049	0.0261783491499598	NADH-cytochrome b5 reductase-like protein	0
MELO3C007081	0.00267470348746146	0.0261783491499598	SIT4 phosphatase-associated family protein	1
MELO3C014687	0.00269195405579215	0.0263315505932833	Structural maintenance of chromosomes protein	1
MELO3C023385	0.00270256906142263	0.0264222952445721	molybdate transporter 2	1
MELO3C023358	0.00270407856419341	0.0264239720753368	Ubiquitin fusion degradation 1 protein	1
MELO3C006439	0.00270856493483707	0.0264476999835899	1-aminocyclopropane-1-carboxylate oxidase homolog 1-like	0
MELO3C022497	0.00270918512667995	0.0264476999835899	40S ribosomal protein S13	0
MELO3C015093	0.00271896315900721	0.0265169399640659	Fasciclin-like arabinogalactan protein 16	1
MELO3C026723	0.00271827361883736	0.0265169399640659	Plastidal glycolate/glycerate translocator 1, chloroplastic	0
MELO3C010744	0.00272509819331868	0.0265636546001237	CTD small phosphatase-like protein 2	1
MELO3C014925	0.00272905227228559	0.026570628428043	Glycerophosphodiester phosphodiesterase, putative	0
MELO3C007405	0.00272984986989211	0.026570628428043	peroxisomal membrane protein PMP22	1
MELO3C023569	0.00272901561183836	0.026570628428043	Alpha-N-acetylglucosaminidase	1
MELO3C005103	0.00273416426217743	0.0265885133692798	Cytochrome b-c1 complex subunit Rieske, mitochondrial	1
MELO3C023599	0.00273464015593183	0.0265885133692798	Glutamine synthetase	0
MELO3C011717	0.00273572632368102	0.0265885133692798	Protein kinase-like protein	1
MELO3C013603	0.0027441539772568	0.0266573029497514	Plant/protein (DUF789)	0
MELO3C006153	0.00275443894018501	0.0267440583233598	UDP-galactose/UDP-glucose transporter 2-like	0
MELO3C011263	0.00276183244145933	0.0267500877324082	EEIG1/EHBP1 protein amino-terminal domain protein	1
MELO3C019501	0.00275780114814639	0.0267500877324082	Transmembrane 53	1
MELO3C013331	0.0027606036489658	0.0267500877324082	hippocampus abundant transcript-like protein 1	1
MELO3C015131	0.00276010714569663	0.0267500877324082	Pentatricopeptide repeat-containing family protein	1
MELO3C003861	0.00275803858939361	0.0267500877324082	H/ACA ribonucleoprotein complex non-core subunit NAF1-like isoform X1	1
MELO3C008214	0.00276361792622737	0.0267542600122864	Emb|CAB62340.1	1
MELO3C017228	0.00276531793823609	0.0267576011573859	Replication protein A 70 kDa DNA-binding subunit	0

MELO3C007857	0.00277499196625031	0.0268074015965016	LOW QUALITY PROTEIN: protein HYPER-SENSITIVITY-RELATED 4-like	0
MELO3C022228	0.00277292080975666	0.0268074015965016	Dienelactone hydrolase	1
MELO3C015861	0.00277506452761478	0.0268074015965016	isoamylase 2, chloroplastic	1
MELO3C012418	0.00277589428653835	0.0268074015965016	Tyramine N-feruloyltransferase 4/11	0
MELO3C025494	0.00278404522379472	0.0268729761117898	leukotriene A-4 hydrolase homolog	0
MELO3C013665	0.00278843488334646	0.0269021985887685	mechanosensitive ion channel protein 6-like	0
MELO3C018985	0.00280648064981326	0.0270630792740049	60S acidic ribosomal protein P1	1
MELO3C006949	0.0028143816981141	0.0271260244783091	NADH-ubiquinone oxidoreductase-related	1
MELO3C020733	0.00282827819139519	0.0272333817659014	Hexosyltransferase	1
MELO3C024984	0.00282776638965032	0.0272333817659014	12-oxophytodienoate reductase 3	1
MELO3C006681	0.00283034097739443	0.0272399629447186	bifunctional epoxide hydrolase 2-like	1
MELO3C015682	0.00283388627394909	0.0272607988427767	Zinc finger BED domain-containing protein DAYSLEEPER	0
MELO3C014199	0.00283809781829736	0.0272822307215747	E3 ubiquitin-protein ligase RING1-like	1
MELO3C010350	0.00283887711442787	0.0272822307215747	heme oxygenase 1, chloroplastic	1
MELO3C019326	0.00284198844840122	0.0272988472118073	Glutaredoxin	1
MELO3C011716	0.00285347093160948	0.0273958179039162	TBC1 domain family member 8B	1
MELO3C012175	0.00285815822128543	0.0274274862546968	Thioredoxin-like protein aaed1, chloroplastic	0
MELO3C025490	0.00286245136842622	0.0274553434070177	Protein TONNEAU 1b	1
MELO3C009188	0.00286979849156177	0.0274591329505104	transcription factor DIVARICATA-like	1
MELO3C006858	0.00286606413668511	0.0274591329505104	At5g51840	0
MELO3C016931	0.00286763125209966	0.0274591329505104	Hydroxyproline-rich glycoprotein	1
MELO3C020157	0.00286972839969413	0.0274591329505104	Glycerol-3-phosphate dehydrogenase [NAD(+)]	0
MELO3C018408	0.00286762071520663	0.0274591329505104	methyltransferase-like protein 13	0
MELO3C006576	0.00287199260083404	0.0274668193093808	ARM repeat superfamily protein	0
MELO3C008248	0.00287463929746568	0.0274788245332283	GRF1-interacting factor 3	1
MELO3C013852	0.00287625232888011	0.0274809420624351	Plant/protein	1
MELO3C007689	0.00289790596181549	0.0276681646798411	protein RMD5 homolog A	1
MELO3C008074	0.00289864968973574	0.0276681646798411	No data found	1
MELO3C012268	0.00290928855179373	0.0277428969625178	LEAF RUST 10 DISEASE-RESISTANCE LOCUS RECEPTOR-LIKE PROTEIN KINASE-like 1.2 isoform X4	0
MELO3C011953	0.00290852105031103	0.0277428969625178	Unknown protein	1
MELO3C022246	0.00291399362481704	0.0277743533284323	cytochrome P450 78A9-like	0
MELO3C002232	0.00292148187912489	0.0278188744603845	serine/threonine-protein kinase fray2	0
MELO3C009949	0.00292063003617526	0.0278188744603845	Pentatricopeptide repeat-containing protein	1
MELO3C026782	0.0029315704215952	0.027901486388474	Protein WVD2-like 3	1
MELO3C025699	0.00293717560620022	0.0279413685196763	Mitochondrial carrier protein	1
MELO3C015807	0.00294721274408638	0.0279586801462572	2-oxoglutarate (2OG) and Fe(II)-dependent oxygenase superfamily protein	0
MELO3C023406	0.00294286704306013	0.0279586801462572	Polygalacturonase	0
MELO3C025872	0.00294290350336335	0.0279586801462572	protein NRT1/ PTR FAMILY 8.1-like	1
MELO3C025854	0.00294734785833395	0.0279586801462572	No data found	1
MELO3C022411	0.00294748959767621	0.0279586801462572	No data found	1
MELO3C008481	0.00294454167237668	0.0279586801462572	Glutamate synthase 1 [nadh], chloroplastic	1
MELO3C017624	0.0029620275572394	0.0280830927642443	Superoxide dismutase	0
MELO3C021565	0.00296685498420146	0.0281103720538155	DExH-box ATP-dependent RNA helicase DExH17-like	1
MELO3C022694	0.00296775156879869	0.0281103720538155	Ethylene-responsive transcription factor	0
MELO3C012527	0.00297250118494685	0.0281418628482816	Guanine nucleotide-binding protein beta subunit-like protein	0
MELO3C019044	0.00298063279371774	0.0282044227419728	Tubulin folding cofactor B	1
MELO3C002058	0.00298196540003237	0.0282044227419728	PHD and RING finger domain-containing protein 1	1
MELO3C021929	0.00299072573288184	0.0282602117218581	B3 domain-containing transcription factor VRN1-like	1
MELO3C026077	0.0029907075838328	0.0282602117218581	leucine-rich repeat extensin-like protein 3	0
MELO3C009278	0.00299360468042398	0.0282738875340474	Pectin acetylesterase	1
MELO3C019004	0.00299954481518294	0.0282948581551635	ENTH/ANTH/VHS superfamily protein, putative	0
MELO3C022500	0.00300012319494214	0.0282948581551635	Vacuolar protein sorting 26	1
MELO3C018495	0.00299853266939398	0.0282948581551635	Carbohydrate esterase, putative (DUF303)	1
MELO3C016801	0.00300623854141413	0.028338999978228	aspartic proteinase-like protein 2	1
MELO3C007413	0.00301537223321668	0.0283981409417135	Core-2/I-branching beta-1,6-N-acetylglucosaminyltransferase family protein	1
MELO3C026638	0.0030153881996442	0.0283981409417135	acyl-protein thioesterase 2	0
MELO3C006943	0.00303125387801784	0.0285138619671975	Keratin-associated protein, putative (DUF819)	1
MELO3C017687	0.00303163409125018	0.0285138619671975	solute carrier family 35 member F1	0
MELO3C002719	0.00303345100982744	0.0285138619671975	60S ribosomal protein L18a	1

MELO3C010135	0.00303274871299286	0.0285138619671975	Kelch repeat-containing protein family	1
MELO3C007950	0.00304051349157075	0.0285394966468777	Thiol-disulfide oxidoreductase LTO1	1
MELO3C022482	0.00303891540561274	0.0285394966468777	SWI/SNF complex component SNF12 homolog	0
MELO3C011123	0.00303966505635012	0.0285394966468777	oleosin 1-like	0
MELO3C006635	0.00304572063851438	0.0285701369470703	transcription termination factor MTEF1, chloroplastic-like	0
MELO3C017786	0.00304667114337587	0.0285701369470703	GPI-anchored protein	1
MELO3C007580	0.003050768630666	0.028581418257601	phosphatidylinositol 3,4,5-trisphosphate 3-phosphatase and protein-tyrosine-phosphatase PTEN2A-like	1
MELO3C012211	0.00304978606683126	0.028581418257601	Coiled-coil domain-containing protein 130	0
MELO3C007841	0.00305590903747888	0.0286160016980419	Bacteriophage N4 adsorption B	1
MELO3C009328	0.00306327293243192	0.0286713635746909	Lectin receptor kinase-like protein	1
MELO3C013275	0.00307285130009638	0.0287238455479359	Eukaryotic translation initiation factor 3 subunit A, putative	0
MELO3C004134	0.00307469793348203	0.0287238455479359	leucine aminopeptidase 1-like	1
MELO3C025897	0.00307432554173359	0.0287238455479359	pumilio homolog 1-like	1
MELO3C026715	0.00307034640401294	0.0287238455479359	Tetratricopeptide repeat (TPR)-like superfamily protein	1
MELO3C019546	0.00308152563759556	0.0287740188259455	PRKR-interacting protein 1	0
MELO3C006945	0.00308380034190114	0.0287816507335566	mediator of RNA polymerase II transcription subunit 36a-like	0
MELO3C026015	0.00309308236949102	0.0288546451181285	cyclin-dependent kinase 11B-like	1
MELO3C015954	0.0030947715945715	0.0288567725312524	No data found	1
MELO3C023201	0.0030977794094238	0.0288575686588257	No data found	1
MELO3C025916	0.00309672394330129	0.0288575686588257	Triosephosphate isomerase, putative	0
MELO3C013879	0.00310242322052934	0.0288872023490023	Regulator of nonsense transcripts 1-like protein	1
MELO3C006833	0.00310508976483725	0.0288905872097688	AT-hook motif nuclear-localized protein 1	0
MELO3C019779	0.00310717541311201	0.0288905872097688	U4/U6 small nuclear ribonucleoprotein PRP4-like protein	1
MELO3C003821	0.00310708875855792	0.0288905872097688	agglutinin-like	1
MELO3C006596	0.00312259521677238	0.0290066476651166	squamosa promoter-binding-like protein 7	0
MELO3C016899	0.00312150091819829	0.0290066476651166	Mitochondrial carrier protein	1
MELO3C016315	0.00312509809007677	0.0290162492623066	Unknown protein	1
MELO3C024172	0.00313617279548883	0.0290917221879328	Histone deacetylase	1
MELO3C012716	0.00313511425606883	0.0290917221879328	ribonuclease 2-like	1
MELO3C006546	0.00313962609965124	0.0291100825549354	BRI1 kinase inhibitor 1-like	1
MELO3C007711	0.0031447472936853	0.0291438828263684	U-box domain-containing protein kinase family protein, putative	1
MELO3C011172	0.00314734549239759	0.0291542805484803	Proteasome subunit beta type	1
MELO3C020628	0.00314969349944749	0.0291623520490335	Protein kinase	0
MELO3C003368	0.0031518431083446	0.0291685799187898	Intron maturase, type II family protein	1
MELO3C018128	0.00315436270314007	0.0291782243673598	Pentatricopeptide repeat-containing protein	0
MELO3C026935	0.00315856654564306	0.0292034319802925	Homeobox-leucine zipper HOX24	0
MELO3C011323	0.0031636598807594	0.0292240016708344	No data found	1
MELO3C003790	0.00316375085180232	0.0292240016708344	subtilisin-like protease SBT3.17 isoform X1	0
MELO3C010057	0.00317500236112433	0.0293142223608436	WRKY transcription factor SUSIBA2-like isoform X2	1
MELO3C016435	0.00318004727588184	0.0293470811455095	PHD finger alfin-like protein	0
MELO3C026949	0.00318437434441865	0.0293732876823559	DNA ligase	0
MELO3C004179	0.0031931976062749	0.0294409241486102	RNA polymerase II-associated protein 3	1
MELO3C017665	0.00319763962111685	0.0294681217346882	Ubiquitin-protein ligase, putative	0
MELO3C020958	0.0032001673855715	0.0294776612395762	Shikimate kinase	0
MELO3C026019	0.00321334455151734	0.0295852408148792	Abscisic acid receptor	0
MELO3C027349	0.00321673340123285	0.0296026411653996	MACPF domain NSL1-like protein	1
MELO3C009275	0.00322209073351121	0.0296342880451715	No data found	1
MELO3C025912	0.00322317336174127	0.0296342880451715	Protein kinase	1
MELO3C013566	0.00323029250749773	0.0296859221640636	Indole-3-acetic acid-amido synthetase GH3.3	0
MELO3C006900	0.00323377434712158	0.0297040974796763	No data found	0
MELO3C008985	0.00323792539730006	0.0297284001261175	Glucose-6-phosphate 1-dehydrogenase	1
MELO3C011141	0.00324029178816565	0.0297363022883287	Transcriptional regulatory plant protein, putative	0
MELO3C020113	0.00324422109289979	0.029758533378392	ADP,ATP carrier protein	1
MELO3C023885	0.00324576723815473	0.0297588937726638	Tropinone reductase family protein	1
MELO3C010695	0.00325920601822216	0.0298682411386865	No data found	1
MELO3C011641	0.00326082986585996	0.0298692620690484	gamma-secretase subunit APH1-like	0
MELO3C015999	0.00327258479556591	0.0299630399293608	60S ribosomal protein L22-2	1
MELO3C002240	0.00327636508104368	0.0299837506883835	RING-type E3 ubiquitin transferase	1
MELO3C014270	0.00328035162177276	0.0300063289385781	No data found	1
MELO3C017682	0.00329068344277839	0.0300590690617162	extensin-2	0
MELO3C011626	0.00329055575005754	0.0300590690617162	Ribosomal protein S8	0
MELO3C010882	0.00328785247888019	0.0300590690617162	Origin recognition complex subunit 2 family protein	0
MELO3C015845	0.00329570830198256	0.030079897053516	basic 7S globulin 2	0

MELO3C006367	0.00329600978397937	0.030079897053516	histone-lysine N-methyltransferase family member SUVH9	1
MELO3C016702	0.00330136386296176	0.0301062021308803	translation initiation factor IF-1, chloroplastic	1
MELO3C018564	0.00330194105096393	0.0301062021308803	Protein trichome birefringence-like 12	1
MELO3C017142	0.00330403547657232	0.0301113966898139	tRNA (Ile)-lysidine synthase	1
MELO3C014696	0.00330563892729141	0.0301121140106449	Glycosyltransferase	0
MELO3C026387	0.00331292201755107	0.0301645444557935	Pentatricopeptide repeat-containing protein At3g59040	1
MELO3C024476	0.00332258243518369	0.0302260283252226	alpha carbonic anhydrase 7-like	0
MELO3C011977	0.00332273570783626	0.0302260283252226	polygalacturonase At1g48100	1
MELO3C006104	0.00332623952523958	0.0302439707108455	Atg8-interacting protein 1	1
MELO3C011450	0.00333358893825408	0.0302968467287528	Kelch repeat-containing F-box family protein	0
MELO3C016379	0.00333695453228211	0.0303134843873226	Ultraviolet-B receptor UVR8	1
MELO3C013981	0.00335602505490162	0.030418811552392	40S ribosomal protein S13	0
MELO3C024538	0.00335382112544536	0.030418811552392	zinc finger A20 and AN1 domain-containing stress-associated protein 4	1
MELO3C005084	0.00335625046193033	0.030418811552392	E3 ubiquitin-protein ligase	1
MELO3C021429	0.00335193882671869	0.030418811552392	Ribosomal protein	0
MELO3C004988	0.00335093209097537	0.030418811552392	Protein SIEL	1
MELO3C001354	0.00335814086479347	0.030421983458168	Kinase family protein	1
MELO3C012642	0.00336533823483554	0.0304732071525754	Glucan endo-1,3-beta-glucosidase-like protein 1	1
MELO3C004803	0.00336930114440837	0.0304951092121544	BnaC01g17260D protein	0
MELO3C014283	0.00337200910851509	0.0305056380595807	BIG SEEDS 1	1
MELO3C007612	0.00337643607475258	0.0305317014836486	molybdate-anion transporter	1
MELO3C022717	0.00338495688318097	0.0305947430141606	FHA domain-containing protein FHA2	0
MELO3C012390	0.00339255872463551	0.030635410266496	NAC domain-containing protein 53-like	0
MELO3C003646	0.00339160336545463	0.030635410266496	guanine nucleotide-binding protein subunit gamma 2-like	0
MELO3C007740	0.00339467117104308	0.0306404757572806	40S ribosomal protein S6-like	0
MELO3C012160	0.00339732236416479	0.0306437874748141	Protein BIG GRAIN 1-like E	1
MELO3C015670	0.00339843699782583	0.0306437874748141	Phosphatidylinositol N-acetylglucosaminyltransferase subunit A	0
MELO3C009826	0.0033996930658422	0.0306437874748141	Carboxypeptidase	0
MELO3C020709	0.00340145935932612	0.0306457212077242	K-stimulated pyrophosphate-energized sodium pump protein	0
MELO3C003618	0.00340400756003645	0.0306546946206839	Unknown protein	0
MELO3C003537	0.00340619799978614	0.0306604395158507	WD-40 repeat-containing protein MSI1	0
MELO3C005597	0.00341005728531718	0.0306784743320635	1-aminocyclopropane-1-carboxylate synthase	0
MELO3C012457	0.00341130840210702	0.0306784743320635	Annexin	1
MELO3C005446	0.00342424757612758	0.0307808217482675	60S ribosomal protein L13	1
MELO3C024964	0.00343821174470194	0.03089228559878	E3 ubiquitin-protein ligase	1
MELO3C012627	0.00344637204195242	0.0309515240820911	KRR1 small subunit processome component homolog	0
MELO3C008749	0.00344966036879268	0.0309669739196758	CBS domain-containing protein CBSX6	0
MELO3C025053	0.00345273664238088	0.0309805070197092	lysine-specific demethylase JMJ25	1
MELO3C017141	0.00345887223368579	0.03102146582337	Dynein light chain	0
MELO3C005776	0.00346706651856055	0.0310808427939411	Plant UBX domain-containing protein 10	1
MELO3C011443	0.00346914766687134	0.0310853889623603	Glycosyltransferase	0
MELO3C009159	0.00347745214263795	0.0311456700067832	ALC-interacting protein 1	1
MELO3C019807	0.00348962571938949	0.0312405341487865	Zinc finger (C3HC4-type RING finger) family protein	0
MELO3C004651	0.00349339114977409	0.0312600733198408	DENN (AEX-3) domain-containing protein	1
MELO3C016321	0.00351307924928468	0.0313935756082005	multiple RNA-binding domain-containing protein 1	0
MELO3C021455	0.00351239881555254	0.0313935756082005	BnaC04g30420D protein	0
MELO3C002644	0.00351114986297452	0.0313935756082005	Transcription factor	1
MELO3C013068	0.00352314090533479	0.0314579681657778	No data found	0
MELO3C007737	0.00352347083815385	0.0314579681657778	No data found	1
MELO3C003545	0.00352514241961388	0.0314586704224828	28 kDa ribonucleoprotein	1
MELO3C008002	0.0035312711957558	0.0314849096365604	serine/threonine-protein kinase D6PKL2	0
MELO3C013051	0.00353085892452476	0.0314849096365604	Dead box ATP-dependent RNA helicase, putative	1
MELO3C009284	0.00353465922443519	0.0314952662272863	Protein SLOW GREEN 1, chloroplastic	1
MELO3C006293	0.00354341023305915	0.0314952662272863	Werner Syndrome-like exonuclease	0
MELO3C006679	0.00354132679588104	0.0314952662272863	Dihydrolipoamide acetyltransferase component of pyruvate dehydrogenase complex	0
MELO3C016574	0.00353635905852601	0.0314952662272863	Serine/threonine-protein kinase	1
MELO3C017979	0.00354359621029066	0.0314952662272863	Bifunctional protein FolD	1
MELO3C018634	0.00353843304329915	0.0314952662272863	7-deoxyloganetin glucosyltransferase-like	0
MELO3C012787	0.00354012354896582	0.0314952662272863	Sterol 3-beta-glucosyltransferase	1
MELO3C002187	0.00354604168811656	0.0315028237960477	Plant/protein (DUF789)	0
MELO3C013699	0.00354782004554266	0.0315044505752797	Pectinesterase	1
MELO3C002921	0.00354961794420117	0.0315062493393388	Cysteine proteinase inhibitor	0

MELO3C011266	0.00355690370295292	0.0315425645395677	Histone acetyltransferase	0
MELO3C010886	0.00355680004882486	0.0315425645395677	Succinate dehydrogenase subunit 5, mitochondrial	1
MELO3C009118	0.00356566194604402	0.0316060402928291	TOM1-like protein 2	0
MELO3C003452	0.00357083843738115	0.0316377246746704	Synaptonemal complex protein 1	0
MELO3C027277	0.00357454085905751	0.031648946287679	Polygalacturonase	0
MELO3C006224	0.00357531010014744	0.031648946287679	HOPM interactor 7	1
MELO3C006942	0.00357863116017443	0.0316511025151031	Receptor-like protein kinase, putative	1
MELO3C012303	0.00357875902153149	0.0316511025151031	Trichome birefringence-like protein	0
MELO3C006470	0.00359422249341379	0.0317736347459395	p-loop nucleoside triphosphate hydrolase superfamily protein	0
MELO3C013634	0.00359595157280856	0.0317746969178507	DNA-directed RNA polymerase subunit beta	0
MELO3C016056	0.00360431063231181	0.0318343160454052	monothiol glutaredoxin-S11	1
MELO3C008871	0.00360628755649928	0.0318375381999572	Chaperone protein dnaJ, putative	1
MELO3C020139	0.00361941064351767	0.0319105985709065	No data found	1
MELO3C018700	0.00361828856415125	0.0319105985709065	UDP-glycosyltransferase 74F2-like	0
MELO3C009973	0.00361824768775709	0.0319105985709065	Dead box ATP-dependent RNA helicase, putative	0
MELO3C019010	0.00362104834108679	0.0319107914717193	No data found	0
MELO3C010566	0.00362510291757867	0.0319266674182015	Topoisomerase II-associated protein PAT1	0
MELO3C011769	0.00362608309377821	0.0319266674182015	Pyruvate kinase	1
MELO3C016706	0.00362792550019198	0.031928654502358	E3 ubiquitin-protein ligase RMA3	1
MELO3C012844	0.00363671067198779	0.0319917145038248	Glutathione S-transferase family protein	1
MELO3C017291	0.00364457998267875	0.0320466652172407	40S ribosomal protein S28	1
MELO3C020055	0.00365494902297803	0.0321235372740512	histidine kinase 4-like	1
MELO3C026594	0.00365773426356975	0.0321337161793767	E3 ubiquitin-protein ligase RGLG2	0
MELO3C004333	0.00366799011256524	0.0321861378545134	DCD (Development and Cell Death) domain protein	1
MELO3C003135	0.0036685906279057	0.0321861378545134	Ribonuclease II, chloroplastic/mitochondrial	1
MELO3C026250	0.00366806256004015	0.0321861378545134	Rhodanese-like domain-containing protein 11, chloroplastic	1
MELO3C014100	0.00367353119137726	0.0321994102008483	Heavy metal-associated isoprenylated plant protein 21	1
MELO3C019954	0.00367499471328736	0.0321994102008483	NAC domain-containing protein 17-like	0
MELO3C018086	0.00367393222298185	0.0321994102008483	No data found	0
MELO3C002364	0.00368322380190222	0.0322572003830452	glucuronoxylan 4-O-methyltransferase 1	0
MELO3C007651	0.00368605120965426	0.0322676530760027	BSD domain-containing protein	0
MELO3C017041	0.00369325977155832	0.032289034232494	Protein canopy 1-like	0
MELO3C005067	0.00369064033854793	0.032289034232494	dihydroorotate dehydrogenase (Quinone), mitochondrial-like	1
MELO3C011580	0.00369339856859607	0.032289034232494	Selenoprotein K	0
MELO3C011306	0.00370901783915945	0.0324112359759115	U2 snRNP-associated SURP motif-containing protein	0
MELO3C013737	0.00371380927877951	0.032438752519512	Eukaryotic translation initiation factor 3 subunit A, putative	1
MELO3C009047	0.00371812788353043	0.0324621165215926	Endonuclease/exonuclease/phosphatase family protein	1
MELO3C009362	0.00372330748990279	0.032484415475003	4-coumarate--CoA ligase-like 7	0
MELO3C021694	0.003723971676308	0.032484415475003	equilibrative nucleotide transporter 3-like	0
MELO3C018849	0.0037317716935662	0.0325380835215183	Glycosyltransferase	1
MELO3C004466	0.00373428926178776	0.0325456657683347	Alpha-galactosidase	1
MELO3C012147	0.00373986616904487	0.0325742299591907	Chromatin modification-related protein EAF7	0
MELO3C022715	0.00374086553989794	0.0325742299591907	E3 ubiquitin-protein ligase RNF4-like isoform X1	1
MELO3C018156	0.00374297430987069	0.0325782281382267	HEAT repeat-containing 8	1
MELO3C020756	0.00374575962541046	0.032588108741071	auxin-responsive protein SAUR24-like	0
MELO3C009313	0.00374905481299304	0.0326024145758694	MCM domain-containing protein	0
MELO3C021441	0.00375323054063759	0.0326243617724699	Low molecular weight protein-tyrosine-phosphatase, putative	1
MELO3C019256	0.00375711455194661	0.0326437550754041	Glutamate receptor	0
MELO3C017659	0.00376166987941229	0.03265460151583	Ribosomal protein L15	1
MELO3C023561	0.00376053621892014	0.03265460151583	Zinc finger, PHD-type	0
MELO3C025595	0.00377304170472659	0.0326903479823329	Hydroxyacylglutathione hydrolase 3, mitochondrial-like protein	0
MELO3C024527	0.00377219600226342	0.0326903479823329	Monodehydroascorbate reductase family protein	0
MELO3C021072	0.00376902665796097	0.0326903479823329	p-loop containing nucleoside triphosphate hydrolases superfamily protein, putative	0
MELO3C022135	0.00377269415701442	0.0326903479823329	Dynamin homolog	0
MELO3C003511	0.00377406417538706	0.0326903479823329	No data found	1
MELO3C009659	0.00378297423157448	0.0327359654708158	WD-repeat protein, putative	0
MELO3C012087	0.00378286641513303	0.0327359654708158	At1g69680/T6C23_12	0
MELO3C025844	0.00378430346700454	0.0327359654708158	zinc finger CCCH domain-containing protein 66	0
MELO3C005590	0.00378620329661872	0.0327380599408595	AT-hook motif nuclear-localized protein 1	0
MELO3C017128	0.00379795715646769	0.0328253198613043	two-component response regulator ARR5-like	1
MELO3C023131	0.00380245973358373	0.0328498588270101	Magnesium chelatase subunit	0
MELO3C022307	0.00380791780284617	0.0328826273233096	Pentatricopeptide repeat-containing family protein	1
MELO3C015877	0.00381685302485724	0.0329453804142944	Autophagy-related protein 18g	0

MELO3C018872	0.00382096715178948	0.0329664833030539	eukaryotic translation initiation factor 1A-like	0
MELO3C007206	0.00382538871009896	0.0329902190549102	Receptor-like kinase	0
MELO3C007781	0.0038398486676372	0.0331004676286194	C2 domain-containing family protein	0
MELO3C007981	0.00384716409883801	0.0331397649451927	Plant intracellular ras group-related LRR protein	1
MELO3C026665	0.0038477634826739	0.0331397649451927	BTB/POZ domain-containing protein At5g48800	0
MELO3C011206	0.00384958612008623	0.0331410097147267	dentin sialophosphoprotein-like	1
MELO3C016629	0.00385657378659299	0.0331759691273178	integrator complex subunit 9 homolog isoform X1	0
MELO3C004813	0.00385700668977274	0.0331759691273178	No data found	0
MELO3C002951	0.00386183647055627	0.0331771225999734	Peptidyl-prolyl cis-trans isomerase	0
MELO3C024701	0.00386218060951637	0.0331771225999734	Elongation factor Ts, mitochondrial	1
MELO3C022756	0.00385939753056552	0.0331771225999734	No data found	0
MELO3C006362	0.00387559388006831	0.0332591859056182	Beta-amylase	1
MELO3C016972	0.00388047519379775	0.0332591859056182	stromal cell-derived factor 2-like protein	0
MELO3C026799	0.00387701403635354	0.0332591859056182	Kinase family protein	1
MELO3C005658	0.00387972951477389	0.0332591859056182	O-glucosyltransferase rumi homolog	0
MELO3C002698	0.00388183824560484	0.0332591859056182	Eukaryotic translation initiation factor 4E	0
MELO3C017496	0.00387421851442116	0.0332591859056182	pathogenesis-related protein PR-1	0
MELO3C007029	0.00388454470007149	0.0332679415792332	glycine-rich RNA-binding protein 4, mitochondrial	0
MELO3C026403	0.00388878465702924	0.033289817161539	60S ribosomal protein L27	1
MELO3C012831	0.0038908092763863	0.0332927176773627	WD repeat-containing protein 26	0
MELO3C014561	0.00389493667687124	0.0333068362123798	Hydroxyproline O-arabinosyltransferase 1	1
MELO3C017322	0.00389583227761392	0.0333068362123798	LEAF RUST 10 DISEASE-RESISTANCE LOCUS RECEPTOR-LIKE PROTEIN KINASE-like 1.2 isoform X2	0
MELO3C004334	0.00390896641762595	0.0333732318117167	ERAD-associated E3 ubiquitin-protein ligase HRD1B-like	1
MELO3C006528	0.00391035791241645	0.0333732318117167	At1g05410/T25N20_5	1
MELO3C000756	0.00390717971422494	0.0333732318117167	Alanine--tRNA ligase	1
MELO3C026504	0.00390827463156984	0.0333732318117167	centromere protein V isoform X1	0
MELO3C013878	0.00391222575567463	0.0333747500858826	haloacid dehalogenase-like hydrolase domain-containing protein Sgpp	1
MELO3C025139	0.0039202516660019	0.0334275900689354	No data found	1
MELO3C002556	0.0039218049617562	0.0334275900689354	heterogeneous nuclear ribonucleoprotein U-like protein 1	1
MELO3C008158	0.00393031276265376	0.0334712146397797	Protein PLASTID MOVEMENT IMPAIRED 2	0
MELO3C019983	0.00392989468547922	0.0334712146397797	Wound-responsive family protein	0
MELO3C016939	0.00394970593609312	0.0335715480937751	Protein phosphatase 2c, putative	0
MELO3C008944	0.00394846519055947	0.0335715480937751	ultraviolet-B receptor UVR8 isoform X2	0
MELO3C011989	0.00395059384120378	0.0335715480937751	Unknown protein	1
MELO3C026495	0.00394489756670136	0.0335715480937751	cytochrome P450 CYP82D47-like	0
MELO3C013044	0.00394792703568192	0.0335715480937751	Serine/threonine-protein phosphatase 2A 55 kDa regulatory subunit B	0
MELO3C004163	0.00395312441178808	0.0335786038745818	trafficking protein particle complex subunit 4	1
MELO3C007919	0.00395536602137492	0.0335819377854541	alpha-mannosidase	0
MELO3C022017	0.00395691777946994	0.0335819377854541	Ribosomal protein L18/L5	0
MELO3C011127	0.00395892010502719	0.0335844987775695	receptor-like protein kinase HSL1	0
MELO3C002789	0.00396747730644487	0.0336426403284584	BnaCnng71930D protein	1
MELO3C013221	0.00397472788079656	0.0336507765001755	KH domain-containing protein	1
MELO3C007232	0.00397436879822932	0.0336507765001755	spermidine coumaroyl-CoA acyltransferase	1
MELO3C021281	0.00397525249759023	0.0336507765001755	Beta-D-xylosidase family protein	0
MELO3C018648	0.00397329808233615	0.0336507765001755	Annexin	0
MELO3C009755	0.00399223218178957	0.0336852876960037	Sigma factor binding protein 1, chloroplastic	1
MELO3C006187	0.00398992103329143	0.0336852876960037	Proteasome subunit beta type	1
MELO3C006954	0.00399297475803051	0.0336852876960037	Ornithine cyclodeaminase/mu-crystallin	0
MELO3C026373	0.0039887085281346	0.0336852876960037	Glycosyltransferase	0
MELO3C007648	0.00398694127513544	0.0336852876960037	RuvB-like helicase	0
MELO3C019798	0.00398754437598248	0.0336852876960037	Acyl-CoA N-acyltransferase domain protein	0
MELO3C011236	0.00398898589143037	0.0336852876960037	Peptidyl-prolyl cis-trans isomerase	1
MELO3C018126	0.00399118870471526	0.0336852876960037	Autophagy-related protein 18f	1
MELO3C006817	0.003994972976333	0.0336877546155424	pectinesterase-like	1
MELO3C009105	0.0040092906562702	0.0337845085349958	Receptor-like kinase plant-like protein	0
MELO3C022425	0.00400986824679883	0.0337845085349958	15 kDa selenoprotein	1
MELO3C026103	0.00401371508088511	0.0338024985639232	DUF538 family protein	0
MELO3C016780	0.00401640311312934	0.0338107182784277	ethylene-responsive transcription factor ERF011-like	0
MELO3C006678	0.00402069563885754	0.0338324321141021	DUF581 family protein, putative (DUF581)	0
MELO3C011227	0.00402447276814755	0.0338353821618331	zeaxanthin epoxidase, chloroplastic-like	0

MELO3C023474	0.00402423910770855	0.0338353821618331	Hydroxycinnamoyl-CoA shikimate/quinate hydroxycinnamoyltransferase	0
MELO3C015941	0.00403168091934258	0.0338815602025943	Long cell-linked locus protein, putative, expressed	1
MELO3C011726	0.00404263312343378	0.0339457259093174	Nuclear transcription factor Y subunit B	0
MELO3C017221	0.00404275392874143	0.0339457259093174	Histone deacetylase	1
MELO3C026210	0.00404664750198225	0.0339639785451115	SNF1-related protein kinase regulatory subunit gamma-1	0
MELO3C006574	0.00405142086150934	0.0339895966839201	guanylate kinase 3, chloroplastic-like	1
MELO3C006891	0.00405529113468006	0.0340076197956673	heat stress transcription factor B-2b-like	0
MELO3C002258	0.00406375095139522	0.0340640991252564	No data found	0
MELO3C007940	0.00406921847048769	0.0340954584529747	Protein phosphatase 2c, putative	1
MELO3C009601	0.00408256489346259	0.034175454074849	Dirigent protein	0
MELO3C006406	0.00409087920567841	0.034175454074849	Transducin/WD40 domain-like protein, putative	0
MELO3C008489	0.00408119611396818	0.034175454074849	Serine/threonine-protein kinase stt7, chloroplastic	1
MELO3C018935	0.00409080955661678	0.034175454074849	Unknown protein	1
MELO3C024610	0.004090155111938	0.034175454074849	Iron-sulfur binding oxidoreductase	0
MELO3C011869	0.00408858935710987	0.034175454074849	cytochrome P450 78A5-like	0
MELO3C019649	0.00408633114963042	0.034175454074849	auxin-responsive protein SAUR71	0
MELO3C016540	0.00409820484929724	0.0341932604853279	NAC domain protein	0
MELO3C024466	0.00409776864969524	0.0341932604853279	heavy metal-associated isoprenylated plant protein 3-like isoform X2	0
MELO3C015915	0.00409647381032929	0.0341932604853279	Heme binding	0
MELO3C013444	0.00410871929360257	0.0342665106965191	No data found	0
MELO3C011320	0.00411998198635644	0.0343459367870634	NAD(P)-binding rossmann-fold protein	0
MELO3C009370	0.00412796035380381	0.0343689245477535	ACT domain-containing protein	0
MELO3C024404	0.00412659958826311	0.0343689245477535	Tudor/PWWP/MBT superfamily protein	0
MELO3C015314	0.00412612017060354	0.0343689245477535	protein SRC2-like	0
MELO3C022568	0.00413550035043642	0.0344099668734598	protein indeterminate-domain 5, chloroplastic	0
MELO3C018374	0.00413637456871707	0.0344099668734598	DUF248-1	0
MELO3C024936	0.00413994951308028	0.03442520544582	Cleavage and polyadenylation specificity factor subunit	0
MELO3C005710	0.00414841548622957	0.0344810847801127	heavy metal-associated isoprenylated plant protein 3	0
MELO3C005504	0.00415565745621238	0.0345267476242063	Disease resistance family protein	0
MELO3C021144	0.00415874744190292	0.0345378903406816	squamosa promoter-binding-like protein 8	0
MELO3C014591	0.00417094646782634	0.0346116311413704	cyclin-dependent protein kinase inhibitor SMR3-like	0
MELO3C022382	0.00417453238090104	0.0346116311413704	Succinate--CoA ligase [ADP-forming] subunit beta, mitochondrial	0
MELO3C010664	0.00417184497662493	0.0346116311413704	F28C11.19	0
MELO3C003323	0.00417463696282061	0.0346116311413704	Myosin heavy chain-like protein	0
MELO3C021407	0.00418955137017907	0.0347207091941529	Stem-specific protein TSJT1	0
MELO3C004316	0.00419185506808106	0.0347252289175893	Prefoldin chaperone subunit family protein, putative	0
MELO3C017094	0.00419379751734894	0.0347267535304504	No data found	0
MELO3C011908	0.00419762735150164	0.0347438988117376	Heat shock protein HSP26	0
MELO3C002084	0.00420015070006774	0.0347502204338659	Protein NEGATIVE REGULATOR OF RESISTANCE	0
MELO3C017520	0.00420329844082712	0.0347617005476946	L-allo-threonine aldolase	0
MELO3C027370	0.00420544322376737	0.0347648799607291	O-methyltransferase, putative	0
MELO3C011799	0.00420786589404742	0.0347703529462521	Cytochrome P450	0
MELO3C021944	0.00421779613002127	0.0348378317740652	Flavoprotein wrbA	0
MELO3C013419	0.00423115977641308	0.0349094003953484	30S ribosomal protein S31, mitochondrial	0
MELO3C012361	0.00422999190468754	0.0349094003953484	cell division control protein 2 homolog A	0
MELO3C027137	0.00423176386381408	0.0349094003953484	Gibberellin receptor GID1A	0
MELO3C004239	0.00424349429512305	0.0349623566267773	Zinc finger protein VAR3, chloroplastic	0
MELO3C016852	0.00424135737752129	0.0349623566267773	zinc finger CCCH domain-containing protein 20-like	1
MELO3C007071	0.00424254602009433	0.0349623566267773	WPP domain associated protein	1
MELO3C006348	0.00425488104939142	0.0350415537299546	PHD finger protein ING	1
MELO3C009713	0.00425803339606046	0.0350528976818666	translation factor GUF1 homolog, chloroplastic	1
MELO3C019295	0.00426894623574081	0.0351280913373522	Cellulose synthase family protein	0
MELO3C013835	0.00427577875347029	0.0351696603924552	Heat shock transcription factor family protein	0
MELO3C017571	0.00428197580447165	0.0352059700926356	alanine--glyoxylate aminotransferase 2 homolog 1, mitochondrial	1
MELO3C017989	0.00430088886261248	0.0353173613919892	PXMP2/4 family protein 4	0
MELO3C021636	0.00429798729381359	0.0353173613919892	No data found	1
MELO3C025550	0.00429966579888252	0.0353173613919892	No data found	1
MELO3C004637	0.00431383370119853	0.0354089367269201	pre-mRNA cleavage factor Im 25 kDa subunit 1	1
MELO3C009787	0.00431780204327548	0.0354267854394048	Protein SRC1	0
MELO3C002515	0.00433020588612543	0.0355138023443069	Eukaryotic translation initiation factor-like protein	1
MELO3C024896	0.00433539021546703	0.035541561380348	Calcium-dependent lipid-binding (CaLB domain) family protein	1
MELO3C004382	0.00433957988353706	0.035551505038091	Auxin-responsive protein	0

MELO3C005089	0.00434194979060565	0.035551505038091	40S ribosomal protein S27	1
MELO3C003793	0.0043420036534445	0.035551505038091	GTP-binding protein hflx, putative	1
MELO3C015857	0.00434471017132754	0.0355589229894519	No data found	1
MELO3C017187	0.00435977689092781	0.0356231832101503	Pectinesterase inhibitor	1
MELO3C007635	0.00435740828139641	0.0356231832101503	F-box protein, putative	1
MELO3C008977	0.00435899313719323	0.0356231832101503	Kinesin-like protein	1
MELO3C022236	0.00435478022543923	0.0356231832101503	Cation/H(+) antiporter 11	0
MELO3C019833	0.00436921025270542	0.0356854976346896	Glycine-rich RNA-binding family protein	0
MELO3C025454	0.00438074020671109	0.0357648773635127	2-oxoglutarate dehydrogenase E1 component family protein	0
MELO3C013892	0.00438636358545552	0.0357959894418021	Calcineurin B-like protein	1
MELO3C007055	0.00439030907538485	0.0358133886533562	reticuline oxidase-like protein	1
MELO3C017245	0.004395158508533	0.0358381442547557	squamosa promoter-binding-like protein 6	0
MELO3C020908	0.00439808294774702	0.0358471894903243	Glycosyl hydrolase family 43 protein	1
MELO3C017365	0.004401984544528	0.0358543790682549	DEAD-box ATP-dependent RNA helicase 42	1
MELO3C011106	0.00440441154588012	0.0358543790682549	Pentatricopeptide repeat-containing protein	1
MELO3C012982	0.00440400022067899	0.0358543790682549	Bet1-like SNARE 1-1	0
MELO3C006555	0.00441530169934157	0.0358838655392167	NEDD8-activating enzyme E1 catalytic subunit	1
MELO3C017756	0.0044125107954931	0.0358838655392167	calcium-dependent protein kinase 24	0
MELO3C022535	0.00441084542698378	0.0358838655392167	Methionine adenosyltransferase 2 subunit beta	0
MELO3C011419	0.00441372812875063	0.0358838655392167	Purple acid phosphatase	0
MELO3C011719	0.00441889278353991	0.0358951901894086	Adenylate kinase	0
MELO3C027061	0.00442033027194499	0.0358951901894086	PLATZ transcription factor family protein	1
MELO3C025492	0.00442331481104608	0.0359046626400941	transcription initiation factor TFIID subunit 1-like	0
MELO3C014781	0.00443181098567713	0.0359466902553953	AT5g13970/MAC12_6	1
MELO3C013364	0.00443433490235257	0.0359466902553953	MYB-related transcription factor	1
MELO3C007317	0.00443550104810231	0.0359466902553953	Transmembrane protein, putative	0
MELO3C027082	0.0044357731607878	0.0359466902553953	transcription factor bHLH149-like	1
MELO3C006341	0.00444064861850657	0.0359683622052152	Holliday junction resolvase	0
MELO3C026519	0.00444300260802799	0.0359683622052152	AT-hook motif nuclear-localized protein 10	0
MELO3C013004	0.00444391127554433	0.0359683622052152	protein IQ-DOMAIN 14-like	0
MELO3C007001	0.00444609229565951	0.035971272735346	Peptidylprolyl isomerase	1
MELO3C012080	0.00444939745034345	0.03598327200935	binding partner of ACD11 1	0
MELO3C016733	0.00445369614312496	0.0360032931357245	Estradiol 17-beta-dehydrogenase 1	0
MELO3C017857	0.00447660665509919	0.0361736926479353	Unknown protein	0
MELO3C025196	0.00448195650987304	0.0362021100668641	CTD small phosphatase-like protein	1
MELO3C006795	0.00448602272104126	0.0362201401135911	F-box protein SKIP16	1
MELO3C002811	0.00448958909934571	0.0362341214233668	SWIM zinc finger family protein	0
MELO3C009686	0.00449453289572133	0.0362592034957518	Pleiotropic drug resistance ABC transporter	1
MELO3C018333	0.00451435304406078	0.0364042295905089	Six-bladed beta-propeller, TolB-like protein	0
MELO3C009569	0.00452389862146674	0.0364365717273029	Gb|AAF02136.1	1
MELO3C017023	0.00452304563686967	0.0364365717273029	Catalase	0
MELO3C023402	0.00452320197757028	0.0364365717273029	Biotin carboxyl carrier protein of acetyl-CoA carboxylase	1
MELO3C018884	0.00453160110978612	0.0364688632099291	No data found	0
MELO3C024747	0.00453016901239933	0.0364688632099291	30S ribosomal protein S5, putative	0
MELO3C002054	0.00454481945338836	0.0365603419083367	Movement protein binding protein 2C	1
MELO3C002292	0.00454712501382337	0.0365639950724747	transcription factor MYB86-like	1
MELO3C014381	0.00455362792746339	0.0366013829627491	Arginine/glutamate-rich 1 protein	0
MELO3C017274	0.00455931809361776	0.0366322103461583	G patch domain-containing protein TGH	1
MELO3C005627	0.00457680273778194	0.0367577378074239	UDP-galactose/UDP-glucose transporter 2	1
MELO3C011270	0.0045788351918522	0.0367591122780037	Adenine phosphoribosyltransferase, putative	0
MELO3C021242	0.00458194269778134	0.0367691126934107	YTH domain family protein 2	1
MELO3C022180	0.00458428047942672	0.0367729306207141	Protein DETOXIFICATION	1
MELO3C007661	0.00458836570581656	0.036790756932266	Transmembrane protein, putative	1
MELO3C009581	0.00459335511739778	0.036793997135694	D-lactate dehydrogenase, putative	1
MELO3C021302	0.00459515873505412	0.036793997135694	Phosphatase 2C (PP2C)-like protein	0
MELO3C002611	0.00459421197278376	0.036793997135694	VQ motif-containing protein	0
MELO3C022766	0.00459622213447552	0.036793997135694	50S ribosomal protein L35	0
MELO3C013309	0.00461226279515592	0.0368639930026092	Coiled-coil protein	0
MELO3C007896	0.00461243236161057	0.0368639930026092	DNA ligase 3	0
MELO3C022208	0.00461235112080338	0.0368639930026092	Transmembrane protein, putative	0
MELO3C002241	0.00460760544686867	0.0368639930026092	Protein ROS1	0
MELO3C022174	0.00461874366324821	0.0368845809160894	molybdopterin synthase sulfur carrier subunit	1

MELO3C021458	0.00461777456584467	0.0368845809160894	glucomannan 4-beta-mannosyltransferase 9-like	0
MELO3C014961	0.00462684788511114	0.0369343649486903	No data found	0
MELO3C007108	0.00462896316894279	0.0369363206559399	Auxilin-related protein 2	0
MELO3C024729	0.0046335805594675	0.0369582320149126	NADH dehydrogenase [ubiquinone] iron-sulfur protein 6, mitochondrial	1
MELO3C025893	0.00464191527612789	0.0370097637417238	chaperone protein DnaJ	1
MELO3C010631	0.00465069359190351	0.0370647892439477	replication factor C subunit 5	1
MELO3C018500	0.00466513527941126	0.0371648877100012	TIP41-like family protein	1
MELO3C007936	0.00466850680925801	0.0371767503935631	aspartyl protease family protein 1-like	1
MELO3C014298	0.00468816507599967	0.0372301209290144	CST complex subunit STN1	1
MELO3C006119	0.00467883824833293	0.0372301209290144	Remorin	1
MELO3C025122	0.00469406507564141	0.0372301209290144	Transmembrane protein, putative	0
MELO3C024352	0.00469137170648004	0.0372301209290144	Transcription initiation factor TFIID subunit 9	1
MELO3C012231	0.00468490302386826	0.0372301209290144	Homologous-pairing protein 2-like protein	1
MELO3C011942	0.0046793778862565	0.0372301209290144	E3 ubiquitin-protein ligase	1
MELO3C002254	0.00469046994419164	0.0372301209290144	No data found	0
MELO3C010334	0.00469594567999265	0.0372301209290144	Non-specific serine/threonine protein kinase	1
MELO3C018609	0.00468423052131772	0.0372301209290144	nicotinamidase 1-like	0
MELO3C018637	0.00469303610003224	0.0372301209290144	outer envelope protein 64, mitochondrial	1
MELO3C010982	0.00469150142351815	0.0372301209290144	cysteine proteinase RD19a-like	0
MELO3C010869	0.00470255932622954	0.0372675939541361	Calcium-binding EF-hand	0
MELO3C008126	0.00471205326936386	0.0373278539978607	receptor homology region, transmembrane domain- and RING domain-containing protein 2-like isoform X2	0
MELO3C024467	0.0047202723733617	0.037348183901565	No data found	0
MELO3C005850	0.00472341949742638	0.037348183901565	S-type anion channel SLAH2	1
MELO3C011045	0.00471896157234275	0.037348183901565	Histone H3	1
MELO3C003619	0.00472073883878732	0.037348183901565	serine/arginine-rich splicing factor RSZ22A	1
MELO3C018767	0.00472407531450247	0.037348183901565	Wound-responsive family protein	1
MELO3C006522	0.00474301631824137	0.0374679317075795	Acyl-CoA N-acyltransferases (NAT) superfamily protein, putative	1
MELO3C020620	0.00474164902427332	0.0374679317075795	telomere repeat-binding protein 5-like	0
MELO3C003924	0.00475797865690586	0.0375710997581903	Nuclear speckle splicing regulatory-like protein (DUF2040)	1
MELO3C007388	0.00476193222621446	0.0375724900381318	calcium-dependent protein kinase-like	0
MELO3C022903	0.00476195972279325	0.0375724900381318	No data found	1
MELO3C017526	0.00476558186294107	0.0375860528000093	No data found	0
MELO3C010860	0.00476961101908036	0.0376028135791688	thioredoxin-like 4, chloroplastic	0
MELO3C015779	0.00477524685384889	0.0376322227121555	peptidyl-prolyl cis-trans isomerase CYP63	1
MELO3C006867	0.00478082614067543	0.0376461465120411	ATP-dependent Clp protease ATP-binding subunit clpX	1
MELO3C024282	0.00477892180585116	0.0376461465120411	DUF3820 family protein	1
MELO3C021352	0.00478487268238359	0.0376629934652824	No data found	1
MELO3C025264	0.00480324345966632	0.0377390862236877	Auxin efflux carrier	0
MELO3C026332	0.00480409452460129	0.0377390862236877	DNA helicase INO80-like protein	1
MELO3C024359	0.00479821584987294	0.0377390862236877	40S ribosomal S3-like protein	0
MELO3C021766	0.00480031640730605	0.0377390862236877	Cysteine proteinase inhibitor	0
MELO3C010205	0.00480220260665098	0.0377390862236877	Myosin-binding protein 7	0
MELO3C026379	0.00481892308236753	0.0378405216515612	choline-phosphate cytidylyltransferase 2-like	0
MELO3C004128	0.00482450500558018	0.0378692962461061	hepatoma-derived growth factor-related protein 2-like isoform X1	0
MELO3C006557	0.00482848374613742	0.0378854690117076	ATP-dependent (S)-NAD(P)H-hydrate dehydratase	0
MELO3C014503	0.00484227068846665	0.0379785559279301	Nuclear transcription factor Y subunit B	0
MELO3C004504	0.004853594233164	0.0380522558597681	SPX domain-containing protein 1	0
MELO3C009653	0.00486423822417426	0.0381054504915579	transcription factor bHLH48	1
MELO3C019979	0.00486300975469733	0.0381054504915579	40S ribosomal protein S18	0
MELO3C006846	0.00486680411514517	0.038110433969073	Mitochondrial metalloendopeptidase OMA1	1
MELO3C023373	0.00488233112164127	0.0381563740883631	Aspartate aminotransferase	1
MELO3C020848	0.00488021440735875	0.0381563740883631	AP2-like ethylene-responsive transcription factor TOE3 isoform X1	1
MELO3C021380	0.00487514380395182	0.0381563740883631	Prolyl 4-hydroxylase alpha subunit, putative	0
MELO3C011261	0.0048818429137143	0.0381563740883631	Peroxidase	1
MELO3C009865	0.00488061309291565	0.0381563740883631	No data found	0
MELO3C017766	0.0048895206154731	0.0381974456625705	Ras family	1
MELO3C024047	0.00489669867223619	0.0382383954440461	Kelch repeat-containing F-box family protein	1
MELO3C023098	0.00490672223331468	0.0383015246583919	No data found	1
MELO3C014607	0.00491102235340035	0.038307474285644	Zinc transporter ZTP29	1
MELO3C011936	0.00491136386101831	0.038307474285644	protein-tyrosine-phosphatase MKP1-like	0
MELO3C014848	0.00492368631958517	0.0383581385110405	Zinc finger, RING-type	0

MELO3C004616	0.00492100162867981	0.0383581385110405	No data found	0
MELO3C013809	0.00492199748758904	0.0383581385110405	calcium permeable stress-gated cation channel 1-like	0
MELO3C023525	0.00493771673994492	0.0384457842027261	60S ribosomal protein L6	0
MELO3C024980	0.00493883004315743	0.0384457842027261	No data found	1
MELO3C005683	0.0049435184544383	0.0384671181862498	UDP-N-acetylmuramoyl-L-alanyl-D-glutamate--2, 6-diaminopimelate ligase	0
MELO3C026427	0.00494570982192477	0.0384690127109855	B-cell receptor-associated 31-like protein	1
MELO3C014560	0.00496315380380685	0.0385743110867302	Phospholipase A2	1
MELO3C024468	0.00496279709271841	0.0385743110867302	Thioredoxin, putative	1
MELO3C014666	0.00496701622528295	0.0385853581760918	Dirigent protein	0
MELO3C022914	0.00496848275061024	0.0385853581760918	50S ribosomal protein L15	0
MELO3C002200	0.00497295451208024	0.0386049051332833	ABC transporter A family protein	0
MELO3C005243	0.00498172170978672	0.0386577689770444	purple acid phosphatase 4-like	0
MELO3C004555	0.00498570584906988	0.0386734897145644	At3g13227	1
MELO3C019021	0.00499094402569167	0.0386837337375921	Endoplasmic reticulum-Golgi intermediate compartment 3	1
MELO3C026734	0.00499084688857632	0.0386837337375921	lamin-like protein	0
MELO3C024947	0.00499678096282596	0.0386903771333979	Inner centromere protein, ARK-binding region protein	1
MELO3C016831	0.00499389552060658	0.0386903771333979	RING-type E3 ubiquitin transferase	0
MELO3C024452	0.00499963757377242	0.0386903771333979	No data found	0
MELO3C018867	0.00499926959078445	0.0386903771333979	E6-like protein	0
MELO3C017478	0.00500308520310322	0.0387018917650159	Xyloglucan endotransglucosylase/hydrolase	1
MELO3C020617	0.00500844294115677	0.0387281674412314	Haloacid dehalogenase-like hydrolase	0
MELO3C002030	0.00501632420632747	0.0387739282781844	Glycine-rich RNA-binding protein	0
MELO3C009465	0.00502843552261645	0.0388523369077278	Terminal flower 1	0
MELO3C018257	0.00503800739884341	0.038911070832913	No data found	0
MELO3C002891	0.00504688773087425	0.0389644197799201	Pseudouridine synthase, RsuA/RluB/C/D/E/F	0
MELO3C006299	0.00505397492352333	0.0389713767143541	RNA-directed DNA polymerase (Reverse transcriptase)-related family protein	0
MELO3C022027	0.0050556821683212	0.0389713767143541	40S ribosomal protein S19	0
MELO3C021713	0.00505438158441507	0.0389713767143541	Ubiquinol oxidase	0
MELO3C012854	0.00505464637579456	0.0389713767143541	Long-chain-alcohol oxidase	0
MELO3C010569	0.00506299294919321	0.0390125040006308	Obg-like ATPase 1	1
MELO3C008932	0.00506938195028461	0.0390464992730775	thioredoxin-like 3-1, chloroplastic	1
MELO3C009748	0.00507356902590583	0.0390635145000446	Pentatricopeptide repeat-containing protein At1g80270, mitochondrial	1
MELO3C020574	0.00507969128465335	0.0390954104367183	No data found	1
MELO3C017092	0.00509335428043201	0.0391808196243162	diphthine methyltransferase	0
MELO3C018572	0.00509558321440995	0.0391808196243162	glutamate-1-semialdehyde 2,1-aminomutase 2, chloroplastic-like	0
MELO3C010865	0.00509674037241725	0.0391808196243162	Calcium-binding EF-hand family protein, putative	1
MELO3C002653	0.00510434896997825	0.0392240419486772	No data found	1
MELO3C002679	0.00510933008744363	0.0392470478012152	heat stress transcription factor A-4c	0
MELO3C017563	0.00512088786410558	0.0393052524011742	Protein AE7	1
MELO3C013472	0.0051198180085511	0.0393052524011742	Histone deacetylase	0
MELO3C019542	0.00513228821363398	0.0393774514106673	D-3-phosphoglycerate dehydrogenase	0
MELO3C016667	0.00514137660805702	0.0393847987498828	Random slug protein 5	0
MELO3C012583	0.00513599158009104	0.0393847987498828	nuclear-pore anchor-like	0
MELO3C021691	0.00514153474524282	0.0393847987498828	F-box protein family	0
MELO3C015299	0.00514189399425591	0.0393847987498828	serine/arginine-rich splicing factor SR30	0
MELO3C018610	0.0051432171743353	0.0393847987498828	Fructose-1,6-bisphosphatase	0
MELO3C014936	0.0051599163782603	0.0394820567819693	BRO1 domain-containing protein	0
MELO3C016335	0.00515823944960314	0.0394820567819693	F22C12.19	0
MELO3C022426	0.0051671505635198	0.0395220977842573	Something about silencing protein	0
MELO3C015455	0.00517018623505283	0.0395300069516293	Acyl--UDP-N-acetylglucosamine O-acyltransferase	1
MELO3C012084	0.00517341272002758	0.0395393683466814	40S ribosomal protein S9, putative	0
MELO3C007190	0.00518428034658769	0.0396070996382051	Splicing factor 3B, subunit 5	0
MELO3C024869	0.0051870663759751	0.0396130602703528	No data found	1
MELO3C005803	0.00519167594605396	0.0396329370926246	WAT1-related protein	0
MELO3C014288	0.00520148075471183	0.0396924433635255	VAN3-binding protein	0
MELO3C016221	0.00520810517208448	0.0397171785628582	ABC transporter G family member 14	0
MELO3C010745	0.00520874436567942	0.0397171785628582	mitochondrial import receptor subunit TOM20-like	1
MELO3C020579	0.00521804986638397	0.0397727776191497	Enolase	1
MELO3C013820	0.00522492446332201	0.0397791184372191	bZIP transcription factor 16	1
MELO3C022417	0.00522320791153241	0.0397791184372191	RNA-binding protein 24-B	1
MELO3C004917	0.00522269622442229	0.0397791184372191	sulfite oxidase-like	0

MELO3C006182	0.00523154057570219	0.0398141405894191	Pentatricopeptide repeat-containing protein At1g01970	0
MELO3C012683	0.00524867626788583	0.0399196237807747	Pentatricopeptide repeat-containing protein, mitochondrial	1
MELO3C022310	0.00524944366594116	0.0399196237807747	Histidine kinase	0
MELO3C005215	0.0052570899040556	0.0399623820304827	defensin Ec-AMP-D2-like	0
MELO3C019137	0.00526112589863548	0.0399776742486156	Plant/MNJ7-17 protein, putative	0
MELO3C017906	0.00526885628831797	0.0400210164761506	acyl-protein thioesterase 2	1
MELO3C007409	0.00527492254906536	0.0400516898967673	WRKY family transcription factor	0
MELO3C006221	0.00527834117750325	0.0400544508958836	Glutathione s-transferase, putative	0
MELO3C006760	0.00527934253288698	0.0400544508958836	Chromatin structure-remodeling complex protein BSH	0
MELO3C007195	0.00528427713697965	0.040066299931388	ER lumen protein-retaining receptor	1
MELO3C010941	0.00528496183711913	0.040066299931388	3-ketoacyl-CoA synthase	0
MELO3C008118	0.0052918874227319	0.0400863298080399	Inner membrane protein oxaA	0
MELO3C025023	0.00529572304770753	0.0400863298080399	thioredoxin-like protein slr0233	1
MELO3C003627	0.00529445457556355	0.0400863298080399	Transcriptional adapter 1	0
MELO3C003690	0.00529425199930755	0.0400863298080399	adenine nucleotide transporter BT1, chloroplastic/mitochondrial-like	0
MELO3C011062	0.00531329000863789	0.0402038943986934	Serine hydrolase FSH	1
MELO3C007688	0.00531587170426806	0.0402080238558368	tRNA-dihydrouridine synthase	0
MELO3C011704	0.00532175202668261	0.0402370906489108	RAS-related protein RABC1	1
MELO3C020748	0.00533361546979561	0.0402651268780556	Receptor-like protein kinase	0
MELO3C001920	0.00533117758364088	0.0402651268780556	No data found	0
MELO3C015481	0.00533354470146574	0.0402651268780556	Chloroplastic group IIA intron splicing facilitator CRS1	0
MELO3C011279	0.00532757903706893	0.0402651268780556	Hydroxyproline O-arabinosyltransferase 1	1
MELO3C005634	0.00533638245875689	0.0402706217722545	phosphatidylinositol glycan anchor biosynthesis class U protein-like	0
MELO3C012881	0.00533881960791294	0.0402736243073616	rho-N domain-containing protein 1, chloroplastic isoform X3	1
MELO3C023004	0.00534674243286837	0.040294608949124	casein kinase I-like isoform X1	0
MELO3C004825	0.00534772241914294	0.040294608949124	Ser/thr-rich protein T10 in DGCR region-like protein	1
MELO3C026640	0.00534644158281883	0.040294608949124	Mitogen-activated protein kinase kinase kinase 1 isoform 1	1
MELO3C007000	0.0053577184510808	0.0403545315371452	Katanin p80 WD40 repeat-containing subunit B1 homolog	1
MELO3C012295	0.00536354190955324	0.0403829924406279	Tetratricopeptide repeat-like superfamily protein	0
MELO3C012912	0.00536579815994709	0.0403845837884127	Chlorophyll a-b binding protein, chloroplastic	0
MELO3C002072	0.00536839161606895	0.0403887108669507	Adenine nucleotide alpha hydrolases-like superfamily protein	0
MELO3C014951	0.00538851756489089	0.0405092628051124	tRNA/rRNA methyltransferase family protein	0
MELO3C020489	0.00538680953554949	0.0405092628051124	WRKY transcription factor 1	0
MELO3C005380	0.00539842275126157	0.0405682842141038	protein phosphatase inhibitor 2	0
MELO3C009151	0.00540405465087668	0.0405797244487314	phosphoinositide phosphatase SAC8	0
MELO3C023173	0.00540260609983467	0.0405797244487314	sister chromatid cohesion 1 protein 3	1
MELO3C016700	0.00541295604689029	0.0406186957918544	Inner membrane protein oxaA	0
MELO3C024248	0.00541360366330046	0.0406186957918544	Dynein light chain family protein	0
MELO3C002313	0.00541541475618779	0.0406186957918544	Serine/threonine-protein kinase AFC2	1
MELO3C015113	0.00542243994015512	0.0406559477517553	Protein SMG7	0
MELO3C007235	0.00543615744316983	0.0407433295427556	Protein IQ-DOMAIN 1	0
MELO3C017551	0.00544379027512432	0.0407695920149526	Pentatricopeptide repeat-containing protein	0
MELO3C017169	0.0054419971112214	0.0407695920149526	60S ribosomal protein L34	0
MELO3C002293	0.00544667677743771	0.0407757466556548	Armadillo/beta-catenin repeat family protein	0
MELO3C009170	0.00545100219701766	0.0407926647930662	vacuolar cation/proton exchanger 3-like	0
MELO3C016881	0.00546445639647308	0.0408778596113435	Cytokinin riboside 5'-monophosphate phosphoribohydrolase	0
MELO3C010023	0.00548021836409496	0.0409802470550971	Ycf20-like protein	1
MELO3C022605	0.00548519315338203	0.0410019226291225	thiamine biosynthetic bifunctional enzyme TH1, chloroplastic-like	0
MELO3C006643	0.00548775039087324	0.0410039815297562	E3 ubiquitin-protein ligase	1
MELO3C019156	0.00549336446814186	0.0410039815297562	protein GrpE	0
MELO3C022885	0.00549564783216616	0.0410039815297562	methyl-CpG-binding domain protein 4-like protein	1
MELO3C015423	0.00549259467745444	0.0410039815297562	Damaged dna-binding 2, putative isoform 1	0
MELO3C026577	0.00549584987134866	0.0410039815297562	mitogen-activated protein kinase kinase 3	0
MELO3C022961	0.00549927721920196	0.0410140580823336	4-hydroxyphenylpyruvate dioxygenase	0
MELO3C009329	0.00550540936501021	0.0410288036036176	Peroxidase	0
MELO3C024348	0.00550384303802409	0.0410288036036176	Lipoxygenase	0
MELO3C005298	0.00551011550099556	0.0410336646483313	DELLA protein GAI	0
MELO3C003554	0.00551021715769784	0.0410336646483313	homeobox-leucine zipper protein ATHB-6-like	0
MELO3C009549	0.00551926640667522	0.0410855605975985	No data found	0
MELO3C017925	0.00552454836960814	0.0410939004713338	Myb transcription factor	1
MELO3C022530	0.00552368037194162	0.0410939004713338	Armadillo/beta-catenin repeat family protein	1
MELO3C011897	0.00553231331154147	0.0411361655081448	F-box protein SKIP14	1

MELO3C003453	0.00554160058650854	0.041189713956702	eukaryotic translation initiation factor 3 subunit L-like	1
MELO3C023308	0.0055442020245402	0.0411935461936209	F-box protein At2g16365	1
MELO3C006093	0.00554875124716214	0.0412118421888699	UDP-glycosyltransferase 91A1-like	0
MELO3C006553	0.00555487297960233	0.0412417994263784	3-dehydrosphinganine reductase TSC10A isoform X1	0
MELO3C022742	0.00556230935646029	0.0412814909735943	ATP-dependent DNA helicase, RecQ family protein, expressed	1
MELO3C009753	0.00556782329136662	0.0412913789640253	Transcription factor PERIANTHIA	0
MELO3C005559	0.00556759058409906	0.0412913789640253	transaldolase	0
MELO3C021715	0.00555844146050554 3	0.0413988753886035	E3 ubiquitin-protein ligase COP1-like	0
MELO3C026293	0.00561249329691038	0.041591418431776	DUF1645 family protein	1
MELO3C021818	0.00561839821362631	0.0416195597602798	Protein LIGHT-DEPENDENT SHORT HYPOCOTYLS 10	1
MELO3C013030	0.00562152618538336	0.0416271168485699	Tudor/PWWP/MBT superfamily protein	0
MELO3C017430	0.0056314445582144	0.0416849320015653	Fiber protein Fb15	1
MELO3C007563	0.00564058020111158	0.0416900517933206	Lipase	0
MELO3C026567	0.00563811290088667	0.0416900517933206	Pentatricopeptide repeat-containing protein At4g18975, chloroplastic	1
MELO3C013581	0.00563795363412223	0.0416900517933206	shaggy-related protein kinase eta	0
MELO3C008152	0.00563998177954761	0.0416900517933206	Class I glutamine amidotransferase-like superfamily protein	0
MELO3C022309	0.00564333704074471	0.0416948235008108	Ectonucleotide pyrophosphatase/phosphodiesterase family member 3	1
MELO3C019429	0.00564600559118555	0.0416989395737934	Basic-leucine zipper (BZIP) transcription factor family protein	1
MELO3C014876	0.00565538385941067	0.041752589098879	Kelch repeat-containing F-box family protein	0
MELO3C016778	0.00565933442381517	0.0417661418295686	SPla/RYanodine receptor (SPRY) domain protein	0
MELO3C004117	0.00566929710292929	0.0418240375367018	Carboxypeptidase	0
MELO3C007636	0.00567263519002581	0.0418330367318221	Calcium-transporting ATPase	0
MELO3C020997	0.00568704454460378	0.0419199713723186	Sterol 3-beta-glucosyltransferase	0
MELO3C026499	0.00568866895933029	0.0419199713723186	Zinc finger HIT domain-containing protein 3	0
MELO3C013692	0.00569296709952316	0.0419359967357266	Transmembrane protein, putative	0
MELO3C002261	0.00570743449773126	0.0420268918328466	serine/threonine-protein kinase HT1-like	0
MELO3C009193	0.0057141543213195	0.0420606909026235	Transmembrane protein	0
MELO3C019997	0.0057189492179438	0.0420803010824039	Histone H4	0
MELO3C014390	0.00572324775500266	0.0420962457778575	mavicyanin-like	0
MELO3C026392	0.0057372614827349	0.042183610209431	RING/U-box superfamily protein	1
MELO3C006151	0.0057406825704176	0.0421920901889014	protein-ribulosamine 3-kinase, chloroplastic	0
MELO3C013951	0.00574760326577217	0.0421920901889014	NADH dehydrogenase [ubiquinone] 1 beta subcomplex subunit 8, mitochondrial	1
MELO3C016676	0.00574342477656464	0.0421920901889014	Peptide methionine sulfoxide reductase	0
MELO3C003123	0.00574566882149075	0.0421920901889014	E3 ubiquitin-protein ligase XB3-like	0
MELO3C022650	0.00574909690102454	0.0421920901889014	At1g16840/F17F16.27	0
MELO3C025152	0.00576102443116722	0.0422639195732249	Coronatine-insensitive 1	0
MELO3C009325	0.00577467309870794	0.0423191774837995	POLAR LOCALIZATION DURING ASYMMETRIC DIVISION AND protein	0
MELO3C014035	0.00577498523058584	0.0423191774837995	No data found	1
MELO3C016723	0.00577229566189108	0.0423191774837995	serpin-ZX-like	0
MELO3C012351	0.00577787071656299	0.0423246175005202	L-aminoadipate-semialdehyde dehydrogenase-phosphopantetheinyl transferase-like	0
MELO3C013215	0.00578362349766959	0.0423510494829354	Chaperone DnaJ domain protein	1
MELO3C016017	0.00578589705892163	0.0423519944464949	translocator protein homolog	0
MELO3C002023	0.00580928505066813	0.0425074362599648	DExH-box ATP-dependent RNA helicase DExH14	0
MELO3C007814	0.00582928347011036	0.0426221840989298	protein indeterminate-domain 2-like	0
MELO3C021695	0.0058292778713428	0.0426221840989298	Phosphatidate cytidylyltransferase	0
MELO3C022301	0.00583286609252087	0.0426325952854162	serine/threonine-protein kinase ATG1a isoform X4	1
MELO3C014353	0.00584390830887993	0.0426975009959562	Transmembrane protein, putative	0
MELO3C018739	0.00584621381637895	0.0426985490605281	GPI-anchored protein LORELEI	1
MELO3C011890	0.00585525734603176	0.0427329923602296	DNA-binding storekeeper protein-related	0
MELO3C025877	0.00585523358807216	0.0427329923602296	Glucose-6-phosphate isomerase	0
MELO3C007133	0.00586456153890169	0.0427776942902953	Transmembrane protein	0
MELO3C020666	0.0058657145241845	0.0427776942902953	ATP-dependent clp protease	1
MELO3C004534	0.00587048715416727	0.0427809706934379	Glycine-rich RNA-binding protein, putative	1
MELO3C024909	0.005876180212674	0.0427809706934379	Mitochondrial transcription termination factor family protein	0
MELO3C006765	0.00587699496132954	0.0427809706934379	DEAD-box ATP-dependent RNA helicase 50	0
MELO3C015718	0.00587510034530903	0.0427809706934379	ATP binding protein	1
MELO3C018802	0.00587443787186281	0.0427809706934379	Peroxisome biogenesis protein 22	0
MELO3C012708	0.00588417269765351	0.042817437953559	Pentatricopeptide repeat-containing protein	0

MELO3C004011	0.00590548212715403	0.0429352413293379	No data found	0
MELO3C006191	0.00590581813556534	0.0429352413293379	Katanin p80 WD40 repeat-containing subunit B1 homolog	0
MELO3C010772	0.00590688392788552	0.0429352413293379	clathrin interactor EPSIN 1	1
MELO3C009201	0.00591891723251758	0.0429423338585641	Immediate early response 3-interacting protein 1	0
MELO3C006188	0.00592525493769747	0.0429423338585641	ATP-dependent DNA helicase 2 subunit KU80	0
MELO3C013243	0.00591825048021155	0.0429423338585641	TOM1-like protein 2	1
MELO3C016108	0.0059234494023328	0.0429423338585641	Receptor-like protein kinase	0
MELO3C008056	0.0059159671652691	0.0429423338585641	NAC domain-containing protein 82	1
MELO3C019145	0.00591396721573012	0.0429423338585641	ER membrane protein complex subunit 8/9 homolog	0
MELO3C002690	0.00591329059347701	0.0429423338585641	Myosin heavy chain kinase B	0
MELO3C003396	0.00592368884294037	0.0429423338585641	Phospholipid hydroperoxide glutathione peroxidase	0
MELO3C010378	0.00592824461531416	0.0429482402449888	No data found	1
MELO3C024777	0.00593479565849098	0.0429799337952102	ABC transporter B family protein	0
MELO3C009446	0.00593804692995192	0.0429877158429694	Serine/threonine-protein phosphatase PP1	0
MELO3C026748	0.0059455675826553	0.043026388490238	Enolase	0
MELO3C014562	0.00599556157265702	0.0433154505707741	E3 ubiquitin-protein ligase ICP0	1
MELO3C003917	0.00599045408550714	0.0433154505707741	Heat shock 70 kDa protein	1
MELO3C016296	0.00599404152910388	0.0433154505707741	Chlororespiratory reduction31	1
MELO3C002981	0.00599647789055124	0.0433154505707741	transmembrane emp24 domain-containing protein p24delta9-like	1
MELO3C012239	0.00599508591673292	0.0433154505707741	Bowman-Birk type bran trypsin inhibitor	0
MELO3C018576	0.006001066828351	0.0433327491016833	L-galactose dehydrogenase	1
MELO3C007947	0.00601022964576781	0.0433812098520652	Ankyrin repeat domain-containing protein, chloroplastic	1
MELO3C000960	0.00601217131829979	0.0433812098520652	Peptidase_M22 domain-containing protein	0
MELO3C012636	0.00604022024987105	0.0435676806846981	Unknown protein	0
MELO3C007305	0.00604570718491382	0.0435754274433807	SNF2 domain-containing protein / helicase domain-containing protein / zinc finger protein-like protein	0
MELO3C002619	0.00604427870695745	0.0435754274433807	Mitochondrial carrier protein, expressed	1
MELO3C017434	0.00605024264847209	0.0435922079768973	Oxysterol-binding protein-related protein 4C	0
MELO3C024960	0.00605807790577961	0.0436165607897204	pentatricopeptide repeat-containing protein At5g66520-like	1
MELO3C011968	0.00606024825596196	0.0436165607897204	Lipase	0
MELO3C020484	0.0060595841623905	0.0436165607897204	B3 domain-containing transcription repressor VAL2-like isoform X1	0
MELO3C019453	0.00606717259072709	0.0436504887046518	Unknown protein	0
MELO3C004524	0.00608588071467309	0.0437596014526496	zinc finger CCCH domain-containing protein 39-like	1
MELO3C012929	0.00608677022585591	0.0437596014526496	Transmembrane protein, putative	0
MELO3C021977	0.00610215935596248	0.0438073774112173	Translation factor GUF1 homolog, mitochondrial	0
MELO3C005419	0.00610228848337935	0.0438073774112173	AT-hook motif nuclear-localized protein 6-like	0
MELO3C008275	0.00609738000015136	0.0438073774112173	Translation initiation factor 2 subunit gamma	0
MELO3C018119	0.00610157934889466	0.0438073774112173	CRS2-associated factor 2, mitochondrial	0
MELO3C012855	0.00610856561304385	0.043836505193315	Thioredoxin family protein	0
MELO3C018729	0.00611147585383698	0.0438414590037873	F21O3.6 protein	0
MELO3C004028	0.0061196128433687	0.0438679615403588	Syntaxin/T-SNARE family protein	0
MELO3C024761	0.00611839938520808	0.0438679615403588	GDSL esterase/lipase At2g30310-like	1
MELO3C024178	0.00612424666004419	0.0438852493792499	Histidine--tRNA ligase	0
MELO3C023608	0.00613091710727787	0.0439171135116542	Zinc finger family protein	0
MELO3C025210	0.00613790062530528	0.0439352662012157	gibberellin 2-beta-dioxygenase 2-like	1
MELO3C021934	0.00613720039845989	0.0439352662012157	Unknown protein	0
MELO3C006919	0.00614558306381441	0.0439743188142285	cleavage and polyadenylation specificity factor subunit 2	0
MELO3C018549	0.0061508796175187	0.0439962772786588	DUF21 domain-containing protein	1
MELO3C002746	0.00616727372711723	0.0440975701798835	Pyruvate dehydrogenase E1 component subunit beta	0
MELO3C011357	0.00619072089896822	0.0442492026904536	serine/arginine-rich splicing factor SC35-like	1
MELO3C024739	0.00619905310426472	0.0442927278423024	growth-regulating factor 4-like	1
MELO3C014540	0.00620616913018546	0.0443275349555272	blue copper protein-like	1
MELO3C002036	0.00622651950250241	0.0444568089858714	DUF1118-domain-containing protein	0
MELO3C016913	0.0062308640362656	0.0444628643048621	No data found	1
MELO3C007762	0.00623705673597619	0.0444628643048621	Mediator of RNA polymerase II transcription subunit 26, putative	0
MELO3C021058	0.00623574434668006	0.0444628643048621	cell division control protein 45 homolog	0
MELO3C015155	0.00623862458801827	0.0444628643048621	Scarecrow-like 3	0
MELO3C010763	0.00623461804273584	0.0444628643048621	vacuolar-processing enzyme-like	1
MELO3C027004	0.00624716628925381	0.0445033742420186	poly(A)-specific ribonuclease PARN-like	0
MELO3C026199	0.0062499307886954	0.0445033742420186	Transmembrane protein, putative	1
MELO3C018765	0.00625106892234339	0.0445033742420186	AT4g28240/F26K10_120	0
MELO3C003173	0.00627159763267748	0.0446281016666281	Proteasome subunit alpha type	1

MELO3C011375	0.00627310801694059	0.0446281016666281	BPS1-like protein	1
MELO3C022302	0.00627652237112752	0.044636312678213	protein LHY-like isoform X1	0
MELO3C020793	0.00628178082278441	0.0446576275986931	Amidase, putative	0
MELO3C008503	0.00629332806158112	0.0447075308950235	Protein ABIL2	1
MELO3C012054	0.00629326949914211	0.0447075308950235	Glycine-rich protein	0
MELO3C013884	0.00630182195868945	0.0447517734132175	E3 ubiquitin-protein ligase LAP	0
MELO3C024563	0.00631506277400962	0.0448296817842976	O-linked N-acetylglucosamine transferase, putative	0
MELO3C014872	0.00632247490555671	0.0448500563612929	Lipase	0
MELO3C007513	0.00632190735505112	0.0448500563612929	No data found	0
MELO3C005964	0.00632905007685847	0.044880578085414	Late cornified envelope protein 1E	1
MELO3C013087	0.00633709589246012	0.0449215027926041	5'/3'-nucleotidase SurE	0
MELO3C012701	0.00636922311907195	0.0451003657442134	Cysteine proteinase inhibitor	0
MELO3C018356	0.00636756099341584	0.0451003657442134	Protein WVD2-like 7	0
MELO3C021329	0.00636951373363392	0.0451003657442134	ATP-binding cassette sub-family C member 11	0
MELO3C021253	0.00637146288046764	0.0451003657442134	Beta-glucosidase	1
MELO3C026388	0.00637537403507316	0.0451026197189537	N-acetyl-D-glucosamine kinase-like	0
MELO3C010153	0.00637634889135241	0.0451026197189537	CTP-dependent diacylglycerol kinase 1	0
MELO3C007784	0.00638303272564489	0.0451337319365417	Unknown protein	1
MELO3C009381	0.00639888795602483	0.0452296486197332	splicing factor 3A subunit 2	0
MELO3C016674	0.00642353608518753	0.0453713927562119	cyclin-SDS-like isoform X1	0
MELO3C018174	0.00642233138082371	0.0453713927562119	zinc finger protein CONSTANS-LIKE 4	0
MELO3C004357	0.00642826459136869	0.0453852268631873	No data found	0
MELO3C016498	0.00643136952453571	0.0453852268631873	MACPF domain-containing protein At4g24290	1
MELO3C018412	0.00643238898121734	0.0453852268631873	allene oxide synthase 3-like	0
MELO3C016846	0.00644461626837156	0.0454066095911773	Phosphoribosyl-AMP cyclohydrolase	1
MELO3C025627	0.00644076471782506	0.0454066095911773	Sodium/calcium exchanger family protein	0
MELO3C025613	0.00644431749613228	0.0454066095911773	Tyrosine aminotransferase	0
MELO3C022004	0.00644429970006122	0.0454066095911773	SPX domain protein	1
MELO3C006050	0.00644986291475913	0.0454115548155478	Phosphatidylinositol-4-phosphate 5-kinase family protein	1
MELO3C006253	0.00646031208615239	0.0454115548155478	protein ECERIFERUM 1-like	0
MELO3C010427	0.00645475405348239	0.0454115548155478	aspartate-semialdehyde dehydrogenase	1
MELO3C010381	0.00645743435607238	0.0454115548155478	2-hydroxyacyl-CoA lyase	1
MELO3C016083	0.00645283144289732	0.0454115548155478	Ubiquitin	1
MELO3C002209	0.00645126342186264	0.0454115548155478	Homeobox leucine zipper family protein	1
MELO3C003341	0.00646141419979185	0.0454115548155478	Casein kinase II subunit beta	0
MELO3C009195	0.00646569829267873	0.0454150041623959	OTU domain-containing protein	0
MELO3C014214	0.00646880382342496	0.0454150041623959	ABC transporter G family-like protein	0
MELO3C010810	0.00646732888793111	0.0454150041623959	Sigma factor sigb regulation protein rsbq	0
MELO3C013814	0.00648131394496065	0.0454866627928315	26S proteasome non-ATPase regulatory subunit 13	0
MELO3C002275	0.00649370496098678	0.0455574349110223	anthranilate phosphoribosyltransferase, chloroplastic	0
MELO3C022225	0.00649818775899091	0.0455726953310765	protein NRT1/ PTR FAMILY 5.10-like	1
MELO3C004648	0.00650643547640417	0.045614339447464	Stress-response A/B barrel domain-containing protein UP3	0
MELO3C014127	0.00651810160220068	0.0456522271398093	Actin-related protein 8	0
MELO3C013774	0.00651526241483036	0.0456522271398093	Cystathionine gamma-synthase	0
MELO3C010338	0.00651877464855244	0.0456522271398093	Outward-rectifying potassium channel 4-like protein	1
MELO3C017394	0.00652352679417967	0.0456578253063655	No data found	0
MELO3C011399	0.00652419783353908	0.0456578253063655	LOW QUALITY PROTEIN: transcription factor BIM2	0
MELO3C009480	0.00653901503596366	0.0457291104621977	ABC transporter family protein	1
MELO3C009226	0.00653689188363704	0.0457291104621977	serine/threonine-protein kinase ATG1c	0
MELO3C006727	0.00654713755056613	0.0457697060127895	Neutral/alkaline invertase	0
MELO3C014592	0.00655080438696443	0.0457791351161219	heterogeneous nuclear ribonucleoprotein F	0
MELO3C025386	0.00655608608069769	0.04579983870099	Polyadenylate-binding protein-interacting protein 4	0
MELO3C002931	0.00656237554505812	0.0458275652897287	Paired amphipathic helix SIN3-like protein	1
MELO3C003629	0.00657160924631839	0.0458729395477752	Plasma membrane ATPase	0
MELO3C025085	0.00657351860449662	0.0458729395477752	Class I heat shock protein	0
MELO3C017111	0.00658733845633164	0.0459531427672531	39S ribosomal protein L47, mitochondrial	0
MELO3C000210	0.00659371367780071	0.0459813740900022	Unknown protein	0
MELO3C002863	0.00659694398511679	0.0459876621115677	patellin-4	0
MELO3C010710	0.00660311013512804	0.046014404396134	Short-chain dehydrogenase/reductase	0
MELO3C006770	0.00661343968116468	0.0460196052035173	At1g08580	0
MELO3C014101	0.00661437329406644	0.0460196052035173	Unknown protein	0
MELO3C005578	0.00660977458179657	0.0460196052035173	Amine oxidase	1
MELO3C020940	0.00661550757875262	0.0460196052035173	Pentatricopeptide repeat-containing family protein	0
MELO3C011317	0.00660728708017455	0.0460196052035173	zinc finger protein CONSTANS-LIKE 4	0

MELO3C003039	0.00663998790077891	0.0461736341734094	No data found	1
MELO3C023313	0.00665769860589904	0.0462804962224218	Transmembrane protein, putative	0
MELO3C002412	0.00666469864478825	0.0463128548683755	Ankyrin repeat family protein	0
MELO3C021730	0.00666911679857307	0.0463272555944494	calcium permeable stress-gated cation channel 1-like	0
MELO3C007344	0.0066785985161617	0.0463768080505195	No data found	1
MELO3C019691	0.00668174178677394	0.0463823263785584	Hexosyltransferase	1
MELO3C023315	0.00668561297068715	0.0463928919740339	diaminopimelate decarboxylase 2, chloroplastic-like	0
MELO3C010430	0.00670618584904936	0.0465193060529947	At1g78110	0
MELO3C010243	0.00671615745963616	0.046572118564029	VAMP-like protein YKT61	1
MELO3C016714	0.00672515339221591	0.0466181306924788	protochlorophyllide reductase, chloroplastic	0
MELO3C024515	0.00672876682696899	0.0466268126546704	splicing factor U2af small subunit B-like	0
MELO3C002102	0.00673479236241348	0.046652197251948	Receptor-like kinase	0
MELO3C006703	0.00674630940843268	0.0467155906406511	CoA ligase	0
MELO3C005600	0.0067735201512592	0.046871202383288	Phosphate translocator-related family protein	0
MELO3C022928	0.00677352836102607	0.046871202383288	No data found	0
MELO3C015597	0.00677974577639429	0.0468813723172307	Calcium ion binding	0
MELO3C018604	0.00677908066685062	0.0468813723172307	Ubiquitin-like-specific protease 2	0
MELO3C026067	0.00678676319927907	0.0469134709214429	tRNA (Guanine(9)-N1)-methyltransferase-like	0
MELO3C007325	0.00679902181931435	0.046981764139132	Sugar transporter, putative	0
MELO3C023845	0.00680785721675858	0.0470263631247867	serine/arginine-rich SC35-like splicing factor SCL30	0
MELO3C018418	0.00681891427759185	0.0470862720518047	No data found	0
MELO3C010532	0.00684685289919851	0.0472626696631497	Structural constituent of ribosome, putative	0
MELO3C026628	0.00686069658808242	0.0473416830601117	Zinc finger protein	0
MELO3C022323	0.00686333010384244	0.0473433133848356	proton pump-interactor 1-like	0
MELO3C007871	0.00687289009524761	0.0473761628240995	rRNA adenine N(6)-methyltransferase	0
MELO3C002405	0.00687058154327702	0.0473761628240995	50S ribosomal protein L7/L12	1
MELO3C022636	0.00688113418024483	0.0474164406579397	No data found	0
MELO3C003447	0.00688547634453296	0.04742981246187	Major facilitator superfamily transporter	1
MELO3C015424	0.00690715562065036	0.0475625580028675	Glucan endo-1,3-beta-glucosidase, putative	0
MELO3C016795	0.00692639658527194	0.04767842668614	Clavata3/ESR (CLE) gene family member MtCLE20	1
MELO3C026546	0.00693441822564089	0.0476860043919131	DNA-directed RNA polymerase subunit beta	0
MELO3C014262	0.00696264092237953	0.0476860043919131	60S ribosomal protein L4-like	0
MELO3C020440	0.00696854568206295	0.0476860043919131	UBX domain-containing protein 1	0
MELO3C004152	0.00696272408374665	0.0476860043919131	40S ribosomal protein S23-1	1
MELO3C006100	0.00695734585909258	0.0476860043919131	Ubiquitin-conjugating enzyme, E2	0
MELO3C014870	0.00695033903996145	0.0476860043919131	DSR6	0
MELO3C010475	0.00694843697490344	0.0476860043919131	UDP-glucuronosyltransferase 2B17	0
MELO3C018008	0.0069448281081157	0.0476860043919131	Glycyl-tRNA synthetase beta subunit	1
MELO3C007024	0.00695655689989738	0.0476860043919131	Phenylalanine--tRNA ligase	0
MELO3C025262	0.00696807649833175	0.0476860043919131	AAA+ ATPase domain-containing protein	0
MELO3C003085	0.00696185243230085	0.0476860043919131	Flagellin N-methylase	0
MELO3C022024	0.00693627676482245	0.0476860043919131	Hexosyltransferase	0
MELO3C020840	0.00696181741775093	0.0476860043919131	Formin-like protein	0
MELO3C025883	0.00696229192516018	0.0476860043919131	Gb|AAC95187.1	0
MELO3C025870	0.0069539047423004	0.0476860043919131	Transcription factor	0
MELO3C002552	0.00693441431194941	0.0476860043919131	Wound-responsive family protein	0
MELO3C008234	0.00696379313695883	0.0476860043919131	Transferring glycosyl group transferase	0
MELO3C005532	0.00697466168591299	0.0477113244319694	Pectinesterase	1
MELO3C021323	0.00699292881807612	0.0478197199543578	condensin-2 complex subunit D3	0
MELO3C011016	0.00701159249660366	0.0479307511995243	tubulin beta chain	1
MELO3C011386	0.00701788286723926	0.0479571518149163	DNA gyrase subunit A	1
MELO3C010709	0.0070296723169897	0.048021099477077	telomere-associated protein RIF1-like isoform X2	1
MELO3C026341	0.00704211024903056	0.0480894312960251	ubiquitin-conjugating enzyme E2 22	0
MELO3C006306	0.00704624370381213	0.048101025546694	beta-mannosyltransferase 1	0
MELO3C024211	0.00708416893756425	0.0483432109011598	BTB/POZ domain-containing protein At5g48130	1
MELO3C021434	0.00709534752098828	0.0484027696690838	DNA polymerase epsilon catalytic subunit A	0
MELO3C022219	0.00711140982249026	0.0484955913620028	SPla/RYanodine receptor (SPRY) domain-containing protein	1
MELO3C007597	0.00712542430296725	0.0485743888710046	Indole-3-acetic acid-amido synthetase GH3.3	0
MELO3C017791	0.00713147184175345	0.048598839683502	No data found	0
MELO3C008811	0.007139438811121	0.0486363494587198	importin-5	1
MELO3C024179	0.00715903843773669	0.0487239522278649	zinc finger protein CONSTANS-LIKE 9-like	0
MELO3C018056	0.00715686435559881	0.0487239522278649	Carbonic anhydrase	0
MELO3C011234	0.00715969969949182	0.0487239522278649	GTP-binding nuclear protein	1
MELO3C024853	0.00717709886898354	0.0488182782776459	GTP-binding protein, chloroplastic	0

MELO3C018841	0.00717850423405153	0.0488182782776459	Beta-adaptin-like protein	1
MELO3C022802	0.00718337005107827	0.0488345525434578	Sulfate transporter, putative	0
MELO3C009638	0.00720397515405002	0.0488443099327942	UBP1-associated protein 2C-like	0
MELO3C014057	0.00719121069185757	0.0488443099327942	Plant UBX domain-containing protein 8	0
MELO3C017745	0.00720673118743775	0.0488443099327942	F12F1.11	0
MELO3C014215	0.00719953826615072	0.0488443099327942	No data found	1
MELO3C003108	0.00720218464493627	0.0488443099327942	Histone H2A	0
MELO3C025150	0.00720791735611159	0.0488443099327942	No data found	0
MELO3C021391	0.00719687947412662	0.0488443099327942	Protein ABCI12, chloroplastic	0
MELO3C021274	0.00720832830460949	0.0488443099327942	Outer envelope pore protein 16-2, chloroplastic	0
MELO3C018769	0.00720953787301104	0.0488443099327942	Wound-responsive family protein	1
MELO3C012904	0.00719324434856972	0.0488443099327942	Autophagy-related protein 9	0
MELO3C019780	0.00721681585490708	0.0488768505893552	protein kinase 2B, chloroplastic-like	1
MELO3C010939	0.00722100799204228	0.0488884768031687	FK506-binding protein 4-like	0
MELO3C026824	0.00723804249067217	0.048987012045334	cytochrome P450 714A1-like	0
MELO3C021328	0.00724702951271161	0.0490182548751763	ubiquitin-like-specific protease ESD4	0
MELO3C022348	0.00724762287890601	0.0490182548751763	Protein TIFY 9	1
MELO3C004223	0.00725452501643375	0.0490313533708249	ATP-dependent Clp protease proteolytic subunit	0
MELO3C017562	0.00725386990279486	0.0490313533708249	Random slug protein 5	0
MELO3C008420	0.0072686274147804	0.0491098606960309	Transcriptional corepressor SEUSS	0
MELO3C009316	0.0072779413909807	0.0491559728216409	Interactor of constitutive active ROPs-like protein	0
MELO3C013370	0.00728490803364623	0.0491862047030699	translocase of chloroplast 120, chloroplastic-like	1
MELO3C021385	0.00728849085706462	0.0491935768749724	Phosphatase 2C family protein	1
MELO3C009552	0.00729901228807617	0.0491973357260124	Mads box protein, putative	1
MELO3C020458	0.00729730268308693	0.0491973357260124	cyclin-dependent kinase inhibitor 5-like	1
MELO3C016448	0.00729807390629156	0.0491973357260124	methionine S-methyltransferase	0
MELO3C019257	0.00729310653565496	0.0491973357260124	CDT1-like protein a, chloroplastic	0
MELO3C005288	0.00730395227585312	0.0492138360613522	F-box family protein	0
MELO3C018966	0.00730701020630065	0.0492176482142672	ATP-dependent 6-phosphofructokinase	1
MELO3C006035	0.00731675729151005	0.0492664983805087	Rhodanese-like domain-containing protein 4, chloroplastic	0
MELO3C004603	0.00732905066766798	0.0492894286514099	Protein-tyrosine phosphatase mitochondrial 1	1
MELO3C012007	0.00732642441238118	0.0492894286514099	spermidine synthase	0
MELO3C025324	0.00732887618986666	0.0492894286514099	Leucine-rich repeat extensin-like protein 4	1
MELO3C010766	0.00733014592886683	0.0492894286514099	UPF0587 protein C1orf123 homolog	0
MELO3C019260	0.00733326272891488	0.0492936030065827	Glutamate receptor	0
MELO3C017705	0.00734710733815036	0.0493698614566626	Transducin/WD40 repeat-like superfamily protein	0
MELO3C012421	0.0073514013120205	0.0493819130990112	Cytochrome c oxidase assembly protein COX16	0
MELO3C010584	0.00736507254652774	0.0494569254407944	ribosome maturation protein SBDS	0
MELO3C002071	0.00737535584584981	0.0495091443234833	single-stranded DNA-binding protein, mitochondrial	1
MELO3C005980	0.00738295761679109	0.0495433333245012	Protein ARABIDILLO 1	0
MELO3C020839	0.00739116720083399	0.0495801838855691	glutamine--tRNA ligase-like	0
MELO3C026554	0.007393470127247	0.0495801838855691	alcohol dehydrogenase-like 7	1
MELO3C008219	0.0074119726130466	0.0496873887084377	glyceraldehyde-3-phosphate dehydrogenase	1
MELO3C004992	0.00742737438247398	0.049773741662531	Protein nuclear fusion defective 4	1
MELO3C008610	0.00743112678605029	0.0497819955555316	No data found	0
MELO3C012753	0.00743754746958103	0.0497952801713388	Unknown protein	1
MELO3C021306	0.00743815264091596	0.0497952801713388	ethylene-responsive transcription factor RAP2-3-like	0
MELO3C017009	0.00744176012404185	0.0498025485224339	4-coumarate--CoA ligase family protein	0
MELO3C007097	0.00744929403958527	0.0498360799416564	F-box protein SKIP19	1
MELO3C022759	0.00746050443032131	0.0498941760902186	MOB kinase activator-like 1A	0
MELO3C016549	0.00746559537964697	0.0499113213109844	U3 small nucleolar RNA-associated protein 14 B isoform 3	0

Supplementary Table 2. List of the Differentially Expressed Genes (2068 DEGs) only considering the postharvest ripening time in melon fruit during postharvest storage at 20 5 ^{o}C and 88% relative humidity for 18 d of the near-isogenic line SC10-2 and its parental control ´Piel de Sapo´ (PS) Gene Ontology terms (GO terms) of the six different clusters (named 2 x) obtained according to the differentially expressed gene

Gene ID	pval	qval	Description
MELO3C010748	5,90E-12	1,16E-07	Heat shock transcription factor
MELO3C005540	1,88E-11	1,86E-07	14 kDa proline-rich protein dc2.15
MELO3C023889	7,79E-11	5,13E-07	Ultraviolet-B receptor UVR8
MELO3C003298	6,24E-10	2,94E-06	high mobility group B protein 1
MELO3C018265	7,45E-10	2,94E-06	ADP-ribosylation factor GTPase-activating protein
MELO3C015733	1,56E-09	5,14E-06	Pre-mRNA-splicing factor ATP-dependent RNA helicase
MELO3C003282	3,84E-09	1,08E-05	cleft lip and palate transmembrane protein 1 homolog
MELO3C008669	1,05E-08	2,60E-05	RING-type E3 ubiquitin transferase
MELO3C026279	1,50E-08	3,29E-05	cell division cycle protein 48 homolog
MELO3C018038	2,96E-08	4,66E-05	proline iminopeptidase
MELO3C007022	3,77E-08	4,66E-05	UDP-N-acetylglucosamine diphosphorylase 2-like
MELO3C022036	3,28E-08	4,66E-05	protein LONGIFOLIA 2
MELO3C015789	2,62E-08	4,66E-05	sucrose-binding protein-like
MELO3C023342	2,79E-08	4,66E-05	kinesin-related protein 11-like
MELO3C002468	3,61E-08	4,66E-05	Tobamovirus multiplication protein 1
MELO3C003752	3,53E-08	4,66E-05	gibberellin-regulated protein 11-like
MELO3C003570	4,19E-08	4,87E-05	Protein ROOT PRIMORDIUM DEFECTIVE 1
MELO3C006028	5,64E-08	5,45E-05	cyclic nucleotide-gated ion channel 1
MELO3C021108	5,62E-08	5,45E-05	Peptidylprolyl isomerase
MELO3C002508	5,38E-08	5,45E-05	thioredoxin-like protein CXXS1
MELO3C024028	5,80E-08	5,45E-05	DEAD-box ATP-dependent RNA helicase
MELO3C004023	7,06E-08	6,18E-05	NADPH--cytochrome P450 reductase
MELO3C019973	7,20E-08	6,18E-05	2-C-methyl-D-erythritol 4-phosphate cytidylyltransferase
MELO3C016073	8,21E-08	6,49E-05	Tudor/PWWP/MBT superfamily protein
MELO3C001317	8,13E-08	6,49E-05	Coiled-coil protein (DUF572)
MELO3C003905	9,86E-08	7,31E-05	glycine--tRNA ligase, mitochondrial 1
MELO3C003444	9,99E-08	7,31E-05	transcription factor IWS1
MELO3C022213	1,09E-07	7,43E-05	Myb family transcription factor family protein
MELO3C022533	1,07E-07	7,43E-05	shaggy-related protein kinase theta
MELO3C023449	1,40E-07	9,21E-05	UPF0481 plant-like protein
MELO3C016475	1,70E-07	0,000104363	Chloride channel protein
MELO3C024278	1,74E-07	0,000104363	Mitochondrial carrier protein
MELO3C012356	1,74E-07	0,000104363	Aspartyl aminopeptidase
MELO3C023146	2,03E-07	0,000104556	villin-2-like
MELO3C025783	1,81E-07	0,000104556	receptor-like serine/threonine-protein kinase NCRK
MELO3C010244	2,06E-07	0,000104556	Temperature-induced lipocalin
MELO3C017271	2,05E-07	0,000104556	Acetyl-coenzyme A synthetase
MELO3C017213	1,95E-07	0,000104556	UDP-glucose 6-dehydrogenase
MELO3C003563	1,86E-07	0,000104556	No data found
MELO3C014061	2,13E-07	0,000105194	WPP domain interacting protein, putative
MELO3C004433	2,20E-07	0,000106054	calcium uptake protein 1, mitochondrial-like isoform X1
MELO3C013868	2,32E-07	0,000107032	Cytochrome P450 family ent-kaurenoic acid oxidase
MELO3C019616	2,33E-07	0,000107032	E3 ubiquitin-protein ligase RGLG2
MELO3C006120	2,88E-07	0,000129143	MYB-related transcription factor
MELO3C004799	3,03E-07	0,000132974	splicing factor U2af small subunit B-like
MELO3C017380	3,28E-07	0,000141013	zinc finger CCHC domain-containing protein 7 isoform X3
MELO3C006297	3,64E-07	0,000148781	RNA recognition motif (RRM) containing protein
MELO3C012728	3,67E-07	0,000148781	Vacuolar sorting-associated protein 2-like protein
MELO3C023559	3,89E-07	0,000148781	40S ribosomal protein S27
MELO3C003812	3,77E-07	0,000148781	Glucose-1-phosphate adenylyltransferase
MELO3C012788	3,82E-07	0,000148781	Transcription initiation factor IIF alpha subunit family protein
MELO3C012930	3,92E-07	0,000148781	Zinc knuckle family protein
MELO3C013136	4,05E-07	0,000150962	GDP-L-galactose phosphorylase 1
MELO3C015720	4,16E-07	0,000152121	Smr (Small MutS-related) domain protein
MELO3C022416	4,70E-07	0,000168621	Ubiquitin family protein
MELO3C003875	5,08E-07	0,000179224	Protein phosphatase 2c, putative
MELO3C016754	6,18E-07	0,000214273	Cold regulated gene 27, putative isoform 3
MELO3C004194	6,44E-07	0,000215458	calreticulin
MELO3C022408	6,40E-07	0,000215458	UV-stimulated scaffold protein A homolog
MELO3C013622	6,73E-07	0,000217727	mannan endo-1,4-beta-mannosidase 2
MELO3C011379	6,66E-07	0,000217727	Chaperone protein dnaJ
MELO3C024626	7,24E-07	0,000230696	Protein LIKE COV 1
MELO3C000452	8,00E-07	0,000243073	Coiled-coil protein (DUF572)
MELO3C021903	7,87E-07	0,000243073	Alpha/beta hydrolase-3
MELO3C002485	7,94E-07	0,000243073	Transmembrane protein, putative
MELO3C022066	8,16E-07	0,000244276	Zinc finger CCHC domain-containing protein 8
MELO3C003448	8,87E-07	0,000261442	Methyltransferase-related family protein
MELO3C003331	9,74E-07	0,0002828	BAX inhibitor-1
MELO3C012149	1,01E-06	0,000288475	PLASMODESMATA CALLOSE-BINDING PROTEIN 3
MELO3C013183	1,07E-06	0,00029567	elongation factor-like GTPase 1
MELO3C006997	1,05E-06	0,00029567	galactan beta-1,4-galactosyltransferase GALS3-like
MELO3C021100	1,08E-06	0,00029567	Heat shock 70 kDa protein
MELO3C024188	1,12E-06	0,000299785	ribulose-1,5 bisphosphate carboxylase/oxygenase large subunit N-methyltransferase, chloroplastic
MELO3C009091	1,15E-06	0,000299785	50S ribosomal protein L17
MELO3C014359	1,17E-06	0,000299785	Calcium-binding EF-hand family protein

MELO3C007735	1,15E-06	0,000299785	E3 ubiquitin-protein ligase RING1
MELO3C022511	1,15E-06	0,000299785	synaptotagmin-5
MELO3C013988	1,23E-06	0,000311097	Myelodysplasia-myeloid leukemia factor 1-interacting protein
MELO3C013712	1,34E-06	0,000334119	Fact complex subunit spt16
MELO3C006921	1,37E-06	0,000338067	No data found
MELO3C014555	1,47E-06	0,000358476	splicing factor 3B subunit 6-like protein
MELO3C018149	1,51E-06	0,000364822	Beta-glucosidase, putative
MELO3C002104	1,54E-06	0,000366033	Receptor-like kinase
MELO3C018525	1,56E-06	0,00036677	Myosin heavy chain-like protein
MELO3C005069	1,60E-06	0,00037138	GEM-like protein 4
MELO3C026068	1,65E-06	0,000379411	Transcriptional adapter ADA2b-like protein
MELO3C017897	1,77E-06	0,000398202	Plant/protein
MELO3C015804	1,77E-06	0,000398202	heat stress transcription factor A-6b-like isoform X1
MELO3C022210	1,96E-06	0,000434452	regulator of nonsense transcripts UPF3-like
MELO3C007072	2,12E-06	0,000465214	Caffeoylshikimate esterase
MELO3C008069	2,15E-06	0,000466976	Phosphoinositide phosphatase family protein
MELO3C005382	2,26E-06	0,000478687	luc7-like protein 3
MELO3C024270	2,28E-06	0,000478687	Terpene cyclase/mutase family member
MELO3C020612	2,30E-06	0,000478687	Unknown protein
MELO3C018644	2,26E-06	0,000478687	serine/arginine-rich splicing factor SC35
MELO3C001976	2,35E-06	0,000483125	Pentatricopeptide repeat-containing family protein
MELO3C023857	2,40E-06	0,000488711	GATA zinc finger domain-containing protein 10-like isoform X2
MELO3C002674	2,57E-06	0,000518413	BnaA04g24650D protein
MELO3C015067	2,65E-06	0,000527841	transcription factor LHW
MELO3C021462	2,70E-06	0,000532957	DDT domain-containing protein PTM
MELO3C024775	2,85E-06	0,000552422	Bud13
MELO3C002056	2,83E-06	0,000552422	O-fucosyltransferase family protein
MELO3C005952	3,12E-06	0,000597548	60S acidic ribosomal protein P1-like
MELO3C026898	3,24E-06	0,000614621	Cathepsin B-like cysteine protease
MELO3C022204	3,44E-06	0,000647494	SART-1 family protein DOT2 isoform X2
MELO3C009579	3,54E-06	0,000647539	Myosin-binding protein 7
MELO3C025257	3,54E-06	0,000647539	KH domain-containing family protein
MELO3C005301	3,52E-06	0,000647539	At1g70780
MELO3C014083	3,77E-06	0,000680058	Transmembrane protein, putative
MELO3C025488	3,79E-06	0,000680058	transcription initiation factor TFIID subunit 1-like
MELO3C025502	3,82E-06	0,000680058	Pentatricopeptide repeat-containing protein
MELO3C015322	3,94E-06	0,000689115	cyclin-L1-1
MELO3C011284	3,94E-06	0,000689115	Aspartate aminotransferase
MELO3C017093	4,18E-06	0,000723327	Kinesin light chain
MELO3C009482	4,24E-06	0,000725607	Rho GTPase-activating protein
MELO3C023408	4,26E-06	0,000725607	Lactoylglutathione lyase
MELO3C009461	4,48E-06	0,000737581	Protein LITTLE ZIPPER 4
MELO3C020244	4,48E-06	0,000737581	UTP--glucose-1-phosphate uridylyltransferase
MELO3C002302	4,42E-06	0,000737581	Kinase family protein
MELO3C019941	4,38E-06	0,000737581	T-complex protein 11
MELO3C007207	4,57E-06	0,000746373	Kinase family protein
MELO3C013630	4,62E-06	0,000748551	switch 2 isoform X1
MELO3C006383	5,10E-06	0,000812025	acid phosphatase 1-like
MELO3C006836	5,09E-06	0,000812025	Activating transcription factor 7-interacting 2
MELO3C016101	5,14E-06	0,000812025	UBP1-associated protein 2C
MELO3C017908	5,32E-06	0,000827253	No data found
MELO3C020989	5,28E-06	0,000827253	phosphatidylinositol 4-kinase alpha 1
MELO3C010295	5,46E-06	0,000841847	Armadillo-like helical
MELO3C017364	5,64E-06	0,000856673	Ribosomal protein L19
MELO3C023986	5,61E-06	0,000856673	DNA topoisomerase 2
MELO3C002700	5,84E-06	0,000880994	Serine/threonine-protein kinase PLK4
MELO3C016366	5,94E-06	0,000888531	Phosphatidylcholine transfer protein
MELO3C018948	5,99E-06	0,000889151	Alpha-1,4 glucan phosphorylase
MELO3C024262	6,09E-06	0,000897106	activating signal cointegrator 1 complex subunit 1
MELO3C014178	6,21E-06	0,000905978	Trigger factor
MELO3C007432	6,24E-06	0,000905978	Phosphatidate cytidylyltransferase
MELO3C007139	6,36E-06	0,000909299	la-related protein 6A
MELO3C007499	6,35E-06	0,000909299	protein DA1-related 1-like
MELO3C021534	6,54E-06	0,000909299	homeobox-leucine zipper protein HAT5-like
MELO3C024447	6,54E-06	0,000909299	Protein SEC13 like
MELO3C012136	6,51E-06	0,000909299	Nodulin-related protein 1
MELO3C020875	6,61E-06	0,000909299	CLK4-associating serine/arginine-rich protein
MELO3C022342	6,63E-06	0,000909299	NAC domain-containing protein 83
MELO3C002148	6,45E-06	0,000909299	NF-X1-type zinc finger protein NFXL1
MELO3C006107	6,91E-06	0,000940831	RNA polymerase I-specific transcription initiation factor RRN3
MELO3C009423	7,01E-06	0,000948429	Uridylate kinase
MELO3C003915	7,08E-06	0,000950539	Pentatricopeptide repeat-containing protein
MELO3C013703	7,12E-06	0,000950539	diacylglycerol O-acyltransferase 2-like
MELO3C009276	7,30E-06	0,00096137	Acyl-CoA N-acyltransferase with RING/FYVE/PHD-type zinc finger domain-containing protein
MELO3C005731	7,29E-06	0,00096137	Intracellular protein transport protein USO1-like protein
MELO3C017657	7,42E-06	0,000970741	branchpoint-bridging protein
MELO3C008933	7,84E-06	0,001018808	Zinc finger family protein
MELO3C004591	8,11E-06	0,001046869	Phosphotransferase
MELO3C008910	8,25E-06	0,001058188	transcription termination factor MTEF18, mitochondrial-like
MELO3C009591	8,33E-06	0,001061017	IQ domain-containing protein IQM6
MELO3C006959	8,45E-06	0,001062493	Reticulon-like protein

MELO3C014174	8,41E-06	0,001062493	(S)-ureidoglycine aminohydrolase
MELO3C006602	8,54E-06	0,001066875	serine/threonine-protein kinase RUNKEL
MELO3C017677	8,66E-06	0,001075323	chitinase-like protein 1
MELO3C025526	8,87E-06	0,001089274	Pollen Ole e 1 allergen/extensin
MELO3C011117	8,88E-06	0,001089274	receptor-like protein kinase HSL1
MELO3C024862	9,68E-06	0,001180217	Plant peroxidase
MELO3C014649	9,79E-06	0,001181894	Metal tolerance protein C2
MELO3C023188	9,81E-06	0,001181894	Beta-galactosidase
MELO3C009187	1,01E-05	0,001194634	Transferase family protein
MELO3C005211	1,00E-05	0,001194634	Zinc finger, CCCH-type
MELO3C011825	1,02E-05	0,001194634	nifU-like protein 2, chloroplastic
MELO3C011747	1,01E-05	0,001194634	Protein FAR1-RELATED SEQUENCE 5
MELO3C005262	1,04E-05	0,001220292	PLATZ transcription factor family protein, putative
MELO3C007075	1,06E-05	0,001234544	ADP-ribosylation factor GTPase-activating protein AGD12
MELO3C013128	1,09E-05	0,001251957	Golgin family A protein
MELO3C022707	1,09E-05	0,001251957	Ubiquitin-conjugating enzyme family protein
MELO3C008520	1,13E-05	0,001262069	Cysteine protease
MELO3C017856	1,13E-05	0,001262069	extensin-like
MELO3C007069	1,12E-05	0,001262069	Protein phosphatase 2c, putative
MELO3C025855	1,12E-05	0,001262069	Alkyl transferase
MELO3C017521	1,13E-05	0,001262069	No data found
MELO3C010119	1,15E-05	0,001270454	U11/U12 small nuclear ribonucleoprotein 48 kDa protein
MELO3C012196	1,15E-05	0,001273125	Phospholipid-transporting ATPase
MELO3C011271	1,18E-05	0,001298592	14 kDa proline-rich protein DC2.15
MELO3C013925	1,20E-05	0,001311679	Myb transcription factor
MELO3C018053	1,21E-05	0,001311679	Costars family protein At4g33640
MELO3C016877	1,22E-05	0,001313028	Beta-fructofuranosidase, insoluble isoenzyme CWINV1
MELO3C013369	1,24E-05	0,001313028	Methyltransferase-like protein
MELO3C025451	1,23E-05	0,001313028	Actin-depolymerizing factor family protein
MELO3C013022	1,24E-05	0,001313028	Serine/threonine-protein kinase ATM
MELO3C004278	1,25E-05	0,00131307	mevalonate kinase-like
MELO3C020701	1,24E-05	0,00131307	Myb transcription factor
MELO3C013123	1,27E-05	0,001314742	Syntaxin-51
MELO3C025079	1,27E-05	0,001314742	universal stress protein A-like protein
MELO3C026613	1,26E-05	0,001314742	Tubulin alpha chain
MELO3C025061	1,31E-05	0,001334848	V-type proton ATPase subunit C
MELO3C023417	1,31E-05	0,001334848	DUF4050 family protein
MELO3C000817	1,30E-05	0,001334848	Magnesium transporter MRS2-like protein
MELO3C006260	1,32E-05	0,001336381	Dynamin, putative
MELO3C009296	1,35E-05	0,00135638	Energy-coupling factor transporter ATP-binding EcfA 1
MELO3C023513	1,35E-05	0,00135638	Metal tolerance protein C2
MELO3C006926	1,39E-05	0,001386896	Divalent ion symporter
MELO3C025977	1,44E-05	0,001425409	OBERON-like protein
MELO3C007177	1,45E-05	0,001426946	Transcription factor GTE12
MELO3C017474	1,47E-05	0,001441788	Zinc finger protein
MELO3C021398	1,49E-05	0,00145805	serine incorporator 3
MELO3C016541	1,55E-05	0,001475351	Peroxisomal membrane 22 kDa (Mpv17/PMP22) family protein
MELO3C024844	1,52E-05	0,001475351	At5g24610
MELO3C025256	1,54E-05	0,001475351	protein RETICULATA-RELATED 3, chloroplastic-like
MELO3C019633	1,54E-05	0,001475351	Glyceraldehyde-3-phosphate dehydrogenase
MELO3C026235	1,54E-05	0,001475351	haloacid dehalogenase-like hydrolase domain-containing protein At3g48420
MELO3C014575	1,61E-05	0,001502947	Saccharopine dehydrogenase
MELO3C007083	1,61E-05	0,001502947	187-kDa microtubule-associated protein AIR9
MELO3C025282	1,61E-05	0,001502947	SCARECROW
MELO3C022499	1,59E-05	0,001502947	Myeloid leukemia factor
MELO3C011324	1,61E-05	0,001502947	No data found
MELO3C002677	1,63E-05	0,001510878	NAD(P)-binding Rossmann-fold superfamily protein
MELO3C014530	1,68E-05	0,001520089	Nuclear transcription factor Y subunit C8
MELO3C004492	1,69E-05	0,001520089	methyl-CpG-binding domain-containing protein 11-like
MELO3C020109	1,68E-05	0,001520089	Nop53 protein
MELO3C015263	1,67E-05	0,001520089	Werner syndrome-like exonuclease
MELO3C015197	1,68E-05	0,001520089	Translocation protein Sec62
MELO3C025345	1,68E-05	0,001520089	Polyol transporter 5-like protein
MELO3C026090	1,71E-05	0,001534494	Sec14p-like phosphatidylinositol transfer family protein
MELO3C008330	1,75E-05	0,001565386	S-acyltransferase
MELO3C014749	1,81E-05	0,001606901	Acetyl-coenzyme A synthetase
MELO3C007033	1,81E-05	0,001606901	protein SUPPRESSOR OF FRI 4 isoform X2
MELO3C013248	1,85E-05	0,00160794	nucleolar complex protein 4 homolog
MELO3C023526	1,82E-05	0,00160794	chaperone protein dnaJ GFA2, mitochondrial
MELO3C001987	1,84E-05	0,00160794	cyclic dof factor 3
MELO3C026629	1,84E-05	0,00160794	potassium channel AKT1
MELO3C002226	1,86E-05	0,00161177	polynucleotide 5'-hydroxyl-kinase NOL9
MELO3C015277	1,88E-05	0,001621496	GATA transcription factor 16-like
MELO3C016380	1,90E-05	0,001633533	Laccase
MELO3C003506	1,91E-05	0,001636029	Rhamnogalacturonate lyase family protein
MELO3C013366	1,94E-05	0,001654622	Protein nuclear fusion defective 4
MELO3C010997	1,97E-05	0,001670415	Protein IQ-DOMAIN 32
MELO3C020444	2,03E-05	0,00171292	Purple acid phosphatase
MELO3C017620	2,06E-05	0,001732538	BnaA10g17500D protein
MELO3C024407	2,10E-05	0,001750958	Charged multivesicular body 1
MELO3C020780	2,10E-05	0,001750958	Triosephosphate isomerase

MELO3C014678	2,13E-05	0,001751257	Kelch repeat-containing F-box family protein
MELO3C006313	2,12E-05	0,001751257	Myb family transcription factor APL
MELO3C021113	2,11E-05	0,001751257	asparagine--tRNA ligase, cytoplasmic 2
MELO3C025859	2,14E-05	0,001755197	zinc finger CCCH domain-containing protein 25
MELO3C007825	2,17E-05	0,001755992	random slug protein 5-like
MELO3C025784	2,16E-05	0,001755992	Zinc finger (C3HC4-type RING finger) family protein
MELO3C021782	2,16E-05	0,001755992	alpha-glucosidase
MELO3C004305	2,19E-05	0,001765171	Pre-mRNA-splicing factor SLU7
MELO3C011160	2,21E-05	0,001773889	2-on-2 hemoglobin
MELO3C016552	2,23E-05	0,001775985	Fiber expressed protein
MELO3C011089	2,22E-05	0,001775985	O-fucosyltransferase family protein
MELO3C016074	2,29E-05	0,001811186	No data found
MELO3C025887	2,29E-05	0,001811186	No data found
MELO3C009595	2,32E-05	0,001817184	serine/arginine-rich SC35-like splicing factor SCL33
MELO3C022721	2,32E-05	0,001817184	Ninja-family protein AFP3
MELO3C017346	2,34E-05	0,001823593	alpha-dioxygenase 2
MELO3C007673	2,35E-05	0,001827806	tubulin alpha chain-like
MELO3C013383	2,37E-05	0,001839283	Calcium-binding EF hand family protein
MELO3C024514	2,42E-05	0,0018583	enolase
MELO3C021587	2,42E-05	0,0018583	NAC domain-containing protein 8 isoform X1
MELO3C014507	2,49E-05	0,001907765	F-box family protein
MELO3C004641	2,56E-05	0,001939773	Protein BREVIS RADIX
MELO3C013104	2,57E-05	0,001939773	Upstream activation factor subunit spp27
MELO3C017749	2,58E-05	0,001939773	BAG family molecular chaperone regulator 6-like
MELO3C007609	2,56E-05	0,001939773	Subtilisin-like protease
MELO3C001175	2,58E-05	0,001939773	Glutathione s-transferase
MELO3C017813	2,62E-05	0,00195107	ADP-ribosylation factor GTPase-activating protein AGD3
MELO3C015327	2,61E-05	0,00195107	isoaspartyl peptidase/L-asparaginase
MELO3C002384	2,71E-05	0,00201456	Coiled-coil domain-containing protein SCD2
MELO3C002115	2,75E-05	0,002026023	Poly(A) polymerase
MELO3C011422	2,75E-05	0,002026023	Pentatricopeptide repeat-containing protein
MELO3C015734	2,76E-05	0,002026925	No data found
MELO3C022647	2,77E-05	0,002028876	UDP-glycosyltransferase 89A2-like
MELO3C013870	2,80E-05	0,002034696	Chloroplast 40 kDa outer membrane envelope protein
MELO3C007265	2,80E-05	0,002034696	Protein DEHYDRATION-INDUCED 19
MELO3C006929	2,82E-05	0,002036511	BAHD acyltransferase DCR
MELO3C026502	2,83E-05	0,002036891	Phytochrome
MELO3C015439	2,90E-05	0,002077194	Protein PLASTID MOVEMENT IMPAIRED 1-RELATED 1
MELO3C011285	2,89E-05	0,002077194	60S ribosomal protein L39
MELO3C006736	2,95E-05	0,002099278	Beta-1,3-galactosyltransferase-like protein
MELO3C011144	2,96E-05	0,002099278	Translation initiation factor IF-2
MELO3C020570	3,03E-05	0,002147341	Maternal effect embryo arrest protein
MELO3C014009	3,07E-05	0,002148255	PGR5-like protein 1A, chloroplastic
MELO3C025111	3,05E-05	0,002148255	CoA ligase
MELO3C004669	3,06E-05	0,002148255	Pentatricopeptide repeat-containing protein
MELO3C006493	3,10E-05	0,002161953	ATP sulfurylase
MELO3C004553	3,16E-05	0,002169827	multiprotein-bridging factor 1c
MELO3C008046	3,18E-05	0,002169827	zinc finger CCCH domain-containing protein 38 isoform X1
MELO3C016002	3,17E-05	0,002169827	Arginine/serine-rich splicing factor, putative
MELO3C013664	3,17E-05	0,002169827	Transcriptional elongation regulator MINIYO
MELO3C022436	3,14E-05	0,002169827	Amaranthin-like lectin
MELO3C026107	3,14E-05	0,002169827	No data found
MELO3C008690	3,24E-05	0,002208703	splicing factor 3B subunit 2
MELO3C011843	3,28E-05	0,002219494	No data found
MELO3C010136	3,28E-05	0,002219494	Glycogenin-1
MELO3C014019	3,42E-05	0,002291067	Rhomboid-like protein
MELO3C005581	3,42E-05	0,002291067	Ankyrin repeat/KH domain protein (DUF1442)
MELO3C021786	3,41E-05	0,002291067	Cyclin-T1-like protein
MELO3C025956	3,48E-05	0,00232373	No data found
MELO3C017095	3,49E-05	0,002323867	CASP-like protein
MELO3C009339	3,54E-05	0,00234295	Glycosyl transferase, family 31
MELO3C008596	3,57E-05	0,002359948	S-adenosyl-L-methionine-dependent methyltransferase
MELO3C021119	3,61E-05	0,00237836	Cytochrome b561 and domon domain-containing protein
MELO3C011003	3,62E-05	0,00237836	transcription factor E2FC isoform X3
MELO3C019730	3,74E-05	0,002443832	zinc finger CCCH domain-containing protein 3-like
MELO3C009827	3,85E-05	0,002508953	No data found
MELO3C019522	3,87E-05	0,002510923	Exocyst complex component
MELO3C026239	3,88E-05	0,002510923	Protein tipD, putative
MELO3C012737	3,94E-05	0,002539535	F21O3.15 protein
MELO3C020783	3,95E-05	0,002539535	protein XAP5 CIRCADIAN TIMEKEEPER
MELO3C009967	3,99E-05	0,002557116	cyclin-dependent kinase C-2-like
MELO3C006705	4,03E-05	0,00257263	Binding protein
MELO3C021207	4,04E-05	0,00257263	Signal peptide peptidase-like protein
MELO3C024863	4,14E-05	0,002631109	No data found
MELO3C009222	4,25E-05	0,002692175	Protein RETICULATA, chloroplastic
MELO3C015594	4,32E-05	0,002725898	No data found
MELO3C015603	4,37E-05	0,002745529	E3 ubiquitin-protein ligase RING1-like
MELO3C016303	4,47E-05	0,002801259	ATP-dependent zinc metalloprotease FtsH
MELO3C011196	4,53E-05	0,002833395	ABC1 family protein, expressed
MELO3C002041	4,55E-05	0,002835312	RHOMBOID-like protein 12, mitochondrial
MELO3C016262	4,65E-05	0,002880684	26S proteasome non-ATPase regulatory subunit 8

MELO3C010761	4,65E-05	0,002880684	far upstream element-binding protein 1
MELO3C013810	4,76E-05	0,002891896	At3g49990
MELO3C017946	4,74E-05	0,002891896	bifunctional epoxide hydrolase 2-like
MELO3C022162	4,69E-05	0,002891896	mannan endo-1,4-beta-mannosidase 1-like
MELO3C021771	4,76E-05	0,002891896	exocyst complex component EXO84C
MELO3C026234	4,74E-05	0,002891896	elongator complex protein 3
MELO3C010675	4,74E-05	0,002891896	ATP-citrate synthase alpha chain protein
MELO3C017754	4,84E-05	0,002913268	NAC domain-containing protein
MELO3C024316	4,83E-05	0,002913268	Late embryogenesis abundant protein, LEA-14
MELO3C019225	4,84E-05	0,002913268	Formin-like protein
MELO3C023419	4,93E-05	0,002938396	methyl-CpG-binding domain-containing protein 11
MELO3C020132	4,94E-05	0,002938396	Potassium transporter
MELO3C021228	4,91E-05	0,002938396	tRNA pseudouridine synthase
MELO3C018502	4,91E-05	0,002938396	MAR-binding filament-like protein
MELO3C025812	5,00E-05	0,002963418	ATP-dependent zinc metalloprotease FtsH
MELO3C010297	5,05E-05	0,002983067	Purple acid phosphatase
MELO3C024005	5,08E-05	0,00299654	Acyl-CoA--sterol O-acyltransferase 1
MELO3C007562	5,21E-05	0,003030419	Lipase
MELO3C024545	5,20E-05	0,003030419	Transmembrane 9 superfamily member
MELO3C021979	5,20E-05	0,003030419	Glutaredoxin family protein, putative
MELO3C022786	5,23E-05	0,003030419	Phd finger protein, putative
MELO3C016019	5,23E-05	0,003030419	heat shock factor-binding protein 1
MELO3C013031	5,23E-05	0,003030419	Glutamate dehydrogenase, putative
MELO3C009776	5,30E-05	0,003063321	DNA-directed RNA polymerase II, putative
MELO3C011731	5,41E-05	0,003103925	Ubiquitin carboxyl-terminal hydrolase
MELO3C022901	5,40E-05	0,003103925	Alpha/beta-Hydrolases superfamily protein, putative
MELO3C014309	5,53E-05	0,003104434	Magnesium transporter MRS2-like protein
MELO3C016660	5,43E-05	0,003104434	Flavin-binding kelch domain F box protein
MELO3C012529	5,49E-05	0,003104434	Ras-related Rab7
MELO3C007450	5,49E-05	0,003104434	No data found
MELO3C025278	5,51E-05	0,003104434	Emp24/gp25L/p24 family/GOLD family protein
MELO3C015764	5,52E-05	0,003104434	F-box/LRR-repeat protein 17
MELO3C020957	5,52E-05	0,003104434	GDSL esterase/lipase 5-like
MELO3C010102	5,50E-05	0,003104434	O-linked n-acetylglucosamine transferase, ogt, putative
MELO3C025265	5,59E-05	0,003125624	Unknown protein
MELO3C016917	5,63E-05	0,003130049	Damaged dna-binding 2, putative isoform 1
MELO3C024435	5,62E-05	0,003130049	Poly(A) polymerase
MELO3C022773	5,68E-05	0,003148872	Transmembrane protein, putative
MELO3C017683	5,78E-05	0,00319616	Clathrin interactor EPSIN 2
MELO3C009495	5,81E-05	0,003205231	CASP-like protein
MELO3C024214	5,88E-05	0,003207012	Cytochrome b561 and domon domain-containing protein
MELO3C012242	5,88E-05	0,003207012	ethylene-responsive transcription factor ERF118
MELO3C021273	5,86E-05	0,003207012	Seed maturation protein PM36
MELO3C002469	5,86E-05	0,003207012	BnaC01g13120D protein
MELO3C025779	5,92E-05	0,003220471	Nucleotide/sugar transporter family protein
MELO3C009272	5,94E-05	0,003223467	UNC93-like protein 3
MELO3C005094	6,04E-05	0,003257855	histidine biosynthesis bifunctional protein hisIE, chloroplastic
MELO3C005565	6,03E-05	0,003257855	Elongation factor G, chloroplastic
MELO3C021232	6,15E-05	0,003309755	Novel plant snare, putative
MELO3C010548	6,17E-05	0,003313352	Receptor-like protein kinase
MELO3C023731	6,23E-05	0,003315726	phosphatidylcholine transfer protein-like isoform X1
MELO3C020001	6,20E-05	0,003315726	Mini-chromosome maintenance complex-binding protein
MELO3C019844	6,22E-05	0,003315726	ras-related protein RABC2a-like
MELO3C002885	6,28E-05	0,003331834	transcription factor GTE1
MELO3C024385	6,38E-05	0,003375474	protein indeterminate-domain 7
MELO3C025853	6,51E-05	0,003437938	protein DAMAGED DNA-BINDING 2
MELO3C020626	6,59E-05	0,003471635	Expansin
MELO3C022998	6,69E-05	0,003506	Malate dehydrogenase
MELO3C018749	6,69E-05	0,003506	Phosphatase 2C family protein
MELO3C008321	6,73E-05	0,003517413	Biotin carboxyl carrier protein of acetyl-CoA carboxylase
MELO3C014016	6,77E-05	0,003517802	Phospholipase D
MELO3C017700	6,77E-05	0,003517802	disease resistance protein RGA2-like
MELO3C023018	6,87E-05	0,00352199	splicing factor U2af large subunit B isoform X1
MELO3C004354	6,85E-05	0,00352199	Cc-nbs-lrr resistance protein
MELO3C005945	6,86E-05	0,00352199	Dihydroorotate dehydrogenase (DUF3598)
MELO3C005293	6,82E-05	0,00352199	Phosphoglucomutase, putative
MELO3C003561	6,86E-05	0,00352199	VQ motif-containing protein 9
MELO3C008367	6,97E-05	0,003567809	serine/threonine-protein kinase STY8-like
MELO3C014129	7,03E-05	0,003567921	THO complex subunit 3
MELO3C023560	7,00E-05	0,003567921	PsaB RNA-binding protein
MELO3C021923	7,03E-05	0,003567921	CCG-binding protein 1
MELO3C009879	7,24E-05	0,003665313	Cullin family protein
MELO3C005405	7,26E-05	0,003665515	CDGSH iron-sulfur domain-containing protein NEET
MELO3C016468	7,29E-05	0,003671413	No data found
MELO3C016354	7,36E-05	0,003696337	Short-chain dehydrogenase TIC 32, chloroplastic
MELO3C026097	7,37E-05	0,003696337	Hexosyltransferase
MELO3C008752	7,44E-05	0,003709205	TATA box-binding protein-associated factor RNA polymerase I subunit B
MELO3C005656	7,42E-05	0,003709205	Protein LURP-one-related 11
MELO3C003147	7,53E-05	0,003744722	LOW QUALITY PROTEIN: L-type lectin-domain containing receptor kinase S.4-like
MELO3C026470	7,55E-05	0,003744722	Potassium transporter
MELO3C022501	7,65E-05	0,003777968	SNARE-interacting protein KEULE

MELO3C026141	7,65E-05	0,003777968	ADP-ribosylation factor-like
MELO3C009203	7,74E-05	0,003814164	tubulin beta chain-like
MELO3C014114	7,85E-05	0,003854576	RPM1-interacting protein 4
MELO3C026614	7,87E-05	0,00385474	WD repeat-containing protein 55
MELO3C017384	7,90E-05	0,003863001	tRNA pseudouridine synthase
MELO3C005812	8,05E-05	0,003913918	ARM repeat superfamily protein
MELO3C011099	8,05E-05	0,003913918	Universal stress protein A-like protein
MELO3C025903	8,07E-05	0,003917532	At5g59460
MELO3C004610	8,12E-05	0,003927962	zinc finger CCCH domain-containing protein 20-like
MELO3C007571	8,15E-05	0,003927962	OTU domain-containing protein
MELO3C021116	8,14E-05	0,003927962	No data found
MELO3C019012	8,19E-05	0,00393172	No data found
MELO3C021529	8,20E-05	0,00393172	NHL domain-containing protein, putative
MELO3C019120	8,32E-05	0,003965589	R3H domain-containing protein 1-like isoform X1
MELO3C021999	8,29E-05	0,003965589	Expansin protein
MELO3C012410	8,35E-05	0,003965589	thioredoxin-like 3-2, chloroplastic isoform X8
MELO3C015590	8,37E-05	0,003965589	protochlorophyllide-dependent translocon component 52, chloroplastic-like
MELO3C010165	8,36E-05	0,003965589	Cyclic nucleotide-gated ion channel-like protein
MELO3C009350	8,41E-05	0,003972539	TSL-kinase interacting protein 1
MELO3C023590	8,49E-05	0,004002215	Pheophytinase, chloroplastic
MELO3C015374	8,52E-05	0,004004007	Superoxide dismutase [Cu-Zn]
MELO3C020589	8,72E-05	0,004091828	17 5 kDa class I heat shock protein
MELO3C013736	8,76E-05	0,004101537	basic endochitinase C
MELO3C007483	8,91E-05	0,004151361	ABC transporter family protein
MELO3C021258	8,91E-05	0,004151361	flowering time control protein FCA isoform X2
MELO3C016360	8,94E-05	0,004153313	Transferring glycosyl group transferase
MELO3C023979	8,96E-05	0,004155775	Cellulose synthase
MELO3C004308	9,02E-05	0,004171791	Photosystem II reaction center PsbP family protein
MELO3C011085	9,09E-05	0,004195778	Argininosuccinate lyase
MELO3C005490	9,19E-05	0,004222227	U-box domain-containing protein 35-like isoform X2
MELO3C013455	9,18E-05	0,004222227	Calcium ion-binding protein
MELO3C025582	9,26E-05	0,004241924	Ribosomal protein S5/S7
MELO3C012378	9,28E-05	0,004243844	phosphoglucan phosphatase DSP4, amyloplastic
MELO3C007153	9,32E-05	0,004249426	No data found
MELO3C015704	9,36E-05	0,004249426	Protein trigalactosyldiacylglycerol 2, chloroplastic
MELO3C024344	9,35E-05	0,004249426	DUF1677 family protein (DUF1677)
MELO3C014150	9,44E-05	0,004256592	Fimbrin, putative
MELO3C008197	9,44E-05	0,004256592	Chloride channel protein
MELO3C025034	9,44E-05	0,004256592	peroxiredoxin Q, chloroplastic
MELO3C009895	9,61E-05	0,004324758	Actin cross-linking protein
MELO3C009354	9,65E-05	0,004329302	Glutathione gamma-glutamylcysteinyltransferase 1
MELO3C017560	9,71E-05	0,004337109	Succinate dehydrogenase [ubiquinone] flavoprotein subunit, mitochondrial
MELO3C025468	9,70E-05	0,004337109	ABC transporter B family protein
MELO3C023685	9,76E-05	0,00435218	alcohol dehydrogenase-like
MELO3C026975	9,80E-05	0,00436109	40S ribosomal protein S15a
MELO3C003471	9,87E-05	0,004378557	protein SAWADEE HOMEODOMAIN HOMOLOG 1-like isoform X2
MELO3C005467	0,000100246	0,004438907	At5g07590
MELO3C003508	0,000100674	0,004447917	UDP-glycosyltransferase 91C1
MELO3C013591	0,000102175	0,00450416	Sugar transporter, putative
MELO3C005035	0,000102449	0,004506164	E3 SUMO-protein ligase SIZ1
MELO3C010760	0,000102713	0,004507639	Pollen specific protein sf21
MELO3C010705	0,000102939	0,004507639	T-complex protein 1 subunit epsilon
MELO3C027060	0,000103272	0,004512221	Pectinesterase
MELO3C019722	0,000103716	0,004515705	Protein disulfide-isomerase like 2-2
MELO3C003733	0,000103809	0,004515705	ribonuclease P protein subunit p25-like protein isoform X1
MELO3C014175	0,000105084	0,004551125	Phospho-2-dehydro-3-deoxyheptonate aldolase
MELO3C023808	0,000105023	0,004551125	SAC3/GANP/Nin1/mts3/eIF-3 p25 family isoform 1
MELO3C015339	0,000107667	0,004652752	UDP-N-acetylglucosamine transferase subunit ALG13 homolog
MELO3C026764	0,000108528	0,004659375	Magnesium transporter MRS2-like protein
MELO3C013214	0,00010835	0,004659375	DNA damage-inducible protein 1
MELO3C000826	0,000108179	0,004659375	Transcription factor
MELO3C009076	0,000109346	0,004669937	Nucleolar protein gar2-like protein
MELO3C021461	0,00010932	0,004669937	No data found
MELO3C010245	0,000109483	0,004669937	Two-component response regulator
MELO3C026804	0,000109889	0,00467717	histone-lysine N-methyltransferase, H3 lysine-9 specific SUVH1-like
MELO3C023161	0,000110585	0,004696648	nuclear transcription factor Y subunit A-7-like
MELO3C024366	0,000111579	0,004728701	Mitochondrial carrier protein
MELO3C010189	0,000113033	0,004780062	lactation elevated protein 1
MELO3C006645	0,000115046	0,004851885	No data found
MELO3C013254	0,000115548	0,004851885	Kinase family protein
MELO3C016245	0,000115714	0,004851885	Glycosyl transferase family 1 family protein
MELO3C024450	0,000115488	0,004851885	nuclear pore complex protein NUP35
MELO3C004999	0,000117465	0,004914861	nicotinamide adenine dinucleotide transporter 1, chloroplastic-like
MELO3C009561	0,000118756	0,004916778	iron-sulfur cluster co-chaperone protein HscB, mitochondrial
MELO3C004593	0,000118147	0,004916778	OXS3
MELO3C006651	0,000118406	0,004916778	No data found
MELO3C020294	0,00011852	0,004916778	DNA-directed RNA polymerase subunit beta
MELO3C017104	0,000118047	0,004916778	Trehalose-6-phosphate synthase, putative
MELO3C025594	0,000119502	0,004937323	C2 domain-containing protein
MELO3C017653	0,000120136	0,004942865	Isoaspartyl peptidase/L-asparaginase
MELO3C015496	0,000120135	0,004942865	Plant/F27B13-30 protein

MELO3C003911	0,000121139	0,004973739	protein BONZAI 3
MELO3C003294	0,000123184	0,005040585	vacuolar cation/proton exchanger 3
MELO3C015230	0,000123277	0,005040585	Pectin acetylesterase
MELO3C002075	0,000125653	0,005127117	No data found
MELO3C000994	0,000126324	0,005143843	wall-associated receptor kinase 2-like
MELO3C012076	0,000126973	0,005159631	UDP-galactose/UDP-glucose transporter family protein
MELO3C005797	0,000127327	0,005163393	Unknown protein
MELO3C011601	0,000128223	0,005189103	No data found
MELO3C013346	0,000129469	0,005200251	Phospholipase-like protein (PEARLI 4) family protein
MELO3C008986	0,000129552	0,005200251	No data found
MELO3C015186	0,000128867	0,005200251	Sulfite reductase
MELO3C026522	0,000129123	0,005200251	monosaccharide-sensing protein 2-like
MELO3C003146	0,000130195	0,00520807	L-type lectin-domain containing receptor kinase IV.1-like
MELO3C018455	0,000130274	0,00520807	thioredoxin M3, chloroplastic
MELO3C023484	0,000131214	0,00522447	AP2-like ethylene-responsive transcription factor At1g16060
MELO3C021940	0,000131077	0,00522447	Cold acclimation protein
MELO3C011044	0,000133374	0,005299798	cytochrome c oxidase subunit 6b-1-like
MELO3C016601	0,000133904	0,005310178	No data found
MELO3C011868	0,000134717	0,005331706	Rubber elongation factor protein (REF)
MELO3C016298	0,00013613	0,005366137	Ribosome maturation factor
MELO3C024396	0,000135867	0,005366137	Cytochrome p450
MELO3C019451	0,000136453	0,005368136	Unknown protein
MELO3C006854	0,000137541	0,005397731	transcription factor bHLH118-like
MELO3C003186	0,000138025	0,005397731	Proteasome inhibitor-related
MELO3C022443	0,000137848	0,005397731	flowering time control protein FPA
MELO3C025606	0,000138545	0,005407372	Unknown protein
MELO3C007082	0,000138903	0,005410626	No data found
MELO3C012173	0,000141571	0,005501034	DNA-directed RNA polymerase
MELO3C013046	0,000141781	0,005501034	Kinase family protein
MELO3C009338	0,000142572	0,005520885	60S ribosomal protein L12
MELO3C024885	0,000144879	0,005555765	ATP-dependent DNA helicase
MELO3C019139	0,000144203	0,005555765	Nascent polypeptide-associated complex subunit alpha-like protein
MELO3C015930	0,00014451	0,005555765	Translation initiation factor IF-2
MELO3C003332	0,000143831	0,005555765	BAX inhibitor-1
MELO3C024004	0,000144864	0,005555765	No data found
MELO3C001948	0,000145692	0,0055761	Short-chain dehydrogenase, putative
MELO3C008469	0,000146222	0,00558555	Kinase family protein
MELO3C013883	0,000147575	0,005615542	BOI-related E3 ubiquitin-protein ligase 1
MELO3C025307	0,000147486	0,005615542	Transmembrane 19
MELO3C010053	0,000148287	0,005631773	Isopentenyl diphosphate isomerase
MELO3C006853	0,000149737	0,005640063	receptor-like serine/threonine-protein kinase isoform X2
MELO3C016126	0,000149702	0,005640063	Pathogen-related protein
MELO3C007653	0,000149933	0,005640063	Protein PHLOEM PROTEIN 2-LIKE A10
MELO3C010913	0,000149696	0,005640063	Protein DA1-related 1
MELO3C009782	0,000149106	0,005640063	5-methyltetrahydropteroyltriglutamate-- homocysteine methyltransferase
MELO3C019435	0,000151452	0,005664813	MLO-like protein 4
MELO3C017248	0,000150882	0,005664813	ATP-dependent helicase hrq1 isoform X6
MELO3C010769	0,000151363	0,005664813	Protein EARLY FLOWERING 3
MELO3C026201	0,000152382	0,005688818	non-specific phospholipase C6
MELO3C003975	0,000152984	0,00568979	protein CHLOROPLAST IMPORT APPARATUS 2 isoform X2
MELO3C006594	0,000152844	0,00568979	Inosine-uridine preferring nucleoside hydrolase
MELO3C026248	0,000153686	0,005705154	E3 ubiquitin-protein ligase RGLG2
MELO3C017226	0,00015485	0,005737567	glycine-rich RNA-binding protein 2, mitochondrial-like
MELO3C019470	0,000156016	0,005754372	glutelin type-A 2-like
MELO3C018956	0,000156177	0,005754372	Ubiquitin carboxyl-terminal hydrolase, putative
MELO3C011444	0,000156102	0,005754372	Mitogen-activated protein kinase
MELO3C022658	0,000156684	0,005762284	Ubiquitin-specific protease family C19 protein
MELO3C015111	0,000157133	0,005768053	rho GTPase-activating protein 7
MELO3C006344	0,000157815	0,00578234	GDT1-like protein
MELO3C004542	0,000158277	0,005788536	tRNA (guanine(37)-N1)-methyltransferase
MELO3C005967	0,000160086	0,005843894	At3g15351
MELO3C009171	0,000160419	0,005845212	Mitochondrial carrier protein
MELO3C017884	0,000161451	0,005871985	DUF4050 family protein
MELO3C011588	0,000161995	0,005880967	Phosphatidylinositol-4-phosphate 5-kinase 1-like protein
MELO3C010214	0,00016233	0,005882308	Nucleoid-associated protein At2g24020, chloroplastic
MELO3C023475	0,000163152	0,005890462	pre-mRNA-splicing factor ISY1 homolog
MELO3C018441	0,000163123	0,005890462	presequence protease 1, chloroplastic/mitochondrial-like
MELO3C024138	0,000164805	0,005931329	Auxin response factor
MELO3C011408	0,000164884	0,005931329	nucleolar protein 14 isoform X2
MELO3C009063	0,000165244	0,005933466	serine/threonine-protein kinase Nek6 isoform X1
MELO3C021279	0,000165964	0,005933924	GTP-binding protein SAR1A-like
MELO3C022345	0,000165703	0,005933924	somatic embryogenesis receptor kinase 2-like
MELO3C020557	0,000166158	0,005933924	Tetratricopeptide repeat (TPR)-like superfamily protein
MELO3C013527	0,000166518	0,005936027	1D-myo-inositol 2-amino-2-deoxy-alpha-D-glucopyranoside ligase
MELO3C022196	0,000167781	0,005970265	Kinase family protein
MELO3C013841	0,000168271	0,005970729	nucleolar protein 12
MELO3C007611	0,000168612	0,005970729	Prolyl 4-hydroxylase alpha-like protein
MELO3C022514	0,000168701	0,005970729	UTP:RNA uridylyltransferase 1
MELO3C014719	0,000171133	0,006045972	Aldehyde oxidase, putative
MELO3C014557	0,000171945	0,006048	Peptidyl-prolyl cis-trans isomerase
MELO3C014128	0,000172955	0,006048	Calcium-dependent protein kinase

MELO3C021064	0,000173027	0,006048	malonyl-CoA:anthocyanidin 5-O-glucoside-6''-O-malonyltransferase
MELO3C001849	0,000172465	0,006048	No data found
MELO3C003393	0,000171685	0,006048	Plant intracellular ras group-related LRR protein
MELO3C003842	0,000172433	0,006048	Dead box ATP-dependent RNA helicase, putative
MELO3C018437	0,000173525	0,006054682	Pentatricopeptide repeat-containing protein At5g39710
MELO3C017242	0,000174787	0,006087962	protein COBRA-like
MELO3C018195	0,000175905	0,006116118	Arf GTPase activating protein
MELO3C027373	0,000176765	0,00613522	ADP-ribosylation factor GTPase-activating protein AGD12-like
MELO3C027375	0,000177846	0,006151116	Pectinesterase
MELO3C002689	0,000177821	0,006151116	serine/threonine-protein kinase STY8-like
MELO3C009539	0,000181792	0,006274078	NC domain-containing protein
MELO3C024910	0,000182037	0,006274078	FRIGIDA-like protein
MELO3C008879	0,000182842	0,006279914	Triosephosphate isomerase
MELO3C023255	0,000182737	0,006279914	DNA-directed RNA polymerase subunit beta-beta protein, putative (DUF506)
MELO3C015373	0,000184106	0,006312352	40S ribosomal protein S25
MELO3C011622	0,000184591	0,006318019	Receptor-like kinase
MELO3C003977	0,000188808	0,006428914	Microtubule-associated family protein
MELO3C016696	0,000188295	0,006428914	PROTON PUMP INTERACTOR 1 family protein
MELO3C008440	0,000188691	0,006428914	wall-associated receptor kinase 2-like
MELO3C010877	0,000191246	0,006500733	Phosphatidate phosphatase PAH2
MELO3C004551	0,00019215	0,00651951	ARF guanine-nucleotide exchange factor GNL2
MELO3C009996	0,000192459	0,00651951	dnaJ protein homolog
MELO3C009429	0,000194464	0,006544185	peroxiredoxin-2E-2, chloroplastic
MELO3C012572	0,000194952	0,006544185	CTP synthase
MELO3C003145	0,000194632	0,006544185	Cyclin d, putative
MELO3C005245	0,000195037	0,006544185	Xyloglucan endotransglucosylase/hydrolase
MELO3C025848	0,000195176	0,006544185	Peptidyl-prolyl cis-trans isomerase
MELO3C010275	0,000194973	0,006544185	Serine-rich protein-like protein
MELO3C015450	0,000195936	0,006558527	Pollen-specific protein SF21
MELO3C007624	0,00019699	0,006582664	Acyl-CoA N-acyltransferases (NAT) superfamily protein
MELO3C017898	0,000199382	0,006651329	F-box family protein
MELO3C005252	0,000199914	0,006657858	Ankyrin repeat-containing protein, putative
MELO3C020394	0,000201726	0,006662025	Phospholipid-transporting ATPase
MELO3C019462	0,000200747	0,006662025	Membralin, putative
MELO3C010565	0,000201305	0,006662025	No data found
MELO3C012201	0,000200408	0,006662025	Isoprenylcysteine alpha-carbonyl methylesterase ICME protein
MELO3C004732	0,000201502	0,006662025	Alpha/beta-Hydrolases superfamily protein
MELO3C025049	0,000202498	0,006676334	transcription factor TCP21-like
MELO3C002382	0,000203267	0,006679412	Kinase family protein
MELO3C010235	0,000203253	0,006679412	No data found
MELO3C007086	0,000204456	0,006707317	ABC transporter C family member 12-like
MELO3C006974	0,000205083	0,006716729	Plastid division protein PDV1
MELO3C014007	0,000205522	0,00671996	Superoxide dismutase 1
MELO3C012525	0,000206484	0,00674026	Receptor-like kinase
MELO3C024444	0,000208262	0,006778458	Avr9/Cf-9 rapidly elicited protein
MELO3C002154	0,000208341	0,006778458	Monoglyceride lipase
MELO3C008332	0,000209733	0,006812512	5-formyltetrahydrofolate cyclo-ligase-like protein COG0212
MELO3C010439	0,000212163	0,006880133	structure-specific endonuclease subunit SLX4-like isoform X2
MELO3C024850	0,000213884	0,00692458	60S ribosomal protein L9-like
MELO3C024975	0,000215317	0,006948193	DUF3511 domain protein
MELO3C010798	0,000215009	0,006948193	NADH dehydrogenase (Ubiquinone) iron-sulfur protein 4, mitochondrial
MELO3C011507	0,000215859	0,006954317	Vesicle transport protein GOT1
MELO3C020824	0,000216965	0,006978582	Pre-mRNA-splicing factor syf2
MELO3C011905	0,00021792	0,006997901	RING finger protein
MELO3C005517	0,000218944	0,007019354	Tryptophan RNA-binding attenuator protein-like
MELO3C025798	0,00022376	0,007162141	cytochrome P450 71A1-like
MELO3C024644	0,000224718	0,007181155	50S ribosomal protein L18
MELO3C000425	0,000225399	0,007191293	alanine--tRNA ligase-like
MELO3C016288	0,000228158	0,007267571	F-box/LRR-repeat protein 14
MELO3C011107	0,000229497	0,007298438	Serine hydroxymethyltransferase
MELO3C019777	0,000230207	0,007309266	U4/U6 small nuclear ribonucleoprotein PRP4-like protein
MELO3C018478	0,000231655	0,007343421	kynurenine formamidase
MELO3C002566	0,000232154	0,007347439	Katanin p80 WD40 repeat-containing subunit B1 homolog
MELO3C015502	0,000232658	0,007351626	Integral membrane protein
MELO3C020924	0,00023482	0,007408081	zinc finger protein 830 isoform X1
MELO3C018720	0,00023523	0,007409188	F-box protein MAX2
MELO3C016213	0,000235725	0,007412948	Beta-amylase
MELO3C010512	0,000236489	0,007425151	Plastid transcriptionally active 6
MELO3C005808	0,000237926	0,007446607	No data found
MELO3C000237	0,000237808	0,007446607	Major facilitator superfamily domain-containing protein 12
MELO3C022212	0,000238624	0,007456609	Deoxycytidine kinase
MELO3C010478	0,000239375	0,007468269	Protein-methionine-s-oxide reductase
MELO3C008925	0,000239951	0,007474446	GTPase LSG1-2-like
MELO3C020386	0,000241205	0,007489865	E3 ubiquitin-protein ligase LAP
MELO3C021292	0,000240838	0,007489865	Protein DEHYDRATION-INDUCED 19
MELO3C017799	0,000243307	0,007543272	F2P16 20 protein, putative isoform 1
MELO3C005882	0,000246426	0,007628007	Eukaryotic translation initiation factor 3 subunit 10
MELO3C021339	0,000248214	0,007671325	60S ribosomal protein L13a, putative
MELO3C012651	0,00024916	0,007676646	FRIGIDA-like protein
MELO3C011395	0,000249164	0,007676646	Hydroxyproline O-arabinosyltransferase 1
MELO3C003541	0,00025058	0,007708259	NAD(P)H-hydrate epimerase

MELO3C007691	0,000252707	0,007749561	Auxin-responsive protein
MELO3C003242	0,000252682	0,007749561	Clathrin light chain
MELO3C008236	0,000253956	0,00777579	S-adenosyl-L-methionine-dependent methyltransferases superfamily protein isoform 1
MELO3C010329	0,00025456	0,007782212	methyl-CpG-binding domain-containing protein 11-like
MELO3C007821	0,00025592	0,007787613	U1 small nuclear ribonucleoprotein 70 kDa
MELO3C009994	0,0002553	0,007787613	MD-2-related lipid recognition domain-containing protein / ML domain-containing protein
MELO3C018718	0,000255613	0,007787613	At2g42760
MELO3C015431	0,000257438	0,007821755	40S ribosomal protein S30
MELO3C022114	0,000259465	0,00786941	RmlC-like cupins superfamily protein
MELO3C015929	0,000260097	0,00786941	GTP-binding protein SAR1A
MELO3C025940	0,000260202	0,00786941	CONSTANS-like zinc finger protein
MELO3C019503	0,000260858	0,00787719	zinc-binding alcohol dehydrogenase domain-containing protein 2
MELO3C018203	0,000262	0,007899594	Lysine-specific histone demethylase 1-like protein
MELO3C008295	0,000262691	0,00790837	ABC1-like protein
MELO3C007421	0,000263489	0,00792031	pyrophosphate--fructose 6-phosphate 1-phosphotransferase subunit beta
MELO3C023830	0,000263933	0,007921598	protein-tyrosine-phosphatase MKP1 isoform X1
MELO3C017572	0,000267737	0,008023584	transcription factor TGA1 isoform X1
MELO3C006175	0,000268353	0,008029865	ankyrin repeat and zinc finger domain-containing protein 1
MELO3C016707	0,000269787	0,008060539	Choline transporter-like protein 2
MELO3C002609	0,000270664	0,008074539	serine/threonine-protein kinase HT1-like
MELO3C016016	0,000273434	0,008136071	xyloglucan 6-xylosyltransferase 1
MELO3C023291	0,000273551	0,008136071	glycine-rich RNA-binding protein 1-like
MELO3C026966	0,000275157	0,008158176	2-oxoglutarate (2OG) and Fe(II)-dependent oxygenase superfamily protein
MELO3C020049	0,000275744	0,008158176	Ribosomal protein S5/S7
MELO3C002223	0,000275412	0,008158176	hydroxyproline O-galactosyltransferase GALT6
MELO3C003658	0,000275946	0,008158176	Protein MARD1
MELO3C023667	0,000277469	0,008190939	Tetratricopeptide repeat-containing protein
MELO3C005673	0,000278018	0,0081949	tubulin beta chain-like
MELO3C004105	0,000280336	0,008214178	Cytochrome c oxidase subunit
MELO3C022406	0,000280149	0,008214178	phosphatidylinositol 4-kinase gamma 4
MELO3C002332	0,000279544	0,008214178	Telomere length regulation TEL2
MELO3C015185	0,000280098	0,008214178	MP domain-containing protein
MELO3C026398	0,00028134	0,008231374	APO protein 1, chloroplastic
MELO3C016868	0,000285092	0,008267658	serine/threonine-protein kinase EDR1
MELO3C026803	0,00028349	0,008267658	S-acyltransferase
MELO3C023464	0,000284025	0,008267658	sister chromatid cohesion protein PDS5 homolog B-B-like
MELO3C026155	0,000284337	0,008267658	(+)-neomenthol dehydrogenase
MELO3C003695	0,000284827	0,008267658	ethylene-responsive transcription factor SHINE 2-like
MELO3C003768	0,000285069	0,008267658	Auxin response factor
MELO3C010928	0,000285792	0,00827581	PPPDE putative thiol peptidase family protein
MELO3C017784	0,000287022	0,008283948	Pentatricopeptide repeat-containing family protein
MELO3C005754	0,000287719	0,008283948	PHD finger family protein
MELO3C023306	0,000286822	0,008283948	adoMet-dependent rRNA methyltransferase spb1 isoform X1
MELO3C002328	0,000287751	0,008283948	zinc finger CCCH domain-containing protein 43
MELO3C024596	0,000288618	0,008294506	DNA polymerase
MELO3C011402	0,000288957	0,008294506	D-aminoacyl-tRNA deacylase
MELO3C024192	0,00029184	0,00834476	Fasciclin-like arabinogalactan protein
MELO3C006413	0,000291842	0,00834476	Clathrin interactor EPSIN 2
MELO3C026221	0,00029224	0,00834476	protein PLASTID TRANSCRIPTIONALLY ACTIVE 10-like
MELO3C011090	0,000292398	0,00834476	Unknown protein
MELO3C025449	0,000294384	0,008389297	Zinc finger C3H1 domain-containing protein, putative
MELO3C024544	0,000294894	0,00839174	Cell division FtsZ-1, chloroplastic-like protein
MELO3C013188	0,000296733	0,008410413	Pentatricopeptide repeat-containing protein
MELO3C018461	0,000296828	0,008410413	E3 ubiquitin-protein ligase MARCH6
MELO3C003817	0,000296781	0,008410413	DNA polymerase epsilon catalytic subunit A
MELO3C010524	0,000297643	0,008421422	arabinosyltransferase XEG113
MELO3C016542	0,000298955	0,008446441	peptidyl-prolyl cis-trans isomerase CYP37, chloroplastic
MELO3C016140	0,000300483	0,008465387	Solanesyl diphosphate synthase, putative
MELO3C026030	0,000300216	0,008465387	Protein phosphatase-2c, putative
MELO3C005238	0,000301079	0,008470097	GAGA-binding transcriptional activator
MELO3C016717	0,000303125	0,008515536	COP1-interacting protein, putative
MELO3C011640	0,0003039	0,008525163	Zinc finger, C6HC-type
MELO3C009566	0,000305243	0,008550704	Protein WVD2-like 4
MELO3C014089	0,00030836	0,008607261	caffeic acid 3-O-methyltransferase 1-like
MELO3C026025	0,00030857	0,008607261	Dehydration responsive element binding transcription factor
MELO3C021759	0,000308348	0,008607261	lecithin-cholesterol acyltransferase-like 4
MELO3C003825	0,000312163	0,008695208	Cysteine/Histidine-rich C1 domain family protein, putative
MELO3C001954	0,000313336	0,008715584	Glycosyltransferase
MELO3C009550	0,000314264	0,00871686	33 kDa ribonucleoprotein, chloroplastic
MELO3C015514	0,000314106	0,00871686	12-oxophytodienoate reductase 3
MELO3C011256	0,00031477	0,008718633	DEAD-box ATP-dependent RNA helicase-like protein
MELO3C011173	0,000316606	0,008757205	Gamma-glutamylcyclotransferase
MELO3C014658	0,000321415	0,008832526	Peroxidase
MELO3C014394	0,000321565	0,008832526	Ribosomal N-lysine methyltransferase 5
MELO3C007492	0,000321389	0,008832526	elongation of fatty acids protein 3-like
MELO3C008785	0,000320693	0,008832526	BTB/POZ domain protein
MELO3C009886	0,000320267	0,008832526	plant cysteine oxidase 2
MELO3C004434	0,000323167	0,00886421	Serine-rich protein-like protein
MELO3C016314	0,000324657	0,00888041	Aldose 1-epimerase, putative
MELO3C023996	0,000324312	0,00888041	RNA polymerase sigma factor sigD, chloroplastic
MELO3C020587	0,000326013	0,008892853	No data found

MELO3C017165	0,000325784	0,008892853	HVA22-like protein
MELO3C006813	0,000326594	0,008896413	monocopper oxidase-like protein SKS1
MELO3C009670	0,000328256	0,008917104	PHD-finger protein
MELO3C016015	0,000327885	0,008917104	AAA-type ATPase family protein
MELO3C005588	0,000329536	0,008939583	No data found
MELO3C009624	0,000330877	0,008963643	Actin family protein
MELO3C006418	0,000334017	0,009036314	Ankyrin repeat-containing protein
MELO3C015563	0,000337528	0,009118805	TATA-box-binding protein
MELO3C014619	0,000339532	0,009141554	IRK-interacting protein-like
MELO3C022488	0,000339917	0,009141554	tubulin-folding cofactor D
MELO3C020622	0,000339005	0,009141554	Rab5-interacting family protein
MELO3C010714	0,000340222	0,009141554	two-component response regulator ARR11
MELO3C015375	0,000341602	0,00916616	Sodium/hydrogen exchanger
MELO3C000065	0,000343344	0,009198122	V-type proton ATPase proteolipid subunit
MELO3C019816	0,000343724	0,009198122	Amino acid transporter family protein
MELO3C008494	0,000344946	0,009218319	E3 ubiquitin-protein ligase
MELO3C016573	0,000346012	0,009221845	Serine/threonine-protein kinase
MELO3C001121	0,000345871	0,009221845	Aspartate aminotransferase
MELO3C013921	0,000347074	0,009237694	Protein-tyrosine phosphatase mitochondrial 1-like protein
MELO3C019404	0,000348394	0,009241571	phytosulfokine receptor 2
MELO3C008018	0,000347799	0,009241571	Like-COV protein
MELO3C021608	0,000348624	0,009241571	zinc finger protein CONSTANS-LIKE 6
MELO3C001996	0,000350501	0,009278878	NAC domain-containing protein 100-like
MELO3C000201	0,000355846	0,009407762	dof zinc finger protein DOF1.5-like
MELO3C023990	0,00035901	0,009478731	Methyltransferase
MELO3C002872	0,000359765	0,009485971	Short-chain dehydrogenase/reductase family protein
MELO3C022068	0,000360452	0,009491434	proline-rich receptor-like protein kinase PERK8
MELO3C017755	0,000361737	0,009512585	zinc finger protein CONSTANS-LIKE 15-like
MELO3C024871	0,000362308	0,009514927	serine/threonine-protein phosphatase 4 regulatory subunit 2 isoform X1
MELO3C009836	0,000363929	0,009544809	Saccharopine dehydrogenase-like protein
MELO3C022005	0,000367548	0,00962694	Phosphate transporter PHO1-like protein
MELO3C002767	0,000371429	0,009715694	Nuclear-interacting partner of ALK
MELO3C022359	0,00037247	0,009730034	F3H9.20 protein
MELO3C012956	0,000374173	0,009761609	Protein MARD1
MELO3C007909	0,000376025	0,00979698	Armadillo repeat only protein
MELO3C026835	0,000376753	0,009803012	Pentatricopeptide repeat-containing protein At2g30100, chloroplastic
MELO3C025349	0,000377451	0,00980825	subtilisin-like protease SBT6.1
MELO3C019688	0,000378015	0,009810011	Peroxisomal and mitochondrial division factor 2
MELO3C002886	0,000379322	0,009822965	Alpha-taxilin
MELO3C017480	0,000379509	0,009822965	Xyloglucan endotransglucosylase/hydrolase
MELO3C024457	0,00038239	0,009884581	ATP-dependent zinc metalloprotease FtsH
MELO3C015290	0,000386293	0,009972425	peptidyl-prolyl cis-trans isomerase G
MELO3C026263	0,000387563	0,00997912	DEAD-box ATP-dependent RNA helicase-like protein
MELO3C011208	0,000387115	0,00997912	acetylglutamate kinase, chloroplastic
MELO3C004100	0,000389113	0,010005992	WD-repeat protein, putative
MELO3C014565	0,000391002	0,01003445	Homeobox domain-containing protein
MELO3C006950	0,000391236	0,01003445	Pentatricopeptide repeat-containing protein At4g21190
MELO3C021280	0,000394794	0,010112568	Calmodulin-binding transcription activator
MELO3C012670	0,000397299	0,010150395	Ribosomal protein S5/S7
MELO3C012411	0,000397107	0,010150395	pumilio homolog 4
MELO3C011773	0,000399887	0,010203324	Oxidoreductase/transition metal ion-binding protein (DUF3531)
MELO3C025346	0,000403884	0,010291994	Sugar/inositol transporter
MELO3C003659	0,000407065	0,010359693	Glucan endo-1,3-beta-glucosidase, putative
MELO3C005971	0,00040998	0,010393714	E3 ubiquitin-protein ligase BRE1-like 1
MELO3C022868	0,000409725	0,010393714	No data found
MELO3C012283	0,000409036	0,010393714	Small ubiquitin-related modifier
MELO3C003078	0,000410585	0,010395704	Protein MODIFIER OF SNC1 11
MELO3C018487	0,000411533	0,01040636	Lipase
MELO3C010774	0,000415371	0,010489987	Zinc finger CCCH domain-containing protein
MELO3C023409	0,000416908	0,010515345	BEL1-like homeodomain protein 7
MELO3C024982	0,000417648	0,01052057	Farnesyl diphosphate synthase
MELO3C007441	0,000419687	0,010527378	RING-type E3 ubiquitin transferase
MELO3C025102	0,000419977	0,010527378	Phytoene synthase
MELO3C015627	0,00042005	0,010527378	serrate RNA effector molecule
MELO3C011110	0,000418692	0,010527378	transcription factor bHLH93-like
MELO3C008732	0,000421822	0,010558394	No data found
MELO3C019813	0,000425661	0,010640976	Lysine-specific demethylase REF6
MELO3C017753	0,000427866	0,010642221	Glycerophosphodiester phosphodiesterase, putative
MELO3C007398	0,000427556	0,010642221	5'-adenylylsulfate reductase
MELO3C023163	0,000427278	0,010642221	Polygalacturonase inhibitor
MELO3C020808	0,000427603	0,010642221	Choline transporter-related family protein
MELO3C013429	0,000430502	0,010654347	kinesin-related protein 11
MELO3C005147	0,00043159	0,010654347	NADPH:QUINONE OXIDOREDUCTASE family protein
MELO3C012447	0,000430274	0,010654347	Scarecrow-like 3
MELO3C011986	0,000431246	0,010654347	Polygalacturonase
MELO3C008209	0,000430571	0,010654347	Ankyrin
MELO3C011212	0,000430422	0,010654347	Photosystem II reaction center PsbP family protein
MELO3C019630	0,000435381	0,010734505	ribosomal RNA large subunit methyltransferase I
MELO3C011139	0,000437758	0,010779657	Nuclear pore complex protein NUP85
MELO3C017711	0,000441544	0,010859341	Proline--tRNA ligase
MELO3C021670	0,000443308	0,01088614	Nuclear inhibitor of protein phosphatase 1

MELO3C003312	0,000443736	0,01088614	Protein kinase superfamily protein
MELO3C013779	0,000446718	0,010945695	2-keto-3-deoxy-L-rhamnonate aldolase
MELO3C013139	0,000447584	0,010947544	prohibitin-1, mitochondrial
MELO3C013615	0,000447902	0,010947544	E3 ubiquitin-protein ligase RMA1H1
MELO3C008959	0,000451143	0,011013129	1-acyl-sn-glycerol-3-phosphate acyltransferase
MELO3C027064	0,000453055	0,011037513	Pentatricopeptide repeat-containing protein
MELO3C015385	0,00045326	0,011037513	Pentatricopeptide repeat-containing protein
MELO3C006051	0,000453925	0,011040104	BTB/POZ domain-containing protein POB1
MELO3C006241	0,000457096	0,011089916	protein NRT1/ PTR FAMILY 7.3-like
MELO3C025549	0,000456881	0,011089916	vesicle-fusing ATPase
MELO3C007767	0,000462486	0,011197199	Lipoxygenase y domain-containing protein 1
MELO3C007931	0,000462652	0,011197199	Protein preY, mitochondrial, putative
MELO3C021742	0,000463278	0,011198624	Glycine cleavage system H, mitochondrial
MELO3C014297	0,000466624	0,011265711	type I inositol polyphosphate 5-phosphatase 4
MELO3C003017	0,000469162	0,01130037	Alpha/beta-Hydrolases superfamily protein
MELO3C019820	0,000469204	0,01130037	Glycerol-3-phosphate dehydrogenase
MELO3C020830	0,000469883	0,011302944	BZIP transcription factor, putative (DUF630 and DUF632)
MELO3C020835	0,000472388	0,011349391	Unknown protein
MELO3C017432	0,000475584	0,011405846	At1g16840/F17F16.27
MELO3C018510	0,000475893	0,011405846	somatic embryogenesis receptor kinase 1-like
MELO3C007248	0,000478865	0,011433429	Transcription factor VOZ1
MELO3C020721	0,000478166	0,011433429	triacylglycerol lipase SDP1
MELO3C003313	0,000478841	0,011433429	Membrane steroid-binding protein
MELO3C012873	0,00047936	0,011433429	NAC domain protein
MELO3C024951	0,000481456	0,011455744	cellulose synthase-like protein E6
MELO3C005757	0,000481084	0,011455744	Luminal binding heat shock protein 70
MELO3C013974	0,000483505	0,011463072	Hsp70-Hsp90 organizing protein 3
MELO3C018052	0,000482496	0,011463072	dynamin-related protein 3A-like
MELO3C011576	0,000483087	0,011463072	zinc finger protein CONSTANS-LIKE 6
MELO3C024558	0,00048545	0,01149538	sorting nexin 1
MELO3C009133	0,00048648	0,011505988	Receptor-like kinase
MELO3C005703	0,000487478	0,011506551	Beta-carotene 3-hydroxylase
MELO3C012960	0,000487669	0,011506551	BZIP protein, putative
MELO3C011675	0,000489723	0,011541219	Cmp-sialic acid transporter, putative
MELO3C009250	0,000492684	0,011564161	Laccase
MELO3C004186	0,000492599	0,011564161	Unknown protein
MELO3C006280	0,000492176	0,011564161	60S ribosomal protein L37a
MELO3C015098	0,000493039	0,011564161	Tubulin beta chain
MELO3C014358	0,000494212	0,01157792	transcription initiation factor TFIID subunit 6-like
MELO3C010630	0,00049758	0,011643018	40S ribosomal protein S8
MELO3C011793	0,000502871	0,011742725	transcription termination factor MTERF9, chloroplastic-like
MELO3C001962	0,00050303	0,011742725	protein REVEILLE 2-like
MELO3C007833	0,000504272	0,011751999	ATPase family AAA domain-containing protein 3
MELO3C009797	0,000504618	0,011751999	HSP20-like chaperones superfamily protein
MELO3C008099	0,000506949	0,011792393	eukaryotic translation initiation factor 2D
MELO3C005518	0,000507675	0,011795371	3-isopropylmalate dehydratase small subunit 3-like
MELO3C005679	0,000509158	0,011815931	Tyrosine--tRNA ligase
MELO3C013315	0,000512098	0,011863977	O-methyltransferase, putative
MELO3C026026	0,00051243	0,011863977	PRA1 family protein
MELO3C007495	0,000515516	0,011921451	protein LYK5-like
MELO3C000254	0,00051635	0,011926777	Auxin response factor
MELO3C016915	0,000518351	0,011959004	copper-transporting ATPase PAA2, chloroplastic isoform X1
MELO3C026443	0,000520272	0,011989319	No data found
MELO3C025885	0,000521179	0,011996228	ras-related protein Rab11C
MELO3C003880	0,000522313	0,012008341	Histone deacetylase complex subunit
MELO3C009562	0,000524514	0,012044923	Pentatricopeptide repeat-containing protein
MELO3C009408	0,000526576	0,01204955	Tetratricopeptide repeat (TPR)-like superfamily protein
MELO3C017544	0,000525788	0,01204955	DNA-directed RNA polymerase III subunit RPC5
MELO3C023481	0,000527659	0,01204955	nudix hydrolase 3-like
MELO3C023412	0,000526748	0,01204955	O-fucosyltransferase family protein
MELO3C013645	0,000527767	0,01204955	Alanine--tRNA ligase
MELO3C015350	0,000528832	0,012059945	Sugar transporter ERD6-like protein
MELO3C013600	0,000530899	0,012093112	O-methyltransferase, putative
MELO3C013757	0,000533573	0,012140022	Proteasome subunit alpha type
MELO3C012622	0,000536651	0,012169726	peptidyl-prolyl cis-trans isomerase CYP59
MELO3C015860	0,000536727	0,012169726	Calcium permeable stress-gated cation channel 1
MELO3C021858	0,000536048	0,012169726	WEB family protein At3g02930, chloroplastic
MELO3C025585	0,000538898	0,012204926	bifunctional nitrilase/nitrile hydratase NIT4A
MELO3C009758	0,000540825	0,012230611	Amino acid transporter family protein
MELO3C017878	0,000541271	0,012230611	Protein LURP-one-related 17
MELO3C014176	0,00054293	0,0122525	30S ribosomal protein S6
MELO3C005869	0,000544101	0,0122525	Bidirectional sugar transporter SWEET
MELO3C017320	0,000543557	0,0122525	Zinc finger protein, putative
MELO3C006320	0,000545691	0,01227432	Type 1 membrane protein, putative isoform 1
MELO3C010964	0,000547068	0,012291283	Cyclin-T1-like protein
MELO3C005520	0,000548142	0,012301423	Ribosomal protein L15
MELO3C013437	0,000550127	0,012331966	V-type proton ATPase subunit a
MELO3C025989	0,00055226	0,012354603	Kinase superfamily protein
MELO3C010052	0,000552388	0,012354603	Basic leucine zipper/W2 domain protein
MELO3C013946	0,000560347	0,012494896	Small heat shock protein, chloroplastic
MELO3C015198	0,000560559	0,012494896	Pentatricopeptide repeat-containing protein

MELO3C025813	0,000559301	0,012494896	Polyadenylate-binding protein-interacting protein 3
MELO3C004597	0,000562498	0,012509883	DUF1005 family protein (DUF1005)
MELO3C002817	0,000562464	0,012509883	No data found
MELO3C005300	0,000565577	0,012564217	BnaC07g20870D protein
MELO3C009966	0,000573553	0,012727086	ADP-ribosylation factor-like
MELO3C002816	0,000574467	0,012733052	obg-like ATPase 1
MELO3C021588	0,000578257	0,01280268	CRS1/YhbY (CRM) domain protein
MELO3C009038	0,000579828	0,01280876	adenylosuccinate synthetase, chloroplastic
MELO3C011138	0,000579399	0,01280876	Ultraviolet-B receptor UVR8
MELO3C004437	0,000581551	0,012832462	Methyltransferase-related family protein
MELO3C003057	0,000585005	0,012894272	Phosphatidylinositol-4-phosphate 5-kinase, putative
MELO3C012628	0,000585702	0,012895245	BOI-related E3 ubiquitin-protein ligase 1-like
MELO3C021552	0,000587182	0,012899069	universal stress protein A-like protein
MELO3C019948	0,000586876	0,012899069	Oxidoreductase family protein
MELO3C003916	0,000590103	0,012905799	Cellulose synthase
MELO3C019527	0,000589502	0,012905799	CBS domain-containing protein CBSX1, chloroplastic
MELO3C019163	0,00058932	0,012905799	ABC transporter F family-like protein
MELO3C017347	0,000589846	0,012905799	Actin-interacting protein 1-2
MELO3C006802	0,000591331	0,012918363	Protein DEHYDRATION-INDUCED 19
MELO3C004505	0,000592869	0,012937653	Ribosomal protein L31
MELO3C014849	0,000597937	0,013033838	Alpha/beta hydrolase-3
MELO3C003120	0,000600664	0,013048329	SLT1
MELO3C011752	0,00060038	0,013048329	E3 ubiquitin ligase BIG BROTHER-related
MELO3C022609	0,000601905	0,013048329	No data found
MELO3C021408	0,000599518	0,013048329	Protein trichome birefringence-like 10
MELO3C002159	0,000601837	0,013048329	Nascent polypeptide-associated complex subunit beta
MELO3C005439	0,000603103	0,013059956	NO-associated protein 1, chloroplastic/mitochondrial
MELO3C011193	0,00060643	0,013117619	COP9 signalosome complex subunit 5b
MELO3C017300	0,000607829	0,013119132	AT-rich interactive domain-containing protein 5A, putative
MELO3C017091	0,000607555	0,013119132	Pleckstrin homology domain-containing family M member 3
MELO3C013710	0,000611069	0,013174678	Auxin efflux carrier
MELO3C023725	0,000616646	0,013210354	Protein ROOT PRIMORDIUM DEFECTIVE 1
MELO3C014306	0,000615127	0,013210354	signal recognition particle 9 kDa protein
MELO3C003945	0,000616214	0,013210354	Protein trichome birefringence
MELO3C023492	0,000614151	0,013210354	Receptor kinase
MELO3C012100	0,000616737	0,013210354	ribonuclease 3-like
MELO3C003726	0,000614743	0,013210354	Methyltransferase
MELO3C003326	0,000619344	0,013251824	Ataxin-10
MELO3C002819	0,000620421	0,013260494	eukaryotic translation initiation factor 3 subunit A-like
MELO3C009101	0,000623036	0,013301987	B3 domain-containing transcription repressor VAL2
MELO3C008052	0,000624482	0,013318459	No data found
MELO3C022930	0,000627924	0,013377414	mitotic spindle checkpoint protein MAD1
MELO3C025637	0,000630045	0,013382351	Mannosyltransferase
MELO3C017968	0,000629519	0,013382351	LOW QUALITY PROTEIN: translocase of chloroplast 159, chloroplastic-like
MELO3C010651	0,000630188	0,013382351	No data found
MELO3C006948	0,000634012	0,013449086	Protein SGT1 homolog
MELO3C010273	0,000635076	0,013457201	Transmembrane protein
MELO3C009380	0,000638714	0,013501767	ras-related protein RABC2a
MELO3C015796	0,000639351	0,013501767	Acetyl-CoA carboxylase, putative
MELO3C023200	0,000639914	0,013501767	Receptor-like protein kinase
MELO3C008088	0,000639383	0,013501767	phospholipase SGR2
MELO3C002470	0,00064277	0,013547571	Patatin
MELO3C008775	0,000644342	0,013566207	Elongation factor 4
MELO3C009735	0,000646709	0,013588861	NF-kappa-B-activating protein
MELO3C023114	0,000646794	0,013588861	Cellulose synthase
MELO3C013343	0,000648394	0,013608008	FAD-dependent urate hydroxylase-like
MELO3C014732	0,000652227	0,013620321	Pyruvate kinase
MELO3C016464	0,000649795	0,013620321	No data found
MELO3C013440	0,000651079	0,013620321	PHD domain-containing protein/BAH domain-containing protein
MELO3C005745	0,000652429	0,013620321	Abhydrolase_5 domain-containing protein
MELO3C009779	0,000650797	0,013620321	S-adenosyl-L-methionine-dependent methyltransferases superfamily protein
MELO3C017467	0,00065854	0,01373337	Syntaxin/T-SNARE family protein
MELO3C010693	0,000663173	0,013815404	Lysine ketoglutarate reductase trans-splicing protein (DUF707)
MELO3C006268	0,000670702	0,013942832	10 kDa chaperonin isoform X1
MELO3C003638	0,000670016	0,013942832	replication protein A 32 kDa subunit A-like
MELO3C017902	0,000676531	0,014049225	monothiol glutaredoxin-S15, mitochondrial
MELO3C014090	0,000679738	0,014100991	No data found
MELO3C024333	0,000689727	0,014293207	DNA-binding protein, putative
MELO3C023776	0,000692692	0,014335035	Laminin subunit gamma-1
MELO3C017757	0,000693923	0,014335035	Inositol transporter 1
MELO3C016033	0,000693729	0,014335035	glutathione S-transferase-like
MELO3C011944	0,00069511	0,01434455	Beta-1,4-mannosyl-glycoprotein 4-beta-N-acetylglucosaminyltransferase
MELO3C023442	0,000695857	0,014344959	glycerol kinase
MELO3C008149	0,000702007	0,014454388	LEAF RUST 10 DISEASE-RESISTANCE LOCUS RECEPTOR-LIKE PROTEIN KINASE-like 1.4 isoform X1
MELO3C011488	0,000702629	0,014454388	ylmG homolog protein 2, chloroplastic
MELO3C021436	0,000709823	0,014587203	60S acidic ribosomal protein P2B-like
MELO3C019873	0,000712436	0,01462568	3-oxoacyl-[acyl-carrier-protein] synthase-like protein
MELO3C017254	0,0007278	0,014925576	Sterile alpha motif domain-containing family protein
MELO3C015750	0,000730788	0,014971299	No data found
MELO3C007472	0,000737797	0,015099226	LRR receptor-like serine/threonine-protein kinase GSO1 isoform X1
MELO3C014454	0,000743376	0,015119403	Receptor-like protein kinase

MELO3C007690	0,000741216	0,015119403	No data found
MELO3C002180	0,000743002	0,015119403	mRNA splicing factor, Cwf18
MELO3C018494	0,000741174	0,015119403	Protein TIC 21, chloroplastic
MELO3C017385	0,000742664	0,015119403	pollen receptor-like kinase 1
MELO3C018120	0,000740158	0,015119403	Purple acid phosphatase
MELO3C014722	0,000746062	0,015120083	ethylene-responsive transcription factor RAP2-11
MELO3C019369	0,000746633	0,015120083	50S ribosomal protein L9
MELO3C016139	0,000748004	0,015120083	Mitogen-activated protein kinase
MELO3C009005	0,000746916	0,015120083	Unknown protein
MELO3C022074	0,000747376	0,015120083	Tryptophan synthase-related
MELO3C018732	0,000744619	0,015120083	Histone-lysine N-methyltransferase, H3 lysine-36 specific
MELO3C016152	0,000750497	0,015154969	Gibberellin 2-oxidase
MELO3C013338	0,00075512	0,015201698	RNA-binding protein 39 isoform X1
MELO3C007743	0,000754472	0,015201698	Polyadenylate-binding 2
MELO3C023304	0,000754129	0,015201698	Isoflavone reductase like
MELO3C011482	0,000757284	0,01522973	ATP-citrate synthase beta chain protein 2-like
MELO3C007152	0,000760376	0,015276373	Leucine-rich receptor-like protein kinase family protein
MELO3C017131	0,000764993	0,015353508	General negative regulator of transcription subunit 4
MELO3C008233	0,000766033	0,015358769	Thylakoid lumenal 15 kDa protein 1, chloroplastic
MELO3C021404	0,000767416	0,015370886	Heavy metal-associated isoprenylated plant protein 21
MELO3C023047	0,000770707	0,015405551	glutamyl-tRNA(Gln) amidotransferase subunit B, chloroplastic/mitochondrial
MELO3C027308	0,000770119	0,015405551	alanine--tRNA ligase-like
MELO3C011759	0,000772506	0,015410315	transcription factor DIVARICATA
MELO3C026198	0,000771969	0,015410315	Gamma carbonic anhydrase-like 1, mitochondrial
MELO3C013173	0,000780326	0,01553626	NAC domain-containing protein 17-like
MELO3C007494	0,000780392	0,01553626	Hexosyltransferase
MELO3C017115	0,000781959	0,015551777	succinate dehydrogenase subunit 7B, mitochondrial-like
MELO3C020978	0,000785857	0,015597885	Adenylyl cyclase-associated protein
MELO3C002034	0,000785617	0,015597885	ninja-family protein 6-like isoform X2
MELO3C005942	0,000788048	0,015605062	Kinase family protein
MELO3C016383	0,00078938	0,015605062	RING-type E3 ubiquitin transferase
MELO3C012713	0,000788594	0,015605062	Zinc finger, CCCH-type
MELO3C001997	0,000788804	0,015605062	Galactoside 2-alpha-L-fucosyltransferase
MELO3C016562	0,000790211	0,015605875	At4g33560
MELO3C024241	0,000794484	0,015658951	Kinesin-like protein
MELO3C026760	0,000794199	0,015658951	Arabinogalactan protein
MELO3C021368	0,00080597	0,015869496	DnaJ subfamily B member 14
MELO3C008285	0,000806924	0,015872456	eukaryotic translation initiation factor 3 subunit F
MELO3C026027	0,000808771	0,015892961	Macrophage migration inhibitory factor family protein
MELO3C001994	0,000811478	0,015930293	thioredoxin-like 1-2, chloroplastic
MELO3C009588	0,000814919	0,015934492	Downstream neighbor of Son
MELO3C005199	0,000814794	0,015934492	charged multivesicular body protein 7 isoform X1
MELO3C015422	0,000812644	0,015934492	Arginine--tRNA ligase
MELO3C025799	0,000814018	0,015934492	Alpha-ketoglutarate-dependent dioxygenase AlkB
MELO3C002271	0,000822787	0,016072425	F-box protein SKIP16
MELO3C009961	0,000827069	0,01614011	At1g23710
MELO3C021384	0,000828633	0,016154657	Cox19-like CHCH family protein
MELO3C009148	0,00083221	0,016208388	Methionine aminopeptidase,related
MELO3C011847	0,000834449	0,016235996	60S ribosomal protein L5
MELO3C017833	0,000835285	0,01623626	Golgi SNAP receptor complex member 1-1
MELO3C018360	0,000837062	0,016254804	No data found
MELO3C014230	0,000837903	0,016255158	Ethylene insensitive 2
MELO3C004480	0,000841204	0,016303183	No data found
MELO3C010421	0,000847224	0,016397526	Random slug protein 5
MELO3C022059	0,000847733	0,016397526	Pentatricopeptide repeat-containing protein
MELO3C020963	0,000849397	0,016413642	WRKY family transcription factor
MELO3C012715	0,00085277	0,016462712	mediator of RNA polymerase II transcription subunit 19a-like
MELO3C009771	0,000855185	0,01648973	Ectonucleotide pyrophosphatase/phosphodiesterase family member 3
MELO3C006154	0,000856674	0,01648973	Cyclin-D-binding Myb-like transcription factor 1
MELO3C023367	0,000856226	0,01648973	DNA repair protein XRCC1
MELO3C013587	0,000858523	0,016493166	No data found
MELO3C017416	0,000858187	0,016493166	Cyclin-dependent protein kinase inhibitor SMR15
MELO3C002651	0,000861593	0,016536046	protein SCAR3
MELO3C013541	0,000864234	0,016570635	No data found
MELO3C002314	0,000873986	0,016741364	cytochrome P450 71A1-like
MELO3C017945	0,000876911	0,016781123	bifunctional epoxide hydrolase 2-like
MELO3C007181	0,000880809	0,016839406	MADS box transcription factor AGAMOUS
MELO3C019564	0,000883614	0,01687668	High chlorophyll fluorescence phenotype 173
MELO3C012722	0,000891105	0,016964184	Pentatricopeptide repeat-containing family protein
MELO3C007800	0,00089249	0,016964184	Receptor protein kinase, putative
MELO3C007986	0,000892438	0,016964184	Histidine phosphatase family (Branch 1) protein
MELO3C022783	0,000891729	0,016964184	transmembrane protein 50A
MELO3C003344	0,000890474	0,016964184	3-isopropylmalate dehydratase large subunit
MELO3C004366	0,000900021	0,017090883	Prenylyltransferase superfamily protein
MELO3C004577	0,000902227	0,017099894	CRS2-associated factor 1, chloroplastic
MELO3C010042	0,000901754	0,017099894	endoribonuclease Dicer homolog 2 isoform X2
MELO3C010456	0,000904831	0,017125726	Phosphatidylinositol-4-phosphate 5-kinase, putative
MELO3C020789	0,000905325	0,017125726	Nucleoporin NUP188 like
MELO3C017960	0,000907356	0,017147725	NADH dehydrogenase [ubiquinone] iron-sulfur protein 5-B
MELO3C003222	0,0009085	0,017152936	mRNA-capping enzyme
MELO3C006412	0,000910434	0,01717303	60S ribosomal protein L14, putative

MELO3C025255	0,00091322	0,017209147	Zinc transporter
MELO3C014273	0,000917455	0,017236905	Pentatricopeptide repeat-containing protein family
MELO3C013965	0,000916457	0,017236905	Flavin-containing monooxygenase
MELO3C022639	0,000915894	0,017236905	No data found
MELO3C009914	0,000918184	0,017236905	Alpha-mannosidase
MELO3C020591	0,000923743	0,01732478	Glycosyltransferase
MELO3C015748	0,00092849	0,017397286	transcription factor EMB1444
MELO3C019253	0,000930162	0,017412104	thioredoxin domain-containing protein 9 homolog
MELO3C019858	0,000933305	0,017454393	No data found
MELO3C014611	0,0009373	0,017512516	Pre-mRNA-splicing factor CWC22
MELO3C009455	0,000940284	0,017551679	BZIP transcription factor family protein
MELO3C002363	0,00094684	0,017650564	TITAN-like protein
MELO3C003671	0,000947369	0,017650564	SPOC domain/transcription elongation factor S-II, putative
MELO3C004204	0,00095	0,017666245	Importin subunit alpha
MELO3C008058	0,000949138	0,017666245	mitogen-activated protein kinase kinase kinase YODA isoform X1
MELO3C018476	0,000953839	0,01772094	cyclin-D3-3
MELO3C013769	0,000956211	0,017748314	Seven transmembrane receptor
MELO3C004279	0,00096026	0,017756725	RING zinc finger family protein
MELO3C014018	0,000957996	0,017756725	Pentatricopeptide repeat-containing protein family
MELO3C007047	0,000959447	0,017756725	Protein kinase
MELO3C026518	0,000958725	0,017756725	Photosystem II reaction center PsbP family protein
MELO3C010055	0,000964219	0,01781324	4-hydroxy-4-methyl-2-oxoglutarate aldolase
MELO3C016246	0,000969134	0,017870612	Kinase family protein
MELO3C025917	0,000968892	0,017870612	CAX-interacting protein 4
MELO3C016469	0,000970779	0,01788425	zinc finger CCCH domain-containing protein 5
MELO3C002741	0,000973931	0,017925603	Protein TIFY 5A
MELO3C003375	0,000975079	0,01793001	Two-component response regulator-like protein APRR2
MELO3C013406	0,000976852	0,017945908	tRNA-dihydrouridine(47) synthase [NAD(P)(+)]
MELO3C019504	0,000978735	0,017952113	Meiosis arrest female protein 1-like protein
MELO3C010686	0,000979008	0,017952113	Alanine aminotransferase 2
MELO3C003973	0,000982277	0,017995345	SNW/SKI-interacting protein-like
MELO3C009172	0,000986526	0,018006515	RING finger protein
MELO3C017703	0,000986533	0,018006515	disease resistance protein RGA2-like
MELO3C007010	0,000985587	0,018006515	phosphatidate cytidylyltransferase, mitochondrial isoform X1
MELO3C010353	0,000986326	0,018006515	protein NRT1/ PTR FAMILY 6.2-like
MELO3C022144	0,000992835	0,018104803	TMV resistance protein N-like
MELO3C014850	0,000995059	0,018128608	No data found
MELO3C009334	0,000999425	0,01819137	Methyltransferase type 11
MELO3C021622	0,001003418	0,01823046	Elicitor-responsive protein 1
MELO3C002464	0,001003114	0,01823046	polyadenylate-binding protein RBP45-like
MELO3C014604	0,001005214	0,01824629	F16F4.11 protein
MELO3C009663	0,001009648	0,018276383	1-acyl-sn-glycerol-3-phosphate acyltransferase-like protein
MELO3C014161	0,001009339	0,018276383	aspartic proteinase A1-like
MELO3C010286	0,001008161	0,018276383	pyrophosphate-energized vacuolar membrane proton pump
MELO3C027408	0,001010878	0,018281896	polygalacturonase-like
MELO3C014346	0,001017641	0,018370564	protein PALE CRESS, chloroplastic
MELO3C018950	0,001016798	0,018370564	Chaperone protein DNAj, putative
MELO3C016923	0,001022046	0,018401207	No data found
MELO3C015867	0,001022134	0,018401207	E3 ubiquitin ligase-like protein
MELO3C008092	0,001020377	0,018401207	50S ribosomal protein L14, putative
MELO3C010601	0,001025788	0,018433383	LysM domain-containing GPI-anchored protein 1
MELO3C010958	0,001025271	0,018433383	Gamma carbonic anhydrase 1, mitochondrial
MELO3C015747	0,001032087	0,018529709	At3g60850
MELO3C015692	0,001037635	0,018612402	Brefeldin A-inhibited guanine nucleotide-exchange protein
MELO3C013076	0,001042091	0,018675371	casein kinase I
MELO3C006189	0,001045776	0,018713312	Glutathione S-transferase
MELO3C020825	0,001046103	0,018713312	Phospholipase-like protein
MELO3C015518	0,001051409	0,018791208	Acyl-CoA N-acyltransferase (NAT) superfamily protein
MELO3C008773	0,001052661	0,01879657	Succinate dehydrogenase assembly factor 2, mitochondrial
MELO3C008766	0,001057254	0,018861521	sister chromatid cohesion 1 protein 4 isoform X1
MELO3C014895	0,001064445	0,018972668	squamosa promoter-binding-like protein 13A
MELO3C022014	0,001066831	0,018998061	WRKY transcription factor, putative
MELO3C000075	0,00107158	0,01906543	Myosin heavy chain-like protein, putative
MELO3C015304	0,001074501	0,019094858	60S ribosomal protein L22-2
MELO3C018768	0,001075167	0,019094858	Wound-responsive family protein
MELO3C013175	0,00108687	0,019285347	Pentatricopeptide repeat-containing family protein
MELO3C017440	0,001088108	0,019289993	U3 small nucleolar RNA-associated protein 25-like
MELO3C024226	0,00109041	0,019313455	Sulfate transporter 3.1
MELO3C009261	0,001093328	0,019347793	Peptide transporter family protein
MELO3C014027	0,001103763	0,019442977	Cytochrome P450 family protein
MELO3C025232	0,001102913	0,019442977	Ubiquitin-conjugating enzyme, E2
MELO3C015946	0,001106583	0,019442977	GATA transcription factor-like protein
MELO3C023413	0,001105341	0,019442977	Signal peptidase I
MELO3C002757	0,001104571	0,019442977	signal recognition particle 14 kDa protein
MELO3C017149	0,001102634	0,019442977	Pentatricopeptide repeat-containing protein
MELO3C018617	0,001106334	0,019442977	Pentatricopeptide repeat-containing protein
MELO3C011484	0,001104414	0,019442977	Spermidine synthase
MELO3C011088	0,001108133	0,019452898	mechanosensitive ion channel protein 3, chloroplastic-like
MELO3C006088	0,001117354	0,019562608	50S ribosomal protein L5, chloroplastic
MELO3C012391	0,001117266	0,019562608	NAC domain-containing protein 16
MELO3C020942	0,001115702	0,019562608	PQ-loop repeat family protein / transmembrane family protein

MELO3C006409	0,001125418	0,019651524	Glycolipid transfer protein domain-containing protein
MELO3C016775	0,001123501	0,019651524	Leucine-rich repeat receptor-like protein kinase family
MELO3C010517	0,001125381	0,019651524	WAT1-related protein
MELO3C007103	0,001130481	0,019689543	Protein plastid transcriptionally active 12
MELO3C005918	0,001128976	0,019689543	NPL4 family protein
MELO3C020806	0,001131583	0,019689543	Peptidyl-prolyl cis-trans isomerase
MELO3C017223	0,001130983	0,019689543	Mitochondrial carrier protein, putative
MELO3C021345	0,001136978	0,019761011	cullin-1
MELO3C010985	0,001137691	0,019761011	B-box zinc finger protein 20-like
MELO3C020834	0,00113984	0,019780936	Unknown protein
MELO3C004448	0,001143358	0,019824557	DNA helicase
MELO3C013773	0,001144942	0,019834607	Mediator of RNA polymerase II transcription subunit
MELO3C022477	0,001146898	0,019851081	Protein nuclear fusion defective 4
MELO3C002144	0,001148916	0,019868609	Receptor-like kinase 1
MELO3C006294	0,001154872	0,019954119	Dna repair helicase xpb1
MELO3C004015	0,001156853	0,019970875	Pentatricopeptide repeat-containing family protein
MELO3C007433	0,001159232	0,019994482	fumarylacetoacetase
MELO3C008815	0,001162718	0,02001964	nucleolar MIF4G domain-containing protein 1
MELO3C008313	0,00116263	0,02001964	UTP--glucose-1-phosphate uridylyltransferase 3, chloroplastic
MELO3C014315	0,001169638	0,020034938	Bifunctional DNA-directed RNA polymerase subunit beta-beta
MELO3C027330	0,001170708	0,020034938	Caffeic acid O-methyltransferase
MELO3C008801	0,001169091	0,020034938	H/ACA ribonucleoprotein complex subunit
MELO3C005079	0,001166811	0,020034938	protein ASPARTIC PROTEASE IN GUARD CELL 2
MELO3C005332	0,001165013	0,020034938	CDP-diacylglycerol--serine O-phosphatidyltransferase 1
MELO3C021456	0,001170444	0,020034938	histone deacetylase HDT1-like
MELO3C003305	0,001167299	0,020034938	Protein CDI
MELO3C004439	0,001173596	0,02006408	Protein phosphatase 2c, putative
MELO3C005367	0,001174443	0,02006408	dehydration-responsive element-binding protein 1D-like
MELO3C014091	0,001178037	0,020108075	caffeic acid 3-O-methyltransferase-like
MELO3C017255	0,001182788	0,020171749	BSD domain-containing protein
MELO3C021620	0,001185964	0,02020329	transcription initiation factor TFIID subunit 7
MELO3C005651	0,001186684	0,02020329	30S ribosomal S1
MELO3C004142	0,001189887	0,020211881	Unknown protein
MELO3C016826	0,001188294	0,020211881	At4g33800
MELO3C002219	0,001190259	0,020211881	HIPL1 protein-like isoform X1
MELO3C006314	0,001193205	0,020244514	60S ribosomal protein L13a, putative
MELO3C024505	0,001194936	0,02025648	SRSF protein kinase 1-like
MELO3C006160	0,001197871	0,020288819	Histone deacetylase complex subunit SAP18
MELO3C018758	0,001202	0,020341295	Secretory carrier-associated membrane protein
MELO3C005704	0,001205731	0,020386969	Beta-carotene hydroxylase
MELO3C015202	0,001210885	0,02045661	zinc finger A20 and AN1 domain-containing stress-associated protein 4-like
MELO3C026288	0,001212665	0,020469162	Serine/threonine-protein phosphatase 2A 55 kDa regulatory subunit B
MELO3C017581	0,001216996	0,02052472	inositol-3-phosphate synthase
MELO3C009583	0,001222917	0,020606981	E3 ubiquitin-protein ligase BAH1-like protein, putative
MELO3C017358	0,001226322	0,020646745	C2 domain-containing protein
MELO3C024222	0,00122875	0,020670004	aldo-keto reductase family 4 member C9-like
MELO3C023338	0,001234763	0,020744986	cysteine proteinase RD19a-like
MELO3C022494	0,001235308	0,020744986	No data found
MELO3C009234	0,001237827	0,020744988	SUPERMAN-like zinc finger protein
MELO3C008598	0,001240561	0,020744988	Lecithin:cholesterol acyltransferase family protein
MELO3C017939	0,00123777	0,020744988	Ribosomal protein L19
MELO3C022819	0,001239145	0,020744988	Myosin heavy chain-like protein, putative
MELO3C012004	0,001240427	0,020744988	Xyloglucan endotransglucosylase/hydrolase
MELO3C013829	0,001245009	0,020801755	Calmodulin family protein
MELO3C005849	0,001247648	0,020828226	p-loop containing nucleoside triphosphate hydrolases superfamily protein
MELO3C008947	0,001248718	0,020828498	CBS domain-containing protein
MELO3C016623	0,001251995	0,020865521	NAD(P)H dehydrogenase (Quinone)
MELO3C006145	0,001255715	0,02090987	F-box protein PP2-A13
MELO3C026304	0,001256932	0,020912504	nuclear cap-binding protein subunit 2
MELO3C013750	0,001262209	0,020982623	SKP1-like protein 1B
MELO3C003826	0,001266017	0,021028241	No data found
MELO3C018434	0,001269051	0,021060915	Armadillo repeat-containing protein, putative
MELO3C013489	0,001281695	0,021236976	monosaccharide-sensing protein 2
MELO3C010223	0,00128181	0,021236976	WRKY transcription factor
MELO3C014447	0,001297412	0,021444979	Nuclear ribonuclease Z
MELO3C022094	0,001296764	0,021444979	T-complex protein 1 subunit zeta 1
MELO3C005201	0,001297623	0,021444979	multicopper oxidase LPR1-like
MELO3C006420	0,001299336	0,021455341	Cotton fiber protein
MELO3C007127	0,001302118	0,021483309	9-cis-epoxycarotenoid dioxygenase
MELO3C014307	0,001311889	0,021626452	PRA1 family protein
MELO3C008076	0,001313603	0,021636651	No data found
MELO3C014258	0,00131955	0,021716499	IQ-domain 1
MELO3C005913	0,001328415	0,021844183	Auxin-responsive family protein
MELO3C017730	0,001329905	0,021850495	Pentatricopeptide repeat-containing family protein
MELO3C016550	0,001332312	0,021871848	Unknown protein
MELO3C002227	0,001334843	0,021895188	Unknown protein
MELO3C009467	0,001336203	0,021899309	Alpha/beta-Hydrolases superfamily protein
MELO3C023985	0,001340004	0,021943403	RNA/RNP complex-1-interacting phosphatase, putative
MELO3C012131	0,001342593	0,021962024	eukaryotic translation initiation factor 5A-like
MELO3C018180	0,001343365	0,021962024	tRNA (guanine(37)-N1)-methyltransferase
MELO3C005779	0,001350039	0,022052878	Metal-dependent protein hydrolase

MELO3C004645	0,001354559	0,022099308	40S ribosomal S3-like protein
MELO3C013149	0,001355635	0,022099308	UPF0505 protein C16orf62 homolog isoform X1
MELO3C007899	0,001357906	0,022099308	WD repeat-containing protein 82
MELO3C026058	0,001357441	0,022099308	Non-specific serine/threonine protein kinase
MELO3C005214	0,001360416	0,022099308	Defensin
MELO3C026194	0,001361813	0,022099308	No data found
MELO3C018688	0,001360022	0,022099308	dynamin-like protein ARC5
MELO3C010731	0,001361834	0,022099308	cyclin-dependent kinase G-2 isoform X1
MELO3C010640	0,00136367	0,022110937	zinc finger CCCH domain-containing protein 1
MELO3C005711	0,001366829	0,022131961	heavy metal-associated isoprenylated plant protein 3-like
MELO3C021185	0,001367208	0,022131961	Peptidase M48
MELO3C016149	0,001369639	0,022153147	Cationic amino acid transporter, putative
MELO3C015695	0,001377374	0,022260026	Expansin
MELO3C019011	0,001378575	0,022261231	copper-transporting ATPase PAA1, chloroplastic isoform X1
MELO3C006759	0,001385022	0,022347062	Ca2+-activated RelA/SpoT-like protein
MELO3C013780	0,001388796	0,022389659	Early nodulin-like protein 1
MELO3C001656	0,001392959	0,022438453	Unknown protein
MELO3C005389	0,001395363	0,022458857	NADH dehydrogenase [ubiquinone] 1 alpha subcomplex subunit 12
MELO3C018264	0,001399616	0,022508972	No data found
MELO3C003423	0,001400854	0,022510545	Zinc finger CCCH domain protein
MELO3C007413	0,001405347	0,02255593	Core-2/I-branching beta-1,6-N-acetylglucosaminyltransferase family protein
MELO3C021308	0,001405962	0,02255593	Multiple organellar RNA editing factor 8, chloroplastic/mitochondrial
MELO3C013745	0,001413439	0,02265747	Phosphatase 2C family protein
MELO3C013760	0,001414678	0,022658937	26S proteasome non-ATPase regulatory subunit 4 homolog
MELO3C014687	0,001418108	0,022695105	Structural maintenance of chromosomes protein
MELO3C021360	0,001419955	0,022695105	Pentatricopeptide repeat-containing family protein
MELO3C002687	0,001420383	0,022695105	dynamin-related protein 4C-like
MELO3C004084	0,001428955	0,022709919	No data found
MELO3C006202	0,00143051	0,022709919	Peptidase_M22 domain-containing protein
MELO3C019501	0,001430486	0,022709919	Transmembrane 53
MELO3C017880	0,001423996	0,022709919	Glucan endo-1,3-beta-glucosidase
MELO3C025272	0,001429508	0,022709919	AT3g54190/F24B22_150
MELO3C004833	0,001425696	0,022709919	crooked neck-like protein 1
MELO3C008116	0,001429946	0,022709919	Magnesium transporter NIPA
MELO3C011498	0,001426771	0,022709919	Splicing factor u2af large subunit, putative
MELO3C021563	0,001441577	0,022867225	isocitrate dehydrogenase [NADP]
MELO3C010599	0,001442786	0,022868044	Gamma-glutamylcyclotransferase
MELO3C002717	0,001445458	0,022892023	prefoldin subunit 6
MELO3C005939	0,001448732	0,022925487	nucleoside diphosphate kinase
MELO3C022399	0,00145033	0,022932398	alcohol dehydrogenase-like
MELO3C004475	0,001453822	0,022939204	arogenate dehydrogenase 1, chloroplastic-like
MELO3C000251	0,001453758	0,022939204	Protein LAZ1
MELO3C002821	0,001454245	0,022939204	Unknown protein
MELO3C004467	0,001460846	0,02302494	Exostosin family protein
MELO3C005926	0,001468715	0,023093668	protein BONZAI 1
MELO3C005821	0,001467018	0,023093668	mRNA, clone: RTFL01-46-D12
MELO3C022448	0,001467626	0,023093668	Metal tolerance protein
MELO3C013702	0,001471309	0,023116053	kinesin-like calmodulin-binding protein
MELO3C016558	0,001475647	0,023129006	Cyclic nucleotide-gated ion channel, putative
MELO3C007269	0,001475218	0,023129006	Auxin repressed protein
MELO3C020749	0,001473578	0,023129006	amidophosphoribosyltransferase, chloroplastic-like
MELO3C018985	0,001478932	0,023162115	60S acidic ribosomal protein P1
MELO3C019053	0,001482362	0,023197442	Ectonucleotide pyrophosphatase/phosphodiesterase family member 3
MELO3C015954	0,001488106	0,023261476	No data found
MELO3C021295	0,001489848	0,023261476	Transducin family protein/WD-40 repeat protein
MELO3C003394	0,001489988	0,023261476	Protein LSD1
MELO3C012730	0,001497104	0,023335688	Structural maintenance of chromosomes protein
MELO3C002092	0,001496421	0,023335688	Receptor-like kinase
MELO3C017167	0,001501045	0,023378654	Transmembrane protein
MELO3C023251	0,001504394	0,023393301	callose synthase 5
MELO3C020927	0,001505539	0,023393301	Molybdenum cofactor sulfurase
MELO3C019661	0,00150409	0,023393301	No data found
MELO3C022124	0,001507441	0,023404444	Glycerophosphodiester phosphodiesterase GDPD4
MELO3C016608	0,001511362	0,023428483	Transmembrane protein, putative
MELO3C005331	0,001510473	0,023428483	Acyl-[acyl-carrier-protein] hydrolase
MELO3C009587	0,001521811	0,023553483	S-adenosyl-L-methionine-dependent methyltransferases superfamily protein
MELO3C005136	0,001521725	0,023553483	Protein EARLY RESPONSIVE TO DEHYDRATION 15
MELO3C025590	0,001526407	0,023587651	NF-kappa-B inhibitor-like protein 2 isoform 2
MELO3C009872	0,001525706	0,023587651	Gibberellin-regulated family protein
MELO3C003416	0,001529192	0,023612208	Unknown protein
MELO3C004564	0,001534372	0,023673689	protein NUCLEAR FUSION DEFECTIVE 6, chloroplastic/mitochondrial-like isoform X2
MELO3C016884	0,001539685	0,023737111	Methyltransferase
MELO3C004273	0,001542611	0,023745402	Mitochondrial Rho GTPase
MELO3C010727	0,001542628	0,023745402	3-oxoacyl-[acyl-carrier-protein] reductase 4
MELO3C023503	0,001549719	0,023827649	Unknown protein
MELO3C018573	0,001550384	0,023827649	Inorganic pyrophosphatase
MELO3C019724	0,001557475	0,023918018	Triacylglycerol lipase 2, putative
MELO3C014888	0,001567833	0,024026857	yrdC domain-containing protein, mitochondrial isoform X2
MELO3C012545	0,001569051	0,024026857	phosphatidylinositol 4-kinase alpha 1-like
MELO3C003249	0,001569429	0,024026857	target of Myb protein 1 isoform X1
MELO3C004944	0,001569178	0,024026857	polyadenylation and cleavage factor homolog 4 isoform X2

MELO3C021217	0,001571244	0,024036012	MACPF domain-containing CAD1-like protein
MELO3C009149	0,001572553	0,024037418	Copper chaperone SCO1/SenC
MELO3C024337	0,001576201	0,024074551	transmembrane protein 87B isoform X2
MELO3C003487	0,00157823	0,024086905	receptor-like protein kinase HAIKU2
MELO3C019026	0,001585064	0,024172538	Phosphate transporter
MELO3C004134	0,001588934	0,024178861	leucine aminopeptidase 1-like
MELO3C023358	0,001586845	0,024178861	Ubiquitin fusion degradation 1 protein
MELO3C011654	0,001589152	0,024178861	RING zinc finger protein-like
MELO3C007617	0,001591437	0,024194985	At5g67390
MELO3C006316	0,001593731	0,024211227	cytochrome b5
MELO3C020369	0,001597715	0,024215862	60S ribosomal protein L37a
MELO3C006870	0,001595901	0,024215862	ethylene-responsive transcription factor ERF027
MELO3C018106	0,001596976	0,024215862	ABC transporter B family protein
MELO3C004281	0,001605072	0,024290084	mevalonate kinase-like
MELO3C024916	0,001604299	0,024290084	Agenet domain-containing protein / bromo-adjacent domain-containing protein, putative
MELO3C019333	0,001606757	0,02429697	DUF679 domain membrane protein
MELO3C011011	0,001610571	0,024336007	Transducin/WD40 repeat-like superfamily protein
MELO3C007254	0,001613304	0,024340055	guanylate-binding protein 2
MELO3C005103	0,00161323	0,024340055	Cytochrome b-c1 complex subunit Rieske, mitochondrial
MELO3C016315	0,001620821	0,024434804	Unknown protein
MELO3C020836	0,001625795	0,024472427	transportin-1
MELO3C026715	0,001625262	0,024472427	Tetratricopeptide repeat (TPR)-like superfamily protein
MELO3C005511	0,001628068	0,024487975	palmitoyl-protein thioesterase 1-like
MELO3C007328	0,001631145	0,024515588	Wound-responsive family protein
MELO3C004321	0,001634236	0,024534462	Vat protein
MELO3C007405	0,001634885	0,024534462	peroxisomal membrane protein PMP22
MELO3C025308	0,001637045	0,024548219	auxin-responsive protein IAA16-like
MELO3C008847	0,001648475	0,024700867	M50 family peptidase
MELO3C002167	0,001652239	0,024723069	Succinate--CoA ligase [ADP-forming] subunit alpha, mitochondrial
MELO3C017207	0,001652461	0,024723069	LYR motif-containing protein 4
MELO3C005109	0,00165439	0,024733189	alpha-mannosidase
MELO3C010057	0,001655678	0,024733726	WRKY transcription factor SUSIBA2-like isoform X2
MELO3C012445	0,001657268	0,024738761	ATP synthase subunit d, mitochondrial
MELO3C002118	0,001660133	0,024762816	Elongation factor 1 alpha
MELO3C002390	0,00166271	0,024763845	At5g44650
MELO3C022228	0,001662029	0,024763845	Dienelactone hydrolase
MELO3C020733	0,001666156	0,024777792	Hexosyltransferase
MELO3C018306	0,001665461	0,024777792	Mitogen-activated protein kinase
MELO3C009506	0,00166957	0,024782586	secoisolariciresinol dehydrogenase-like
MELO3C025490	0,001670243	0,024782586	Protein TONNEAU 1b
MELO3C025725	0,001669696	0,024782586	RNA binding (RRM/RBD/RNP motifs) family protein
MELO3C025872	0,001673066	0,024805848	protein NRT1/ PTR FAMILY 8.1-like
MELO3C009188	0,001675463	0,02482275	transcription factor DIVARICATA-like
MELO3C013738	0,00167882	0,02483522	Ganglioside-induced differentiation-associated protein 2
MELO3C002312	0,00167825	0,02483522	cytochrome P450 71A1-like
MELO3C002646	0,001687107	0,024939126	Transcription initiation factor IIB
MELO3C021845	0,001689148	0,02495062	Cytochrome P450
MELO3C026143	0,001694488	0,025010794	Unknown protein
MELO3C023540	0,001697192	0,025022503	Unknown protein
MELO3C011172	0,001697815	0,025022503	Proteasome subunit beta type
MELO3C006949	0,001709312	0,025138388	NADH-ubiquinone oxidoreductase-related
MELO3C012597	0,00171077	0,025138388	Defective in cullin neddylation protein
MELO3C002016	0,00170755	0,025138388	zinc finger protein ZAT4-like
MELO3C026657	0,001709578	0,025138388	Glycine-rich protein
MELO3C006136	0,00171365	0,025161981	Signal recognition particle 54 kDa protein
MELO3C009119	0,001718851	0,025219605	Protein LURP-one-related 15
MELO3C009318	0,001727588	0,02528348	Ribonuclease P protein subunit p29
MELO3C023310	0,001728325	0,02528348	Glucose-1-phosphate adenylyltransferase
MELO3C018521	0,001726606	0,02528348	DNA polymerase kappa
MELO3C019818	0,001724792	0,02528348	DVL8
MELO3C009278	0,0017382	0,025405911	Pectin acetylesterase
MELO3C009019	0,001741661	0,025405911	Rhodanese-like domain-containing family protein
MELO3C023309	0,001739777	0,025405911	SNF1-related protein kinase regulatory subunit gamma-1-like
MELO3C009949	0,00174184	0,025405911	Pentatricopeptide repeat-containing protein
MELO3C009275	0,001749203	0,02541754	No data found
MELO3C006005	0,001751647	0,02541754	Bifunctional fucokinase/fucose pyrophosphorylase
MELO3C006569	0,001747599	0,02541754	Cytochrome P450 family protein
MELO3C016483	0,001744253	0,02541754	phosphoribosylamine--glycine ligase
MELO3C016879	0,001748919	0,02541754	Cytochrome P450, putative
MELO3C005299	0,001746783	0,02541754	C2 domain-containing protein
MELO3C012967	0,00175148	0,02541754	At5g57230
MELO3C017043	0,001755354	0,025433964	Glutamate receptor
MELO3C022231	0,001755155	0,025433964	Corepressor
MELO3C021047	0,001762342	0,025479124	nucleolin-like
MELO3C021370	0,001762177	0,025479124	PAX-interacting protein 1
MELO3C003456	0,001761414	0,025479124	Alpha/beta-Hydrolases superfamily protein
MELO3C004139	0,00176555	0,025506839	Ubiquitin carboxyl-terminal hydrolase, putative
MELO3C018495	0,001768672	0,025533265	Carbohydrate esterase, putative (DUF303)
MELO3C017838	0,001777557	0,025642781	Ubiquitin system component Cue
MELO3C005286	0,001783225	0,025687028	Mediator of RNA polymerase II transcription subunit 23
MELO3C019947	0,001782242	0,025687028	Oxidoreductase family protein

MELO3C020860	0,001789058	0,025752271	DNA polymerase
MELO3C002240	0,001807554	0,025999557	RING-type E3 ubiquitin transferase
MELO3C009032	0,001813381	0,026064389	fructokinase-like 2, chloroplastic
MELO3C013353	0,001817417	0,026103398	heavy metal-associated isoprenylated plant protein 26-like
MELO3C007081	0,001821971	0,026149788	SIT4 phosphatase-associated family protein
MELO3C014099	0,001824298	0,026164165	BnaC03g71690D protein
MELO3C022021	0,001827571	0,026192087	Lysine--trna ligase
MELO3C025593	0,001834197	0,026267986	Pentatricopeptide repeat-containing family protein
MELO3C016931	0,001837696	0,026276854	Hydroxyproline-rich glycoprotein
MELO3C017462	0,001838808	0,026276854	(DL)-glycerol-3-phosphatase 2
MELO3C008248	0,001836651	0,026276854	GRF1-interacting factor 3
MELO3C006943	0,001845063	0,026347185	Keratin-associated protein, putative (DUF819)
MELO3C005446	0,001846912	0,026354528	60S ribosomal protein L13
MELO3C016951	0,001854951	0,02639962	Glutathione peroxidase
MELO3C011952	0,001855104	0,02639962	UDP-galactose:fucoside alpha-3-galactosyltransferase
MELO3C008389	0,001855419	0,02639962	RNA-binding protein 2
MELO3C003593	0,001853717	0,02639962	Bromo-adjacent-like (BAH) domain protein
MELO3C002589	0,001869205	0,026576627	At2g47960/T9J23.10
MELO3C010716	0,001872575	0,026605377	Protein HHL1, chloroplastic
MELO3C006367	0,001875238	0,026624071	histone-lysine N-methyltransferase family member SUVH9
MELO3C023469	0,001878526	0,026651592	Protein LOW PSII ACCUMULATION 3, chloroplastic
MELO3C008040	0,001881556	0,026675408	RING-type E3 ubiquitin transferase
MELO3C017808	0,001885382	0,026702269	Protein NEOXANTHIN-DEFICIENT 1
MELO3C026053	0,001887507	0,026702269	WEB family protein At2g38370
MELO3C010350	0,001886706	0,026702269	heme oxygenase 1, chloroplastic
MELO3C023473	0,001895232	0,02679237	Phosphatase 2C family protein
MELO3C007011	0,001898043	0,026793748	No data found
MELO3C013051	0,001897813	0,026793748	Dead box ATP-dependent RNA helicase, putative
MELO3C006598	0,001903585	0,026833623	serine/arginine-rich SC35-like splicing factor SCL28
MELO3C016379	0,00190291	0,026833623	Ultraviolet-B receptor UVR8
MELO3C011705	0,001905403	0,026840092	Pyruvate dehydrogenase E1 component subunit alpha
MELO3C022411	0,001916373	0,026975379	No data found
MELO3C013859	0,001926227	0,027063223	CAAX amino terminal protease
MELO3C013331	0,001924304	0,027063223	hippocampus abundant transcript-like protein 1
MELO3C017481	0,001926725	0,027063223	Xyloglucan endotransglucosylase/hydrolase
MELO3C007612	0,001929109	0,027077453	molybdate-anion transporter
MELO3C018999	0,001934757	0,02710801	Transmembrane protein, putative
MELO3C026015	0,001938149	0,02710801	cyclin-dependent kinase 11B-like
MELO3C015999	0,001937128	0,02710801	60S ribosomal protein L22-2
MELO3C011885	0,001937355	0,02710801	Lipoxygenase
MELO3C027092	0,0019373	0,02710801	DExH-box ATP-dependent RNA helicase DExH12-like
MELO3C023885	0,001943686	0,027166205	Tropinone reductase family protein
MELO3C025699	0,001945414	0,027171132	Mitochondrial carrier protein
MELO3C014825	0,001948929	0,027200989	Steroid nuclear receptor, ligand-binding
MELO3C011716	0,001953014	0,027238758	TBC1 domain family member 8B
MELO3C017836	0,001960071	0,027306672	UPF0326 protein
MELO3C011206	0,001960649	0,027306672	dentin sialophosphoprotein-like
MELO3C019899	0,001972807	0,027456636	AMMECR1 family
MELO3C004391	0,001978193	0,027512209	PRA1 family protein
MELO3C011977	0,001982034	0,027546231	polygalacturonase At1g48100
MELO3C006681	0,001986267	0,027579088	bifunctional epoxide hydrolase 2-like
MELO3C007737	0,001987191	0,027579088	No data found
MELO3C019326	0,001990879	0,027610857	Glutaredoxin
MELO3C002372	0,002008671	0,027838061	heavy metal-associated isoprenylated plant protein 3-like
MELO3C026247	0,002012254	0,027868159	Raffinose synthase
MELO3C002897	0,002014896	0,027885197	Nuclear receptor corepressor 1
MELO3C011109	0,002016465	0,027887376	Octicosapeptide/Phox/Bem1p
MELO3C017786	0,002018683	0,027898511	GPI-anchored protein
MELO3C010755	0,002023602	0,027946928	At5g11810
MELO3C009159	0,002035301	0,028051229	ALC-interacting protein 1
MELO3C014488	0,002035415	0,028051229	Cyclin T1 family protein
MELO3C021929	0,002034457	0,028051229	B3 domain-containing transcription factor VRN1-like
MELO3C026782	0,002039701	0,028090688	Protein WVD2-like 3
MELO3C011984	0,002046965	0,028171092	pyrrolidone-carboxylate peptidase
MELO3C003852	0,00205307	0,028226406	DNA ligase-like protein
MELO3C003861	0,002053843	0,028226406	H/ACA ribonucleoprotein complex non-core subunit NAF1-like isoform X1
MELO3C019561	0,002059087	0,028228772	At1g78995
MELO3C017979	0,002059733	0,028228772	Bifunctional protein FolD
MELO3C012218	0,00205906	0,028228772	Two-component response regulator
MELO3C018406	0,002057861	0,028228772	Cytochrome c biogenesis protein
MELO3C006528	0,002063123	0,028235108	At1g05410/T25N20_5
MELO3C002785	0,002062723	0,028235108	epimerase family protein SDR39U1 homolog, chloroplastic-like
MELO3C024673	0,002067343	0,028235108	Trihelix transcription factor
MELO3C019810	0,002067002	0,028235108	Adenosine kinase
MELO3C003511	0,002064632	0,028235108	No data found
MELO3C012160	0,002082866	0,028427444	Protein BIG GRAIN 1-like E
MELO3C010420	0,002085005	0,028436991	DUF581 family protein, putative (DUF581)
MELO3C001323	0,002089158	0,02844162	transmembrane protein 184C
MELO3C017259	0,002087757	0,02844162	Protoheme IX farnesyltransferase, mitochondrial
MELO3C003545	0,002089665	0,02844162	28 kDa ribonucleoprotein
MELO3C022500	0,002094619	0,02848941	Vacuolar protein sorting 26

MELO3C003292	0,002110998	0,028692428	protein N-methyltransferase NNT1 isoform X1
MELO3C020906	0,002112654	0,028695185	60S ribosomal protein L26-1-like
MELO3C021441	0,002119311	0,028765823	Low molecular weight protein-tyrosine-phosphatase, putative
MELO3C009687	0,002121381	0,028767693	No data found
MELO3C023402	0,002122362	0,028767693	Biotin carboxyl carrier protein of acetyl-CoA carboxylase
MELO3C026403	0,002124813	0,028781161	60S ribosomal protein L27
MELO3C014272	0,002126328	0,028781935	Pyruvate kinase
MELO3C009328	0,00213544	0,028885477	Lectin receptor kinase-like protein
MELO3C010600	0,002138232	0,028903446	DNA ligase 1 isoform X3
MELO3C013822	0,002143379	0,028953215	Unknown protein
MELO3C017142	0,002151301	0,029040357	tRNA (Ile)-lysidine synthase
MELO3C025073	0,002156608	0,029092111	GRIP and coiled-coil domain-containing protein 1
MELO3C023201	0,002162151	0,029146973	No data found
MELO3C018368	0,002174462	0,029292935	omega-hydroxypalmitate O-feruloyl transferase
MELO3C008318	0,002183195	0,029390538	Dehydration-responsive element-binding protein 2C
MELO3C022425	0,002187971	0,029434771	15 kDa selenoprotein
MELO3C023799	0,002193667	0,029491311	12-oxophytodienoate reductase 3
MELO3C023753	0,002198867	0,029541101	BnaC06g27400D protein
MELO3C008985	0,002200413	0,029541772	Glucose-6-phosphate 1-dehydrogenase
MELO3C015941	0,002203298	0,029560419	Long cell-linked locus protein, putative, expressed
MELO3C016253	0,002213095	0,029671694	Zinc finger protein, putative
MELO3C018365	0,002215524	0,029684113	GDP-Man:Man(3)GlcNAc(2)-PP-Dol alpha-1,2-mannosyltransferase
MELO3C021777	0,002218623	0,029705479	Vesicle-associated membrane protein, putative
MELO3C015151	0,002226652	0,02977262	Alanine glyoxylate aminotransferase
MELO3C010737	0,002225506	0,02977262	RING-type E3 ubiquitin transferase
MELO3C014860	0,002232141	0,029805646	Transcription factor GTE8
MELO3C018042	0,002230883	0,029805646	Phosphoglycerate mutase-like protein 1
MELO3C012695	0,002239626	0,029885381	la-related protein 6B isoform X1
MELO3C007232	0,00224746	0,029969679	spermidine coumaroyl-CoA acyltransferase
MELO3C010695	0,002255474	0,030056245	No data found
MELO3C026636	0,002257047	0,030056923	Protein arginine N-methyltransferase
MELO3C006754	0,0022639	0,030107586	SWI/SNF-related matrix-associated actin-dependent regulator of chromatin subfamily A-like protein 1
MELO3C000756	0,00226318	0,030107586	Alanine--tRNA ligase
MELO3C025854	0,002276317	0,030252349	No data found
MELO3C023370	0,002278528	0,030261358	No data found
MELO3C011263	0,002281069	0,03027475	EEIG1/EHBP1 protein amino-terminal domain protein
MELO3C004533	0,00230233	0,030536406	GDP-mannose transporter, putative
MELO3C009284	0,002314987	0,030667975	Protein SLOW GREEN 1, chloroplastic
MELO3C005759	0,002315355	0,030667975	30S ribosomal protein S6 alpha, chloroplastic
MELO3C002058	0,002320837	0,030709077	PHD and RING finger domain-containing protein 1
MELO3C018569	0,002321785	0,030709077	peptide methionine sulfoxide reductase B5-like
MELO3C018591	0,002323123	0,030709077	Transcription factor, putative
MELO3C012457	0,002324859	0,030711465	Annexin
MELO3C014588	0,002329523	0,030720166	Calcium-dependent protein kinase
MELO3C004461	0,002328875	0,030720166	protein TOPLESS
MELO3C007580	0,002330184	0,030720166	phosphatidylinositol 3,4,5-trisphosphate 3-phosphatase and protein-tyrosine-phosphatase PTEN2A-like
MELO3C012642	0,002340501	0,030835587	Glucan endo-1,3-beta-glucosidase-like protein 1
MELO3C007613	0,0023421	0,030836086	acyl-CoA-binding domain-containing protein 3
MELO3C008074	0,002345054	0,030854414	No data found
MELO3C026711	0,002357921	0,031003045	Protein FAM32A-like
MELO3C026250	0,002366285	0,031092325	Rhodanese-like domain-containing protein 11, chloroplastic
MELO3C016308	0,00236964	0,031115699	myosin-11-like
MELO3C011105	0,002372222	0,031128911	Chaperone protein dnaJ
MELO3C022382	0,002378877	0,031195509	Succinate--CoA ligase [ADP-forming] subunit beta, mitochondrial
MELO3C003426	0,002381324	0,031206873	Inositol-tetrakisphosphate 1-kinase
MELO3C024108	0,002390668	0,031302545	OBERON-like protein
MELO3C017571	0,002393379	0,031302545	alanine--glyoxylate aminotransferase 2 homolog 1, mitochondrial
MELO3C012634	0,002392484	0,031302545	Receptor-like protein kinase
MELO3C011989	0,002396412	0,031321469	Unknown protein
MELO3C019411	0,002402097	0,031367529	Kinase superfamily protein
MELO3C016970	0,002408407	0,031367529	Chaperone protein
MELO3C026046	0,002406738	0,031367529	alpha-ketoglutarate-dependent dioxygenase AlkB-like
MELO3C003278	0,002403885	0,031367529	PHD finger protein At1g33420
MELO3C022568	0,002409466	0,031367529	protein indeterminate-domain 5, chloroplastic
MELO3C017274	0,002405103	0,031367529	G patch domain-containing protein TGH
MELO3C019815	0,002415556	0,031426095	Receptor-like protein kinase
MELO3C012361	0,002418655	0,0314457	cell division control protein 2 homolog A
MELO3C023445	0,00242176	0,031465348	F-box/LRR-repeat protein 14
MELO3C008977	0,00242354	0,031467785	Kinesin-like protein
MELO3C009290	0,002430501	0,031537432	Phosphatidate phosphatase PAH1
MELO3C020988	0,002436848	0,031599023	Unknown protein
MELO3C015664	0,00244087	0,031630406	RING-type E3 ubiquitin transferase
MELO3C004459	0,002445923	0,031675097	actin-related protein 6
MELO3C014877	0,002454349	0,031763391	DNA/RNA-binding protein KIN17
MELO3C006546	0,00245917	0,031784128	BRI1 kinase inhibitor 1-like
MELO3C010794	0,002457811	0,031784128	No data found
MELO3C019871	0,002461341	0,031791379	Phytol kinase
MELO3C006362	0,002466494	0,031837123	Beta-amylase
MELO3C006224	0,002471833	0,031843597	HOPM interactor 7
MELO3C016382	0,002470672	0,031843597	small nuclear ribonucleoprotein Sm D2-like
MELO3C025893	0,002470417	0,031843597	chaperone protein DnaJ

MELO3C002644	0,002480634	0,03193614	Transcription factor
MELO3C009581	0,002484269	0,03196211	D-lactate dehydrogenase, putative
MELO3C018344	0,00248821	0,031991964	No data found
MELO3C008115	0,002491333	0,032011282	5'-3' exonuclease
MELO3C006942	0,002496694	0,032054016	Receptor-like protein kinase, putative
MELO3C017094	0,002497905	0,032054016	No data found
MELO3C024357	0,002500774	0,032069996	transcription initiation factor TFIID subunit 12b
MELO3C011216	0,002506002	0,032116174	Photosynthetic NDH subcomplex B 3
MELO3C009748	0,002525227	0,032323842	Pentatricopeptide repeat-containing protein At1g80270, mitochondrial
MELO3C016056	0,002528753	0,032323842	monothiol glutaredoxin-S11
MELO3C026427	0,002527159	0,032323842	B-cell receptor-associated 31-like protein
MELO3C025897	0,002525532	0,032323842	pumilio homolog 1-like
MELO3C012604	0,002533219	0,032358543	Phosphoglycerate kinase
MELO3C010664	0,002534744	0,032358543	F28C11.19
MELO3C016031	0,002536861	0,032364646	glutathione S-transferase-like
MELO3C016574	0,00253857	0,032365535	Serine/threonine-protein kinase
MELO3C007940	0,002540917	0,032374558	Protein phosphatase 2c, putative
MELO3C014321	0,002547808	0,032420527	2-methyl-6-phytyl-1,4-hydroquinone methyltransferase, chloroplastic
MELO3C011104	0,002547373	0,032420527	Glucose-6-phosphate isomerase
MELO3C006158	0,002565104	0,032556707	lysophospholipid acyltransferase LPEAT2 isoform X1
MELO3C011769	0,002564335	0,032556707	Pyruvate kinase
MELO3C025550	0,002564713	0,032556707	No data found
MELO3C020003	0,002561197	0,032556707	40S ribosomal protein S26
MELO3C016706	0,002573575	0,032622291	E3 ubiquitin-protein ligase RMA3
MELO3C020533	0,002573546	0,032622291	Ran-binding protein 1
MELO3C015210	0,002582759	0,032717708	ETHYLENE INSENSITIVE 3-like 3 protein
MELO3C006348	0,002586612	0,032745518	PHD finger protein ING
MELO3C006055	0,002590276	0,032749907	Aldose 1-epimerase
MELO3C001354	0,002590061	0,032749907	Kinase family protein
MELO3C014730	0,002592731	0,032759975	N utilization substance B
MELO3C006104	0,002599318	0,03278029	Atg8-interacting protein 1
MELO3C023317	0,002598954	0,03278029	phosphatidylinositol/phosphatidylcholine transfer protein SFH8-like
MELO3C011045	0,002596188	0,03278029	Histone H3
MELO3C022715	0,002602778	0,032802982	E3 ubiquitin-protein ligase RNF4-like isoform X1
MELO3C006785	0,002604786	0,032807344	U11/U12 small nuclear ribonucleoprotein 35 kDa protein
MELO3C005776	0,002606831	0,03281218	Plant UBX domain-containing protein 10
MELO3C021348	0,002612184	0,032840187	E3 ubiquitin-protein ligase Topors
MELO3C011550	0,002612382	0,032840187	transcription factor HBP-1b(C38) isoform X2
MELO3C006555	0,00261696	0,032861199	NEDD8-activating enzyme E1 catalytic subunit
MELO3C006817	0,002620451	0,032861199	pectinesterase-like
MELO3C018616	0,002618082	0,032861199	Alkyl transferase
MELO3C003793	0,002620709	0,032861199	GTP-binding protein hflx, putative
MELO3C015779	0,002624553	0,032888516	peptidyl-prolyl cis-trans isomerase CYP63
MELO3C003924	0,00263039	0,032919884	Nuclear speckle splicing regulatory-like protein (DUF2040)
MELO3C015791	0,002629404	0,032919884	Pentatricopeptide repeat-containing protein
MELO3C004163	0,002635886	0,032948877	trafficking protein particle complex subunit 4
MELO3C011320	0,002636044	0,032948877	NAD(P)-binding rossmann-fold protein
MELO3C003135	0,002638042	0,032952998	Ribonuclease II, chloroplastic/mitochondrial
MELO3C026799	0,002650628	0,033089282	Kinase family protein
MELO3C022000	0,002660118	0,033186779	KH domain-containing protein
MELO3C007601	0,00266637	0,033223806	Lysine-rich arabinogalactan protein 18
MELO3C011236	0,002666451	0,033223806	Peptidyl-prolyl cis-trans isomerase
MELO3C012844	0,002668541	0,033228888	Glutathione S-transferase family protein
MELO3C009572	0,00267166	0,033246763	ABC transporter family protein
MELO3C016114	0,002679947	0,033286969	Protein ROOT INITIATION DEFECTIVE 3
MELO3C017128	0,002678091	0,033286969	two-component response regulator ARR5-like
MELO3C003532	0,0026795	0,033286969	Pesticidal crystal cry8Ba protein
MELO3C004441	0,002681757	0,033288505	RING-H2 finger protein ATL16
MELO3C014706	0,002688709	0,033291105	Argonaute
MELO3C022174	0,002686306	0,033291105	molybdopterin synthase sulfur carrier subunit
MELO3C023622	0,002688572	0,033291105	Short-chain dehydrogenase/reductase
MELO3C023451	0,002686991	0,033291105	BRCA1-associated protein
MELO3C026897	0,002693668	0,03333161	thioredoxin-like 1-1, chloroplastic
MELO3C013125	0,002696375	0,033344218	Lipid-binding serum glycoprotein family protein, putative
MELO3C013852	0,002701952	0,033392271	Plant/protein
MELO3C024701	0,002722685	0,033627463	Elongation factor Ts, mitochondrial
MELO3C024086	0,002730488	0,033681705	70 kDa heat shock protein
MELO3C022386	0,002729666	0,033681705	50S ribosomal protein L14
MELO3C014100	0,002733928	0,033703091	Heavy metal-associated isoprenylated plant protein 21
MELO3C013699	0,002735738	0,033704361	Pectinesterase
MELO3C017906	0,002748047	0,033834902	acyl-protein thioesterase 2
MELO3C009047	0,002752363	0,033866931	Endonuclease/exonuclease/phosphatase family protein
MELO3C017993	0,002756806	0,033900477	40S ribosomal protein S29
MELO3C025710	0,002766025	0,033992675	Nuclear factor related to kappa-B-binding protein
MELO3C005084	0,002768466	0,034001512	E3 ubiquitin-protein ligase
MELO3C016434	0,002785114	0,034043854	protein STICHEL
MELO3C027219	0,002778258	0,034043854	Hydroxycinnamoyl-CoA shikimate/quinate hydroxycinnamoyltransferase
MELO3C008932	0,002780255	0,034043854	thioredoxin-like 3-1, chloroplastic
MELO3C021604	0,00278398	0,034043854	glycerol-3-phosphate dehydrogenase [NAD(+)]
MELO3C002736	0,002774689	0,034043854	Calcyclin-binding protein
MELO3C017478	0,002785704	0,034043854	Xyloglucan endotransglucosylase/hydrolase

MELO3C010631	0,002785354	0,034043854	replication factor C subunit 5
MELO3C018156	0,002778243	0,034043854	HEAT repeat-containing 8
MELO3C018637	0,002795115	0,03413774	outer envelope protein 64, mitochondrial
MELO3C014008	0,002799344	0,034147159	Adenosine monophosphate-protein transferase and cysteine protease ibpA
MELO3C007572	0,002797667	0,034147159	AP2-like ethylene-responsive transcription factor TOE3
MELO3C018716	0,002801119	0,034147712	ras-related protein Rab11D
MELO3C014199	0,002811106	0,034248325	E3 ubiquitin-protein ligase RING1-like
MELO3C013444	0,002818216	0,034313781	No data found
MELO3C016186	0,002820951	0,03431424	No data found
MELO3C016198	0,002821729	0,03431424	No data found
MELO3C009755	0,002830707	0,034386002	Sigma factor binding protein 1, chloroplastic
MELO3C010334	0,002831112	0,034386002	Non-specific serine/threonine protein kinase
MELO3C020848	0,002843447	0,034514594	AP2-like ethylene-responsive transcription factor TOE3 isoform X1
MELO3C014298	0,002848395	0,034553407	CST complex subunit STN1
MELO3C011496	0,002862369	0,034701612	BRCT domain DNA repair protein
MELO3C019673	0,002864285	0,034703532	BOI-related E3 ubiquitin-protein ligase 1-like
MELO3C005244	0,00287285	0,034764654	ABC transporter F family member 3
MELO3C027082	0,002872432	0,034764654	transcription factor bHLH149-like
MELO3C014560	0,002886753	0,034890143	Phospholipase A2
MELO3C011106	0,002886027	0,034890143	Pentatricopeptide repeat-containing protein
MELO3C023727	0,002889946	0,034907366	CDT1-like protein a, chloroplastic
MELO3C017963	0,00289547	0,034952714	Lycopene beta-cyclase
MELO3C027349	0,002897783	0,034959267	MACPF domain NSL1-like protein
MELO3C006867	0,002901755	0,034967061	ATP-dependent Clp protease ATP-binding subunit clpX
MELO3C024404	0,00290197	0,034967061	Tudor/PWWP/MBT superfamily protein
MELO3C006795	0,002905902	0,034993084	F-box protein SKIP16
MELO3C007935	0,002914473	0,035049105	Peroxidase
MELO3C011717	0,002914359	0,035049105	Protein kinase-like protein
MELO3C021242	0,002915878	0,035049105	YTH domain family protein 2
MELO3C019488	0,002921813	0,035099083	Pentatricopeptide repeat-containing protein
MELO3C021247	0,002929612	0,035171372	Dihydrolipoyl dehydrogenase
MELO3C007934	0,002950461	0,035383526	methyltransferase-like protein 23 isoform X3
MELO3C023224	0,002950867	0,035383526	Glutathione-S-transferase
MELO3C013878	0,002957395	0,035401287	haloacid dehalogenase-like hydrolase domain-containing protein Sgpp
MELO3C010569	0,002957726	0,035401287	Obg-like ATPase 1
MELO3C005260	0,002957489	0,035401287	Vacuolar iron transporter 1
MELO3C013221	0,002962542	0,035416003	KH domain-containing protein
MELO3C020139	0,00296188	0,035416003	No data found
MELO3C022885	0,002964338	0,035416035	methyl-CpG-binding domain protein 4-like protein
MELO3C008871	0,002966193	0,035416771	Chaperone protein dnaJ, putative
MELO3C021452	0,002968697	0,03542525	No data found
MELO3C017319	0,002971065	0,0354321	BnaA06g03540D protein
MELO3C013260	0,002980565	0,035473547	protein LAZ1 isoform X1
MELO3C013879	0,002977994	0,035473547	Regulator of nonsense transcripts 1-like protein
MELO3C007001	0,002983521	0,035473547	Peptidylprolyl isomerase
MELO3C020574	0,002982642	0,035473547	No data found
MELO3C024984	0,002982609	0,035473547	12-oxophytodienoate reductase 3
MELO3C006957	0,002986868	0,035491975	DUF21 domain-containing protein
MELO3C019021	0,002990581	0,035514727	Endoplasmic reticulum-Golgi intermediate compartment 3
MELO3C024729	0,002999388	0,035597902	NADH dehydrogenase [ubiquinone] iron-sulfur protein 6, mitochondrial
MELO3C016890	0,003010612	0,035709654	aminopeptidase M1
MELO3C010886	0,003017045	0,035764474	Succinate dehydrogenase subunit 5, mitochondrial
MELO3C027370	0,003021861	0,035778621	O-methyltransferase, putative
MELO3C025196	0,003020505	0,035778621	CTD small phosphatase-like protein
MELO3C022180	0,003023713	0,035779094	Protein DETOXIFICATION
MELO3C019044	0,003030012	0,035832154	Tubulin folding cofactor B
MELO3C024869	0,003033633	0,035853509	No data found
MELO3C014561	0,003046338	0,035942705	Hydroxyproline O-arabinosyltransferase 1
MELO3C012284	0,003044031	0,035942705	Zinc finger, B-box
MELO3C018849	0,00304664	0,035942705	Glycosyltransferase
MELO3C014781	0,003053533	0,03600252	AT5g13970/MAC12_6
MELO3C008481	0,003067925	0,036149299	Glutamate synthase 1 [nadh], chloroplastic
MELO3C011261	0,003069643	0,036149299	Peroxidase
MELO3C007950	0,003073946	0,03617543	Thiol-disulfide oxidoreductase LTO1
MELO3C023110	0,003077357	0,03617543	Alkaline alpha galactosidase
MELO3C023308	0,003076209	0,03617543	F-box protein At2g16365
MELO3C007661	0,003080611	0,036192143	Transmembrane protein, putative
MELO3C025139	0,003083892	0,036209142	No data found
MELO3C015862	0,003094223	0,036308865	Unknown protein
MELO3C012787	0,003098021	0,036331842	Sterol 3-beta-glucosyltransferase
MELO3C006983	0,003103923	0,036379454	Protein phosphatase 2C
MELO3C003418	0,00312099	0,036557785	PLATZ transcription factor family protein
MELO3C025651	0,00312838	0,036611552	Intracellular protein transport protein USO1, putative
MELO3C002117	0,003129288	0,036611552	T-complex protein 1 subunit delta
MELO3C017551	0,003135065	0,036657431	Pentatricopeptide repeat-containing protein
MELO3C011955	0,003151726	0,036830441	Tetratricopeptide-like helical
MELO3C007043	0,003158388	0,036886457	UDP-glucose 4-epimerase, putative
MELO3C024047	0,003169067	0,036989311	Kelch repeat-containing F-box family protein
MELO3C003323	0,003174141	0,037026649	Myosin heavy chain-like protein
MELO3C004576	0,003176483	0,037030643	sugar transport protein 14-like
MELO3C013476	0,003178234	0,037030643	phototropin-2

MELO3C011323	0,003180577	0,037036095	No data found
MELO3C014607	0,003194901	0,037110629	Zinc transporter ZTP29
MELO3C013949	0,003200132	0,037110629	Ribosomal protein L20
MELO3C013891	0,003198512	0,037110629	AT5g47090/K14A3_4
MELO3C024474	0,003199865	0,037110629	zinc finger protein 593
MELO3C005504	0,0031908	0,037110629	Disease resistance family protein
MELO3C022307	0,003194397	0,037110629	Pentatricopeptide repeat-containing family protein
MELO3C002719	0,003197284	0,037110629	60S ribosomal protein L18a
MELO3C016702	0,003207778	0,037177474	translation initiation factor IF-1, chloroplastic
MELO3C012906	0,003217846	0,037272286	CDT1-like protein a, chloroplastic
MELO3C017430	0,003244779	0,037562214	Fiber protein Fb15
MELO3C016083	0,003254038	0,037647333	Ubiquitin
MELO3C020055	0,003260646	0,037701701	histidine kinase 4-like
MELO3C013359	0,003263656	0,037714419	Ubiquitin-conjugating enzyme, E2
MELO3C012180	0,00326865	0,037750045	ruBisCO large subunit-binding protein subunit beta, chloroplastic-like
MELO3C016846	0,003282629	0,037889324	Phosphoribosyl-AMP cyclohydrolase
MELO3C003619	0,003300998	0,038079098	serine/arginine-rich splicing factor RSZ22A
MELO3C007340	0,003313583	0,038201954	NAD(P)H dehydrogenase (Quinone) FQR1-like
MELO3C023222	0,003316953	0,038218502	ABC transporter-like protein
MELO3C022442	0,003319357	0,0382239	At1g08760
MELO3C024172	0,003325012	0,038233085	Histone deacetylase
MELO3C022903	0,003325963	0,038233085	No data found
MELO3C003874	0,003325589	0,038233085	cytochrome P450 734A1-like
MELO3C004825	0,00333147	0,038274119	Ser/thr-rich protein T10 in DGCR region-like protein
MELO3C009653	0,003335391	0,03829688	transcription factor bHLH48
MELO3C009569	0,003341995	0,038336453	Gb|AAF02136.1
MELO3C013245	0,003345101	0,038336453	40S ribosomal protein S11-like
MELO3C007947	0,003346602	0,038336453	Ankyrin repeat domain-containing protein, chloroplastic
MELO3C026640	0,003346185	0,038336453	Mitogen-activated protein kinase kinase kinase 1 isoform 1
MELO3C006187	0,003373939	0,038382447	Proteasome subunit beta type
MELO3C013411	0,003359761	0,038382447	NADP dependent sorbitol 6-phosphate dehydrogenase family protein
MELO3C017651	0,003365623	0,038382447	Receptor-like kinase
MELO3C011897	0,003364709	0,038382447	F-box protein SKIP14
MELO3C002607	0,003368718	0,038382447	Sulfate/thiosulfate import ATP-binding protein cysA, putative
MELO3C002313	0,003361391	0,038382447	Serine/threonine-protein kinase AFC2
MELO3C017221	0,003372724	0,038382447	Histone deacetylase
MELO3C020002	0,003354814	0,038382447	Protein IDA
MELO3C011279	0,003373493	0,038382447	Hydroxyproline O-arabinosyltransferase 1
MELO3C010865	0,003371209	0,038382447	Calcium-binding EF-hand family protein, putative
MELO3C010744	0,003353091	0,038382447	CTD small phosphatase-like protein 2
MELO3C003368	0,003371584	0,038382447	Intron maturase, type II family protein
MELO3C004651	0,003388972	0,038411752	DENN (AEX-3) domain-containing protein
MELO3C013243	0,003386839	0,038411752	TOM1-like protein 2
MELO3C013737	0,00339013	0,038411752	Eukaryotic translation initiation factor 3 subunit A, putative
MELO3C026387	0,003383352	0,038411752	Pentatricopeptide repeat-containing protein At3g59040
MELO3C015852	0,003381614	0,038411752	adenylate isopentenyltransferase 3, chloroplastic
MELO3C021352	0,003385027	0,038411752	No data found
MELO3C012869	0,003384461	0,038411752	Adaptin ear-binding coat-associated protein, putative
MELO3C011787	0,003395586	0,038451502	No data found
MELO3C019429	0,00339882	0,038466072	Basic-leucine zipper (BZIP) transcription factor family protein
MELO3C006925	0,003401941	0,038479344	mitogen-activated protein kinase kinase kinase YODA-like
MELO3C006522	0,003406663	0,038510695	Acyl-CoA N-acyltransferases (NAT) superfamily protein, putative
MELO3C014459	0,003412741	0,038513275	Serine/threonine phosphatase
MELO3C002381	0,003410916	0,038513275	Bidirectional sugar transporter SWEET
MELO3C015616	0,003409437	0,038513275	BnaA04g07840D protein
MELO3C006846	0,003415532	0,038514691	Mitochondrial metalloendopeptidase OMA1
MELO3C011704	0,003416767	0,038514691	RAS-related protein RABC1
MELO3C008489	0,003421744	0,03854879	Serine/threonine-protein kinase stt7, chloroplastic
MELO3C026175	0,003426007	0,03857481	Long chain base biosynthesis protein
MELO3C011882	0,003434884	0,038652717	RING-type E3 ubiquitin transferase
MELO3C021636	0,003446073	0,038756546	No data found
MELO3C012052	0,003452074	0,038801943	dnaJ homolog subfamily B member 1
MELO3C018126	0,003462355	0,038895368	Autophagy-related protein 18f
MELO3C020666	0,003464992	0,038902854	ATP-dependent clp protease
MELO3C013892	0,003475055	0,038971525	Calcineurin B-like protein
MELO3C002722	0,003474179	0,038971525	3-oxoacyl-[acyl-carrier-protein] synthase
MELO3C025912	0,003482485	0,03901055	Protein kinase
MELO3C018739	0,003480823	0,03901055	GPI-anchored protein LORELEI
MELO3C019827	0,00348579	0,039025439	MEF2BNB-like protein
MELO3C007008	0,003505922	0,039206378	cytochrome c6, chloroplastic
MELO3C007106	0,003505337	0,039206378	Remorin family protein
MELO3C009713	0,00351416	0,039276258	translation factor GUF1 homolog, chloroplastic
MELO3C009747	0,003531004	0,039397631	Zinc finger (C3HC4-type RING finger) family protein, putative
MELO3C025091	0,003530344	0,039397631	protein REVEILLE 1-like isoform X1
MELO3C005532	0,003527148	0,039397631	Pectinesterase
MELO3C015131	0,003533209	0,039399968	Pentatricopeptide repeat-containing family protein
MELO3C027061	0,003535623	0,039404641	PLATZ transcription factor family protein
MELO3C011942	0,003539061	0,03942071	E3 ubiquitin-protein ligase
MELO3C016296	0,003541354	0,039424015	Chlororespiratory reduction31
MELO3C014270	0,003548068	0,039432076	No data found
MELO3C004534	0,003544491	0,039432076	Glycine-rich RNA-binding protein, putative

MELO3C007344	0,003547741	0,039432076	No data found
MELO3C014260	0,00356425	0,039481967	Interactor of constitutive active ROPs-like protein
MELO3C006765	0,003561252	0,039481967	DEAD-box ATP-dependent RNA helicase 50
MELO3C008503	0,003567236	0,039481967	Protein ABIL2
MELO3C016694	0,00356367	0,039481967	VQ motif-containing protein
MELO3C012088	0,003568551	0,039481967	sphinganine C4-monooxygenase 2
MELO3C022354	0,00356635	0,039481967	Light-regulated protein, putative
MELO3C015093	0,003557723	0,039481967	Fasciclin-like arabinogalactan protein 16
MELO3C010763	0,003555075	0,039481967	vacuolar-processing enzyme-like
MELO3C008037	0,003570997	0,039486906	Ubiquinol-cytochrome C chaperone family protein
MELO3C002653	0,003573311	0,039490386	No data found
MELO3C007055	0,003581872	0,039540431	reticuline oxidase-like protein
MELO3C015718	0,003581143	0,039540431	ATP binding protein
MELO3C002891	0,003585267	0,039540431	Pseudouridine synthase, RsuA/RluB/C/D/E/F
MELO3C002981	0,003585848	0,039540431	transmembrane emp24 domain-containing protein p24delta9-like
MELO3C012083	0,003592586	0,039584422	Actin-binding LIM protein 1, putative
MELO3C010745	0,003593846	0,039584422	mitochondrial import receptor subunit TOM20-like
MELO3C017766	0,003610937	0,039717805	Ras family
MELO3C020908	0,003610566	0,039717805	Glycosyl hydrolase family 43 protein
MELO3C022417	0,003611989	0,039717805	RNA-binding protein 24-B
MELO3C012428	0,003616813	0,03974872	mRNA-decapping enzyme subunit 2-like
MELO3C022004	0,003620939	0,039771924	SPX domain protein
MELO3C004466	0,003624832	0,039792552	Alpha-galactosidase
MELO3C024980	0,003638813	0,039923839	No data found
MELO3C020601	0,00364269	0,039944192	Protein phosphatase 2C
MELO3C013403	0,003646581	0,039964669	auxin-responsive protein SAUR36-like
MELO3C007784	0,003649542	0,039974931	Unknown protein
MELO3C026293	0,003656398	0,040027832	DUF1645 family protein
MELO3C026249	0,003662455	0,040071928	E3 ubiquitin-protein ligase RGLG2
MELO3C026102	0,003665971	0,040088183	Rhodanese-like domain-containing protein 6
MELO3C024088	0,003673788	0,040151428	F-box family protein, putative
MELO3C015825	0,00367858	0,04018157	F-box protein, putative
MELO3C007635	0,003691045	0,040295438	F-box protein, putative
MELO3C017844	0,003701289	0,040360967	calcineurin subunit B
MELO3C023195	0,003703179	0,040360967	NAC domain-containing protein 2
MELO3C025023	0,003700209	0,040360967	thioredoxin-like protein slr0233
MELO3C016913	0,003713995	0,040418482	No data found
MELO3C010482	0,003712349	0,040418482	F-box protein 7
MELO3C024352	0,003714595	0,040418482	Transcription initiation factor TFIID subunit 9
MELO3C005089	0,0037201	0,040456085	40S ribosomal protein S27
MELO3C019497	0,003727132	0,040510255	Tubby-like F-box protein
MELO3C023221	0,003736333	0,040587924	DNA cross-link repair family protein
MELO3C025053	0,003746829	0,040657217	lysine-specific demethylase JMJ25
MELO3C011399	0,003746213	0,040657217	LOW QUALITY PROTEIN: transcription factor BIM2
MELO3C004637	0,003756844	0,040671892	pre-mRNA cleavage factor Im 25 kDa subunit 1
MELO3C016852	0,003760096	0,040671892	zinc finger CCCH domain-containing protein 20-like
MELO3C021385	0,003760539	0,040671892	Phosphatase 2C family protein
MELO3C020532	0,003759449	0,040671892	Potassium transporter
MELO3C015523	0,003757061	0,040671892	Cysteine protease
MELO3C018576	0,003753217	0,040671892	L-galactose dehydrogenase
MELO3C010023	0,003766895	0,040718344	Ycf20-like protein
MELO3C007547	0,003777406	0,040809619	AT3g50560/T20E23_160
MELO3C003813	0,003780437	0,040820042	Mannan endo-1,4-beta-mannosidase-like protein
MELO3C015455	0,003791053	0,040912299	Acyl--UDP-N-acetylglucosamine O-acyltransferase
MELO3C009308	0,003803179	0,040971692	LRR receptor-like kinase
MELO3C024282	0,003804855	0,040971692	DUF3820 family protein
MELO3C021366	0,00380155	0,040971692	Acyl carrier protein
MELO3C012881	0,003803284	0,040971692	rho-N domain-containing protein 1, chloroplastic isoform X3
MELO3C024947	0,003815395	0,041062803	Inner centromere protein, ARK-binding region protein
MELO3C004524	0,003821849	0,041109857	zinc finger CCCH domain-containing protein 39-like
MELO3C005600	0,003831717	0,041193563	Phosphate translocator-related family protein
MELO3C024761	0,003834984	0,041206251	GDSL esterase/lipase At2g30310-like
MELO3C019691	0,003841997	0,041242606	Hexosyltransferase
MELO3C010338	0,003842544	0,041242606	Outward-rectifying potassium channel 4-like protein
MELO3C010688	0,003849725	0,041297244	F-box protein At1g70590
MELO3C024739	0,003857873	0,041362184	growth-regulating factor 4-like
MELO3C009560	0,003869597	0,041400198	Polyketide cyclase/dehydrase/lipid transport superfamily protein
MELO3C004555	0,003869804	0,041400198	At3g13227
MELO3C024926	0,003865295	0,041400198	two-pore potassium channel 1 isoform X1
MELO3C002209	0,003866952	0,041400198	Homeobox leucine zipper family protein
MELO3C004423	0,00387519	0,041435366	protease 2
MELO3C016067	0,003886455	0,041533337	Mitochondrial processing peptidase beta subunit
MELO3C022388	0,003895212	0,041584413	Pre-mRNA-processing factor 39
MELO3C021783	0,003899657	0,041584413	Peroxisome biogenesis protein 1
MELO3C026222	0,003897988	0,041584413	Transcription factor GTE10
MELO3C023969	0,003899371	0,041584413	Unknown protein
MELO3C021407	0,0039026	0,041593331	Stem-specific protein TSJT1
MELO3C021846	0,00390593	0,041606376	cytochrome P450 89A2-like
MELO3C007841	0,003917636	0,041708569	Bacteriophage N4 adsorption B
MELO3C010378	0,003926868	0,041741601	No data found
MELO3C005360	0,00392708	0,041741601	mediator of RNA polymerase II transcription subunit 36a-like

MELO3C005850	0,003925023	0,041741601	S-type anion channel SLAH2
MELO3C002789	0,003938719	0,041842795	BnaCnng71930D protein
MELO3C024960	0,003956688	0,041913419	pentatricopeptide repeat-containing protein At5g66520-like
MELO3C026392	0,003958903	0,041913419	RING/U-box superfamily protein
MELO3C008056	0,003957199	0,041913419	NAC domain-containing protein 82
MELO3C019135	0,003951906	0,041913419	4-alpha-glucanotransferase DPE2
MELO3C021253	0,003960223	0,041913419	Beta-glucosidase
MELO3C011386	0,003948698	0,041913419	DNA gyrase subunit A
MELO3C022742	0,003952049	0,041913419	ATP-dependent DNA helicase, RecQ family protein, expressed
MELO3C022225	0,003974648	0,04204356	protein NRT1/ PTR FAMILY 5.10-like
MELO3C015024	0,003977944	0,042055892	RING-type E3 ubiquitin transferase
MELO3C002556	0,003983689	0,0420941	heterogeneous nuclear ribonucleoprotein U-like protein 1
MELO3C003039	0,003992429	0,042163897	No data found
MELO3C013929	0,004016596	0,042396446	Unknown protein
MELO3C019002	0,00402459	0,042458132	Annexin
MELO3C012683	0,004034378	0,042538673	Pentatricopeptide repeat-containing protein, mitochondrial
MELO3C024468	0,004043191	0,042608845	Thioredoxin, putative
MELO3C007936	0,004053995	0,042677153	aspartyl protease family protein 1-like
MELO3C005650	0,004052481	0,042677153	Dead box ATP-dependent RNA helicase, putative
MELO3C010427	0,004077216	0,042853085	aspartate-semialdehyde dehydrogenase
MELO3C007195	0,004077084	0,042853085	ER lumen protein-retaining receptor
MELO3C002292	0,004074355	0,042853085	transcription factor MYB86-like
MELO3C004334	0,004082556	0,042886386	ERAD-associated E3 ubiquitin-protein ligase HRD1B-like
MELO3C012231	0,004086041	0,042900167	Homologous-pairing protein 2-like protein
MELO3C026332	0,004092545	0,042945629	DNA helicase INO80-like protein
MELO3C003917	0,004095247	0,042951162	Heat shock 70 kDa protein
MELO3C013792	0,004109432	0,043077059	Ribosomal protein L28
MELO3C006643	0,004132745	0,043229655	E3 ubiquitin-protein ligase
MELO3C010381	0,00413255	0,043229655	2-hydroxyacyl-CoA lyase
MELO3C024538	0,004127031	0,043229655	zinc finger A20 and AN1 domain-containing stress-associated protein 4
MELO3C011908	0,004132723	0,043229655	Heat shock protein HSP26
MELO3C012400	0,004137771	0,043259309	pentatricopeptide repeat-containing protein At2g22070
MELO3C017187	0,004145526	0,043294547	Pectinesterase inhibitor
MELO3C023569	0,004145485	0,043294547	Alpha-N-acetylglucosaminidase
MELO3C009178	0,004153711	0,043339304	No data found
MELO3C012716	0,0041542	0,043339304	ribonuclease 2-like
MELO3C009268	0,004161762	0,043387488	SLT1
MELO3C021818	0,004163213	0,043387488	Protein LIGHT-DEPENDENT SHORT HYPOCOTYLS 10
MELO3C020579	0,004171474	0,043450658	Enolase
MELO3C007517	0,004177658	0,043492126	Mitochondrial pyruvate carrier
MELO3C014384	0,004183069	0,043525516	ABSCISIC ACID-INSENSITIVE 5-like protein 4 isoform X1
MELO3C026567	0,004192935	0,043582254	Pentatricopeptide repeat-containing protein At4g18975, chloroplastic
MELO3C022309	0,004191627	0,043582254	Ectonucleotide pyrophosphatase/phosphodiesterase family member 3
MELO3C022301	0,004197551	0,043607279	serine/threonine-protein kinase ATG1a isoform X4
MELO3C003173	0,004207307	0,043685655	Proteasome subunit alpha type
MELO3C017343	0,004218144	0,043775159	Protein DETOXIFICATION
MELO3C017925	0,004233382	0,043910224	Myb transcription factor
MELO3C015891	0,004238724	0,043942551	U1 small nuclear ribonucleoprotein C
MELO3C023098	0,004242721	0,04396091	No data found
MELO3C009370	0,004260693	0,043990453	ACT domain-containing protein
MELO3C006875	0,004249928	0,043990453	BAG family molecular chaperone regulator 1-like
MELO3C014035	0,00425177	0,043990453	No data found
MELO3C017623	0,004256934	0,043990453	Metacaspase-1
MELO3C005067	0,004263392	0,043990453	dihydroorotate dehydrogenase (Quinone), mitochondrial-like
MELO3C024371	0,004262261	0,043990453	Hydroxyproline-rich glycoprotein family protein
MELO3C011742	0,004252653	0,043990453	No data found
MELO3C018549	0,004260993	0,043990453	DUF21 domain-containing protein
MELO3C009480	0,004270564	0,044018463	ABC transporter family protein
MELO3C013951	0,004268865	0,044018463	NADH dehydrogenase [ubiquinone] 1 beta subcomplex subunit 8, mitochondrial
MELO3C007097	0,004276916	0,044042639	F-box protein SKIP19
MELO3C018374	0,004278249	0,044042639	DUF248-1
MELO3C010135	0,0042796	0,044042639	Kelch repeat-containing protein family
MELO3C019168	0,004293298	0,04416059	Metacaspase-9
MELO3C017365	0,004301125	0,044218068	DEAD-box ATP-dependent RNA helicase 42
MELO3C011234	0,004308579	0,044271653	GTP-binding nuclear protein
MELO3C007000	0,004317741	0,044319683	Katanin p80 WD40 repeat-containing subunit B1 homolog
MELO3C019226	0,004317006	0,044319683	transcription factor ILR3-like
MELO3C023373	0,004327562	0,044397416	Aspartate aminotransferase
MELO3C019907	0,004348841	0,044592553	40S ribosomal protein S17
MELO3C010243	0,004352503	0,044606949	VAMP-like protein YKT61
MELO3C022007	0,00436531	0,044714989	transmembrane emp24 domain-containing protein p24delta9
MELO3C022530	0,004370793	0,044747951	Armadillo/beta-catenin repeat family protein
MELO3C022219	0,00437392	0,044756755	SPla/RYanodine receptor (SPRY) domain-containing protein
MELO3C020562	0,004381523	0,044811338	No data found
MELO3C014562	0,004383797	0,044811393	E3 ubiquitin-protein ligase ICP0
MELO3C003447	0,004388805	0,044839378	Major facilitator superfamily transporter
MELO3C015857	0,004393219	0,044861266	No data found
MELO3C002619	0,004397541	0,044882192	Mitochondrial carrier protein, expressed
MELO3C014283	0,004405154	0,044891527	BIG SEEDS 1
MELO3C007793	0,004410314	0,044891527	cytochrome P450 CYP736A12-like
MELO3C023173	0,004408955	0,044891527	sister chromatid cohesion 1 protein 3

MELO3C005182	0,004412094	0,044891527	Short-chain dehydrogenase/reductase family protein
MELO3C005421	0,004410409	0,044891527	GTF2H2
MELO3C025324	0,00440425	0,044891527	Leucine-rich repeat extensin-like protein 4
MELO3C020541	0,004415679	0,044904867	Omega-3 fatty acid desaturase
MELO3C024896	0,004425602	0,044973267	Calcium-dependent lipid-binding (CaLB domain) family protein
MELO3C007660	0,00442696	0,044973267	DUF21 domain-containing-like protein
MELO3C002171	0,004433773	0,04501932	LOW QUALITY PROTEIN: probable metal-nicotianamine transporter YSL5
MELO3C006119	0,004436391	0,045022754	Remorin
MELO3C010522	0,004443462	0,045071359	Zinc knuckle family protein
MELO3C016498	0,004450952	0,045078873	MACPF domain-containing protein At4g24290
MELO3C007981	0,004451051	0,045078873	Plant intracellular ras group-related LRR protein
MELO3C024434	0,004448586	0,045078873	protein IQ-DOMAIN 14-like
MELO3C007689	0,004468911	0,045229993	protein RMD5 homolog A
MELO3C008214	0,004470553	0,045229993	Emb|CAB62340.1
MELO3C018008	0,004484931	0,045352224	Glycyl-tRNA synthetase beta subunit
MELO3C012753	0,004495256	0,045433371	Unknown protein
MELO3C011357	0,004510552	0,045564646	serine/arginine-rich splicing factor SC35-like
MELO3C020113	0,004517785	0,045614382	ADP,ATP carrier protein
MELO3C002044	0,004521056	0,045624084	DNA polymerase alpha subunit B
MELO3C015727	0,004533629	0,045727594	Maternal effect embryo arrest 60
MELO3C013370	0,004542785	0,045796557	translocase of chloroplast 120, chloroplastic-like
MELO3C004636	0,004562754	0,045956283	T-complex protein 1 subunit beta
MELO3C018966	0,004563283	0,045956283	ATP-dependent 6-phosphofructokinase
MELO3C026199	0,0045674	0,045974302	Transmembrane protein, putative
MELO3C019056	0,004577074	0,046048208	two-component response regulator ARR8-like
MELO3C011953	0,004581695	0,046071233	Unknown protein
MELO3C014991	0,004592244	0,046153801	MLP-like protein 28
MELO3C016801	0,004595981	0,046167865	aspartic proteinase-like protein 2
MELO3C016795	0,004616259	0,046347994	Clavata3/ESR (CLE) gene family member MtCLE20
MELO3C009312	0,004637357	0,046443786	Pentatricopeptide repeat-containing protein At3g09650, chloroplastic
MELO3C020458	0,004640894	0,046443786	cyclin-dependent kinase inhibitor 5-like
MELO3C013215	0,004637275	0,046443786	Chaperone DnaJ domain protein
MELO3C007647	0,004642262	0,046443786	xyloglucan 6-xylosyltransferase 1
MELO3C000279	0,004642023	0,046443786	Late cornified envelope protein 1E
MELO3C008114	0,004641918	0,046443786	TSA: Wollemia nobilis Ref_Wollemi_Transcript_28887_1569 transcribed RNA sequence
MELO3C018767	0,004631049	0,046443786	Wound-responsive family protein
MELO3C004603	0,004650444	0,046502086	Protein-tyrosine phosphatase mitochondrial 1
MELO3C005627	0,004658441	0,046558473	UDP-galactose/UDP-glucose transporter 2
MELO3C005404	0,004661356	0,046564044	LOW QUALITY PROTEIN: xyloglucan galactosyltransferase XLT2
MELO3C018500	0,004666952	0,04659638	TIP41-like family protein
MELO3C025210	0,004670139	0,046604633	gibberellin 2-beta-dioxygenase 2-like
MELO3C026171	0,004684672	0,046726052	Phosphate carrier, mitochondrial
MELO3C008513	0,004697722	0,046832565	FAST kinase domain-containing 3
MELO3C013820	0,004711581	0,046872055	bZIP transcription factor 16
MELO3C011375	0,00471355	0,046872055	BPS1-like protein
MELO3C010991	0,004708747	0,046872055	No data found
MELO3C003453	0,004711087	0,046872055	eukaryotic translation initiation factor 3 subunit L-like
MELO3C003821	0,004712946	0,046872055	agglutinin-like
MELO3C004992	0,004716173	0,046874535	Protein nuclear fusion defective 4
MELO3C017563	0,004720256	0,046891514	Protein AE7
MELO3C015861	0,00473689	0,047033107	isoamylase 2, chloroplastic
MELO3C018841	0,00474106	0,047050848	Beta-adaptin-like protein
MELO3C012033	0,004754153	0,047146974	Neurofilament heavy protein
MELO3C002083	0,00475552	0,047146974	Bowman-Birk type bran trypsin inhibitor
MELO3C023385	0,004763871	0,047206067	molybdate transporter 2
MELO3C004333	0,00477455	0,047288161	DCD (Development and Cell Death) domain protein
MELO3C003581	0,004779227	0,047310758	signal peptide peptidase
MELO3C005964	0,004786932	0,047363283	Late cornified envelope protein 1E
MELO3C010772	0,004792676	0,047396378	clathrin interactor EPSIN 1
MELO3C013364	0,004797805	0,047423351	MYB-related transcription factor
MELO3C011490	0,004807445	0,047494858	Myosin
MELO3C011715	0,004821563	0,047586732	CDP-diacylglycerol--glycerol-3-phosphate 3-phosphatidyltransferase 2
MELO3C025943	0,004819407	0,047586732	RPM1-interacting protein 4
MELO3C024211	0,004835288	0,047626989	BTB/POZ domain-containing protein At5g48130
MELO3C018935	0,004829019	0,047626989	Unknown protein
MELO3C005513	0,004833075	0,047626989	E3 ubiquitin-protein ligase HOS1
MELO3C025354	0,004832401	0,047626989	Late embryogenesis abundant protein
MELO3C010709	0,004851085	0,047758765	telomere-associated protein RIF1-like isoform X2
MELO3C007871	0,00485956	0,047818358	rRNA adenine N(6)-methyltransferase
MELO3C004179	0,004867492	0,047872556	RNA polymerase II-associated protein 3
MELO3C007325	0,00487634	0,047934223	Sugar transporter, putative
MELO3C015459	0,004878616	0,047934223	Cytidine deaminase
MELO3C021353	0,004882791	0,047951391	Chromatin remodeling factor, putative
MELO3C021565	0,004892331	0,048017693	DExH-box ATP-dependent RNA helicase DExH17-like
MELO3C011062	0,004894406	0,048017693	Serine hydrolase FSH
MELO3C015103	0,004900855	0,04805709	Histone deacetylase
MELO3C014540	0,004906707	0,048066291	blue copper protein-like
MELO3C006050	0,004905261	0,048066291	Phosphatidylinositol-4-phosphate 5-kinase family protein
MELO3C009984	0,004909095	0,048066291	Zinc finger CCCH domain-containing protein 41
MELO3C009686	0,004920878	0,048110111	Pleiotropic drug resistance ABC transporter
MELO3C022845	0,004920763	0,048110111	RING-type E3 ubiquitin transferase

MELO3C002054	0,00491912	0,048110111	Movement protein binding protein 2C
MELO3C016817	0,004932507	0,048184439	Calcium-transporting ATPase
MELO3C010960	0,00493336	0,048184439	Proteasome subunit alpha type
MELO3C005578	0,004939104	0,048216689	Amine oxidase
MELO3C020276	0,004949485	0,048270311	Tobamovirus multiplication 1
MELO3C018564	0,004948426	0,048270311	Protein trichome birefringence-like 12
MELO3C011383	0,004955995	0,04830994	DNA-directed RNA polymerase subunit beta
MELO3C004152	0,004959362	0,04831891	40S ribosomal protein S23-1
MELO3C022348	0,004994168	0,048634032	Protein TIFY 9
MELO3C006574	0,005016799	0,048830338	guanylate kinase 3, chloroplastic-like
MELO3C007071	0,005035167	0,048946423	WPP domain associated protein
MELO3C004988	0,00503616	0,048946423	Protein SIEL
MELO3C011016	0,005035252	0,048946423	tubulin beta chain
MELO3C005710	0,005041507	0,048948249	heavy metal-associated isoprenylated plant protein 3
MELO3C017291	0,005040338	0,048948249	40S ribosomal protein S28
MELO3C008219	0,005046262	0,048948249	glyceraldehyde-3-phosphate dehydrogenase
MELO3C019779	0,005045138	0,048948249	U4/U6 small nuclear ribonucleoprotein PRP4-like protein
MELO3C002071	0,005049346	0,048954117	single-stranded DNA-binding protein, mitochondrial
MELO3C024964	0,005065109	0,049058772	E3 ubiquitin-protein ligase
MELO3C010806	0,005063283	0,049058772	DNA excision repair protein ERCC-8
MELO3C026554	0,005078	0,049159522	alcohol dehydrogenase-like 7
MELO3C002931	0,00508282	0,049182075	Paired amphipathic helix SIN3-like protein
MELO3C014724	0,00509845	0,049274668	Mitochondrial carrier family
MELO3C014519	0,005095436	0,049274668	BEL1-like homeodomain protein 1
MELO3C012470	0,00510131	0,049274668	two-component response regulator ORR9-like
MELO3C002405	0,00510237	0,049274668	50S ribosomal protein L7/L12
MELO3C006249	0,005116632	0,049340898	No data found
MELO3C007711	0,005112354	0,049340898	U-box domain-containing protein kinase family protein, putative
MELO3C002385	0,005116723	0,049340898	Transcription factor Inducer of CBF expression 1
MELO3C011167	0,00512558	0,049402188	basic leucine zipper 9
MELO3C013378	0,005138683	0,049422864	Unknown protein
MELO3C013419	0,005140238	0,049422864	30S ribosomal protein S31, mitochondrial
MELO3C014215	0,005140167	0,049422864	No data found
MELO3C002515	0,005137092	0,049422864	Eukaryotic translation initiation factor-like protein
MELO3C024016	0,005132207	0,049422864	Metal-dependent phosphohydrolase
MELO3C005696	0,005146382	0,049457856	E3 ubiquitin-protein ligase RHA1B
MELO3C015130	0,005149257	0,04946142	polygalacturonase-like
MELO3C014379	0,005165809	0,049596282	Protein RETICULATA-RELATED 1, chloroplastic
MELO3C016899	0,005169158	0,049604328	Mitochondrial carrier protein
MELO3C006092	0,005178299	0,04966489	Glycoside hydrolase family 28 protein/polygalacturonase family protein
MELO3C003072	0,005180499	0,04966489	Thioredoxin-like protein AAED1, chloroplastic
MELO3C009552	0,005195047	0,049780192	Mads box protein, putative
MELO3C000885	0,005198453	0,049788673	auxin-responsive protein SAUR71-like
MELO3C008811	0,005201536	0,049794056	importin-5
MELO3C009970	0,005205874	0,04981144	polygalacturonase At1g48100
MELO3C014419	0,005215486	0,049855095	Unknown protein
MELO3C017659	0,005213556	0,049855095	Ribosomal protein L15
MELO3C018769	0,005218299	0,049857856	Wound-responsive family protein
MELO3C019780	0,005232823	0,049972446	protein kinase 2B, chloroplastic-like

Supplementary Table 2.B Gene Ontology terms (GO terms) of the cluster 2.1 obtained considering the comparison between lines the postharvest ripening time fruit during storage at 20.5°C and 88% relative humidity for 18 d the near-isogenic line SC10-2 and its parental "Piel de Sapo" obtained according to the differentially expressed gene pattern (Supl. Table 2.A)

GO ID	GO Name	GO Category	FDR	P-Value	SC10-2	PS	Non Annot Test	Non Annot Reference	TestSet Sequences	RefSet Sequences
GO 0006415	translational termination	BIOLOGICAL_PROCESS	7,88E-13	4,17E-16	35	146	592	16355	MELO3C020906; MELO3C015999; MELO3C017939; MELO3C020049; MELO3C021339; MELO3C009338; MELO3C020003; MELO3C005952; MELO3C004645; MELO3C021436; MELO3C007635; MELO3C026403; MELO3C016083; MELO3C017993; MELO3C015431; MELO3C012967; MELO3C017659; MELO3C019907; MELO3C010630; MELO3C013245; MELO3C005089; MELO3C012131; MELO3C012670; MELO3C006412; MELO3C006314; MELO3C005446; MELO3C017291;	MELO3C011276; MELO3C010222; MELO3C006088; MELO3C014262; MELO3C024506; MELO3C006245; MELO3C003258; MELO3C022601; MELO3C020141; MELO3C022441; MELO3C023012; MELO3C010867; MELO3C016201; MELO3C016049; MELO3C025030; MELO3C011956; MELO3C016963; MELO3C013984; MELO3C007740; MELO3C013981; MELO3C002294; MELO3C011040; MELO3C023703; MELO3C006411; MELO3C014391; MELO3C005844; MELO3C023820;
GO 0006414	translational elongation	BIOLOGICAL_PROCESS	1,61E-12	1,02E-15	36	161	591	16340	MELO3C020906; MELO3C015999; MELO3C017939; MELO3C020049; MELO3C021339; MELO3C009338; MELO3C020003; MELO3C005952; MELO3C004645; MELO3C021436; MELO3C007635; MELO3C026403; MELO3C016083; MELO3C017993; MELO3C015431; MELO3C012967; MELO3C018985; MELO3C017659; MELO3C019907; MELO3C010630; MELO3C013245; MELO3C005089; MELO3C012131; MELO3C012670; MELO3C006412; MELO3C006314; MELO3C005446;	MELO3C008660; MELO3C011276; MELO3C010222; MELO3C006088; MELO3C014262; MELO3C024506; MELO3C006245; MELO3C003258; MELO3C022601; MELO3C020141; MELO3C022441; MELO3C020023; MELO3C023012; MELO3C010867; MELO3C016201; MELO3C025030; MELO3C011956; MELO3C016963; MELO3C014306; MELO3C007740; MELO3C013981; MELO3C002294; MELO3C005565; MELO3C011040; MELO3C023703; MELO3C006411; MELO3C005844;
GO 0003735	structural constituent of ribosome	MOLECULAR_FUNCTION	7,01E-10	1,19E-12	44	310	583	16191	MELO3C020906; MELO3C015999; MELO3C017939; MELO3C020049; MELO3C021339; MELO3C009338; MELO3C020003; MELO3C005952; MELO3C004645; MELO3C020369; MELO3C021436; MELO3C007635; MELO3C026403; MELO3C004505; MELO3C022386; MELO3C002405; MELO3C024644; MELO3C005759; MELO3C015373; MELO3C017993; MELO3C015431; MELO3C012967; MELO3C018985; MELO3C017659; MELO3C019907; MELO3C010630; MELO3C013245;	MELO3C011310; MELO3C020704; MELO3C006088; MELO3C002164; MELO3C012084; MELO3C014262; MELO3C024506; MELO3C020945; MELO3C006400; MELO3C003258; MELO3C006766; MELO3C024747; MELO3C020141; MELO3C022441; MELO3C003811; MELO3C001514; MELO3C025276; MELO3C016201; MELO3C025030; MELO3C016688; MELO3C014824; MELO3C020836; MELO3C007740; MELO3C013981; MELO3C009489; MELO3C002294; MELO3C025609;
GO 0022625	cytosolic large ribosomal subunit	CELLULAR_COMPONENT	3,67E-09	7,00E-12	27	124	600	16377	MELO3C020906; MELO3C015999; MELO3C017939; MELO3C021339; MELO3C009338; MELO3C005952; MELO3C020369; MELO3C021436; MELO3C007635; MELO3C026403; MELO3C022386; MELO3C016083; MELO3C012967; MELO3C017659; MELO3C011285; MELO3C006412; MELO3C006314; MELO3C005520; MELO3C005446; MELO3C023201; MELO3C024850; MELO3C016198; MELO3C002719; MELO3C011847; MELO3C009091; MELO3C006280; MELO3C015304	MELO3C006088; MELO3C014262; MELO3C024506; MELO3C006245; MELO3C006922; MELO3C022601; MELO3C022441; MELO3C001514; MELO3C023012; MELO3C016201; MELO3C025030; MELO3C011956; MELO3C012254; MELO3C002294; MELO3C006411; MELO3C005844; MELO3C004995; MELO3C023820; MELO3C006657; MELO3C020556; MELO3C025168; MELO3C000241; MELO3C023260; MELO3C011448; MELO3C016459; MELO3C011720; MELO3C002668;

GO 0046686	response to cadmium ion	BIOLOGICAL_PROCESS	1,84E-04	8,95E-07	22	160	605	16341	MELO3C011256; MELO3C005293; MELO3C013214; MELO3C013411; MELO3C004194; MELO3C009038; MELO3C009203; MELO3C003173; MELO3C006241; MELO3C011284; MELO3C003344; MELO3C024514; MELO3C005757; MELO3C021247; MELO3C008879; MELO3C002117; MELO3C022382; MELO3C018573; MELO3C002816; MELO3C015385; MELO3C010599; MELO3C011107	MELO3C013974; MELO3C006086; MELO3C021919; MELO3C017817; MELO3C020429; MELO3C003491; MELO3C003370; MELO3C008541; MELO3C005395; MELO3C004980; MELO3C009910; MELO3C007698; MELO3C005674; MELO3C009633; MELO3C009915; MELO3C002444; MELO3C019040; MELO3C003536; MELO3C026800; MELO3C021113; MELO3C024461; MELO3C017134; MELO3C018623; MELO3C026360; MELO3C011712; MELO3C019318; MELO3C006493;
GO 0016071	mRNA metabolic process	BIOLOGICAL_PROCESS	4,59E-04	2,52E-06	38	415	589	16086	MELO3C020906; MELO3C015999; MELO3C011256; MELO3C010960; MELO3C017939; MELO3C020049; MELO3C021339; MELO3C009338; MELO3C020003; MELO3C005952; MELO3C004645; MELO3C021436; MELO3C007635; MELO3C026403; MELO3C016083; MELO3C016382; MELO3C016262; MELO3C017993; MELO3C012967; MELO3C017659; MELO3C019907; MELO3C010630; MELO3C013245; MELO3C005089; MELO3C008332; MELO3C012670; MELO3C006412;	MELO3C020705; MELO3C004580; MELO3C014262; MELO3C013051; MELO3C002045; MELO3C020824; MELO3C003258; MELO3C007978; MELO3C006767; MELO3C026246; MELO3C017771; MELO3C016201; MELO3C015113; MELO3C025030; MELO3C017775; MELO3C019837; MELO3C020836; MELO3C007740; MELO3C002294; MELO3C002173; MELO3C020718; MELO3C006411; MELO3C006416; MELO3C008956; MELO3C008955; MELO3C019964; MELO3C016459;
GO 0000287	magnesium ion binding	MOLECULAR_FUNCTION	0,002863815	2,48E-05	21	186	606	16315	MELO3C005293; MELO3C010286; MELO3C014732; MELO3C007153; MELO3C010794; MELO3C009038; MELO3C012196; MELO3C020579; MELO3C024514; MELO3C006736; MELO3C004439; MELO3C021385; MELO3C024982; MELO3C021563; MELO3C020244; MELO3C018573; MELO3C022494; MELO3C005939; MELO3C020394; MELO3C011704; MELO3C013745	MELO3C005271; MELO3C020829; MELO3C013336; MELO3C018628; MELO3C018507; MELO3C005396; MELO3C008426; MELO3C024509; MELO3C022605; MELO3C024508; MELO3C001595; MELO3C004226; MELO3C003379; MELO3C026007; MELO3C002448; MELO3C026005; MELO3C026006; MELO3C025552; MELO3C026004; MELO3C002727; MELO3C015076; MELO3C000372; MELO3C000130; MELO3C011713; MELO3C019677; MELO3C013218; MELO3C014943;
GO 0004775	succinate-CoA ligase (ADP-forming) activity	MOLECULAR_FUNCTION	0,002863815	2,52E-05	4	2	623	16499	MELO3C002167; MELO3C022382; MELO3C010675; MELO3C011482	MELO3C021268; MELO3C015245
GO 0009651	response to salt stress	BIOLOGICAL_PROCESS	0,00360577	3,28E-05	18	146	609	16355	MELO3C012136; MELO3C012445; MELO3C004194; MELO3C009203; MELO3C011044; MELO3C005147; MELO3C011172; MELO3C026629; MELO3C004105; MELO3C024514; MELO3C008879; MELO3C027349; MELO3C017242; MELO3C018573; MELO3C015098; MELO3C016033; MELO3C015186; MELO3C015374	MELO3C021918; MELO3C006086; MELO3C017935; MELO3C013454; MELO3C004580; MELO3C012085; MELO3C022725; MELO3C008666; MELO3C006648; MELO3C002203; MELO3C026009; MELO3C024345; MELO3C007739; MELO3C026245; MELO3C017134; MELO3C024222; MELO3C019039; MELO3C010625; MELO3C012925; MELO3C026482; MELO3C016738; MELO3C002170; MELO3C012099; MELO3C012097; MELO3C007067; MELO3C009123; MELO3C005444;

GO 0006096	glycolytic process	BIOLOGICAL_PROCESS	0,005205084	5,29E-05	12	72	615	16429	MELO3C020780; MELO3C014732; MELO3C007421; MELO3C007986; MELO3C020579; MELO3C012604; MELO3C018966; MELO3C024514; MELO3C011104; MELO3C022998; MELO3C008219; MELO3C008879	MELO3C005271; MELO3C009351; MELO3C007772; MELO3C013010; MELO3C008221; MELO3C025916; MELO3C009438; MELO3C024509; MELO3C024508; MELO3C024866; MELO3C006964; MELO3C009439; MELO3C019872; MELO3C017175; MELO3C025275; MELO3C018027; MELO3C019634; MELO3C011367; MELO3C020837; MELO3C003381; MELO3C004591; MELO3C014272; MELO3C025969; MELO3C024519; MELO3C021720; MELO3C016050; MELO3C016095;
GO 0022627	cytosolic small ribosomal subunit	CELLULAR_COMPONENT	0,009406002	1,08E-04	13	91	614	16410	MELO3C019907; MELO3C010630; MELO3C013245; MELO3C005089; MELO3C012670; MELO3C020049; MELO3C020003; MELO3C017291; MELO3C004645; MELO3C015373; MELO3C017993; MELO3C015431; MELO3C025582	MELO3C011310; MELO3C004020; MELO3C002481; MELO3C009036; MELO3C003890; MELO3C012084; MELO3C005830; MELO3C009315; MELO3C009716; MELO3C001556; MELO3C020141; MELO3C022363; MELO3C010867; MELO3C017338; MELO3C019879; MELO3C002091; MELO3C003061; MELO3C020759; MELO3C013981; MELO3C009489; MELO3C025609; MELO3C023703; MELO3C019490; MELO3C001168; MELO3C024359; MELO3C006733; MELO3C003986;
GO 0002119	nematode larval development	BIOLOGICAL_PROCESS	0,010270399	1,20E-04	25	273	602	16228	MELO3C011256; MELO3C010243; MELO3C008285; MELO3C010960; MELO3C016707; MELO3C011193; MELO3C009338; MELO3C007433; MELO3C020369; MELO3C006949; MELO3C022488; MELO3C016262; MELO3C017993; MELO3C011285; MELO3C005421; MELO3C004278; MELO3C025549; MELO3C023201; MELO3C002118; MELO3C002717; MELO3C003905; MELO3C022094; MELO3C006280; MELO3C025061; MELO3C013822	MELO3C011795; MELO3C012522; MELO3C006760; MELO3C002166; MELO3C002045; MELO3C004344; MELO3C019031; MELO3C026800; MELO3C019034; MELO3C025275; MELO3C016321; MELO3C014708; MELO3C015235; MELO3C019956; MELO3C020836; MELO3C008157; MELO3C002173; MELO3C004473; MELO3C014153; MELO3C013185; MELO3C023545; MELO3C008835; MELO3C023306; MELO3C023427; MELO3C006657; MELO3C024757; MELO3C003703;
GO 0009792	embryo development ending in birth or egg hatching	BIOLOGICAL_PROCESS	0,010669712	1,25E-04	31	374	596	16127	MELO3C011256; MELO3C010243; MELO3C008285; MELO3C010960; MELO3C002180; MELO3C012361; MELO3C011193; MELO3C009338; MELO3C007433; MELO3C005679; MELO3C020369; MELO3C006949; MELO3C019253; MELO3C022488; MELO3C020860; MELO3C017993; MELO3C011285; MELO3C005421; MELO3C004278; MELO3C025549; MELO3C023201; MELO3C002118; MELO3C024352; MELO3C002717; MELO3C003905; MELO3C022094; MELO3C006280;	MELO3C010584; MELO3C011795; MELO3C012522; MELO3C009592; MELO3C006760; MELO3C002166; MELO3C002045; MELO3C004344; MELO3C019031; MELO3C022562; MELO3C018062; MELO3C026800; MELO3C026245; MELO3C018187; MELO3C019034; MELO3C025275; MELO3C014708; MELO3C015235; MELO3C015599; MELO3C019956; MELO3C006096; MELO3C008151; MELO3C020836; MELO3C008157; MELO3C002173; MELO3C004473; MELO3C014153;

GO 0006099	tricarboxylic acid cycle	BIOLOGICAL_PROCESS	0,029273395	4,00E-04	7	31	620	16470	MELO3C021563; MELO3C022382; MELO3C017560; MELO3C011482; MELO3C002167; MELO3C021247; MELO3C022998	MELO3C012389; MELO3C017938; MELO3C007674; MELO3C014221; MELO3C013153; MELO3C003577; MELO3C025636; MELO3C022343; MELO3C005539; MELO3C017175; MELO3C019711; MELO3C025076; MELO3C018724; MELO3C014824; MELO3C019879; MELO3C002350; MELO3C023506; MELO3C007968; MELO3C021268; MELO3C021545; MELO3C006734; MELO3C005348; MELO3C016050; MELO3C016095; MELO3C005968; MELO3C019300; MELO3C019243;
GO 0005618	cell wall	CELLULAR_COMPONENT	0,030634705	4,34E-04	28	351	599	16150	MELO3C013699; MELO3C012004; MELO3C011256; MELO3C009133; MELO3C012100; MELO3C020049; MELO3C005757; MELO3C016067; MELO3C017478; MELO3C010686; MELO3C009203; MELO3C005089; MELO3C012670; MELO3C021404; MELO3C005201; MELO3C004597; MELO3C009429; MELO3C008879; MELO3C007609; MELO3C017480; MELO3C021782; MELO3C025324; MELO3C017481; MELO3C017242; MELO3C017560; MELO3C023188; MELO3C025582;	MELO3C015914; MELO3C020704; MELO3C007057; MELO3C013055; MELO3C026806; MELO3C005316; MELO3C002047; MELO3C008946; MELO3C003810; MELO3C021595; MELO3C021471; MELO3C019039; MELO3C018862; MELO3C018743; MELO3C008032; MELO3C009120; MELO3C005561; MELO3C012099; MELO3C009488; MELO3C009367; MELO3C012097; MELO3C005560; MELO3C012096; MELO3C004477; MELO3C008159; MELO3C009924; MELO3C010919;
GO 0003878	ATP citrate synthase activity	MOLECULAR_FUNCTION	0,031860458	4,62E-04	3	2	624	16499	MELO3C010675; MELO3C011482; MELO3C002167	MELO3C021268; MELO3C015245
GO 0008340	determination of adult lifespan	BIOLOGICAL_PROCESS	0,032223247	4,81E-04	11	80	616	16421	MELO3C014007; MELO3C011256; MELO3C023201; MELO3C006949; MELO3C008285; MELO3C010960; MELO3C020860; MELO3C016262; MELO3C022094; MELO3C004278; MELO3C011104	MELO3C016329; MELO3C010584; MELO3C012522; MELO3C014221; MELO3C006121; MELO3C005753; MELO3C007214; MELO3C024822; MELO3C008306; MELO3C004945; MELO3C025755; MELO3C025796; MELO3C020783; MELO3C004827; MELO3C025275; MELO3C015199; MELO3C019712; MELO3C022280; MELO3C027174; MELO3C013814; MELO3C011830; MELO3C017627; MELO3C010795; MELO3C009840; MELO3C015928; MELO3C014153; MELO3C022219;
GO 0031018	endocrine pancreas development	BIOLOGICAL_PROCESS	0,032223247	4,78E-04	4	7	623	16494	MELO3C023201; MELO3C017993; MELO3C009338; MELO3C017291	MELO3C014237; MELO3C017184; MELO3C006662; MELO3C017169; MELO3C018512; MELO3C023127; MELO3C017290
GO 0010181	FMN binding	MOLECULAR_FUNCTION	0,057904252	9,44E-04	6	26	621	16475	MELO3C007340; MELO3C011062; MELO3C003541; MELO3C023799; MELO3C016623; MELO3C015514	MELO3C008482; MELO3C013476; MELO3C008481; MELO3C004023; MELO3C009759; MELO3C022683; MELO3C022684; MELO3C008805; MELO3C022681; MELO3C024281; MELO3C018625; MELO3C018626; MELO3C010940; MELO3C017636; MELO3C008075; MELO3C007124; MELO3C006296; MELO3C006011; MELO3C009702; MELO3C021944; MELO3C005229; MELO3C003644; MELO3C025720; MELO3C017461; MELO3C025861; MELO3C007808

GO 0004776	succinate-CoA ligase (GDP-forming) activity	MOLECULAR_FUNCTION	0,076614304	0,001337993	2	0	625	16501	MELO3C022382; MELO3C002167	
GO 0003861	3-isopropylmalate dehydratase activity	MOLECULAR_FUNCTION	0,076614304	0,001337993	2	0	625	16501	MELO3C005518; MELO3C003344	
GO 0040002	collagen and cuticulin-based cuticle development	BIOLOGICAL_PROCESS	0,086570236	0,001530189	3	4	624	16497	MELO3C016707; MELO3C019253; MELO3C012361	MELO3C016321; MELO3C023052; MELO3C008151; MELO3C015126
GO 0048046	apoplast	CELLULAR_COMPONENT	0,08752412	0,001574841	18	203	609	16298	MELO3C012004; MELO3C009038; MELO3C011284; MELO3C024514; MELO3C021247; MELO3C008879; MELO3C007609; MELO3C020780; MELO3C017480; MELO3C021782; MELO3C017481; MELO3C023188; MELO3C015186; MELO3C012604; MELO3C017478; MELO3C009250; MELO3C011107; MELO3C010686	MELO3C011430; MELO3C007058; MELO3C013055; MELO3C007059; MELO3C003137; MELO3C026800; MELO3C001998; MELO3C015470; MELO3C015472; MELO3C010901; MELO3C007061; MELO3C007064; MELO3C007065; MELO3C008274; MELO3C007062; MELO3C007063; MELO3C005561; MELO3C007068; MELO3C009247; MELO3C009367; MELO3C005565; MELO3C010919; MELO3C025840; MELO3C026259; MELO3C019168; MELO3C011329; MELO3C010114;
GO 0004298	threonine-type endopeptidase activity	MOLECULAR_FUNCTION	0,099790014	0,001869478	5	20	622	16481	MELO3C010960; MELO3C011172; MELO3C003173; MELO3C013757; MELO3C006187	MELO3C011880; MELO3C006131; MELO3C007920; MELO3C021745; MELO3C021746; MELO3C000704; MELO3C025735; MELO3C023267; MELO3C025755; MELO3C026800; MELO3C000762; MELO3C006517; MELO3C019011; MELO3C019010; MELO3C019012; MELO3C027069; MELO3C024343; MELO3C010635; MELO3C026360; MELO3C011449
GO 0015631	tubulin binding	MOLECULAR_FUNCTION	0,099790014	0,001869478	5	20	622	16481	MELO3C022488; MELO3C013702; MELO3C002717; MELO3C017221; MELO3C006602	MELO3C004390; MELO3C010584; MELO3C006171; MELO3C018707; MELO3C007036; MELO3C007584; MELO3C022016; MELO3C001970; MELO3C022478; MELO3C006723; MELO3C022166; MELO3C022751; MELO3C024792; MELO3C016297; MELO3C024150; MELO3C017720; MELO3C018910; MELO3C011800; MELO3C019823; MELO3C011830
GO 0000084	mitotic S phase	BIOLOGICAL_PROCESS	0,102607716	0,001954846	9	68	618	16433	MELO3C016083; MELO3C010960; MELO3C003638; MELO3C020860; MELO3C016262; MELO3C020001; MELO3C012361; MELO3C010631; MELO3C004448	MELO3C009313; MELO3C002481; MELO3C014021; MELO3C014020; MELO3C008864; MELO3C004864; MELO3C025879; MELO3C025755; MELO3C026800; MELO3C005912; MELO3C023372; MELO3C010507; MELO3C010828; MELO3C018501; MELO3C012407; MELO3C013814; MELO3C017458; MELO3C006096; MELO3C015926; MELO3C007066; MELO3C007144; MELO3C012492; MELO3C002892; MELO3C025923; MELO3C025646; MELO3C021204; MELO3C019642;

GO 0040010	positive regulation of growth rate	BIOLOGICAL_PROCESS	0,110013724	0,002155258	20	241	607	16260	MELO3C011256; MELO3C010243; MELO3C008285; MELO3C011285; MELO3C009338; MELO3C005421; MELO3C007433; MELO3C026614; MELO3C017291; MELO3C020369; MELO3C023201; MELO3C006949; MELO3C002118; MELO3C024352; MELO3C002717; MELO3C003905; MELO3C017993; MELO3C006280; MELO3C025061; MELO3C013822	MELO3C012522; MELO3C009592; MELO3C006760; MELO3C002045; MELO3C004344; MELO3C018187; MELO3C019034; MELO3C025275; MELO3C016321; MELO3C014708; MELO3C026482; MELO3C019956; MELO3C021808; MELO3C020836; MELO3C004473; MELO3C014153; MELO3C013185; MELO3C004353; MELO3C023545; MELO3C023306; MELO3C006657; MELO3C002738; MELO3C025044; MELO3C017661; MELO3C018512; MELO3C016456; MELO3C015246;
GO 0006094	gluconeogenesis	BIOLOGICAL_PROCESS	0,110013724	0,002165808	7	43	620	16458	MELO3C020780; MELO3C011284; MELO3C012604; MELO3C021604; MELO3C011104; MELO3C022998; MELO3C008879	MELO3C012444; MELO3C012389; MELO3C009351; MELO3C007674; MELO3C007772; MELO3C003491; MELO3C025916; MELO3C004980; MELO3C005333; MELO3C003577; MELO3C003214; MELO3C003215; MELO3C023354; MELO3C005539; MELO3C017175; MELO3C019634; MELO3C014724; MELO3C011710; MELO3C011367; MELO3C013203; MELO3C012375; MELO3C009147; MELO3C011682; MELO3C003265; MELO3C007687; MELO3C004433; MELO3C003266;
GO 0005774	vacuolar membrane	CELLULAR_COMPONENT	0,110013724	0,002147824	14	145	613	16356	MELO3C013489; MELO3C011279; MELO3C010286; MELO3C010991; MELO3C006320; MELO3C026614; MELO3C022448; MELO3C006926; MELO3C026522; MELO3C000065; MELO3C016067; MELO3C012604; MELO3C025061; MELO3C024192	MELO3C014821; MELO3C015914; MELO3C007695; MELO3C011151; MELO3C002042; MELO3C005831; MELO3C026800; MELO3C021595; MELO3C024346; MELO3C025035; MELO3C025310; MELO3C025157; MELO3C016044; MELO3C012405; MELO3C010992; MELO3C013467; MELO3C013102; MELO3C014796; MELO3C005561; MELO3C004075; MELO3C005441; MELO3C007980; MELO3C007100; MELO3C004477; MELO3C009887; MELO3C003783; MELO3C004874;
GO 0006069	ethanol oxidation	BIOLOGICAL_PROCESS	0,115059486	0,00227732	4	12	623	16489	MELO3C023685; MELO3C022399; MELO3C014749; MELO3C026554	MELO3C023687; MELO3C005792; MELO3C004383; MELO3C026553; MELO3C017100; MELO3C017125; MELO3C004430; MELO3C019622; MELO3C002189; MELO3C027151; MELO3C005081; MELO3C025328
GO 0035046	pronuclear migration	BIOLOGICAL_PROCESS	0,117208756	0,002381888	3	5	624	16496	MELO3C019253; MELO3C012361; MELO3C020860	MELO3C022016; MELO3C005064; MELO3C019956; MELO3C006723; MELO3C004458
GO 0051903	S-(hydroxymethyl)glutathione dehydrogenase activity	MOLECULAR_FUNCTION	0,117208756	0,002381888	3	5	624	16496	MELO3C023685; MELO3C026554; MELO3C022399	MELO3C002189; MELO3C005792; MELO3C026553; MELO3C027151; MELO3C026552

GO 0051086	chaperone mediated protein folding independent of cofactor	BIOLOGICAL_PROCESS	0,132668929	0,002892654	4	13	623	16488	MELO3C002117; MELO3C009624; MELO3C022094; MELO3C010705	MELO3C014127; MELO3C015615; MELO3C008567; MELO3C021633; MELO3C003128; MELO3C004458; MELO3C023558; MELO3C004636; MELO3C026888; MELO3C017295; MELO3C023852; MELO3C018683; MELO3C023264
GO 0007018	microtubule-based movement	BIOLOGICAL_PROCESS	0,14661594	0,00328355	9	74	618	16427	MELO3C009203; MELO3C024241; MELO3C007673; MELO3C023342; MELO3C015098; MELO3C005673; MELO3C013429; MELO3C013702; MELO3C008977	MELO3C017936; MELO3C017937; MELO3C005594; MELO3C015839; MELO3C014142; MELO3C004267; MELO3C020741; MELO3C020742; MELO3C005479; MELO3C007217; MELO3C009715; MELO3C005678; MELO3C021238; MELO3C003218; MELO3C023013; MELO3C015272; MELO3C002528; MELO3C010629; MELO3C015273; MELO3C018025; MELO3C017377; MELO3C010988; MELO3C016369; MELO3C010147; MELO3C010787; MELO3C009760; MELO3C004273;
GO 0004807	triose-phosphate isomerase activity	MOLECULAR_FUNCTION	0,16359848	0,003916322	2	1	625	16500	MELO3C020780; MELO3C008879	MELO3C025916
GO 0050625	2-hydroxy-1,4-benzoquinone reductase activity	MOLECULAR_FUNCTION	0,16359848	0,003916322	2	1	625	16500	MELO3C007340; MELO3C016623	MELO3C025861
GO 0004733	pyridoxamine-phosphate oxidase activity	MOLECULAR_FUNCTION	0,16359848	0,003916322	2	1	625	16500	MELO3C011062; MELO3C003541	MELO3C006011
GO 0016328	lateral plasma membrane	CELLULAR_COMPONENT	0,16359848	0,003916322	2	1	625	16500	MELO3C017242; MELO3C022488	MELO3C007829
GO 0000022	mitotic spindle elongation	BIOLOGICAL_PROCESS	0,179478323	0,004445166	4	15	623	16486	MELO3C009338; MELO3C011285; MELO3C006280; MELO3C020369	MELO3C014237; MELO3C007036; MELO3C003342; MELO3C009600; MELO3C025755; MELO3C004807; MELO3C023594; MELO3C024782; MELO3C016981; MELO3C024150; MELO3C024020; MELO3C026580; MELO3C015269; MELO3C017744; MELO3C012667
GO 0005852	eukaryotic translation initiation factor 3 complex	CELLULAR_COMPONENT	0,19261379	0,004831654	3	7	624	16494	MELO3C011193; MELO3C008285; MELO3C003453	MELO3C026327; MELO3C017707; MELO3C009841; MELO3C019434; MELO3C015553; MELO3C022038; MELO3C007050
GO 0019773	proteasome core complex, alpha-subunit complex	CELLULAR_COMPONENT	0,19261379	0,004831654	3	7	624	16494	MELO3C003173; MELO3C010960; MELO3C013757	MELO3C026800; MELO3C024343; MELO3C007920; MELO3C021745; MELO3C021746; MELO3C026360; MELO3C025735
GO 0009825	multidimensional cell growth	BIOLOGICAL_PROCESS	0,21338209	0,00539779	4	16	623	16485	MELO3C012004; MELO3C007325; MELO3C017242; MELO3C007207	MELO3C012114; MELO3C002081; MELO3C005631; MELO3C007324; MELO3C021737; MELO3C001364; MELO3C002553; MELO3C024898; MELO3C020643; MELO3C023374; MELO3C015782; MELO3C011913; MELO3C015783; MELO3C015784; MELO3C015785; MELO3C011732
GO 0009846	pollen germination	BIOLOGICAL_PROCESS	0,246779923	0,006477712	4	17	623	16484	MELO3C008285; MELO3C004551; MELO3C019522; MELO3C013702	MELO3C015989; MELO3C014698; MELO3C005099; MELO3C003581; MELO3C021702; MELO3C009734; MELO3C000736; MELO3C022308; MELO3C004336; MELO3C006326; MELO3C024874; MELO3C020044; MELO3C012924; MELO3C019825; MELO3C015654; MELO3C015689; MELO3C024093

GO 0042450	arginine biosynthetic process via ornithine	BIOLOGICAL_PROCESS	0,267436664	0,007642665	2	2	625	16499	MELO3C011085; MELO3C011208	MELO3C023629; MELO3C003523
GO 0018279	protein N-linked glycosylation via asparagine	BIOLOGICAL_PROCESS	0,267436664	0,007321952	7	55	620	16446	MELO3C003812; MELO3C023310; MELO3C011944; MELO3C025637; MELO3C021279; MELO3C024447; MELO3C013822	MELO3C009473; MELO3C007374; MELO3C002165; MELO3C002166; MELO3C007137; MELO3C021632; MELO3C009914; MELO3C009912; MELO3C026524; MELO3C023850; MELO3C026763; MELO3C020220; MELO3C018343; MELO3C010625; MELO3C017413; MELO3C026482; MELO3C017019; MELO3C004196; MELO3C015929; MELO3C024710; MELO3C017661; MELO3C024194; MELO3C010319; MELO3C015246; MELO3C016018; MELO3C013830; MELO3C014202;
GO 0006272	leading strand elongation	BIOLOGICAL_PROCESS	0,267436664	0,007642665	2	2	625	16499	MELO3C010631; MELO3C020860	MELO3C014021; MELO3C010507
GO 0004634	phosphopyruvate hydratase activity	MOLECULAR_FUNCTION	0,267436664	0,007642665	2	2	625	16499	MELO3C020579; MELO3C024514	MELO3C017268; MELO3C026748
GO 0004133	glycogen debranching enzyme activity	MOLECULAR_FUNCTION	0,267436664	0,007642665	2	2	625	16499	MELO3C015861; MELO3C019135	MELO3C017391; MELO3C020949
GO 0008541	proteasome regulatory particle, lid subcomplex	CELLULAR_COMPONENT	0,267436664	0,007642665	2	2	625	16499	MELO3C016262; MELO3C011193	MELO3C025923; MELO3C013814
GO 0000015	phosphopyruvate hydratase complex	CELLULAR_COMPONENT	0,267436664	0,007642665	2	2	625	16499	MELO3C020579; MELO3C024514	MELO3C017268; MELO3C026748
GO 0034515	proteasome storage granule	CELLULAR_COMPONENT	0,285040264	0,008387087	3	9	624	16492	MELO3C016262; MELO3C011193; MELO3C010960	MELO3C025755; MELO3C026800; MELO3C020453; MELO3C018764; MELO3C021746; MELO3C010635; MELO3C011449; MELO3C013814; MELO3C025923
GO 0030170	pyridoxal phosphate binding	MOLECULAR_FUNCTION	0,330546323	0,010250854	11	123	616	16378	MELO3C018948; MELO3C023373; MELO3C000251; MELO3C020927; MELO3C011284; MELO3C026175; MELO3C001121; MELO3C011107; MELO3C010686; MELO3C020444; MELO3C001323	MELO3C005392; MELO3C013732; MELO3C010464; MELO3C020429; MELO3C010461; MELO3C004980; MELO3C002561; MELO3C023659; MELO3C007698; MELO3C009117; MELO3C017490; MELO3C026404; MELO3C022321; MELO3C024500; MELO3C011959; MELO3C016200; MELO3C016448; MELO3C011960; MELO3C013583; MELO3C004355; MELO3C022699; MELO3C018082; MELO3C026534; MELO3C019443; MELO3C017386; MELO3C019203; MELO3C010754;
GO 0005509	calcium ion binding	MOLECULAR_FUNCTION	0,358334546	0,011491889	16	211	611	16290	MELO3C014016; MELO3C014588; MELO3C004194; MELO3C010794; MELO3C013892; MELO3C014150; MELO3C006158; MELO3C005757; MELO3C006759; MELO3C019002; MELO3C022494; MELO3C019820; MELO3C017844; MELO3C013702; MELO3C014658; MELO3C012457	MELO3C003372; MELO3C004465; MELO3C008705; MELO3C024866; MELO3C025712; MELO3C023415; MELO3C005319; MELO3C002967; MELO3C019035; MELO3C019036; MELO3C020263; MELO3C015597; MELO3C016569; MELO3C010348; MELO3C020719; MELO3C014279; MELO3C013982; MELO3C023542; MELO3C007507; MELO3C020277; MELO3C016330; MELO3C016333; MELO3C018876; MELO3C018877; MELO3C013504; MELO3C018517; MELO3C018879;

GO 0005982	starch metabolic process	BIOLOGICAL_PROCESS	0,376688631	0,012200119	4	21	623	16480	MELO3C003812; MELO3C005293; MELO3C011104; MELO3C019135	MELO3C009960; MELO3C014105; MELO3C011972; MELO3C005396; MELO3C006585; MELO3C006552; MELO3C011682; MELO3C020949; MELO3C007155; MELO3C012071; MELO3C005795; MELO3C002455; MELO3C023105; MELO3C021412; MELO3C025149; MELO3C026536; MELO3C024754; MELO3C024175; MELO3C022275; MELO3C017942; MELO3C017735
GO 0016882	cyclo-ligase activity	MOLECULAR_FUNCTION	0,37679878	0,012429782	2	3	625	16498	MELO3C016483; MELO3C008332	MELO3C005781; MELO3C017138; MELO3C017137
GO 0019843	rRNA binding	MOLECULAR_FUNCTION	0,37679878	0,012522737	8	77	619	16424	MELO3C024850; MELO3C010630; MELO3C005759; MELO3C013245; MELO3C011847; MELO3C009091; MELO3C012967; MELO3C008801	MELO3C010584; MELO3C011276; MELO3C011310; MELO3C004020; MELO3C003890; MELO3C009795; MELO3C006682; MELO3C006088; MELO3C012480; MELO3C012084; MELO3C006245; MELO3C020945; MELO3C021312; MELO3C022601; MELO3C001556; MELO3C022485; MELO3C003811; MELO3C019631; MELO3C025474; MELO3C019879; MELO3C003061; MELO3C025609; MELO3C005844; MELO3C005800; MELO3C004995; MELO3C003986; MELO3C025845;
GO 0008878	glucose-1-phosphate adenylyltransferase activity	MOLECULAR_FUNCTION	0,37679878	0,012429782	2	3	625	16498	MELO3C003812; MELO3C023310	MELO3C006552; MELO3C024175; MELO3C021412
GO 0019781	NEDD8 activating enzyme activity	MOLECULAR_FUNCTION	0,37679878	0,012429782	2	3	625	16498	MELO3C011193; MELO3C006555	MELO3C008213; MELO3C014386; MELO3C013230
GO 0004069	L-aspartate 2-oxoglutarate aminotransferase activity	MOLECULAR_FUNCTION	0,384072065	0,013141879	3	11	624	16490	MELO3C023373; MELO3C001121; MELO3C011284	MELO3C015944; MELO3C010464; MELO3C008136; MELO3C010461; MELO3C018037; MELO3C004980; MELO3C006840; MELO3C005597; MELO3C003577; MELO3C017998; MELO3C026051
GO 0051087	chaperone binding	MOLECULAR_FUNCTION	0,384072065	0,013141879	3	11	624	16490	MELO3C005757; MELO3C002717; MELO3C022488	MELO3C004390; MELO3C006948; MELO3C009561; MELO3C010013; MELO3C014179; MELO3C011373; MELO3C019156; MELO3C022725; MELO3C009611; MELO3C022478; MELO3C011830
GO 0009664	plant-type cell wall organization	BIOLOGICAL_PROCESS	0,387087609	0,013315355	5	34	622	16467	MELO3C012004; MELO3C021999; MELO3C020626; MELO3C017242; MELO3C010524	MELO3C010062; MELO3C021619; MELO3C011350; MELO3C020005; MELO3C003134; MELO3C005613; MELO3C001993; MELO3C017181; MELO3C024488; MELO3C025996; MELO3C024487; MELO3C016062; MELO3C026188; MELO3C020143; MELO3C003916; MELO3C015695; MELO3C025095; MELO3C012108; MELO3C011732; MELO3C016517; MELO3C016916; MELO3C014013; MELO3C025907; MELO3C008552; MELO3C020810; MELO3C005962; MELO3C006318;

GO 0005978	glycogen biosynthetic process	BIOLOGICAL_PROCESS	0,403293101	0,014009997	4	22	623	16479	MELO3C003812; MELO3C005293; MELO3C023310; MELO3C020244	MELO3C011991; MELO3C013146; MELO3C004270; MELO3C005396; MELO3C009445; MELO3C006552; MELO3C009861; MELO3C007155; MELO3C008045; MELO3C005795; MELO3C002455; MELO3C021412; MELO3C008407; MELO3C008614; MELO3C021249; MELO3C026536; MELO3C025521; MELO3C024175; MELO3C012925; MELO3C018534; MELO3C010862; MELO3C011346
GO 0043161	proteasome-mediated ubiquitin-dependent protein catabolic process	BIOLOGICAL_PROCESS	0,425423227	0,015219417	8	80	619	16421	MELO3C016083; MELO3C010960; MELO3C005918; MELO3C016262; MELO3C012361; MELO3C011193; MELO3C015764; MELO3C005757	MELO3C014542; MELO3C002481; MELO3C022725; MELO3C007137; MELO3C002401; MELO3C025755; MELO3C026800; MELO3C005912; MELO3C023372; MELO3C025232; MELO3C010828; MELO3C025152; MELO3C018501; MELO3C012407; MELO3C013814; MELO3C017338; MELO3C011710; MELO3C006173; MELO3C007383; MELO3C003464; MELO3C006972; MELO3C025923; MELO3C008916; MELO3C019642; MELO3C026177; MELO3C010635; MELO3C011449;
GO 0006351	transcription, DNA-templated	BIOLOGICAL_PROCESS	0,432026982	0,015592845	43	1606	584	14895	MELO3C011256; MELO3C014722; MELO3C007691; MELO3C012242; MELO3C011110; MELO3C009653; MELO3C020848; MELO3C011193; MELO3C020701; MELO3C011172; MELO3C008847; MELO3C002644; MELO3C016083; MELO3C023412; MELO3C020860; MELO3C016660; MELO3C011759; MELO3C023195; MELO3C007181; MELO3C016623; MELO3C009188; MELO3C011003; MELO3C007340; MELO3C011167; MELO3C010057; MELO3C002292; MELO3C006870;	MELO3C007971; MELO3C014266; MELO3C005791; MELO3C014263; MELO3C007974; MELO3C014261; MELO3C006648; MELO3C012081; MELO3C000099; MELO3C016444; MELO3C017775; MELO3C017308; MELO3C021809; MELO3C021804; MELO3C003140; MELO3C007500; MELO3C002299; MELO3C012094; MELO3C005327; MELO3C012091; MELO3C007989; MELO3C007988; MELO3C027103; MELO3C027102; MELO3C017782; MELO3C027101; MELO3C017303;
GO 0005506	iron ion binding	MOLECULAR_FUNCTION	0,432026982	0,015575442	4	320	623	16181	MELO3C005103; MELO3C007611; MELO3C013868; MELO3C006943	MELO3C007174; MELO3C012522; MELO3C007175; MELO3C021914; MELO3C012088; MELO3C007058; MELO3C020028; MELO3C006644; MELO3C004221; MELO3C004584; MELO3C007059; MELO3C025712; MELO3C026802; MELO3C020385; MELO3C023893; MELO3C023530; MELO3C000772; MELO3C015591; MELO3C026487; MELO3C000770; MELO3C015592; MELO3C015593; MELO3C015595; MELO3C015596; MELO3C026484; MELO3C016686; MELO3C016687;

GO 0003924	GTPase activity	MOLECULAR_FUNCTION	0,434527948	0,015729102	9	97	618	16404	MELO3C011234; MELO3C002118; MELO3C024544; MELO3C025885; MELO3C009203; MELO3C007673; MELO3C015098; MELO3C005673; MELO3C002687	MELO3C011312; MELO3C003370; MELO3C021514; MELO3C023931; MELO3C026889; MELO3C018587; MELO3C015755; MELO3C015756; MELO3C003261; MELO3C004074; MELO3C014156; MELO3C007220; MELO3C005565; MELO3C013185; MELO3C013183; MELO3C003786; MELO3C013180; MELO3C000761; MELO3C026259; MELO3C016695; MELO3C006063; MELO3C019819; MELO3C018848; MELO3C013158; MELO3C014400; MELO3C004440; MELO3C021977;
GO 0005768	endosome	CELLULAR_COMPONENT	0,437568879	0,016070745	7	65	620	16436	MELO3C006926; MELO3C010243; MELO3C010772; MELO3C004391; MELO3C025783; MELO3C026614; MELO3C018758	MELO3C014821; MELO3C011795; MELO3C009473; MELO3C014542; MELO3C005199; MELO3C007457; MELO3C012481; MELO3C014180; MELO3C004945; MELO3C025310; MELO3C004827; MELO3C026440; MELO3C013816; MELO3C012728; MELO3C015433; MELO3C006171; MELO3C010795; MELO3C023828; MELO3C024558; MELO3C005328; MELO3C004874; MELO3C018195; MELO3C016491; MELO3C026971; MELO3C025682; MELO3C026096; MELO3C022490;
GO 0005525	GTP binding	MOLECULAR_FUNCTION	0,448993888	0,016680446	17	237	610	16264	MELO3C011234; MELO3C009038; MELO3C009203; MELO3C007673; MELO3C005673; MELO3C002167; MELO3C021279; MELO3C002687; MELO3C009966; MELO3C002118; MELO3C024544; MELO3C025885; MELO3C022382; MELO3C002816; MELO3C015098; MELO3C011704; MELO3C010569	MELO3C011312; MELO3C003370; MELO3C012760; MELO3C021114; MELO3C012529; MELO3C011684; MELO3C004471; MELO3C003261; MELO3C014156; MELO3C020959; MELO3C015929; MELO3C005565; MELO3C006896; MELO3C013185; MELO3C007742; MELO3C013183; MELO3C021803; MELO3C018080; MELO3C013180; MELO3C000761; MELO3C026259; MELO3C016695; MELO3C019844; MELO3C006063; MELO3C019819; MELO3C018848; MELO3C013158;
GO 0009098	leucine biosynthetic process	BIOLOGICAL_PROCESS	0,463366121	0,018195262	2	4	625	16497	MELO3C005518; MELO3C003344	MELO3C017853; MELO3C024817; MELO3C014221; MELO3C020296
GO 0006977	DNA damage response, signal transduction by p53 class mediator resulting in cell cycle arrest	BIOLOGICAL_PROCESS	0,463366121	0,018118465	4	24	623	16477	MELO3C016083; MELO3C010960; MELO3C016262; MELO3C012361	MELO3C011983; MELO3C002481; MELO3C011470; MELO3C021746; MELO3C014086; MELO3C000704; MELO3C004136; MELO3C021715; MELO3C025923; MELO3C025417; MELO3C005738; MELO3C023476; MELO3C026239; MELO3C003316; MELO3C025755; MELO3C026800; MELO3C005912; MELO3C020453; MELO3C018099; MELO3C019642; MELO3C019587; MELO3C019731; MELO3C013814; MELO3C016699
GO 0006103	2-oxoglutarate metabolic process	BIOLOGICAL_PROCESS	0,463366121	0,018195262	2	4	625	16497	MELO3C021563; MELO3C011284	MELO3C025076; MELO3C004980; MELO3C003577; MELO3C019166

GO 0016762	xyloglucan xyloglucosyl transferase activity	MOLECULAR_FUNCTION	0,463366121	0,018118465	4	24	623	16477	MELO3C012004; MELO3C017480; MELO3C017481; MELO3C017478	MELO3C014469; MELO3C014468; MELO3C014467; MELO3C014466; MELO3C014465; MELO3C002480; MELO3C009367; MELO3C004087; MELO3C003441; MELO3C024704; MELO3C005245; MELO3C021686; MELO3C004941; MELO3C018292; MELO3C026945; MELO3C001951; MELO3C026755; MELO3C017482; MELO3C021685; MELO3C018033; MELO3C011706; MELO3C017476; MELO3C018785; MELO3C017479
GO 0004090	carbonyl reductase (NADPH) activity	MOLECULAR_FUNCTION	0,463366121	0,018195262	2	4	625	16497	MELO3C002872; MELO3C001948	MELO3C019918; MELO3C014897; MELO3C021704; MELO3C020605
GO 0009331	glycerol-3-phosphate dehydrogenase complex	CELLULAR_COMPONENT	0,463366121	0,018195262	2	4	625	16497	MELO3C021604; MELO3C019820	MELO3C026337; MELO3C020158; MELO3C020157; MELO3C005116
GO 0009629	response to gravity	BIOLOGICAL_PROCESS	0,483810141	0,019151672	3	13	624	16488	MELO3C005293; MELO3C008847; MELO3C025282	MELO3C008088; MELO3C005396; MELO3C002781; MELO3C002354; MELO3C000009; MELO3C021982; MELO3C025310; MELO3C017043; MELO3C004827; MELO3C024155; MELO3C026110; MELO3C013815; MELO3C017414
GO 0004022	alcohol dehydrogenase (NAD) activity	MOLECULAR_FUNCTION	0,483810141	0,019151672	3	13	624	16488	MELO3C023685; MELO3C026554; MELO3C022399	MELO3C014897; MELO3C005792; MELO3C011043; MELO3C005482; MELO3C003251; MELO3C005521; MELO3C008767; MELO3C007314; MELO3C002189; MELO3C005129; MELO3C004714; MELO3C026553; MELO3C027151
GO 0004497	monooxygenase activity	MOLECULAR_FUNCTION	0,49629696	0,020391656	3	265	624	16236	MELO3C016879; MELO3C024396; MELO3C015590	MELO3C016329; MELO3C018628; MELO3C014027; MELO3C012088; MELO3C002043; MELO3C021118; MELO3C013050; MELO3C000537; MELO3C007856; MELO3C000655; MELO3C002720; MELO3C026802; MELO3C003933; MELO3C003932; MELO3C023530; MELO3C023533; MELO3C003934; MELO3C015591; MELO3C026487; MELO3C015592; MELO3C015593; MELO3C015595; MELO3C015596; MELO3C026484; MELO3C016685; MELO3C018623; MELO3C011799;
GO 0046658	anchored component of plasma membrane	CELLULAR_COMPONENT	0,49629696	0,020424758	4	25	623	16476	MELO3C021119; MELO3C017242; MELO3C024192; MELO3C010601	MELO3C002461; MELO3C005751; MELO3C020643; MELO3C022861; MELO3C003659; MELO3C018862; MELO3C014428; MELO3C018888; MELO3C010006; MELO3C013347; MELO3C011860; MELO3C005561; MELO3C013101; MELO3C005361; MELO3C013264; MELO3C012392; MELO3C020855; MELO3C024938; MELO3C006813; MELO3C004636; MELO3C025700; MELO3C002219; MELO3C018774; MELO3C012714; MELO3C016635

GO 0019083	viral transcription	BIOLOGICAL_PROCESS	0,526860835	0,022082651	6	54	621	16447	MELO3C023201; MELO3C017993; MELO3C009338; MELO3C005421; MELO3C024352; MELO3C017291	MELO3C010981; MELO3C016968; MELO3C008106; MELO3C021758; MELO3C008589; MELO3C008105; MELO3C002888; MELO3C022087; MELO3C020022; MELO3C017775; MELO3C017579; MELO3C015712; MELO3C014237; MELO3C014358; MELO3C008157; MELO3C002173; MELO3C014155; MELO3C003222; MELO3C020474; MELO3C017184; MELO3C026776; MELO3C003707; MELO3C018512; MELO3C009890; MELO3C015937; MELO3C006662; MELO3C005694;
GO 1903050	regulation of proteolysis involved in cellular protein catabolic process	BIOLOGICAL_PROCESS	0,554297243	0,023649485	5	40	622	16461	MELO3C011193; MELO3C016083; MELO3C010960; MELO3C016262; MELO3C012361	MELO3C013750; MELO3C014684; MELO3C002481; MELO3C004484; MELO3C014086; MELO3C022725; MELO3C025417; MELO3C005733; MELO3C025413; MELO3C023476; MELO3C025755; MELO3C024685; MELO3C026800; MELO3C005615; MELO3C005912; MELO3C024402; MELO3C025232; MELO3C016464; MELO3C026580; MELO3C012407; MELO3C013814; MELO3C017338; MELO3C013359; MELO3C011345; MELO3C011983; MELO3C014573; MELO3C021746;
GO 0051287	NAD binding	MOLECULAR_FUNCTION	0,554297243	0,023760625	6	55	621	16446	MELO3C010427; MELO3C021563; MELO3C021604; MELO3C019633; MELO3C010727; MELO3C008219	MELO3C006085; MELO3C021919; MELO3C011431; MELO3C006164; MELO3C014221; MELO3C009956; MELO3C024942; MELO3C005116; MELO3C023217; MELO3C017213; MELO3C025076; MELO3C025791; MELO3C027054; MELO3C017853; MELO3C015407; MELO3C014752; MELO3C022537; MELO3C022538; MELO3C020158; MELO3C020157; MELO3C026337; MELO3C024039; MELO3C002813; MELO3C027223; MELO3C013505; MELO3C011129; MELO3C019405;
GO 0006123	mitochondrial electron transport, cytochrome c to oxygen	BIOLOGICAL_PROCESS	0,561936534	0,02486129	2	5	625	16496	MELO3C004105; MELO3C011044	MELO3C015922; MELO3C003366; MELO3C016120; MELO3C018157; MELO3C006242
GO 0032012	regulation of ARF protein signal transduction	BIOLOGICAL_PROCESS	0,561936534	0,02486129	2	5	625	16496	MELO3C004551; MELO3C006224	MELO3C023883; MELO3C012923; MELO3C012924; MELO3C006181; MELO3C015692
GO 0005086	ARF guanyl-nucleotide exchange factor activity	MOLECULAR_FUNCTION	0,561936534	0,02486129	2	5	625	16496	MELO3C004551; MELO3C006224	MELO3C023883; MELO3C012923; MELO3C012924; MELO3C006181; MELO3C015692
GO 0005751	mitochondrial respiratory chain complex IV	CELLULAR_COMPONENT	0,561936534	0,02486129	2	5	625	16496	MELO3C004105; MELO3C011044	MELO3C015922; MELO3C003366; MELO3C016926; MELO3C014946; MELO3C016120
GO 0043601	nuclear replisome	CELLULAR_COMPONENT	0,561936534	0,02486129	2	5	625	16496	MELO3C020001; MELO3C020860	MELO3C022319; MELO3C017228; MELO3C027184; MELO3C024596; MELO3C001937
GO 0033179	proton-transporting V-type ATPase, V0 domain	CELLULAR_COMPONENT	0,561936534	0,02486129	2	5	625	16496	MELO3C000065; MELO3C010991	MELO3C010992; MELO3C009887; MELO3C013122; MELO3C011225; MELO3C003677

GO 0005960	glycine cleavage complex	CELLULAR_COMPONENT	0,561936534	0,02486129	2	5	625	16496	MELO3C021247; MELO3C021742	MELO3C003386; MELO3C003734; MELO3C002444; MELO3C006734; MELO3C010754
GO 0008237	metallopeptidase activity	MOLECULAR_FUNCTION	0,569490972	0,025353183	10	114	617	16387	MELO3C012356; MELO3C008052; MELO3C009148; MELO3C018441; MELO3C016890; MELO3C016067; MELO3C011193; MELO3C004134; MELO3C006846; MELO3C008847	MELO3C006089; MELO3C014386; MELO3C003139; MELO3C022843; MELO3C019273; MELO3C017011; MELO3C026003; MELO3C010623; MELO3C016738; MELO3C000768; MELO3C005965; MELO3C026539; MELO3C023149; MELO3C005688; MELO3C015483; MELO3C004918; MELO3C023023; MELO3C004919; MELO3C013276; MELO3C014882; MELO3C003474; MELO3C006466; MELO3C025899; MELO3C026225; MELO3C000673; MELO3C004605; MELO3C026224;
GO 0005351	sugar proton symporter activity	MOLECULAR_FUNCTION	0,571343664	0,025761262	5	41	622	16460	MELO3C013489; MELO3C011675; MELO3C025345; MELO3C026522; MELO3C004576	MELO3C008582; MELO3C008581; MELO3C014485; MELO3C020608; MELO3C000836; MELO3C003830; MELO3C024689; MELO3C000832; MELO3C007756; MELO3C018040; MELO3C019030; MELO3C007815; MELO3C021377; MELO3C017055; MELO3C015350; MELO3C009081; MELO3C010946; MELO3C017699; MELO3C017655; MELO3C000070; MELO3C017656; MELO3C013415; MELO3C011676; MELO3C012554; MELO3C006595; MELO3C013485; MELO3C007980;
GO 0042817	pyridoxal metabolic process	BIOLOGICAL_PROCESS	0,583238357	0,036606726	1	0	626	16501	MELO3C003541	
GO 0048482	plant ovule morphogenesis	BIOLOGICAL_PROCESS	0,583238357	0,036606726	1	0	626	16501	MELO3C010913	
GO 0015680	intracellular copper ion transport	BIOLOGICAL_PROCESS	0,583238357	0,036606726	1	0	626	16501	MELO3C014007	
GO 0046087	cytidine metabolic process	BIOLOGICAL_PROCESS	0,583238357	0,036606726	1	0	626	16501	MELO3C015459	
GO 0006898	receptor-mediated endocytosis	BIOLOGICAL_PROCESS	0,583238357	0,0330493S	10	125	617	16376	MELO3C010243; MELO3C002118; MELO3C008285; MELO3C002717; MELO3C003905; MELO3C009338; MELO3C025549; MELO3C026614; MELO3C013822; MELO3C018758	MELO3C011795; MELO3C016968; MELO3C006760; MELO3C011151; MELO3C006121; MELO3C002045; MELO3C008306; MELO3C022166; MELO3C026888; MELO3C025310; MELO3C015235; MELO3C015512; MELO3C021808; MELO3C017707; MELO3C013982; MELO3C008151; MELO3C020836; MELO3C004074; MELO3C014153; MELO3C023545; MELO3C005963; MELO3C023306; MELO3C023427; MELO3C006657; MELO3C017020; MELO3C007903; MELO3C016297;
GO 0006616	SRP-dependent cotranslational protein targeting to membrane, translocation	BIOLOGICAL_PROCESS	0,583238357	0,036606726	1	0	626	16501	MELO3C005757	
GO 0030950	establishment or maintenance of actin cytoskeleton polarity	BIOLOGICAL_PROCESS	0,583238357	0,036606726	1	0	626	16501	MELO3C026614	
GO 0046292	formaldehyde metabolic process	BIOLOGICAL_PROCESS	0,583238357	0,036606726	1	0	626	16501	MELO3C022399	
GO 0010812	negative regulation of cell-substrate adhesion	BIOLOGICAL_PROCESS	0,583238357	0,036606726	1	0	626	16501	MELO3C022488	

GO 0007409	axonogenesis	BIOLOGICAL_PROCESS	0,583238357	0,030460745	7	75	620	16426	MELO3C007673; MELO3C012361; MELO3C018841; MELO3C011193; MELO3C002609; MELO3C009624; MELO3C020978	MELO3C006283; MELO3C003092; MELO3C011354; MELO3C014785; MELO3C014383; MELO3C007015; MELO3C022407; MELO3C002124; MELO3C022842; MELO3C021633; MELO3C008306; MELO3C023852; MELO3C024269; MELO3C018025; MELO3C019315; MELO3C025790; MELO3C013739; MELO3C017734; MELO3C012526; MELO3C004594; MELO3C003341; MELO3C022219; MELO3C005123; MELO3C020439; MELO3C004635; MELO3C021683; MELO3C026613;
GO 0006420	arginyl-tRNA aminoacylation	BIOLOGICAL_PROCESS	0,583238357	0,036606726	1	0	626	16501	MELO3C015422	
GO 0006121	mitochondrial electron transport, succinate to ubiquinone	BIOLOGICAL_PROCESS	0,583238357	0,036606726	1	0	626	16501	MELO3C017560	
GO 0006127	glycerophosphate shuttle	BIOLOGICAL_PROCESS	0,583238357	0,036606726	1	0	626	16501	MELO3C019820	
GO 0019563	glycerol catabolic process	BIOLOGICAL_PROCESS	0,583238357	0,036606726	1	0	626	16501	MELO3C019820	
GO 0008643	carbohydrate transport	BIOLOGICAL_PROCESS	0,583238357	0,027238541	8	90	619	16411	MELO3C013489; MELO3C025345; MELO3C026522; MELO3C012076; MELO3C013591; MELO3C007325; MELO3C004576; MELO3C004533	MELO3C008582; MELO3C008581; MELO3C004222; MELO3C005631; MELO3C021558; MELO3C011150; MELO3C007818; MELO3C016280; MELO3C022166; MELO3C019030; MELO3C002966; MELO3C007815; MELO3C015350; MELO3C026441; MELO3C027013; MELO3C010946; MELO3C017655; MELO3C010269; MELO3C017656; MELO3C011115; MELO3C011875; MELO3C008674; MELO3C004591; MELO3C007980; MELO3C013186; MELO3C009724; MELO3C004111;
GO 0007310	oocyte dorsal/ventral axis specification	BIOLOGICAL_PROCESS	0,583238357	0,036606726	1	0	626	16501	MELO3C011193	
GO 0006470	protein dephosphorylation	BIOLOGICAL_PROCESS	0,583238357	0,027068299	7	73	620	16428	MELO3C004439; MELO3C012378; MELO3C021385; MELO3C007580; MELO3C011704; MELO3C006736; MELO3C013745	MELO3C020829; MELO3C013336; MELO3C018507; MELO3C008426; MELO3C004587; MELO3C003574; MELO3C024667; MELO3C002645; MELO3C026602; MELO3C023893; MELO3C026166; MELO3C018500; MELO3C011713; MELO3C026163; MELO3C010744; MELO3C009960; MELO3C015408; MELO3C013860; MELO3C016939; MELO3C009840; MELO3C006852; MELO3C021405; MELO3C023626; MELO3C007940; MELO3C020114; MELO3C003222; MELO3C008478;
GO 0008347	glial cell migration	BIOLOGICAL_PROCESS	0,583238357	0,036606726	1	0	626	16501	MELO3C011193	
GO 0031115	negative regulation of microtubule polymerization	BIOLOGICAL_PROCESS	0,583238357	0,036606726	1	0	626	16501	MELO3C022488	
GO 0042149	cellular response to glucose starvation	BIOLOGICAL_PROCESS	0,583238357	0,036606726	1	0	626	16501	MELO3C005757	
GO 0007229	integrin-mediated signaling pathway	BIOLOGICAL_PROCESS	0,583238357	0,036606726	1	0	626	16501	MELO3C007690	

GO 0040035	hermaphrodite genitalia development	BIOLOGICAL_PROCESS	0,583238357	0,035053154	10	127	617	16374	MELO3C011256; MELO3C008285; MELO3C019253; MELO3C022488; MELO3C016707; MELO3C012361; MELO3C002717; MELO3C011193; MELO3C022094; MELO3C026614	MELO3C009592; MELO3C006760; MELO3C006121; MELO3C004344; MELO3C019031; MELO3C022166; MELO3C024586; MELO3C026888; MELO3C016321; MELO3C014708; MELO3C015235; MELO3C019956; MELO3C021808; MELO3C015647; MELO3C008151; MELO3C008157; MELO3C002173; MELO3C000924; MELO3C006498; MELO3C004873; MELO3C007466; MELO3C008835; MELO3C023823; MELO3C023427; MELO3C006657; MELO3C024757; MELO3C007903;
GO 0006084	acetyl-CoA metabolic process	BIOLOGICAL_PROCESS	0,583238357	0,030564468	3	16	624	16485	MELO3C021247; MELO3C011482; MELO3C004278	MELO3C013864; MELO3C012235; MELO3C014017; MELO3C006661; MELO3C003131; MELO3C025919; MELO3C014031; MELO3C007940; MELO3C003445; MELO3C021268; MELO3C013081; MELO3C006734; MELO3C022343; MELO3C006529; MELO3C019872; MELO3C015245
GO 0046827	positive regulation of protein export from nucleus	BIOLOGICAL_PROCESS	0,583238357	0,036606726	1	0	626	16501	MELO3C007207	
GO 0010342	endosperm cellularization	BIOLOGICAL_PROCESS	0,583238357	0,036606726	1	0	626	16501	MELO3C006602	
GO 0060904	regulation of protein folding in endoplasmic reticulum	BIOLOGICAL_PROCESS	0,583238357	0,036606726	1	0	626	16501	MELO3C005757	
GO 0010312	detoxification of zinc ion	BIOLOGICAL_PROCESS	0,583238357	0,036606726	1	0	626	16501	MELO3C022448	
GO 0048759	xylem vessel member cell differentiation	BIOLOGICAL_PROCESS	0,583238357	0,036606726	1	0	626	16501	MELO3C011484	
GO 0001556	oocyte maturation	BIOLOGICAL_PROCESS	0,583238357	0,036606726	1	0	626	16501	MELO3C012361	
GO 0034333	adherens junction assembly	BIOLOGICAL_PROCESS	0,583238357	0,036606726	1	0	626	16501	MELO3C022488	
GO 0010266	response to vitamin B1	BIOLOGICAL_PROCESS	0,583238357	0,036606726	1	0	626	16501	MELO3C020562	
GO 0043154	negative regulation of cysteine-type endopeptidase activity involved in apoptotic process	BIOLOGICAL_PROCESS	0,583238357	0,036606726	1	0	626	16501	MELO3C005757	
GO 0010299	detoxification of cobalt ion	BIOLOGICAL_PROCESS	0,583238357	0,036606726	1	0	626	16501	MELO3C022448	
GO 0048730	epidermis morphogenesis	BIOLOGICAL_PROCESS	0,583238357	0,036606726	1	0	626	16501	MELO3C006929	
GO 0015966	diadenosine tetraphosphate biosynthetic process	BIOLOGICAL_PROCESS	0,583238357	0,036606726	1	0	626	16501	MELO3C003905	
GO 0034484	raffinose catabolic process	BIOLOGICAL_PROCESS	0,583238357	0,036606726	1	0	626	16501	MELO3C023110	
GO 0004301	epoxide hydrolase activity	MOLECULAR_FUNCTION	0,583238357	0,036606726	1	0	626	16501	MELO3C017946	
GO 0030942	endoplasmic reticulum signal peptide binding	MOLECULAR_FUNCTION	0,583238357	0,036606726	1	0	626	16501	MELO3C002757	
GO 0050311	sulfite reductase (ferredoxin) activity	MOLECULAR_FUNCTION	0,583238357	0,036606726	1	0	626	16501	MELO3C015186	
GO 0016532	superoxide dismutase copper chaperone activity	MOLECULAR_FUNCTION	0,583238357	0,036606726	1	0	626	16501	MELO3C014007	
GO 0050201	fucokinase activity	MOLECULAR_FUNCTION	0,583238357	0,036606726	1	0	626	16501	MELO3C006005	
GO 0008908	isochorismatase activity	MOLECULAR_FUNCTION	0,583238357	0,036606726	1	0	626	16501	MELO3C011747	
GO 0004637	phosphoribosylamine-glycine ligase activity	MOLECULAR_FUNCTION	0,583238357	0,036606726	1	0	626	16501	MELO3C016483	
GO 0052636	arabinosyltransferase activity	MOLECULAR_FUNCTION	0,583238357	0,036606726	1	0	626	16501	MELO3C010524	
GO 0035259	glucocorticoid receptor binding	MOLECULAR_FUNCTION	0,583238357	0,036606726	1	0	626	16501	MELO3C012231	
GO 0016859	cis-trans isomerase activity	MOLECULAR_FUNCTION	0,583238357	0,03131995	6	59	621	16442	MELO3C014557; MELO3C021108; MELO3C025848; MELO3C023224; MELO3C020806; MELO3C007001	MELO3C011036; MELO3C012489; MELO3C013896; MELO3C017816; MELO3C010261; MELO3C013375; MELO3C015916; MELO3C006285; MELO3C008222; MELO3C021912; MELO3C009952; MELO3C002126; MELO3C007778; MELO3C026524; MELO3C003338; MELO3C019631; MELO3C024662; MELO3C017776; MELO3C025192; MELO3C016887; MELO3C011236; MELO3C008553; MELO3C006176; MELO3C004752; MELO3C022335; MELO3C023984; MELO3C016495;
GO 0050347	trans-octaprenyltranstransferase activity	MOLECULAR_FUNCTION	0,583238357	0,036606726	1	0	626	16501	MELO3C016140	
GO 0019706	protein-cysteine S-palmitoyltransferase activity	MOLECULAR_FUNCTION	0,583238357	0,036606726	1	0	626	16501	MELO3C010243	
GO 0047115	trans-1,2-dihydrobenzene-1,2-diol dehydrogenase activity	MOLECULAR_FUNCTION	0,583238357	0,036606726	1	0	626	16501	MELO3C019948	

GO 0005319	lipid transporter activity	MOLECULAR_FUNCTION	0,583238357	0,031398208	4	29	623	16472	MELO3C006409; MELO3C015704; MELO3C012196; MELO3C020394	MELO3C016505; MELO3C012044; MELO3C011330; MELO3C002064; MELO3C014000; MELO3C020821; MELO3C002065; MELO3C008403; MELO3C002188; MELO3C021055; MELO3C023696; MELO3C025675; MELO3C000372; MELO3C011559; MELO3C012726; MELO3C012236; MELO3C000868; MELO3C022654; MELO3C024378; MELO3C025304; MELO3C025224; MELO3C017660; MELO3C018077; MELO3C017661; MELO3C019921; MELO3C018710; MELO3C017027;
GO 0005302	L-tyrosine transmembrane transporter activity	MOLECULAR_FUNCTION	0,583238357	0,036606726	1	0	626	16501	MELO3C006926	
GO 0004334	fumarylacetoacetase activity	MOLECULAR_FUNCTION	0,583238357	0,036606726	1	0	626	16501	MELO3C007433	
GO 0005354	galactose transmembrane transporter activity	MOLECULAR_FUNCTION	0,583238357	0,036606726	1	0	626	16501	MELO3C004576	
GO 0052591	sn-glycerol-3-phosphate ubiquinone-8 oxidoreductase activity	MOLECULAR_FUNCTION	0,583238357	0,036606726	1	0	626	16501	MELO3C019820	
GO 0005125	cytokine activity	MOLECULAR_FUNCTION	0,583238357	0,036606726	1	0	626	16501	MELO3C011104	
GO 0051499	D-aminoacyl-tRNA deacylase activity	MOLECULAR_FUNCTION	0,583238357	0,036606726	1	0	626	16501	MELO3C011402	
GO 0016002	sulfite reductase activity	MOLECULAR_FUNCTION	0,583238357	0,036606726	1	0	626	16501	MELO3C015186	
GO 0004364	glutathione transferase activity	MOLECULAR_FUNCTION	0,583238357	0,030564468	3	16	624	16485	MELO3C016031; MELO3C016033; MELO3C023224	MELO3C011334; MELO3C009300; MELO3C009299; MELO3C020204; MELO3C022821; MELO3C017341; MELO3C001978; MELO3C016032; MELO3C016166; MELO3C016034; MELO3C023220; MELO3C016167; MELO3C016168; MELO3C016169; MELO3C011714; MELO3C016349
GO 0004126	cytidine deaminase activity	MOLECULAR_FUNCTION	0,583238357	0,036606726	1	0	626	16501	MELO3C015459	
GO 0004369	glycerol-3-phosphate oxidase activity	MOLECULAR_FUNCTION	0,583238357	0,036606726	1	0	626	16501	MELO3C019820	
GO 0005153	interleukin-8 receptor binding	MOLECULAR_FUNCTION	0,583238357	0,036606726	1	0	626	16501	MELO3C005679	
GO 0015088	copper uptake transmembrane transporter activity	MOLECULAR_FUNCTION	0,583238357	0,036606726	1	0	626	16501	MELO3C018494	
GO 0004073	aspartate-semialdehyde dehydrogenase activity	MOLECULAR_FUNCTION	0,583238357	0,036606726	1	0	626	16501	MELO3C010427	
GO 0030331	estrogen receptor binding	MOLECULAR_FUNCTION	0,583238357	0,036606726	1	0	626	16501	MELO3C012231	
GO 0004177	aminopeptidase activity	MOLECULAR_FUNCTION	0,583238357	0,028388178	4	28	623	16473	MELO3C012356; MELO3C004134; MELO3C009148; MELO3C016890	MELO3C005470; MELO3C023479; MELO3C006206; MELO3C026225; MELO3C023478; MELO3C026003; MELO3C026224; MELO3C015673; MELO3C012427; MELO3C004172; MELO3C001380; MELO3C002074; MELO3C006077; MELO3C004255; MELO3C013085; MELO3C004135; MELO3C000768; MELO3C020895; MELO3C020334; MELO3C005688; MELO3C007807; MELO3C016891; MELO3C023023; MELO3C018038; MELO3C016894; MELO3C016895; MELO3C023481;
GO 0008893	guanosine-3',5'-bis(diphosphate) 3'-diphosphatase activity	MOLECULAR_FUNCTION	0,583238357	0,036606726	1	0	626	16501	MELO3C006759	
GO 0030797	24-methylenesterol C-methyltransferase activity	MOLECULAR_FUNCTION	0,583238357	0,036606726	1	0	626	16501	MELO3C003726	
GO 0047705	bilirubin oxidase activity	MOLECULAR_FUNCTION	0,583238357	0,036606726	1	0	626	16501	MELO3C005201	
GO 0032442	phenylcoumaran benzylic ether reductase activity	MOLECULAR_FUNCTION	0,583238357	0,036606726	1	0	626	16501	MELO3C023304	
GO 0047837	D-xylose 1-dehydrogenase (NADP+) activity	MOLECULAR_FUNCTION	0,583238357	0,036606726	1	0	626	16501	MELO3C019948	
GO 0034618	arginine binding	MOLECULAR_FUNCTION	0,583238357	0,036606726	1	0	626	16501	MELO3C011208	

GO 0043565	sequence-specific DNA binding	MOLECULAR_FUNCTION	0,583238357	0,036287843	5	324	622	16177	MELO3C025282; MELO3C011167; MELO3C010057; MELO3C007181; MELO3C024192	MELO3C011432; MELO3C010223; MELO3C011550; MELO3C005791; MELO3C014384; MELO3C024507; MELO3C008942; MELO3C013173; MELO3C022209; MELO3C001991; MELO3C025714; MELO3C007736; MELO3C006887; MELO3C022205; MELO3C002723; MELO3C025951; MELO3C020145; MELO3C018187; MELO3C017415; MELO3C019715; MELO3C023092; MELO3C011797; MELO3C015239; MELO3C017429; MELO3C003140; MELO3C002050; MELO3C006891;
GO 0003841	1-acylglycerol-3-phosphate O-acyltransferase activity	MOLECULAR_FUNCTION	0,583238357	0,032354424	2	6	625	16495	MELO3C009663; MELO3C008959	MELO3C014054; MELO3C025383; MELO3C010918; MELO3C014475; MELO3C009182; MELO3C012571
GO 0004814	arginine-tRNA ligase activity	MOLECULAR_FUNCTION	0,583238357	0,036606726	1	0	626	16501	MELO3C015422	
GO 0003977	UDP-N-acetylglucosamine diphosphorylase activity	MOLECULAR_FUNCTION	0,583238357	0,036606726	1	0	626	16501	MELO3C007022	
GO 0080007	S-nitrosoglutathione reductase activity	MOLECULAR_FUNCTION	0,583238357	0,036606726	1	0	626	16501	MELO3C022399	
GO 0010487	thermospermine synthase activity	MOLECULAR_FUNCTION	0,583238357	0,036606726	1	0	626	16501	MELO3C011484	
GO 0034020	neoxanthin synthase activity	MOLECULAR_FUNCTION	0,583238357	0,036606726	1	0	626	16501	MELO3C017963	
GO 0000026	alpha-1,2-mannosyltransferase activity	MOLECULAR_FUNCTION	0,583238357	0,036606726	1	0	626	16501	MELO3C025637	
GO 0016830	carbon-carbon lyase activity	MOLECULAR_FUNCTION	0,583238357	0,035904578	0	110	627	16391		MELO3C018628; MELO3C013057; MELO3C003491; MELO3C003259; MELO3C026007; MELO3C022321; MELO3C018340; MELO3C026005; MELO3C002329; MELO3C026006; MELO3C026004; MELO3C024189; MELO3C000130; MELO3C015998; MELO3C014547; MELO3C004110; MELO3C012252; MELO3C007227; MELO3C024519; MELO3C023787; MELO3C019050; MELO3C025446; MELO3C023786; MELO3C000483; MELO3C018994; MELO3C006580; MELO3C010162;
GO 0010297	heteropolysaccharide binding	MOLECULAR_FUNCTION	0,583238357	0,036606726	1	0	626	16501	MELO3C019135	
GO 0005875	microtubule associated complex	CELLULAR_COMPONENT	0,583238357	0,033428346	6	60	621	16441	MELO3C011256; MELO3C022094; MELO3C013429; MELO3C005757; MELO3C010631; MELO3C023342	MELO3C005594; MELO3C006121; MELO3C009957; MELO3C024627; MELO3C021317; MELO3C004268; MELO3C008589; MELO3C003774; MELO3C026888; MELO3C026800; MELO3C018185; MELO3C025310; MELO3C010507; MELO3C015199; MELO3C017338; MELO3C012723; MELO3C009841; MELO3C005122; MELO3C014153; MELO3C005289; MELO3C025923; MELO3C022897; MELO3C022898; MELO3C007668; MELO3C017141; MELO3C004518; MELO3C007903;
GO 0034099	luminal surveillance complex	CELLULAR_COMPONENT	0,583238357	0,036606726	1	0	626	16501	MELO3C005757	
GO 0009842	cyanelle	CELLULAR_COMPONENT	0,583238357	0,036606726	1	0	626	16501	MELO3C016140	
GO 0009930	longitudinal side of cell surface	CELLULAR_COMPONENT	0,583238357	0,036606726	1	0	626	16501	MELO3C017242	
GO 0042555	MCM complex	CELLULAR_COMPONENT	0,583238357	0,036606726	1	0	626	16501	MELO3C020001	
GO 0008305	integrin complex	CELLULAR_COMPONENT	0,583238357	0,036606726	1	0	626	16501	MELO3C007690	
GO 0031672	A band	CELLULAR_COMPONENT	0,583238357	0,036606726	1	0	626	16501	MELO3C011193	

GO 0009526	plastid envelope	CELLULAR_COMPONENT	0,583238357	0,028872683	21	328	606	16173	MELO3C005293; MELO3C015704; MELO3C008052; MELO3C011284; MELO3C006344; MELO3C002785; MELO3C006943; MELO3C020780; MELO3C023222; MELO3C018494; MELO3C015590; MELO3C008959; MELO3C018573; MELO3C020001; MELO3C010727; MELO3C019026; MELO3C015186; MELO3C015594; MELO3C019871; MELO3C009171; MELO3C011104	MELO3C011311; MELO3C009474; MELO3C014389; MELO3C003373; MELO3C006088; MELO3C007298; MELO3C006523; MELO3C004223; MELO3C005432; MELO3C001992; MELO3C026802; MELO3C003811; MELO3C001998; MELO3C015591; MELO3C015592; MELO3C025036; MELO3C022680; MELO3C015593; MELO3C017772; MELO3C015595; MELO3C017774; MELO3C010229; MELO3C015596; MELO3C026000; MELO3C009480; MELO3C006094; MELO3C004471;
GO 0031429	box H/ACA snoRNP complex	CELLULAR_COMPONENT	0,583238357	0,036606726	1	0	626	16501	MELO3C008801	
GO 0018444	translation release factor complex	CELLULAR_COMPONENT	0,583238357	0,036606726	1	0	626	16501	MELO3C002118	
GO 0009316	3-isopropylmalate dehydratase complex	CELLULAR_COMPONENT	0,583238357	0,036606726	1	0	626	16501	MELO3C005518	
GO 0042175	nuclear outer membrane-endoplasmic reticulum membrane network	CELLULAR_COMPONENT	0,583238357	0,03313727	13	182	614	16319	MELO3C010960; MELO3C016706; MELO3C010794; MELO3C009663; MELO3C007931; MELO3C021108; MELO3C025637; MELO3C005757; MELO3C005405; MELO3C006926; MELO3C020541; MELO3C005918; MELO3C013822	MELO3C017815; MELO3C009197; MELO3C006089; MELO3C009630; MELO3C020821; MELO3C002165; MELO3C002166; MELO3C006007; MELO3C021634; MELO3C026524; MELO3C022166; MELO3C026800; MELO3C022321; MELO3C018461; MELO3C025156; MELO3C018066; MELO3C019034; MELO3C017413; MELO3C015597; MELO3C012527; MELO3C017019; MELO3C025390; MELO3C010621; MELO3C008270; MELO3C014306; MELO3C015756; MELO3C016219;
GO 0034663	endoplasmic reticulum chaperone complex	CELLULAR_COMPONENT	0,583238357	0,036606726	1	0	626	16501	MELO3C005757	
GO 0045263	proton-transporting ATP synthase complex, coupling factor F(o)	CELLULAR_COMPONENT	0,583238357	0,035005647	3	17	624	16484	MELO3C012445; MELO3C000065; MELO3C010991	MELO3C010992; MELO3C000827; MELO3C007468; MELO3C022944; MELO3C001387; MELO3C000965; MELO3C001566; MELO3C000995; MELO3C002745; MELO3C003769; MELO3C004618; MELO3C015443; MELO3C027395; MELO3C027032; MELO3C027031; MELO3C011269; MELO3C013404
GO 0045271	respiratory chain complex I	CELLULAR_COMPONENT	0,583238357	0,028388178	4	28	623	16473	MELO3C005389; MELO3C006949; MELO3C013951; MELO3C017960	MELO3C012488; MELO3C012522; MELO3C012486; MELO3C002086; MELO3C024729; MELO3C026725; MELO3C022540; MELO3C023357; MELO3C025258; MELO3C017010; MELO3C019212; MELO3C016861; MELO3C010701; MELO3C022919; MELO3C014894; MELO3C009702; MELO3C000924; MELO3C009644; MELO3C006999; MELO3C025525; MELO3C026758; MELO3C023322; MELO3C020331; MELO3C022394; MELO3C025540; MELO3C017388; MELO3C023063;
GO 0010005	cortical microtubule, transverse to long axis	CELLULAR_COMPONENT	0,583238357	0,036606726	1	0	626	16501	MELO3C012361	
GO 0033162	melanosome membrane	CELLULAR_COMPONENT	0,583238357	0,036606726	1	0	626	16501	MELO3C006926	
GO 0005923	bicellular tight junction	CELLULAR_COMPONENT	0,583238357	0,036606726	1	0	626	16501	MELO3C022488	

GO 0009570	chloroplast stroma	CELLULAR_COMPONENT	0,595676803	0,037450468	22	361	605	16140	MELO3C018948; MELO3C012378; MELO3C005293; MELO3C012410; MELO3C009038; MELO3C011284; MELO3C005147; MELO3C003344; MELO3C009429; MELO3C008879; MELO3C020780; MELO3C020562; MELO3C018573; MELO3C010727; MELO3C016033; MELO3C015186; MELO3C010427; MELO3C018455; MELO3C014749; MELO3C011208; MELO3C010686; MELO3C011104	MELO3C013732; MELO3C021919; MELO3C012764; MELO3C002161; MELO3C008146; MELO3C006088; MELO3C009475; MELO3C013172; MELO3C004223; MELO3C005674; MELO3C003137; MELO3C001992; MELO3C008946; MELO3C003811; MELO3C001998; MELO3C003814; MELO3C021355; MELO3C016680; MELO3C016681; MELO3C017890; MELO3C024189; MELO3C015231; MELO3C025397; MELO3C019036; MELO3C017774; MELO3C015233; MELO3C011439;
GO 2001141	regulation of RNA biosynthetic process	BIOLOGICAL_PROCESS	0,596654655	0,037575097	41	1472	586	15029	MELO3C011256; MELO3C014722; MELO3C007691; MELO3C012242; MELO3C011110; MELO3C009653; MELO3C020848; MELO3C020701; MELO3C011172; MELO3C008847; MELO3C002644; MELO3C016083; MELO3C023412; MELO3C020860; MELO3C016660; MELO3C011759; MELO3C023195; MELO3C007181; MELO3C016623; MELO3C009188; MELO3C011003; MELO3C007340; MELO3C011167; MELO3C010057; MELO3C002292; MELO3C006870; MELO3C012231;	MELO3C014029; MELO3C007971; MELO3C005791; MELO3C003372; MELO3C014263; MELO3C007974; MELO3C013173; MELO3C014261; MELO3C007736; MELO3C012081; MELO3C006887; MELO3C002049; MELO3C026008; MELO3C000099; MELO3C010904; MELO3C010906; MELO3C010905; MELO3C019712; MELO3C016202; MELO3C016444; MELO3C015355; MELO3C025151; MELO3C017775; MELO3C019715; MELO3C017308; MELO3C021809; MELO3C003140;
GO 0000323	lytic vacuole	CELLULAR_COMPONENT	0,60175772	0,037960161	4	31	623	16470	MELO3C006926; MELO3C010243; MELO3C025061; MELO3C023569	MELO3C015218; MELO3C014920; MELO3C014821; MELO3C013676; MELO3C003291; MELO3C025752; MELO3C025972; MELO3C020442; MELO3C004827; MELO3C025355; MELO3C018764; MELO3C017653; MELO3C026440; MELO3C017414; MELO3C014458; MELO3C006034; MELO3C005243; MELO3C004353; MELO3C008897; MELO3C004477; MELO3C004874; MELO3C026977; MELO3C026898; MELO3C026415; MELO3C025645; MELO3C026971; MELO3C022495;
GO 2000243	positive regulation of reproductive process	BIOLOGICAL_PROCESS	0,611865368	0,039760302	3	18	624	16483	MELO3C016660; MELO3C012361; MELO3C011104	MELO3C011221; MELO3C011771; MELO3C011299; MELO3C002050; MELO3C006121; MELO3C014473; MELO3C004398; MELO3C007457; MELO3C006520; MELO3C022995; MELO3C019031; MELO3C004944; MELO3C024578; MELO3C022443; MELO3C018187; MELO3C025183; MELO3C026161; MELO3C014514
GO 0015780	nucleotide-sugar transport	BIOLOGICAL_PROCESS	0,611865368	0,040605375	2	7	625	16494	MELO3C011675; MELO3C004533	MELO3C010474; MELO3C013485; MELO3C013186; MELO3C020559; MELO3C011623; MELO3C011676; MELO3C007756
GO 0008615	pyridoxine biosynthetic process	BIOLOGICAL_PROCESS	0,611865368	0,040605375	2	7	625	16494	MELO3C011062; MELO3C003541	MELO3C020384; MELO3C013732; MELO3C025766; MELO3C009168; MELO3C006011; MELO3C024240; MELO3C025846

GO 0007023	post-chaperonin tubulin folding pathway	BIOLOGICAL_PROCESS	0,611865368	0,040605375	2	7	625	16494	MELO3C007673; MELO3C022488	MELO3C026613; MELO3C017607; MELO3C018025; MELO3C018532; MELO3C022478; MELO3C011830; MELO3C014723
GO 0009298	GDP-mannose biosynthetic process	BIOLOGICAL_PROCESS	0,611865368	0,040605375	2	7	625	16494	MELO3C003812; MELO3C023310	MELO3C006552; MELO3C024175; MELO3C020220; MELO3C017126; MELO3C026482; MELO3C021412; MELO3C005458
GO 0005544	calcium-dependent phospholipid binding	MOLECULAR_FUNCTION	0,611865368	0,040605375	2	7	625	16494	MELO3C019002; MELO3C012457	MELO3C012455; MELO3C012456; MELO3C018326; MELO3C015135; MELO3C026608; MELO3C018327; MELO3C018648
GO 0004365	glyceraldehyde-3-phosphate dehydrogenase (NAD+) (phosphorylating) activity	MOLECULAR_FUNCTION	0,611865368	0,040605375	2	7	625	16494	MELO3C008219; MELO3C019633	MELO3C012598; MELO3C012599; MELO3C014752; MELO3C017044; MELO3C002342; MELO3C002343; MELO3C024866
GO 0005199	structural constituent of cell wall	MOLECULAR_FUNCTION	0,611865368	0,040605375	2	7	625	16494	MELO3C022068; MELO3C025324	MELO3C027328; MELO3C006506; MELO3C021194; MELO3C004550; MELO3C007279; MELO3C021192; MELO3C018704
GO 0004723	calcium-dependent protein serine/threonine phosphatase activity	MOLECULAR_FUNCTION	0,611865368	0,040605375	2	7	625	16494	MELO3C017844; MELO3C013892	MELO3C023443; MELO3C019099; MELO3C014069; MELO3C026598; MELO3C018436; MELO3C022260; MELO3C007998
GO 0000139	Golgi membrane	CELLULAR_COMPONENT	0,611865368	0,040465342	9	108	618	16393	MELO3C010243; MELO3C011675; MELO3C001997; MELO3C010135; MELO3C019691; MELO3C019026; MELO3C006736; MELO3C004533; MELO3C026614	MELO3C017935; MELO3C009473; MELO3C017818; MELO3C004583; MELO3C011272; MELO3C008782; MELO3C020821; MELO3C007456; MELO3C020428; MELO3C021517; MELO3C024503; MELO3C024227; MELO3C009914; MELO3C005799; MELO3C021595; MELO3C019674; MELO3C021590; MELO3C018066; MELO3C021591; MELO3C027332; MELO3C013979; MELO3C008270; MELO3C011676; MELO3C015756; MELO3C018919; MELO3C007101; MELO3C004074;
GO 2000112	regulation of cellular macromolecule biosynthetic process	BIOLOGICAL_PROCESS	0,613024982	0,040747215	43	1527	584	14974	MELO3C011256; MELO3C014722; MELO3C007691; MELO3C012242; MELO3C011110; MELO3C009653; MELO3C020848; MELO3C020701; MELO3C011172; MELO3C008847; MELO3C002644; MELO3C016083; MELO3C023412; MELO3C020860; MELO3C016660; MELO3C011759; MELO3C023195; MELO3C007181; MELO3C016623; MELO3C009188; MELO3C011003; MELO3C007340; MELO3C011167; MELO3C010057; MELO3C002292; MELO3C006870; MELO3C012231;	MELO3C014029; MELO3C007971; MELO3C020705; MELO3C005791; MELO3C003372; MELO3C014263; MELO3C007974; MELO3C013173; MELO3C014261; MELO3C007736; MELO3C012081; MELO3C006887; MELO3C002049; MELO3C026008; MELO3C000099; MELO3C010904; MELO3C010906; MELO3C010905; MELO3C019712; MELO3C016202; MELO3C016444; MELO3C015355; MELO3C025151; MELO3C019715; MELO3C017308; MELO3C021809; MELO3C003140;

GO 0048199	vesicle targeting, to, from or within Golgi	BIOLOGICAL_PROCESS	0,619619031	0,041513426	4	32	623	16469	MELO3C004551; MELO3C021279; MELO3C024447; MELO3C009966	MELO3C013434; MELO3C006782; MELO3C023339; MELO3C021556; MELO3C009912; MELO3C023630; MELO3C020980; MELO3C025796; MELO3C024225; MELO3C026763; MELO3C018343; MELO3C012923; MELO3C012528; MELO3C019856; MELO3C010666; MELO3C007042; MELO3C009240; MELO3C004196; MELO3C007300; MELO3C009269; MELO3C012991; MELO3C007583; MELO3C015929; MELO3C005422; MELO3C005423; MELO3C009969; MELO3C023883;
GO 0005741	mitochondrial outer membrane	CELLULAR_COMPONENT	0,619619031	0,041513426	4	32	623	16469	MELO3C010745; MELO3C019820; MELO3C005405; MELO3C016067	MELO3C020808; MELO3C013775; MELO3C014885; MELO3C024929; MELO3C015839; MELO3C020905; MELO3C004681; MELO3C009893; MELO3C020821; MELO3C025739; MELO3C000215; MELO3C017471; MELO3C019213; MELO3C019776; MELO3C017676; MELO3C017019; MELO3C017439; MELO3C007542; MELO3C004273; MELO3C014531; MELO3C016818; MELO3C021943; MELO3C006378; MELO3C003464; MELO3C002035; MELO3C020973; MELO3C018052;
GO 0015035	protein disulfide oxidoreductase activity	MOLECULAR_FUNCTION	0,63535636	0,042769543	6	64	621	16437	MELO3C019722; MELO3C019326; MELO3C017902; MELO3C018455; MELO3C012410; MELO3C016056	MELO3C010860; MELO3C009478; MELO3C011352; MELO3C008421; MELO3C005790; MELO3C007253; MELO3C022405; MELO3C009556; MELO3C001994; MELO3C026569; MELO3C024468; MELO3C025752; MELO3C014909; MELO3C021350; MELO3C021351; MELO3C017411; MELO3C012969; MELO3C017410; MELO3C019913; MELO3C008750; MELO3C012053; MELO3C009882; MELO3C005763; MELO3C022339; MELO3C007026; MELO3C005206; MELO3C026855;
GO 0048316	seed development	BIOLOGICAL_PROCESS	0,646422686	0,043582901	10	134	617	16367	MELO3C007609; MELO3C003768; MELO3C022399; MELO3C008959; MELO3C022488; MELO3C020848; MELO3C012361; MELO3C010913; MELO3C015764; MELO3C016019	MELO3C006243; MELO3C021518; MELO3C007451; MELO3C003650; MELO3C006402; MELO3C008942; MELO3C022204; MELO3C005714; MELO3C006925; MELO3C005957; MELO3C025310; MELO3C021196; MELO3C011830; MELO3C012653; MELO3C005162; MELO3C015649; MELO3C006530; MELO3C002052; MELO3C014670; MELO3C003389; MELO3C004632; MELO3C006811; MELO3C026934; MELO3C024874; MELO3C002738; MELO3C017662; MELO3C019205;

GO 0032201	telomere maintenance via semi-conservative replication	BIOLOGICAL_PROCESS	0,660678447	0,04482376	3	19	624	16482	MELO3C010631; MELO3C003638; MELO3C020860	MELO3C005384; MELO3C014021; MELO3C014020; MELO3C008864; MELO3C002892; MELO3C022319; MELO3C026949; MELO3C025879; MELO3C025646; MELO3C010507; MELO3C024596; MELO3C001937; MELO3C025142; MELO3C014529; MELO3C017228; MELO3C015225; MELO3C027184; MELO3C014528; MELO3C017458
GO 0045454	cell redox homeostasis	BIOLOGICAL_PROCESS	0,665413214	0,045616041	9	113	618	16388	MELO3C017902; MELO3C019253; MELO3C012410; MELO3C016056; MELO3C019722; MELO3C019326; MELO3C018455; MELO3C021247; MELO3C009429	MELO3C010860; MELO3C009478; MELO3C008421; MELO3C005790; MELO3C011030; MELO3C011393; MELO3C009872; MELO3C009519; MELO3C001994; MELO3C024103; MELO3C024468; MELO3C021350; MELO3C025034; MELO3C021351; MELO3C017411; MELO3C010625; MELO3C017410; MELO3C009882; MELO3C002450; MELO3C022339; MELO3C005206; MELO3C000126; MELO3C026897; MELO3C016053; MELO3C016055; MELO3C010633; MELO3C012465;
GO 0046700	heterocycle catabolic process	BIOLOGICAL_PROCESS	0,681717933	0,047117042	1	151	626	16350	MELO3C002118	MELO3C016969; MELO3C020705; MELO3C010461; MELO3C006121; MELO3C013051; MELO3C002562; MELO3C024905; MELO3C002203; MELO3C006767; MELO3C018062; MELO3C004867; MELO3C000014; MELO3C023775; MELO3C023136; MELO3C020380; MELO3C017771; MELO3C015199; MELO3C015113; MELO3C017811; MELO3C017810; MELO3C016736; MELO3C012257; MELO3C008154; MELO3C014554; MELO3C010350; MELO3C021769; MELO3C008435;
GO 0044270	cellular nitrogen compound catabolic process	BIOLOGICAL_PROCESS	0,684298913	0,047440282	1	152	626	16349	MELO3C002118	MELO3C016969; MELO3C020705; MELO3C010461; MELO3C006121; MELO3C013051; MELO3C002562; MELO3C024905; MELO3C006767; MELO3C018062; MELO3C004867; MELO3C000014; MELO3C023775; MELO3C023136; MELO3C020380; MELO3C017771; MELO3C015199; MELO3C015113; MELO3C017811; MELO3C017810; MELO3C016736; MELO3C012257; MELO3C008154; MELO3C014554; MELO3C010350; MELO3C021769; MELO3C008435; MELO3C023545;
GO 0042023	DNA endoreduplication	BIOLOGICAL_PROCESS	0,699756525	0,049548806	2	8	625	16493	MELO3C011003; MELO3C012361	MELO3C019031; MELO3C012214; MELO3C008916; MELO3C018187; MELO3C012492; MELO3C026580; MELO3C014639; MELO3C002168

GO 0009695	jasmonic acid biosynthetic process	BIOLOGICAL_PROCESS	0,699756525	0,049548806	2	8	625	16493	MELO3C002470; MELO3C015514	MELO3C004955; MELO3C009362; MELO3C012388; MELO3C010910; MELO3C004565; MELO3C008062; MELO3C018734; MELO3C002346
GO 0007043	cell-cell junction assembly	BIOLOGICAL_PROCESS	0,699756525	0,049548806	2	8	625	16493	MELO3C007673; MELO3C022488	MELO3C007829; MELO3C026613; MELO3C006574; MELO3C018025; MELO3C018532; MELO3C006575; MELO3C015103; MELO3C014723
GO 0000578	embryonic axis specification	BIOLOGICAL_PROCESS	0,699756525	0,049548806	2	8	625	16493	MELO3C003768; MELO3C011193	MELO3C025389; MELO3C024028; MELO3C005946; MELO3C024874; MELO3C005099; MELO3C007036; MELO3C024782; MELO3C019956
GO 0046474	glycerophospholipid biosynthetic process	BIOLOGICAL_PROCESS	0,699756525	0,049164821	4	34	623	16467	MELO3C007931; MELO3C008959; MELO3C025637; MELO3C012545	MELO3C013830; MELO3C007010; MELO3C012286; MELO3C020821; MELO3C020987; MELO3C005332; MELO3C022308; MELO3C020989; MELO3C005634; MELO3C021052; MELO3C015670; MELO3C026440; MELO3C017214; MELO3C013319; MELO3C017019; MELO3C010621; MELO3C011215; MELO3C015647; MELO3C011047; MELO3C013842; MELO3C009088; MELO3C009186; MELO3C013982; MELO3C014212; MELO3C008992; MELO3C005285; MELO3C006258;
GO 0016161	beta-amylase activity	MOLECULAR_FUNCTION	0,699756525	0,049548806	2	8	625	16493	MELO3C006362; MELO3C016213	MELO3C014105; MELO3C022740; MELO3C022739; MELO3C023067; MELO3C018794; MELO3C021362; MELO3C021214; MELO3C013887

Supplementary Table 2.C Gene Ontology terms (GO terms) of the cluster 2.2 obtained considering the comparison between lines the postharvest ripening time fruit during storage at 20.5°C and 88% relative humidity for 18 d the near-isogenic line SC10-2 and its parental ''Piel de Sapo'' obtained according to the differentially expressed gene pattern (Supl. Table 2.A)

GO ID	GO Name	GO Category	FDR	P-Value	SC10-2	PS	Non Annot Test	Non Annot Reference	TestSet Sequences	RefSet Sequences
GO:0004370	glycerol kinase activity	MOLECULAR_FUNCTION	0 459917717	4 87E-05	2	0	118	17008	MELO3C023442; MELO3C004084	
GO:0043069	negative regulation of programmed cell death	BIOLOGICAL_PROCESS	1	0 030471862	2	37	118	16971	MELO3C003331; MELO3C017623	MELO3C002481; MELO3C011470; MELO3C006121; MELO3C007237; MELO3C003332; MELO3C005976; MELO3C004622; MELO3C025417; MELO3C022346; MELO3C005757; MELO3C025413; MELO3C016083; MELO3C005912; MELO3C025752; MELO3C021057; MELO3C023972; MELO3C009939; MELO3C004827; MELO3C024340; MELO3C025355; MELO3C005718; MELO3C011710; MELO3C013522; MELO3C011983; MELO3C012376; MELO3C011021; MELO3C004950;
GO:0043622	cortical microtubule organization	BIOLOGICAL_PROCESS	1	0 034546914	1	4	119	17004	MELO3C002054	MELO3C007829; MELO3C014496; MELO3C002717; MELO3C023374
GO:0006954	inflammatory response	BIOLOGICAL_PROCESS	1	0 041312923	1	5	119	17003	MELO3C026027	MELO3C026028; MELO3C015103; MELO3C017426; MELO3C018756; MELO3C022821
GO:0042780	tRNA 3'-end processing	BIOLOGICAL_PROCESS	1	0 027733554	1	3	119	17005	MELO3C014447	MELO3C020738; MELO3C010582; MELO3C024265
GO:0010017	red or far-red light signaling pathway	BIOLOGICAL_PROCESS	1	0 026260641	2	34	118	16974	MELO3C026502; MELO3C014459	MELO3C009692; MELO3C006046; MELO3C014684; MELO3C012221; MELO3C006142; MELO3C014386; MELO3C011250; MELO3C003075; MELO3C006225; MELO3C021715; MELO3C003574; MELO3C024805; MELO3C026506; MELO3C004148; MELO3C002742; MELO3C005738; MELO3C002705; MELO3C005939; MELO3C019731; MELO3C010769; MELO3C025191; MELO3C014699; MELO3C008213; MELO3C009202; MELO3C005120; MELO3C002793; MELO3C006717;
GO:0010497	plasmodesmata-mediated intercellular transport	BIOLOGICAL_PROCESS	1	0 041312923	1	5	119	17003	MELO3C002054	MELO3C018455; MELO3C002933; MELO3C014025; MELO3C010974; MELO3C012843
GO:0010375	stomatal complex patterning	BIOLOGICAL_PROCESS	1	0 020872515	1	2	119	17006	MELO3C002054	MELO3C021111; MELO3C020718
GO:0070838	divalent metal ion transport	BIOLOGICAL_PROCESS	1	0 019826524	2	29	118	16979	MELO3C016817; MELO3C014607	MELO3C007271; MELO3C003950; MELO3C008308; MELO3C024920; MELO3C007636; MELO3C020600; MELO3C022448; MELO3C024289; MELO3C020683; MELO3C009917; MELO3C025057; MELO3C025255; MELO3C019215; MELO3C017953; MELO3C010795; MELO3C010794; MELO3C012595; MELO3C004374; MELO3C006259; MELO3C006257; MELO3C026832; MELO3C009809; MELO3C026378; MELO3C015780; MELO3C021780; MELO3C010753; MELO3C018734;
GO:0009959	negative gravitropism	BIOLOGICAL_PROCESS	1	0 027733554	1	3	119	17005	MELO3C008088	MELO3C025310; MELO3C008847; MELO3C024155
GO:0006659	phosphatidylserine biosynthetic process	BIOLOGICAL_PROCESS	1	0 013963465	1	1	119	17007	MELO3C005332	MELO3C012286

GO:0009408	response to heat	BIOLOGICAL_PROCESS	1	4 24E-04	5	85	115	16923	MELO3C016970; MELO3C025139; MELO3C013946; MELO3C009996; MELO3C003917	MELO3C013974; MELO3C008263; MELO3C005873; MELO3C005035; MELO3C008589; MELO3C014183; MELO3C005674; MELO3C020589; MELO3C018780; MELO3C026886; MELO3C018023; MELO3C018660; MELO3C001916; MELO3C019039; MELO3C012925; MELO3C010748; MELO3C015312; MELO3C016449; MELO3C012455; MELO3C012136; MELO3C012456; MELO3C015608; MELO3C012331; MELO3C009840; MELO3C014230; MELO3C005884; MELO3C008677;
GO:0009660	amyloplast organization	BIOLOGICAL_PROCESS	1	0 013963465	1	1	119	17007	MELO3C008088	MELO3C025310
GO:0045038	protein import into chloroplast thylakoid membrane	BIOLOGICAL_PROCESS	1	0 020872515	1	2	119	17006	MELO3C006136	MELO3C020652; MELO3C018772
GO:0006433	prolyl-tRNA aminoacylation	BIOLOGICAL_PROCESS	1	0 020872515	1	2	119	17006	MELO3C017711	MELO3C019492; MELO3C005193
GO:0033345	asparagine catabo ic process via L-aspartate	BIOLOGICAL_PROCESS	1	0 013963465	1	1	119	17007	MELO3C017653	MELO3C006131
GO:0009590	detection of gravity	BIOLOGICAL_PROCESS	1	0 020872515	1	2	119	17006	MELO3C008088	MELO3C005293; MELO3C005396
GO:0009753	response to jasmonic acid	BIOLOGICAL_PROCESS	1	0 00858548	3	57	117	16951	MELO3C010774; MELO3C006120; MELO3C011885	MELO3C006086; MELO3C006046; MELO3C014386; MELO3C006765; MELO3C020701; MELO3C005674; MELO3C024348; MELO3C008625; MELO3C017292; MELO3C001913; MELO3C017134; MELO3C025152; MELO3C012527; MELO3C011439; MELO3C015436; MELO3C010353; MELO3C004231; MELO3C005840; MELO3C020637; MELO3C021643; MELO3C006934; MELO3C021645; MELO3C004513; MELO3C026577; MELO3C024357; MELO3C010910; MELO3C016852;
GO:0006516	glycoprotein catabolic process	BIOLOGICAL_PROCESS	1	0 034546914	1	4	119	17004	MELO3C017653	MELO3C001609; MELO3C026905; MELO3C016787; MELO3C015327
GO:0006517	protein deglycosylation	BIOLOGICAL_PROCESS	1	0 007006072	1	0	119	17008	MELO3C017653	
GO:0051604	protein maturation	BIOLOGICAL_PROCESS	1	0 022309646	2	31	118	16977	MELO3C017653; MELO3C016970	MELO3C005470; MELO3C009174; MELO3C006089; MELO3C012220; MELO3C008520; MELO3C004285; MELO3C022725; MELO3C020322; MELO3C020686; MELO3C003576; MELO3C023413; MELO3C006206; MELO3C022525; MELO3C025156; MELO3C017891; MELO3C004827; MELO3C025353; MELO3C014926; MELO3C015335; MELO3C011874; MELO3C011641; MELO3C013522; MELO3C013881; MELO3C006131; MELO3C009684; MELO3C025349; MELO3C025589;
GO:0006013	mannose metabolic process	BIOLOGICAL_PROCESS	1	0 041312923	1	5	119	17003	MELO3C005109	MELO3C016048; MELO3C026482; MELO3C009914; MELO3C007919; MELO3C009913
GO:0007586	digestion	BIOLOGICAL_PROCESS	1	0 048031907	1	6	119	17002	MELO3C015523	MELO3C012302; MELO3C012071; MELO3C005751; MELO3C017002; MELO3C019036; MELO3C022495
GO:0035071	salivary gland cell autophagic cell death	BIOLOGICAL_PROCESS	1	0 034546914	1	4	119	17004	MELO3C015523	MELO3C026898; MELO3C022308; MELO3C007891; MELO3C025809
GO:0032515	negative regulation of phosphoprotein phosphatase activity	BIOLOGICAL_PROCESS	1	0 007006072	1	0	119	17008	MELO3C018500	
GO:0007030	Golgi organization	BIOLOGICAL_PROCESS	1	0 00419236	2	12	118	16996	MELO3C008088; MELO3C004825	MELO3C021320; MELO3C005918; MELO3C008037; MELO3C025044; MELO3C008782; MELO3C024284; MELO3C021946; MELO3C022038; MELO3C006811; MELO3C015756; MELO3C016416; MELO3C022305

GO:0017006	protein-tetrapyrrole linkage	BIOLOGICAL_PROCESS	1	0 048031907	1	6	119	17002	MELO3C026502	MELO3C006717; MELO3C024196; MELO3C024195; MELO3C026506; MELO3C002705; MELO3C015204
GO:0051865	protein autoubiquitination	BIOLOGICAL_PROCESS	1	0 041312923	1	5	119	17003	MELO3C025853	MELO3C011752; MELO3C022725; MELO3C010168; MELO3C011153; MELO3C023546
GO:0006072	glycerol-3-phosphate metabolic process	BIOLOGICAL_PROCESS	1	0 00132592	2	6	118	17002	MELO3C023442; MELO3C004084	MELO3C026337; MELO3C021604; MELO3C020158; MELO3C019820; MELO3C020157; MELO3C005116
GO:0031648	protein destabilization	BIOLOGICAL_PROCESS	1	0 007006072	1	0	119	17008	MELO3C015523	
GO:0048510	regulation of timing of transition from vegetative to reproductive phase	BIOLOGICAL_PROCESS	1	0 034546914	1	4	119	17004	MELO3C022388	MELO3C027290; MELO3C019330; MELO3C013793; MELO3C009465
GO:0002949	tRNA threonylcarbamoyladenosine modification	BIOLOGICAL_PROCESS	1	0 007006072	1	0	119	17008	MELO3C006202	
GO:0016404	15-hydroxyprostaglandin dehydrogenase (NAD) activity	MOLECULAR_FUNCTION	1	0 007006072	1	0	119	17008	MELO3C019503	
GO:0004144	diacylglycerol O-acyltransferase activity	MOLECULAR_FUNCTION	1	0 020872515	1	2	119	17006	MELO3C013703	MELO3C004632; MELO3C018460
GO:0003846	2-acylglycerol O-acyltransferase activity	MOLECULAR_FUNCTION	1	0 007006072	1	0	119	17008	MELO3C013703	
GO:0042781	3'-tRNA processing endoribonuclease activity	MOLECULAR_FUNCTION	1	0 020872515	1	2	119	17006	MELO3C014447	MELO3C020738; MELO3C024265
GO:0046872	metal ion binding	MOLECULAR_FUNCTION	1	0 031268561	28	2666	92	14342	MELO3C008088; MELO3C014447; MELO3C012284; MELO3C004441; MELO3C025917; MELO3C006202; MELO3C009996; MELO3C025855; MELO3C005711; MELO3C026249; MELO3C025853; MELO3C011216; MELO3C018569; MELO3C009380; MELO3C009583; MELO3C009561; MELO3C016817; MELO3C013383; MELO3C022715; MELO3C004139; MELO3C006418; MELO3C005109; MELO3C025940; MELO3C019503; MELO3C010774; MELO3C011885; MELO3C014459;	MELO3C018628; MELO3C004460; MELO3C005792; MELO3C012088; MELO3C006644; MELO3C020945; MELO3C004465; MELO3C005316; MELO3C003137; MELO3C003139; MELO3C005315; MELO3C005319; MELO3C015590; MELO3C015591; MELO3C015592; MELO3C015593; MELO3C015594; MELO3C015110; MELO3C015595; MELO3C015596; MELO3C019951; MELO3C015597; MELO3C015599; MELO3C018624; MELO3C017777; MELO3C017309; MELO3C014279;
GO:0004827	proline-tRNA ligase activity	MOLECULAR_FUNCTION	1	0 020872515	1	2	119	17006	MELO3C017711	MELO3C019492; MELO3C005193
GO:0045547	dehydrodolichyl diphosphate synthase activity	MOLECULAR_FUNCTION	1	0 020872515	1	2	119	17006	MELO3C025855	MELO3C021891; MELO3C018615
GO:0050178	phenylpyruvate tautomerase activity	MOLECULAR_FUNCTION	1	0 007006072	1	0	119	17008	MELO3C026027	
GO:0003948	N4-(beta-N-acetylglucosaminyl)-L-asparaginase activity	MOLECULAR_FUNCTION	1	0 007006072	1	0	119	17008	MELO3C017653	
GO:0050221	prostaglandin-E2 9-reductase activity	MOLECULAR_FUNCTION	1	0 020872515	1	2	119	17006	MELO3C026155	MELO3C015622; MELO3C011853
GO:0033743	peptide-methionine (R)-S-oxide reductase activity	MOLECULAR_FUNCTION	1	0 013963465	1	1	119	17007	MELO3C018569	MELO3C016676
GO:0008020	G-protein coupled photoreceptor activity	MOLECULAR_FUNCTION	1	0 041312923	1	5	119	17003	MELO3C026502	MELO3C006717; MELO3C024196; MELO3C024195; MELO3C026506; MELO3C002705
GO:0004197	cysteine-type endopeptidase activity	MOLECULAR_FUNCTION	1	0 017468633	2	27	118	16981	MELO3C015523; MELO3C017623	MELO3C010982; MELO3C008520; MELO3C007578; MELO3C023338; MELO3C021359; MELO3C017053; MELO3C024402; MELO3C024666; MELO3C025355; MELO3C016781; MELO3C010702; MELO3C015576; MELO3C015577; MELO3C015578; MELO3C013438; MELO3C010763; MELO3C015634; MELO3C012403; MELO3C013563; MELO3C006275; MELO3C005564; MELO3C026898; MELO3C018473; MELO3C019168; MELO3C010976; MELO3C018636; MELO3C015701
GO:0008834	di-trans poly-cis-decaprenylcistransferase activity	MOLECULAR_FUNCTION	1	0 020872515	1	2	119	17006	MELO3C025855	MELO3C021891; MELO3C018615
GO:0008798	beta-aspartyl-peptidase activity	MOLECULAR_FUNCTION	1	0 034546914	1	4	119	17004	MELO3C017653	MELO3C001609; MELO3C016787; MELO3C006131; MELO3C015327
GO:0004557	alpha-galactosidase activity	MOLECULAR_FUNCTION	1	0 034546914	1	4	119	17004	MELO3C020139	MELO3C020138; MELO3C011771; MELO3C010698; MELO3C011770
GO:0005262	calcium channel activity	MOLECULAR_FUNCTION	1	0 034546914	1	4	119	17004	MELO3C016817	MELO3C017043; MELO3C022020; MELO3C018734; MELO3C007977
GO:0003882	CDP-diacylglycerol-serine O-phosphatidyltransferase activity	MOLECULAR_FUNCTION	1	0 013963465	1	1	119	17007	MELO3C005332	MELO3C012286
GO:0004605	phosphatidate cytidylyltransferase activity	MOLECULAR_FUNCTION	1	0 027733554	1	3	119	17005	MELO3C007432	MELO3C020525; MELO3C021695; MELO3C021145

GO:0047268	galactinol-raffinose galactosyltransferase activity	MOLECULAR_FUNCTION	1	0 048031907	1	6	119	17002	MELO3C026247	MELO3C015912; MELO3C009979; MELO3C002287; MELO3C025599; MELO3C023110; MELO3C010314
GO:0034511	U3 snoRNA binding	MOLECULAR_FUNCTION	1	0 013963465	1	1	119	17007	MELO3C017440	MELO3C013185
GO:0005764	lysosome	CELLULAR_COMPONENT	1	0 011186588	2	21	118	16987	MELO3C017653; MELO3C015523	MELO3C014821; MELO3C003291; MELO3C006034; MELO3C005243; MELO3C004353; MELO3C008897; MELO3C004477; MELO3C026977; MELO3C023569; MELO3C006926; MELO3C026898; MELO3C026415; MELO3C025645; MELO3C025752; MELO3C025972; MELO3C020442; MELO3C026971; MELO3C025355; MELO3C018764; MELO3C014818; MELO3C026110
GO:0031983	vesicle lumen	CELLULAR_COMPONENT	1	0 007006072	1	0	119	17008	MELO3C015523	
GO:0042718	yolk granule	CELLULAR_COMPONENT	1	0 007006072	1	0	119	17008	MELO3C015523	
GO:0016602	CCAAT-binding factor complex	CELLULAR_COMPONENT	1	0 034546914	1	4	119	17004	MELO3C023161	MELO3C009551; MELO3C015320; MELO3C023554; MELO3C007077
GO:0045169	fusome	CELLULAR_COMPONENT	1	0 020872515	1	2	119	17006	MELO3C015523	MELO3C006951; MELO3C024150
GO:0005783	endoplasmic reticulum	CELLULAR_COMPONENT	1	0 011232603	8	425	112	16583	MELO3C008088; MELO3C016817; MELO3C019333; MELO3C017653; MELO3C014607; MELO3C013703; MELO3C015523; MELO3C014459	MELO3C019959; MELO3C012088; MELO3C003372; MELO3C020821; MELO3C002165; MELO3C002166; MELO3C006405; MELO3C009914; MELO3C006525; MELO3C025156; MELO3C017891; MELO3C024187; MELO3C018740; MELO3C017652; MELO3C017413; MELO3C025390; MELO3C016449; MELO3C016219; MELO3C018518; MELO3C002052; MELO3C003263; MELO3C003383; MELO3C017661; MELO3C019722; MELO3C017542; MELO3C016696; MELO3C015246;

Supplementary Table 2.D Gene Ontology terms (GO terms) of the cluster 2.3 obtained considering the comparison between lines the postharvest ripening time fruit during storage at 20.5°C and 88% relative humidity for 18 d the near-isogenic line SC 0-2 and its parental 'Piel de Sapo'' obtained according to the differentially expressed gene pattern (Supl. Table 2.A)

GO ID	GO Name	GO Category	FDR	P-Value	SC10-2	PS	Non Annot Test	Non Annot Reference	TestSet Sequences	RefSet Sequences
GO:0006287	base-excision repair gap-fil ing	BIOLOGICAL_PROCESS	1	0 021251752	1	0	63	16764	MELO3C024596	
GO:0045004	DNA replication proofreading	BIOLOGICAL_PROCESS	1	0 021251752	1	0	63	16764	MELO3C024596	
GO:0009832	plant-type cell wa l biogenesis	BIOLOGICAL_PROCESS	1	0 023114647	3	26	61	16738	MELO3C007450; MELO3C008069; MELO3C018365	MELO3C005051; MELO3C017818; MELO3C0 0062; MELO3C007036; MELO3C005791; MELO3C023836; MELO3C026947; MELO3C026188; MELO3C023551; MELO3C023374; MELO3C003916; MELO3C022385; MELO3C0 6301; MELO3C013319; MELO3C0 0524; MELO3C012573; MELO3C009322; MELO3C009189; MELO3C002672; MELO3C003783; MELO3C003488; MELO3C003569; MELO3C020651; MELO3C017242; MELO3C026156; MELO3C0 6777
GO:0007259	JAK-STAT cascade	BIOLOGICAL_PROCESS	1	0 04205 081	1	1	63	1676	MELO3C022219	MELO3C005634
GO:0002119	nematode larval development	BIOLOGICAL_PROCESS	1	0 03798 651	12	286	352	16478	MELO3C003924; MELO3C010640; MELO3C026234; MELO3C024596; MELO3C017365; MELO3C011383; MELO3C015322; MELO3C011139; MELO3C011206; MELO3C012622; MELO3C002556; MELO3C003842	MELO3C011795; MELO3C012522; MELO3C006760; MELO3C002166; MELO3C002045; MELO3C004344; MELO3C019031; MELO3C026800; MELO3C019034; MELO3C025275; MELO3C0 6321; MELO3C014708; MELO3C015235; MELO3C019956; MELO3C020836; MELO3C008157; MELO3C002173; MELO3C004473; MELO3C014153; MELO3C013185; MELO3C023545; MELO3C008835; MELO3C023306; MELO3C023427; MELO3C006657; MELO3C024757; MELO3C003703;
GO:0018315	molybdenum incorporation into molybdenum-molybdopterin complex	BIOLOGICAL_PROCESS	1	0 021251752	1	0	63	16764	MELO3C022174	
GO:0010031	circumnutation	BIOLOGICAL_PROCESS	1	0 04205 081	1	1	63	1676	MELO3C010769	MELO3C001999
GO:0006297	nucleotide-excision repair DNA gap fi ling	BIOLOGICAL_PROCESS	1	0 044412945	2	14	62	16750	MELO3C018521; MELO3C024596	MELO3C014021; MELO3C014020; MELO3C008864; MELO3C026949; MELO3C025879; MELO3C003638; MELO3C0 0507; MELO3C001937; MELO3C025142; MELO3C014529; MELO3C017228; MELO3C014528; MELO3C017458; MELO3C0 0631
GO:0000348	mRNA branch site recognition	BIOLOGICAL_PROCESS	1	0 04205 081	1	1	63	1676	MELO3C017365	MELO3C011256
GO:004 631	RNA polyadenylation	BIOLOGICAL_PROCESS	1	0 02582 813	2	10	62	16754	MELO3C022443; MELO3C024435	MELO3C005162; MELO3C004944; MELO3C008873; MELO3C021828; MELO3C008722; MELO3C002045; MELO3C027241; MELO3C021974; MELO3C002115; MELO3C011126
GO:0009965	leaf morphogenesis	BIOLOGICAL_PROCESS	1	0 027567914	3	28	61	16736	MELO3C021534; MELO3C017813; MELO3C005971	MELO3C006085; MELO3C007098; MELO3C011771; MELO3C007870; MELO3C004347; MELO3C022204; MELO3C024446; MELO3C020860; MELO3C015173; MELO3C001957; MELO3C025450; MELO3C017559; MELO3C013621; MELO3C0 6916; MELO3C011142; MELO3C013287; MELO3C007121; MELO3C020854; MELO3C014670; MELO3C002670; MELO3C007500; MELO3C004752; MELO3C024898; MELO3C0 8380; MELO3C007207; MELO3C003009; MELO3C023064;
GO:0040007	growth	BIOLOGICAL_PROCESS	1	0 044484447	18	508	346	16256	MELO3C014358; MELO3C008481; MELO3C010640; MELO3C008069; MELO3C011383; MELO3C005971; MELO3C002556; MELO3C003842; MELO3C003924; MELO3C026234; MELO3C022174; MELO3C017365; MELO3C019225; MELO3C015322; MELO3C010769; MELO3C011139; MELO3C011206; MELO3C012622	MELO3C021918; MELO3C006760; MELO3C002166; MELO3C002045; MELO3C004344; MELO3C006648; MELO3C025275; MELO3C019953; MELO3C0 6321; MELO3C026482; MELO3C019956; MELO3C021808; MELO3C020836; MELO3C005561; MELO3C002173; MELO3C004473; MELO3C014153; MELO3C013185; MELO3C004353; MELO3C008835; MELO3C006657; MELO3C006415; MELO3C025044; MELO3C017661; MELO3C0 0913; MELO3C0 8512; MELO3C0 6456;

GO:0006662	glycerol ether metabolic process	BIOLOGICAL_PROCESS	1	0 035039541	3	31	61	1673	MELO3C008932; MELO3C026897; MELO3C025023	MELO3C0 0860; MELO3C007211; MELO3C008421; MELO3C003791; MELO3C015939; MELO3C009894; MELO3C008127; MELO3C007873; MELO3C006026; MELO3C004822; MELO3C001994; MELO3C022106; MELO3C008888; MELO3C026569; MELO3C024468; MELO3C025752; MELO3C021431; MELO3C002508; MELO3C0 0009; MELO3C012969; MELO3C0 6516; MELO3C012410; MELO3C011340; MELO3C004371; MELO3C012053; MELO3C007026; MELO3C0 0490;
GO:0006541	glutamine metabolic process	BIOLOGICAL_PROCESS	1	0 021047312	3	25	61	16739	MELO3C012572; MELO3C020749; MELO3C008481	MELO3C022828; MELO3C013152; MELO3C026828; MELO3C0 8290; MELO3C007757; MELO3C009759; MELO3C0 8382; MELO3C023599; MELO3C024486; MELO3C024189; MELO3C024485; MELO3C013218; MELO3C012434; MELO3C012156; MELO3C011485; MELO3C008152; MELO3C005680; MELO3C006577; MELO3C006993; MELO3C025766; MELO3C025645; MELO3C011808; MELO3C020230; MELO3C019622; MELO3C012435
GO:0071281	cellular response to iron ion	BIOLOGICAL_PROCESS	1	0 011586716	2	6	62	16758	MELO3C014230; MELO3C014099	MELO3C015210; MELO3C019550; MELO3C015531; MELO3C026952; MELO3C0 6340; MELO3C003906
GO:0060250	germ-line stem-cell niche homeostasis	BIOLOGICAL_PROCESS	1	0 021251752	1	0	63	16764	MELO3C022219	
GO:003 048	chromatin silencing by sma l RNA	BIOLOGICAL_PROCESS	1	4 50E-04	2	0	62	16764	MELO3C022443; MELO3C014706	
GO:0009631	cold acclimation	BIOLOGICAL_PROCESS	1	0 004316803	2	3	62	1676	MELO3C021940; MELO3C026068	MELO3C011972; MELO3C0 8668; MELO3C015546
GO:0060152	microtubule-based peroxisome localization	BIOLOGICAL_PROCESS	1	0 021251752	1	0	63	16764	MELO3C021783	
GO:0044765	single-organism transport	BIOLOGICAL_PROCESS	1	0 037521218	8	740	356	16024	MELO3C004999; MELO3C021783; MELO3C017343; MELO3C018720; MELO3C014230; MELO3C016149; MELO3C011139; MELO3C007613	MELO3C014028; MELO3C005550; MELO3C012087; MELO3C004222; MELO3C006883; MELO3C007731; MELO3C005311; MELO3C004465; MELO3C008709; MELO3C006409; MELO3C017891; MELO3C025277; MELO3C015350; MELO3C0 0900; MELO3C019951; MELO3C017655; MELO3C0 0901; MELO3C017414; MELO3C0 6326; MELO3C017656; MELO3C0 6689; MELO3C019956; MELO3C020836; MELO3C004591; MELO3C007980; MELO3C014397; MELO3C002052;
GO:005 697	protein delipidation	BIOLOGICAL_PROCESS	1	0 021251752	1	0	63	16764	MELO3C008520	
GO:004 603	cellular amide metabolic process	BIOLOGICAL_PROCESS	1	0 048516947	8	727	356	16037	MELO3C023047; MELO3C008099; MELO3C014611; MELO3C021113; MELO3C026234; MELO3C017364; MELO3C014706; MELO3C000756	MELO3C020704; MELO3C020705; MELO3C002164; MELO3C012084; MELO3C014262; MELO3C004345; MELO3C004587; MELO3C020945; MELO3C006400; MELO3C004344; MELO3C005674; MELO3C004226; MELO3C004347; MELO3C005679; MELO3C003258; MELO3C006648; MELO3C006766; MELO3C025279; MELO3C025156; MELO3C017891; MELO3C025276; MELO3C0 6200; MELO3C017653; MELO3C0 6201; MELO3C024061; MELO3C015598; MELO3C025030;
GO:0019419	sulfate reduction	BIOLOGICAL_PROCESS	1	0 04205 081	1	1	63	1676	MELO3C007398	MELO3C002450
GO:0019544	arginine catabolic process to glutamate	BIOLOGICAL_PROCESS	1	0 04205 081	1	1	63	1676	MELO3C017571	MELO3C002752
GO:0006071	glycerol metabolic process	BIOLOGICAL_PROCESS	1	0 034627522	2	12	62	16752	MELO3C022124; MELO3C017753	MELO3C007806; MELO3C013101; MELO3C001925; MELO3C024364; MELO3C001926; MELO3C002033; MELO3C019820; MELO3C014925; MELO3C013703; MELO3C011029; MELO3C021466; MELO3C004632
GO:0010051	xylem and phloem pattern formation	BIOLOGICAL_PROCESS	1	0 04964 023	2	15	62	16749	MELO3C007450; MELO3C017813	MELO3C012125; MELO3C009584; MELO3C002670; MELO3C005236; MELO3C004752; MELO3C006307; MELO3C024898; MELO3C022204; MELO3C003768; MELO3C003009; MELO3C025774; MELO3C019573; MELO3C0 6850; MELO3C0 6301; MELO3C0 8952

GO:0006470	protein dephosphorylation	BIOLOGICAL_PROCESS	1	0 007099285	6	74	358	16690	MELO3C020601; MELO3C004603; MELO3C007940; MELO3C006983; MELO3C013921; MELO3C023473	MELO3C020829; MELO3C013336; MELO3C0 8507; MELO3C008426; MELO3C004587; MELO3C003574; MELO3C024667; MELO3C002645; MELO3C026602; MELO3C023893; MELO3C026166; MELO3C0 8500; MELO3C011713; MELO3C026163; MELO3C0 0744; MELO3C012378; MELO3C009960; MELO3C007580; MELO3C015408; MELO3C013860; MELO3C0 6939; MELO3C009840; MELO3C006852; MELO3C021405; MELO3C023626; MELO3C020114; MELO3C003222;
GO:0034517	ribophagy	BIOLOGICAL_PROCESS	1	0 021251752	1	0	63	16764	MELO3C011731	
GO:0001736	estab ishment of planar polarity	BIOLOGICAL_PROCESS	1	0 04205 081	1	1	63	1676	MELO3C014230	MELO3C005892
GO:0016807	cysteine-type carboxypeptidase activity	MOLECULAR_FUNCTION	1	0 021251752	1	0	63	16764	MELO3C008520	
GO:0050281	serine-glyoxylate transaminase activity	MOLECULAR_FUNCTION	1	0 04205 081	1	1	63	1676	MELO3C015151	MELO3C014568
GO:0008865	fructokinase activity	MOLECULAR_FUNCTION	1	0 011586716	2	6	62	16758	MELO3C015750; MELO3C009032	MELO3C022452; MELO3C015749; MELO3C020278; MELO3C003755; MELO3C005395; MELO3C009200
GO:0003723	RNA binding	MOLECULAR_FUNCTION	1	0 044838422	26	789	338	15975	MELO3C011498; MELO3C009550; MELO3C005650; MELO3C009713; MELO3C013051; MELO3C005651; MELO3C025897; MELO3C022443; MELO3C019630; MELO3C026221; MELO3C015750; MELO3C014706; MELO3C012428; MELO3C019858; MELO3C016468; MELO3C016469; MELO3C012622; MELO3C008099; MELO3C014358; MELO3C005382; MELO3C007821; MELO3C013183; MELO3C003842; MELO3C024435; MELO3C017365; MELO3C026398	MELO3C014025; MELO3C020705; MELO3C014263; MELO3C012084; MELO3C003135; MELO3C002045; MELO3C020945; MELO3C026246; MELO3C015110; MELO3C019953; MELO3C019951; MELO3C019957; MELO3C017309; MELO3C012099; MELO3C005565; MELO3C013185; MELO3C009922; MELO3C007743; MELO3C007741; MELO3C006657; MELO3C026259; MELO3C015360; MELO3C0 8872; MELO3C019964; MELO3C0 8874; MELO3C017303; MELO3C015126;
GO:0046905	phytoene synthase activity	MOLECULAR_FUNCTION	1	0 021251752	1	0	63	16764	MELO3C025102	
GO:0032440	2-alkenal reductase [NAD(P)] activity	MOLECULAR_FUNCTION	1	0 037244384	2	341	62	1642	MELO3C017385; MELO3C023492	MELO3C002280; MELO3C014387; MELO3C007179; MELO3C008942; MELO3C022209; MELO3C004465; MELO3C001991; MELO3C024986; MELO3C004228; MELO3C022205; MELO3C021359; MELO3C019030; MELO3C015350; MELO3C020263; MELO3C0 8865; MELO3C017655; MELO3C014948; MELO3C017656; MELO3C015359; MELO3C0 0352; MELO3C013982; MELO3C002050; MELO3C011440; MELO3C011682; MELO3C007980; MELO3C006890; MELO3C0 0351;
GO:0004553	hydrolase activity hydrolyzing O-glycosyl compounds	MOLECULAR_FUNCTION	1	0 026860295	2	366	62	16398	MELO3C022162; MELO3C011977	MELO3C014148; MELO3C011430; MELO3C014147; MELO3C013055; MELO3C025718; MELO3C005431; MELO3C005438; MELO3C009914; MELO3C009913; MELO3C007734; MELO3C003813; MELO3C015470; MELO3C019035; MELO3C015471; MELO3C015472; MELO3C019036; MELO3C006092; MELO3C026480; MELO3C013622; MELO3C009488; MELO3C009367; MELO3C005560; MELO3C006777; MELO3C009924; MELO3C027109; MELO3C026811; MELO3C025840;
GO:0003735	structural constituent of ribosome	MOLECULAR_FUNCTION	1	0 007957351	1	353	63	1641	MELO3C017364	MELO3C011310; MELO3C020704; MELO3C006088; MELO3C002164; MELO3C012084; MELO3C014262; MELO3C024506; MELO3C020945; MELO3C006400; MELO3C003258; MELO3C006766; MELO3C024747; MELO3C020141; MELO3C022441; MELO3C003811; MELO3C001514; MELO3C025276; MELO3C0 6201; MELO3C025030; MELO3C0 8985; MELO3C0 6688; MELO3C014824; MELO3C017659; MELO3C020836; MELO3C007740; MELO3C013981; MELO3C009489;
GO:0051538	3 iron 4 su fur cluster binding	MOLECULAR_FUNCTION	1	0 04205 081	1	1	63	1676	MELO3C008481	MELO3C009759
GO:0008720	D-lactate dehydrogenase activity	MOLECULAR_FUNCTION	1	0 021251752	1	0	63	16764	MELO3C009581	
GO:0008444	CDP-diacylglycerol-glycerol-3-phosphate 3-phosphatidyltransferase activity	MOLECULAR_FUNCTION	1	0 04205 081	1	1	63	1676	MELO3C011715	MELO3C007382
GO:0004760	serine-pyruvate transaminase activity	MOLECULAR_FUNCTION	1	0 04205 081	1	1	63	1676	MELO3C015151	MELO3C014568

GO:0004485	methylcrotonoyl-CoA carboxylase activity	MOLECULAR_FUNCTION	1	0 04205 081	1	1	63	1676	MELO3C015796	MELO3C0 8456
GO:0008453	alanine-glyoxylate transaminase activity	MOLECULAR_FUNCTION	1	0 004316803	2	3	62	1676	MELO3C015151; MELO3C017571	MELO3C014568; MELO3C026045; MELO3C009117
GO:0008607	phosphorylase kinase regulator activity	MOLECULAR_FUNCTION	1	0 04205 081	1	1	63	1676	MELO3C026234	MELO3C025450
GO:0004402	histone acetyltransferase activity	MOLECULAR_FUNCTION	1	0 027567914	3	28	61	16736	MELO3C026234; MELO3C002885; MELO3C026222	MELO3C007593; MELO3C013698; MELO3C011851; MELO3C011774; MELO3C013356; MELO3C009471; MELO3C006243; MELO3C007211; MELO3C014860; MELO3C013253; MELO3C004100; MELO3C009635; MELO3C007015; MELO3C009633; MELO3C022788; MELO3C017030; MELO3C0 0806; MELO3C015474; MELO3C012527; MELO3C005161; MELO3C005162; MELO3C0 0476; MELO3C007627; MELO3C004615; MELO3C001964; MELO3C002318; MELO3C026433;
GO:0004008	copper-exporting ATPase activity	MOLECULAR_FUNCTION	1	0 02582 813	2	10	62	16754	MELO3C019011; MELO3C016915	MELO3C000189; MELO3C019010; MELO3C019012; MELO3C0 8643; MELO3C005665; MELO3C007027; MELO3C008846; MELO3C020853; MELO3C008845; MELO3C003996
GO:0017153	sodium:dicarboxylate symporter activity	MOLECULAR_FUNCTION	1	0 04205 081	1	1	63	1676	MELO3C017343	MELO3C023446
GO:0033741	adenylyl-sulfate reductase (glutathione) activity	MOLECULAR_FUNCTION	1	0 04205 081	1	1	63	1676	MELO3C007398	MELO3C002450
GO:0004861	cyclin-dependent protein serine/threonine kinase inhibitor activity	MOLECULAR_FUNCTION	1	0 04205 081	1	1	63	1676	MELO3C020458	MELO3C026998
GO:0004458	D-lactate dehydrogenase (cytochrome) activity	MOLECULAR_FUNCTION	1	0 04205 081	1	1	63	1676	MELO3C009581	MELO3C0 6408
GO:0004355	glutamate synthase (NADPH) activity	MOLECULAR_FUNCTION	1	0 04205 081	1	1	63	1676	MELO3C008481	MELO3C009759
GO:0004354	glutamate dehydrogenase (NADP) activity	MOLECULAR_FUNCTION	1	0 021251752	1	0	63	16764	MELO3C013031	
GO:0019154	glycolate dehydrogenase activity	MOLECULAR_FUNCTION	1	0 021251752	1	0	63	16764	MELO3C009581	
GO:0008949	oxalyl-CoA decarboxylase activity	MOLECULAR_FUNCTION	1	0 021251752	1	0	63	16764	MELO3C010381	
GO:190 681	sulfur compound binding	MOLECULAR_FUNCTION	1	0 046452118	3	35	61	16729	MELO3C010381; MELO3C015796; MELO3C007613	MELO3C024609; MELO3C013153; MELO3C007612; MELO3C005894; MELO3C000358; MELO3C008625; MELO3C000599; MELO3C026205; MELO3C026007; MELO3C026005; MELO3C026006; MELO3C026004; MELO3C001913; MELO3C025454; MELO3C0 6066; MELO3C019218; MELO3C012235; MELO3C012993; MELO3C004231; MELO3C009145; MELO3C003386; MELO3C003265; MELO3C007227; MELO3C003266; MELO3C020531; MELO3C021742; MELO3C013081;
GO:0004044	amidophosphoribosyltransferase activity	MOLECULAR_FUNCTION	1	0 04205 081	1	1	63	1676	MELO3C020749	MELO3C025646
GO:0008889	glycerophosphodiester phosphodiesterase activity	MOLECULAR_FUNCTION	1	0 008813139	2	5	62	16759	MELO3C022124; MELO3C017753	MELO3C007806; MELO3C002033; MELO3C014925; MELO3C013101; MELO3C011029
GO:0047499	calcium-independent phospho ipase A2 activity	MOLECULAR_FUNCTION	1	0 021251752	1	0	63	16764	MELO3C020721	
GO:0019786	Atg8-specific protease activity	MOLECULAR_FUNCTION	1	0 021251752	1	0	63	16764	MELO3C008520	
GO:0010293	abscisic aldehyde oxidase activity	MOLECULAR_FUNCTION	1	0 04205 081	1	1	63	1676	MELO3C014719	MELO3C014717
GO:0080048	GDP-D-glucose phosphorylase activity	MOLECULAR_FUNCTION	1	0 021251752	1	0	63	16764	MELO3C013136	
GO:0004689	phosphorylase kinase activity	MOLECULAR_FUNCTION	1	0 04205 081	1	1	63	1676	MELO3C008469	MELO3C023218
GO:0003755	peptidyl-prolyl cis-trans isomerase activity	MOLECULAR_FUNCTION	1	0 038575996	4	56	60	16708	MELO3C015779; MELO3C016542; MELO3C014178; MELO3C012622	MELO3C011036; MELO3C012489; MELO3C013896; MELO3C017816; MELO3C0 0261; MELO3C013375; MELO3C015916; MELO3C006285; MELO3C008222; MELO3C021912; MELO3C009952; MELO3C002126; MELO3C007778; MELO3C026524; MELO3C003338; MELO3C019631; MELO3C024662; MELO3C017776; MELO3C025192; MELO3C0 6887; MELO3C011236; MELO3C014557; MELO3C008553; MELO3C006176; MELO3C004752; MELO3C025848; MELO3C022335;
GO:0004602	glutathione peroxidase activity	MOLECULAR_FUNCTION	1	0 014689493	2	7	62	16757	MELO3C015857; MELO3C016951	MELO3C014348; MELO3C017729; MELO3C015858; MELO3C015859; MELO3C005666; MELO3C022821; MELO3C005667
GO:0004604	phosphoadenylyl-sulfate reductase (thioredoxin) activity	MOLECULAR_FUNCTION	1	0 04205 081	1	1	63	1676	MELO3C007398	MELO3C002450
GO:004 625	delta DNA polymerase complex	CELLULAR_COMPONENT	1	0 021251752	1	0	63	16764	MELO3C024596	
GO:0015030	Cajal body	CELLULAR_COMPONENT	1	0 039403779	2	13	62	1675	MELO3C017365; MELO3C014706	MELO3C012871; MELO3C004440; MELO3C023809; MELO3C022928; MELO3C017908; MELO3C006422; MELO3C005127; MELO3C004018; MELO3C008801; MELO3C026433; MELO3C019034; MELO3C017696; MELO3C022370
GO:0030140	trans-Golgi network transport vesicle	CELLULAR_COMPONENT	1	0 011586716	2	6	62	16758	MELO3C003242; MELO3C017813	MELO3C025730; MELO3C013605; MELO3C024167; MELO3C007298; MELO3C005579; MELO3C008306

GO:0008287	protein serine/threonine phosphatase complex	CELLULAR_COMPONENT	1	0 03101136	4	52	60	16712	MELO3C020601; MELO3C007940; MELO3C006983; MELO3C023473	MELO3C020829; MELO3C013336; MELO3C0 8507; MELO3C008221; MELO3C008426; MELO3C024667; MELO3C023893; MELO3C026288; MELO3C011713; MELO3C013337; MELO3C015408; MELO3C020837; MELO3C0 6939; MELO3C006852; MELO3C023626; MELO3C008478; MELO3C024635; MELO3C021246; MELO3C006736; MELO3C004439; MELO3C024478; MELO3C013745; MELO3C009093; MELO3C011765; MELO3C006581; MELO3C014325; MELO3C009297;
GO:0000815	ESCRT III complex	CELLULAR_COMPONENT	1	0 04205_081	1	1	63	1676	MELO3C005199	MELO3C004945
GO:0009508	plastid chromosome	CELLULAR_COMPONENT	1	0 018106304	2	8	62	16756	MELO3C026221; MELO3C010512	MELO3C019372; MELO3C006321; MELO3C017774; MELO3C002396; MELO3C007103; MELO3C022303; MELO3C003216; MELO3C025888
GO:0019031	viral envelope	CELLULAR_COMPONENT	1	0 02582_813	2	10	62	16754	MELO3C017968; MELO3C013370	MELO3C013688; MELO3C013687; MELO3C013686; MELO3C014389; MELO3C014321; MELO3C019997; MELO3C005059; MELO3C019996; MELO3C020500; MELO3C013766
GO:0009570	chloroplast stroma	CELLULAR_COMPONENT	1	0 005873914	17	366	347	16398	MELO3C009550; MELO3C009032; MELO3C008481; MELO3C007398; MELO3C014178; MELO3C011196; MELO3C008932; MELO3C009713; MELO3C023469; MELO3C022228; MELO3C023047; MELO3C019011; MELO3C026897; MELO3C015151; MELO3C025023; MELO3C011825; MELO3C016951	MELO3C013732; MELO3C021919; MELO3C012764; MELO3C002161; MELO3C008146; MELO3C006088; MELO3C009475; MELO3C013172; MELO3C004223; MELO3C005674; MELO3C003137; MELO3C001992; MELO3C008946; MELO3C003811; MELO3C001998; MELO3C003814; MELO3C021355; MELO3C0 6680; MELO3C0 6681; MELO3C017890; MELO3C024189; MELO3C015231; MELO3C025397; MELO3C019036; MELO3C017774; MELO3C015233; MELO3C011439;
GO:0009571	proplastid stroma	CELLULAR_COMPONENT	1	0 021251752	1	0	63	16764	MELO3C023469	
GO:0005775	vacuolar lumen	CELLULAR_COMPONENT	1	0 04205_081	1	1	63	1676	MELO3C008520	MELO3C025752
GO:0044391	ribosomal subunit	CELLULAR_COMPONENT	1	0 034251243	1	283	63	1648	MELO3C017364	MELO3C011310; MELO3C006088; MELO3C012084; MELO3C014262; MELO3C024506; MELO3C020141; MELO3C022441; MELO3C001514; MELO3C0 6201; MELO3C025030; MELO3C017659; MELO3C013984; MELO3C013981; MELO3C009489; MELO3C002294; MELO3C006412; MELO3C025609; MELO3C006411; MELO3C005446; MELO3C006657; MELO3C024994; MELO3C025168; MELO3C022691; MELO3C0 8512; MELO3C011448; MELO3C0 6459; MELO3C024071;

Supplementary Table 2.E Gene Ontology terms (GO terms) of the cluster 2.4 obtained considering the comparison between lines the postharvest ripening time fruit during storage at 20.5°C and 88% relative humidity for 18 d the near-isogenic line SC10-2 and its parental "Piel de Sapo" obtained according to the differentially expressed gene pattern (Supl. Table 2.A)

GO ID	GO Name	GO Category	FDR	P-Value	SC10-2	PS	Non Annot Test	Non Annot Reference	TestSet Sequences	RefSet Sequences
GO 0071011	precatalytic spliceosome	CELLULAR_COMPONENT	0,191781685	1,83E-04	6	41	301	16780	MELO3C026304; MELO3C008076; MELO3C024028; MELO3C014555; MELO3C008690; MELO3C020824	MELO3C012489; MELO3C011851; MELO3C002181; MELO3C013333; MELO3C008488; MELO3C008344; MELO3C014122; MELO3C004440; MELO3C022928; MELO3C008023; MELO3C004123; MELO3C002120; MELO3C006787; MELO3C024822; MELO3C024685; MELO3C023475; MELO3C017338; MELO3C009580; MELO3C011414; MELO3C012449; MELO3C009381; MELO3C012622; MELO3C012214; MELO3C013443; MELO3C008151; MELO3C008332; MELO3C015907;
GO 0008270	zinc ion binding	MOLECULAR_FUNCTION	0,502199987	5,85E-04	40	1237	267	15584	MELO3C007075; MELO3C007033; MELO3C025859; MELO3C026803; MELO3C022786; MELO3C006802; MELO3C002148; MELO3C004305; MELO3C025977; MELO3C004944; MELO3C002767; MELO3C018461; MELO3C018265; MELO3C024385; MELO3C017131; MELO3C015891; MELO3C026640; MELO3C003619; MELO3C017657; MELO3C010985; MELO3C019616; MELO3C008330; MELO3C015867; MELO3C013587; MELO3C015627; MELO3C013440; MELO3C014199;	MELO3C004460; MELO3C005792; MELO3C014022; MELO3C007732; MELO3C005559; MELO3C009914; MELO3C007735; MELO3C003139; MELO3C009913; MELO3C026249; MELO3C010904; MELO3C015110; MELO3C019951; MELO3C018864; MELO3C017536; MELO3C018624; MELO3C017777; MELO3C017537; MELO3C021804; MELO3C021806; MELO3C004472; MELO3C012095; MELO3C004232; MELO3C002297; MELO3C002055; MELO3C004237; MELO3C004239;
GO 0005689	U12-type spliceosomal complex	CELLULAR_COMPONENT	0,614567138	8,46E-04	3	8	304	16813	MELO3C014555; MELO3C008690; MELO3C006785	MELO3C019829; MELO3C017020; MELO3C001824; MELO3C015907; MELO3C006787; MELO3C024822; MELO3C016998; MELO3C023823
GO 0047938	glucose-6-phosphate 1-epimerase activity	MOLECULAR_FUNCTION	0,64064555	9,49E-04	2	1	305	16820	MELO3C016314; MELO3C006055	MELO3C004001
GO 0006406	mRNA export from nucleus	BIOLOGICAL_PROCESS	0,826988708	0,001475555	4	24	303	16797	MELO3C026304; MELO3C003078; MELO3C015733; MELO3C014129	MELO3C011256; MELO3C014532; MELO3C013443; MELO3C020407; MELO3C005265; MELO3C005694; MELO3C004622; MELO3C021931; MELO3C021887; MELO3C016280; MELO3C022166; MELO3C009808; MELO3C005946; MELO3C015492; MELO3C025497; MELO3C025498; MELO3C019034; MELO3C026441; MELO3C011924; MELO3C015113; MELO3C013879; MELO3C012713; MELO3C015447; MELO3C016756
GO 0031053	primary miRNA processing	BIOLOGICAL_PROCESS	0,826988708	0,001876102	2	2	305	16819	MELO3C026304; MELO3C015627	MELO3C005929; MELO3C015158

GO 2000241	regulation of reproductive process	BIOLOGICAL_PROCESS	1	0,03397942	5	95	302	16726	MELO3C026304; MELO3C004944; MELO3C011550; MELO3C007033; MELO3C015733	MELO3C006243; MELO3C012361; MELO3C006121; MELO3C007457; MELO3C020900; MELO3C006520; MELO3C005035; MELO3C009633; MELO3C004347; MELO3C024822; MELO3C019031; MELO3C018062; MELO3C022443; MELO3C021157; MELO3C018187; MELO3C026243; MELO3C020263; MELO3C025152; MELO3C017216; MELO3C015512; MELO3C026161; MELO3C017812; MELO3C025191; MELO3C005161; MELO3C021929; MELO3C005162; MELO3C008151;
GO 0019919	peptidyl-arginine methylation, to asymmetrical-dimethyl arginine	BIOLOGICAL_PROCESS	1	0,017923867	1	0	306	16821	MELO3C026636	
GO 0002121	inter-male aggressive behavior	BIOLOGICAL_PROCESS	1	0,035527497	1	1	306	16820	MELO3C015733	MELO3C026612
GO 0031119	tRNA pseudouridine synthesis	BIOLOGICAL_PROCESS	1	0,004579945	2	4	305	16817	MELO3C021228; MELO3C017384	MELO3C004192; MELO3C019957; MELO3C021593; MELO3C011820
GO 0000184	nuclear-transcribed mRNA catabolic process, nonsense-mediated decay	BIOLOGICAL_PROCESS	1	0,044805879	2	17	305	16804	MELO3C026304; MELO3C024028	MELO3C015714; MELO3C011145; MELO3C013051; MELO3C008956; MELO3C006767; MELO3C021931; MELO3C008955; MELO3C026612; MELO3C026327; MELO3C007816; MELO3C025497; MELO3C003804; MELO3C025498; MELO3C026263; MELO3C015113; MELO3C013879; MELO3C026290
GO 0045893	positive regulation of transcription, DNA-templated	BIOLOGICAL_PROCESS	1	0,049494568	4	73	303	16748	MELO3C010748; MELO3C007103; MELO3C004553; MELO3C012788	MELO3C013015; MELO3C006760; MELO3C005791; MELO3C008304; MELO3C006520; MELO3C007015; MELO3C004622; MELO3C003216; MELO3C022562; MELO3C017295; MELO3C019433; MELO3C019554; MELO3C017650; MELO3C024460; MELO3C015512; MELO3C017429; MELO3C015209; MELO3C006131; MELO3C020474; MELO3C003429; MELO3C015360; MELO3C024352; MELO3C016099; MELO3C011649; MELO3C015367; MELO3C015885; MELO3C018910;
GO 0048367	shoot system development	BIOLOGICAL_PROCESS	1	0,043991757	9	235	298	16586	MELO3C018195; MELO3C004944; MELO3C015627; MELO3C011550; MELO3C007033; MELO3C010350; MELO3C016101; MELO3C008248; MELO3C022204	MELO3C006085; MELO3C021918; MELO3C006880; MELO3C008942; MELO3C006520; MELO3C022209; MELO3C005674; MELO3C004347; MELO3C007615; MELO3C006888; MELO3C022443; MELO3C003937; MELO3C026243; MELO3C020263; MELO3C025152; MELO3C013857; MELO3C021929; MELO3C013621; MELO3C002050; MELO3C006890; MELO3C002052; MELO3C020718; MELO3C007500; MELO3C023546; MELO3C007746; MELO3C008956; MELO3C008955;
GO 0000740	nuclear membrane fusion	BIOLOGICAL_PROCESS	1	0,017923867	1	0	306	16821	MELO3C023526	
GO 0051410	detoxification of nitrogen compound	BIOLOGICAL_PROCESS	1	0,035527497	1	1	306	16820	MELO3C025585	MELO3C021201

GO 0006606	protein import into nucleus	BIOLOGICAL_PROCESS	1	0,039165002	3	39	304	16782	MELO3C004204; MELO3C016308; MELO3C020533	MELO3C012585; MELO3C008488; MELO3C012584; MELO3C012087; MELO3C004123; MELO3C021613; MELO3C005895; MELO3C014681; MELO3C005893; MELO3C016280; MELO3C022166; MELO3C000796; MELO3C000453; MELO3C026441; MELO3C024782; MELO3C013982; MELO3C014532; MELO3C020836; MELO3C004174; MELO3C004173; MELO3C009840; MELO3C011020; MELO3C010592; MELO3C012192; MELO3C006015; MELO3C000249; MELO3C005424;
GO 0009658	chloroplast organization	BIOLOGICAL_PROCESS	1	0,036841102	3	38	304	16783	MELO3C023560; MELO3C006974; MELO3C013476	MELO3C013793; MELO3C008920; MELO3C020966; MELO3C003135; MELO3C007638; MELO3C008847; MELO3C002785; MELO3C020500; MELO3C020985; MELO3C003878; MELO3C005838; MELO3C015693; MELO3C025397; MELO3C010707; MELO3C019337; MELO3C010989; MELO3C014926; MELO3C024185; MELO3C011812; MELO3C014943; MELO3C019509; MELO3C009680; MELO3C014156; MELO3C005683; MELO3C003560; MELO3C026919; MELO3C005565;
GO 0009408	response to heat	BIOLOGICAL_PROCESS	1	0,005582333	6	84	301	16737	MELO3C013974; MELO3C018950; MELO3C010748; MELO3C004553; MELO3C023526; MELO3C020589	MELO3C008263; MELO3C005873; MELO3C005035; MELO3C008589; MELO3C014183; MELO3C005674; MELO3C009996; MELO3C018780; MELO3C026886; MELO3C018023; MELO3C018660; MELO3C001916; MELO3C019039; MELO3C012925; MELO3C015312; MELO3C016449; MELO3C012455; MELO3C012136; MELO3C012456; MELO3C015608; MELO3C012331; MELO3C009840; MELO3C014230; MELO3C005884; MELO3C008677; MELO3C009127; MELO3C020872;
GO 2000011	regulation of adaxial/abaxial pattern formation	BIOLOGICAL_PROCESS	1	0,017923867	1	0	306	16821	MELO3C015627	
GO 0002474	antigen processing and presentation of peptide antigen via MHC class I	BIOLOGICAL_PROCESS	1	0,038566615	4	67	303	16754	MELO3C022707; MELO3C025232; MELO3C013359; MELO3C009879	MELO3C012564; MELO3C020827; MELO3C021718; MELO3C002481; MELO3C002361; MELO3C009310; MELO3C003650; MELO3C022725; MELO3C006565; MELO3C007214; MELO3C021950; MELO3C005757; MELO3C016083; MELO3C005912; MELO3C010625; MELO3C012407; MELO3C014436; MELO3C014876; MELO3C009880; MELO3C014395; MELO3C003660; MELO3C006972; MELO3C006615; MELO3C025768; MELO3C019642; MELO3C022053; MELO3C016132;
GO 0090630	activation of GTPase activity	BIOLOGICAL_PROCESS	1	0,035527497	1	1	306	16820	MELO3C018195	MELO3C013721

GO 0006986	response to unfolded protein	BIOLOGICAL_PROCESS	1	0,018771079	2	10	305	16811	MELO3C022707; MELO3C010748	MELO3C021891; MELO3C007383; MELO3C010795; MELO3C012198; MELO3C018660; MELO3C009730; MELO3C006478; MELO3C012527; MELO3C017118; MELO3C005757
GO 0047497	mitochondrion transport along microtubule	BIOLOGICAL_PROCESS	1	0,035527497	1	1	306	16820	MELO3C004273	MELO3C015839
GO 0045071	negative regulation of viral genome replication	BIOLOGICAL_PROCESS	1	0,017923867	1	0	306	16821	MELO3C026304	
GO 0051085	chaperone mediated protein folding requiring cofactor	BIOLOGICAL_PROCESS	1	0,035527497	1	1	306	16820	MELO3C023526	MELO3C007116
GO 0031124	mRNA 3'-end processing	BIOLOGICAL_PROCESS	1	0,005969919	3	18	304	16803	MELO3C026304; MELO3C004944; MELO3C015733	MELO3C005161; MELO3C011256; MELO3C005162; MELO3C008873; MELO3C009412; MELO3C005265; MELO3C021828; MELO3C008722; MELO3C002045; MELO3C006125; MELO3C021974; MELO3C002115; MELO3C004637; MELO3C024435; MELO3C022443; MELO3C005946; MELO3C027241; MELO3C011126
GO 0019933	cAMP-mediated signaling	BIOLOGICAL_PROCESS	1	0,035527497	1	1	306	16820	MELO3C006948	MELO3C026602
GO 0007094	mitotic spindle assembly checkpoint	BIOLOGICAL_PROCESS	1	0,036476381	2	15	305	16806	MELO3C025232; MELO3C013359	MELO3C011895; MELO3C014684; MELO3C014573; MELO3C003047; MELO3C006972; MELO3C022930; MELO3C004622; MELO3C005866; MELO3C005733; MELO3C024685; MELO3C017066; MELO3C017087; MELO3C026580; MELO3C017995; MELO3C012437
GO 0001666	response to hypoxia	BIOLOGICAL_PROCESS	1	0,025279833	2	12	305	16809	MELO3C024028; MELO3C010748	MELO3C025534; MELO3C025535; MELO3C008938; MELO3C011021; MELO3C017087; MELO3C009145; MELO3C004189; MELO3C007039; MELO3C026482; MELO3C015302; MELO3C013879; MELO3C021953
GO 0055062	phosphate ion homeostasis	BIOLOGICAL_PROCESS	1	0,035527497	1	1	306	16820	MELO3C010297	MELO3C007283
GO 0009963	positive regulation of flavonoid biosynthetic process	BIOLOGICAL_PROCESS	1	0,035527497	1	1	306	16820	MELO3C027219	MELO3C016879
GO 0051382	kinetochore assembly	BIOLOGICAL_PROCESS	1	0,017923867	1	0	306	16821	MELO3C006948	
GO 0042542	response to hydrogen peroxide	BIOLOGICAL_PROCESS	1	0,002685504	3	13	304	16808	MELO3C013974; MELO3C010748; MELO3C020589	MELO3C013522; MELO3C016937; MELO3C002020; MELO3C007439; MELO3C006536; MELO3C002338; MELO3C005923; MELO3C018023; MELO3C012939; MELO3C012925; MELO3C017883; MELO3C021171; MELO3C017636
GO 0048644	muscle organ morphogenesis	BIOLOGICAL_PROCESS	1	0,017923867	1	0	306	16821	MELO3C008076	
GO 0006206	pyrimidine nucleobase metabolic process	BIOLOGICAL_PROCESS	1	0,04055957	2	16	305	16805	MELO3C005067; MELO3C022212	MELO3C018607; MELO3C014554; MELO3C012330; MELO3C005122; MELO3C014189; MELO3C002362; MELO3C003165; MELO3C009854; MELO3C023314; MELO3C002149; MELO3C003814; MELO3C011808; MELO3C015352; MELO3C015199; MELO3C010935; MELO3C013218
GO 0000350	generation of catalytic spliceosome for second transesterification step	BIOLOGICAL_PROCESS	1	0,017923867	1	0	306	16821	MELO3C015733	
GO 0010267	production of ta-siRNAs involved in RNA interference	BIOLOGICAL_PROCESS	1	0,013103927	2	8	305	16813	MELO3C015627; MELO3C014129	MELO3C010254; MELO3C011257; MELO3C015492; MELO3C005929; MELO3C010042; MELO3C022813; MELO3C023207; MELO3C012127
GO 0010362	negative regulation of anion channel activity by blue light	BIOLOGICAL_PROCESS	1	0,035527497	1	1	306	16820	MELO3C013476	MELO3C025720

GO 0006787	porphyrin-containing compound catabolic process	BIOLOGICAL_PROCESS	1	0,032563635	2	14	305	16807	MELO3C010350; MELO3C023590	MELO3C016736; MELO3C019918; MELO3C014286; MELO3C006434; MELO3C008435; MELO3C024905; MELO3C020912; MELO3C007554; MELO3C025347; MELO3C004867; MELO3C022310; MELO3C005616; MELO3C018440; MELO3C025982
GO 0043097	pyrimidine nucleoside salvage	BIOLOGICAL_PROCESS	1	0,017923867	1	0	306	16821	MELO3C022212	
GO 0006419	alanyl-tRNA aminoacylation	BIOLOGICAL_PROCESS	1	0,010607789	2	7	305	16814	MELO3C000425; MELO3C027308	MELO3C012870; MELO3C010097; MELO3C024031; MELO3C000756; MELO3C018624; MELO3C027271; MELO3C013645
GO 0040022	feminization of hermaphroditic germ-line	BIOLOGICAL_PROCESS	1	0,008348753	2	6	305	16815	MELO3C026304; MELO3C015733	MELO3C006787; MELO3C005946; MELO3C021157; MELO3C009413; MELO3C017216; MELO3C015907
GO 0000209	protein polyubiquitination	BIOLOGICAL_PROCESS	1	0,009420097	5	67	302	16754	MELO3C018461; MELO3C022707; MELO3C025232; MELO3C013359; MELO3C009879	MELO3C012564; MELO3C011153; MELO3C020827; MELO3C021718; MELO3C002481; MELO3C002361; MELO3C009310; MELO3C003650; MELO3C022725; MELO3C006565; MELO3C007214; MELO3C021950; MELO3C016083; MELO3C005912; MELO3C012407; MELO3C014436; MELO3C014876; MELO3C009880; MELO3C014395; MELO3C003660; MELO3C006972; MELO3C006615; MELO3C025768; MELO3C026578; MELO3C019642; MELO3C022053; MELO3C002738;
GO 0007525	somatic muscle development	BIOLOGICAL_PROCESS	1	0,035527497	1	1	306	16820	MELO3C018265	MELO3C025387
GO 0007638	mechanosensory behavior	BIOLOGICAL_PROCESS	1	0,017923867	1	0	306	16821	MELO3C008076	
GO 0006369	termination of RNA polymerase II transcription	BIOLOGICAL_PROCESS	1	0,036476381	2	15	305	16806	MELO3C026304; MELO3C015733	MELO3C008873; MELO3C003340; MELO3C002045; MELO3C008589; MELO3C006125; MELO3C021974; MELO3C002115; MELO3C004637; MELO3C017020; MELO3C024435; MELO3C005946; MELO3C001923; MELO3C016377; MELO3C016378; MELO3C011126
GO 0032526	response to retinoic acid	BIOLOGICAL_PROCESS	1	0,017923867	1	0	306	16821	MELO3C026102	
GO 0045451	pole plasm oskar mRNA localization	BIOLOGICAL_PROCESS	1	0,035527497	1	1	306	16820	MELO3C024028	MELO3C005946
GO 0010198	synergid death	BIOLOGICAL_PROCESS	1	0,017923867	1	0	306	16821	MELO3C023526	
GO 0009640	photomorphogenesis	BIOLOGICAL_PROCESS	1	0,010927009	3	23	304	16798	MELO3C023560; MELO3C013440; MELO3C020783	MELO3C027290; MELO3C009584; MELO3C007283; MELO3C006046; MELO3C014684; MELO3C003141; MELO3C005593; MELO3C008232; MELO3C020865; MELO3C000307; MELO3C005179; MELO3C000009; MELO3C004148; MELO3C000029; MELO3C026327; MELO3C021982; MELO3C002738; MELO3C024155; MELO3C019731; MELO3C010759; MELO3C016115; MELO3C011159; MELO3C017834

GO 0006370	7-methylguanosine mRNA capping	BIOLOGICAL_PROCESS	1	0,028283234	3	34	304	16787	MELO3C026304; MELO3C009776; MELO3C012788	MELO3C010981; MELO3C010201; MELO3C005694; MELO3C021758; MELO3C008589; MELO3C002888; MELO3C022087; MELO3C020022; MELO3C017775; MELO3C015158; MELO3C019837; MELO3C017579; MELO3C027194; MELO3C015712; MELO3C007284; MELO3C013741; MELO3C008774; MELO3C008157; MELO3C002173; MELO3C006473; MELO3C008414; MELO3C005421; MELO3C003222; MELO3C007526; MELO3C020474; MELO3C026776; MELO3C023983;
GO 0009644	response to high light intensity	BIOLOGICAL_PROCESS	1	0,005185079	3	17	304	16804	MELO3C013974; MELO3C010748; MELO3C020589	MELO3C009241; MELO3C006079; MELO3C005482; MELO3C006384; MELO3C002020; MELO3C011150; MELO3C024348; MELO3C006536; MELO3C005923; MELO3C018023; MELO3C026365; MELO3C010229; MELO3C012925; MELO3C017883; MELO3C021171; MELO3C017876; MELO3C011885
GO 0006259	DNA metabolic process	BIOLOGICAL_PROCESS	1	0,011324473	4	678	303	16143	MELO3C009776; MELO3C026141; MELO3C010378; MELO3C010806	MELO3C006760; MELO3C020706; MELO3C014263; MELO3C013053; MELO3C014021; MELO3C002044; MELO3C014020; MELO3C006520; MELO3C004226; MELO3C002168; MELO3C003016; MELO3C008825; MELO3C008704; MELO3C004227; MELO3C008829; MELO3C003019; MELO3C027337; MELO3C026127; MELO3C027214; MELO3C025396; MELO3C025395; MELO3C017775; MELO3C010901; MELO3C018624; MELO3C014035; MELO3C002173; MELO3C008833;
GO 0010188	response to microbial phytotoxin	BIOLOGICAL_PROCESS	1	0,035527497	1	1	306	16820	MELO3C002148	MELO3C004372
GO 0006221	pyrimidine nucleotide biosynthetic process	BIOLOGICAL_PROCESS	1	0,04920819	2	18	305	16803	MELO3C009423; MELO3C005067	MELO3C008043; MELO3C012572; MELO3C005122; MELO3C014189; MELO3C006256; MELO3C006993; MELO3C009854; MELO3C023314; MELO3C002149; MELO3C002338; MELO3C024340; MELO3C016297; MELO3C015352; MELO3C005939; MELO3C017855; MELO3C015940; MELO3C011305; MELO3C013218
GO 0042752	regulation of circadian rhythm	BIOLOGICAL_PROCESS	1	0,008348753	2	6	305	16815	MELO3C025049; MELO3C020783	MELO3C015209; MELO3C025357; MELO3C005120; MELO3C004018; MELO3C025191; MELO3C011754
GO 0010155	regulation of proton transport	BIOLOGICAL_PROCESS	1	0,035527497	1	1	306	16820	MELO3C016696	MELO3C025720
GO 0004665	prephenate dehydrogenase (NADP+) activity	MOLECULAR_FUNCTION	1	0,017923867	1	0	306	16821	MELO3C004475	

GO 0016758	transferase activity, transferring hexosyl groups	MOLECULAR_FUNCTION	1	0,011308174	1	391	306	16430	MELO3C017104	MELO3C018629; MELO3C019719; MELO3C020949; MELO3C002165; MELO3C002287; MELO3C002166; MELO3C005795; MELO3C002047; MELO3C005799; MELO3C026247; MELO3C026369; MELO3C016445; MELO3C018627; MELO3C021805; MELO3C012097; MELO3C004474; MELO3C012096; MELO3C007749; MELO3C018630; MELO3C018632; MELO3C026373; MELO3C024194; MELO3C018631; MELO3C018634; MELO3C016697; MELO3C025283; MELO3C018635;
GO 0016881	acid-amino acid ligase activity	MOLECULAR_FUNCTION	1	0,009142966	4	42	303	16779	MELO3C015867; MELO3C022707; MELO3C025232; MELO3C013359	MELO3C016407; MELO3C011378; MELO3C006100; MELO3C011153; MELO3C006046; MELO3C014684; MELO3C020827; MELO3C005691; MELO3C009310; MELO3C011072; MELO3C005277; MELO3C005674; MELO3C026704; MELO3C007439; MELO3C005733; MELO3C009417; MELO3C021530; MELO3C021252; MELO3C024782; MELO3C026341; MELO3C014115; MELO3C009120; MELO3C007283; MELO3C020814; MELO3C005683; MELO3C006555; MELO3C006710;
GO 0018822	nitrile hydratase activity	MOLECULAR_FUNCTION	1	0,017923867	1	0	306	16821	MELO3C025585	
GO 0080079	cellobiose glucosidase activity	MOLECULAR_FUNCTION	1	0,017923867	1	0	306	16821	MELO3C021253	
GO 0047172	shikimate O-hydroxycinnamoyltransferase activity	MOLECULAR_FUNCTION	1	0,035527497	1	1	306	16820	MELO3C027219	MELO3C023474
GO 0004402	histone acetyltransferase activity	MOLECULAR_FUNCTION	1	0,017693064	3	28	304	16793	MELO3C014860; MELO3C004100; MELO3C010806	MELO3C007593; MELO3C013698; MELO3C011851; MELO3C011774; MELO3C013356; MELO3C009471; MELO3C006243; MELO3C007211; MELO3C013253; MELO3C009635; MELO3C007015; MELO3C009633; MELO3C002885; MELO3C022788; MELO3C017030; MELO3C026222; MELO3C015474; MELO3C012527; MELO3C005161; MELO3C005162; MELO3C010476; MELO3C007627; MELO3C004615; MELO3C001964; MELO3C002318; MELO3C026234; MELO3C026433;
GO 0000170	sphingosine hydroxylase activity	MOLECULAR_FUNCTION	1	0,035527497	1	1	306	16820	MELO3C012088	MELO3C008543
GO 0033862	UMP kinase activity	MOLECULAR_FUNCTION	1	0,035527497	1	1	306	16820	MELO3C009423	MELO3C008043
GO 0050638	taxadien-5-alpha-ol O-acetyltransferase activity	MOLECULAR_FUNCTION	1	0,035527497	1	1	306	16820	MELO3C018368	MELO3C025311
GO 0080061	indole-3-acetonitrile nitrilase activity	MOLECULAR_FUNCTION	1	0,017923867	1	0	306	16821	MELO3C025585	

GO 0005096	GTPase activator activity	MOLECULAR_FUNCTION	1	0,009142966	4	42	303	16779	MELO3C018195; MELO3C007075; MELO3C011716; MELO3C018265	MELO3C012464; MELO3C013850; MELO3C002160; MELO3C013431; MELO3C004462; MELO3C014242; MELO3C004980; MELO3C025639; MELO3C006548; MELO3C004547; MELO3C003413; MELO3C003977; MELO3C021110; MELO3C006408; MELO3C022488; MELO3C017792; MELO3C018264; MELO3C020360; MELO3C025077; MELO3C019359; MELO3C015111; MELO3C002808; MELO3C027373; MELO3C017654; MELO3C017813; MELO3C017779; MELO3C013721;
GO 0051741	2-methyl-6-phytyl-1,4-benzoquinone methyltransferase activity	MOLECULAR_FUNCTION	1	0,017923867	1	0	306	16821	MELO3C014321	
GO 0015220	choline transmembrane transporter activity	MOLECULAR_FUNCTION	1	0,017923867	1	0	306	16821	MELO3C020808	
GO 0051082	unfolded protein binding	MOLECULAR_FUNCTION	1	0,021826864	7	148	300	16673	MELO3C004636; MELO3C013792; MELO3C008871; MELO3C018950; MELO3C009408; MELO3C023526; MELO3C011379	MELO3C013215; MELO3C013333; MELO3C014661; MELO3C020425; MELO3C007610; MELO3C009996; MELO3C008428; MELO3C003534; MELO3C026888; MELO3C004506; MELO3C026886; MELO3C024104; MELO3C019433; MELO3C001916; MELO3C017379; MELO3C018866; MELO3C004194; MELO3C014551; MELO3C009245; MELO3C010230; MELO3C020799; MELO3C005449; MELO3C002214; MELO3C023267; MELO3C006935; MELO3C007908; MELO3C016178;
GO 0004697	protein kinase C activity	MOLECULAR_FUNCTION	1	0,04920819	2	18	305	16803	MELO3C007047; MELO3C013476	MELO3C012376; MELO3C012751; MELO3C002781; MELO3C004520; MELO3C006602; MELO3C005408; MELO3C023003; MELO3C001920; MELO3C024168; MELO3C001921; MELO3C005407; MELO3C025720; MELO3C015495; MELO3C017135; MELO3C001919; MELO3C010857; MELO3C016889; MELO3C021090
GO 0050662	coenzyme binding	MOLECULAR_FUNCTION	1	0,048984136	1	314	306	16507	MELO3C008985	MELO3C006085; MELO3C016329; MELO3C007053; MELO3C021919; MELO3C007054; MELO3C007051; MELO3C011431; MELO3C013057; MELO3C007057; MELO3C007055; MELO3C007056; MELO3C007612; MELO3C013171; MELO3C006405; MELO3C008946; MELO3C025712; MELO3C007613; MELO3C002842; MELO3C026007; MELO3C002843; MELO3C020385; MELO3C002844; MELO3C026005; MELO3C026006; MELO3C026004; MELO3C027332; MELO3C013979;
GO 0047427	cyanoalanine nitrilase activity	MOLECULAR_FUNCTION	1	0,017923867	1	0	306	16821	MELO3C025585	
GO 0004813	alanine-tRNA ligase activity	MOLECULAR_FUNCTION	1	0,010607789	2	7	305	16814	MELO3C000425; MELO3C027308	MELO3C012870; MELO3C010097; MELO3C024031; MELO3C000756; MELO3C018624; MELO3C027271; MELO3C013645
GO 0047558	3-cyanoalanine hydratase activity	MOLECULAR_FUNCTION	1	0,017923867	1	0	306	16821	MELO3C025585	

GO 0004034	aldose 1-epimerase activity	MOLECULAR_FUNCTION	1	0,008348753	2	6	305	16815	MELO3C016314; MELO3C006055	MELO3C017161; MELO3C004001; MELO3C017162; MELO3C017363; MELO3C017448; MELO3C009884
GO 0005366	myo-inositol proton symporter activity	MOLECULAR_FUNCTION	1	0,017923867	1	0	306	16821	MELO3C017757	
GO 0031624	ubiquitin conjugating enzyme binding	MOLECULAR_FUNCTION	1	0,035527497	1	1	306	16820	MELO3C018461	MELO3C023546
GO 0071522	ureidoglycine aminohydrolase activity	MOLECULAR_FUNCTION	1	0,017923867	1	0	306	16821	MELO3C014174	
GO 0047205	quinate O-hydroxycinnamoyltransferase activity	MOLECULAR_FUNCTION	1	0,017923867	1	0	306	16821	MELO3C027219	
GO 0080124	pheophytinase activity	MOLECULAR_FUNCTION	1	0,017923867	1	0	306	16821	MELO3C023590	
GO 0004137	deoxycytidine kinase activity	MOLECULAR_FUNCTION	1	0,017923867	1	0	306	16821	MELO3C022212	
GO 0008420	CTD phosphatase activity	MOLECULAR_FUNCTION	1	0,035527497	1	1	306	16820	MELO3C010744	MELO3C007164
GO 0033730	arogenate dehydrogenase (NADP+) activity	MOLECULAR_FUNCTION	1	0,017923867	1	0	306	16821	MELO3C004475	
GO 0042624	ATPase activity, uncoupled	MOLECULAR_FUNCTION	1	0,034590522	3	37	304	16784	MELO3C024028; MELO3C015733; MELO3C017908	MELO3C015615; MELO3C005694; MELO3C004004; MELO3C002023; MELO3C011192; MELO3C021972; MELO3C004027; MELO3C007659; MELO3C017150; MELO3C022562; MELO3C023476; MELO3C026888; MELO3C021157; MELO3C017450; MELO3C024243; MELO3C016189; MELO3C023052; MELO3C024284; MELO3C017528; MELO3C009324; MELO3C015907; MELO3C010251; MELO3C026913; MELO3C025549; MELO3C002213; MELO3C022910; MELO3C002633;
GO 0009882	blue light photoreceptor activity	MOLECULAR_FUNCTION	1	0,035527497	1	1	306	16820	MELO3C013476	MELO3C025720
GO 0016277	[myelin basic protein]-arginine N-methyltransferase activity	MOLECULAR_FUNCTION	1	0,017923867	1	0	306	16821	MELO3C026636	
GO 0004842	ubiquitin-protein transferase activity	MOLECULAR_FUNCTION	1	0,01225715	7	131	300	16690	MELO3C018461; MELO3C011882; MELO3C005490; MELO3C022707; MELO3C025232; MELO3C007711; MELO3C003563	MELO3C003490; MELO3C012003; MELO3C004460; MELO3C011153; MELO3C013694; MELO3C020827; MELO3C014022; MELO3C020149; MELO3C012481; MELO3C022725; MELO3C005277; MELO3C022726; MELO3C026528; MELO3C024469; MELO3C022842; MELO3C007339; MELO3C021512; MELO3C026527; MELO3C004903; MELO3C018740; MELO3C012406; MELO3C012407; MELO3C014427; MELO3C008310; MELO3C020316; MELO3C014270; MELO3C023546;
GO 0004726	non-membrane spanning protein tyrosine phosphatase activity	MOLECULAR_FUNCTION	1	0,035527497	1	1	306	16820	MELO3C021441	MELO3C009840
GO 0071007	U2-type catalytic step 2 spliceosome	CELLULAR_COMPONENT	1	0,017923867	1	0	306	16821	MELO3C015733	

GO 0005730	nucleolus	CELLULAR_COMPONENT	1	0,026607121	10	245	297	16576	MELO3C006160; MELO3C024028; MELO3C015627; MELO3C006154; MELO3C024474; MELO3C016101; MELO3C011408; MELO3C004553; MELO3C004204; MELO3C022204	MELO3C010584; MELO3C011795; MELO3C021919; MELO3C006760; MELO3C003491; MELO3C002168; MELO3C021598; MELO3C024989; MELO3C004227; MELO3C018062; MELO3C019034; MELO3C017650; MELO3C016321; MELO3C014706; MELO3C024180; MELO3C008032; MELO3C010355; MELO3C008157; MELO3C002173; MELO3C014153; MELO3C013185; MELO3C002299; MELO3C023545; MELO3C008835; MELO3C023306; MELO3C006657; MELO3C026259;
GO 0005846	nuclear cap binding complex	CELLULAR_COMPONENT	1	0,017923867	1	0	306	16821	MELO3C026304	
GO 0005783	endoplasmic reticulum	CELLULAR_COMPONENT	1	0,014998725	15	418	292	16403	MELO3C012088; MELO3C022707; MELO3C003282; MELO3C015929; MELO3C003581; MELO3C004023; MELO3C004366; MELO3C003313; MELO3C006316; MELO3C006959; MELO3C022783; MELO3C018461; MELO3C024474; MELO3C012716; MELO3C016696	MELO3C019959; MELO3C003372; MELO3C020821; MELO3C002165; MELO3C002166; MELO3C006405; MELO3C009914; MELO3C006525; MELO3C025156; MELO3C017891; MELO3C024187; MELO3C018740; MELO3C017653; MELO3C017652; MELO3C017413; MELO3C025390; MELO3C016449; MELO3C016219; MELO3C018518; MELO3C002052; MELO3C003263; MELO3C003383; MELO3C017661; MELO3C019722; MELO3C017542; MELO3C015246; MELO3C015126;
GO 0010445	nuclear dicing body	CELLULAR_COMPONENT	1	0,035527497	1	1	306	16820	MELO3C015627	MELO3C005929
GO 0009707	chloroplast outer membrane	CELLULAR_COMPONENT	1	0,04920819	2	18	305	16803	MELO3C021253; MELO3C006974	MELO3C015416; MELO3C017968; MELO3C006133; MELO3C004471; MELO3C016719; MELO3C004591; MELO3C004474; MELO3C002387; MELO3C020610; MELO3C024587; MELO3C017360; MELO3C018772; MELO3C019874; MELO3C014409; MELO3C014605; MELO3C011502; MELO3C011415; MELO3C013766
GO 0009706	chloroplast inner membrane	CELLULAR_COMPONENT	1	0,044030549	3	41	304	16780	MELO3C016354; MELO3C014321; MELO3C014379	MELO3C011311; MELO3C011950; MELO3C014389; MELO3C006105; MELO3C011150; MELO3C006344; MELO3C005999; MELO3C020500; MELO3C026802; MELO3C023998; MELO3C020560; MELO3C004867; MELO3C005838; MELO3C026723; MELO3C023994; MELO3C023131; MELO3C021073; MELO3C021074; MELO3C010989; MELO3C017774; MELO3C010229; MELO3C014578; MELO3C015704; MELO3C016817; MELO3C010074; MELO3C014596; MELO3C023747;
GO 0009705	plant-type vacuole membrane	CELLULAR_COMPONENT	1	0,025279833	2	12	305	16809	MELO3C016475; MELO3C017757	MELO3C011146; MELO3C008088; MELO3C025972; MELO3C026522; MELO3C026971; MELO3C007980; MELO3C003783; MELO3C012405; MELO3C010334; MELO3C008406; MELO3C009170; MELO3C022448

GO 0016607	nuclear speck	CELLULAR_COMPONENT	1	0,016191216	3	27	304	16794	MELO3C024028; MELO3C015627; MELO3C017908	MELO3C011256; MELO3C012489; MELO3C008488; MELO3C004440; MELO3C022928; MELO3C014086; MELO3C005035; MELO3C024822; MELO3C002326; MELO3C016008; MELO3C014823; MELO3C005382; MELO3C015826; MELO3C013781; MELO3C023809; MELO3C023427; MELO3C024757; MELO3C021320; MELO3C017365; MELO3C026275; MELO3C019500; MELO3C016115; MELO3C012616; MELO3C010637; MELO3C019702; MELO3C014459; MELO3C012579
GO 0000151	ubiquitin ligase complex	CELLULAR_COMPONENT	1	0,038140521	6	132	301	16689	MELO3C006948; MELO3C007711; MELO3C011882; MELO3C005490; MELO3C014129; MELO3C009879	MELO3C012003; MELO3C013212; MELO3C013694; MELO3C008023; MELO3C003650; MELO3C020149; MELO3C022725; MELO3C002045; MELO3C022726; MELO3C006647; MELO3C002960; MELO3C026528; MELO3C006645; MELO3C007339; MELO3C021512; MELO3C007855; MELO3C026527; MELO3C019281; MELO3C003537; MELO3C022166; MELO3C025152; MELO3C022280; MELO3C012406; MELO3C012527; MELO3C012407; MELO3C018869; MELO3C017705;
GO 0030692	Noc4p-Nop14p complex	CELLULAR_COMPONENT	1	0,017923867	1	0	306	16821	MELO3C011408	
GO 0000243	commitment complex	CELLULAR_COMPONENT	1	0,017923867	1	0	306	16821	MELO3C026304	
GO 0010168	ER body	CELLULAR_COMPONENT	1	0,017923867	1	0	306	16821	MELO3C012716	

Supplementary Table 2.F Gene Ontology terms (GO terms) of the cluster 2.5 obtained considering the comparison between lines the postharvest ripening time fruit during storage at 20.5°C and 88% relative humidity for 18 d the near-isogenic line SC10-2 and its parental "Piel de Sapo" obtained according to the differentially expressed gene pattern (Supl. Table 2.A)

GO ID	GO Name	GO Category	FDR	P-Value	SC10-2	PS	Non Annot Test	Non Annot Reference	TestSet Sequences	RefSet Sequences
GO 0016308	1-phosphatidylinositol-4-phosphate 5-kinase activity	MOLECULAR_FUNCTION	0,304197153	2,25E-04	3	7	214	16904	MELO3C010456; MELO3C006050; MELO3C003057	MELO3C019075; MELO3C000333; MELO3C012475; MELO3C014374; MELO3C005148; MELO3C009382; MELO3C010116
GO 0055114	oxidation-reduction process	BIOLOGICAL_PROCESS	0,340910349	3,28E-04	7	1688	210	15223	MELO3C024222; MELO3C013829; MELO3C019404; MELO3C009886; MELO3C023986; MELO3C011601; MELO3C001994	MELO3C018628; MELO3C002280; MELO3C005792; MELO3C012088; MELO3C006644; MELO3C004465; MELO3C005795; MELO3C012080; MELO3C015590; MELO3C015591; MELO3C015592; MELO3C015593; MELO3C017772; MELO3C015595; MELO3C015596; MELO3C024061; MELO3C018623; MELO3C018625; MELO3C018626; MELO3C002293; MELO3C007980; MELO3C004475; MELO3C007984; MELO3C008836; MELO3C020952; MELO3C003149; MELO3C005329;
GO 0033169	histone H3-K9 demethylation	BIOLOGICAL_PROCESS	0,404853209	9,43E-04	2	2	215	16909	MELO3C025053; MELO3C019813	MELO3C002327; MELO3C004836
GO 0008270	zinc ion binding	MOLECULAR_FUNCTION	0,404853209	5,80E-04	31	1246	186	15665	MELO3C009670; MELO3C009234; MELO3C014562; MELO3C006367; MELO3C009914; MELO3C022568; MELO3C005513; MELO3C004524; MELO3C002646; MELO3C018264; MELO3C022066; MELO3C012628; MELO3C025053; MELO3C010522; MELO3C013879; MELO3C017755; MELO3C019813; MELO3C009984; MELO3C013883; MELO3C009101; MELO3C025725; MELO3C003423; MELO3C021348; MELO3C021462; MELO3C017380; MELO3C021047; MELO3C017320;	MELO3C004460; MELO3C005792; MELO3C014022; MELO3C007732; MELO3C005559; MELO3C007735; MELO3C003139; MELO3C009913; MELO3C026249; MELO3C010904; MELO3C015110; MELO3C019951; MELO3C018864; MELO3C017536; MELO3C018624; MELO3C017777; MELO3C017537; MELO3C021804; MELO3C021806; MELO3C004472; MELO3C012095; MELO3C004232; MELO3C002297; MELO3C002055; MELO3C004237; MELO3C004239; MELO3C004238;
GO 0031491	nucleosome binding	MOLECULAR_FUNCTION	0,404853209	9,43E-04	2	2	215	16909	MELO3C021353; MELO3C004459	MELO3C021352; MELO3C009890
GO 0005524	ATP binding	MOLECULAR_FUNCTION	0,705878947	0,00310521	41	2020	176	14891	MELO3C016868; MELO3C014687; MELO3C005094; MELO3C013254; MELO3C002382; MELO3C008489; MELO3C003057; MELO3C020666; MELO3C021353; MELO3C006925; MELO3C023098; MELO3C026025; MELO3C019411; MELO3C018344; MELO3C026263; MELO3C018106; MELO3C013879; MELO3C009480; MELO3C012730; MELO3C027092; MELO3C004591; MELO3C005565; MELO3C009328; MELO3C014272; MELO3C003146; MELO3C003222; MELO3C023986;	MELO3C014269; MELO3C003133; MELO3C004463; MELO3C007972; MELO3C006648; MELO3C007978; MELO3C008825; MELO3C003139; MELO3C008829; MELO3C026243; MELO3C019951; MELO3C000093; MELO3C025392; MELO3C015599; MELO3C018624; MELO3C020958; MELO3C008832; MELO3C008831; MELO3C002299; MELO3C008835; MELO3C005329; MELO3C008838; MELO3C026256; MELO3C024079; MELO3C019967; MELO3C019939; MELO3C019938;

GO 0008353	RNA polymerase II carboxy-terminal domain kinase activity	MOLECULAR_FUNCTION	0,780094579	0,00520173	3	25	214	16886	MELO3C022196; MELO3C019411; MELO3C002382	MELO3C007454; MELO3C002140; MELO3C012361; MELO3C009014; MELO3C002003; MELO3C004567; MELO3C007615; MELO3C001212; MELO3C004349; MELO3C001378; MELO3C006605; MELO3C020186; MELO3C022286; MELO3C017059; MELO3C015376; MELO3C025274; MELO3C014702; MELO3C013799; MELO3C008774; MELO3C009967; MELO3C007623; MELO3C024972; MELO3C017342; MELO3C026178; MELO3C011886
GO 0043044	ATP-dependent chromatin remodeling	BIOLOGICAL_PROCESS	0,788464754	0,00542445	2	7	215	16904	MELO3C021353; MELO3C004459	MELO3C021352; MELO3C021430; MELO3C007903; MELO3C007894; MELO3C006760; MELO3C005059; MELO3C007648
GO 0006972	hyperosmotic response	BIOLOGICAL_PROCESS	0,819860774	0,01136775	2	11	215	16900	MELO3C008815; MELO3C025349	MELO3C004428; MELO3C009971; MELO3C010211; MELO3C006142; MELO3C006721; MELO3C012085; MELO3C008666; MELO3C004127; MELO3C024239; MELO3C002752; MELO3C013249
GO 0032790	ribosome disassembly	BIOLOGICAL_PROCESS	0,819860774	0,01266931	1	0	216	16911	MELO3C005565	
GO 0007126	meiotic nuclear division	BIOLOGICAL_PROCESS	0,819860774	0,00816862	5	93	212	16818	MELO3C023475; MELO3C014687; MELO3C023986; MELO3C004459; MELO3C014877	MELO3C012361; MELO3C003892; MELO3C006201; MELO3C024822; MELO3C004027; MELO3C016280; MELO3C018062; MELO3C003338; MELO3C026602; MELO3C005714; MELO3C026127; MELO3C021157; MELO3C019674; MELO3C018187; MELO3C019510; MELO3C021272; MELO3C024265; MELO3C024782; MELO3C015113; MELO3C017258; MELO3C015235; MELO3C017338; MELO3C015434; MELO3C017216; MELO3C012446; MELO3C010743; MELO3C008594;
GO 0034551	mitochondrial respiratory chain complex III assembly	BIOLOGICAL_PROCESS	0,819860774	0,01266931	1	0	216	16911	MELO3C008037	
GO 0045843	negative regulation of striated muscle tissue development	BIOLOGICAL_PROCESS	0,819860774	0,01266931	1	0	216	16911	MELO3C015103	
GO 0018996	molting cycle, collagen and cuticulin-based cuticle	BIOLOGICAL_PROCESS	0,819860774	0,0089881	3	31	214	16880	MELO3C008815; MELO3C023475; MELO3C003222	MELO3C015218; MELO3C014920; MELO3C010960; MELO3C008488; MELO3C006662; MELO3C004440; MELO3C007374; MELO3C004123; MELO3C009413; MELO3C004945; MELO3C026800; MELO3C025972; MELO3C025310; MELO3C023594; MELO3C016321; MELO3C024020; MELO3C017216; MELO3C013218; MELO3C010795; MELO3C008690; MELO3C007085; MELO3C014153; MELO3C023127; MELO3C017291; MELO3C005963; MELO3C023427; MELO3C017290;
GO 0030183	B cell differentiation	BIOLOGICAL_PROCESS	0,819860774	0,01266931	1	0	216	16911	MELO3C015103	
GO 0048577	negative regulation of short-day photoperiodism, flowering	BIOLOGICAL_PROCESS	0,819860774	0,01266931	1	0	216	16911	MELO3C019813	
GO 0048579	negative regulation of long-day photoperiodism, flowering	BIOLOGICAL_PROCESS	0,819860774	0,01266931	1	0	216	16911	MELO3C019813	
GO 0030538	embryonic genitalia morphogenesis	BIOLOGICAL_PROCESS	0,819860774	0,01266931	1	0	216	16911	MELO3C013879	
GO 0035103	sterol regulatory element binding protein cleavage	BIOLOGICAL_PROCESS	0,819860774	0,01266931	1	0	216	16911	MELO3C025349	
GO 0001570	vasculogenesis	BIOLOGICAL_PROCESS	0,819860774	0,01266931	1	0	216	16911	MELO3C015103	
GO 0010600	regulation of auxin biosynthetic process	BIOLOGICAL_PROCESS	0,819860774	0,01266931	1	0	216	16911	MELO3C025091	
GO 0003696	satellite DNA binding	MOLECULAR_FUNCTION	0,819860774	0,01266931	1	0	216	16911	MELO3C023986	
GO 0004636	phosphoribosyl-ATP diphosphatase activity	MOLECULAR_FUNCTION	0,819860774	0,01266931	1	0	216	16911	MELO3C005094	
GO 0004635	phosphoribosyl-AMP cyclohydrolase activity	MOLECULAR_FUNCTION	0,819860774	0,01266931	1	0	216	16911	MELO3C005094	
GO 0004651	polynucleotide 5'-phosphatase activity	MOLECULAR_FUNCTION	0,819860774	0,01266931	1	0	216	16911	MELO3C003222	
GO 0004572	mannosyl-oligosaccharide 1,3-1,6-alpha-mannosidase activity	MOLECULAR_FUNCTION	0,819860774	0,01266931	1	0	216	16911	MELO3C009914	
GO 0008139	nuclear localization sequence binding	MOLECULAR_FUNCTION	0,819860774	0,01266931	1	0	216	16911	MELO3C020836	
GO 0017077	oxidative phosphorylation uncoupler activity	MOLECULAR_FUNCTION	0,819860774	0,01266931	1	0	216	16911	MELO3C014724	

GO 0003918	DNA topoisomerase type II (ATP-hydrolyzing) activity	MOLECULAR_FUNCTION	0,819860774	0,00969922	2	10	215	16901	MELO3C019163; MELO3C023986	MELO3C022420; MELO3C011386; MELO3C003071; MELO3C019089; MELO3C014153; MELO3C024924; MELO3C014639; MELO3C019090; MELO3C024756; MELO3C024755
GO 0004484	mRNA guanylyltransferase activity	MOLECULAR_FUNCTION	0,819860774	0,01266931	1	0	216	16911	MELO3C003222	
GO 0008672	2-dehydro-3-deoxyglucarate aldolase activity	MOLECULAR_FUNCTION	0,819860774	0,01266931	1	0	216	16911	MELO3C013779	
GO 0004743	pyruvate kinase activity	MOLECULAR_FUNCTION	0,819860774	0,00672422	2	8	215	16903	MELO3C014272; MELO3C011769	MELO3C005271; MELO3C014732; MELO3C003381; MELO3C018027; MELO3C019624; MELO3C024509; MELO3C024508; MELO3C006964
GO 0034990	nuclear mitotic cohesin complex	CELLULAR_COMPONENT	0,819860774	0,01266931	1	0	216	16911	MELO3C012730	
GO 0008623	CHRAC	CELLULAR_COMPONENT	0,819860774	0,01266931	1	0	216	16911	MELO3C023986	
GO 0000800	lateral element	CELLULAR_COMPONENT	0,819860774	0,01266931	1	0	216	16911	MELO3C014687	
GO 0016246	RNA interference	BIOLOGICAL_PROCESS	0,861424734	0,014041	3	37	214	16874	MELO3C020836; MELO3C013879; MELO3C014035	MELO3C011257; MELO3C007894; MELO3C014221; MELO3C005153; MELO3C014440; MELO3C010042; MELO3C005757; MELO3C021974; MELO3C026304; MELO3C003636; MELO3C023332; MELO3C007816; MELO3C015492; MELO3C016262; MELO3C019378; MELO3C001957; MELO3C019712; MELO3C025450; MELO3C014706; MELO3C012127; MELO3C014129; MELO3C010254; MELO3C015627; MELO3C008151; MELO3C015907; MELO3C013185; MELO3C022813;
GO 0010171	body morphogenesis	BIOLOGICAL_PROCESS	0,898501477	0,01512608	4	71	213	16840	MELO3C003222; MELO3C020836; MELO3C004459; MELO3C014877	MELO3C009592; MELO3C014221; MELO3C002120; MELO3C004344; MELO3C004622; MELO3C007816; MELO3C022488; MELO3C025310; MELO3C019034; MELO3C018102; MELO3C025275; MELO3C019997; MELO3C014708; MELO3C019996; MELO3C013814; MELO3C017216; MELO3C012449; MELO3C019956; MELO3C014153; MELO3C000924; MELO3C022016; MELO3C023865; MELO3C008835; MELO3C007829; MELO3C007903; MELO3C023741; MELO3C026971;
GO 0030955	potassium ion binding	MOLECULAR_FUNCTION	0,959488919	0,0170587	2	14	215	16897	MELO3C014272; MELO3C011769	MELO3C005271; MELO3C020719; MELO3C014732; MELO3C003381; MELO3C004198; MELO3C012593; MELO3C024509; MELO3C024508; MELO3C023606; MELO3C006964; MELO3C018027; MELO3C019624; MELO3C024471; MELO3C012911
GO 0000184	nuclear-transcribed mRNA catabolic process, nonsense-mediated decay	BIOLOGICAL_PROCESS	1	0,02371263	2	17	215	16894	MELO3C026263; MELO3C013879	MELO3C015714; MELO3C011145; MELO3C013051; MELO3C008956; MELO3C006767; MELO3C021931; MELO3C008955; MELO3C026304; MELO3C026612; MELO3C026327; MELO3C007816; MELO3C024028; MELO3C025497; MELO3C003804; MELO3C025498; MELO3C015113; MELO3C026290
GO 0070830	bicellular tight junction assembly	BIOLOGICAL_PROCESS	1	0,04972657	1	3	216	16908	MELO3C006574	MELO3C007829; MELO3C006575; MELO3C022488

GO 0006383	transcription from RNA polymerase III promoter	BIOLOGICAL_PROCESS	1	0,03672829	2	22	215	16889	MELO3C002646; MELO3C017544	MELO3C021804; MELO3C014058; MELO3C012297; MELO3C008157; MELO3C002173; MELO3C009662; MELO3C007348; MELO3C012480; MELO3C021758; MELO3C013095; MELO3C009776; MELO3C023634; MELO3C026899; MELO3C015360; MELO3C003707; MELO3C017782; MELO3C019700; MELO3C017775; MELO3C016456; MELO3C017579; MELO3C015712; MELO3C017658
GO 0006265	DNA topological change	BIOLOGICAL_PROCESS	1	0,02864406	2	19	215	16892	MELO3C019163; MELO3C023986	MELO3C014689; MELO3C009682; MELO3C011386; MELO3C003071; MELO3C005694; MELO3C009586; MELO3C014153; MELO3C019090; MELO3C024756; MELO3C024755; MELO3C006788; MELO3C022750; MELO3C022420; MELO3C019089; MELO3C003609; MELO3C003608; MELO3C014639; MELO3C016965; MELO3C012446
GO 0000398	mRNA splicing, via spliceosome	BIOLOGICAL_PROCESS	1	0,02876654	5	130	212	16781	MELO3C012730; MELO3C023475; MELO3C019779; MELO3C022000; MELO3C014877	MELO3C010981; MELO3C012489; MELO3C013333; MELO3C004580; MELO3C008023; MELO3C021758; MELO3C002045; MELO3C020824; MELO3C006125; MELO3C023531; MELO3C018062; MELO3C000014; MELO3C020022; MELO3C017775; MELO3C011313; MELO3C013741; MELO3C014555; MELO3C010355; MELO3C008151; MELO3C008157; MELO3C002173; MELO3C023428; MELO3C008798; MELO3C006416; MELO3C023545; MELO3C023823; MELO3C023427;
GO 0032776	DNA methylation on cytosine	BIOLOGICAL_PROCESS	1	0,0375306	1	2	216	16909	MELO3C025053	MELO3C022551; MELO3C015649
GO 2000034	regulation of seed maturation	BIOLOGICAL_PROCESS	1	0,0375306	1	2	216	16909	MELO3C009101	MELO3C005929; MELO3C020484
GO 0071456	cellular response to hypoxia	BIOLOGICAL_PROCESS	1	0,02517885	1	1	216	16910	MELO3C013879	MELO3C026482
GO 0045739	positive regulation of DNA repair	BIOLOGICAL_PROCESS	1	0,0375306	1	2	216	16909	MELO3C026332	MELO3C002326; MELO3C016858
GO 0007062	sister chromatid cohesion	BIOLOGICAL_PROCESS	1	0,03124992	2	20	215	16891	MELO3C012730; MELO3C014687	MELO3C006251; MELO3C009682; MELO3C013696; MELO3C008766; MELO3C009536; MELO3C006327; MELO3C005824; MELO3C016064; MELO3C016065; MELO3C018187; MELO3C020001; MELO3C010507; MELO3C023581; MELO3C024243; MELO3C017664; MELO3C017663; MELO3C017258; MELO3C015235; MELO3C011228; MELO3C010631
GO 0006406	mRNA export from nucleus	BIOLOGICAL_PROCESS	1	0,04867873	2	26	215	16885	MELO3C013879; MELO3C012713	MELO3C011256; MELO3C020407; MELO3C005694; MELO3C003078; MELO3C004622; MELO3C021931; MELO3C026304; MELO3C016280; MELO3C022166; MELO3C015492; MELO3C025497; MELO3C025498; MELO3C019034; MELO3C026441; MELO3C015113; MELO3C015733; MELO3C014129; MELO3C014532; MELO3C013443; MELO3C005265; MELO3C021887; MELO3C009808; MELO3C005946; MELO3C011924; MELO3C015447; MELO3C016756
GO 0010106	cellular response to iron ion starvation	BIOLOGICAL_PROCESS	1	0,02517885	1	1	216	16910	MELO3C017320	MELO3C017166

GO 0007091	metaphase/anaphase transition of mitotic cell cycle	BIOLOGICAL_PROCESS	1	0,02864406	2	19	215	16892	MELO3C012730; MELO3C022930	MELO3C011895; MELO3C014684; MELO3C014573; MELO3C003047; MELO3C006972; MELO3C002234; MELO3C004622; MELO3C005866; MELO3C005733; MELO3C024685; MELO3C017066; MELO3C017087; MELO3C025232; MELO3C026580; MELO3C017995; MELO3C015235; MELO3C012437; MELO3C010920; MELO3C013359
GO 0032049	cardiolipin biosynthetic process	BIOLOGICAL_PROCESS	1	0,02517885	1	1	216	16910	MELO3C007010	MELO3C013700
GO 0010030	positive regulation of seed germination	BIOLOGICAL_PROCESS	1	0,04972657	1	3	216	16908	MELO3C009101	MELO3C020484; MELO3C004632; MELO3C009627
GO 0006569	tryptophan catabolic process	BIOLOGICAL_PROCESS	1	0,04972657	1	3	216	16908	MELO3C012201	MELO3C023775; MELO3C010461; MELO3C024595
GO 0031055	chromatin remodeling at centromere	BIOLOGICAL_PROCESS	1	0,04972657	1	3	216	16908	MELO3C023986	MELO3C006760; MELO3C005059; MELO3C017558
GO 0016233	telomere capping	BIOLOGICAL_PROCESS	1	0,0375306	1	2	216	16909	MELO3C014298	MELO3C018187; MELO3C006292
GO 0010495	long-distance posttranscriptional gene silencing	BIOLOGICAL_PROCESS	1	0,02517885	1	1	216	16910	MELO3C014035	MELO3C017106
GO 0046488	phosphatidylinositol metabolic process	BIOLOGICAL_PROCESS	1	0,0422135	3	58	214	16853	MELO3C010456; MELO3C006050; MELO3C003057	MELO3C013178; MELO3C007931; MELO3C020821; MELO3C024309; MELO3C020987; MELO3C020989; MELO3C025637; MELO3C005634; MELO3C019075; MELO3C000333; MELO3C022481; MELO3C015670; MELO3C026365; MELO3C026440; MELO3C017214; MELO3C019875; MELO3C022480; MELO3C017019; MELO3C010621; MELO3C010667; MELO3C015647; MELO3C011047; MELO3C016737; MELO3C013982; MELO3C009840; MELO3C008992; MELO3C005285;
GO 0019318	hexose metabolic process	BIOLOGICAL_PROCESS	1	0,04860452	5	151	212	16760	MELO3C014272; MELO3C011769; MELO3C009914; MELO3C014724; MELO3C013829	MELO3C005272; MELO3C009351; MELO3C005396; MELO3C003491; MELO3C010186; MELO3C020949; MELO3C004980; MELO3C002287; MELO3C024509; MELO3C020428; MELO3C004465; MELO3C024508; MELO3C009913; MELO3C020780; MELO3C025275; MELO3C027332; MELO3C020263; MELO3C019557; MELO3C012925; MELO3C016048; MELO3C026482; MELO3C013979; MELO3C010862; MELO3C011710; MELO3C006491; MELO3C020837; MELO3C003381;
GO 0030466	chromatin silencing at silent mating-type cassette	BIOLOGICAL_PROCESS	1	0,04972657	1	3	216	16908	MELO3C013879	MELO3C022562; MELO3C009773; MELO3C010882
GO 0071044	histone mRNA catabolic process	BIOLOGICAL_PROCESS	1	0,0375306	1	2	216	16909	MELO3C013879	MELO3C011748; MELO3C017087
GO 0042078	germ-line stem cell division	BIOLOGICAL_PROCESS	1	0,02517885	1	1	216	16910	MELO3C008815	MELO3C008594
GO 0006346	methylation-dependent chromatin silencing	BIOLOGICAL_PROCESS	1	0,02517885	1	1	216	16910	MELO3C014035	MELO3C017558
GO 0005506	iron ion binding	MOLECULAR_FUNCTION	1	0,03808894	0	324	217	16587		MELO3C007174; MELO3C012522; MELO3C007175; MELO3C021914; MELO3C012088; MELO3C007058; MELO3C020028; MELO3C006644; MELO3C004221; MELO3C007611; MELO3C004584; MELO3C007059; MELO3C025712; MELO3C026802; MELO3C020385; MELO3C023893; MELO3C023530; MELO3C000772; MELO3C015591; MELO3C026487; MELO3C000770; MELO3C015592; MELO3C015593; MELO3C015595; MELO3C015596; MELO3C026484; MELO3C016686;
GO 0000182	rDNA binding	MOLECULAR_FUNCTION	1	0,0375306	1	2	216	16909	MELO3C023986	MELO3C012480; MELO3C020235

GO 0000156	phosphorelay response regulator activity	MOLECULAR_FUNCTION	1	0,04557323	2	25	215	16886	MELO3C017128; MELO3C020055	MELO3C005250; MELO3C009770; MELO3C004183; MELO3C010245; MELO3C003075; MELO3C005156; MELO3C005336; MELO3C000311; MELO3C001999; MELO3C017472; MELO3C019056; MELO3C010624; MELO3C021290; MELO3C013758; MELO3C016937; MELO3C012031; MELO3C006451; MELO3C006693; MELO3C012470; MELO3C022310; MELO3C025982; MELO3C005927; MELO3C003906; MELO3C010714; MELO3C016975
GO 0003680	AT DNA binding	MOLECULAR_FUNCTION	1	0,02517885	1	1	216	16910	MELO3C012730	MELO3C022471
GO 0051721	protein phosphatase 2A binding	MOLECULAR_FUNCTION	1	0,04972657	1	3	216	16908	MELO3C013879	MELO3C002748; MELO3C022178; MELO3C015113
GO 0047800	cysteamine dioxygenase activity	MOLECULAR_FUNCTION	1	0,04972657	1	3	216	16908	MELO3C009886	MELO3C017267; MELO3C008836; MELO3C013579
GO 0016435	rRNA (guanine) methyltransferase activity	MOLECULAR_FUNCTION	1	0,0375306	1	2	216	16909	MELO3C023306	MELO3C002238; MELO3C015412
GO 0000400	four-way junction DNA binding	MOLECULAR_FUNCTION	1	0,02517885	1	1	216	16910	MELO3C023986	MELO3C015928
GO 0008138	protein tyrosine/serine/threonine phosphatase activity	MOLECULAR_FUNCTION	1	0,02371263	2	17	215	16894	MELO3C023830; MELO3C003222	MELO3C012378; MELO3C009960; MELO3C014446; MELO3C007580; MELO3C009840; MELO3C021405; MELO3C004587; MELO3C020114; MELO3C002645; MELO3C004603; MELO3C026602; MELO3C019894; MELO3C018474; MELO3C026166; MELO3C011936; MELO3C026163; MELO3C013921
GO 0004385	guanylate kinase activity	MOLECULAR_FUNCTION	1	0,04972657	1	3	216	16908	MELO3C006574	MELO3C018452; MELO3C006575; MELO3C023150
GO 0003729	mRNA binding	MOLECULAR_FUNCTION	1	0,01917371	2	15	215	16896	MELO3C012411; MELO3C023986	MELO3C011157; MELO3C005382; MELO3C015714; MELO3C020705; MELO3C011385; MELO3C005482; MELO3C023836; MELO3C008722; MELO3C024822; MELO3C008956; MELO3C008955; MELO3C017020; MELO3C021296; MELO3C019953; MELO3C017841
GO 0003955	NAD(P)H dehydrogenase (quinone) activity	MOLECULAR_FUNCTION	1	0,0375306	1	2	216	16909	MELO3C007950	MELO3C005147; MELO3C012476
GO 0008780	acyl-[acyl-carrier-protein]-UDP-N-acetylglucosamine O-acyltransferase activity	MOLECULAR_FUNCTION	1	0,02517885	1	1	216	16910	MELO3C015455	MELO3C007369
GO 0009884	cytokinin receptor activity	MOLECULAR_FUNCTION	1	0,04972657	1	3	216	16908	MELO3C020055	MELO3C005250; MELO3C022310; MELO3C025982
GO 0004864	protein phosphatase inhibitor activity	MOLECULAR_FUNCTION	1	0,04972657	1	3	216	16908	MELO3C021670	MELO3C002748; MELO3C022178; MELO3C005380
GO 0003743	translation initiation factor activity	MOLECULAR_FUNCTION	1	0,04989364	4	105	213	16806	MELO3C002646; MELO3C002819; MELO3C002817; MELO3C006107	MELO3C010981; MELO3C010222; MELO3C020828; MELO3C004345; MELO3C004344; MELO3C020786; MELO3C023779; MELO3C020380; MELO3C000253; MELO3C019434; MELO3C014706; MELO3C016963; MELO3C012127; MELO3C017707; MELO3C011321; MELO3C006494; MELO3C014155; MELO3C010197; MELO3C012131; MELO3C002698; MELO3C023701; MELO3C015360; MELO3C018872; MELO3C018874; MELO3C014439; MELO3C011371; MELO3C002822;
GO 0008650	rRNA (uridine-2'-O-)-methyltransferase activity	MOLECULAR_FUNCTION	1	0,02517885	1	1	216	16910	MELO3C023306	MELO3C009184

GO 0004725	protein tyrosine phosphatase activity	MOLECULAR_FUNCTION	1	0,04557323	2	25	215	16886	MELO3C023830; MELO3C003222	MELO3C018606; MELO3C014446; MELO3C010061; MELO3C002645; MELO3C023674; MELO3C004603; MELO3C026602; MELO3C026166; MELO3C019876; MELO3C019734; MELO3C011936; MELO3C019875; MELO3C026163; MELO3C024481; MELO3C007580; MELO3C011186; MELO3C013860; MELO3C009840; MELO3C021405; MELO3C020114; MELO3C021441; MELO3C018474; MELO3C018159; MELO3C014438; MELO3C013921
GO 0000325	plant-type vacuole	CELLULAR_COMPONENT	1	0,02955212	3	50	214	16861	MELO3C011601; MELO3C013437; MELO3C013829	MELO3C002042; MELO3C022009; MELO3C024902; MELO3C020983; MELO3C020984; MELO3C022448; MELO3C026522; MELO3C015314; MELO3C012405; MELO3C010983; MELO3C011599; MELO3C007980; MELO3C003783; MELO3C001488; MELO3C009809; MELO3C026971; MELO3C016010; MELO3C016011; MELO3C024398; MELO3C026330; MELO3C009170; MELO3C011600; MELO3C011894; MELO3C008088; MELO3C010286; MELO3C012542; MELO3C009852;
GO 0000812	Swr1 complex	CELLULAR_COMPONENT	1	0,0375306	1	2	216	16909	MELO3C004459	MELO3C007894; MELO3C007648
GO 0005829	cytosol	CELLULAR_COMPONENT	1	0,02743781	3	734	214	16177	MELO3C020836; MELO3C013175; MELO3C007800	MELO3C021918; MELO3C014028; MELO3C004343; MELO3C014021; MELO3C012084; MELO3C014262; MELO3C004344; MELO3C004347; MELO3C005679; MELO3C005559; MELO3C008944; MELO3C007739; MELO3C026245; MELO3C025275; MELO3C016201; MELO3C026360; MELO3C026482; MELO3C025030; MELO3C018985; MELO3C010901; MELO3C018624; MELO3C017659; MELO3C016569; MELO3C019956; MELO3C018518; MELO3C002294; MELO3C003263;
GO 0031314	extrinsic component of mitochondrial inner membrane	CELLULAR_COMPONENT	1	0,04972657	1	3	216	16908	MELO3C007010	MELO3C013534; MELO3C018763; MELO3C022197
GO 0000118	histone deacetylase complex	CELLULAR_COMPONENT	1	0,0375306	1	2	216	16909	MELO3C015103	MELO3C016865; MELO3C021442
GO 0031410	cytoplasmic vesicle	CELLULAR_COMPONENT	1	0,02912388	12	1687	205	15224	MELO3C003659; MELO3C012201; MELO3C008037; MELO3C025255; MELO3C025594; MELO3C013780; MELO3C009328; MELO3C003146; MELO3C008815; MELO3C013769; MELO3C005513; MELO3C007800	MELO3C015119; MELO3C002280; MELO3C012088; MELO3C002286; MELO3C012085; MELO3C026249; MELO3C026243; MELO3C017775; MELO3C015599; MELO3C025391; MELO3C003142; MELO3C003144; MELO3C004477; MELO3C014270; MELO3C005328; MELO3C020951; MELO3C008838; MELO3C017300; MELO3C019962; MELO3C019939; MELO3C020928; MELO3C014249; MELO3C012068; MELO3C014246; MELO3C003595; MELO3C012061; MELO3C004445;
GO 0005935	cellular bud neck	CELLULAR_COMPONENT	1	0,0375306	1	2	216	16909	MELO3C020836	MELO3C013504; MELO3C013982

Supplementary Table 2.G Gene Ontology terms (GO terms) of the cluster 2.6 obtained considering the comparison between lines the postharvest ripening time fruit during storage at 20.5°C and 88% relative humidity for 18 d the near-isogenic line SC10-2 and its parental "Piel de Sapo" obtained according to the differentially expressed gene pattern (Supl. Table 2.A)

GO ID	GO Name	GO Category	FDR	P-Value	SC10-2	PS	Non Annot Test	Non Annot Reference	TestSet Sequences	RefSet Sequences
GO 0016206	catechol O-methyltransferase activity	MOLECULAR_FUNCTION	0,281888732	5,97E-05	2	1	75	17050	MELO3C027330; MELO3C014089	MELO3C024861
GO 0042446	hormone biosynthetic process	BIOLOGICAL_PROCESS	0,510918541	1,62E-04	4	57	73	16994	MELO3C027330; MELO3C027370; MELO3C014089; MELO3C013315	MELO3C011158; MELO3C012321; MELO3C013411; MELO3C013410; MELO3C007417; MELO3C022404; MELO3C024861; MELO3C025355; MELO3C024222; MELO3C016881; MELO3C009362; MELO3C002170; MELO3C009521; MELO3C009124; MELO3C000525; MELO3C021600; MELO3C002775; MELO3C002776; MELO3C004955; MELO3C000487; MELO3C019323; MELO3C012817; MELO3C014719; MELO3C019324; MELO3C014716; MELO3C017668; MELO3C016416;
GO 0015095	magnesium ion transmembrane transporter activity	MOLECULAR_FUNCTION	0,659113425	4,13E-04	2	5	75	17046	MELO3C026764; MELO3C000817	MELO3C026733; MELO3C000103; MELO3C011418; MELO3C019432; MELO3C004841
GO 0006968	cellular defense response	BIOLOGICAL_PROCESS	0,94386839	0,004495563	1	0	76	17051	MELO3C006765	
GO 0071395	cellular response to jasmonic acid stimulus	BIOLOGICAL_PROCESS	0,94386839	0,002016649	2	13	75	17038	MELO3C006765; MELO3C024357	MELO3C006046; MELO3C012221; MELO3C005466; MELO3C004610; MELO3C020450; MELO3C026577; MELO3C025152; MELO3C012527; MELO3C016852; MELO3C011439; MELO3C010774; MELO3C015436; MELO3C017559
GO 0071947	protein deubiquitination involved in ubiquitin-dependent protein catabolic process	BIOLOGICAL_PROCESS	0,94386839	0,004495563	1	0	76	17051	MELO3C018956	
GO 0010247	detection of phosphate ion	BIOLOGICAL_PROCESS	0,94386839	0,004495563	1	0	76	17051	MELO3C005035	
GO 0010400	rhamnogalacturonan I side chain metabolic process	BIOLOGICAL_PROCESS	0,94386839	0,004495563	1	0	76	17051	MELO3C003916	
GO 0070485	dehydro-D-arabinono-1,4-lactone biosynthetic process	BIOLOGICAL_PROCESS	0,94386839	0,004495563	1	0	76	17051	MELO3C018576	
GO 2000311	regulation of AMPA receptor activity	BIOLOGICAL_PROCESS	0,94386839	0,004495563	1	0	76	17051	MELO3C018956	
GO 0034498	early endosome to Golgi transport	BIOLOGICAL_PROCESS	0,94386839	0,004495563	1	0	76	17051	MELO3C024558	
GO 2000070	regulation of response to water deprivation	BIOLOGICAL_PROCESS	0,94386839	0,004495563	1	0	76	17051	MELO3C005035	
GO 0047834	D-threo-aldose 1-dehydrogenase activity	MOLECULAR_FUNCTION	0,94386839	0,004495563	1	0	76	17051	MELO3C018576	
GO 0005290	L-histidine transmembrane transporter activity	MOLECULAR_FUNCTION	0,94386839	0,004495563	1	0	76	17051	MELO3C002619	
GO 0035255	ionotropic glutamate receptor binding	MOLECULAR_FUNCTION	0,94386839	0,004495563	1	0	76	17051	MELO3C018956	
GO 0050235	pyridoxal 4-dehydrogenase activity	MOLECULAR_FUNCTION	0,94386839	0,004495563	1	0	76	17051	MELO3C018576	
GO 0045290	D-arabinose 1-dehydrogenase [NAD(P)+] activity	MOLECULAR_FUNCTION	0,94386839	0,004495563	1	0	76	17051	MELO3C018576	
GO 0019151	galactose 1-dehydrogenase activity	MOLECULAR_FUNCTION	0,94386839	0,004495563	1	0	76	17051	MELO3C018576	
GO 0010349	L-galactose dehydrogenase activity	MOLECULAR_FUNCTION	0,94386839	0,004495563	1	0	76	17051	MELO3C018576	
GO 0047816	D-arabinose 1-dehydrogenase (NAD) activity	MOLECULAR_FUNCTION	0,94386839	0,004495563	1	0	76	17051	MELO3C018576	
GO 0000172	ribonuclease MRP complex	CELLULAR_COMPONENT	0,94386839	0,004495563	1	0	76	17051	MELO3C009318	
GO 0005655	nucleolar ribonuclease P complex	CELLULAR_COMPONENT	0,94386839	0,004495563	1	0	76	17051	MELO3C009318	
GO 0007098	centrosome cycle	BIOLOGICAL_PROCESS	1	0,026675887	1	5	76	17046	MELO3C013369	MELO3C015782; MELO3C024150; MELO3C022094; MELO3C019034; MELO3C010920
GO 0016925	protein sumoylation	BIOLOGICAL_PROCESS	1	0,026675887	1	5	76	17046	MELO3C005035	MELO3C005717; MELO3C025617; MELO3C014183; MELO3C023325; MELO3C024782
GO 0046854	phosphatidylinositol phosphorylation	BIOLOGICAL_PROCESS	1	0,0397492	1	8	76	17043	MELO3C020989	MELO3C012544; MELO3C008054; MELO3C013045; MELO3C020987; MELO3C026141; MELO3C012545; MELO3C010667; MELO3C021931
GO 0030259	lipid glycosylation	BIOLOGICAL_PROCESS	1	0,044068338	1	9	76	17042	MELO3C015339	MELO3C011311; MELO3C010079; MELO3C020997; MELO3C004474; MELO3C010080; MELO3C002112; MELO3C002113; MELO3C012787; MELO3C008339

GO 0034727	piecemeal microautophagy of nucleus	BIOLOGICAL_PROCESS	1	0,0397492	1	8	76	17043	MELO3C024558	MELO3C019565; MELO3C004827; MELO3C008520; MELO3C025809; MELO3C022280; MELO3C022308; MELO3C023607; MELO3C007214
GO 0030001	metal ion transport	BIOLOGICAL_PROCESS	1	0,016770116	4	214	73	16837	MELO3C026764; MELO3C014309; MELO3C000817; MELO3C002372	MELO3C010221; MELO3C007854; MELO3C008943; MELO3C007853; MELO3C020822; MELO3C009910; MELO3C022329; MELO3C005316; MELO3C004225; MELO3C005315; MELO3C026802; MELO3C022448; MELO3C009917; MELO3C016324; MELO3C008392; MELO3C005687; MELO3C001880; MELO3C009809; MELO3C021364; MELO3C027105; MELO3C009927; MELO3C026378; MELO3C014007; MELO3C015218; MELO3C014920; MELO3C007271; MELO3C014000;
GO 0010113	negative regulation of systemic acquired resistance	BIOLOGICAL_PROCESS	1	0,008971177	1	1	76	17050	MELO3C005035	MELO3C002630
GO 0040025	vulval development	BIOLOGICAL_PROCESS	1	0,006510321	2	25	75	17026	MELO3C013369; MELO3C018956	MELO3C013015; MELO3C010882; MELO3C007894; MELO3C006500; MELO3C002045; MELO3C022308; MELO3C019031; MELO3C016262; MELO3C024265; MELO3C024782; MELO3C016321; MELO3C004390; MELO3C006171; MELO3C015904; MELO3C004473; MELO3C023325; MELO3C023545; MELO3C004459; MELO3C017020; MELO3C007903; MELO3C003703; MELO3C026234; MELO3C024552; MELO3C010839; MELO3C011206
GO 0000050	urea cycle	BIOLOGICAL_PROCESS	1	0,035410803	1	7	76	17044	MELO3C002619	MELO3C003814; MELO3C011085; MELO3C002352; MELO3C002353; MELO3C013218; MELO3C026229; MELO3C003523
GO 0019853	L-ascorbic acid biosynthetic process	BIOLOGICAL_PROCESS	1	0,013426929	1	2	76	17049	MELO3C018576	MELO3C026482; MELO3C004377
GO 0032258	CVT pathway	BIOLOGICAL_PROCESS	1	0,0397492	1	8	76	17043	MELO3C024558	MELO3C019565; MELO3C008520; MELO3C025809; MELO3C022280; MELO3C022308; MELO3C023607; MELO3C007214; MELO3C008406
GO 0010187	negative regulation of seed germination	BIOLOGICAL_PROCESS	1	0,026675887	1	5	76	17046	MELO3C023484	MELO3C009889; MELO3C007222; MELO3C024155; MELO3C006547; MELO3C010435
GO 0045053	protein retention in Golgi apparatus	BIOLOGICAL_PROCESS	1	0,017862908	1	3	76	17048	MELO3C018052	MELO3C013753; MELO3C015420; MELO3C006811
GO 0010337	regulation of salicylic acid metabolic process	BIOLOGICAL_PROCESS	1	0,017862908	1	3	76	17048	MELO3C005035	MELO3C027349; MELO3C002099; MELO3C016008
GO 0016559	peroxisome fission	BIOLOGICAL_PROCESS	1	0,035410803	1	7	76	17044	MELO3C018052	MELO3C022531; MELO3C019045; MELO3C010926; MELO3C011193; MELO3C006147; MELO3C015136; MELO3C006810
GO 0000422	mitophagy	BIOLOGICAL_PROCESS	1	0,03105306	1	6	76	17045	MELO3C024558	MELO3C022280; MELO3C023607; MELO3C007214; MELO3C019565; MELO3C008520; MELO3C025809

GO 0006379	mRNA cleavage	BIOLOGICAL_PROCESS	1	0,0397492	1	8	76	17043	MELO3C009318	MELO3C005162; MELO3C008873; MELO3C005929; MELO3C021828; MELO3C008722; MELO3C002045; MELO3C027241; MELO3C021974
GO 0071446	cellular response to salicylic acid stimulus	BIOLOGICAL_PROCESS	1	0,0397492	1	8	76	17043	MELO3C006765	MELO3C020450; MELO3C013621; MELO3C008938; MELO3C005061; MELO3C022341; MELO3C007039; MELO3C018037; MELO3C012836
GO 0010104	regulation of ethylene-activated signaling pathway	BIOLOGICAL_PROCESS	1	0,026675887	1	5	76	17046	MELO3C024357	MELO3C007039; MELO3C016937; MELO3C015961; MELO3C003906; MELO3C016866
GO 0006065	UDP-glucuronate biosynthetic process	BIOLOGICAL_PROCESS	1	0,026675887	1	5	76	17046	MELO3C017213	MELO3C016068; MELO3C003703; MELO3C011431; MELO3C020244; MELO3C011346
GO 0060625	regulation of protein deneddylation	BIOLOGICAL_PROCESS	1	0,008971177	1	1	76	17050	MELO3C016464	MELO3C014386
GO 0009736	cytokinin-activated signaling pathway	BIOLOGICAL_PROCESS	1	0,048368299	1	10	76	17041	MELO3C024357	MELO3C004183; MELO3C016937; MELO3C024563; MELO3C014230; MELO3C003198; MELO3C025617; MELO3C016973; MELO3C010714; MELO3C017877; MELO3C024439
GO 0045900	negative regulation of translational elongation	BIOLOGICAL_PROCESS	1	0,008971177	1	1	76	17050	MELO3C014306	MELO3C002757
GO 0006614	SRP-dependent cotranslational protein targeting to membrane	BIOLOGICAL_PROCESS	1	0,048368299	1	10	76	17041	MELO3C014306	MELO3C002757; MELO3C004130; MELO3C024550; MELO3C006951; MELO3C023371; MELO3C006136; MELO3C017841; MELO3C011898; MELO3C006747; MELO3C005757
GO 0050826	response to freezing	BIOLOGICAL_PROCESS	1	0,013426929	1	2	76	17049	MELO3C005035	MELO3C021253; MELO3C022358
GO 0008988	rRNA (adenine-N6-)-methyltransferase activity	MOLECULAR_FUNCTION	1	0,017862908	1	3	76	17048	MELO3C013369	MELO3C010154; MELO3C007871; MELO3C006150
GO 0000064	L-ornithine transmembrane transporter activity	MOLECULAR_FUNCTION	1	0,008971177	1	1	76	17050	MELO3C002619	MELO3C024239
GO 0008234	cysteine-type peptidase activity	MOLECULAR_FUNCTION	1	0,034577805	2	63	75	16988	MELO3C019168; MELO3C018956	MELO3C007571; MELO3C010982; MELO3C017814; MELO3C009196; MELO3C012000; MELO3C005793; MELO3C004340; MELO3C011193; MELO3C009559; MELO3C007578; MELO3C002321; MELO3C023338; MELO3C021359; MELO3C017053; MELO3C024666; MELO3C026400; MELO3C025355; MELO3C016165; MELO3C010702; MELO3C019434; MELO3C015634; MELO3C012403; MELO3C014753; MELO3C004472; MELO3C021328; MELO3C005564; MELO3C002334;
GO 0004430	1-phosphatidylinositol 4-kinase activity	MOLECULAR_FUNCTION	1	0,013426929	1	2	76	17049	MELO3C020989	MELO3C008054; MELO3C012545
GO 0008239	dipeptidyl-peptidase activity	MOLECULAR_FUNCTION	1	0,017862908	1	3	76	17048	MELO3C023481	MELO3C015446; MELO3C023479; MELO3C023478
GO 0003979	UDP-glucose 6-dehydrogenase activity	MOLECULAR_FUNCTION	1	0,013426929	1	2	76	17049	MELO3C017213	MELO3C016068; MELO3C011431
GO 0032266	phosphatidylinositol-3-phosphate binding	MOLECULAR_FUNCTION	1	0,017862908	1	3	76	17048	MELO3C024558	MELO3C026612; MELO3C020154; MELO3C003655
GO 0016633	galactonolactone dehydrogenase activity	MOLECULAR_FUNCTION	1	0,013426929	1	2	76	17049	MELO3C018576	MELO3C020737; MELO3C020736
GO 0004652	polynucleotide adenylyltransferase activity	MOLECULAR_FUNCTION	1	0,035410803	1	7	76	17044	MELO3C002115	MELO3C017806; MELO3C024435; MELO3C013730; MELO3C009952; MELO3C023722; MELO3C026172; MELO3C011126

GO 0004526	ribonuclease P activity	MOLECULAR_FUNCTION	1	0,022279198	1	4	76	17047	MELO3C009318	MELO3C016319; MELO3C023673; MELO3C025708; MELO3C010071
GO 0008312	7S RNA binding	MOLECULAR_FUNCTION	1	0,035410803	1	7	76	17044	MELO3C014306	MELO3C018272; MELO3C002757; MELO3C024550; MELO3C006136; MELO3C017841; MELO3C011898; MELO3C006747
GO 0005047	signal recognition particle binding	MOLECULAR_FUNCTION	1	0,022279198	1	4	76	17047	MELO3C014306	MELO3C011981; MELO3C004130; MELO3C015126; MELO3C011898
GO 0047763	caffeate O-methyltransferase activity	MOLECULAR_FUNCTION	1	0,013426929	1	2	76	17049	MELO3C014089	MELO3C024861; MELO3C009403
GO 0033843	xyloglucan 6-xylosyltransferase activity	MOLECULAR_FUNCTION	1	0,022279198	1	4	76	17047	MELO3C007647	MELO3C006664; MELO3C017190; MELO3C017191; MELO3C000841
GO 0004564	beta-fructofuranosidase activity	MOLECULAR_FUNCTION	1	0,048368299	1	10	76	17041	MELO3C016877	MELO3C004170; MELO3C013379; MELO3C006727; MELO3C005363; MELO3C024384; MELO3C009488; MELO3C005560; MELO3C012360; MELO3C024083; MELO3C024383
GO 0005524	ATP binding	MOLECULAR_FUNCTION	1	0,021994726	3	2058	74	14993	MELO3C006765; MELO3C013076; MELO3C016434	MELO3C014269; MELO3C003133; MELO3C004463; MELO3C007972; MELO3C006648; MELO3C007978; MELO3C008825; MELO3C003139; MELO3C008829; MELO3C026243; MELO3C019951; MELO3C000093; MELO3C025392; MELO3C015599; MELO3C018624; MELO3C020958; MELO3C008832; MELO3C008831; MELO3C014272; MELO3C003146; MELO3C002299; MELO3C008835; MELO3C005329; MELO3C008838; MELO3C026256; MELO3C024079; MELO3C019967;
GO 0019789	SUMO transferase activity	MOLECULAR_FUNCTION	1	0,013426929	1	2	76	17049	MELO3C005035	MELO3C025617; MELO3C024782
GO 0015189	L-lysine transmembrane transporter activity	MOLECULAR_FUNCTION	1	0,008971177	1	1	76	17050	MELO3C002619	MELO3C002398
GO 0004452	isopentenyl-diphosphate delta-isomerase activity	MOLECULAR_FUNCTION	1	0,022279198	1	4	76	17047	MELO3C023481	MELO3C023478; MELO3C008717; MELO3C023479; MELO3C010053
GO 0015181	arginine transmembrane transporter activity	MOLECULAR_FUNCTION	1	0,008971177	1	1	76	17050	MELO3C002619	MELO3C002398
GO 0004577	N-acetylglucosaminyldiphosphodolichol N-acetylglucosaminyltransferase activity	MOLECULAR_FUNCTION	1	0,008971177	1	1	76	17050	MELO3C015339	MELO3C013839
GO 0044297	cell body	CELLULAR_COMPONENT	1	0,035410803	1	7	76	17044	MELO3C018956	MELO3C008571; MELO3C009840; MELO3C016990; MELO3C009668; MELO3C005662; MELO3C018534; MELO3C017338
GO 0043541	UDP-N-acetylglucosamine transferase complex	CELLULAR_COMPONENT	1	0,008971177	1	1	76	17050	MELO3C015339	MELO3C013839
GO 0009507	chloroplast	CELLULAR_COMPONENT	1	0,046022234	2	1593	75	15458	MELO3C006765; MELO3C003916	MELO3C018628; MELO3C020948; MELO3C020949; MELO3C002287; MELO3C003135; MELO3C005795; MELO3C003137; MELO3C003139; MELO3C015590; MELO3C015591; MELO3C015592; MELO3C026246; MELO3C015593; MELO3C017772; MELO3C015594; MELO3C025397; MELO3C015595; MELO3C017774; MELO3C015596; MELO3C017776; MELO3C018622; MELO3C017309; MELO3C002291; MELO3C014278; MELO3C004471; MELO3C007986; MELO3C004475;

GO 0005669	transcription factor TFIID complex	CELLULAR_COMPONENT	1	0,035410803	1	7	76	17044	MELO3C024357	MELO3C016968; MELO3C003391; MELO3C024352; MELO3C021620; MELO3C010016; MELO3C000238; MELO3C024537
GO 0009360	DNA polymerase III complex	CELLULAR_COMPONENT	1	0,013426929	1	2	76	17049	MELO3C016434	MELO3C007194; MELO3C014529
GO 0005768	endosome	CELLULAR_COMPONENT	1	0,041648667	2	70	75	16981	MELO3C024558; MELO3C018956	MELO3C014821; MELO3C011795; MELO3C009473; MELO3C014542; MELO3C005199; MELO3C007457; MELO3C012481; MELO3C014180; MELO3C004945; MELO3C006926; MELO3C025310; MELO3C004827; MELO3C026440; MELO3C013816; MELO3C012728; MELO3C015433; MELO3C006171; MELO3C010795; MELO3C004391; MELO3C023828; MELO3C005328; MELO3C004874; MELO3C026614; MELO3C018195; MELO3C016491; MELO3C026971; MELO3C025682;
GO 0042406	extrinsic component of endoplasmic reticulum membrane	CELLULAR_COMPONENT	1	0,013426929	1	2	76	17049	MELO3C015339	MELO3C011649; MELO3C018518
GO 0000407	pre-autophagosomal structure	CELLULAR_COMPONENT	1	0,03105306	1	6	76	17045	MELO3C024558	MELO3C007534; MELO3C022308; MELO3C023607; MELO3C007214; MELO3C019565; MELO3C025809
GO 0005785	signal recognition particle receptor complex	CELLULAR_COMPONENT	1	0,008971177	1	1	76	17050	MELO3C014306	MELO3C004130
GO 0005786	signal recognition particle, endoplasmic reticulum targeting	CELLULAR_COMPONENT	1	0,035410803	1	7	76	17044	MELO3C014306	MELO3C002757; MELO3C024550; MELO3C017841; MELO3C015126; MELO3C011898; MELO3C006747; MELO3C013306

Supplementary Table 3. List of the Differentially Expressed Genes (909 DEGs) considering the postharvest ripening time and the effect of the introgression over time in melon fruit of the near-isogenic line SC10-2 and its parental control ´Piel de Sapo´ (PS) during postharvest storage at 20 5 ^{o}C and 88% relative humidity for 18 d

Gene ID	pval	qval	Description
MELO3C018099	6.98878999116914e-09	8.62635084597496e-06	No data found
MELO3C021514	8.24147254885332e-08	3.77341577131167e-05	No data found
MELO3C012331	1.44328094586754e-07	5.37799158489398e-05	dnaJ protein homolog
MELO3C007204	2.70307014549331e-07	8.47348131799166e-05	60S ribosomal protein L11-like
MELO3C023537	5.4337361676815e-07	0.00012691733086263	zinc finger A20 and AN1 domain-containing stress-associated protein 8-like
MELO3C012146	7.17645318282223e-07	0.000149187130429007	14-3-3 protein, putative
MELO3C020880	2.09783662086238e-06	0.000312158869772302	Pathogenesis-related protein 1
MELO3C026045	2.71888340064308e-06	0.000365273661763947	alanine--glyoxylate aminotransferase 2 homolog 2, mitochondrial-like
MELO3C012074	3.70429519958027e-06	0.000425326313351806	Ubiquitin-conjugating enzyme, E2
MELO3C007827	4.27775306732769e-06	0.00047169877077526	pyridine nucleotide-disulfide oxidoreductase domain-containing protein 2-like
MELO3C013000	4.45895326350865e-06	0.000478586239136045	Malic enzyme
MELO3C016805	4.5614759661694e-06	0.000480700689972296	No data found
MELO3C000673	4.68826114552456e-06	0.000482679936310805	ATP-dependent zinc metalloprotease FtsH
MELO3C026738	6.6257926438773e-06	0.000608617576390385	Acyl-CoA N-acyltransferase (NAT) superfamily protein
MELO3C022065	7.89187488892118e-06	0.0006773432768121	Nuclear matrix constituent protein 1
MELO3C011963	7.81226541701763e-06	0.0006773432768121	anthranilate phosphoribosyltransferase
MELO3C026410	8.27649747914272e-06	0.000689673201331601	transcription factor PIF4-like
MELO3C026689	1.01759043160676e-05	0.000788974717069347	LRR receptor-like kinase, putative
MELO3C007614	1.15006113516891e-05	0.00086458369524327	Leucine-rich repeat family protein
MELO3C026749	1.20811670227816e-05	0.000896958524559827	DNA helicase
MELO3C009315	1.23509541338773e-05	0.00090491340308527	Ribosomal protein S12
MELO3C016855	1.24174151722167e-05	0.00090491340308527	CRG16
MELO3C017720	1.5829999835848e-05	0.00104557413631492	protein farnesyltransferase/geranylgeranyltransferase type-1 subunit alpha
MELO3C013093	1.62023783316645e-05	0.0010508747649051	glyoxylate/succinic semialdehyde reductase 2, chloroplastic-like
MELO3C021107	1.93475282579403e-05	0.00118295459927574	Peptidylprolyl isomerase
MELO3C012243	2.02363198715805e-05	0.00121105176104195	tetraketide alpha-pyrone reductase 2-like
MELO3C012748	2.83333883075443e-05	0.00148385868132083	Lysine-specific demethylase
MELO3C024292	3.02042248422341e-05	0.00153552012010767	O-fucosyltransferase family protein
MELO3C013470	3.44618684419151e-05	0.00168046281446761	Ankyrin repeat domain-containing 2-like protein
MELO3C024586	3.89204117599018e-05	0.00180760621925962	Ribosomal protein S8e/ribosomal biogenesis NSA2
MELO3C018394	4.6087660756533e-05	0.00201368409796631	Abscisic acid receptor
MELO3C015043	4.71004272699638e-05	0.00204436557836157	DnaJ-like protein
MELO3C025391	4.83084956899305e-05	0.00207353939040731	No data found
MELO3C025056	4.8402534760128e-05	0.00207353939040731	zinc finger CCCH domain-containing protein 53-like
MELO3C024376	4.90235715564502e-05	0.00208656576437141	Eukaryotic initiation factor 4A (ATP-dependent RNA helicase eIF4A)
MELO3C009292	5.42517615724769e-05	0.00222633555573646	ABC transporter G family member 20
MELO3C022693	5.60978884305285e-05	0.00227958271319858	GDSL esterase/lipase 5
MELO3C021332	6.05753663890374e-05	0.00238547596635887	40S ribosomal protein S21
MELO3C005992	6.3408310252755e-05	0.00246211971008436	homeobox-leucine zipper protein ATHB-7
MELO3C020255	6.65873213148149e-05	0.00253378229026258	3-phosphoinositide-dependent protein kinase-1
MELO3C025026	7.38424094659518e-05	0.00271924112679749	abscisic stress-ripening protein 2-like
MELO3C013084	7.63203350274688e-05	0.0027671089367998	Aminopeptidase
MELO3C025654	8.41080056708243e-05	0.00292498547025566	Transmembrane protein
MELO3C005828	8.65793669142523e-05	0.00296335514244293	SKP1-like protein 21
MELO3C005872	8.92453339496058e-05	0.00303555374175946	Polypyrimidine tract binding protein, putative
MELO3C006670	9.2026495270625 1e-05	0.00307398449987238	Translationally-controlled tumor protein homolog
MELO3C012943	9.46720039655125e-05	0.00313704262804514	ADP,ATP carrier protein
MELO3C010021	9.6358700537813e-05	0.00317694153075337	ER membrane protein complex subunit 10
MELO3C021901	0.000102486479856445	0.00328012097486915	Alpha/beta hydrolase-3
MELO3C013261	0.000104022481609345	0.00329094438804991	No data found
MELO3C003906	0.000107750928353134	0.00338431427849777	Ethylene receptor
MELO3C002085	0.000113224239913556	0.00346676823884159	ethylene-responsive transcription factor ERF071
MELO3C024324	0.000116198570528248	0.00352495494601283	Chaperone protein DnaJ
MELO3C022837	0.000116753774780598	0.00352564265770953	Cysteine-rich repeat secretory protein 60
MELO3C010776	0.000116715602386908	0.00352564265770953	Branched-chain-amino-acid aminotransferase
MELO3C001165	0.000124820210286147	0.00368471499692246	eukaryotic translation initiation factor 3 subunit M
MELO3C016924	0.000125729655771067	0.00369128273352684	pentatricopeptide repeat-containing protein At4g33170-like
MELO3C023989	0.000126739273406784	0.00369715496382656	Methyltransferase
MELO3C007246	0.000136437561226055	0.00384148920539927	28 kDa heat/acid-stable phosphoprotein-like protein
MELO3C023033	0.000141418977736452	0.00392810603560785	heterogeneous nuclear ribonucleoprotein 1-like
MELO3C019087	0.000146130882510365	0.00398610331311767	UDP-glycosyltransferase 76E2-like
MELO3C013563	0.000146093610227327	0.00398610331311767	Metacaspase-5
MELO3C005692	0.000146809861828023	0.00399910063619536	E3 ubiquitin-protein ligase At3g02290-like
MELO3C024861	0.000151226502948631	0.00407445048667466	Caffeic acid O-methyltransferase
MELO3C018160	0.000152143725675513	0.00407691511311494	factor of DNA methylation 1-like
MELO3C008974	0.000155525458351624	0.00413387924224256	60S ribosomal protein L35a
MELO3C002163	0.000164730021437798	0.00426283287985112	E3 ubiquitin-protein ligase RING1-like
MELO3C014217	0.000167148322577915	0.00427592256812336	Telomere repeat-binding protein 4
MELO3C005001	0.000170562545132369	0.00434637381137955	dof zinc finger protein DOF5.3-like
MELO3C020583	0.000173737441671706	0.0044017019494474	Neutral ceramidase
MELO3C014799	0.000175285251514445	0.00442673712552274	TRANSPORT INHIBITOR RESPONSE 1 protein, putative
MELO3C022562	0.00017556921672901	0.00442824579972059	protein CHROMATIN REMODELING 19 isoform X1
MELO3C006239	0.000194745937404539	0.0048075468972528	Receptor protein kinase, putative
MELO3C022684	0.000194616340531306	0.0048075468972528	peroxisomal (S)-2-hydroxy-acid oxidase GLO4-like
MELO3C024902	0.000197626941677576	0.00484235046053404	ABC subfamily C transporter
MELO3C022540	0.000216005163480082	0.00519433149706969	NADH dehydrogenase [ubiquinone] 1 beta subcomplex subunit 7
MELO3C019629	0.000220238525441285	0.00524667145831115	ALA-interacting subunit 3-like
MELO3C019921	0.000224478914295334	0.00530926236936354	Phospholipid-transporting ATPase
MELO3C011682	0.00023316957210473	0.00547828218461161	Fructose-1,6-bisphosphatase
MELO3C005111	0.00023446163867713	0.00548351994895583	Coiled-coil protein
MELO3C014614	0.000235860026803869	0.00549292413838397	Leucine-rich repeat receptor-like protein kinase family
MELO3C017008	0.000239417539566356	0.00552722123260604	Ubiquitin family protein
MELO3C024688	0.000240582824529545	0.00554407258066976	TATA-binding protein-associated factor 2N
MELO3C009127	0.000241609568591317	0.00556124402110712	WRKY family transcription factor family protein
MELO3C007425	0.000247283160818346	0.0056205337601488	1-aminocyclopropane-1-carboxylate oxidase 1

MELO3C002351	0.000259527766881318	0.00580454571703188	Receptor protein kinase-like protein
MELO3C013766	0.000277047881957371	0.00602295331887094	Translocase of chloroplast
MELO3C022679	0.000277183104936407	0.00602295331887094	oligouridylate-binding protein 1B-like
MELO3C005002	0.000281040859585691	0.00607916312810274	Interactor of constitutive active ROPs-like protein
MELO3C012349	0.000282115086382206	0.00609572302074638	replication protein A 14 kDa subunit B-like
MELO3C008097	0.000282891183413736	0.00610581200135287	Polyprotein
MELO3C022353	0.000283476774613156	0.0061117716395581	tRNA dimethylallyltransferase
MELO3C020850	0.000287415273795277	0.00616304477978603	Filament-like plant protein 7
MELO3C003771	0.000289095891857327	0.00616328919688229	Mitochondrial 39S ribosomal protein L53
MELO3C007084	0.000290601122250878	0.00617769813060558	BTB/POZ domain-containing protein
MELO3C012335	0.00030093175099899	0.00634386020921778	Uricase
MELO3C002298	0.00030226452811033	0.00635973082156247	Methylthioribose-1-phosphate isomerase
MELO3C004818	0.000313659812932854	0.00651363579980119	S-adenosyl-L-methionine-dependent methyltransferase superfamily protein
MELO3C025628	0.000319630051430653	0.00660290155408364	Aspartyl/glutamyl-tRNA (Asn/Gln) amidotransferase subunit B
MELO3C017698	0.00034384648671526	0.00697905885523091	Vesicle transport protein GOT1
MELO3C021510	0.000345680560706607	0.00699471864077334	Ferredoxin-thioredoxin reductase catalytic chain
MELO3C007119	0.000364741286312031	0.00730555341113216	E3 ubiquitin-protein ligase arkadia-A, putative
MELO3C026919	0.000385875008708902	0.00765125054918887	RuBisCO large subunit-binding protein subunit alpha, chloroplastic
MELO3C006096	0.000388869747816378	0.00769517900764094	DNA replication complex GINS protein SLD5
MELO3C006726	0.000393613047360519	0.00775021343202681	Galactokinase
MELO3C023350	0.000393498277305726	0.00775021343202681	GATA transcription factor
MELO3C005861	0.000394326202309614	0.00775296869722632	Hexosyltransferase
MELO3C020610	0.000397760016506599	0.00776020694699844	protein TOC75-3, chloroplastic
MELO3C021139	0.000416728063664884	0.00798238170586701	No data found
MELO3C005875	0.000415414077330256	0.00798238170586701	Curved DNA-binding protein
MELO3C012171	0.000417125825128095	0.00798238170586701	phosphatidylinositol 4-kinase gamma 5
MELO3C008086	0.00042505111070712	0.00809656108130136	Delta-aminolevulinic acid dehydratase
MELO3C025753	0.000438646630847916	0.0082897916867134	elongation factor 1-alpha
MELO3C006289	0.000446332049387155	0.00840287096601232	Unknown protein
MELO3C023876	0.000456434521640348	0.00855230110804101	glycerol-3-phosphate acyltransferase 5-like
MELO3C009542	0.00046017704841339	0.00859657502875971	BEL1-like homeodomain protein 1
MELO3C009490	0.000477551177120339	0.00880593669182967	Ribosomal protein S11
MELO3C026433	0.000478847432524576	0.00882160256056703	U4/U6 small nuclear ribonucleoprotein PRP4-like protein
MELO3C026780	0.000482363906618488	0.00886692143153668	Ribosomal protein S19
MELO3C019735	0.000492040262321525	0.00894906064744133	1-aminocyclopropane-1-carboxylate oxidase
MELO3C026705	0.000490305274858382	0.00894906064744133	Vesicle-associated membrane protein, putative
MELO3C013938	0.000499419243035093	0.00902351976145818	Protein transport protein Sec16B
MELO3C011070	0.000500007962388027	0.00902351976145818	Rhamnogalacturonate lyase
MELO3C013436	0.000502109941717843	0.00903935208658677	DNA helicase
MELO3C012073	0.000503847273066516	0.00906236775572916	SNF1-related kinase regulatory subunit gamma 1
MELO3C008245	0.000504765109731187	0.00906236922916473	Delta-1-pyrroline-5-carboxylate synthetase
MELO3C023998	0.000507430810900544	0.00908544975927003	Protein RETICULATA-RELATED 4, chloroplastic
MELO3C006430	0.000517174720864766	0.00920981385244208	ethylene-responsive transcription factor 1B
MELO3C008866	0.000517893399529346	0.00921430337595049	Plasma-membrane choline transporter family protein
MELO3C005720	0.000530338114349549	0.0093264892433564	Late embryogenesis abundant protein
MELO3C008491	0.000531797074916351	0.00934382600758276	Zinc finger protein CONSTANS
MELO3C009346	0.000538853443754816	0.00942651619399203	translin
MELO3C007391	0.000540671539647652	0.00944931171371813	Glycosyl transferase, family 31
MELO3C025062	0.000544142102876677	0.00947406635026766	transcription initiation factor TFIID subunit 11-like
MELO3C003567	0.000545821213981501	0.00948892883355692	Glycosyltransferase
MELO3C012178	0.000548063155305423	0.00951115927427662	protein PHYLLO, chloroplastic isoform X1
MELO3C022260	0.000550317736865757	0.00952517527200863	CDPK-related kinase 3 isoform X1
MELO3C008806	0.000551102874571718	0.00953041214528622	Echinoderm microtubule-associated protein-like 6
MELO3C005706	0.000567796577401691	0.00971699705988388	40S ribosomal protein S10-1
MELO3C002714	0.000579702326297893	0.00988647775652598	60S ribosomal protein L18a-like protein
MELO3C024760	0.000592163910059229	0.00997836609194515	RNA polymerase sigma factor sigA
MELO3C011805	0.000592819805662836	0.00998090225237456	No data found
MELO3C018462	0.000600683577282934	0.0100436026132101	Polyadenylate-binding protein
MELO3C005899	0.000607220982714818	0.0101086526857278	Protein yippee-like
MELO3C011873	0.000621061425400415	0.0102808654980692	60S ribosomal protein L17
MELO3C017030	0.000630415357957714	0.0103750607535891	Bromodomain-containing protein
MELO3C015270	0.000642051019905554	0.0104878954442637	single-stranded DNA-binding protein, mitochondrial
MELO3C018027	0.000645454282273139	0.0105173899510002	Pyruvate kinase
MELO3C012452	0.000667682946013937	0.0107902195406569	CSC1-like protein isoform X1
MELO3C001971	0.000668754302383112	0.0107902195406569	HVA22-like protein
MELO3C007012	0.000677563644158052	0.0108878799092574	DNA polymerase eta
MELO3C000881	0.000697534212565021	0.0111004054504002	Unknown protein
MELO3C013007	0.000705481661930962	0.0111962038589772	profilin-like
MELO3C008775	0.000711395060906339	0.0112574848219866	Elongation factor 4
MELO3C007667	0.000719402723322826	0.0113207046875717	Epidermal patterning factor-like protein
MELO3C009128	0.000720765197783857	0.0113240985608858	F-box/LRR-repeat protein 15
MELO3C019498	0.000730368821527216	0.0113934074694637	Tubby-like F-box protein
MELO3C014062	0.000737302663945227	0.0114563259718759	Tir-nbs resistance protein
MELO3C004589	0.000738241873302403	0.0114619015376173	Mitochondrial import inner membrane translocase subunit Tim17-like protein
MELO3C017561	0.000741241733906883	0.0114728845422048	Gras family transcription factor
MELO3C003678	0.000746920851982136	0.0115331820999181	DNA-directed RNA polymerase subunit beta
MELO3C003086	0.000755050317633899	0.0116405064191662	protein GPR107
MELO3C021326	0.000766461351612402	0.0117888202749169	Peroxisomal fatty acid beta-oxidation multifunctional protein
MELO3C015233	0.000766447720925711	0.0117888202749169	ABC1-like kinase
MELO3C025645	0.000773924241273871	0.0118566152606867	gamma-glutamyl hydrolase 2-like
MELO3C015686	0.000774471299118229	0.0118566152606867	Lectin receptor kinase
MELO3C002662	0.00078275615172041	0.0119187750503673	Receptor kinase, putative
MELO3C023644	0.000784187854190543	0.0119225443154391	subtilisin-like protease SBT3.17
MELO3C007281	0.00078421110262572	0.0119225443154391	Transmembrane protein, putative
MELO3C021170	0.00079612896994774	0.0120388598985436	BTB/POZ domain-containing protein POB1
MELO3C015844	0.000797345327828602	0.012048028216746	DNA repair helicase
MELO3C013761	0.000803412442861307	0.0120892909496463	MLO-like protein
MELO3C026224	0.000806198958957616	0.0120946682916889	Aspartyl aminopeptidase family protein
MELO3C011018	0.000812005118265402	0.0121487038489571	Thaumatin-like protein 1
MELO3C016522	0.000815966088231534	0.0121714739300738	Unknown protein
MELO3C007143	0.000819606583127408	0.0121977471063928	NAD(P)-binding domain-containing protein

MELO3C001947	0.000841859856859473	0.0124352208774254	eukaryotic translation initiation factor 3 subunit G-like
MELO3C016408	0.000849878202600962	0.0124919222927065	D-2-hydroxyglutarate dehydrogenase, mitochondrial-like
MELO3C024287	0.000858057790619982	0.0125439869644173	GATA transcription factor 24-like
MELO3C022319	0.000857819419544437	0.0125439869644173	DNA primase large subunit
MELO3C020710	0.000855996771340739	0.0125439869644173	THO complex subunit 4A
MELO3C003439	0.000864308651512991	0.0126158400286253	NAD(P)-binding rossmann-fold protein
MELO3C013707	0.000869260816383277	0.0126787532221221	Thioredoxin reductase
MELO3C018689	0.000892082156492835	0.0129257010334387	nuclear transcription factor Y subunit C-2
MELO3C010903	0.00089679269942633	0.0129749150336781	thylakoidal processing peptidase 1, chloroplastic-like
MELO3C025720	0.00090037014311295	0.0129920969393496	phototropin-1
MELO3C010183	0.000904336723108301	0.0129920969393496	glycine-rich cell wall structural protein 2-like
MELO3C003139	0.000913198703413887	0.013059204340131	ATP-dependent zinc metalloprotease FtsH
MELO3C020172	0.000915802238327545	0.0130774970388508	Hydroxyacylglutathione hydrolase
MELO3C007144	0.000921378557700914	0.0131286472842968	DNA helicase
MELO3C018046	0.000926412561525591	0.0131718658585809	Zinc transport ZntB
MELO3C025347	0.000928175455473412	0.0131874367411111	Short-chain dehydrogenase/reductase
MELO3C009770	0.000931788216151919	0.0132197453166553	two-component response regulator ORR9-like
MELO3C015926	0.000935266432297022	0.0132500550727646	DNA helicase
MELO3C007917	0.000939995495577994	0.013286163190543	thiosulfate sulfurtransferase 18 isoform X1
MELO3C004539	0.000946307413841607	0.0133322132934015	serine/threonine protein phosphatase 2A 57 kDa regulatory subunit B' iota isoform-like
MELO3C005046	0.000947141386938188	0.0133322132934015	protein indeterminate-domain 2
MELO3C007646	0.000954499819987076	0.0133975955543175	heptahelical transmembrane protein 4-like
MELO3C012016	0.00097897348711995	0.0136153150684027	MLP-like protein 423
MELO3C005915	0.000986201687010468	0.0136581326204556	Mitochondrial import inner membrane translocase subunit Tim17/Tim22/Tim23 family protein
MELO3C025944	0.000985917354598187	0.0136581326204556	ABC1 family protein
MELO3C016811	0.000987087449194402	0.0136608199258166	Ubiquitin system component Cue
MELO3C015770	0.000999619597627954	0.0137301972062592	phospholipase A1-Igamma1, chloroplastic-like isoform X1
MELO3C007467	0.00100905049094524	0.0138099363448909	No data found
MELO3C007316	0.00101829843398527	0.0139089177661161	Transmembrane protein, putative
MELO3C001943	0.00103568118847042	0.0140667073781726	17. class I heat shock protein
MELO3C024239	0.0010406075041931	0.0140953069960971	Mitochondrial carrier protein
MELO3C010959	0.00104181627537914	0.014102007966047	Adenosine kinase, putative
MELO3C014116	0.0010524633137019	0.0142168932847461	poly(A)-specific ribonuclease PARN
MELO3C021598	0.0010608705730426	0.0142852160059244	pre-rRNA-processing protein ESF2
MELO3C010821	0.00106381826751312	0.0143018018823121	Glutamyl-tRNA (Gln) amidotransferase subunit A
MELO3C013824	0.00106573213139216	0.0143080515723071	inactive poly [ADP-ribose] polymerase RCD1-like
MELO3C000254	0.00107265318236205	0.014391187295155	Auxin response factor
MELO3C013964	0.00107467152470697	0.0144084778964277	Flavin-containing monooxygenase
MELO3C019125	0.00107877740647	0.0144537143828874	WAT1-related protein At5g07050-like
MELO3C002134	0.00109141215498465	0.0145872662731249	protection of telomeres protein 1a-like isoform X1
MELO3C008124	0.0010950939938712	0.0146128454628124	SNARE associated Golgi protein family
MELO3C020616	0.00110160610411703	0.0146898169819089	Haloacid dehalogenase-like hydrolase
MELO3C004713	0.00111704118586142	0.0148355389237238	Ribosomal protein
MELO3C019140	0.00112109638180102	0.0148595083563484	Nascent polypeptide-associated complex subunit alpha-like protein
MELO3C006995	0.00112951941137085	0.0149353473849775	DNA helicase
MELO3C025511	0.00116227454348072	0.0152506151645319	elongation factor 1-alpha-like
MELO3C003420	0.0011601994899415	0.0152506151645319	Ring finger protein, putative
MELO3C024554	0.00117317342071144	0.0153437098580332	Chaperone dnaJ-like protein
MELO3C018981	0.00117475910333109	0.0153529891038268	UNC93-like protein
MELO3C026230	0.00117574360508321	0.0153529891038268	Ribonuclease J
MELO3C026886	0.00121509032211076	0.0157562828439694	Chaperone DnaJ
MELO3C007914	0.00122356487409925	0.015796148569604	calmodulin-lysine N-methyltransferase isoform X1
MELO3C007724	0.00123610608361802	0.0158993585323115	Pesticidal crystal cry8Ba protein
MELO3C003675	0.00123674154707298	0.0158993585323115	Protein TIFY 8
MELO3C022009	0.00125751310639199	0.0160950267907553	Vesicle transport v-SNARE family protein
MELO3C010375	0.00126258066098428	0.0161389679441932	DNA ligase
MELO3C026013	0.00126215947958241	0.0161389679441932	Plectin-like protein
MELO3C008252	0.00126698624011023	0.016174344703256	Protease inhibitor/seed storage/lipid transfer family protein
MELO3C014398	0.00127170983656311	0.0162085217333131	Myosin-binding protein 1
MELO3C016882	0.00128643995485178	0.0163277009436811	Magnesium transporter NIPA
MELO3C023961	0.00128738672658923	0.0163292231621135	ras-related protein RABA4c isoform X1
MELO3C011040	0.00129103487176252	0.0163649856755058	40S ribosomal protein S6-like
MELO3C006507	0.00129529568976838	0.0163979452418178	40S ribosomal protein S3a
MELO3C014190	0.00130600334466013	0.0165017658692853	DUF4408 domain protein
MELO3C016300	0.00132248461135576	0.0166461877352294	UDP-glucose 4-epimerase family protein
MELO3C012715	0.00132243173147539	0.0166461877352294	mediator of RNA polymerase II transcription subunit 19a-like
MELO3C005294	0.00132249068593726	0.0166461877352294	Myosin-binding protein 2
MELO3C021556	0.00132370263701453	0.0166508301773249	ADP-ribosylation factor-like
MELO3C012296	0.00133013796895898	0.0166786633326799	Unknown protein
MELO3C015409	0.00134065781250059	0.0167467749140254	ABC transporter B family protein
MELO3C003846	0.00135074087660314	0.0168514097106983	Glucan endo-1,3-beta-glucosidase, putative
MELO3C009873	0.00136459747634987	0.0169920779069569	zinc-finger homeodomain protein 9-like
MELO3C015398	0.00136911537600959	0.017026863703283	cysteine synthase-like
MELO3C008375	0.00138251768956899	0.0171288217385809	Unknown protein
MELO3C017272	0.00138518236716068	0.0171403299304863	Ethylene-responsive transcription factor
MELO3C006587	0.0013871485080218	0.0171431763985747	Endonuclease/exonuclease/phosphatase family protein
MELO3C027346	0.00139863809916196	0.0171921631272379	Indole-3-acetic acid-amido synthetase GH3.3
MELO3C016965	0.00140646424613533	0.0172416278069067	Formin-like protein
MELO3C017133	0.00141800169024686	0.0172971682400774	No data found
MELO3C008096	0.00142424626433679	0.0173305233976508	Galactose-binding domain-like protein
MELO3C019524	0.0014304129339574	0.017373447129597	40S ribosomal protein S16
MELO3C011834	0.00143661881258605	0.0174273863204926	Protein EI24 like
MELO3C022932	0.00145937989094569	0.0175954172565851	Auxin response factor
MELO3C015477	0.00146228225489542	0.0176089099097132	No data found
MELO3C014281	0.0014702360035872	0.0176508758874429	Aldo/keto reductase, putative
MELO3C021914	0.00146823354847903	0.0176508758874429	peroxidase 10-like
MELO3C007497	0.0014780779626572	0.0177234740039569	Transcription termination factor family protein
MELO3C002416	0.00148622342396076	0.017777968746094	Ankyrin repeat family protein
MELO3C021536	0.00151639341105281	0.0180296529048055	Quinone oxidoreductase-like protein
MELO3C003457	0.00152415156525021	0.018078359917193	protein EMBRYONIC FLOWER 1-like isoform X3
MELO3C021148	0.00153136859350866	0.0181146196894978	Autophagy-related protein

MELO3C025035	0.00153071881752509	0.0181146196894978	lecithin-cholesterol acyltransferase-like 1
MELO3C020427	0.00153376154089113	0.018127023740909	DEAD-box ATP-dependent RNA helicase 42-like
MELO3C022392	0.00153951311588807	0.018173248371592	Cytochrome oxidase complex assembly protein
MELO3C011439	0.00154415748059011	0.0182171840407253	6,7-dimethyl-8-ribityllumazine synthase
MELO3C010197	0.00157227802397697	0.0184785490735071	Tetratricopeptide repeat (TPR)-like superfamily protein
MELO3C010403	0.00157447526897514	0.0184865113477943	LOW QUALITY PROTEIN: LEAF RUST 10 DISEASE-RESISTANCE LOCUS RECEPTOR-LIKE PROTEIN KINASE-like 1.4
MELO3C024313	0.00158260126212806	0.0185349689647406	AT-rich interactive domain-containing protein 4-like
MELO3C014944	0.00158975633025693	0.0185423015211278	homeobox-leucine zipper protein HAT22-like
MELO3C016193	0.00158896575333467	0.0185423015211278	Lysine-specific histone demethylase 1
MELO3C022042	0.00159143253219463	0.0185423015211278	DUF2039 family protein
MELO3C019491	0.00160887864625414	0.0186904378734547	Nucleolar complex protein 2 homolog
MELO3C007099	0.00160852551941759	0.0186904378734547	Nucleoporin protein Ndc1-Nup
MELO3C020159	0.00160703147890584	0.0186904378734547	transmembrane protein 87A
MELO3C023852	0.00164327417852994	0.0189672833148964	Actin family protein
MELO3C013753	0.00168358970314475	0.0193016055803562	Vacuolar protein sorting-associated protein 35
MELO3C024001	0.00169134873987065	0.0193637369644669	MADS-box transcription factor
MELO3C003770	0.0016973381454457	0.019401769103248	TLD-domain nucleolar protein
MELO3C009090	0.00173121000396637	0.0196392051611116	Kinase family protein
MELO3C019490	0.00173728752931601	0.0196392051611116	40S ribosomal protein S16
MELO3C005455	0.00173406833228484	0.0196392051611116	origin of replication complex subunit 3
MELO3C008195	0.00173319093407187	0.0196392051611116	Katanin p60 atpase-containing subunit a1
MELO3C016494	0.00174848962342988	0.019709430121642	Polygalacturonase
MELO3C017294	0.00174730515676302	0.019709430121642	Carbon catabolite repressor protein 4 like 3
MELO3C015470	0.00175565135908395	0.0197675933241442	beta-galactosidase
MELO3C021264	0.00177097699103468	0.0198834704922933	Ubiquitin-conjugating enzyme, E2
MELO3C018459	0.00179830009973014	0.0201216026456491	40S ribosomal protein S16
MELO3C025142	0.00180918499272109	0.0202090466183534	Proliferating cell nuclear antigen
MELO3C002604	0.00183522225955302	0.0204536142234269	DUF2921 family protein
MELO3C008786	0.00185244710486099	0.0206223099627394	Rhomboid protein, putative
MELO3C026593	0.00186878067212692	0.0207573394228541	Surfeit locus protein 2 (SURF2)
MELO3C012493	0.00187295993871484	0.0207687174787643	Choline/ethanolamine kinase
MELO3C012420	0.00187233804376197	0.0207687174787643	No data found
MELO3C012852	0.00188039613797097	0.0208203232473985	Protein BREAST CANCER SUSCEPTIBILITY 1-like protein
MELO3C015177	0.00188263980533365	0.0208292736781705	60S ribosomal protein L13a, putative
MELO3C008032	0.00188467890401967	0.020840158832858	Actin
MELO3C018413	0.00188895876601003	0.0208569116575077	Allene oxide synthase
MELO3C023862	0.0019068491527422	0.0210027680620675	Factor of DNA methylation 1
MELO3C025744	0.00190635644741377	0.0210027680620675	Zinc finger family protein, putative
MELO3C020588	0.00196327140921926	0.0214806908923386	17.5 kDa class I heat shock protein
MELO3C008516	0.00196685604928237	0.0214960930366782	Guanosine nucleotide diphosphate dissociation inhibitor
MELO3C019814	0.00201274196770884	0.0218719472185081	ABC transporter G family member
MELO3C006934	0.00202201822291359	0.021892587246618	protein REVEILLE 6-like isoform X2
MELO3C007228	0.00202308834498344	0.021892587246618	GDSL esterase/lipase
MELO3C014417	0.00204144586045041	0.0220188499716194	sugar transporter ERD6-like 7
MELO3C018781	0.0020542658700694	0.0220967846775603	Leucine-rich repeat family protein
MELO3C011972	0.00208045004987989	0.0223176578137305	Alpha-glucan water dikinase, chloroplastic
MELO3C009600	0.00209252401614957	0.022398513167988	60S ribosomal protein L21
MELO3C013539	0.00209583349110565	0.0224217852740224	vesicle-associated protein 4-2-like
MELO3C010198	0.00210011636188545	0.0224554401899706	DNA-directed RNA polymerase subunit beta
MELO3C002268	0.00211346018252012	0.0225736750376365	Iron-sulfur cluster assembly protein
MELO3C026887	0.00212116551042296	0.022643728467753	Tryptophan synthase, alpha chain
MELO3C011763	0.0021263565296451	0.0226746301857241	LRR receptor-like kinase
MELO3C021153	0.00213199409674547	0.0227224778287244	Arginine--tRNA ligase
MELO3C025491	0.00215106029913348	0.0228516889981641	transcription initiation factor TFIID subunit 1-like
MELO3C015457	0.00216212621458034	0.0229445623921263	K(+) efflux antiporter
MELO3C002598	0.00217096035433062	0.0230012317798688	E3 ubiquitin-protein ligase RMA1H1-like
MELO3C009489	0.0021885277242305	0.0231377055812785	Ribosomal protein S11
MELO3C003496	0.00219345078663657	0.0231525705960907	Phosphoglycerate mutase-like protein 1
MELO3C011042	0.00220196138837392	0.0232175843347552	VQ motif-containing protein 9
MELO3C019361	0.00220806422194508	0.0232695092418321	fasciclin-like arabinogalactan protein 7
MELO3C006212	0.00222542135216774	0.0233900193102506	tRNA (Guanine-N(7)-)-methyltransferase
MELO3C009757	0.00222821468022771	0.0234069211275623	Amino acid transporter family protein
MELO3C008970	0.00223264451449334	0.023440986983907	vacuolar protein sorting-associated protein 20 homolog 2-like
MELO3C015292	0.00225207974747366	0.0236199272081026	Epoxide hydrolase 2
MELO3C005976	0.00225640094494073	0.0236526869753898	Protein AATF
MELO3C007466	0.00225882808818756	0.0236530201026597	RNA cytidine acetyltransferase
MELO3C007270	0.00226366852216031	0.023678596209822	Ring finger protein, putative
MELO3C008100	0.00229727735813157	0.0239287608363609	gibberellin receptor GID1B
MELO3C022165	0.00231035379912992	0.0239890521445934	Actin-binding LIM protein 1, putative
MELO3C018492	0.00231232472788601	0.0239969001844565	Cinnamyl alcohol dehydrogenase
MELO3C006106	0.00232061450614851	0.0240576461322451	U-box domain-containing protein kinase family protein, putative
MELO3C016952	0.00234128339180883	0.0241830573770045	eukaryotic translation initiation factor-like
MELO3C017817	0.0023669444389276	0.0243335688310157	transaldolase
MELO3C003722	0.00237262336257049	0.0243792605553614	serine/threonine-protein kinase STY46-like isoform X1
MELO3C013034	0.00238546539224549	0.0244603094659689	Charged multivesicular body 1
MELO3C019725	0.00239709679529321	0.0245540791546917	ethylene-responsive transcription factor 3-like
MELO3C023404	0.00240231684114978	0.0245947927920513	DNA replication complex GINS protein PSF1
MELO3C021521	0.00240698686863405	0.0246043393730093	WAT1-related protein
MELO3C026286	0.00240990356136972	0.0246086791279682	Protein MICRORCHIDIA 6
MELO3C027184	0.00242276758035198	0.0246889767514816	DNA primase
MELO3C004761	0.00243983236026302	0.0248134188898108	CBS domain-containing protein CBSX1, chloroplastic
MELO3C018797	0.00243837045809947	0.0248134188898108	Cysteine-rich receptor-kinase-like protein
MELO3C009908	0.00245124923270912	0.0249021199057471	Type I inositol polyphosphate 5-phosphatase, putative
MELO3C011264	0.00245758550501518	0.0249280206155854	Histone acetyltransferase
MELO3C009639	0.00246576674180576	0.0249496524561083	Squamosa promoter binding protein
MELO3C010493	0.00246180150676134	0.0249496524561083	Aldehyde dehydrogenase
MELO3C019827	0.00246720498745034	0.0249496524561083	MEF2BNB-like protein
MELO3C019500	0.00249021021586082	0.0251170385868414	Protein-protein interaction regulator family protein
MELO3C018683	0.00249307436724266	0.0251330912091247	Actin
MELO3C011084	0.00250020007177665	0.0251920669477128	Ribosomal RNA small subunit methyltransferase A
MELO3C004381	0.00251245552795387	0.025251137008428	Auxin-responsive protein

MELO3C023844	0.00252223327356038	0.0253107646948902	2-oxoglutarate dehydrogenase E1 component family protein
MELO3C019704	0.00252200355091303	0.0253107646948902	Serine/threonine protein phosphatase 7 long form
MELO3C018460	0.00253286875232273	0.0253659355931144	O-acyltransferase WSD1-like
MELO3C016014	0.0025571448957098	0.0255184712205016	thiamine pyrophosphokinase 1
MELO3C002277	0.0025908406468802	0.0257506350957408	Glutathione transport system permease protein gsiD
MELO3C026572	0.00260563742446895	0.0258067871092464	Proline transporter
MELO3C003818	0.00260420294403418	0.0258067871092464	Tubby-like F-box protein
MELO3C024244	0.00261508509481012	0.0258485062749775	Ribosomal protein L37
MELO3C017158	0.00262413446791454	0.0258938185759979	Serine/threonine-protein kinase atr
MELO3C007785	0.00263134950686683	0.0259431666044565	RING-H2 zinc finger protein RHA2a
MELO3C009532	0.0026377958393965	0.025943562933669	NDR1/HIN1-like protein 12
MELO3C021618	0.00263523784937714	0.025943562933669	ribosomal RNA large subunit methyltransferase E-like
MELO3C027119	0.00263408267344634	0.025943562933669	1-aminocyclopropane-1-carboxylate oxidase 2
MELO3C026901	0.00263783859288103	0.025943562933669	HNH endonuclease
MELO3C004385	0.00265207979831772	0.0260253671353869	pathogenesis-related protein PR-4-like
MELO3C004519	0.00267496625574049	0.0261783491499598	NADH-cytochrome b5 reductase-like protein
MELO3C006439	0.00270856493483707	0.0264476999835899	1-aminocyclopropane-1-carboxylate oxidase homolog 1-like
MELO3C022497	0.00270918512667995	0.0264476999835899	40S ribosomal protein S13
MELO3C014925	0.00272905227228559	0.026570628428043	Glycerophosphodiester phosphodiesterase, putative
MELO3C023599	0.00273464015593183	0.0265885133692798	Glutamine synthetase
MELO3C013603	0.0027441539772568	0.0266573029497514	Plant/protein (DUF789)
MELO3C006153	0.00275443894018501	0.0267440583233598	UDP-galactose/UDP-glucose transporter 2-like
MELO3C017228	0.00276531793823609	0.0267576011573859	Replication protein A 70 kDa DNA-binding subunit
MELO3C007857	0.00277499196625031	0.0268074015965016	LOW QUALITY PROTEIN: protein HYPER-SENSITIVITY-RELATED 4-like
MELO3C012418	0.00277589428653835	0.0268074015965016	Tyramine N-feruloyltransferase 4/11
MELO3C025494	0.00278404522379472	0.0268729761117898	leukotriene A-4 hydrolase homolog
MELO3C013665	0.00278843488334646	0.0269021985887685	mechanosensitive ion channel protein 6-like
MELO3C015682	0.00283388627394909	0.0272607988427767	Zinc finger BED domain-containing protein DAYSLEEPER
MELO3C012175	0.00285815822128543	0.0274274862546968	Thioredoxin-like protein aaed1, chloroplastic
MELO3C020157	0.00286972839969413	0.0274591329505104	Glycerol-3-phosphate dehydrogenase [NAD(+)]
MELO3C018408	0.00286762071520663	0.0274591329505104	methyltransferase-like protein 13
MELO3C006576	0.00287199260083404	0.0274668193093808	ARM repeat superfamily protein
MELO3C012268	0.00290928855179373	0.0277428969625178	LEAF RUST 10 DISEASE-RESISTANCE LOCUS RECEPTOR-LIKE PROTEIN KINASE-like 1.2 isoform X4
MELO3C022246	0.00291399362481704	0.0277743533284323	cytochrome P450 78A9-like
MELO3C002232	0.00292148187912489	0.0278188744603845	serine/threonine-protein kinase fray2
MELO3C015807	0.00294721274408638	0.0279586801462572	2-oxoglutarate (2OG) and Fe(II)-dependent oxygenase superfamily protein
MELO3C023406	0.00294286704306013	0.0279586801462572	Polygalacturonase
MELO3C017624	0.0029620275572394	0.0280830927642443	Superoxide dismutase
MELO3C022694	0.00296775156879869	0.0281103720538155	Ethylene-responsive transcription factor
MELO3C012527	0.00297250118494685	0.0281418628482816	Guanine nucleotide-binding protein beta subunit-like protein
MELO3C026077	0.0029907075838328	0.0282602117218581	leucine-rich repeat extensin-like protein 3
MELO3C019004	0.00299954481518294	0.0282948581551635	ENTH/ANTH/VHS superfamily protein, putative
MELO3C026638	0.0030153881996442	0.0283981409417135	acyl-protein thioesterase 2
MELO3C017687	0.00303163409125018	0.0285138619671975	solute carrier family 35 member F1
MELO3C022482	0.00303891540561274	0.0285394966468777	SWI/SNF complex component SNF12 homolog
MELO3C011123	0.00303966505635012	0.0285394966468777	oleosin 1-like
MELO3C006635	0.00304572063851438	0.0285701369470703	transcription termination factor MTEF1, chloroplastic-like
MELO3C012211	0.00304978606683126	0.028581418257601	Coiled-coil domain-containing protein 130
MELO3C013275	0.00307285130009638	0.0287238455479359	Eukaryotic translation initiation factor 3 subunit A, putative
MELO3C019546	0.00308152563759556	0.0287740188259455	PRKR-interacting protein 1
MELO3C006945	0.00308380034190114	0.0287816507335566	mediator of RNA polymerase II transcription subunit 36a-like
MELO3C025916	0.00309672394330129	0.0288557686588257	Triosephosphate isomerase, putative
MELO3C006833	0.00310508976483725	0.0288905872097688	AT-hook motif nuclear-localized protein 1
MELO3C006596	0.00312259521677238	0.0290066476651166	squamosa promoter-binding-like protein 7
MELO3C020628	0.00314969349944749	0.0291623520490335	Protein kinase
MELO3C026935	0.00315856654564306	0.0292034319802925	Homeobox-leucine zipper HOX24
MELO3C003790	0.00316375085180232	0.0292240016708344	subtilisin-like protease SBT3.17 isoform X1
MELO3C016435	0.00318004727588184	0.0293470811455095	PHD finger alfin-like protein
MELO3C026949	0.00318437434441865	0.0293732876823559	DNA ligase
MELO3C017665	0.00319763962111685	0.0294681217346882	Ubiquitin-protein ligase, putative
MELO3C020958	0.0032001673855715	0.0294776612395762	Shikimate kinase
MELO3C026019	0.00321334455151734	0.0295852408148792	Abscisic acid receptor
MELO3C013566	0.00323029250749773	0.0296859221640636	Indole-3-acetic acid-amido synthetase GH3.3
MELO3C006900	0.00323377434712158	0.0297040974796763	No data found
MELO3C011141	0.00324029178816565	0.0297363022883287	Transcriptional regulatory plant protein, putative
MELO3C011641	0.00326082986585996	0.0298692620690484	gamma-secretase subunit APH1-like
MELO3C017682	0.00329068344277839	0.0300590690617162	extensin-2
MELO3C011626	0.00329055575005754	0.0300590690617162	Ribosomal protein S8
MELO3C010882	0.00328785247888019	0.0300590690617162	Origin recognition complex subunit 2 family protein
MELO3C015845	0.00329570830198256	0.030079897053516	basic 7S globulin 2
MELO3C014696	0.00330563892729141	0.0301121140106449	Glycosyltransferase
MELO3C024476	0.00332258243518369	0.0302260283252226	alpha carbonic anhydrase 7-like
MELO3C011450	0.00333358893825408	0.0302968467287528	Kelch repeat-containing F-box family protein
MELO3C013981	0.00335602505490162	0.030418811552392	40S ribosomal protein S13
MELO3C021429	0.00335193882671869	0.030418811552392	Ribosomal protein
MELO3C022717	0.00338495688318097	0.0305947430141606	FHA domain-containing protein FHA2
MELO3C012390	0.00339255872463551	0.030635410266496	NAC domain-containing protein 53-like
MELO3C003646	0.00339160336545463	0.030635410266496	guanine nucleotide-binding protein subunit gamma 2-like
MELO3C007740	0.00339467117104308	0.0306404757572806	40S ribosomal protein S6-like
MELO3C015670	0.00339843699782583	0.0306437874748141	Phosphatidylinositol N-acetylglucosaminyltransferase subunit A
MELO3C009826	0.0033996930658422	0.0306437874748141	Carboxypeptidase
MELO3C020709	0.00340145935932612	0.0306457212077242	K-stimulated pyrophosphate-energized sodium pump protein
MELO3C003618	0.00340400756003645	0.0306546946206839	Unknown protein
MELO3C003537	0.00340619799978614	0.0306604395158507	WD-40 repeat-containing protein MSI1
MELO3C005597	0.00341005728531718	0.0306784743320635	1-aminocyclopropane-1-carboxylate synthase
MELO3C012627	0.00344637204195242	0.0309515240820911	KRR1 small subunit processome component homolog
MELO3C008749	0.00344966036879268	0.0309669739196758	CBS domain-containing protein CBSX6
MELO3C017141	0.00345887223368579	0.03102146582337	Dynein light chain
MELO3C011443	0.00346914766687134	0.0310853889623603	Glycosyltransferase
MELO3C019807	0.00348962571938949	0.0312405341487865	Zinc finger (C3HC4-type RING finger) family protein
MELO3C016321	0.00351307924928468	0.0313935756082005	multiple RNA-binding domain-containing protein 1

MELO3C013068	0.00352314090533479	0.0314579681657778	No data found
MELO3C008002	0.0035312711957558	0.0314849096365604	serine/threonine-protein kinase D6PKL2
MELO3C006293	0.00354341023305915	0.0314952662272863	Werner Syndrome-like exonuclease
MELO3C006679	0.00354132679588104	0.0314952662272863	Dihydrolipoamide acetyltransferase component of pyruvate dehydrogenase complex
MELO3C018634	0.00353843304329915	0.0314952662272863	7-deoxyloganetin glucosyltransferase-like
MELO3C002187	0.00354604168811656	0.0315028237960477	Plant/protein (DUF789)
MELO3C002921	0.00354961794420117	0.0315062493393388	Cysteine proteinase inhibitor
MELO3C011266	0.00355690370295292	0.0315425645395677	Histone acetyltransferase
MELO3C009118	0.00356566194604402	0.0316060402928291	TOM1-like protein 2
MELO3C003452	0.00357083843738115	0.0316377246746704	Synaptonemal complex protein 1
MELO3C027277	0.00357454085905751	0.031648946287679	Polygalacturonase
MELO3C012303	0.00357875902153149	0.0316511025151031	Trichome birefringence-like protein
MELO3C006470	0.00359422249341379	0.0317736347459395	p-loop nucleoside triphosphate hydrolase superfamily protein
MELO3C013634	0.00359595157280856	0.0317746969178507	DNA-directed RNA polymerase subunit beta
MELO3C018700	0.00361828856415125	0.0319105985709065	UDP-glycosyltransferase 74F2-like
MELO3C009973	0.00361824768775709	0.0319105985709065	Dead box ATP-dependent RNA helicase, putative
MELO3C019010	0.00362104834108679	0.0319107914717193	No data found
MELO3C010566	0.00362510291757867	0.0319266674182015	Topoisomerase II-associated protein PAT1
MELO3C026594	0.00365773426356975	0.0321337161793767	E3 ubiquitin-protein ligase RGLG2
MELO3C019954	0.00367499471328736	0.0321994102008483	NAC domain-containing protein 17-like
MELO3C018086	0.00367393222298185	0.0321994102008483	No data found
MELO3C002364	0.00368322380190222	0.0322572003830452	glucuronoxylan 4-O-methyltransferase 1
MELO3C007651	0.00368605120965426	0.0322676530760027	BSD domain-containing protein
MELO3C017041	0.00369325977155832	0.032289034232494	Protein canopy 1-like
MELO3C011580	0.00369339856859607	0.032289034232494	Selenoprotein K
MELO3C011306	0.00370901783915945	0.0324112359759115	U2 snRNP-associated SURP motif-containing protein
MELO3C009362	0.00372330748990279	0.032484415475003	4-coumarate--CoA ligase-like 7
MELO3C021694	0.003723971676308	0.032484415475003	equilibrative nucleotide transporter 3-like
MELO3C012147	0.00373986616904487	0.0325742299591907	Chromatin modification-related protein EAF7
MELO3C020756	0.00374575962541046	0.032588108741071	auxin-responsive protein SAUR24-like
MELO3C009313	0.00374905481299304	0.0326024145758694	MCM domain-containing protein
MELO3C019256	0.00375711455194661	0.0326437550754041	Glutamate receptor
MELO3C023561	0.00376053621892014	0.03265460151583	Zinc finger, PHD-type
MELO3C025595	0.00377304170472659	0.0326903479823329	Hydroxyacylglutathione hydrolase 3, mitochondrial-like protein
MELO3C024527	0.00377219600226342	0.0326903479823329	Monodehydroascorbate reductase family protein
MELO3C021072	0.00376902665796097	0.0326903479823329	p-loop containing nucleoside triphosphate hydrolases superfamily protein, putative
MELO3C022135	0.00377269415701442	0.0326903479823329	Dynamin homolog
MELO3C009659	0.00378297423157448	0.0327359654708158	WD-repeat protein, putative
MELO3C025844	0.00378430346700454	0.0327359654708158	zinc finger CCCH domain-containing protein 66
MELO3C005590	0.00378620329661872	0.0327380599408595	AT-hook motif nuclear-localized protein 1
MELO3C023131	0.00380245973358373	0.0328498588270101	Magnesium chelatase subunit
MELO3C015877	0.00381685302485724	0.0329453804142944	Autophagy-related protein 18g
MELO3C018872	0.00382096715178948	0.0329664833030539	eukaryotic translation initiation factor 1A-like
MELO3C007206	0.00382538871009896	0.0329902190549102	Receptor-like kinase
MELO3C007781	0.0038398486676372	0.0331004676286194	C2 domain-containing family protein
MELO3C026665	0.0038477634826739	0.0331397649451927	BTB/POZ domain-containing protein At5g48800
MELO3C016629	0.00385657378659299	0.0331759691273178	integrator complex subunit 9 homolog isoform X1
MELO3C004813	0.00385700668977274	0.0331759691273178	No data found
MELO3C002951	0.00386183647055627	0.0331771225999734	Peptidyl-prolyl cis-trans isomerase
MELO3C022756	0.00385939753056552	0.0331771225999734	No data found
MELO3C016972	0.00388047519379775	0.0332591859056182	stromal cell-derived factor 2-like protein
MELO3C005658	0.00387972951477389	0.0332591859056182	O-glucosyltransferase rumi homolog
MELO3C002698	0.00388183824560484	0.0332591859056182	Eukaryotic translation initiation factor 4E
MELO3C017496	0.00387421851442116	0.0332591859056182	pathogenesis-related protein PR-1
MELO3C007029	0.00388454470007149	0.0332679415792332	glycine-rich RNA-binding protein 4, mitochondrial
MELO3C012831	0.0038908092763863	0.0332927176773627	WD repeat-containing protein 26
MELO3C017322	0.00389583227761392	0.0333068362123798	LEAF RUST 10 DISEASE-RESISTANCE LOCUS RECEPTOR-LIKE PROTEIN KINASE-like 1.2 isoform X2
MELO3C026504	0.00390827463156984	0.0333732318117167	centromere protein V isoform X1
MELO3C008158	0.00393031276265376	0.0334712146397797	Protein PLASTID MOVEMENT IMPAIRED 2
MELO3C019983	0.00392989468547922	0.0334712146397797	Wound-responsive family protein
MELO3C016939	0.00394970593609312	0.0335715480937751	Protein phosphatase 2c, putative
MELO3C008944	0.00394846519055947	0.0335715480937751	ultraviolet-B receptor UVR8 isoform X2
MELO3C026495	0.00394489756670136	0.0335715480937751	cytochrome P450 CYP82D47-like
MELO3C013044	0.00394792703568192	0.0335715480937751	Serine/threonine-protein phosphatase 2A 55 kDa regulatory subunit B
MELO3C007919	0.00395536602137492	0.0335819377854541	alpha-mannosidase
MELO3C022017	0.00395691777946994	0.0335819377854541	Ribosomal protein L18/L5
MELO3C011127	0.00395892010502719	0.0335844987775695	receptor-like protein kinase HSL1
MELO3C021281	0.00397525249759023	0.0336507765001755	Beta-D-xylosidase family protein
MELO3C018648	0.00397329808233615	0.0336507765001755	Annexin
MELO3C006954	0.00399297475803051	0.0336852876960037	Ornithine cyclodeaminase/mu-crystallin
MELO3C026373	0.0039887085281346	0.0336852876960037	Glycosyltransferase
MELO3C007648	0.00398694127513544	0.0336852876960037	RuvB-like helicase
MELO3C019798	0.00398754437598248	0.0336852876960037	Acyl-CoA N-acyltransferase domain protein
MELO3C009105	0.0040092906562702	0.0337845085349958	Receptor-like kinase plant-like protein
MELO3C026103	0.00401371508088511	0.0338024985639232	DUF538 family protein
MELO3C016780	0.00401640311312934	0.0338107182784277	ethylene-responsive transcription factor ERF011-like
MELO3C006678	0.00402069563885754	0.0338324321141021	DUF581 family protein, putative (DUF581)
MELO3C011227	0.00402447276814755	0.0338353821618331	zeaxanthin epoxidase, chloroplastic-like
MELO3C023474	0.00402423910770855	0.0338353821618331	Hydroxycinnamoyl-CoA shikimate/quinate hydroxycinnamoyltransferase
MELO3C011726	0.00404263312343378	0.0339457259093174	Nuclear transcription factor Y subunit B
MELO3C026210	0.00404664750198225	0.0339639785451115	SNF1-related protein kinase regulatory subunit gamma-1
MELO3C006891	0.00405529113468006	0.0340076197956673	heat stress transcription factor B-2b-like
MELO3C002258	0.00406375095139522	0.0340640991252564	No data found
MELO3C009601	0.00408256489346259	0.034175454074849	Dirigent protein
MELO3C006406	0.00409087920567841	0.034175454074849	Transducin/WD40 domain-like protein, putative
MELO3C024610	0.004090155111938	0.034175454074849	Iron-sulfur binding oxidoreductase
MELO3C011869	0.00408858935710987	0.034175454074849	cytochrome P450 78A5-like
MELO3C019649	0.00408633114963042	0.034175454074849	auxin-responsive protein SAUR71
MELO3C016540	0.00409820484929724	0.0341932604853279	NAC domain protein
MELO3C024466	0.00409776864969524	0.0341932604853279	heavy metal-associated isoprenylated plant protein 3-like isoform X2
MELO3C015915	0.00409647381032929	0.0341932604853279	Heme binding

MELO3C013444	0.00410871929360257	0.0342665106965191	No data found
MELO3C011320	0.00411998193635644	0.0343459367870634	NAD(P)-binding rossmann-fold protein
MELO3C009370	0.00412796035380381	0.0343689245477535	ACT domain-containing protein
MELO3C024404	0.00412659958826311	0.0343689245477535	Tudor/PWWP/MBT superfamily protein
MELO3C015314	0.00412612017060354	0.0343689245477535	protein SRC2-like
MELO3C022568	0.00413550035043642	0.0344099668734598	protein indeterminate-domain 5, chloroplastic
MELO3C018374	0.00413637456871707	0.0344099668734598	DUF248-1
MELO3C024936	0.00413994951308028	0.03442520544582	Cleavage and polyadenylation specificity factor subunit
MELO3C005710	0.00414841548622957	0.0344810847801127	heavy metal-associated isoprenylated plant protein 3
MELO3C005504	0.00415565745621238	0.0345267476242063	Disease resistance family protein
MELO3C021144	0.00415874744190292	0.0345378903406816	squamosa promoter-binding-like protein 8
MELO3C014591	0.00417094646782634	0.0346116311413704	cyclin-dependent protein kinase inhibitor SMR3-like
MELO3C022382	0.00417453238090104	0.0346116311413704	Succinate--CoA ligase [ADP-forming] subunit beta, mitochondrial
MELO3C003323	0.00417463696282061	0.0346116311413704	Myosin heavy chain-like protein
MELO3C021407	0.00418955137017907	0.0347207091941529	Stem-specific protein TSJT1
MELO3C004316	0.00419185506808106	0.0347252289175893	Prefoldin chaperone subunit family protein, putative
MELO3C017094	0.00419379751734894	0.0347267535304504	No data found
MELO3C011908	0.00419762735150164	0.0347438988117376	Heat shock protein HSP26
MELO3C002084	0.00420015070006774	0.0347502204338659	Protein NEGATIVE REGULATOR OF RESISTANCE
MELO3C017520	0.00420329844082712	0.0347617005476946	L-allo-threonine aldolase
MELO3C027370	0.00420544322376737	0.0347648799607291	O-methyltransferase, putative
MELO3C011799	0.00420786589404742	0.0347703529462521	Cytochrome P450
MELO3C021944	0.00421779613002127	0.0348378317740652	Flavoprotein wrbA
MELO3C013419	0.00423115977641308	0.0349094003953484	30S ribosomal protein S31, mitochondrial
MELO3C012361	0.00422999190468754	0.0349094003953484	cell division control protein 2 homolog A
MELO3C027137	0.00423176386381408	0.0349094003953484	Gibberellin receptor GID1A
MELO3C004239	0.00424349429512305	0.0349623566267773	Zinc finger protein VAR3, chloroplastic
MELO3C019295	0.00426894623574081	0.0351280913373522	Cellulose synthase family protein
MELO3C013835	0.00427577875347029	0.0351696603924552	Heat shock transcription factor family protein
MELO3C017989	0.00430088886261248	0.0353173613919892	PXMP2/4 family protein 4
MELO3C009787	0.00431780204327548	0.0354267854394048	Protein SRC1
MELO3C004382	0.00433957988353706	0.035551505038091	Auxin-responsive protein
MELO3C022236	0.00435478022543923	0.0356231832101503	Cation/H(+) antiporter 11
MELO3C019833	0.00436921025270542	0.0356854976346896	Glycine-rich RNA-binding family protein
MELO3C025454	0.00438074020671109	0.0357648773635127	2-oxoglutarate dehydrogenase E1 component family protein
MELO3C017245	0.004395158508533	0.0358381442547557	squamosa promoter-binding-like protein 6
MELO3C012982	0.00440400022067899	0.0358543790682549	Bet1-like SNARE 1-1
MELO3C017756	0.0044125107954931	0.0358838655392167	calcium-dependent protein kinase 24
MELO3C022535	0.00441084542698378	0.0358838655392167	Methionine adenosyltransferase 2 subunit beta
MELO3C011419	0.00441372812875063	0.0358838655392167	Purple acid phosphatase
MELO3C011719	0.00441889278353991	0.0358951901894086	Adenylate kinase
MELO3C025492	0.00442331481104608	0.0359046626400941	transcription initiation factor TFIID subunit 1-like
MELO3C007317	0.00443550104810231	0.0359466902553953	Transmembrane protein, putative
MELO3C006341	0.00444064861850657	0.0359683622052152	Holliday junction resolvase
MELO3C026519	0.00444300260802799	0.0359683622052152	AT-hook motif nuclear-localized protein 10
MELO3C013004	0.00444391127554433	0.0359683622052152	protein IQ-DOMAIN 14-like
MELO3C012080	0.00444939745034345	0.03598327200935	binding partner of ACD11 1
MELO3C016733	0.00445369614312496	0.0360032931357245	Estradiol 17-beta-dehydrogenase 1
MELO3C017857	0.00447660665509919	0.0361736926479353	Unknown protein
MELO3C002811	0.00448958909934571	0.0362341214233668	SWIM zinc finger family protein
MELO3C018333	0.00451435304406078	0.0364042295905089	Six-bladed beta-propeller, TolB-like protein
MELO3C017023	0.00452304563686967	0.0364365717273029	Catalase
MELO3C018884	0.00453160110978612	0.0364688632099291	No data found
MELO3C024747	0.00453016901239933	0.0364688632099291	30S ribosomal protein S5, putative
MELO3C014381	0.00455362792746339	0.0366013829627491	Arginine/glutamate-rich 1 protein
MELO3C011270	0.0045788351918522	0.0367591122780037	Adenine phosphoribosyltransferase, putative
MELO3C021302	0.00459515873505412	0.036793997135694	Phosphatase 2C (PP2C)-like protein
MELO3C002611	0.00459421197278376	0.036793997135694	VQ motif-containing protein
MELO3C022766	0.00459622213447552	0.036793997135694	50S ribosomal protein L35
MELO3C013309	0.00461226279515592	0.0368639930026092	Coiled-coil protein
MELO3C007896	0.00461243236161057	0.0368639930026092	DNA ligase 3
MELO3C022208	0.00461235112080338	0.0368639930026092	Transmembrane protein, putative
MELO3C002241	0.00460760544686867	0.0368639930026092	Protein ROS1
MELO3C021458	0.00461777456584467	0.0368845809160894	glucomannan 4-beta-mannosyltransferase 9-like
MELO3C014961	0.00462684788511114	0.0369343649486903	No data found
MELO3C007108	0.00462896316894279	0.0369363206559399	Auxilin-related protein 2
MELO3C025122	0.00469406507564141	0.0372301209290144	Transmembrane protein, putative
MELO3C002254	0.00469046994419164	0.0372301209290144	No data found
MELO3C018609	0.00468423052131772	0.0372301209290144	nicotinamidase 1-like
MELO3C010982	0.00469150142351815	0.0372301209290144	cysteine proteinase RD19a-like
MELO3C010869	0.00470255932622954	0.0372675939541361	Calcium-binding EF-hand
MELO3C008126	0.00471205326936386	0.0373278539978607	receptor homology region, transmembrane domain- and RING domain-containing protein 2-like isoform X2
MELO3C024467	0.0047202723733617	0.037348183901565	No data found
MELO3C020620	0.00474164902427332	0.0374679317075795	telomere repeat-binding protein 5-like
MELO3C007388	0.00476193222621446	0.0375724900381318	calcium-dependent protein kinase-like
MELO3C017526	0.00476558186294107	0.0375860528000093	No data found
MELO3C010860	0.00476961101908036	0.0376028135791688	thioredoxin-like 4, chloroplastic
MELO3C025264	0.00480324345966632	0.0377390862236877	Auxin efflux carrier
MELO3C024359	0.00479821584987294	0.0377390862236877	40S ribosomal S3-like protein
MELO3C021766	0.00480031640730605	0.0377390862236877	Cysteine proteinase inhibitor
MELO3C010205	0.00480220260665098	0.0377390862236877	Myosin-binding protein 7
MELO3C026379	0.00481892308236753	0.0378405216515612	choline-phosphate cytidylyltransferase 2-like
MELO3C004128	0.00482450500558018	0.0378692962461061	hepatoma-derived growth factor-related protein 2-like isoform X1
MELO3C006557	0.00482848374613742	0.0378854690117076	ATP-dependent (S)-NAD(P)H-hydrate dehydratase
MELO3C014503	0.00484227068846665	0.0379785559279301	Nuclear transcription factor Y subunit B
MELO3C004504	0.004853594233164	0.0380522558597681	SPX domain-containing protein 1
MELO3C019979	0.00486300975469733	0.0381054504915579	40S ribosomal protein S18
MELO3C021380	0.00487514380395182	0.0381563740883631	Prolyl 4-hydroxylase alpha subunit, putative
MELO3C009865	0.00488061309291565	0.0381563740883631	No data found
MELO3C011936	0.00491136386101831	0.038307474285644	protein-tyrosine-phosphatase MKP1-like
MELO3C014848	0.00492368631958517	0.0383581385110405	Zinc finger, RING-type

MELO3C004616	0.00492100162867981	0.0383581385110405	No data found
MELO3C013809	0.00492199748758904	0.0383581385110405	calcium permeable stress-gated cation channel 1-like
MELO3C023525	0.00493771673994492	0.0384457842027261	60S ribosomal protein L6
MELO3C005683	0.0049435184544383	0.0384671181862498	UDP-N-acetylmuramoyl-L-alanyl-D-glutamate--2, 6-diaminopimelate ligase
MELO3C014666	0.00496701622528295	0.0385853581760918	Dirigent protein
MELO3C022914	0.00496848275061024	0.0385853581760918	50S ribosomal protein L15
MELO3C002200	0.00497295451208024	0.0386049051332833	ABC transporter A family protein
MELO3C005243	0.00498172170978672	0.0386577689770444	purple acid phosphatase 4-like
MELO3C026734	0.00499084688857632	0.0386837337375921	lamin-like protein
MELO3C016831	0.00499389552060658	0.0386903771333979	RING-type E3 ubiquitin transferase
MELO3C024452	0.00499963757377242	0.0386903771333979	No data found
MELO3C018867	0.00499926959078445	0.0386903771333979	E6-like protein
MELO3C020617	0.00500844294115677	0.0387281674412314	Haloacid dehalogenase-like hydrolase
MELO3C002030	0.00501632420632747	0.0387739282781844	Glycine-rich RNA-binding protein
MELO3C009465	0.00502843552261645	0.0388523369077278	Terminal flower 1
MELO3C018257	0.00503800739884341	0.038911070832913	No data found
MELO3C002891	0.00504688773087425	0.0389644197799201	Pseudouridine synthase, RsuA/RluB/C/D/E/F
MELO3C006299	0.00505397492352333	0.0389713767143541	RNA-directed DNA polymerase (Reverse transcriptase)-related family protein
MELO3C022027	0.0050556821683212	0.0389713767143541	40S ribosomal protein S19
MELO3C021713	0.00505438158441507	0.0389713767143541	Ubiquinol oxidase
MELO3C012854	0.00505464637579456	0.0389713767143541	Long-chain-alcohol oxidase
MELO3C017092	0.00509335428043201	0.0391808196243162	diphthine methyltransferase
MELO3C018572	0.00509558321440995	0.0391808196243162	glutamate-1-semialdehyde 2,1-aminomutase 2, chloroplastic-like
MELO3C002679	0.00510933008744363	0.0392470478012152	heat stress transcription factor A-4c
MELO3C013472	0.0051198180085511	0.0393052524011742	Histone deacetylase
MELO3C019542	0.00513228821363398	0.0393774514106673	D-3-phosphoglycerate dehydrogenase
MELO3C016667	0.00514137660805702	0.0393847987498828	Random slug protein 5
MELO3C012583	0.00513599158009104	0.0393847987498828	nuclear-pore anchor-like
MELO3C021691	0.00514153474524282	0.0393847987498828	F-box protein family
MELO3C015299	0.00514189399425591	0.0393847987498828	serine/arginine-rich splicing factor SR30
MELO3C018610	0.0051432171743353	0.0393847987498828	Fructose-1,6-bisphosphatase
MELO3C014936	0.0051599163782603	0.0394820567819693	BRO1 domain-containing protein
MELO3C022426	0.0051671505635198	0.0395220977842573	Something about silencing protein
MELO3C012084	0.00517341272002758	0.0395393683466814	40S ribosomal protein S9, putative
MELO3C007190	0.00518428034658769	0.0396070996382051	Splicing factor 3B, subunit 5
MELO3C005803	0.00519167594605396	0.0396329370926246	WAT1-related protein
MELO3C014288	0.00520148075471183	0.0396924433635255	VAN3-binding protein
MELO3C016221	0.00520810517208448	0.0397171785628582	ABC transporter G family member 14
MELO3C004917	0.00522269622442229	0.0397791184372191	sulfite oxidase-like
MELO3C006182	0.00523154057570219	0.0398141405894191	Pentatricopeptide repeat-containing protein At1g01970
MELO3C022310	0.00524944366594116	0.0399196237807747	Histidine kinase
MELO3C005215	0.0052570899040556	0.0399623820304827	defensin Ec-AMP-D2-like
MELO3C019137	0.00526112589863548	0.0399776742486156	Plant/MNJ7-17 protein, putative
MELO3C007409	0.00527492254906536	0.0400516898967673	WRKY family transcription factor
MELO3C006221	0.00527834117750325	0.0400544508958836	Glutathione s-transferase, putative
MELO3C006760	0.00527934253288698	0.0400544508958836	Chromatin structure-remodeling complex protein BSH
MELO3C010941	0.00528496183711913	0.040066299931388	3-ketoacyl-CoA synthase
MELO3C008118	0.0052918874227319	0.0400863298080399	Inner membrane protein oxaA
MELO3C003627	0.00529445457556355	0.0400863298080399	Transcriptional adapter 1
MELO3C003690	0.00529425199930755	0.0400863298080399	adenine nucleotide transporter BT1, chloroplastic/mitochondrial-like
MELO3C007688	0.00531587170426806	0.0402080238558368	tRNA-dihydrouridine synthase
MELO3C020748	0.00533361546979561	0.0402651268780556	Receptor-like protein kinase
MELO3C001920	0.00533117758364088	0.0402651268780556	No data found
MELO3C015481	0.00533354470146574	0.0402651268780556	Chloroplastic group IIA intron splicing facilitator CRS1
MELO3C005634	0.00533638245875689	0.0402706217722545	phosphatidylinositol glycan anchor biosynthesis class U protein-like
MELO3C023004	0.00534674243286837	0.040294608949124	casein kinase I-like isoform X1
MELO3C012295	0.00536354190955324	0.0403829924406279	Tetratricopeptide repeat-like superfamily protein
MELO3C012912	0.00536579815994709	0.0403845837884127	Chlorophyll a-b binding protein, chloroplastic
MELO3C002072	0.00536839161606895	0.0403887108669507	Adenine nucleotide alpha hydrolases-like superfamily protein
MELO3C014951	0.00538851756489089	0.0405092628051124	tRNA/rRNA methyltransferase family protein
MELO3C020489	0.00538680953554949	0.0405092628051124	WRKY transcription factor 1
MELO3C005380	0.00539842275126157	0.0405682842141038	protein phosphatase inhibitor 2
MELO3C009151	0.00540405465087668	0.0405797244487314	phosphoinositide phosphatase SAC8
MELO3C016700	0.00541295604689029	0.0406186957918544	Inner membrane protein oxaA
MELO3C024248	0.00541360366330046	0.0406186957918544	Dynein light chain family protein
MELO3C015113	0.00542243994015512	0.0406559477517553	Protein SMG7
MELO3C007235	0.00543615744316983	0.0407433295427556	Protein IQ-DOMAIN 1
MELO3C017551	0.00544379027512432	0.0407695920149526	Pentatricopeptide repeat-containing protein
MELO3C017169	0.0054419971112214	0.0407695920149526	60S ribosomal protein L34
MELO3C002293	0.00544667677743771	0.0407757466556548	Armadillo/beta-catenin repeat family protein
MELO3C009170	0.00545100219701766	0.0407926647930662	vacuolar cation/proton exchanger 3-like
MELO3C016881	0.00546445639647308	0.0408778596113435	Cytokinin riboside 5'-monophosphate phosphoribohydrolase
MELO3C022605	0.00548519315338203	0.0410019226291225	thiamine biosynthetic bifunctional enzyme TH1, chloroplastic-like
MELO3C019156	0.00549336446814186	0.0410039815297562	protein GrpE
MELO3C015423	0.00549259467745444	0.0410039815297562	Damaged dna-binding 2, putative isoform 1
MELO3C026577	0.00549584987134866	0.0410039815297562	mitogen-activated protein kinase kinase 3
MELO3C022961	0.00549927721920196	0.0410140580823336	4-hydroxyphenylpyruvate dioxygenase
MELO3C009329	0.00550540936501021	0.0410288036036176	Peroxidase
MELO3C024348	0.00550384303802409	0.0410288036036176	Lipoxygenase
MELO3C005298	0.00551011550099556	0.0410336646483313	DELLA protein GAI
MELO3C003554	0.00551021715769784	0.0410336646483313	homeobox-leucine zipper protein ATHB-6-like
MELO3C009549	0.00551926640667522	0.0410855605975985	No data found
MELO3C006093	0.00554875124716214	0.0412118421888699	UDP-glycosyltransferase 91A1-like
MELO3C006553	0.00555487297960233	0.0412417994263784	3-dehydrosphinganine reductase TSC10A isoform X1
MELO3C009753	0.00556782329136662	0.0412913789640253	Transcription factor PERIANTHIA
MELO3C005559	0.00556759058409906	0.0412913789640253	transaldolase
MELO3C021715	0.00558441460505543	0.0413988753886035	E3 ubiquitin-protein ligase COP1-like
MELO3C007563	0.00564058020111158	0.0416900517933206	Lipase
MELO3C013581	0.00563795363412223	0.0416900517933206	shaggy-related protein kinase eta
MELO3C008152	0.00563998177954761	0.0416900517933206	Class I glutamine amidotransferase-like superfamily protein
MELO3C014876	0.00565538385941067	0.041752589098879	Kelch repeat-containing F-box family protein

MELO3C016778	0.00565933442381517	0.0417661418295686	SPla/RYanodine receptor (SPRY) domain protein
MELO3C004117	0.00566929710292929	0.0418240375367018	Carboxypeptidase
MELO3C007636	0.00567263519002581	0.0418330367318221	Calcium-transporting ATPase
MELO3C020997	0.00568704454460378	0.0419199713723186	Sterol 3-beta-glucosyltransferase
MELO3C026499	0.00568866895933029	0.0419199713723186	Zinc finger HIT domain-containing protein 3
MELO3C013692	0.00569296709952316	0.0419359967357266	Transmembrane protein, putative
MELO3C002261	0.00570743449773126	0.0420268918328466	serine/threonine-protein kinase HT1-like
MELO3C009193	0.0057141543213195	0.0420606909026235	Transmembrane protein
MELO3C019997	0.0057189492179438	0.0420803010824039	Histone H4
MELO3C014390	0.00572324775500266	0.0420962457778575	mavicyanin-like
MELO3C006151	0.0057406825704176	0.0421920901889014	protein-ribulosamine 3-kinase, chloroplastic
MELO3C016676	0.00574342477656464	0.0421920901889014	Peptide methionine sulfoxide reductase
MELO3C003123	0.00574566882149075	0.0421920901889014	E3 ubiquitin-protein ligase XB3-like
MELO3C025152	0.00576102443116722	0.0422639195732249	Coronatine-insensitive 1
MELO3C009325	0.00577467309870794	0.0423191774837995	POLAR LOCALIZATION DURING ASYMMETRIC DIVISION AND protein
MELO3C016723	0.00577229566189108	0.0423191774837995	serpin-ZX-like
MELO3C012351	0.00577787071656299	0.0423246175005202	L-aminoadipate-semialdehyde dehydrogenase-phosphopantetheinyl transferase-like
MELO3C016017	0.00578589705892163	0.0423519944464949	translocator protein homolog
MELO3C002023	0.00580928505066813	0.0425074362599648	DExH-box ATP-dependent RNA helicase DExH14
MELO3C007814	0.00582928347011036	0.0426221840989298	protein indeterminate-domain 2-like
MELO3C021695	0.0058292778713428	0.0426221840989298	Phosphatidate cytidylyltransferase
MELO3C014353	0.00584390830887993	0.0426975009959562	Transmembrane protein, putative
MELO3C011890	0.00585525734603176	0.0427329923602296	DNA-binding storekeeper protein-related
MELO3C025877	0.00585523358807216	0.0427329923602296	Glucose-6-phosphate isomerase
MELO3C007133	0.00586456153890169	0.0427776942902953	Transmembrane protein
MELO3C024909	0.005876180212674	0.0427809706934379	Mitochondrial transcription termination factor family protein
MELO3C006765	0.00587699496132954	0.0427809706934379	DEAD-box ATP-dependent RNA helicase 50
MELO3C018802	0.00587443787186281	0.0427809706934379	Peroxisome biogenesis protein 22
MELO3C012708	0.00588417269765351	0.042817437953559	Pentatricopeptide repeat-containing protein
MELO3C004011	0.00590548212715403	0.0429352413293379	No data found
MELO3C006191	0.00590581813556534	0.0429352413293379	Katanin p80 WD40 repeat-containing subunit B1 homolog
MELO3C009201	0.00591891723251758	0.0429423338585641	Immediate early response 3-interacting protein 1
MELO3C006188	0.00592525493769747	0.0429423338585641	ATP-dependent DNA helicase 2 subunit KU80
MELO3C016108	0.0059234494023328	0.0429423338585641	Receptor-like protein kinase
MELO3C019145	0.00591396721573012	0.0429423338585641	ER membrane protein complex subunit 8/9 homolog
MELO3C002690	0.00591329059347701	0.0429423338585641	Myosin heavy chain kinase B
MELO3C003396	0.00592368884294037	0.0429423338585641	Phospholipid hydroperoxide glutathione peroxidase
MELO3C024777	0.00593479565849098	0.0429799337952102	ABC transporter B family protein
MELO3C009446	0.00593804692995192	0.0429877158429694	Serine/threonine-protein phosphatase PP1
MELO3C026748	0.0059455675826553	0.043026388490238	Enolase
MELO3C012239	0.00599508591673292	0.0433154505707741	Bowman-Birk type bran trypsin inhibitor
MELO3C000960	0.00601217131829979	0.0433812098520652	Peptidase_M22 domain-containing protein
MELO3C012636	0.00604022024987105	0.0435676806846981	Unknown protein
MELO3C007305	0.00604570718491382	0.0435754274433807	SNF2 domain-containing protein / helicase domain-containing protein / zinc finger protein-like protein
MELO3C017434	0.00605024264847209	0.0435922079768973	Oxysterol-binding protein-related protein 4C
MELO3C011968	0.00606024825596196	0.0436165607897204	Lipase
MELO3C020484	0.0060595841623905	0.0436165607897204	B3 domain-containing transcription repressor VAL2-like isoform X1
MELO3C019453	0.00606717259072709	0.0436504887046518	Unknown protein
MELO3C012929	0.00608677022585591	0.0437596014526496	Transmembrane protein, putative
MELO3C021977	0.00610215935596248	0.0438073774112173	Translation factor GUF1 homolog, mitochondrial
MELO3C005419	0.00610228848337935	0.0438073774112173	AT-hook motif nuclear-localized protein 6-like
MELO3C008275	0.00609738000015136	0.0438073774112173	Translation initiation factor 2 subunit gamma
MELO3C018119	0.00610157934889466	0.0438073774112173	CRS2-associated factor 2, mitochondrial
MELO3C012855	0.00610856561304385	0.043836505193315	Thioredoxin family protein
MELO3C004028	0.0061196128433687	0.0438679615403588	Syntaxin/T-SNARE family protein
MELO3C024178	0.00612424666004419	0.0438852493792499	Histidine--tRNA ligase
MELO3C023608	0.00613091710727787	0.0439171135116542	Zinc finger family protein
MELO3C021934	0.00613720039845989	0.0439352662012157	Unknown protein
MELO3C006919	0.00614558306381441	0.0439743188142285	cleavage and polyadenylation specificity factor subunit 2
MELO3C002746	0.00616727372711723	0.0440975701798835	Pyruvate dehydrogenase E1 component subunit beta
MELO3C002036	0.00622651950250241	0.0444568089858714	DUF1118-domain-containing protein
MELO3C007762	0.00623705673597619	0.0444628643048621	Mediator of RNA polymerase II transcription subunit 26, putative
MELO3C021058	0.00623574434668006	0.0444628643048621	cell division control protein 45 homolog
MELO3C015155	0.00623862458801827	0.0444628643048621	Scarecrow-like 3
MELO3C027004	0.00624716628925381	0.0445033742420186	poly(A)-specific ribonuclease PARN-like
MELO3C022302	0.00627652237112752	0.044636312678213	protein LHY-like isoform X1
MELO3C020793	0.00628178082278441	0.0446576275986931	Amidase, putative
MELO3C012054	0.00629326949914211	0.0447075308950235	Glycine-rich protein
MELO3C013884	0.00630182195868945	0.0447517734132175	E3 ubiquitin-protein ligase LAP
MELO3C024563	0.00631506277400962	0.0448296817842976	O-linked N-acetylglucosamine transferase, putative
MELO3C014872	0.00632247490555671	0.0448500563612929	Lipase
MELO3C007513	0.00632190735505112	0.0448500563612929	No data found
MELO3C013087	0.00633709589246012	0.0449215027926041	5'/3'-nucleotidase SurE
MELO3C012701	0.00636922311907195	0.0451003657442134	Cysteine proteinase inhibitor
MELO3C018356	0.00636756099341584	0.0451003657442134	Protein WVD2-like 7
MELO3C021329	0.00636951373363392	0.0451003657442134	ATP-binding cassette sub-family C member 11
MELO3C026388	0.00637537403507316	0.0451026197189537	N-acetyl-D-glucosamine kinase-like
MELO3C010153	0.00637634889135241	0.0451026197189537	CTP-dependent diacylglycerol kinase 1
MELO3C009381	0.00639888795602483	0.0452296486197332	splicing factor 3A subunit 2
MELO3C016674	0.00642353608518753	0.0453713927562119	cyclin-SDS-like isoform X1
MELO3C018174	0.00642233138082371	0.0453713927562119	zinc finger protein CONSTANS-LIKE 4
MELO3C004357	0.00642826459136869	0.0453852268631873	No data found
MELO3C018412	0.00643238898121734	0.0453852268631873	allene oxide synthase 3-like
MELO3C025627	0.00644076471782506	0.0454066095911773	Sodium/calcium exchanger family protein
MELO3C025613	0.00644431749613228	0.0454066095911773	Tyrosine aminotransferase
MELO3C006253	0.00646031208615239	0.0454115548155478	protein ECERIFERUM 1-like
MELO3C003341	0.00646141419979185	0.0454115548155478	Casein kinase II subunit beta
MELO3C009195	0.00646569829267873	0.0454150041623959	OTU domain-containing protein
MELO3C014214	0.00646880382342496	0.0454150041623959	ABC transporter G family-like protein
MELO3C010810	0.00646732888793111	0.0454150041623959	Sigma factor sigb regulation protein rsbq
MELO3C013814	0.00648131394496065	0.0454866627928315	26S proteasome non-ATPase regulatory subunit 13

MELO3C002275	0.00649370496098678	0.0455574349110223	anthranilate phosphoribosyltransferase, chloroplastic
MELO3C004648	0.00650643547640417	0.045614339447464	Stress-response A/B barrel domain-containing protein UP3
MELO3C014127	0.00651810160220068	0.0456522271398093	Actin-related protein 8
MELO3C013774	0.00651526241483036	0.0456522271398093	Cystathionine gamma-synthase
MELO3C017394	0.00652352679417967	0.0456578253063655	No data found
MELO3C011399	0.00652419783353908	0.0456578253063655	LOW QUALITY PROTEIN: transcription factor BIM2
MELO3C009226	0.00653689188363704	0.0457291104621977	serine/threonine-protein kinase ATG1c
MELO3C006727	0.00654713755056613	0.0457697060127895	Neutral/alkaline invertase
MELO3C014592	0.00655080438696443	0.0457791351161219	heterogeneous nuclear ribonucleoprotein F
MELO3C025386	0.00655608608069769	0.04579983870099	Polyadenylate-binding protein-interacting protein 4
MELO3C003629	0.00657160924631839	0.0458729395477752	Plasma membrane ATPase
MELO3C025085	0.00657351860449662	0.0458729395477752	Class I heat shock protein
MELO3C017111	0.00658733845633164	0.0459531427672531	39S ribosomal protein L47, mitochondrial
MELO3C000210	0.00659371367780071	0.0459813740900022	Unknown protein
MELO3C002863	0.00659694398511679	0.0459876621115677	patellin-4
MELO3C010710	0.00660311013512804	0.046014404396134	Short-chain dehydrogenase/reductase
MELO3C014101	0.00661437329406644	0.0460196052035173	Unknown protein
MELO3C020940	0.00661550757875262	0.0460196052035173	Pentatricopeptide repeat-containing family protein
MELO3C011317	0.00660728708017455	0.0460196052035173	zinc finger protein CONSTANS-LIKE 4
MELO3C023313	0.00665769860589904	0.0462804962224218	Transmembrane protein, putative
MELO3C002412	0.00666469864478825	0.0463128548683755	Ankyrin repeat family protein
MELO3C021730	0.00666911679857307	0.0463272555944494	calcium permeable stress-gated cation channel 1-like
MELO3C023315	0.00668561297068715	0.0463928919740339	diaminopimelate decarboxylase 2, chloroplastic-like
MELO3C016714	0.00672515339221591	0.0466181306924788	protochlorophyllide reductase, chloroplastic
MELO3C024515	0.00672876682696899	0.0466268126546704	splicing factor U2af small subunit B-like
MELO3C002102	0.00673479236241348	0.046652197251948	Receptor-like kinase
MELO3C006703	0.00674630940843268	0.0467155906406511	CoA ligase
MELO3C005600	0.0067735201512592	0.046871202383288	Phosphate translocator-related family protein
MELO3C022928	0.00677352836102607	0.046871202383288	No data found
MELO3C015597	0.00677974577639429	0.0468813723172307	Calcium ion binding
MELO3C018604	0.00677908066685062	0.0468813723172307	Ubiquitin-like-specific protease 2
MELO3C026067	0.00678676319927907	0.0469134709214429	tRNA (Guanine(9)-N1)-methyltransferase-like
MELO3C007325	0.00679902181931435	0.046981764139132	Sugar transporter, putative
MELO3C023845	0.00680785721675858	0.0470263631247867	serine/arginine-rich SC35-like splicing factor SCL30
MELO3C018418	0.00681891427759185	0.0470862720518047	No data found
MELO3C010532	0.00684685289919851	0.0472626696631497	Structural constituent of ribosome, putative
MELO3C026628	0.00686069658808242	0.0473416830601117	Zinc finger protein
MELO3C022323	0.00686333010384244	0.0473433133848356	proton pump-interactor 1-like
MELO3C007871	0.00687289009524761	0.0473761628240995	rRNA adenine N(6)-methyltransferase
MELO3C022636	0.00688113418024483	0.0474164406579397	No data found
MELO3C015424	0.00690715562065036	0.0475625580028675	Glucan endo-1,3-beta-glucosidase, putative
MELO3C026546	0.00693441822564089	0.0476860043919131	DNA-directed RNA polymerase subunit beta
MELO3C014262	0.00696264092237953	0.0476860043919131	60S ribosomal protein L4-like
MELO3C020440	0.00696854568206295	0.0476860043919131	UBX domain-containing protein 1
MELO3C006100	0.00695734585909258	0.0476860043919131	Ubiquitin-conjugating enzyme, E2
MELO3C014870	0.00695033903996145	0.0476860043919131	DSR6
MELO3C010475	0.00694843697490344	0.0476860043919131	UDP-glucuronosyltransferase 2B17
MELO3C007024	0.00695655689989738	0.0476860043919131	Phenylalanine--tRNA ligase
MELO3C025262	0.00696807649833175	0.0476860043919131	AAA+ ATPase domain-containing protein
MELO3C003085	0.00696185243230085	0.0476860043919131	Flagellin N-methylase
MELO3C022024	0.00693627676482245	0.0476860043919131	Hexosyltransferase
MELO3C020840	0.00696181741775093	0.0476860043919131	Formin-like protein
MELO3C025870	0.0069539047423004	0.0476860043919131	Transcription factor
MELO3C002552	0.00693441431194941	0.0476860043919131	Wound-responsive family protein
MELO3C008234	0.00696379313695883	0.0476860043919131	Transferring glycosyl group transferase
MELO3C021323	0.00699292881807612	0.0478197199543578	condensin-2 complex subunit D3
MELO3C026341	0.00704211024903056	0.0480894312960251	ubiquitin-conjugating enzyme E2 22
MELO3C006306	0.00704624370381213	0.048101025546694	beta-mannosyltransferase 1
MELO3C021434	0.00709534752098828	0.0484027696690838	DNA polymerase epsilon catalytic subunit A
MELO3C007597	0.00712542430296725	0.0485743888710046	Indole-3-acetic acid-amido synthetase GH3.3
MELO3C017791	0.00713147184175345	0.048598839683502	No data found
MELO3C024179	0.00715903843773669	0.0487239522278649	zinc finger protein CONSTANS-LIKE 9-like
MELO3C018056	0.00715686435559881	0.0487239522278649	Carbonic anhydrase
MELO3C024853	0.00717709886898354	0.0488182782776459	GTP-binding protein, chloroplastic
MELO3C022802	0.00718337005107827	0.0488345525434578	Sulfate transporter, putative
MELO3C009638	0.00720397515405002	0.0488443099327942	UBP1-associated protein 2C-like
MELO3C014057	0.00719121069185757	0.0488443099327942	Plant UBX domain-containing protein 8
MELO3C003108	0.00720218464493627	0.0488443099327942	Histone H2A
MELO3C025150	0.00720791735611159	0.0488443099327942	No data found
MELO3C021391	0.00719687947412662	0.0488443099327942	Protein ABCI12, chloroplastic
MELO3C021274	0.00720832830460949	0.0488443099327942	Outer envelope pore protein 16-2, chloroplastic
MELO3C012904	0.00719324434856972	0.0488443099327942	Autophagy-related protein 9
MELO3C010939	0.00722100799204228	0.0488884768031687	FK506-binding protein 4-like
MELO3C026824	0.00723804249067217	0.048987012045334	cytochrome P450 714A1-like
MELO3C021328	0.00724702951271161	0.0490182548751763	ubiquitin-like-specific protease ESD4
MELO3C004223	0.00725452501643375	0.0490313533708249	ATP-dependent Clp protease proteolytic subunit
MELO3C017562	0.00725386990279486	0.0490313533708249	Random slug protein 5
MELO3C008420	0.0072686274147804	0.0491098606960309	Transcriptional corepressor SEUSS
MELO3C009316	0.0072779413909807	0.0491559728216409	Interactor of constitutive active ROPs-like protein
MELO3C016448	0.00729807390629156	0.0491973357260124	methionine S-methyltransferase
MELO3C019257	0.00729310653565496	0.0491973357260124	CDT1-like protein a, chloroplastic
MELO3C005288	0.00730395227585312	0.0492138360613522	F-box family protein
MELO3C006035	0.00731675729151005	0.0492664983805087	Rhodanese-like domain-containing protein 4, chloroplastic
MELO3C012007	0.00732642441238118	0.0492894286514099	spermidine synthase
MELO3C010766	0.00733014592886683	0.0492894286514099	UPF0587 protein C1orf123 homolog
MELO3C019260	0.00733326272891488	0.0492936030065827	Glutamate receptor
MELO3C017705	0.00734710733815036	0.0493698614566626	Transducin/WD40 repeat-like superfamily protein
MELO3C012421	0.0073514013120205	0.0493819130990112	Cytochrome c oxidase assembly protein COX16
MELO3C010584	0.00736507254652774	0.0494569254407944	ribosome maturation protein SBDS
MELO3C005980	0.00738295761679109	0.0495433333245012	Protein ARABIDILLO 1
MELO3C020839	0.00739116720083399	0.0495801838855691	glutamine--tRNA ligase-like

MELO3C008610	0.00743112678605029	0.0497819955555316	No data found
MELO3C021306	0.00743815264091596	0.0497952801713388	ethylene-responsive transcription factor RAP2-3-like
MELO3C017009	0.00744176012404185	0.0498025485224339	4-coumarate--CoA ligase family protein
MELO3C022759	0.00746050443032131	0.0498941760902186	MOB kinase activator-like 1A
MELO3C016549	0.00746559537964697	0.0499113213109844	U3 small nucleolar RNA-associated protein 14 B isoform 3

Supplementary Table 4. Functionality of differentially expressed genes transcripts from RNA-seq (23 DEGs) that were exclusive to the effect of introgression over time in the near-isogenic line (NIL) SC10-2 fruit (n = 3) of melon and its parental control ´Piel de Sapo´ (PS) during postharvest ripening at 20.5 ºC and 88% relative humidity for 18 d.

Gene ID	Functionality*
MELO3C009178	kinase activity, Similar to Probable LRR receptor-like serine/threonine-protein kinase At3g47570 (*Arabidopsis* thaliana) (uniprot_sprot:sp|C0LGP4|Y3475_ARATH)
MELO3C007517	Similar to Brain protein 44-like protein (Homo sapiens) (uniprot_sprot:sp|Q9Y5U8|BR44L_HUMAN)
MELO3C014384	protein dimerization activity, sequence-specific DNA binding, sequence-specific DNA binding transcription factor activity.
MELO3C017343	sodium:dicarboxylate symporter activity, antiporter activity, drug transmembrane transporter activity.
MELO3C024371	Similar to Putative uncharacterized protein (Glycine max) (uniref90:UniRef90_C6THY2)
MELO3C011742	Similar to Putative uncharacterized protein (Vitis vinifera) (uniref90:UniRef90_A5AT31)
MELO3C020541	delta12-fatty acid dehydrogenase activity.
MELO3C024434	Similar to Putative uncharacterized protein (Ricinus communis) (uniref90:UniRef90_B9RQD6)
MELO3C026171	integral to membrane, mitochondrial inner membrane.
MELO3C010991	proton-transporting ATPase activity, rotational mechanism, hydrogen ion transporting ATP synthase activity, rotational mechanism.
MELO3C002083	Similar to Putative uncharacterized protein (Glycine max) (uniref90:UniRef90_C6SZD6)
MELO3C011490	ATP binding, actin binding, motor activity.
MELO3C011715	CDP-diacylglycerol-glycerol-3-phosphate 3-phosphatidyltransferase activity.
MELO3C005513	metal ion binding, zinc ion binding, protein binding, ubiquitin-protein ligase activity.
MELO3C021353	regulation of transcription, DNA-dependent, ATP-dependent chromatin remodeling.
MELO3C011383	ribonucleoside binding, DNA-directed RNA polymerase activity, DNA binding.
MELO3C014724	gluconeogenesis, glucose metabolic process, carbohydrate metabolic process.
MELO3C014519	sequence-specific DNA binding, sequence-specific DNA binding transcription factor activity.
MELO3C002385	regulation of transcription, DNA-dependent.
MELO3C013378	No data found
MELO3C003072	oxidoreductase activity, antioxidant activity.
MELO3C000885	auxin mediated signaling pathway.
MELO3C009970	cellular cell wall organization, carbohydrate metabolic process.

(*According to www.melonomics net, New Melonomics (v3.5))

Supplementary Table 5. Expression levels of differentially expressed genes in melon fruit of the near-isogenic line SC10-2 and its parental control 'Piel de Sapo' (PS) during postharvest storage at 20.5°C and 88% relative humidity for 18 d. *, **; ***, ****: significance at P ≤ 0.05, 0.01, 0.001 or 0.0001, respectively. Gene code according with Melonomics 4.0

		Expression levels of the lines over time (mean ±SE, n=3)										ANOVA significance		
		PS					SC10-2							
Gene ID	Gene abbreviation	0	4	8	12	16	0	4	8	12	16	Ripening time (RT)	Introgression (I)	RT x I
MELO3C024348	*Cm* LOX18	5,1 ±0,7	5,6 ±0,2	1,6 ±0,2	2,4 ±0,1	4,2 ±0,1	33 ±4,5	17,2 ±2,3	6,7 ±1,1	5,8 ±0,5	27,1 ±8,0	**	****	NS
MELO3C019735	*Cm* ACO2	45,7 ±5,0	53,0 ±5,1	38,0 ±0,5	25,1 ±0,8	13,6 ±0,5	32,7 ±5,4	17,5 ±0,3	12,8 ±1,1	9,5 ±0,4	9,1 ±0,8	***	****	NS
MELO3C019548	*Cm* ADH1	4,2 ±0,17	4,4 ±0,11	5,0 ±0,13	5,0 ±0,14	3,4 ±0,5	4,1 ±0,1	3,8 ±0,1	3,2 ±0,1	3,3 ±0,1	3,1 ±0,3	*	**	*
MELO3C018492	*Cm* CAD1	55,8 ±4,1	151,0 ±0,4	252,9 ±20,5	172,0 ±36,4	166,2 ±17,2	19,4 ±4,5	48,0 ±5,7	44,8 ±1,6	52,3 ±3,5	56,2 ±10,4	**	****	*
MELO3C010910	*Cm* AOS	4,7 ±0,0	5,7 ±0,1	5,1 ±0,1	6,0 ±0,1	5,6 ±0,3	7,8 ±0,2	7,2 ±0,3	5,7 ±0,2	5,8 ±0,1	6,5 ±0,2	*	****	**
MELO3C016259	*Cm* SWEET7	0,5 ±0,3	1,6 ±0,2	0,5 ±0,2	0,5 ±0,6	0,9 ±0,9	0,2 ±0,1	2,0 ±0,4	3,4 ±0,2	3,0 ±0,2	2,3 ±0,1	*	**	*
MELO3C008075	*Cm* OPR2	2,3 ±0,2	2,8 ±0,1	2,5 ±0,1	2,7 ±0,0	2,2 ±0,2	4,0 ±0,1	4,6 ±0,1	3,9 ±0,2	3,1 ±0,2	3,8 ±0,1	****	NS	NS
MELO3C020508	*Cm* DFR4	3.1 ±0,1	2,6 ±0,1	2,6 ±0,1	3,0 ±0,1	1,2 ±0.3	4,2 ±0,1	3,77 ±0,0	4,2 ±0,1	4,5 ±0,1	4,3 ±0,5	**	****	*
MELO3C012476	*Cm* NADH1	2,5 ±0,1	2,4 ±0,0	1,7 ±0,1	1,6 ±0,1	0,7 ±0,1	0,3 ±0,0	0,8 ±0,0	0,7 ±0,1	1,0 ±0,1	0,7 ±0,1	*	**	NS
MELO3C017811	*Cm* PAL	0,6 ±0,7	0,5 ±0,1	0,5 ±0,2	0,4 ±0,2	0,1 ±0,0	2,0 ±0,2	2,1 ±0,1	1,3 ±0,1	1,8 ±0,1	2,5 ±0,2	NS	****	NS
MELO3C009127	*Cm* WRKY33	7,3 ±1,3	46,7 ±7,8	12,4 ±0,1	10,8 ±1,5	28,2 ±4,8	56,3 ±5,5	207,4 ±13,7	60,4 ±7,1	34,1 ±2,8	33,4 ±1,0	**	****	*
MELO3C023350	*Cm* GATA5	5,1 ±0,1	5,0 ±0,1	4,6 ±0,1	4,7 ±0,1	4,3 ±0,1	6,2 ±0,3	6,8 ±0,1	5,6 ±0,1	5,3 ±0,1	5,0 ±0,0	***	****	NS
MELO3C005630	*Cm* ERF027	0,0 ±0,0	0,0 ±0,0	0,0 ±0,0	0,0 ±0,0	0,0 ±0,0	3,4 ±0,6	2,0 ±0,4	0,2 ±0,1	0,7 ±0,2	1,8 ±0,7	*	**	*
MELO3C012086	*Cm* TCP15	1,7 ±0,0	2,1 ±0,1	2,0 ±0,1	1,4 ±0,3	0,0 ±0,0	3,3 ±0,2	3,3 ±0.1	3,2 ±0,1	2,7 ±0,1	3,1 ±0,1	*	****	NS
MELO3C011939	*Cm* GDSL esterase/lipase	1,6 ±0,0	1,0 ±0,1	1,0 ±0,1	0,9 ±0,1	0,1 ±0,0	4,2 ±0,1	4,5 ±0,0	4,3 ±0,0	3,9 ±0,0	4,1 ±0,1	***	****	*
MELO3C013101	*Cm* GDPDL4	30,2 ±1,4	27,1 ±1,2	11,3 ±0,8	46,6 ±1,8	28,6 ±1,4	81,2 ±2,3	67,1 ±1,5	58,2 ±2,1	20,1 ±0,8	34,1 ±1,2	*	****	****
MELO3C016540	*Cm* NAC18	677,9 ±31,6	766,9 ±6,8	719,8 ±3,0	639,3 ±32,2	733,9 ±34,3	177,0 ±32,8	240,4 ±11,3	380,4 ±30,4	564,7 ±20,6	491,8 ±3,0	*	****	**
MELO3C005591	*Cm* ACT	17,1 ±0,5	37,2 ±0,9	20,1 ±2,1	38,2 ±2,1	32,1 ±1,6	78,8 ±2,4	100,2 ±0,8	32,2 ±1,8	24,6 ±2,1	40,2 ±2,1	*	***	**
MELO3C017560	*Cm* SDHA	68,2 ±2,4	46,1 ±0,5	46,8 ±0,3	46,8 ±1,1	54,6 ±0,3	67,3 ±1,2	48,1 ±1,2	44,7 ±0,9	44,9 ±0,62	56,9 ±2,4	****	NS	NS
MELO3C021563	*Cm* NADP	39,9 ±2,2	21,8 ±0,2	25,0 ±0,9	23,0 ±1,4	26,0 ±0,4	36,9 ±1,5	22,0 ±0,3	22,1 ±0,9	18,5 ±0,7	24,6 ±0,3	****	NS	NS
MELO3C018576	*Cm* L-GalDH	36,0 ±0,8	30,7 ±0,2	30,5 ±1,2	44,9 ±1,0	48,1 ±0,6	34,3 ±1,2	34,8 ±1,0	36,6 ±0,1	40,6 ±0,1	39,1 ±1,2	***	NS	NS
MELO3C004377	*Cm* GME	78,6 ±2,1	87,1 ±0,3	92,4 ±0,9	81,3 ±5,7	92,2 ±4,7	77,1 ±1,7	90,4 ±2,0	99,2 ±1,6	97,2 ±2,6	84,7 ±0,4	*	NS	NS
MELO3C010675	*Cm* ACLA-1	88,0 ±2,7	37,5 ±1,0	39,5 ±0,7	34,3 ±1,4	42,4 ±1,3	90,1 ±6,8	36,9 ±1,7	43,6 ±1,1	41,0 ±1,0	67,2 ±7,2	****	NS	NS
MELO3C011482	*Cm* ACLB-2	46,1 ±3,0	18,7 ±0,3	25,9 ±0,9	40,3 ±2,4	48,8 ±1,8	44,3 ±3,2	16,6 ±0,1	15,3 ±0,4	21,0 ±1,0	32,6 ±3,7	***	*	NS
MELO3C002167	*Cm* SCOA	65,1 ±3,1	38,7 ±0,3	39,4 ±1,0	43,9 ±2.0	51,5 ±0,4	64,2 ±2,0	46,0 ±2,1	43,0 ±1,2	38,0 ±0,2	52,0 ±3,6	****	NS	NS
MELO3C005518	*Cm* IPMI3	56,3 ±2,5	30,1 ±0,4	28,2 ±0,9	38,0 ±0,3	34,0 ±0,7	57,0 ±1,4	40,2 ±0,8	35,2 ±0,7	30,8 ±0,8	40,8 ±2,9	****	NS	NS
MELO3C003344	*Cm* IIL1	105,2 ±3,6	54,0 ±0,1	54,4 ±0,7	50,6 ±1,3	68,8 ±1,2	69,9 ±1,3	55,8 ±0,6	50,8 ±0,1	51,1 ±0,8	49,2 ±2,3	****	**	***
MELO3C007433	*Cm* FAH	52,0 ±2,1	29,6 ±0,2	27,6 ±0,2	30,9 ±1,1	34,0 ±0,6	36,6 ±1,4	26,0 ±0,3	25,2 ±0,9	23,5 ±0,8	30,5 ±1,0	****	**	NS
MELO3C009970	*Cm* DHL92	1,0 ±0,1	0,3 ±0,1	0,1 ±0,1	0,2 ±0,1	0,5 ±0,1	1,1 ±0,0	0,3 ±0,1	0,5 ±0,1	0,3 ±0,0	0,2 ±0,1	***	NS	NS
MELO3C007517	*Cm* MPC1	44,8 ±0,5	31,7 ±1,0	30,2 ±1,3	32,8 ±1,9	37,0 ±0,9	48,3 ±1,8	34,1 ±1,0	39,7 ±0,9	32,4 ±1,2	37,1 ±2,0	***	NS	NS
MELO3C017343	*Cm* DTX	25,7 ±2,1	38,7 ±2,3	34,4 ±2,1	28,4 ±2,5	33,0 ±0,8	17,8 ±1,2	28,9 ±1,1	32,0 ±0,6	36,7 ±0,7	26,7 ±1,4	*	NS	NS
MELO3C014384	*Cm* ABREX1	46,0 ±1,5	50,5 ±0,7	52,2 ±2,9	50 ±1,6	47,7 ±0,5	39,7 ±2,1	43,7 ±0,7	47,3 ±0,3	49,0 ±1,0	45,9 ±1,3	NS	*	NS
MELO3C000885	*Cm* IAA71	1,4 ±0,3	0,6 ±0,2	0,0 ±0,0	0,3 ±0,2	0,2 ±0,1	1,9 ±0,3	0,2 ±0,1	0,4 ±0,1	0,2 ±0,1	0,3 ±0,1	**	NS	NS
MELO3C024001	*Cm* MADS-box	9,6 ±0,6	6,1 ±1,0	6,7 ±0,4	6,1 ±0,6	5,2 ±0,1	6,2 ±0,6	3,6 ±0,4	2,9 ±0,3	2,1 ±0,1	1,3 ±0,1	**	***	NS
MELO3C010686	*Cm* ALT-2	89,9 ±4,7	46,6 ±3,1	59,5 ±0,2	49,9 ±3,0	53,6 ±2,1	71,8 ±2,7	41,1 ±1,3	42,3 ±1,2	39,2 ±0,8	47,0 ±0,3	****	**	NS

LIST OF REFERENCES:

REFERENCES:

Abrahão, C., Miguel, A.C.A., Dias, J.R. P.S., Spoto, M.H.F., da Silva, P.P.M., 2009. Consumer profile evaluation by quality function development for melon. Ciência e Tecnologia de Alimentos. 2, 716–720. http://www.scielo.br/pdf/cta/v29n4/03.pdf

Aggarwal, C.C., Yu, P.S., 2001. Outlier detection for high dimensional data. ACM Sigmoid Rec. 30, 37–46. DOI:10.1145/376284.375668.

Agilent Technologies, Retention time locking with the MSD productivity ChemStation. Technical overview 2008. Available online: http://www.chem.agilent.com/Library/technicaloverviews/Public/5989-8574EN.pdf (accessed on 28 March 2018).

Aguilar-Martinez J.A., Poza-Carrión C., Cubas P., 2007. Arabidopsis BRANCHED1 acts as an integrator of branching signals within axillary buds. Plant Cell. 19, 458–472. DOI: 10.1105/tpc.106.048934

Alexander, L., Grierson, D., 2002. Ethylene biosynthesis and action in tomato: a model for climacteric fruit ripening. J. Exp. Bot. 53, 2039–2055. DOI: 10.1093/jxb/erf072

Allwood, J.W., Cheung, W., Xu, Y., Mumm R., de Vos, R.C.H., Deborde, C., Biais, B., Maucourt, M., Berger, Y., Schaffer, A.A., Rolin, D., Moing, A., Hall, R.D., Goodacre, R., 2014. Metabolomics in melon: A new opportunity for aroma analysis. Phytochem. 99, 61–72. DOI: 10.1016/j.phytochem.2013.12.010

Allwood, J.W., Erban, A., de Koning, S., Dunn, W.B., Luedemann, A., Lommen, A., Kay, L., Löscher, R., Kopka, J., Goodacre, R., 2009. Inter-laboratory reproducibility of fast gas chromatography–electron impact–time of flight mass spectrometry (GC-EI-TOF/MS) based plant metabolomics. Metabolomics. 5, 479–496. DOI: 10.1007/s11306-009-0169-z

Amaro, A.L., Fundo, J.F., Oliveira, A., Beaulieu, J.C., Fernández-Trujillo, J.P., Almeida, D. P.F., 2013. 1-Methylcyclopropene effects on temporal changes of aroma volatiles and phytochemicals of fresh-cut cantaloupe. J. Sci. Food Agric. 93, 828–837. DOI: 10.1002/jsfa.5804

Andreou, A., Feussner, I., 2009. Lipoxygenases–structure and reaction mechanism. Phytochem. 70, 1504-1510. DOI: 10.1016/j.phytochem.2009.05.008.

Andrews, S., 2010. FastQC: a quality control tool for high throughput sequence data. Babraham Bioinf. Available online at: http://www.bioinformatics.babraham.ac.uk/projects/fastqc

Araújo, W.L., Nunes-Nesi, A., Nikoloski, Z., Sweetlove, L.J., Fernie, A.R., 2012. Metabolic control and regulation of the tricarboxylic acid cycle in photosynthetic and heterotrophic plant tissues. Plant Cell Environ. 35, 1-21. DOI: 10.1111/j.1365-3040.2011.02332.x

Aravind, L., Koonin, E.V., 1999. Gleaning non-trivial structural, functional and evolutionary information about proteins by iterative database searches. J. Mol. Biol. 287, 1023-1040. DOI: 10.1006/jmbi.1999.2653

Argyris, J.M., Pujol, M., Martín-Hernández,, A.M., Garcia-Mas, J., 2015a. Combined use of genetic and genomics resources to understand virus resistance and fruit quality traits in melon. Physiol. Plant. 155, 4-11. DOI: 10.1111/ppl.12323

Argyris, J.M., Ruiz-Herrera, A., Madriz-Masis, P., Sansaverino, W., Morata, J., Pujol, M., Ramos-Onsins, S., Garcia-Mas, J., 2015b. Use of targeted SNP selection for an improved anchoring of the melon (*Cucumis melo* L.) scaffold genome assembly. BMC Genom. 16, 4. DOI: 10.1186/s12864-014-1196-3

Artés, F., Escriche, A.J., Martínez, J.A., Marín, J.G., 1993. Quality factors in 4 varieties of melon (*Cucumis melo* L.). J. Food Qual. 16, 91-100. DOI: 10.1111/j.1745-4557.1993.tb00352.x

Atsumi, S., Hanai, T., Liao, J.C. 2008. Non-fermentative pathways for synthesis of branched-chain higher alcohols as biofuels. Nature. 451, 86-89. DOI: 10.1038/nature06450

Aubert, C., Bourger, N., 2004. Investigation of volatiles in *Charentais* cantaloupe melons (*Cucumis melo* var. *cantaloupensis*). Characterization of aroma constituents in some cultivars. J. Agric. Food Chem. 52, 4522-4528.

Aurand, R., Faurobert, M., Page, D., Maingonnat, J. F., Brunel, B., Causse, M., 2012. Anatomical and biochemical trait network underlying genetic variations in tomato fruit texture. Euphytica. 187, 99–116. DOI: 10.1007/s10681-012-0760-7

Ayub, R., Guis, M., Ben Amor, M., Gillot, L., Roustan, J.P., Latché, A., Bouzayen, M., Pech, J.C., 1996. Expression of ACC oxidase antisense gene inhibits ripening of cantaloupe melon fruits. Nat. Biotechnol. 14, 862–866. DOI: 10.1038/nbt0796-862

Barba, C., Thomas-Danguin, T., Guichard, E., 2017. Comparison of stir bar sorptive extraction in the liquid and vapour phases, solvent-assisted flavour evaporation and headspace solid-phase microextraction for the (non)-targeted analysis of volatiles in fruit juice. LWT-Food Sci. Technol. 85 Part B, 334–344. DOI: 10.1016/j.lwt.2016.09.015.

Baron, L.J.R., Yolando, R., Aramburu, M., Gil, P., Pérez-Elortonda, P.J., Albisu, M., Najera, A.I., Renobales, M., Fernández-García, F., 2007. Volatile composition and sensory properties of industrially produced *Idiazabal* cheese. Intl. Dairy J. 17, 1401–1414. DOI: 10.1080/10942912.2010.528110

Barry, C.S., Llop-Tous, M.I., Grierson, D., 2000. The regulation of 1-aminocyclopropane-1-carboxylic acid synthase gene expression during the transition from system-1 to system-2 ethylene synthesis in tomato. Plant Physiol. 123, 979–986. DOI: 10.1104/pp.123.3.979

Beaulieu, J.C., 2005. Within-season volatile and quality differences in stored fresh-cut cantaloupe cultivars. J. Agric. Food Chem. 53, 8679–8687. DOI: 10.1021/jf050241w

Beaulieu, J.C., 2006. Volatile changes in cantaloupe during growth, maturation, and in stored fresh-cuts prepared from fruit harvested at various maturities. J. Amer. Soc. Hort. Sci. 131, 127–139. DOI: 10.21273/JASHS.131.1.127

Beaulieu, J.C., Grimm, C.C., 2001. Identification of volatile compounds in cantaloupe at various developmental stages using solid phase microextraction. J. Agri. Food Chem. 49, 1345–1352. DOI: 10.1021/jf0005768

Bernillon, S., Biais, B., Deborde, C., Maucourt, M., Cabasson, C., Gibon, Y., Hansen, T.H., Husted, S., De Vos, R.C.H., Mumm, R., Jonker, H., Ward, J.L., Miller, S.J., Baker, J.M., Burger, J., Tadmor, Y., Beale, M.H., Schjoerring, J.K., Schaffer, A.A., Rolin, D., Hall, R.D.,

Moing, A., 2013. Metabolomic and elemental profiling of melon fruit quality as affected by genotype and environment. Metabolomics. 9, 57–77. DOI: 10.1007/s11306-012-0429-1

Biais, B., Allwood, J.W., Deborde, C., Xu, Y., Maucourt, M., Beauvoit, B., Dunn, W.B., Jacob, D., Goodacre, R., Rolin, D., Moing, A., 2009. 1H NMR, GC-EI-TOFMS, and data set correlation for fruit metabolomics: Application to spatial metabolite analysis in melon. Anal. Chem. 81, 2884–2894, DOI:10.1021/ac9001996.

Bianchi, L., Guerrero, L., Gratacós-Cubarsí, M., Claret, A., Argyris, J., Garcia-Mas, J., Hortós, M., 2016. Textural properties of different melon (*Cucumis melo* L.) fruit types: sensory and physical-chemical evaluation. Scientia Hort. 201, 46-56. DOI: 10.1016/j.scienta.2016.01.028

Bianco, V.V., Pratt, H.K., 1977. Compositional changes in muskmelons during Development and in response to Ethylene treatment. J. Amer. Soc. Hort. Sci. 102, 127-133.

Blanca, J., Esteras, C., Ziarsolo, P., Perez, D., Fernandez-Pedrosa, V., Collado, C., Rodriguez, de Pablos R., Ballester A., Roig C., Canizares J, Picó, B., 2012. Transcriptome sequencing for SNP discovery across *Cucumis melo*. BMC Genomics. 13, 280. DOI: 10.1186/1471-2164-13-280.

Blanca, J., Cañizares, J., Ziarsolo, P., Esteras, C., Mir, G., Nuez, F., Garcia-Mas, J., Picó, M.B., 2011. Melon transcriptome characterization. SSRs and SNPs discovery for high throughput genotyping across the species. The Plant Genome 4, 118-131.

Boatright, J., Negre, F., Chen, X., Kish, C.M., Wood, B., Peel, G., 2004. Understanding in vivo benzenoid metabolism in petunia petal tissue. Plant. Physiol. 135, 1993–2011. DOI: 10.1104/pp.104.045468.

Boualem, A., Fergany, M., Fernández, R., Troadec, C., Martin, A., Morin, H., Sari, M.A., Collin, F., Flowers, J.M., Pitrat, M., Purugganan, M.D., Dogimont, C., Bendahmane, A., 2008. A conserved mutation in an ethylene biosynthesis enzyme leads to andromonoecy in melons. Science. 321, 836–838.

Burger, Y., Saar, U., Katzir, N., Paris, H.S., Yeselson, Y., Levin, I., Schaffer, A.A., 2002. A Single Recessive Gene for Sucrose Accumulation in *Cucumis melo* fruit.

J. Amer. Soc. Hort. Sci. 127, 938-943. DOI : 10.21273/JASHS.127.6.938

Burzynski-Chang, E.A., Ryona, I., Reisch, B.I., Gonda, I., Foolad, M.R., Giovannoni, J.J., Sacks, G.L., 2018. HS-SPME-GC-MS analyses of volatiles in plant populations—Quantitating compound individual matrix effects. Molecules. 23, 2436. DOI: 10.3390/molecules23102436

Buttery, R.G., Seifert, R.M., Ling, L.C., Soderstrom, E.L., Ogawa, J.M., Turnbaugh, J.G., 1982. Additional aroma components of Honey Dew, melon. J. Agric. Food Chem. 30, 1208-1211. DOI : 10.1021/jf00114a051

Canales, I., Fernández-Trujillo, J.P., Bueso, M.C., Zarid, M., 2018. Volatile changes in non-climacteric melons with introgression in linkage group X at three stages of maturity. Acta Hortic. (ISHS). 1194, 351–356. DOI:10.17660/ActaHortic.2018.1194.50.

Castro, G.E., Perpiñá, G., Esteras, C., Monforte, A.J., Picó, M.B., 2016. A new introgression line collection to improve 'Piel de Sapo' melons. Acta Hort. 1151, 81-86. DOI: 10.17660/ActaHortic.2017.1151.14.

Causse, M., 2008. Genetic background of flavour: the case of the tomato. In: Bruckner B and Wyllie SG (Eds), Fruit and vegetable flavour: Recent advances and future prospects. 12, 229-253. Woodhead Pub. Ltd., Abington, UK.

Causse, M., Saliba-Colombani, V., Lecomte, L., Duffe, P., Rousselle, P., Buret, M., 2002. QTL analysis of fruit quality in fresh market tomato: a few chromosome regions control the variation of sensory and instrumental traits. J. Exp. Bot. 53, 2089-2098. DOI: 10.1093/jxb/erf058

Chambers, E., Koppel, K., 2013. Associations of volatile compounds with sensory aroma and flavor: The complex nature of flavor. Molecules. 18, 4887–4905, DOI:10.3390/molecules18054887.

Chaparro-Torres, L.A., Bueso, M.C., Fernández-Trujillo, J.P., 2016. Aroma volatiles obtained at harvest by HS-SPME/GC-MS and INDEX/MS-E-nose fingerprint discriminate climacteric behavior in melon fruit. J. Sci. Food Agric. 96, 2352-2365. DOI: 10.1002/jsfa.7350.

Chemindustry. Chemical Information Search. Available online: http://www.chemindustry.com/apps/chemicals (accessed on 28 March 2018).

Chen, H., Cao, S., Jin, Y., Tang, Y. Qi, H., 2016. The relationship between *Cm*ADHs and the diversity of volatile organic compounds of three aroma types of melon (*Cucumis melo*). Front Physiol. **7**, 254. DOI: 10.3389/fphys.2016.00254.

Cheng, Y., Zhou, W., El Sheery, N.I., Peters, C., Li, M., Wang, X., et al., 2011. Characterization of the *Arabidopsis* glycerophosphodiester phosphodiesterase (GDPD) family reveals a role of the plastid-localized AtGDPD1 in maintaining cellular phosphate homeostasis under phosphate starvation. Plant J. 67, 746-746. DOI: 10.1111/j.1365-313X.2011.04538.x

Chipman, D.M., Shaanan, B., 2001. The ACT domain family. Curr. Opin. Struct. Biol. 11, 694-700. DOI: 10.1016/S0959-440X(01)00272-X

Clepet, C., Joobeur, T., Zheng, Y., Jublot, D., Huang, M., Truniger, V., Boualem, A., Hernández-González, M.E., Dolcet-Sanjuan, R., Portnoy, V., Mascarell-Creus, A., Caño-Delgado, A., Katzir, N., Bendahmane, A., Giovannoni, J.J., Aranda, M.A., Garcia-Mas, J., Fei, Z., 2011. Analysis of expressed sequence tags generated from full-length enriched cDNA libraries of melon. BMC Genomics. 12, 252. DOI:10.1186/1471-2164-12-252

Condurso, C., Verzera, A., Dima, G., Tripodi, G., Crinó, P., Paratore, A., Romano, D., 2012. Effects of different rootstock on aroma volatile compounds and carotenoid content of melon fruits. Scientia Hort. 148, 9-26. DOI: 10.1016/j.scienta.2012.09.015

Conesa, A., Götz, S., García-Gómez, J.M., Terol, J., Talón, M., Robles, M., 2005. Blast2GO: a universal tool for annotation, visualization and analysis in functional genomics research. Bioinformat. 21, 3674-3676. DOI: 10.1093/bioinformatics/bti610

Cuevas, H.E., Staub, J.E., Simon, P.W., Zalapa, J.E., McCreight, J.D., 2008. Mapping of genetic loci that regulated quantity of β-carotene in fruit of U.S. Western Shipping melon (*Cucumis melo* L.). Theor. Appl. Genet. 117, 1345–1359.

Dahmani-Mardas, F., Troadec, C., Boualem, A., Leveque, S., Alsadon, A., Aldoss, A., Dogimont, C., Bendahmane, A., 2010. Engineering melon plants with improved fruit shelf life using the TILLING approach. PLoS One. 5, e15776. DOI: 10.1371/journal.pone.0015776

Daminato, M., Guzzo, F., Casadoro, G., 2013. A SHATTERPROOF-like gene controls ripening in non-climacteric strawberries, and auxin and abscisic acid antagonistically affect its expression. J. Exp. Bot. 64, 3775–3786. DOI: 10.1093/jxb/ert214

Diallinas, G., Kanellis, A.K., 1994. A phenylalanine ammonia-lyase gene from melon fruit: cDNA cloning, sequence and expression in response to development and wounding. Plant Mol. Biol. 26, 473-479. DOI: 10.1007/BF00039557

Diaz, A., Fergany, M., Formisano, G., Ziarsolo, P., Blanca, J., Fei, Z., Staub, J.E., Zalapa, J.E., Cuevas, H.E., Dace, G., Oliver M, Boissot, N., Dogimont, C., Pitrat, M., Hofstede, R., van Koert, P., Harel-Beja, R., Tzuri, G., Portnoy, V., Cohen, S., Schaffer, A., Katzir, N., Xu, Y., Zhang, H., Fukino, N., Matsumoto, S., Garcia-Mas, J., Monforte, A.J., 2011. A consensus linkage map for molecular markers and quantitative trait loci associated with economically important traits in melon (*Cucumis melo* L.). BMC Plant Biol. 11, 111. DOI : 10.1186/1471-2229-11-111

Dima, G., Tripodi, G., Condurso, C. Verzera, A., 2014. Volatile constituents of mini-watermelon fruits. J. Essential Oil Res. 26, 323-327. DOI: 10.1080/10412905.2014.933449

Dos-Santos, N., Bueso, M.C., Fernández-Trujillo, J.P., 2013. Aroma volatiles as biomarkers of textural differences at harvest in non-climacteric near-isogenic lines of melon. Food Res. Intl. 5, 1801–1812. DOI: 10.1016/j.foodres.2013.09.031

Dos-Santos, N., Jiménez-Araujo, A., Rodríguez-Arcos, R., Fernández-Trujillo, J.P., 2011. Cell wall polysaccharides of near-isogenic lines of melon and their inbred parentals which show differential flesh firmness and physiological behavior. J. Agric. Food Chem. 59, 7773–7784. DOI: 10.1021/jf201155a

Dos-Santos, N., Obando, J., Ostos, I., Melgarejo, L.M., Moreno, E., Monforte, A.J., et al., 2007. Optimización de la extracción de ácidos orgánicos en pulpa liofilizada de melón y análisis por cromatografía líquida de alta eficiencia. In: Rabasseda J and Martín de la Hinojosa MI (coord.). Congreso IV IBEROLAB, Ministerio de Cultura, Pesca y Alimentación, Madrid, pp. 203-211. http://www.iberolab.org/opencms/export/sites/Iberolab/comunicaciones/Comunicaciones/documentos_comunicaciones/Requisitos_Tecnicos_0039.pdf

Eduardo, I., Arús, P., Monforte, A.J., 2005. Development of a genomic library of near isogenic lines (NILs) in melon (*Cucumis melo* L.) from the exotic accession PI161375. Theor. Appl. Genet. 112, 139–148. DOI: 10.1007/s00122-005-0116-y

Eduardo, I., Arús, P., Monforte, A.J., Obando, J., Fernández-Trujillo, J.P., Martínez, J.A., Alarcón, A.L., Álvarez, J.M., van der Knaap, E., 2007. Estimating the genetic architecture of fruit quality traits in melon (*Cucumis melo* L.) using a genomic library of near-isogenic lines. J. Amer. Soc. Hort. Sci. 132, 1–10. DOI: 10.21273/JASHS.132.1.80

Eisenreich, W., Bacher, A., Arigoni, D., Rohdich, F., 2004. Biosynthesis of isoprenoids via the non-mevalonate pathway. Cell Mol. Life Sci. 61, 1401-1426. DOI: 10.1007/s00018-004-3381-z

Ellis, J., Dodds, P., Pryor, T., 2000. Structure, function and evolution of plant disease resistance genes. Curr. Opin. Plant Biol. 3, 278–284. DOI : 10.1016/S1369-5266(00)00080-7

El-Shewy, A.A., 1999. Response of mango trees to foliar spray with urea and some micronutrients under El-Fayoum governorate conditions. Ann. Agric. Sci. (Moshtohor). 37, 1721-1732.

http://srv4.eulc.edu.eg/eulc_v5/libraries/start.aspx?fn=DigitalLibraryViewIssues&ScopeID=1.&item_id=11719108.64.

Escribano, S., Lázaro, A., 2012. Sensorial characteristics of Spanish traditional melon genotypes: has the flavor of melon changed in the last century? Europ. Food Res. Technol. 234, 581–592. DOI: 10.1007/s00217-012-1661-7

Escribano, S., Sánchez, F.J., Lázaro, A., 2010. Establishment of a sensory characterization protocol for melon (*Cucumis melo* L.) and its correlation with physical–chemical attributes: indications for future genetic improvements. Europ. Food Res. Technol. 231, 611–621. DOI: 10.1007/s00217-010-1313-8

Escudero, A.A., Zarid, M., Bueso, M.C., Fernández-Trujillo, J.P., 2018. Aroma volatiles during non-climacteric melon ripening and potential association with flesh firmness. Acta Hortic. (ISHS). 1194, 363–366. DOI:10.17660/ActaHortic.2018.1194.52.

Eshed, Y., Zamir, D., 1995. An introgression line population of Lycopersicon pennellii in the cultivated tomato enables the identification and fine mapping of yield-associated QTL. Genetics. 141, 1147–1162.

Espino-Díaz, M., Sepúlveda, D.R., González-Aguilar, G., Olivas, G.I., 2016. Biochemistry of apple aroma: A review. Food Technol. Biotechnol. 54, 375–397. DOI: 10.17113/ftb.54.04.16.4248

Esteras, C., Formisano, G., Roig, C., Díaz, A., Blanca, J., Garcia-Mas, J., Gómez-Guillamón, M., López-Sesé, A., Lazaro, A., Monforte, A., Pico, B., 2013. SNP genotyping in melons: genetic variation, population structure, and linkage disequilibrium. Theor. Appl. Genet 126, 1285–1303.

Esteras, C., Rambla, J.L., Sánchez, G., López-Gresa, M.P., González-Mas, M.C., Fernández-Trujillo, J.P., Bellés, J.M., Granell, A., Picó, M.B., 2018. Fruit flesh volatile and carotenoid profile analysis within the *Cucumis melo* L. species reveals unexploited variability for future genetic breeding. J. Sci. Food Agric. 98, 3915-3925. DOI:10.1002/jsfa.8909.

Ezura, H., Ariizumi, T., Garcia-Mas, J., Rose, J., et al., 2006. Functional genomic and biotechnology in *Solanaceae* and *Cucurbitaceae* crops.. Biotechnology in Agriculture and Forestry.DOI: 10.1007/978-3-662-48535-4.

Ezura, H., Owino, W.O., 2008. Melon, an alternative model plant for elucidating fruit ripening. Plant Sci. 175, 121-129. DOI: 10.1016/j.plantsci.2008.02.004

Fatland, B.L., Ke, J., Anderson, M.D., Mentzen, W.I., Cui, L.W., Allred, C.C., Johnston, J.L., Nikolau, B.J., Wurtele, E.S., et al., 2002. Molecular characterization of a heteromeric ATP-citrate lyase that generates cytosolic acetyl-coenzyme A in *Arabidopsis*. Plant Physiol. 130, 740-756. DOI: 10.1104/pp.008110

Fernández-Trujillo, J.P., Bueso, M.C., Hernández, M.S., 2012a. Quality oriented breeding using sensory attributes in melon: the case of climacteric and non-climactereic near-isogenic lines obtained from non-climacteric parents. Acta Hort. (ISHS) 934, 975-984. DOI: 10.17660/ActaHortic.2012.934.130

Fernández-Trujillo, J.P., Dos-Santos, N., Martínez-Alcaraz, R., Le Bleis, I., 2013. Non-destructive assessment of aroma volatiles from a climacteric near-isogenic line of melon obtained by headspace sorptive bar extraction. Foods 2, 401-414. DOI: 10.3390/foods2030401

Fernández-Trujillo, J.P., Fernández-Talavera, M., Ruiz-León, M.T., Roca, M.J., Dos-Santos, N., 2012. Aroma volatiles during whole melon ripening in a climacteric near-isogenic line and its inbred non-climacteric parents. Acta Hort. (ISHS) 934, 951-958. DOI: 10.17660/ActaHortic.2012.934.127

Fernández-Trujillo, J.P., Lester, G., Dos-Santos, N., Martínez, J.A., Esteva, J., Jifon, J.L., et al., 2013. Pre- and postharvest muskmelon fruit cracking: causes and potential remedies. Hort. Technol. 23, 266-275. DOI: 10.21273/HORTTECH.23.3.266Fernández-Trujillo, J.P., Obando, J., Martínez, J.A., Alarcon, A.L., Eduardo, I., Arús, P., Monforte, A.J., 2007. Mapping fruit susceptibility to postharvest physiological disorders and decay using a collection of near-isogenic lines of melon. J. Amer. Soc. Hort. Sci. 132, 739-748. DOI : 10.21273/JASHS.132.5.739

Fernández-Trujillo, J.P., Obando-Ulloa, J.M., Martínez, J.A., Moreno, E., García-Mas, J., Monforte, A.J., 2008. Climacteric or non-climacteric behavior in melon fruit 2. Linking climacteric pattern and main postharvest disorders and decay in a set of near-isogenic lines. Postharvest Biol. Technol. 50, 125-134. DOI: 10.1016/j.postharvbio.2008.04.007

Fernández-Trujillo, J.P., Obando-Ulloa, J.M., Monforte, A.J., Sanmartín, P., Kessler, M., Bueso, M.C., 2009. Métodos estadísticos multivariantes aplicables a estudios de calidad postcosecha del fruto de melón. In Proceedings of the Fifth Virtual Iberoamerican Congress on Quality Management in Laboratories, Congress V IBEROLAB, Madrid, Spain, 5 April 2009; Alsina, I., Martín de la Hinojosa, M.I., Hooghuis, H. (eds.). Madrid, Min. Med. AMB. Medio Rural y Marino: Madrid, Spain, 2009, pp. 13–21. Available online: http://www.iberolab.org/opencms/export/sites/IberolabV/comunicaciones/Comunicaciones/documentos_comunicaciones/Requisitos_Tecnicos_0003.pdf (accessed on 28 March 2018).

Fernández-Trujillo, J.P., Zarid, M., Bueso, M.C., 2018. Methodology to remove strong outliers of non-climacteric melon fruit aroma at harvest obtained by HS-SPME GC-MS analysis. Separations. 5, 30. DOI:10.3390/separations5020030

Ferrer, M.J., Obando, J., Moreno, E., Monforte, A.J., Fernández-Trujillo, J.P., 2007. Diferencias de calidad sensorial asociadas al comportamiento climatérico o no climatérico del melón mediante líneas casi isogénicas. Aitep07. Congreso Iberoamericano de Tecnología Postcosecha y Agroexportaciones. Cartagena Mayo-Junio 2007. Comunicación oral. In: Grupo de Postrecolección y Refrigeración and AITEP (eds.). V Cong. Iberoamer. Tecnol. Postc. Agroep., pp. 504-514. www.horticom. com/pd/imagenes/68/929/68929.pdf.

Filzmoser, P., Gschwandtner, M., 2018. Mvoutlier: Multivariate outlier detection based on robust methods. R Package Version 2.0.8. Available online: https://CRAN.R-project.org/package=mvoutlier (accessed on 29 March 2018).

Flores, F., Yahyaoui, F.E., Billerbeck, G., Romojaro, F., Latché, A., Bouzayen, M., Pech, J.C., C., Ambid., 2002. Role of ethylene in the biosynthetic pathway of aliphatic ester Aroma volatiles in Charentais Cantaloupe melons. Expt. Bot. 53, 201-206. DOI : 10.1093/jexbot/53.367.201

Fraser, M.E., James, M.N.G., Bridger, W.A., Wolodko, W.T., 1999. A detailed structural description of *Escherichia coli* succinyl-CoA synthetase1. J. Mol. Biol. 285, 1633–1653. DOI: 10.1006/jmbi.1998.2324

Fredes, A., Sales, C., Barreda, M., Valcárcel, M., Roselló, S., Beltrán, J., 2016. Quantification of prominent volatile compounds responsible for muskmelon and watermelon aroma by purge and trap extraction followed by gas chromatography-mass spectrometry determination. Food Chem. 190, 689–700. DOI:10.1016/j.foodchem.2015.06.011.

Freilich, S., Lev, S., Gonda, I., Reuveni, E., Portnoy, V., Oren, E., et al., 2015. Systems approach for exploring the intricate associations between sweetness, color and aroma in melon fruits. BMC Plant Biol. 15, 71. DOI: 10.1186/s12870-015-0449-x

Fu, J., Frazee, A.C., Collado-Torres, L., Jaffe, A.E., Leek, J.T., 2018. Ballgown: Flexible, isoform-level differential expression analysis. R package version 2.12.0.

Galpaz, N., Burger, Y., Lavee,T., Tzuri, G., Sherman, A., Melamed, T., Eshed, R., Meir, A., Portnoy, V., Bar, E., Shimoni-Shor, E., Feder, A., Saar, Y., Saar, U., Baumkoler, F., Lewinsohn, E., Schaffer, A.A., Katzir, N., Tadmor, Y., 2013. Genetic and chemical characterization of an EMS induced mutation in *Cucumis melo* CRTISO gene. Arch. Biochem. Biophys. 15, 117-25. DOI: 10.1016/j.abb.2013.08.006.

Galpaz, N., Gonda, I., Shem-Tov, D., Barad, O., Tzuri, G., Lev, S., et al., 2018. Deciphering genetic factors that determine melon fruit-quality traits using RNA-seq-based high-resolution QTL and eQTL mapping. The Plant J. 94, 169-191. DOI: 10.1111/tpj.13838

Galpaz, N., Gonda, I., Shem-Tov, D., Barad, O., Tzuri, G., Lev, S., Fei, Z., Xu, Y., Lombardi, N., Mao, L., Jiao, C., Harel-Beja, R., Doron-Faigenboim, A., Tzfadia, O., Bar, E., Meir, A., Saar, U., Fait, A., Halperin, E., Kenigswald, M., Fallik, E., Kol, G., Ronen, G., Burger, Y., Gur, A., Tadmor, Y., Portnoy, V., Schaffer, A., Lewinsohn, E., Giovannoni, J., Katzir, N., 2018. Deciphering genetic factors that determine melon fruit-quality traits using RNA-seq-based high-resolution QTL and eQTL mapping. The Plant J. 94, 169-191. DOI: https://doi.org/10.1111/tpj.13838

Gang, D.R., Wang, J., Dudareva, N., Nam, K.H., Simon, J.E., Lewinsohn, E., Pichersky, E., 2001. An investigation of the storage and biosynthesis of phenylpropenes in sweet basil. Plant Physiol. 125, 539-555. DOI: 10.1104/pp.125.2.539

Gao, Z.F., Petreikov, M., Zamski, E., Schaffer, A.A., 1999. Carbohydrate metabolism during early fruit development of sweet melon (*Cucumis melo*). Physiol. Plant. 106, 1-8.

Gao, Z.F., Schaffer, A.A., 1999. A novel alkaline alpha-galactosidase from melon fruit with a substrate preference for raffinose. Plant Physiol. 119, 979-987.

Garcia-Mas, J., Benjak, A., Sanseverino, W., Bourgeois, M., Mir, G. et al., 2012. The genome of melon (*Cucumis melo* L.). Proc. Natl. Acad. Sci. USA. 109, 11872–11877.

Garcia-Mas, J., Puigdomenech, P., 2016. Melon genome sequence. In : Functional genomics and biotechnology in *Solanaceae* and *Cucurbitaceae* crops., Biotechnology in Agriculture and Forestry vol. 70, pp. 15-29 Springer, Berlin, Heidelberg. DOI : 10.1007/978-3-662-48535-4_2

Gaude, N., Nakamura, Y., Scheible, W.R., Ohta, H., Dormann, P., 2008. Phospholipase C5 (NPC5) is involved in galactolipid accumulation during phosphate limitation in leaves of *Arabidopsis*. Plant J. 56, 28–39. DOI: 10.1111/j.1365-313X.2008.03582.x

Ge, W., Song, Y., Zhang, C., Zhang, Y., Burlingame, A.L., Guo, Y., Proteomic analyses of apoplastic proteins from germinating Arabidopsis thaliana pollen. Biochim. Biophys. Acta. 1814, 1964–1973. DOI: 10.1016/j.bbapap.2011.07.013.

Gilbert, L., Alhagdow, M., Nunes-Nesi, A., Quemener, B., Guillon, F., Bouchet, B., Faurobert, M., Gouble, B., Page, D., García, V., Petit, J., Stevens, R., Causse, M., Fernie, A.R., Lahaye, M., Rothan, C., Baldet, P., 2009. GDP-D-mannose 3,5-epimerase (GME) plays a key role at the intersection of ascorbate and non-cellulosic cell-wall biosynthesis in tomato. Plant J. 60, 499-508. DOI: 10.1111/j.1365-313X.2009.03972.x.

Giovannoni, J., 2001. Molecular biology of fruit maturation and ripening. Annual Review of Plant Physiol. Plant Mol. Biol. 52, 725-749.

Girard, A.L., Mounet, F., Lemaire-Chamley, M., Gaillard, C., Elmorjani, K., Vivancos, J., Runavol, J.L., Quemener, B., Petit, J., Germain, V., Rothan, C., Marion, D., Bakan,B., 2012. Tomato GDSL1 is required for cutin deposition in the fruit cuticle. Plant Cell 24, 3119–3134. DOI: 10.1105/tpc.112.101055

Giraud, E., Ng, S., Carrie, C., Duncan, O., Low, J., Lee, C.P., Van Aken, O., Millar, A.H., Murcha, M., Whelan, J., 2010. TCP transcription factors link the regulation of genes encoding mitochondrial proteins with the circadian clock in *Arabidopsis thaliana*. Plant Cell. 22, 3921–3934. DOI: 10.1105/tpc.110.074518

Goff, S.A., Klee, H. J., 2006. Plant volatile compounds: sensory cues for health and nutritional value. Science 311, 815–819. DOI: 10.1126/science.1112614

Goldman, A., 2002. Melons for the passionate grower. Artisan, New York, NY. pp. 176.

Gomes, H., Fundo, J., Obando-Ulloa, J.M., Almeida, D.P.F., Fernández-Trujillo, J.P., 2010. The genetic background of quality and cell wall changes in fresh-cut melons. Acta Hort. (ISHS) 877, 1011–1018. DOI: 10.17660/ActaHortic.2010.877.136

Gonda, I., Bar, E., Portnoy, V., Lev, S., Burger, J., Schaffer, A.A., Tadmor, Y., Gepstein, S., Giovannoni, J.J., Katzir, N., Lewinsohn, E., 2010. Branched-chain and aromatic amino acid catabolism into aroma volatiles in *Cucumis melo* L. fruit. J. Exp. Bot. 61, 1111-23. DOI: 10.1093/jxb/erp390.

Gonda, I., Davidovich-Rikanati, R., Bar, E., Lev, S., Jhirad, P., Meshulam, Y., Wissotsky, G., Portnoy, V., Burger, J., Schaffer, A., Tadmor, Y., Giovannoni, J.J., Fei, Z., Fait, A., Katzir, N., Lewinsohn, E., 2018. Differential metabolism of L-phenylalanine in the formation of aromatic volatiles in melon (*Cucumis melo* L.) fruit. Phytochem. 148, 122-131. DOI: 10.1016/j.phytochem.2017.12.018

Gonda, I., Lev, S., Bar, E., Sikron, N., Portnoy, V., Davidovich-Rikanati, R., Burger, J., Schaffer, A.A., Tadmor, Y., Giovannonni, J.J., Huang, M., Fei, Z., Katzir, N., Fait, A., Lewinsohn, E., 2013. Catabolism of L–methionine in the formation of sulfur and other volatiles in melon (*Cucumis melo* L.) fruit. The Plant J. 74, 458-472. DOI: 10.1111/tpj.12149

González, M., Xu, M., Esteras, C., Roig, C., Monforte, A.J., Troadec, C., et al., 2011. Towards a TILLING platform for functional genomics in ´Piel de Sapo´ melons. BMC Res. Notes. 4, 289. DOI: 10.1186/1756-0500-4-289.

González, V.M., Rodríguez-Moreno, L., Centeno, E., Benjak, A., Garcia-Mas, J., Puigdomènech, P., Aranda, M.A. 2010. Genome-wide BAC-end sequencing of *Cucumis melo* using two BAC libraries. BMC Genomics. 11, 618. DOI: 10.1186/1471-2164-11-618

Gonzalez-Ibeas, D., Blanca, J., Donaire, L., Saladie, M., Mascarell-Creus, A., Cano-Delgado, A., GarciaMas, J., Llave, C., Aranda, M., 2011. Analysis of the melon (*Cucumis melo*) small RNAome by high-throughput pyrosequencing. BMC Genomics. 12, 393. DOI : 10.1186/1471-2164-12-393

Gonzalez-Ibeas, D., Canizares, J., Aranda, M., 2012. Microarray analysis shows that recessive resistance to Watermelon mosaic virus in melon is associated with the induction of defense response genes. Mol. Plant Microbe. Interact. 25, 107–118. DOI: 10.1094/MPMI-07-11-0193

Grubbs, F., 1969. Procedures for detecting outlying observations in samples. Technometrics 11, 1–21. DOI:10.2307/1266761.

Gruer, M.J., Artymiuk, P.J., Guest, J.R., 1997. The aconitase family: three structural variations on a common theme. Trends Biochem. Sci. 22, 3-6. DOI: 10.1016/S0968-0004(96)10069-4

Güler, Z., Karaca, F., Yetisir, H., 2013. Volatile compounds and sensory properties in various melons, which were chosen from different species and different locations, grown in Turkey. Intl. J. Food Prop. 16, 168-179. DOI:10.1080/10942912.2010.528110.

Gull, D.D., 1988. Harvesting and handling. In: Hochmuth, G.J., Florida Cooperative Extension Service. Muskmelon Production Guide for Florida. University of Florida Cooperative Extension Service Institute of Food and Agricultural Sciences, Gainesville, FL.

Guo, S., Zhang, J., Sun, H., Salse, J., Lucas, W., et al., 2012. The draft genome of watermelon (*Citrullus lanatus*) and resequencing of 20 diverse accessions. Nat. Genet. 45, 51–58. DOI : 10.1038/ng.2470.

Guo, W.J., Nagy, R., Chen, H.Y., Pfrunder, S., Yu, Y.C., Santelia, D., et al., 2014. SWEET17, a facilitative transporter, mediates fructose transport across the tonoplast of *Arabidopsis* roots and leaves. Plant Physiol. 164, 777–789. DOI: 10.1104/pp.113.232751.

Guo, X., Xu, J., Cui, X., Chen, H., Qi, H., 2017. iTRAQ-based protein profiling and fruit quality changes at different development stages of oriental melon. BMC Plant Biol. 17, 28. DOI: 10.1186/s12870-017-0977-7

Hairdry, G.A., Jalal-ud-Din, B., Ghaffoor, A., Munir, M., 1997. Effect of NAA on fruit drop, yield and quality of mango, *Mangifera indica* cultivars Langra. Scientif. Khyber. 10, 13-20. DOI: 10.9790/2380-081218795

Hammani, K., Gobert, A., Hleibieh, K., Choulier, L., Small, I., Giege, P., 2011. An *Arabidopsis* dual-localized pentatricopeptide repeat protein interacts with nuclear proteins involved in gene expression regulation. Plant Cell. 23, 730–740. DOI: 10.1105/tpc.110.081638

Han, C., Ren, C., Zhi, T., Zhou, Z., Liu, Y., Chen, F., Peng, W., Xie, D., 2013. Disruption of fumarylacetoacetate hydrolase causes spontaneous cell death under short-day conditions in *Arabidopsis*. Plant Physiol. 162**,**1956-1964. DOI: 10.1104/pp.113.216804

Hancock, R.D., Viola, R., 2005. Biosynthesis and catabolism of L-ascorbic acid in plants. Crit. Rev. Plant Sci. 24, 167–188. DOI: 10.1080/07352680591002165

Hayashi, S., Ishii, T., Matsunaga, T., Tominaga, R., Kuromori, T., Wada, T., Shinozaki, K., Hirayama, T., 2008. The glycerophosphoryl diester phosphodiesterase-like proteins SHV3 and its homologs play important roles in cell wall organization. Plant Cell Physiol. 49, 1522-1535. DOI: 10.1093/pcp/pcn120.

Hong, S.J., Lee, S.K., Oh, S.H., 2011. Aroma volatile changes of netted muskmelon (*Cucumis melo* L.) fruit during developmental stages. J. Hort. Environ. Biotechnol. 52, 590–595. DOI:10.1007/s13580-011-0090-z.

Howe, E.A., Sinha, R., Schlauch, D., Quackenbush, J., 2011. RNA-Seq analysis in MeV. Bioinformat. 27, 3209–3210. DOI: 10.1093/bioinformatics/btr490

Hua, C., Linling, L., Shuiyuan, C., Fuliang, C., Feng, X., Honghui, Y., Conghua, W., 2013. Molecular cloning and characterization of three genes encoding dihydroflavonol-4-reductase from *Ginkgo biloba* in anthocyanin biosynthetic pathway. PLoS ONE 8, e72017. DOI: 10.1371/journal.pone.0072017

Hubbard, N.L., Pharr, D.M., Huber, S.C., 1990. Sucrose metabolism in ripening muskmelon fruit as affected by leaf area. J. Amer. Soc. Hort. Sci. 115, 798-802. DOI: 10.21273/JASHS.115.5.798

Iqbal, M., Khan, M.Q., Jalal-ud-Din, Rehman, K., Munir, M., 2009. Effect of foliar application of NAA on fruit drop, yield and physic-chemical characteristic of guava (*Psidium guajava* L.) red flesh cultivar. J. Agric. Res. 47, 259-269. http://www.scialert.net/fulltext/?doi=ajpp.2012.243.251

Irigoyen, A., Ortigosa, M., Juansaras, I., Oneca, M., Torre, P., 2007. Influence of an adjunct culture of *Lactobacillus* on the free amino acids and volatile compounds in a Roncal-type ewe's-milk cheese. Food Chem. 100, 71–80. DOI: 10.1016/j.foodchem.2005.09.011

Jaakola, L., Poole, M., Jones, M.O., Kämäräinen-Karppinen, T., Koskimäki, J.J., Hohtola, A., Häggman, H., Fraser, P.D., Manning, K., King, G.J., Thomson, H., Seymour, G.B., 2010. A SQUAMOSA MADS box gene involved in the regulation of anthocyanin accumulation in bilberry fruits. Plant Physiol. 153, 1619-1629. DOI: 10.1104/pp.110.158279

Jayaprakasam, B., Seeram, N.P., Nair, M.G., 2003. Anticancer and anti-inflammatory activities of cucurbitacins from *Cucurbita andreana*. Cancer Letters 189, 11-16. DOI: 10.1016/S0304-3835(02)00497-4

Jeffrey, C., 1990. Systematics of the *Cucurbitaceae*: an Overview. In: Bates D.M., Robinson, R.W., Jeffrey, C. (eds.), Biology and Utilization of the *Cucurbitaceae*. Cornell University Press, Ithaca, New York, pp. 449-463.

Jeong, M.J., Shih, M.C., 2003. Interaction of a GATA factor with cis-acting elements involved in light regulation of nuclear genes encoding chloroplast glyceraldehyde-3-phosphate dehydrogenase in *Arabidopsis*. Biochem. Biophys. Res. Comm. 300, 555–562. DOI: 10.1016/S0006-291X(02)02892-9

Jin, Y., Zhang, C., Liu, W., Tang, Y., Qi, H., Chen, H., Cao, S., 2016. The alcohol dehydrogenase gene family in melon (*Cucumis melo* L.): Bioinformatic analysis and expression patterns. Front. Plant Sci. **7**, 670. DOI: 10.3389/fpls.2016.00670

Juttner, F., Leonhardt, J., Mohren, S., 1983. Environmental factors mecting the formation of mesityloxide, dimethylallylic alcohol and other volatile compounds excreted by *Anabaena*

cylindrica. J. Gen. Microbiol. 129, 407-412. DOI: https://doi.org/10.1099/00221287-129-2-407

Kays, S.J., Paull, R.E., 2004. Postharvest biology. Exon Press. Athens, Georgia, USA.

Kemp, T.R., Stoltz, L.P., and D.E. Knavel., 1972. Volatile components of muskmelon fruit. J. Agric. Food Chem. 20, 196-198. DOI: 10.1021/jf60180a031

Kendall, S.A., T.J. Ng., 1988. Genetic variation of ethylene production in harvested muskmelon fruits. Hortscience 23, 759-761.

Kende, A., Lim, P.P., Lai, F., Jessop, M., Swindale, L., Oliver, M., Hurr, B., Rickett, D., Baxter, C., 2019. High throughput quantitative volatile profiling of melons with silicone rod extraction – thermal desorption – GC–MS for plant breeding line selection. Food Chem. 270, 368-374. DOI: 10.1016/j.foodchem.2018.07.101

Kerje, T., Grum, M., 2000. The origin of melon, *Cucumis melo*: a review of the literature. In: Katzir, N., Paris, H.S. (eds.). The 7th EUCARPIA Meeting on Cucurbit Genetics & Breeding. ISHS, Maale Ha Hamisha, Israel, pp. 37-44.

Kim, D., Langmead, B. Salzberg, S.L., 2015. HISAT: a fast spliced aligner with low memory requirements. Nat. Meth. 12, 357-360. DOI: 10.1038/nmeth.3317

Kirkbride, J.H., 1993. Biosystematic monograph of the *genus Cucumis* (Cucurbitaceae). Parkway Publ, Boone. North Carolina, USA, 159 p.

Klein, J.D., 1989. Ethylene biosynthesis in heat treated apples. In: Clijsters, H., de Proft, M., Marcelle, R., van Poucke, M. (eds.), Biochemical and physiological aspects of ethylene production in lower and higher plants, pp. 184-190. Kluwer Academic, Dordrecht, Netherlands.

Komsta, L. 2011. Outliers: Tests for outliers. R Package Version 0.14. Available online: https://CRAN.R-project.org/package=outliers (accessed on 28 March 2018).

Kuhn, M., Wing, J., Weston, S., Williams, A., Keefer, C., Engelhardt, A., Cooper, T., Mayer, Z., Kenkel, B., 2016. The R Core Team; et al. Package 'Caret'. Classification and Regression Training. R Package Version 6.0-78. Available online: http://CRAN.R-project.org/package=caret (accessed on 28 March 2018).

Kunst, L., Jetter, R., Samuels, A. L., 2006. Biosynthesis and transport of plant cuticular waxes. In: Riederer, M., Müller, M. (eds.). Biology of the Plant Cuticle. Ann. Plant. Rev. 23:, 182–215. DOI: 10.1002/9781119312994.apr0233

Kyriacou, M. C., Leskovar, D. I., Colla, G., Rouphael, Y., 2018. Watermelon and melon fruit quality: The genotypic and agro-environmental factors implicated. Scientia Hort. 234, 393-408. DOI : 10.1016/j.scienta.2018.01.032

Lázaro, A., De Lorenzo, C., 2015. Texture analysis in melon landraces through instrumental and sensory methods. Intl. J. Food Prop. 18, 1575-1583. DOI: 10.1080/10942912.2014.923441

Lê, S., Josse, J., Husson, F., 2008. FactoMineR: An R package for multivariate analysis. J. Stat. Softw. 25, 1–18.

Lester, G., Shellie, K.C., 1992. Postharvest sensory and physicochemical attributes of Honey Dew melon fruits. Hortscience 27, 1012-1014. DOI: 10.21273/HORTSCI.27.9.1012

Li, M., Qin, C., Welti, R., Wang, X., 2006. Double knockouts of phospholipases Dzeta1 and Dzeta2 in Arabidopsis affect root elongation during phosphate-limited growth but do not affect root hair patterning. Plant Physiol. 140, 761–770. DOI: 10.1104/pp.105.070995

Li, Y., Qi, H., Jin, Y., Tian, X., Sui, L., Qiu, Y., 2016. Role of ethylene in the biosynthesis pathway of related-aroma volatiles derived from fatty acids in oriental sweet melon. J. Amer. Soc. Hort. Sci. 141, 327-338. DOI: 10.21273/JASHS.141.4.327

Liavonchanka, A., Feussner, I., 2006. Lipoxygenases: occurrence, functions and catalysis. J. Plant Physiol. 163, 348–357. DOI: 10.1016/j.jplph.2005.11.006

Lingwood, D., Simons, K., 2010. Lipid rafts as a membrane-organizing principle. Science 5961, 46-50. DOI: 10.1126/science.1174621.

Liu, L., Kakihara, F., Kato, M., 2004. Characterization of six varieties of *Cucumis melo* L. based on morphological and physiological characters, including shelf-life of fruit. Euphytica 135, 305-313.

Liu, M., Diretto, G., Pirrello, J., Roustan, J.P., Li, Z., Giuliano, G., Regad, F., Bouzayen, M., 2014. The chimeric repressor version of an Ethylene Response Factor (ERF) family member, Sl-ERF.B3, shows contrasting effects on tomato fruit ripening. New Phytol. 201, 206-218. DOI: 10.1111/nph.12771.

Lu, W., Mao, L., Chen, J., Han, X., Ren, X., Ying, T., Luo, Z., 2018. Interaction of abscisic acid and auxin on gene expression involved in banana ripening. Acta Physiol. Plant. 40, 46. DOI: 10.1007/s11738-018-2621-z

Luan, F., Delannay, I., Staub, J.E., 2008. Chinese melon (*Cucumis melo* L.) diversity analyses provide strategies for germplasm curation, genetic improvement, and evidentiary support of domestication patterns. Euphytica. 164, 445–461. DOI : 10.1007/s10681-008-9699-0

Mahmuda, K. M., Ueda Y., 2008. Bioconversion of aliphatic and aromatic alcohols to their corresponding esters in melons (*Cucumis melo* L., cv. Prince melon and cv. Earls favorite melon). Postharvest Biol. Technol. 50, 18–24. DOI: 10.1016/j.postharvbio.2008.02.015

Manríquez, D., El-Sharkawy, I., Flores, F.B., El-Yahyaoui, F., Regad, F., Bouzayen, M., Latché, A., Pech, J.C., 2006. Two highly divergent alcohol dehydrogenases of melon exhibit fruit ripening-specific expression and distinct biochemical characteristics. Plant Mol. Biol. 61, 675–685. DOI: 10.1007/s11103-006-0040-9

Martin, A., Troadec, C., Boualem, A., Rajab, M., Fernández, R., Morin, H., Pitrat, M., Dogimont, C., Bendahmane, A., 2009. A transposon-induced epigenetic change leads to sex determination in melon. Nature 461, 1135–1138.

Mascarell-Creus, A., Cañizares, J., Vilarrasa-Blasi, J., Mora-Garcia, S., Blanca, J., González-Ibeas, D., Saladié, M., Roig, C., Deleu, W., Picó-Sirvent, B., López-Bigas, N., Aranda, M.A., Garcia-Mas, J., Nuez, F., Puigdomenech, P., Caño-Delgado, A., 2009. An oligobased microarray offers novel transcriptomic approaches for the analysis of pathogen resistance and fruit quality traits in melon (*Cucumis melo* L.). BMC Genomics. 10, 467. DOI: 1186/1471-2164-10-467.

Mathieu, S., Dal Cin, V., Fei, Z., Li, H., Bliss, P., Taylor, M.G., Klee, H.J., Tieman, D.M., 2009. Flavour compounds in tomato fruits: identification of loci and potential pathways affecting volatile composition. J. Expt. Bot. 60, 325-337. DOI : 10.1093/jxb/ern294

Matich, A., Rowan, D., 2007. Pathway analysis of branched-chain ester biosynthesis in apple using deuterium labeling and enantioselective gas chromatography-mass spectrometry. J. Agric. Food Chem. 55, 2727-2735. DOI: 10.1021/jf063018n

McCollum, T.G., Huber, D.J, and Cantliffe, D.J., 1988. Soluble sugar accumulation and activity of related enzymes during muskmelon fruit-development. J. Amer. Soc. Hort. Sci. 113, 399-403.

Melo, A.M.P., Bandeiras, T.M., Teixeira, M., 2004. New insights into type II NAD(P)H:quinone oxidoreductases. Microbiol. Mol. Biol. Rev. 68, 603–616. DOI: 10.1128/MMBR.68.4.603-616.2004

MEV, Multi experiment viewer. TM4 MeV stand-alone client (2018). http://mev.tm4.org/#/welcome. Download at: https://sourceforge.net/projects/mev-tm4/ (accesed on 5 October 2018).

Mitchell, D.E., Madore, M.A., 1992. Patterns of assimilate production and translocation in muskmelon (*Cucumis melo* L.).2. Low-temperature effects. Plant Physiology. 99, 966-971.

Moing, A., Aharoni, A., Biais, B., Rogachev, I., Meir, S., Brodsky, L., 2011. Extensive metabolic cross-talk in melon fruit revealed by spatial and developmental combinatorial metabolomics. New Phytol. 190, 683–696 DOI: 10.1111/j.1469-8137.2010.03626.x.

Moller, I. M., 2001. Plant mitochondria and oxidative stress: Electron Transport, NADPH turnover, and metabolism of reactive oxygen species. Plant Physiol. Plant Mol. Biol. 52, 561-591. DOI: 10.1146/annurev.arplant.52.1.561

Monforte, A.J., Garcia-Mas, J., Arús, P., 2003. *Cucumis melo* L. intraspecific classification based on microsatellite variation. Plant Breed. 122, 153–157.

Monforte, A.J., Oliver, M., Gonzalo, M.J., Alvarez, J.M., Dolcet-Sanjuan, R., Arus, P., 2004. Identification of quantitative trait loci involved in fruit quality traits in melon (*Cucumis melo* L.). Theor. Appl. Genet. 108, 750–758.

Moreno, E., Obando, J., Dos-Santos, N., Fernández-Trujillo, J.P., Monforte, A.J., Garcia-Mas, J., 2008. Candidate genes and QTLs for fruit ripening and softening in melon. Theor. Appl. Genet. 116, 589–602. DOI:10.1007/s00122-007-0694-y

Moummou, H., Tonfack, L.B., Chervin, C., Benichou, M., Youmbi, E., Ginies, C., et al., 2012. Functional characterization of *Slsc*ADH1, a fruit-ripening-associated short-chain alcohol dehydrogenase of tomato. J. Plant. Physiol. 169, 1435–1444. DOI: 10.1016/j.jplph.2012.06.007

Nakamura, Y., Awai, K., Masuda, T., Yoshioka, Y., Tkamiya, K., Ohta, H., 2005. A novel phosphatidylcholine-hydrolyzing phospholipase C induced by phosphate starvation in *Arabidopsis*. J. Biol. Chem. 280, 7469–7476. DOI: 10.1074/jbc.M408799200

Nakamura, Y., Koizumi, R., Shui, G., Shimojima, M., Wenk, M., Ito, T., Ohta, H., 2009. *Arabidopsis* lipins mediate eukaryotic pathway of lipid metabolism and cope critically with phosphate starvation. Proc. Natl. Acad. Sci. USA. 106, 20978–20983. DOI: 10.1073/pnas.0907173106

Nakata, E., Staub, J.E., López-Sesé, A., Katzir, N., 2005. Genetic diversity in Japanese melon (*Cucumis melo* L.) as assessed by random amplified polymorphic DNA and simple sequence repeat markers. Genet. Resour. Crop. Evol. 52, 405–419.

National Institute of Standards and Technology. U.S. Department of Commerce. NIST Chemistry WebBook, SRD 69. 2017. Available online: http://webbook.nist.gov/chemistry/cas-ser/ (accessed on 28 March 2018).

Nattaporn, W., Pranee, A., 2011. Effect of pectinase on volatile and functional bioactive compounds in the flesh and placenta of 'Sunlady' cantaloupe. Intl. Food Res. J. 18, 819–827.

Naudin, C., 1859. Essais d'une monographiedes espèces et des varieties du genre *Cucumis*. Ann. Sci. Nat. 11, 5–87 (in French).

Navarro, V., 1997. The search of the long life in melon. In: Namesny, A. (ed.), Compendios de Horticultura 10. Melones, pp. 35–40. Reus, Spain: Ed. Horticultura (Chapter 4).

Negri, A. S., Allegra, D., Simoni, L., Rusconi, F., Tonelli, C., Espen L., Galbiati, M., 2015. Comparative analysis of fruit aroma patterns in the domesticated wild strawberries "Profumata di Tortona" (*F. moschata*) and "Regina delle Valli" (*F. vesca*). Front. Plant Sci. 6, 56. DOI: 10.3389/fpls.2015.00056

Nimmakayala, P., Tomason, Y.R., Abburi, V.L., Alvarado, A., Saminathan, T., Vajja, V.G., Salazar, G., Panicker, G.K., Levi, A., Wechter, W.P., McCreight, J.D., Korol, A.B., Ronin, Y., Garcia-Mas, J., Reddy, U.K., 2016. Genome-wide differentiation of various melon horticultural groups for use in GWAS for fruit firmness and construction of a high-resolution genetic map. Front. Plant Sci. 7, 1437. DOI: 10.3389/fpls.2016.01437.

Obando, J., Fernández-Trujillo, J.P., Martínez, J.A, Alarcón, A.L., Eduardo, I., Arús, P., Monforte, A.J., 2008. Identification of melon fruit quality quantitative trait loci using near-isogenic lines. J. Amer. Soc. Hort. Sci. 133, 139-151. DOI: 10.21273/JASHS.133.1.139

Obando-Ulloa, J.M., Eduardo, I., Monforte, A.J., Fernández-Trujillo, J.P., 2009. Identification of QTLs related to sugar and organic acid composition in melon using near-isogenic lines. Scientia Hort. 121, 425-433. DOI: 10.1016/j.scienta.2009.02.023

Obando-Ulloa, J.M., Jowkar, M.M., Moreno, E., Souri, M.K., Martínez, J. A., Bueso, M.C., García-Mas, J., Monforte, A.J., Fernández-Trujillo, J.P., 2009. Discrimination of climacteric and non-climacteric melon fruit at harvest or at senescence stage by quality traits. J. Sci. Food Agric. 89, 1743-1753. DOI: https://doi.org/10.1002/jsfa.3651

Obando-Ulloa, J.M., Moreno, E., García-Mas, J., Nicolai, B., Lammertyn, J., Monforte, A.J., Fernández-Trujillo, J.P., 2008. Climacteric or non-climacteric behavior in melon fruit 1. Aroma volatiles. Postharvest Biol. Technol. 49, 27-37. DOI: 10.1016/j.postharvbio.2007.11.004

Obando-Ulloa, J.M., Nicolai, B., Lammertyn, J., Bueso, M.C., Monforte, A.J., Fernández-Trujillo, J.P., 2009. Aroma volatiles associated with the senescence of climacteric or non-climacteric melon fruit. Postharvest Biol. Technol. 52, 146-155. DOI: 10.1016/j.postharvbio.2008.11.007

Obando-Ulloa, J.M., Ruiz, J., Monforte, A.J., Fernández-Trujillo, J.P., 2010. Aroma profile of a collection of near-isogenic lines of melon. Food Chem. 118, 815-822. DOI: 10.1016/j.foodchem.2009.05.068

Oh, S., Lim, B.S., Hong, S.J., Lee, S.K., 2011. Aroma volatile changes of netted muskmelon (*Cucumis melo* L.) fruit during developmental stages. Hortic. Environ. Biotechnol. 52, 590–595. DOI:10.1007/s13580-011-0090-z.

Osorio, S., Muñoz, C., Valpuesta, V., 2010. Physiology and biochemistry of fruit flavors. In: Hui Y.H. (Ed.). Handbook of Fruit and Vegetable Flavors. John Wiley & Sons, Inc., Hoboken, N.J., USA, pp. 25-44. DOI: 10.1002/9780470622834.ch2

Pang, X.L., Guo, X.F., Qin, Z.H., Yao, Y.B., Hu, X.S., Wu, J.H., 2012. Identification of aroma-active compounds in Jiashi muskmelon juice by GC-O-MS and OAV calculation. J. Agric. Food Chem. 60, 4179–4185. DOI: 10.1021/jf300149m

Pangalo, K.J. 1929. Critical review of the main literature on the taxonomy, geography and origin of cultivated and partially wild melons. Trudy Prikl. Bot. 23, 397-442. [in Russian and translated into English for USDA by G. Saad in 1986].

Paris, K.M., Zalapa, J.E., McCreight, J.D., Staub, J.E., 2008. Genetic dissection of fruit quality components in melon (*Cucumis melo* L.) using a RIL population derived from exotic and elite US Western Shipping germplasm. Mol. Breed. 22, 405–419. DOI: 10.1007/s11032-008-9185-3

Park, S.O., Hwang, H.Y., Crosby, K.M., 2009. A genetic linkage map including loci for male sterility, sugars, and ascorbic acid in melon. J. Amer. Soc. Hort. Sci. 134, 67-76. DOI: 10.1007/s00122-010-1327-4

Paul, V., Pandey, R., Srivastava, G.C., 2012. The fading distinctions between classical patterns of ripening in climacteric and non-climacteric fruit and the ubiquity of ethylene. An overview. J. Food Sci. Technol. 49, 1-21. DOI: 10.1007/s13197-011-0293-4

Pech, J.C., Bouzayen, M., Latché, A., 2008. Climacteric fruit ripening: ethylene-dependent and independent regulation of ripening pathways in melon fruit. Plant Sci. 175, 114-120. DOI: 10.1016/j.plantsci.2008.01.003

Pech, J.C., Latché, A., Van der Rest, B., 2008b. Genes involved in the biosynthesis of aroma volatiles and biotechnological applications. In Fruit and vegetable flavour: recent advances and future prospects. Woodhead Publishing Ltd, Cambridge, Inglaterra. pp. 254-271.

Pereira, L., Ruggieri, V., Pérez, S., Alexiou, K.G., Fernández, M., Jahrmann, M., Pujol, M., Garcia-Mas, J., 2018. QTL mapping of melon fruit quality traits using a high-density GBS-based genetic map. BMC Plant Biol. 18, 324. DOI: 10.1186/s12870-018-1537-5

Perin, C., Gomez-Jimenez, M., Hagen, L., Dogimont, C., Pech, J.C., Latche, A., Pitrat, M., Lelievre, J.M. 2002a. Molecular and genetic characterization of a nonclimacteric phenotype in melon reveals two loci conferring altered ethylene response in fruit. Plant Physiol. 129, 300-309.

Perin, C., Hagen, L.S., Giovinazzo, N., Besombes, D., Dogimont, C., Pitrat, M., 2002b. Genetic control of fruit shape acts prior to anthesis in melon (*Cucumis melo* L.). Mol. Genet. Genom. 266, 933-941.

Perotti, V.E., Moreno, A.S., Podestá, F.E., 2014. Physiological aspects of fruit ripening: The mitochondrial connection. Mitochondrion 17, 1-6. DOI: 10.1016/j.mito.2014.04.010

Perpiñá, G., Cebolla-Cornejo, J., Esteras, C., Monforte, A.J. Picó, B., 2017. 'MAK-10': A long shelf-life *Charentais* breeding line developed by introgression of a genomic region from Makuwa melon. Hort. Sci. 52, 1633-1638. DOI: 10.21273/HORTSCI12068-17

Perpiñá, G., Esteras, C., Gibon, Y., Monforte, A.J., Picó, B., 2016. A new genomic library of melon introgression lines in a cantaloupe genetic background for dissecting desirable agronomical traits. BMC Plant Biol. 16, 154. DOI: 10.1186/s12870-016-0842-0

Perry, P.L., Wang, Y., Lin, J., 2009. Analysis of honeydew melon (*Cucumis melo* var. *inodorus*) flavour and GC-MS/MS identification of (E, Z)-2,6-nonadienyl acetate. Flavour Fragr. J. 24, 341–347. DOI:10.1002/ffj.1947

Pertea, M., Pertea, G.M., Antonescu, C.M., Chang, T.C., Mendell, J.T., Salzberg, S.L., 2015. StringTie enables improved reconstruction of a transcriptome from RNA-seq reads. Nat. Biotechnol. 33, 290-295. DOI: 10.1038/nbt.3122

Pilati, S., Perazzolli, M., Malossini, A., Cestaro, A., Demattè, L., Fontana, P., Dal Ri, A., Viola, R., Velasco, R., Moser, C., 2007. Genome-wide transcriptional analysis of grapevine berry ripening reveals a set of genes similarly modulated during three seasons and the occurrence of an oxidative burst at veraison. BMC Genom. 8, 428. DOI: 10.1186/1471-2164-8-428

Pirrello, J., Prasad, B.C., Zhang, W., Chen, K., Mila, I., Zouine, M., Latché, A., Pech, J.C., Ohme-Takagi, M., Regad, F., Bouzayen, M., 2011. Functional analysis and binding affinity of tomato ethylene response factors provide insight on the molecular bases of plant differential responses to ethylene. BMC Plant Biol. 12, 190. DOI: 10.1186/1471-2229-12-190

Pitrat, M., 2017. Melon genetic resources: phenotypic diversity and horticultural taxonomy. In: Grumet, R., Katzir, N., Garcia-Mas, J., (Eds) Genetics and genomics of the *Cucurbitaceae*. Springer, New York. pp 409-415. DOI: https://dx.doi.org/10.1007/7397_2017_1

Polster, J., Schieberle, P., 2017. Structure–odor correlations in homologous series of mercaptoalkanols. J. Agric. Food Chem. 65, 4329–4340. DOI: 10.1021/acs.jafc.7b01266

Portnoy, V., Benyamini, Y., Bar, E., Harel-Beja, R., Gepstein, S., Giovannoni, J.J., Schaffer, A.A., Burger, J., Tadmor, Y., Lewinsohn, E., et al., 2008. The molecular and biochemical basis for varietal variation in sesquiterpene content in melon (*Cucumis melo* L.) rinds. Plant Mol. Biol. 66, 647–661, DOI:10.1007/s11103-008-9296-6.

Portnoy, V., Diber, A., Pollock, S., Karchi, H., Lev, S., Tzuri, G., Harel-Beja, R., Forer, R., Portnoy, V., Lewinsohn, E., Tadmor, Y., Burger, J., Schaffer, A., Katzir, N. 2011. Use of non-normalized, non-amplified cDNA for 454-based RNA sequencing of fleshy melon fruit. Plant Genome. 4, 36–46. https://dl.sciencesocieties.org/publications/tpg/pdfs/4/1/36

Pratt, H., 1971. Melons. In: Hulme, A. (ed.), Biochemistry of Fruits and their Products, Vol 2. Academic Press, London. pp. 207-232.

Pratt, H.K., Goeschl, J.D., Martin, F.W., 1977. Fruit growth and development, ripening, and role of ethylene in Honey Dew muskmelon. J. Amer. Soc. Hort. Sci. 102, 203-210.

Qi, H., Guan, X., Li, Y., Jing, P., 2012. Effect of grafting on 2-methyl-1-butyl acetate biosynthesis in oriental sweet melon (*Cucumis melo* var. Makuwa makino) peel and flesh tissues. Acta Hort. 93, 271–277. DOI: 10.17660/ActaHortic.2012.932.39

R Core Team, 2018. R: A Language and environment for statistical computing. R foundation for statistical computing, Vienna, Austria. https://www.R-project.org/

Reiter, W.D., Vauzin, G.F., 2001. Molecular genetics of nucleotide sugar interconversion pathways in plants. Plant Mol. Biol. 47, 95–113. DOI: 10.1023/A:1010671129803

Ríos, P., Argyris, J., Vegas, J., Leida, C., Kenigswald, M., Tzuri, G., Troadec, C., Bendahmane, A., Katzir, N., Picó, B., Monforte, A.J., Garcia-Mas, J., 2017. ETHQV6.3 is involved in melon climacteric fruit ripening and is encoded by a NAC domain transcription factor. Plant J. 91, 671–683. DOI: 10.1111/tpj.13596

Ro, K., Zou, C., Wang, Z., Yin, G., 2015. Outlier detection for high dimensional data. Biometrika 102, 589–599. DOI:10.1093/biomet/asv021.

Robinson, R.W., Decker-Walters, D.S., 1999. Cucurbits. CAB International, Wallingford, New York, N.Y. pp 226.

Rodriguez-Moreno, L., Gonzalez, V., Benjak, A., Marti, M., Puigdomenech, P., Aranda, M., Garcia-Mas, J., 2011. Determination of the melon chloroplast and mitochondrial genome sequences reveals that the largest reported mitochondrial genome in plants contains a significant amount of DNA having a nuclear origin. BMC Genomics. 12, 424. DOI : 10.1186/1471-2164-12-424

Rose, J.K.C., Hadfield, K.A., Labavitch, J.M., Bennett, A.B., 1998. Temporal sequence of cell wall disassembly in rapidly ripening melon fruit. Plant Physiol. 117, 345–361. DOI: 10.1104/pp.117.2.345

Rowan, D.D., Allen, J.M., Fielder, S., Hunt, M.B.J., 1999. Biosynthesis of straight-chain ester volatiles in Red Delicious and Granny Smith apples using deuterium-labeled precursors. Agric. Food Chem. 47, 2553-2562. DOI: 10.1021/jf9809028

Rowan, D.D., Lane, H.P., Allen, J.M., Fielder, S., Hunt, M.B., 1996. Biosynthesis of 2-methylbutyl, 2-methyl-2-butenyl, and 2-methylbutanoate esters in Red Delicious and Granny Smith apples using deuterium-labeled substrates. J. Agric. Food Chem. 44, 3276–3285. DOI: 10.1021/jf9508209

Saladié, M., Cañizares J., Phillips, M. A., Rodriguez-Concepcion, M., Larrigaudière, C., Gibon, Y., Lunn, J.E., Garcia-Mas, J., 2015. Comparative transcriptional profiling analysis of developing melon (*Cucumis melo* L.) fruit from climacteric and non-climacteric varieties. BMC Genom. 16: 440. DOI:10.1186/s12864-015-1649-3

Sams, C.E., 1999. Preharvest factors affecting postharvest texture. Postharvest Biol Technol. 15, 249–254. DOI: 10.1016/S0925-5214(98)00098-2

Sánchez, L.B., Galperin, M., Muller, M., 2000. Acetyl-CoA synthetase from the amitochondriate eukaryote Giardia lamblia belongs to the newly recognized superfamily of acyl-CoA synthetases (nucleoside diphosphate-forming). J. Biol. Chem. 275, 5794–5803. DOI: 10.1074/jbc.275.8.5794

Sanz, C., Olías, J.M., Pérez, A.G., 1997. Aroma biochemistry of fruits and vegetables. In: Tomás-Barberán, F.A., Robins, R.J. (eds.). Phytochemistry of fruit and vegetables. Oxford, UK: Clarendon Press, pp. 125–155.

Sanz, C., Pérez, A.G., 2010. Plant metabolic pathways and flavor biosynthesis. In: Hui Y.H. (ed.). Handbook of Fruit and Vegetable Flavors. Hoboken, NJ, USA: John Wiley & Sons, Inc., pp. 129–155. DOI: 10.1002/9780470622834.ch9

Sattler, S.E., Funnell-Harris, D.L., Pedersen, J.F., 2010. Brown midrib mutations and their importance to the utilization of maize, sorghum, and pearl millet lignocellulosic tissues. Plant Sci. 178, 229–238. DOI: 10.1016/j.plantsci.2010.01.001

Schaffer, R.J., Friel, E.N., Souleyre, E.J., Bolitho, K., Thodey, K., Ledger, S., Bowen, J.H., Ma J.H., Nain B., Cohen, D., Gleave, A.P., Crowhurst, R.N., Janssen, B.J., Yao J.L., Newcomb, R.D., 2007. A genomics approach reveals that aroma production in apple is controlled by ethylene predominantly at the final step in each biosynthetic pathway. Plant Physiol. 144, 1899-1912. DOI: 10.1104/pp.106.093765

Schwab, W., Davidovich-Rikanati, R., Lewinsohn, E., 2008. Biosynthesis of plant-derived flavor compounds. Plant J. 54, 712-32. DOI: 10.1111/j.1365-313X.2008.03446.x.

Seymour, G.B. and McGlasson, W.B. 1993. Melons. In : Seymour, G., Taylor, J., Tucker, G. (eds.). Biochemistry of fruit ripening. Chapman & Hall, London, pp. 273- 290.

Seymour, G.B., Ryder, C.D., Cevik, V., Hammond, J.P., Popovich, A., King, G.J., et al., 2011. A SEPALLATA gene is involved in the development and ripening of strawberry (*Fragaria x ananassa* Duch.) fruit, a non-climacteric tissue. J. Exp. Bot. 62, 1179-1188. DOI: 10.1093/jxb/erq360

Shalit, M., Katzir, N., Tadmor, Y., Larkov, O., Burger, Y., Shalekhet, F., Lastochkin, E., Ravid, U., Amar, O., Edelstein, M., et al., 2001. Acetyl-CoA: Alcohol acetyltransferase activity and aroma formation in ripening melon fruits. J. Agric. Food Chem. 49, 794–799, DOI:10.1021/jf001075p.

Shammai A, Petreikov M, Yeselson Y, Faigenboim A, Moy-Komemi, M, et al., 2018. Natural genetic variation for expression of a SWEET transporter among wild species of *Solanum lycopersicum* (tomato) determines the hexose composition of ripening tomato fruit. Plant J. 96, 343-357. DOI: 10.1111/tpj.14035

Shapiro, S.S., Wilk, M.B., 1965. An analysis of variance test for complete samples. Biometrika 52, 591–611. DOI: 10.1093/biomet/52.3-4.591.

Sharma, M.K., Kumar, R., Solanke, A.U., Sharma, R., Tyagi, A.K., Sharma, A.K., 2010. Identification, phylogeny, and transcript profiling of ERF family genes during development and abiotic stress treatments in tomato. Mol. Genet. Genom. 284, 455-475. DOI: 10.1007/s00438-010-0580-1

Shin, A.Y., Kim, Y.M., Koo, N., Lee, S.M., Nahm, S., Kwon, S.Y., 2017. Transcriptome analysis of the oriental melon (*Cucumis melo* L. var. makuwa) during fruit development. Peer. J. 5, e2834. DOI: 10.7717/peerj.2834

Shiomi, S., Yamamoto, M., Nakamura, R., Inaba, A., 1999. Expression of ACC synthase and ACC oxidase genes in melons harvested at different stages of maturity. J. Jap. Soc. Hort. Sci. 68, 10-17. DOI : 10.2503/jjshs.68.10

Sinclair, J.W., Park, S.O., Lester, G.E., Yoo, K.S., Crosby, K.M., 2006. Identification and confirmation of RAPD markers and *andromonoecious* associated with quantitative trait loci

for sugars in melon. J. Amer. Soc. Hort. Sci. 131, 360–371. DOI: 10.21273/JASHS.131.3.360

Singh, T.K., Drake, M.A., Cadwallader, K.R., 2003. Flavor of cheddar cheese: a chemical and sensory perspective. Comprehensive Rev. Food Sci. Food Saf. 2, 139–162. DOI: 10.1111/j.1541-4337.2003.tb00021.x

Smit, B.A., Engels, W.J., Smit, G., 2009. Branched chain aldehydes: production and breakdown pathways and relevance for flavour in foods. Appl. Microbiol. Biotechnol. 81, 987-999. DOI: 10.1007/s00253-008-1758-x.

Soteriou, G.A., Siomos, A.S., Gerasopoulos, D., Rouphael, Y., Gerogiadou, S., Kyriacou, M.C., 2017. Biochemical and histological contribution to textual changes in watermelon fruit modulated by grafting. Scientia Hort. 237, 133-140. DOI: 10.1016/j.foodchem.2017.05.083.

Strassner, J., Schaller, F., Frick, U.B., Howe, G.A., Weiler, E.W., Amrhein, N., Macheroux, P., Schaller, A., 2002. Characterization and cDNA-microarray expression analysis of 12-oxophytodienoate reductases reveals differential roles for octadecanoid biosynthesis in the local versus the systemic wound response. Plant J. 32, 585-601. DOI: 10.1046/j.1365-313X.2002.01449.x

Tang, M., Zhao, H., Bie, Z., Li, Q., Xie, J., Shi, X., Yi, H., Sun, Y., 2012. Effect of different potassium levels on growth and quality in two melon cultivars and two growing-seasons. J. Food. Agric. Environ. 10, 570-575.

Tang, Y., Zhang, C., Cao, S., Wang, X. Qi, H., 2015. The Effect of *Cm*LOXs on the production of volatile organic compounds in four aroma types of melon (*Cucumis melo*). PLoS ONE 10, e0143567. DOI: 10.1371/journal.pone.0143567

Tarze, A., Deniaud, A., Le Bras, M., Maillier, E., Molle, D., Larochette, N., Zamzami, N., Jan, G., Kroemer, G., Brenner, C., 2007. GAPDH, a novel regulator of the pro-apoptotic mitochondrial membrane permeabilization. Oncogene 26, 2606–2620. DOI: 10.1038/sj.onc.1210074. PMID 17072346.

The Good Scent Co. Available online: http://www.thegoodscentscompany.com/search2.html (accessed on 28 March 2018).

Tijet, N., Schneider, C., Muller, B.L. Brash, A.R., 2001. Biogenesis of volatile aldehydes from fatty acid hydroperoxides: molecular cloning of a hydroperoxide lyase (CYP74C) with specificity for both the 9-and 13-hydroperoxides of linoleic and linolenic acids. Arch. Biochem. Biophys. 386, 281–289. DOI: 10.1006/abbi.2000.2218

Tijskens, L.M.M., Dos-Santos, N., Jowkar, M.M., Obando, J., Moreno, E., Schouten, R.E., Monforte, A.J., Fernández Trujillo, J.P., 2009. Postharvest firmness behaviour of near-isogenic lines of melon. Postharvest Biol. Technol. 51, 320–326. DOI:10.1016/j.postharvbio.2008.06.001.

Till, B., Reynolds, S., Greene, E., Codomo, C., Enns, L., Johnson, J., Burtner, C., Odden, A., Young, K., Taylor, N., Henikoff, J., Comai, L., Henikoff, S., 2003. Large-scale discovery of induced point mutations with high-throughput TILLING. Genome Res. 13, 524–530. DOI :10.1101/gr.977903

Torrigiani, P., Fregola, F., Ziosi, V., Ruiz, K.B., Kondo, S., Costa, G., 2012. Differential expression of allene oxide synthase (AOS), and jasmonate relationship with ethylene

biosynthesis in seed and mesocarp of developing peach fruit. Postharvest Biol. Technol. 63, 67–73. DOI: 10.1016/j.postharvbio.2011.08.008

Tukey, J.W., 1977. Exploratory Data Analysis; Addison-Wesley Pub. Co.: Boston, MA, USA.

Ueda, Y., Fujishita, N., Chachin, K., 1997. Presence of alcohol acetyltransferase in melons (*Cucumis melo* L.). Postharvest Biol. Technol. 10, 121-126. DOI: 10.1016/S0925-5214(96)01303-8

Vallone, S., Sivertsen, H., Anthon, G.E., Barrett, D.M., Mitcham, E.J., Ebeler, S.E., 2013. An integrated approach for flavour quality evaluation in muskmelon (*Cucumis melo* L. reticulatus group) during ripening. Food Chem. 139, 171–183. DOI : 10.1016/j.foodchem.2012.12.042

Van den Dool, H., Kratz, P.D., 1963. A generalization of the retention index system including linear temperature programmed gas–liquid partition chromatography. J. Chrom. 11, 463–471, DOI:10.1016/S0021-9673(01)80947-X.

Van Moerkercke, A., Schauvinhold, I., Pichersky, E., Haring, M.A., Schurink, R.C., 2009. A plant thiolase involved in benzoic acid biosynthesis and volatile benzoid production. Plant. J. 60, 292-3-2. DOI: 10.1111/j.1365-313X.2009.03953.x

Verzera, A., Dima, G., Tripodi, G., Condurso, C., Crinò, P., Romano, D., Mazzaglia, A., Lanza, C.M., Restuccia, C., Paratore, A., 2014. Aroma and sensory quality of honeydew melon fruits (*Cucumis melo* L. subsp. melo var. *inodorus* H. Jacq.) in relation to different rootstocks. Scientia Hort. 169, 118-124. DOI: 10.1016/j.scienta.2014.02.008

Verzera, A., Dima, G., Tripodi, G., Ziino, M., Lanza, C.M., Mazzaglia, A., 2011. Fast quantitative determination of aroma volatile constituents in melon fruits by headspace solid–phase microextraction and gas chromatography mass spectrometry. Food Anal. Meth. 4, 141–149. DOI: 10.1007/s12161-010-9159-z

Volk, G.M., Haritatos, E.E., Turgeon, R., 2003. Galactinol synthase gene expression in melon. J. Amer. Soc. Hort. Sci. 128, 8-15. DOI: 10.21273/JASHS.128.1.0008

Wan, H., Yuan, W., Bo, K., Shen, J., Pang, X., Chen, J., 2013. Genome-wide analysis of NBS-encoding disease resistance genes in *Cucumis sativus* and phylogenetic study of NBS-encoding genes in *Cucurbitaceae* crops. BMC Genomics. 14, 109. DOI: 10.1186/1471-2164-14-109

Wang, L., Zhang, X., Wang, L., Tian, Y., Jia, N., Chen, S., Shi, N.B., Huang, X., Zhou, C., Yu, Y., Zhang, Z.Q., Pang, X.A., 2017. Regulation of ethylene-responsive SlWRKYs involved in color change during tomato fruit ripening. Sci. Rep. 7, 16674. DOI: 10.1038/s41598-017-16851-y

Wang, Y., Wyllie, S.G., Leach, D.N., 1996. Chemical changes during the development and ripening of the fruit of *Cucumis melo* (Cv. Makdimon). J. Agric. Food Chem. 44, 210-216. https://pubs.acs.org/doi/10.1021/jf9503568

Wang, Y.H., Thomas, C.E., Dean, R.A., 1997. A genetic map of melon (*Cucumis melo* L.) based on amplified fragment length polymorphism (AFLP) markers. Theor. Appl. Genet. 95, 791–798. DOI : 10.1007/s001220050627

Wasternack, C., Hause, B., 2002. Jasmonates and octadecanoids: signals in plant stress responses and development. Prog. Nucleic Acid Res. Mol. Biol. 72, 165-221. DOI: 10.1016/S0079-6603(02)72070-9

Watanabe, K., Saito, T., Hirota, S., Takahashi, B., Fujishita, N., 1991. Carotenoid- pigments in orange, light orange, green and white flesh colored fruits of melon (*Cucumis melo* L). J. Jap. Soc. Food Sci. Technol. 38, 153-159. DOI : 10.3136/nskkk1962.38.153

Wien, H.C., 1997. The Cucurbits: Cucumber, melon, squash and pumpkin. In: Wien, H.C. (ed.). The physiology of vegetable crops. CAB Int., New York, NY, pp 345-386.

Wüst, M. 2018. Smell of stress: Identification of induced biochemical pathways affecting the volatile composition and flavor quality of crops. J. Agric. Food Chem. 66, 3616–3618, DOI:10.1021/acs.jafc.8b00522.

Wyllie, S.G., Leach, D.N., Wang, Y.M., Shewfelt, R.L., 1995. Key aroma compounds in melons - Their development and cultivar dependence. Fruit Flavors 596, 248-257. https://pubs.acs.org/doi/pdf/10.1021/bk-1995-0596.ch022

Yabumoto, K., Jennings, W.G., Yamaguchi, M., 1977. Volatile constituents of Cantaloupe, *Cucumis melo*, and their biogenesis. J. Food Sci. 42, 32-37.

Yabumoto, K., Yamaguchi, M., Jennings, W.G., 1978. Production of volatile compounds by muskmelon, *Cucumis melo*. Food Chem. 3, 7-16. DOI : 10.1016/0308-8146(78)90042-0

Yagi, T., Di Bernardo, S., Nakamuro-Ogiso, E., Kao, M.C., Seo, B.B. Matsuno-Yagi, A., 2004. NADH dehydrogenases (NADH:quinone oxidoreductase). In: Zannoni D. (ed.), Respiration in archaea and bacteria, vol. 1, pp. 15-40. Kluwer Pub., Dordrecht, The Netherlands.

Yahyaoui, F.E.L., Wongs-Aree, C., Latche, A., Hackett, R., Grierson, D., Pech, J.C. 2002. Molecular and biochemical characteristics of a gene encoding an alcohol acyl-transferase involved in the generation of aroma volatile esters during melon ripening. Europ. J. Biochem. 269, 2359-2366. DOI : 10.1046/j.1432-1033.2002.02892.x

Yamaguchi, M., Hughes, D.L., Yabumoto, K., Jennings, W.G., 1977. Quality of cantaloupe muskmelons - Variability and attributes. Scientia Horticulturae. 6, 59-70.

Yanaka, N., 2007. Mammalian glycerophosphodiester phosphodiesterases. Biosci. Biotechnol. Biochem. 71, 1811-1818. DOI: 10.1271/bbb.70062

Yang, L., Li, D., Li, Y., Gu, X., Huang, S., Garcia-Mas, J., Weng, Y., 2013. A 1,681-locus consensus genetic map of cultivated cucumber including 67 NB-LRR resistance gene homolog and ten gene loci. BMC Plant Biol. 13, 53.

Yano, R., Nonaka, S., Ezura, H., 2018. Melonet-DB, a grand RNA-seq gene expression atlas in melon (*Cucumis melo* L.). Plant Cell Physiol. 59, e4. DOI: 10.1093/pcp/pcx193

Zala, D., Hinckelmann, M.V., Yu, H., Lyra da Cunha, M.M., Liot, G., Cordelières, F.P., Marco, S., Saudou, F., 2013. Vesicular glycolysis provides on-board energy for fast axonal transport. Cell. 152, 479–491. DOI: 10.1016/j.cell.2012.12.029

Zalapa, J.E., Staub, J.E., McCreight, J.D., Chung, S.M., Cuevas, H., 2007. Detection of QTL for yieldrelated traits using recombinant inbred lines derived from exotic and elite US Western Shipping melon germplasm. Theor. Appl. Genet. 114, 1185–1201.

Zhang, C., Cao, S., Jin, Y., Ju, L., Chen, Q., Xing, Q., Qi, H., 2017. Melon 13-lipoxygenase *Cm*LOX18 may be involved in C6 volatiles biosynthesis in fruit. Sci. Rep. **7**, 2816. DOI: 10.1038/s41598-017-02559-6

Zhang, C., Hou, Y., Hao, Q., Chen, H., Chen, L., Yuan, S., Shan, Z., Zhang, X., Yang, Z., Qiu, D., Zhou, X., Huang, W., 2015a. Genome-wide survey of the soybean GATA transcription factor gene family and expression analysis under low nitrogen stress. PLoS ONE. 10, e0125174. DOI: 10.1371/journal.pone.0125174

Zhang, H., Wang, H., Yi, H., Zhai, W., Wang, W. Fu, Q., 2016. Transcriptome profiling of *Cucumis melo* fruit development and ripening. Hort. Res. 3, 16014. DOI: 10.1038/hortres.2016.14

Zhang, Z., Jiang, S., Wang, N., Li, M., Ji, X., Sun, S., Liu, J., Wang, D., Xu, H., Qi, S., Wu, S., Fei, Z., Feng, S. Chen, X., 2015b. Identification of differentially expressed genes associated with apple fruit ripening and softening by suppression subtractive hybridization. PLoS ONE. 10, e0146061. DOI:10.1371/journal.pone.0146061

Zheng, X.Y., Wolff, D.W., 2000. Ethylene production, shelf-life and Eevidence of RFLP polymorphisms linked to ethylene genes in melon (*Cucumis melo* L.). Theor. Appl. Genet. 101, 613-624.

Zhou, Y., Liu, L., Huang, W., Yuan, M., Li, Z., Zhou, F., Li, X., Lin, Y., 2014. Overexpression of OsSWEET5 in rice causes growth retardation and precocious senescence. PLoS ONE. 9, e94210. DOI: 10.1371/journal.pone.0094210

Zhu, M., Chen, G., Zhou, S., Tu, Y., Wang, Y., Dong, T., Hu, Z., 2013. A new tomato NAC (NAM/ATAF1/2/CUC2) transcription factor, SlNAC4, functions as a positive regulator of fruit ripening and carotenoid accumulation. Plant Cell Physiol. 55, 119–135. DOI: 10.1093/pcp/pct162